CELL BIOLOGY AND INSTRUMENTATION: UV RADIATION, NITRIC OXIDE AND CELL DEATH IN PLANTS

NATO Science Series

A series presenting the results of scientific meetings supported under the NATO Science Programme.

The series is published by IOS Press and Springer Science and Business Media in conjunction with the NATO Public Diplomacy Division.

Sub-Series

I.	Life and Behavioural Sciences	IOS Press
II.	Mathematics, Physics and Chemistry	Springer Science and Business Media
III.	Computer and Systems Sciences	IOS Press
IV.	Earth and Environmental Sciences	Springer Science and Business Media
V.	Science and Technology Policy	IOS Press

The NATO Science Series continues the series of books published formerly as the NATO ASI Series.

The NATO Science Programme offers support for collaboration in civil science between scientists of countries of the Euro-Atlantic Partnership Council. The types of scientific meeting generally supported are "Advanced Study Institutes" and "Advanced Research Workshops", although other types of meeting are supported from time to time. The NATO Science Series collects together the results of these meetings. The meetings are co-organized by scientists from NATO countries and scientists from NATO's Partner countries – countries of the CIS and Central and Eastern Europe.

Advanced Study Institutes are high-level tutorial courses offering in-depth study of latest advances in a field.
Advanced Research Workshops are expert meetings aimed at critical assessment of a field, and identification of directions for future action.

As a consequence of the restructuring of the NATO Science Programme in 1999, the NATO Science Series has been re-organized and there are currently five sub-series as noted above. Please consult the following web sites for information on previous volumes published in the series, as well as details of earlier sub-series:

http://www.nato.int/science
http://www.springeronline.nl
http://www.iospress.nl
http://www.wtv-books.de/nato_pco.htm

Series I. Life and Behavioural Sciences – Vol. 371 ISSN: 1566-7693

Cell Biology and Instrumentation: UV Radiation, Nitric Oxide and Cell Death in Plants

Edited by

Yaroslav Blume

National Academy of Sciences of Ukraine, Institute of Cell Biology and Genetic Engineering, Kyiv, Ukraine

Don J. Durzan

University of California, Department of Plant Sciences, One Shields Ave. MS 6, Davis, California, USA

and

Petro Smertenko

National Academy of Sciences of Ukraine, Institute of Semiconductor Physics, Kyiv, Ukraine

IOS Press

Amsterdam • Berlin • Oxford • Tokyo • Washington, DC

Published in cooperation with NATO Public Diplomacy Division

Proceedings of the NATO Advanced Research Workshop on
Cell Biology and Instrumentation: UV Radiation, Nitric Oxide and Cell Death in Plants
Yalta, Ukraine
8–11 September 2004

ISBN 1-58603-574-6
Library of Congress Control Number: 2005937746

Publisher
IOS Press
Nieuwe Hemweg 6B
1013 BG Amsterdam
Netherlands
fax: +31 20 687 0019
e-mail: order@iospress.nl

Distributor in the UK and Ireland
IOS Press/Lavis Marketing
73 Lime Walk
Headington
Oxford OX3 7AD
England
fax: +44 1865 750079

Distributor in the USA and Canada
IOS Press, Inc.
4502 Rachael Manor Drive
Fairfax, VA 22032
USA
fax: +1 703 323 3668
e-mail: iosbooks@iospress.com

PRINTED IN THE NETHERLANDS

Cell Biology and Instrumentation: UV Radiation, Nitric Oxide and Cell Death in Plants
Y. Blume et al. (Eds.)
IOS Press, 2006

Preface

The contributions from speakers and the poster presentations for the Advanced Research Workshop (ARW), "Cell Biology and Instrumentation: UV Radiation, Nitric Oxide and Cell Death in Plants" are archived in this volume. The ARW was held at the Hotel "MRIYA", Yalta, Ukraine, from 8 to 11, September 2004. The ARW was organized to create links among scientists from NATO and Partner countries to stabilize and sustain their scientific communities. Contributions were received from the European Union, the Eastern European countries of the Former Soviet Union, and the USA.

The main aims of the Workshop were to introduce new theoretical developments and instrumentation for cell biology, update our understanding of the effects of UV radiation, and evaluate how plants use UV signals to protect against damage and enhance their productivity.

Cellular processes, signaled by UV radiation, contribute to the behavior of plants under various and different stresses in the environment. The importance of the free radical, nitric oxide (NO) was identified as a key early signal in this process. Stress-induced NO can be protective, produce physiological disorders, DNA damage, and programmed cell death (apoptosis).

This volume is divided into three parts: Instrumentation and Ecological Aspects, Effects of UV Radiation, Nitric oxide and Plant stress, and Plant Stress and Programmed Cell Death.

The Workshop:

(i) Evaluates case histories, and introduces new instruments for the non-invasive sensing and imaging of UV-stress-related damage in vegetation
(ii) Identifies the cell biological hazards of UV radiation coupled to other environmental stresses
(iii) Examines how UV light may relate to the production of NO by plants in terms of DNA damage, error-prone repair cell cycles, and the multiple mechanisms of programmed cell death

The oral and poster papers presented during the four-day meeting are included.

All attendees express their sincere gratitude to the NATO International Scientific Exchange Programme, whose financial support made the meeting possible. We also thank the agency ITEM (Intelligence, Technology, Materials) in Kyiv whose director Dr. L. Chernyshov professionally helped us to organise the workshop. We thank V. Stepanov, N. Sukach, and P. Karpov for their clerical and technical assistance, which ensured the conference and social arrangements ran smoothly.

Yaroslav Blume, *Kyiv, Ukraine*
Don Durzan, *Davis, USA*
Petro Smertenko, *Kyiv, Ukraine*

Invited Lectures

ANDREEV Igor
Institute of Molecular Biology & Genetics
National Academy of Sciences of Ukraine
Akad. Zabolotnogo Str., 150
03143 Kyiv, Ukraine
Tel: +380 (44) 2660798
Fax: 380 (44) 2660759
E-mail: i.o.andreev@imbg.org.ua

BLUME Yaroslav B.
Institute of Cell Biology and Genetic Engineering
Acad. Zabolotny Str., 148
03143, Kiev, Ukraine
Tel./Fax: + 380 (44) 266 7104
E-mail: cellbio@cellbio.freenet.viaduk.net and yablume@univ.kiev.ua

BLUMTHALER Mario
Institute for Medical Physics
Muellerstr. 44
Innsbruck, 6020, Austria
Tel: +43-512-5073556
Fax: 43-512-5072860
E-mail: Mario.Blumthaler@uibk.ac.at

BOZHKOV Peter
Swedish University of Agricultural Sciences
Box 7080
SE-75007 Uppsala, Sweden
E-mail: peter.bozhkov@vbsg.slu.se

BRIT Anne
Section of Plant Biology
University of California
One Shields Ave
Davis, CA 95616 USA
Tel: 530 752-0699
Fax: 30 752-5410
E-mail: abbritt@ucdavis.edu

DELEDONE Massimo
Verona University
Strada le Grazie, 15
37134 Verona, Italy

Tel.: +39 045 8027962
Fax: +39 045 8027929
E-mail: massimo.delledonne@univr.it

DORDAS Christos
Aristotle University of Thessaloniki
School of Agriculture
Laboratory of Agronomy
54124 Thessaloniki, Grece
Tel: 302310-998602
Fax: 302310-998634
E-mail: chdordas@agro.auth.gr

DURZAN Don
Department of Plant Sciences MS 6
University of California
One Shields Avenue
Davis, California, 95616 USA
Tel.: (530) 752-0399
Fax: (530) 752-0399
E-mail: djdurzan@ucdavis.edu

FLUHR Robert
Department of Plant Sciences
Weizmann Institute of Science
Rehovot, Israel 76100
Tel.: 972-8-9342175
Fax: 972-8-9344181
E-mail: robert.fluhr@weizmann.ac.il

GALLOIS Patrick
University of Manchester
3.614 Stopford building, Oxford road, Manchester
M13 9PT UK
Tel.: +44 161 275 3922
Fax: +44 161 275 3916
E-mail: patrick.gallois@man.ac.uk

GARDINER Brian G.
British Antarctic Survey
Madingley Road
Cambridge CB3 0ET U.K.
Tel.: + 44 1223 221494 (direct line)
Tel.: + 44 1223 221400 (switchboard)
Fax: + 44 1223 221279 (department)
Fax: + 44 1223 362616 (institute)
E-mail: brian.gardiner@bas.ac.uk

HAVEL Ladislav
Department of Botany and Plant Physiology
Faculty of Agronomy, Mendel University of Agriculture and Forestry in Brno

Zemedelska 1
613 00 Brno, Czech Republic
E-mail: lhavel@mendelu

IAKIMOVA Elena T.
AgroBioInstitute
8 Dragan Tzankov Blvd
1164 Sofia, Bulgaria
Tel.: (+359) 2 963 54 07
Fax: (+359) 2 963 54 08
elena_iakimova@hotmail.com
E-mail: elena_iakimova@abi.bg

MATKOWSKI Adam
Dept. Pharmaceutical Biology and Botany
Medical University in Wroclaw
Al. Jana Kochanowskiego 10, 51–601 Wroclaw, Poland
E-mail: am9@biol.am.wroc.pl

MELNIKOVA Irina
Research Centre for Ecological Safety
Russian Academy of Sciences
Korpusnaya St., 18, St. Petersburg
197100 Russia
Tel.: + 7 (812) 370 1972
Fax: + 7 (812) 370-19-72
E-mail: Irina.Melnikova@pobox.spbu.ru

MÜHLENBOCK Per
Department of Botany
Stockholm University
10405, Stockholm, Sweden

NEILL Steven J.
Director, Centre for Research in Plant Science
Faculty of Applied Sciences
University of the West of England (UWE)
Coldharbour Lane
Bristol, BS16 1QY
Tel.: +44(0)117 3282149
Fax: +44(0)117 3282904
E-mail: Steven.Neill@uwe.ac.uk

OTVOS Krisztina
Laboratory of Cell Division and Differentiation
Institute of Plant Biology
Biological Research Centre
Hungarian Academy of Sciences
Temesvari krt. 62
Szeged, Hungary
Tel.: 36 62 432 232
Fax: 36 62 433 434

de PINTO Maria Concetta
Dipartimento di Biologia e Patologia Vegetale
Universita degli Studi di Bari
Via Orabona 4
I – 70126 Bari, Italy
Tel.: +39 080 5442170
Fax: +39 080 5442167
E-mail: depinto@botanica.uniba.it

SLINEY David H.
US Center for Health Promotion and Preventive Medicine
Laser/Optical Radiation
MCHB-TS-OLO (Bldg. E-1950)
MD 21010 Aberdeen Proving Ground, USA
Tel.: +1-410-4363002
Fax: +1-410-4365054
E-mail: David.Sliney@apg.amedd.army.mil and David.Sliney@att.net

SMERTENKO Petro
National Academy of Sciences of Ukraine
Institute of Semiconductors Physics
Prospekt Nauki 45
03028 Kyiv-28, Ukraine
Tel.: +380-44-2656477
Fax: +380-44-265 8342
E-mail: petro_smertenko@eureka.kiev.ua and eureka@merydian.kiev.ua

VALERO Francisco P.J.
Atmospheric Research Laboratory
Center for Atmospheric Sciences
Scripps Institution of Oceanography
University of California, San Diego
9500 Gilman Drive, MC 0242
La Jolla, CA 92093-0242
Tel.: (858) 534-2701
Fax: (858) 822-0517
E-mail: fvalero@ucsd.edu

WENDEHENNE David
UMR INRA 1088/CNRS 5184/
Universite de Bourgogne
Plante-Microbe-Environnement
17 rue Sully, BP 86510, 21065 Dijon Cedex
France
Tel.: 333 80 69 37 21
Fax: 333 80 69 32 26
E-mail: wendehen@dijon.inra.fr

Poster Presentations

GALCHINETSKI Leonid
STC “Institute for Single Crystals”
60 Lenin Ave.
61001 Kharkov
Ukraine
Tel.: (0572) 30 83 93
E-mail: stcri@isc.kharkov.com

KOLESNEVA Kate
Institute of Biophysics and Cell Engineering
of National Academy of Sciences of Belarus
27, Akademicheskaya Str.
220072, Minsk
Belarus
Tel.: 375-17-2841749
Fax: 375-17-2842359
E-mail: ipb@biobel.bas-net.by
kolesneva_kate@mail.ru

MARTÍNEZ M. Carmen
Autonomous University of Barcelona
Biochemistry and Molecular Biology Dpt.
Fac. Ciencias.
Bellaterra (Barcelona), 08193, Spain
Tel.: +34 93 5813422
Fax: +34 93 5811264
E-mail: carmen.martinez@uab.es

MÜHLENBOCK Per
Department of Botany
Stockholm University
10405, Stockholm, Sweden
E-mail: Per.Muhlenbock@botan.su.se

RAFANELLI Claudio
C.N.R. – Institute of Atmospheric Sciences and Climate – Section of Rome
Area della Ricerca “Roma – Tor Vergata” – via del Fosso del Cavaliere, 100 – Rome
00133 Italy
Tel.: +39 064993 4284
Fax: +39 064993 4291
E-mail: c.rafanelli@isac.cnr.it

SOBOLEVSKI Piotr
Institute of Geophysics, Geophysical Observatory at Belsk
Polish Academy of Sciences
Ks. Janusza 64
01-452 Warsaw
Poland
Tel.: (+48) 48 6642056 int. 52
(+48) 48 6611373
E-mail: pss@ra.onet.pl, piotrs@igf.edu.pl

STEPANOV Vladymir
National Academy of Sciences of Ukraine
Institute of Semiconductors Physics
Prospekt Nauki 45
03028 Kyiv-28, Ukraine
Tel.: +380-44-2655757
Fax: +380-44-265 8342
E-mail: class@class.semicond.kiev.ua

VELIGURA Alina
Kiev National Taras Shevchenko University
64, Vladimirskaya Str., Kiev 01033
Ukraine
Tel.: +38 044 266 06 10
Fax: +38 044 239 31 00
E-mail: alinav@bigmir.net

ZAMYATNIN Andrey
Natural Sciences Center of A.M. Prokhorov
General Physics Institute, RAS
Vavilov Str., 38, Bld. L-2, Moscow, 119991
Russia
Tel.: +46 18 67 3370
Fax: 46 18 67 3279
E-mail: andrey.zamyatnin@vbsg.slu.se

Contributed Papers

GALATCHI Liviu-Daniel
Ovidius State University
str. Dezrobirii, nr. 114, bl. IS7, sc. A, et. 4, apt. 16, 900241 Romania
Tel.: +4 0724 216 273
Fax: 41 618 326
E-mail: galatchi@univ-ovidius.ro

TOMKINS Jeffrey
304 Biosystems Resarch Complex
Clemson Univ. Genomics Institute
Clemson, SC 29634, USA
Tel.: 01-864-656-6419
Fax: 01-864-656-4293
E-mail: jtmkns@clemson.edu

Registered Participants

ABDULLAEV Abdumanon
Institute of Plant Physiology and Genetics
Academy of Science of Republic of Tajikistan
ul. Aini 299/2
734063 Dushanbe, Tajikistan
Tel.: +1099-2372-216116
Fax: +1099-2372-214911
E-mail: plant1@ac.tajik.net

AFONIN Viktor Yu.
Institute of Genetics & Cytology
National Academy of Sciences of Belarus
Akademicheskaya str., 27
Minsk, 220072, Belarus
Tel.: +375172842190
Fax: +375172841917
E-mail: viktor_afonin@biobel.bas-net.by

BAYER Galina
Institute of Cell Biology and Genetic Engineering
acad. Zabolotny str., 148
03143, Kiev, Ukraine
Tel./Fax: + 380 (44) 266 7104
E-mail: galinabayer@univ.kiev.ua

BAYER Oleg
Institute of Cell Biology and Genetic Engineering
acad. Zabolotny str., 148
03143, Kiev, Ukraine
Tel./Fax: + 380 (44) 266 7104
E-mail: bayeroleg@univ.kiev.ua

CHEREGI Otilia-Silvia
Institute of Biological Research
Temesvari krt.
PO BOX 521 6701
62 6726 Szeged, Hungary
Tel.: 3662599600
Fax: 3662433434
E-mail: ocheregi@nucleus.szbk.u-szeged.hu

DANYLCHENKO Oksana
Institute of Cell Biology and Genetic Engineering
acad. Zabolotny str., 148
03143, Kyiv, Ukraine
Tel.: +380 (44)2661081
Fax: +380 (44)2667104
E-mail: oksanaukr@yahoo.com

DAVYDOV Olga
Weizmann Institute of Sciences
P.O.B. 26 Rehovot
76100 Israel
Tel.: 97289343340
Fax: 97289344181
E-mail: olga.davydov@weizmann.ac.il

KARPOV Pavel
Institute of Cell Biology and Genetic Engineering
Acad. Zabolotny str., 148
03143, Kiev, Ukraine
Tel.: + 380 (44) 266 1498
Fax: + 380 (44) 266 7104
E-mail: karpov_pavel@univ.kiev.ua

MITROFANOVA Irina
The State Nikita Botanical Garden
Nikita, 334267. Yalta, Crimea, Ukraine
Tel.: +380 (0654) 33 59 08
Fax: +380 (0654) 3353 86
E-mail: flora@gnbs.crimea.ua

NYPORKO Alex
Institute of Cell Biology and Genetic Engineering
Acad. Zabolotny Str., 148
03143, Kiev, Ukraine
Tel./Fax: + 380 (44) 266 7104
E-mail: dfnalex@univ.kiev.ua

PAKHOMOV Alex
Institute of Cell Biology and Genetic Engineering
Acad. Zabolotny Str., 148
03143, Kiev, Ukraine
Tel./Fax: + 380 (44) 266 7104
E-mail: pakhomov@i.kiev.ua

ROSU Ana
Professor in Plant Biotechnology
Faculty of Biotechnology
University of Agronomic Sciences and Veterinary Medicine of Bucharest
Bd. Marasti 59, 71331 Bucharest, Romania

SHEREMET Yaryna
Institute of Cell Biology and Genetic Engineering
acad. Zabolotny Str., 148
03143, Kiev, Ukraine
Tel./Fax: + 380 (44) 266 7104
E-mail: yasheremet@univ.kiev.ua

STELMAKH Oksana
Institute of Cell Biology and Genetic Engineering
Acad. Zabolotny Str., 148
03143, Kiev, Ukraine
Tel./Fax: + 380 (44) 266 7104
E-mail: StelmakhOA@univ.kiev.ua

VITECEK Jan
Department of Botany and Plant Physiology
Faculty of Agronomy, Mendel University of Agriculture and Forestry in Brno
Zemědělská 1
613 00 Brno, Czech Republic
E-mail: vitecek@mendelu.cz

YEMETS Alla
Institute of Cell Biology and Genetic Engineering
Acad. Zabolotny Str., 148, 03143, Kiev, Ukraine
Tel./Fax: + 380 (44) 266 7104
E-mail: alyemets@univ.kiev.ua

Contents

Effects of UV Radiation

Nitric Oxide and Plant Stress

This page intentionally left blank

INSTRUMENTATION AND ECOLOGICAL ASPECTS

This page intentionally left blank

Cell Biology and Instrumentation: UV Radiation, Nitric Oxide and Cell Death in Plants
Y. Blume et al. (Eds.)
IOS Press, 2006

Monitoring the Effects of UV Radiation in Cells and Plants

Don J. DURZAN and Petro SMERTENKO
Department of Plant Science, University of California, MS 6
One Shields Ave. Davis, USA
V.Lashkaryov Institute of Semiconductor Physics,
National Academy of Sciences of Ukraine,
45 Prospect Nauki, Kyiv, 03028 Ukraine

Abstract. Selected properties of plant cell populations are useful but have limitations for the design of UV-monitoring instruments and their utility. Diagnostics based on nitric oxide bursts, dose-dependent DNA damage and cell death continue to evolve. Case histories are needed for the realistic modeling of local and global effects of UV radiation, environmental health and decision-making.

Introduction

Many of the effects of UV-radiation are a function of solar activity, environmental conditions such as rainfall, temperatures, and the genomics of target organisms that determine population changes and environmental health. Once economically feasible models are established, warning signals, hazards and the environmental impacts can be monitored for decision-making purposes. Can the recent theoretical developments at the cellular, plant and population levels, and the use of integrated sets of instruments give us the benefits and early warnings of radiation damage up to a month or season in advance? To achieve this goal, new sensors and instruments, and a bewildering variety of factors will have to be sorted out.

A basic problem in modeling the effects of UV-radiation at the plant level is the need to detect, analyze and sort out huge volumes of low-level signals, and specific systematic responses without a basic and integrated understanding of cell biology. Stresses that occur at the same time may be of biotic and/or abiotic origins, either intended or unintended. We do not yet know how these relate to cellular maintenance, homeostasis, damage and repair processes, plant resilience, adaptive plasticity, and productivity.

At the individual cell level and in the laboratory, the monitoring of the responses to UV-light or to other stresses in three and four dimensions is typically done using laser confocal microscopy [1]. Monitoring individual plants and plant populations under field conditions raises the need for new instruments and strategies that sort out and integrate factors for a wide range of scientific, sustainable and economic objectives.

Instruments for the detection of radiation damage should employ different sensor designs, specific means of detection, and computing resources aimed at a decision-maker. Resources should distinguish between low- and high-level operational tasks for diverse missions. Agriculturists, silviculturists, environmentalists and heath-care professionals may have little experience but may need to know into how UV-radiation and new technological developments can be used to forecast and control hazards. This workshop aims to provide

baseline information for the development and demonstration of UV-monitoring tools that will contribute to such a goal.

1. Cell biology: Nitric oxide, early stress signals and cell death

Improvements in instrumentation are needed to observe and interpret how UV-radiation affects the cellular networks of plants. Modeling of the dose-responses should take advantage of the insights from functional plant genomics [2] and from new virtual imaging technologies [3]. Most current genomic information is based on a flowering mustard plant and on rice. By 2010 the function of every gene in the *Arabidopsis* plant will be worked out. Will we be able to apply this information to other agricultural plants and to forest trees? How can we benefit from data that shows the function of every gene? Where and how are UV-sensitive genes regulated and expressed? How do they interact with each other to give us useful information? How can this information be used to advance our understanding of phenetics or the understanding of trait, population and evolution [4], and environmental health?

Some microscopes designed for in vivo imaging now employ two-photon fluorescence and second-harmonics. This enables the imaging of cellular membranes and their action potentials in live cells. Two-photon tracking reveals the phased transport of molecules in images 250 μm wide. Microscopes can also image to a depth of ca 50 μm, a spatial resolution of 0.6 μm, and a temporal resolution of 0.833 ms. The measurements of the behavior of single molecules now require small sample volumes. However, these assays are costly to perform [5, 6].

The free radical, nitric oxide (NO) is a very early and highly transient metabolic signal in the stress response of cells. Laser confocal microscopy and detecting dyes, or laser photoacoutsic detection, have been effective for monitoring NO bursts in cells and plants respectively. NO is lipid soluble and diffuses in membranes. It leads to protective and or harmful reaction depending on the perturbing conditions. Damaging effects arise from the reaction of NO with other free radicals that may not be produced by enzymatic reactions [7]. With optical methods, the problems due to photodamage and toxicity must be evaluated and ruled out. Fluorescent sensors and combined techniques have produced consistent models to quantify stress and damage [8].

NO is derived from nitrate in the cell, or from an enzyme that uses L-arginine and oxygen to produce NO and citrulline. Historically, the organization of reactions of into amino acid families has employed state-network maps to assess the responses of fruit and forest trees to environmental, nutritional, and pathological changes under field conditions [9,10]. The mapping of physiological states over time will now benefit from the emerging models in metabolomics. Flux-balance analyses have shown that metabolic networks are dominated by several reactions with very high fluxes [11]. Results with *Escherichia coli* are believed by some to represent a universal feature of metabolic activity of all cells. Improved and more specific probes are needed to determine the 'time of flux' for NO reactions leading to UV protection and damage.

In plant development, cell death (apoptosis) performs a myriad of necessary functions from sculpting out organ shapes to adapting plants to various stresses throughout their life histories [12]. Understanding the developmentally programmed cell-death signals and their manifestation is a key step in designing monitoring systems not only for UV radiation, but also for the electromagnetic spectrum.

In the human body, damage due to UV-B radiation may involve the p53 tumor-suppressor protein. This represents one of the most effective natural defenses against cancer. Small-molecule drugs have been designed to activate p53 by preventing the binding

of negative regulators of p53 for a new and effective genotoxic general treatment for cancer [13]. While plants are considered to lack of p53 homolog, proteins having partial amino acid sequences related to human p53 and to the mitotic inhibitor p21 have been detected in conifer cells *cf.* Durzan, Santerre, and Havel; Rotari *et al*. (these proceedings). We do not know if proteins and other metabolites produced by plants under UV-B radiation would offer new pharmacogenomic insights in the treatment of malignancies.

The set of external signals received by a plant cell creates a brief instability that usually consumes a mere fraction of the energy expended relative to the final outcome. After the response to a stimulus, the original physiological state is assumed to return and ready to again respond. However, prior responses may change the ability of a cell or site to respond later. This *fatigue* (time needed for recovery) may require a *summation* of prior stimuli. *Hysteresis* in the response curves becomes evident by the retardation of repeated responses and can lead to the aging of cells.

The time elapsed between the beginning of a stimulus and the end reaction is call the '*reaction time*'. It is made up of the *perception time* (e.g., a small fraction of a second in a cell), the *transmission time* (e.g., 0 to 4 cm per second in a plant), and the *physiological response*, which is variable and far longer depending on the systems response as in the case of morphogenesis. Internal plant correlations that *synchronize* and *coordinate* the physiological rhythms and display a 24-hour periodicity set by light-dark cycles.

The 'metabolic pursuit' or 'tracking curves' of nonlinear fluctuations have a long history in hereditary mechanics [14]. However, when the number (n) of external variable exceeds 7, the phenotypic outcomes become almost incomprehensible. The range of phenotypic expressions in a given environment has been referred to as the '*reaction norm*' [15]. The reaction norms arising from UV-radiation doses have yet to be worked out in models involving adaptive dynamics [16, 17].

In California, coniferous trees dating nearly 5000 years of age have survived at very high elevations where UV-B radiation exposure is high. Live cells are supported by their largely adaptive woody structures comprising dead cells (e.g., tracheids). We do not yet know how species at high elevations are programmed to avoid DNA damage or to express cell death under UV radiation. DNA polymerase δ is required for DNA replication. Replication in plant and animal cells is dependent on the proliferating cell nuclear antigen (PCNA). PCNA activity was useful in distinguishing which conifer cells in a population express apoptosis leading to xylogenesis and/or tracheid formation [18].

2. Physiological Parameters and Instrument Design

Plants track many factors in their environment at the same time, e.g., light intensity, quality, duration, changes in CO_2, oxygen, volatile organic compounds, humidity, water availability, changes in temperature, mechanical forces, etc. The biological role of background terrestrial radiation must also be assessed for different populations, meteorological conditions, developmental rates and absorption of radionucleotides by the leaves and roots especially in polluted areas. Most responses occur in cells, tissues or organs different from those that sense the stimulus. The site of perception is not always the site of final response. The network and stream of signals within a plant or released by plants is continuous, variable, multifunctional and complex. UV doses being a potential contributor to somatic mutation rate can become a concealing factor.

We need new technologies that can sense, record and evaluate many simultaneous 'tracks having multiple physiological outcomes. Examples of questions to ask are:

1. How can UV-B-signal processing be defined?
2. What are the inputs, components, mechanism, and output of the signal?

3. How much does structure constrain the plant's signal processing capability?
4. How can signals be abstracted mathematically and outcomes predicted?
5. How do signal networks contribute to bioenergetics and biological function?
6. How do signals in the blue, green, red and far-red affect the plant's UV response?

We can now look to genomics and bioinformatics to extract and manage the useful biological information.

Table 1. Some characteristics of genomes and methods that may be useful in modeling plant responses.

Characteristic	Analysis method
Complexity	Genomic design and bioinformatics
Environmental monitoring	Biosensors and large-scale integration
Autonomous behavior	Adaptive signal processing & control theory
Robust design	Adaptive cooperativity, stability & pathology
Execution	Transport & kinetic theory, system reliability
Adaptive	Bifurcation functions analysis, optimization
Conservation & change	Evolutionary theory and climate change

'Lab-on-a-chip' technologies are being developed for *high-throughput screening* for the diagnosis of diseases. These chips save time and materials by employing microfluidics, sensors, bioreporters, microelectromechanical (MEM) devices, and nanotechnologies. Competition for intellectual property based on nanotechnology may determine new trends in diagnostics [19].

Another trend is the use of integrated circuits with bioreporters. Circuits may comprise a few thousand microbes on a small silicon chip. Bioluminescent Bioreporter Integrated Circuits (BBICs) use small, rugged, and inexpensive whole-cell biosensors for remote environmental monitoring [20]. BBICs sense UV radiation, ultrasound, ammonia, cadmium, zinc, copper, lead, mercury, proteins, and pollutants. The microbes are the bioluminescent reporters in a chip having a porous barrier, encapsulation matrix, a photodetector, and an integrated circuit. The BBICs can survive in extreme and highly contaminated surroundings. Some devices can scan body-fluids for certain proteins that signal tumors, or even be used as an early warning system for the UV-radiation damage. The understanding of how bacteria act as specific bioreporters can provide important clues for the design of other devices in the monitoring of environmental hazards. This requires a better understanding of the compatibility of living cells in controlled abiotic environments having detectors and integrated circuits.

3. Bridging the gap between instrument design and mission

Convenience and portability has made cost-effective UV-vis instruments an important laboratory and field tool (*cf.* [21]). Instruments provide UV detection, identification of the targets, effects on the target, and support automated informational systems that evaluate the effects of radiation from zero to death on plants.

Discovery continues to bring surprises. Some bats are color blind but are UV-sensitive down to ca 310 nm. Many flowers are strong reflectors of UV light especially in twilight when the spectrum is shifted towards shorter wavelengths. UV vision in bats enables them to search for nectar-producing flowers [23]. This illustrates the unexpected complexity of environmental, mammal and plant interactions.

Spectrophotometry has been integrated with systems that provide unique spectral and reflectance signatures in real times. Some autonomous environment-monitoring systems even use neural networks to recognize common and novel properties [24].

3.1 Some instrument design parameters

UV-vis and global positioning systems have been used to classify mines and assess the need for remediation (*cf*. [25]). For a crop at various elevations, an ideal optoelectronic instrument would detect the radiation, and identify the environmental target rapidly, without the need for an interrogating signal, identifying marks at the targets, or the need for transponders. This instrument could have an optical correlator and a neural processor that could identify a different portion of the overall target indicating an acceptable or hazardous situation.

Within an imaged scene an optical correlator would perform a wide-area search, work out the noise preprocessing, and detect the cells, plants or populations of interest. The neural processor would recognize and classify of targets of interest or concern. Signatures may even characterize threats that are hidden to other methods.

'Signature-less' sensors may be used for components or layers in networks to detect anomalies in data streams (traffic). This may provide fewer false signals (alarms). Plant diagnostics would require new ways for sampling spectral content, population changes, and noise filtering in a changing environment.

Correlation algorithms may bridge signals across different sensor types. Diagnostic parameters are linked to detect 'intrusive' stress factors in the environment. Correlations among data clusters would be used to identify redundant alerts. This may reduce data overload on the instrument's analytical capacity. The goal is to provide a clearer picture of both the nature and extent of the damage.

Image montages may have to be generated for each algorithm. Algorithms could be tiled together on a computer to produce a montage. Algorithms can correct positioning errors among image fields so that inherent errors do not accumulate. Intensity and color-correction algorithms should accommodate fluorescence and various UV-vis modes of operation. The best montaging systems create seamless, focused, and large-scale images automatically to digitally visualize the problem and related to early-warning and decision-making formats.

Light-emitting diodes (LEDs) are now available for the ultraviolet to the infrared [26]. UV LEDs are small, produce little excess heat, and have acceptable speed and peaks at 375 nm. They are used in detection, identification, and for excitation applications. Sequentially fired UV-LEDs using optical and semiconductor engineering have been used in bioaerosol monitoring. However, limitations exist. LED outputs are not always coherent and outputs and cannot provide a narrowband source.

Most fluorescent probes have decay times measured in nanoseconds, which requires the light source to operate in the 100-MHz range. Such speeds are currently beyond the capacities of blue, violet and ultraviolet LEDs. LEDs with emission of only a few milliwatts are inadequate for many large area applications that need intense light sources. With high-current or high flux LEDs heat management becomes problematic. Intelligent and universal controllers are helping to make LED lights more user-friendly [27].

Instruments could be designed to optimize date acquisition and image analysis, provide environmental snapshots, superior resolution in small, rugged packages. Flexibility and modular design for the entire UV or entire electromagnetic spectrum would require reliable signal processing with short integration times, very low noise, high-speed sampling rates with windowing modes, and maximum sensitivity full-frame integration. Some of the existing technological developments and solutions for design and manufacturing may already be available, e.g., NASA commercial technology teams in the USA [24].

3.2. Functional indices in support of environmental health and quality

Since plants use sunlight for photosynthesis, and are exposed to UV radiation, their UV dose-dependent damage and repair mechanisms may also be a function of climate change, self-adaptive capabilities of various genotypes, and genetic variation in plant populations. The annual World Watch Institute Reports (Washington, DC) provide up-to-date review of several indexes related to the importance of solar- and UV-radiation. Interaction among microorganisms, insects, animals and human activities increase the complexity most ecological, environmental, and even some older qualitative societal models [e.g., 22]. Local and possibly global multisensor constellation may someday provide us with supporting indicators, warnings, and situational analysis ultimately linked to economic growth and environmental well-being. An objective appraisal of the status and value of the monitored targets might include monetary units and value to commerce but their value to the public as a whole. Earlier models have attempted a functional integrity of normally forested landscapes with an index that defines how well landowners and governments are protecting the public's interests [28].

Transboundary pollution, deforestation, solar activity, and climate change may also alter the response to UV-radiation. Strategies for addressing solutions to these problems require a dialogue among interested and impacted parties, officials, scientists, layered institutions of mixed types [29]. In practice the formulation of general principles for robust governance of environmental resources remains very challenging especially during times of regional and global conflict. Some situations may have no technical solution or have little or no role for science. An international framework has been suggested to promote access to data obtained from public investment in research, downstream commercialization, and information for decision-makers to address complex and transnational problems [30].

Decision-making and planning can benefit from the state-of-the-art environmental monitoring systems with reference to sets of numerical metrics. For example, can the correlators recognize 98% of the hazards and identify 75% of the targets and damage? How does the extent of radiation damage correlate with instrument and system performance? New designs are needed to incorporate revolutionary and integrated decision-making systems using simulations, field monitoring, and different scenarios.

Unfortunately we still have too little information, diffuse and poorly designed information systems, and an inability to timely analyze the facts of any given situation. We need to capture the totality of the opportunities represented in the information. We need ways to create superior knowledge and operational concepts from the vast continually changing baseline information. Next-generation models, logistics, decision cycles, system effects and human factors will have to be developed and assessed. The emerging policies must be debated for their environmental, economic and political impacts.

4. Conclusions and workshop recommendations: Where do we go from here?

This workshop has contributed to plant cell biology and instrumentation through the advancement of knowledge, and the follow-through from discovery to completion with instrument design and fabrication. The latter was proven suitable for monitoring UV-radiation in the Ukraine. Future technological and research opportunities must achieve a critical mass before they become a high enough priority to continue over the long term.

4.1 Recommendations

1. Identify the cellular mechanisms that give plants their function and structures that deal with the beneficial and harmful responses to UV-radiation. Develop models for gene regulatory networks that govern how plants respond to and integrate multiple stimuli.

2. Continue to develop affordable monitoring instrumentation, screening formats and computational infrastructure to model and assess the benefits and hazards of UV-radiation using case studies at strategic locations.

3. Establish technological showcases based on population health, ecological safety, and biological productivity.

4. Support and speed up the experimental and design work, which is at present being carried on within the constraining limits of the budgets of University and State funds. Encourage the provision of private funds to make contributions for this cause, and obtain the cooperation of laboratories, which have the necessary equipment, bioinformatics systems, responsibilities for environment and health monitoring.

5. Maintain a NATO framework with financial support for knowledge sharing, decision analysis, and entrepreneurial opportunities for future research on population and environmental health especially in the newly independent states.

A good plan vigorously executed today, is usually better than a perfect plan tomorrow.

References

[1] May M., "Advances in cellular image processing". *The Scientist (March)*, vol. 18, pp. 40-43, 2004.
[2] Cullis C.A., "Plant Genomics and Proteomics". Wiley-Liss, Hoboken, NJ. 214 p.p., 2004.
[3] Alfonso B. "Images: scope this out". *Science* vol. 308, p. 173, 2005.
[4] Yablokov A.V., "Phenetics. Evolution, Population, Trait". Columbia University Press. NY., 1986.
[5] Wahl M., "Tools for time-resolved single-molecule measurements". *Biophotonics International*, vol. 11, p.p. 48-53, 2004.
[6] Mur A.J, Santosa E., Laarhoven L.J.J., Holton N.J., Harren F.J.M. and Smith A.R., "Laser photoaccoustic detection allows in planta detection of nitric oxide in tobacco following challenge with avirulent and virulent *Pseudomonas syringae* pathovars". *Plant Physiology*, vol.138, p.p. 1247-1258, 2005.
[7] Durzan D.J. and Pedroso M.C., "Nitric Oxide and Reactive Nitrogen Oxide Species in Plants". *Biotechnology & Genetic Engineering Reviews,* vol. 19, p.p. 293-337, 2002.
[8] Beechem J.M., Johnson I. and Patton W.F., "Fluorescent sensors for systems biology". *Biophotonics International*, p.p. 46-50, 2004.
[9] Durzan D.J., "Molecular Phenogenetics as an Aid to Fruit Breeding". *Proc. Intl Symp. In Vitro Culture and Horticultural Breeding. May 30 - June 3, 1989. Cesena, Italy. Acta Hort*., vol. 280, p.p. 547-556, 1990.
[10] Durzan D.J., "Molecular Bases for Adaptation of Coniferous Trees to Cold Climates". In "Forest Development in Cold Climates". J.N. Alden, S. Odum and J.L. Mastrantonio (eds), NATO, Plenum Press, N.Y., p.p. 15-42, 1993.
[11] Almaas E., Kovács B., Viscek T., Oltval Z.N. and Barabási A.-L., "Global organization of metabolic fluxes in the bacterium *Escherichia coli*". *Nature*, vol. 427, p.p. 839-843.
[12] Havel L. and Durzan D.J., "Apoptosis in plants". *Botanica Acta,* vol. 109, p.p. 268-277, 1996.
[13] Lane D.P. and Fischer P.M., "Turning the key on p53". *Nature*, vol. 427, p.p. 789-790, 2004.
[14] Davis H.T., "Introduction to Nonlinear Differential and Integral Equations". Dover Publications, New York, 1962.
[15] Schlichting C.D. and Pigliucci M., "Phenotypic Evolution. A Reaction Norm Perspective". Sinauer, Sunderland, Massachusetts, 1993.
[16] Staddon J.E.R., "Adaptive Dynamics". MIT Press, Massachusetts, 2001.
[17] Glass L., "Synchronization and rhythmic processes in physiology". *Nature*, vol. 410, p.p. 277-284, 2001.
[18] Havel L., Scarano T. and Durzan D.J., "Xylogenesis in *Cupressus* callus involves apoptosis". *Adv. Hort. Sci*., vol. 11, p.p. 37-40, 1997.
[19] Forman D., "Intellectual Property storm clouds build on horizon". *Smalltimes*, vol. 4, p.p. 21-24, 2004.

[20] Nivens D.E., McKnight T.E., Moser S.A., Osbourn S.J., Simpson M.L. and Sayler G.S., "Bioluminescent bioreporter intergrated circuits: potentially small, rugged and inexpensive whole-cell biosensors for remote environmental monitoring". *J. Applied Micrbiology*, vol. 96, p.p. 33-46, 2004.
[21] Smertenko et.al, "UV and VIS radiation meters for monitoring system". This Workshop.
[22] Odum H.T., "Environment, power and society". Wiley, Interscience, 1971.
[23] Winter Y., Lopez J. and von Helversen O., "Ultraviolet vision in a bat". *Nature*, vol. 425, p.p. 612-614, 2003.
[24] Hand C., "Autonomous environment-monitoring networks". *NASA Tech Brief*s, vol. 28, p.p. 35-36, 2004.
[25] Cleaves K.S., "Spectrophotometry on the rise". *Today's Chemist at Work*, p.p. 17-18, 2003.
[26] Hogan H., "Light sources offer flexibility in bioanalysis". *Biophotonics International*, p.p. 52-55, 2004.
[27] Hardin R.W., "LEDs and controllers speed vision inspections". *Vision Systems Design*, vol. 9, p.p. 17-20, 2004.
[28] Woodwell G.M., The functional integrity of normally forested landscapes: A proposal for an index of environmental capital". *Proc. Natl. Acad. Sci. USA*, vol. 99, p.p. 13600-13605, 2002.
[29] Dietz T., Ostrom and Stern P.C., "The struggle to govern the commons". *Science*, vol. 302, p.p. 1907-1912, 2003.
[30] Artzberger P., Schroeder P., Beaulieu A., Bowker G., Casey K., Laaksonen, Moorman D., Uhlir P. and Wouters P., "An international framework to promote access to data". *Science*, vol. 303, p.p. 1777-1778, 2004.

Cell Biology and Instrumentation: UV Radiation, Nitric Oxide and Cell Death in Plants
Y. Blume et al. (Eds.)
IOS Press, 2006

Photobiological Measurements and Obtaining Action Spectra

David H. SLINEY
Vice-President, International Commission on Illumination (CIE)

Abstract. The main aspects of photobiological measurements and obtaining action spectra have been considered. It has been shown that the proper use of internationally defined quantities and units in scientific publications promotes the best international communication in the science of photobiology and photochemistry. The accuracy and precision of the applied action spectra, measurement techniques and consideration of exposure geometry are of importance. The factors which influence the quality of the original photobiological research, the possible sources of error and the levels of uncertainty in applying laboratory action spectra to human health risk assessment have to be taken into account.

Introduction

The validity of photobiological research depends strongly upon the accuracy and precision of the applied action spectra, measurement techniques and consideration of exposure geometry. It is therefore important to recognize the factors which influence the quality of the original photobiological research, the possible sources of error and the levels of uncertainty in applying laboratory action spectra to human health risk assessment. One need only study the variation in the reported action spectra published by different laboratories for the same biological effect to recognize that the derivation of sound action spectra is surely fraught with some problems. Both biological and physical factors influence the variation in published action spectra. Biological factors which may affect the actual biological effect of exposure to optical radiation include: variation in response among species, variation in response due to individual adaptation, influence of nutritional factors, the biological endpoint applied in each study, and the means and time of assessment of the endpoint in the plant, animal or human subjects. The physical factors which influence any reported action spectrum relate to the accuracy of radiometric and spectroradiometric measurements, the type of light source and the geometry and spectral bandwidth of each exposure used in the biological experiment.

To characterize photobiological phenomena, standardized terms and units are required. Without a uniform set of descriptors, much of the scientific value of publications can be lost. Attempting to achieve an international consensus for a common language has always been difficult, but now with truly international publications, it is all the more important. Since photobiology represents the fusion of several scientific disciplines, it is not surprising that the physical terms used to describe dosimetric concepts (e.g.., surface exposure dose, absorbed dose, dose rate, fluence, etc.) can vary from author to author. There are, however, international organizations that were established to minimize the confusion produced by poor or inconsistent technical terminology. Hopefully all scientific workers will apply the standardized terminology of the International Commission on Illumination, the CIE [1,2].

The International Commission on Illumination, the CIE, has provided international guidance in the science, terminology and measurement of light and optical radiation since 1913. The International Lighting Vocabulary (parts of which are also issued as an ISO or IEC standard) has been an international reference for photobiologists for many decades and the next revision is due to be published later this year. Despite its stature, many research scientists are unfamiliar with some of the subtle distinctions between the widely used dosimetric terms, such as irradiance, radiant exposure, fluence rate and fluence. For example, the standardized radiometric quantity, "radiant fluence," is defined as the radiant energy that passes through the circular cross-sectional area of an extremely small sphere. The photon fluence is the number of photons passing through this area. These quantities are most useful in quantifying a dose within a scattering medium, such as deep within tissue. Although radiant fluence has units of joules per unit area, that same unit applies to "radiant exposure." This latter radiometric quantity is what is frequently measured at the exposed surface of tissue and incorporates an added cosine dependence that is not present in the concept of fluence that captures energy arriving from all directions and entering the tiny dosimetric sphere. Similar distinctions apply to fluence-rate and irradiance. It is also of note that the same definitions apply in ionizing radiation dosimetry. The proper use of internationally defined quantities and units in scientific publications promotes the best international communication in the science of photobiology and photochemistry.

The CIE considers all aspects of the effects of optical radiation and lighting upon materials, plants, animals and humans other than vision. The Division prepares technical reports by technical committees (TCs) and by individual reporters, prepares standards, and promotes scientific meetings and seminars.

In this article the main definitions and very important procedure for determination of action spectra are described for practical use.

1. Main definitions

1.1 Spectral Bands

During the 1930s, the CIE Committee on Photobiology developed a short-hand notation for different spectral bands of interest to the field of photobiology. The CIE has designated 315 to 400 nm as UV-A, 280 to 315 nm as UV-B, and 100-280 nm as UV-C [1, 2]. Light (visible radiation) overlaps the UV-A and IR-A extending at most from about 380 nm to at least 780 nm. (IR-A extends from 770 nm to 1400 nm; IR-B, from 1400 to 3000 nm; and IR-C from 3000 nm to 1 mm). The CIE photobiological bands are summarized in Table 1.

Table 1. CIE Photobiological Spectral Bands

CIE Spectral Band Designation	Wavelength Interval	Characteristics
UV-C	100 nm to 280 nm	Superficial absorption in tissue; significant protein absorption—particularly at 250-280 nm
UV-B	280 nm to 315 nm	Penetrates, still actinic, most photocarcinogenic
UV-A	315 nm to 400 nm	Deeper penetration, less absorption
Light (visible)	380 nm to 780 nm*	Photopic (day) and Scotopic (night) vision
IR-A	780 nm to 1400 nm	Deeply penetrating, water transmits
IR-B	1400 nm to 3000 nm (1.4 μm - 3.0 μm)	Water strongly absorbs, very slight penetration
IR-C	3 μm to 1,000 μm (1 mm or 300 GHz)	Very superficial absorption, generally less than 0.1 mm

*An early definition. Light (visible radiation) is no longer defined as being limited to specific wavelengths, but most generally as that radiation which elicits vision.

1.2 Radiometric Quantities and Units for Describing Exposures

In photobiology, one often speaks of a "dose" of light or ultraviolet radiation. But just what do photobiologists mean by dose? Because energy is absorbed largely near the surface, a surface exposure (accumulated) dose is very useful. The physicist defines radiant exposure (incident on surface) in $J \cdot m^{-2}$ and radiant fluence as the energy that has passed through a unit diametrical area of a microscopic sphere in tissue (or in air when speaking of air disinfection) or in water for water disinfection. Dose-rate can also be expressed either as a surface exposure rate—in terms of irradiance (incident on a surface)--or as a fluence rate (passing through a surface).

There are a number CIE standard radiometric quantities and units that are of value in describing various non-visual effects, and we shall just quickly describe those that are most widely employed. In addition to those quantities designed to describe a source output [radiant energy (CIE/ISO Symbol: Q) and radiant power (also termed "radiant flux" with symbol Φ)], most photobiologists will use several terms to describe exposures, and these will be discussed in more detail. Some of the most useful quantities are also summarized in Table 2.

Radiant exposure is the radiant energy incident on a surface divided by the area (projected to the normal) of the surface. The SI unit is Joules$\cdot m^{-2}$. The CIE/ISO symbol is H. In photobiology radiant exposure is also called the "exposure dose." Although not the most desirable unit, the older $J \cdot cm^{-2}$ is still widely used in photodermatology and ophthalmology, since the dimensions of irradiated areas may be of the order of cm.

Irradiance on a surface is the radiant power incident on a surface divided by the area of the surface. Irradiance multiplied by the exposure duration, the time t in seconds, is the radiant exposure. The CIE/ISO symbol is E. Irradiance is known as the "exposure dose rate" in photobiology. The older $W \cdot cm^{-2}$ is still widely used in photodermatology and ophthalmology, since the dimensions of irradiated areas may be of the order of a centimeter.

Fluence and Fluence Rate are—at least in theory—the most important and useful radiometric concepts in photochemistry and photobiology, since they actually best describe the dose or dose-rate, respectively. However, these terms are frequently misused, and fluence is frequently mistaken for radiant exposure H because the same units of $J \cdot m^{-2}$ are used for both quantities. However, the fundamental definition of fluence differs from that of radiant exposure. Fluence is the radiant energy passing through a small unit area sphere divided by the diametrical area of the sphere, and it does **not** include the cosine response in the irradiance definition, and perhaps most importantly, fluence includes backscatter. This unit was initially designed for use in radiation biology and biochemistry. It is particularly useful in photochemistry and photobiology to describe the microscopic exposure of a molecule in a scattering medium or to describe the photobiologically important dose to bacteria in air or water for UV disinfection calculations. Likewise, fluence rate is also mistaken for irradiance E, since it has the same units of W/m^2, but it includes backscatter and ignores a cosine response. Thus, it is also useful in: photochemistry and photobiology in a scattering medium.

Table 2. Useful Radiometric Quantities and their Units [1,2]

Term	Symbol	Defining Equation	Defining Equation	Unit and abbreviation
Radiant Energy	Q	Energy emitted, transferred, or received in the form of radiation	$Q = \Phi \cdot t$	joule (J)
Radiant Power	Φ	Radiant Energy per unit time	$\Phi = \frac{dQe}{dt}$	watt (W) defined as $J \cdot s^{-1}$
Radiant Exposure (Dose in Photobiology)	H	Radiant energy per unit area incident upon a given surface	$H = \frac{dQe}{dA}$	joules per square meter ($J \cdot m^{-2}$)
Irradiance or Radiant Flux Density (Dose Rate in Photobiology)	E	Radiant power per unit area incident upon a given surface	$E = \frac{d\Phi e}{dA}$	watts per square meter ($W \cdot m^{-2}$)
Fluence	Iᵽ	Radiant Energy emitted by a source per unit solid angle	$I = \frac{d\Phi e}{d\Omega}$	joules per steradian ($J \cdot sr^{-1}$)
Radiant Intensity	I	Radiant Power emitted by a source per unit solid angle	$I = \frac{d\Phi e}{d\Omega}$	watts per steradian ($W \cdot sr^{-1}$)
Radiant Fluence Rate	$E_{e,o}$	Radiant Energy emitted by a source per unit solid angle per source area	$E_{e,o} = \int_{4\pi sr} L_e \, d\Omega$	joules per steradian per square centimeter ($J \cdot sr^{-1} \cdot m^{-2}$)
Radiance[3]	L	Radiant Power emitted by a source per unit solid angle per source area	$L = \frac{d\Phi e}{d\Omega \cdot dA \cdot \cos\theta}$	watts per steradian per square centimeter ($W \cdot sr^{-1} \cdot m^{-2}$)
Optical Density	OD	A logarithmic expression for the attenuation produced by a medium	$OD = -\log_{10}\left(\frac{\Phi_O}{\Phi_L}\right)$	unitless Φ_O is the incident power; Φ_L is the transmitted power

1. The units may be altered to refer to narrow spectral bands in which the term is preceded by the word *spectral* and the unit is then per wavelength interval and the symbol has a subscript λ. For example, spectral irradiance E_λ has units of $W \cdot m^{-2} \cdot m^{-1}$ or more often, $W \cdot cm^{-2} \cdot nm^{-1}$.

2. While the meter is the preferred unit of length, the centimeter is still the most commonly used unit of length for many of the terms below and the nm or μm are most commonly used to express wavelength.

3. At the source $L = \frac{dI}{dA \bullet \cos\theta}$; and at a receptor $L = \frac{dE}{d\Omega \bullet \cos\theta}$

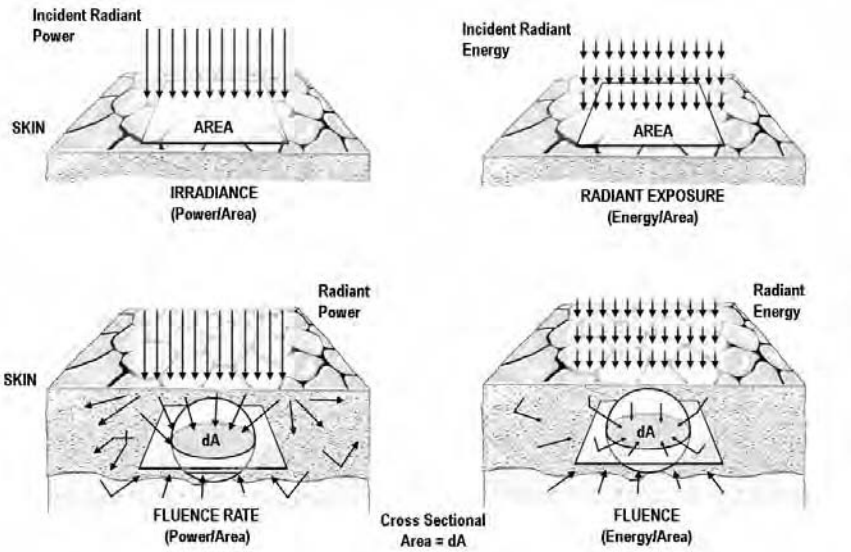

Figure 1. The distinction between irradiance and radiant fluence rate and between radiant exposure and radiant fluence. Both pairs employ the same units of power-per-unit-area and energy-per-unit-area, respectively.

2. Dosimetry and Measurement for Non-Visual Effects

The scientific characterization and measurement of visual effects has been a major focus of the CIE since its inception. The science of photometry has evolved over the last century and the standardized metric for daylight visual response—the lumen—is based upon the well known V(λ) spectral response of the "CIE Standard Observer". However, the scientific characterization and measurement of non-visual effects, such as the synthesis of Vitamin-D, erythema and circadian effects, are less well publicized. The science of photobiology deals with the study of the interaction of optical radiation (ultraviolet, visible and infrared radiation) upon living organisms – both animals and plants. Although everyone is familiar with photobiological effects such as sunburn or photosynthesis, the methods of scientific description and measurement for some of the most familiar photobiological effects require knowledge of specialized action spectra and the characteristics of the effect. Attempts to improve phototherapy of human diseases, protection of health from harmful photobiological effects, and many of the effects of ultraviolet radiation and visible light on plant species require specialized dosimetry. CIE Division 6, which is devoted to photobiology and photochemistry, considers all forms of non-visual effects of light, ultraviolet radiation and infrared radiation upon humans, animals and plants. Most of the non-visual effects are initiated by photochemical interactions that are limited to relatively narrow regions of the optical spectrum and most notably in the ultraviolet and short-wavelength visible parts of the optical spectrum. The description of the relative sensitivity of a biological response as a function of wavelength is termed the *action spectrum*. Instruments can be designed to track the action spectrum of interest, and effective exposures or dose rates can be measured.

3. Action Spectra

The description of dose and dose rate also should not ignore spectral information. Because sufficient photon energy is necessary to elicit a photochemical reaction, the ultraviolet spectrum and light are of primary interest in photobiology. An action spectrum is used to describe a relative response function for eliciting a photobiological or photochemical effect. The action spectrum is normally determined by using mono-chromatic sources to obtain relative exposure doses at each wavelength to produce the defined effect. But it is very important to recognize that the endpoint must be defined! For example, erythema, or sunburn has a different action spectrum depending upon when the skin is examined post-exposure (e.g., 1 h, 4 h, 12 h, 24 h, 48 h, etc.) or the degree of redness. A radiant exposure at the target surface is measured, and an underlying assumption is: reciprocity of irradiance (dose rate) and time. Borrowing from human photobiology, we know that typical action spectra (for erythema, photokeratitis, photic maculopathy of the retina, single-cone vision, etc.) have action spectra that are less than 100 nm in spectral width. The "First Law of Photobiology" described by Kendric Smith was that "Radiant energy must be absorbed to produce a photobiological effect." However, it is always important to recognize that not all of the absorbed energy will produce a photochemical effect.

It is not uncommon for published action spectra of apparently the same effect to sometimes differ, and many are puzzled as to "which is correct?" As it turns out, each may be correct because of different endpoints. The action spectrum will differ in-situ from that measured on an exterior surface if intervening molecules have varying absorption spectra. Consider photosynthesis, vision, erythema (sunburn), etc. Spectral sampling intervals and spectral bandwidth of the source can affect the result. When action spectra differ when derived in different laboratories, think of these factors!

How one plots an action spectrum can reveal different information. It is best to plot the action spectrum both on a linear scale and a semi-log rhythmic scale.

Examples of action spectra are the familiar CIE visual response functions. The scotopic function describes the eye's response to low light levels experience at night and this action spectrum peaks around 505 nm. The photopic luminous efficacy function describes the relative spectral response of the CIE "standard observer" (an average of a number of individuals) to daylight; this response peaks around 555 nm. The entire science of photometry revolves around these CIE luminous efficacy functions as shown in Figure 2.

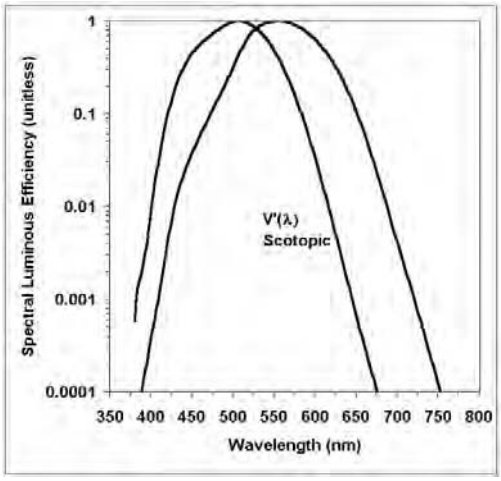

Figure 2. Action Spectra—Example from Photometry.

3.1 Action Spectra: General Aspects

An action spectrum is defined as the relative spectral effectiveness of monochromatic radiation in eliciting a defined response relative to a wavelength of maximal effectiveness. Provided that multiple action spectra do not overlap (i.e., one chromophore is present), weighting a broad spectrum source by an action spectrum can predict the effectiveness of the broad spectrum source. The shape of the action spectrum is determined by a number of factors. The most important factor is the target molecule itself, the chromophore. The action spectrum of a pure solution of the chromophore will provide the fundamental action spectrum; however, other biological factors can alter this fundamental action spectrum. Optical reflection, absorption or scattering prior to absorption of photons by the chromophores will frequently shift the peak of the action spectrum, as in the case of erythema (skin reddening, or "sunburn"). The proteins of the stratum corneum (outermost, horny surface layer) of the skin spectrally filters the UV photons incident upon the skin and tend to block the transmission of wavelengths much less than 295 nm, even though the most important chromophore—DNA—has a spectral absorption peak at a shorter wavelength [3, 4]. Chain effects are also possible, where other biochemistry is initiated by the incident photons. The choice of the measured endpoint for the effect also affects the action spectrum, and the action spectrum for erythema shifts to a narrower curve with a longer wavelength peak if severe, rather than minimal, erythema is the endpoint. The time of assessment of this biological effect and the degree of severity, the means to measure the effect (e.g., visual observation, chemical assay, histology, etc.) also generally affect the action spectrum. Thus we are always left with experimental error and uncertainties. Some of the sources of uncertainties—the variables—in the determination of action spectra include: physical measurement errors of the optical radiation, the area of exposure, exposure duration, distance, the spectral bandwidth (e.g., laser, 1 nm, 5 nm), the number of wavelengths sampled, individual subject (or anatomical site) variations in sensitivity, etc. In addition, as well illustrated by erythema, the target tissue may undergo adaptation (e.g., thickening of the stratum corneum and skin pigmentation) and the type of assessment (e.g., color, method, time delay, etc) influences the result. Although erythema was used in this example, the same types of errors can apply to the determination of plant action spectra.

Thermal effects show very broad spectral dependence and a spot-size dependence. Hence, the thresholds for biological injury and human exposure limits for purely photochemical injury are expressed as a surface exposure dose, i.e., as radiant exposure. The product of the irradiance (or exposure dose rate) E in W/m^2 or W/cm^2 and the exposure duration t is the radiant exposure (or exposure dose) H expressed in J/m^2 or J/cm^2, i.e., $H = E \cdot t$. This product always must result in the same radiant exposure or exposure dose over the total exposure duration to produce a threshold injury. This is termed the Rule of Reciprocity, or the Bunsen-Roscoe Law. Chemical recombination over long periods (normally hours) will lead to reciprocity failure, and in biological tissue, photochemical damage may be repaired by enzymatic and other repair mechanisms and cellular apoptosis.

Where radiant energy is more penetrating, as in the visible and IR-A spectral bands, it is sometimes useful to apply the radiometric concepts of fluence and fluence rate. For all photobiology, it is necessary to employ an action spectrum for photochemical effects. The UV safety function $S(\lambda)$ is also an action spectrum, which is an envelope curve for protection of both eye and skin and is used to spectrally weight the incident UVR to determine an effective irradiance for comparison with the threshold value or exposure limit. With computer spread-sheet programs, one can readily calculate the

spectrally weighted values from a lamp's spectrum with a variety of photochemical action spectra:

$$E_{eff} = \sum E_{\lambda} \cdot S(\lambda) \cdot \Delta\lambda \qquad [1]$$

The exposure limit is then expressed as a permissible effective irradiance E_{eff} or an effective radiant exposure. One then can compare different sources to determine relative effectiveness of the same irradiance from several lamps for a given action spectrum.

3.2 Guidelines for Obtaining Action Spectra

Published photobiological threshold data are frequently plotted as an action spectrum with relative response versus wavelength. Account is generally not taken of the influence of spectral bandwidth of the radiant exposure applied to each wavelength. In the determination of any photobiological action spectrum, the choice of wavelength interval and spectral bandpass are of utmost importance. The accuracy and resolution of the action spectrum are significantly influenced by the choice of the monochromatic source and the number of data points obtained. Ideally, a truly monochromatic source, such as a continuous-wave (CW) laser would be best to assess the response at a particular wavelength, since the spectral bandwidth at each wavelength will be extremely small and therefore afford a very high resolution spectrum. Unfortunately, lasers are expensive, and tunable laser sources in the UV are generally only presently available with repetitively pulsed outputs using non-linear-optical crystals for second-harmonic generation and wavelength tunability. Questions of non-linear responses from very short pulse durations create questions of validity for extrapolating to CW exposures. Thus, most investigators choose an arc-lamp monochromator to produce narrow spectral bands of radiation. The challenges of this technique are more than most scientists appreciate, and it is important to examine spectral threshold data from experiments designed to determine an action spectrum.

To illustrate this problem one can examine the published action spectra for photokeratoconjunctivitis (“snow blindness” or “welder’s flash). Measurements of UV action spectra for photokeratitis can be quite challenging, especially in the 300-320-nm spectral region, as the UV hazard action spectrum, S(λ), which is based upon this research changes quite rapidly with a small change in wavelength in this region, i.e., a tenfold (1,000%) change in less than 7 nm. Typical UV sources that have been used in biological studies of photokeratitis, photokeratoconjunctivitis or erythemal thresholds fall into two general categories:

- low-pressure mercury lamps, which emit very narrow-wavelength line spectra, where the desired wavelengths are isolated by filters or a monochromator; or
- xenon-arc (or mercury-xenon-arc) high-pressure lamps, which employ monochromators to limit the source to the desired narrow wavelength band at the site of exposure [5].

The low-pressure lamp and filter has the disadvantage that only a limited number of wavelengths are available (e.g., at 254, 280, 297, 303, 314, 330, 365, etc. for a mercury lamp). While the xenon arc monochromator is continuously tunable across the wavelengths of interest, the resolution is poor because the slit widths must be great enough to pass enough power.

Significant plotting errors can be introduced when the slit width of the monochromator is not accounted for when plotting the action spectral data [3,5-7]. Threshold data for each spectral bandpass is frequently plotted against the center-wavelength of the bandpass; however, this can misrepresent the true action spectrum. To

derive a true action spectrum from the low-resolution threshold data obtained from monochromator studies, a mathematical convolution is required. The typical monochromator spectral band pass values used in most photobiological experiments vary from about 5 nm to 12 nm. The band pass is traditionally specified at the "full-width-half-maximum" (FWHM) of the "slit function;" however the different published reports are not always clear on the meaning of bandwidths given (particularly the earlier reports), and it is difficult to discern if the "bandwidth" is the base width, the full width at half maximum, or an averaged bandwidth. The slit function is the spectral power distribution of radiant energy emitted at the given wavelength set on the monochromator [8]. For a perfect grating monochromator, the shape is triangular, as shown in Figure 3. Although it would always be desirable to employ a high-resolution monochromator slit-width, such as 0.5 or 1.0 nm, the radiant power that can pass through the slit (the "throughput") is so low that a threshold exposure could require hours. In practice, much larger bandpass values of 5-10 nm are therefore used.

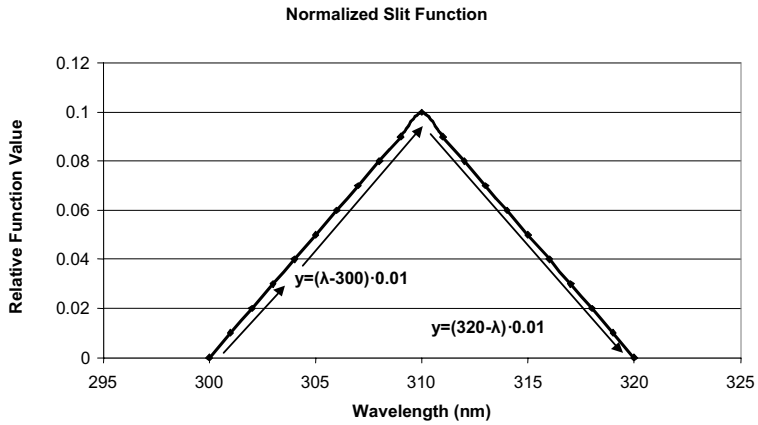

Figure 3. The expected slit function for the 310 nm Pitts human cornea (1973) threshold is shown here. From 300-310 nm, the function is expressed in the top equation; from 310-320 nm the function is expressed in the bottom equation.

When the UV Hazard (ACGIH) action spectrum was developed in 1972 the published threshold data were "corrected" for the impact of the spectral bandwidth of the monochromators. Therefore, when the original published data are plotted along with the UV Exposure (UV Hazard) action spectrum there appears to be a lack of agreement with the original data. By convoluting the threshold data and weighting it with the ACGIH UV Relative Spectral Effectiveness function (S(λ)), it is possible to determine the wavelengths in each bandwidth that are contributing most of the effective dose. Many of the early threshold data were obtained using low-pressure mercury lamps or xenon-arc high-pressure lamps where the desired wavelengths were isolated by monochromators. When comparing these data to the UV Hazard action spectrum, it is necessary to consider the spectral bandwidth for all data and to consider also "stray radiation" and the sources of "stray radiation" in the instrument; e.g. stray light scattered from the gratings in monochromators, leaks in radiometric housing, etc. The use of tunable UV lasers to determine action spectra is needed.

3.3 Special Photobiological Quantities

Once an action spectrum has been established it is possible to build and instrument that has a spectral response that simulates the action spectrum, for example, the action spectrum for erythema. Other specialized instruments that attempt to mimic the response of other photobiological action spectra include plant-growth meters, ultraviolet hazard meters, erythemal meters, blue-light hazard meters, vitamin D meters and so forth.

As an interesting historical note, a half-century ago it was popular to develop specialized photobiological terms and units for measurements made with special instruments. There were units such as the E-Viton and the Erythem and the Finsen; however, the difficulties provided by these specialized terms, quantities and units were such that purists argued that these should not be maintained and that only radiometric quantities plus the photometric quantity, the candela, should be standardized in the SI.

4. An Important Example: Corneal Damage Thresholds

When photokeratitis threshold data [9, 10], corneal damage threshold data [11], and photoconjunctivitis data [12] are compared to the ACGIH UV exposure guidelines [13,14,15] without taking bandwidth into account in the cited thresholds, the 310 and 320 nm data points appear to be located at exposure doses below the ACGIH exposure limits (Fig. 4). The distortion of experimental action spectra was taken into account in deriving the ACGIH exposure limit [16] and action spectra from mercury lines at 297 and 313 nm were used to define the slope. It is not surprising that this safety action spectrum has a

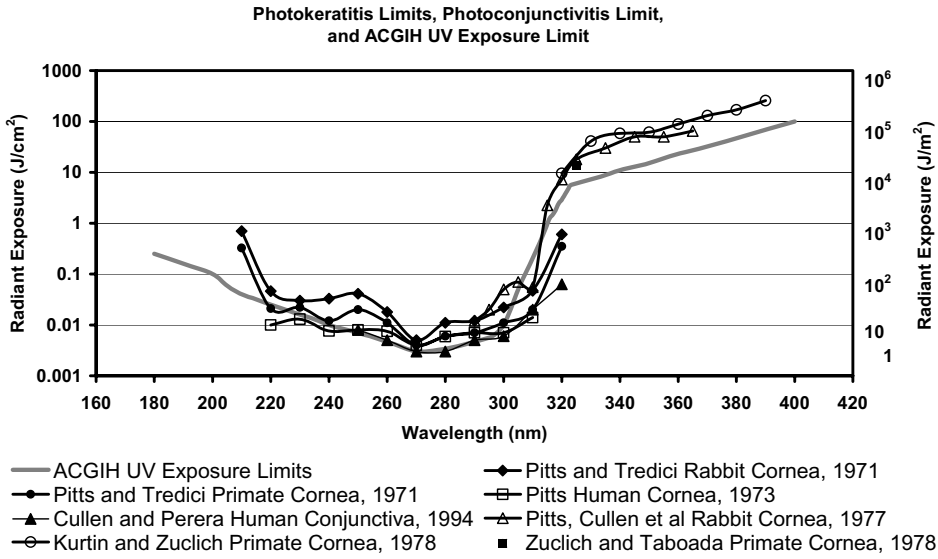

Figure 4. Reported photokeratitis thresholds and the ICNIRP UV exposure limit. Outlying threshold points plotted at the center wavelength of the monochromator are especially apparent in the 300-320 nm wavelength region. The Kurtin and Zuclich 1978 [18], and Zuclich and Taboda 1978 [19] data are included for purposes of comparison.

slope very similar to that obtained for DNA by Peak, Peak, et al. [17].

Threshold data in the 300-320 nm region can be particularly misleading if the data were taken using a monochromator with too large a bandwidth. The Pitts and Tredici 1971 paper reports that data were obtained with "a nominal 9.92-nm bandpass which did not exceed 10 nm for all wavelengths." For the Pitts 1973 data, the report specifies that "full band pass did not exceed 10 nm for all wavebands." The Pitts et al [11] data were obtained with two different monochromators: a single grating monochromator "whose entrance and exit slits were set to provide a 9.96 nanometer full-bandwidth wavelength" (bandwidths were reported as 10.0 nm); and a double grating monochromator "set to pass a full-bandwidth of 6.6 nm; however, all wavebands are reported as 5.0 nm." The Cullen and Perera data were obtained with a 9 nm bandwidth (FWHM). The different published reports are not always clear on the meaning of bandwidths given, i.e., if they are the FWHM, as recommended.

Such large bandwidths do not lead to great plotting errors in the derived action spectrum for wavelengths around 270-280 nm or at wavelengths greater than 330 nm. However, the plotting error is quite noticeable in the 300-320 nm range since the exposure limits in these wavelengths are rapidly increasing—the limits increase by an order of magnitude between 303-310 nm, and another order of magnitude between 310-320 nm. For the threshold points in question, most of the effective dose comes not from the wavelength at the center of the bandwidth, but from the shorter wavelengths. These wavelengths frequently are within the exposure limits.

4.1 Procedure

The slit function was centered at the wavelength of the point being investigated and normalized so that the area under the function corresponded to the value of the exposure dose when the function was weighted by the exposure dose (figure 3). We assumed that the actual arc-spectrum did not significantly vary across the limited bandwidth, which is valid for a xenon arc.

This function was weighted by the exposure dose, and then spectrally weighted by the UV hazard action spectrum $S(\lambda)$ [13] to determine what wavelengths actually were contributing to the actual photobiological effect (Fig. 5).

4.2 Results

Assuming the published bandwidths are the FWHM values, a shift in wavelength occurs for all eight data points examined (Figs 6-10).

For seven of the eight examined data points, the greatest dose comes from a wavelength within the ACGIH/ICNIRP exposure limits. The exception appears to be the "320-nm" threshold for human conjunctivitis from Cullen and Perera's 1994 study. This surprisingly low reported threshold could be due to the contribution of a thermal effect because of the long exposure duration required. Another explanation of this apparent inconsistency might have resulted from short-wavelength stray light in the small, single grating monochromator used in their experiment [12] Figure 11 shows a possible slit function for this data point accounting for stray light, and the resulting effectiveness function. The stray light was estimated for a single grating monochromator with high spectral scatter [6]. Although the stray light does not shift the peak wavelength from 314 nm, which was determined with the "perfect" slit function, the stray light in this estimation does account for 8% of the effective dose.

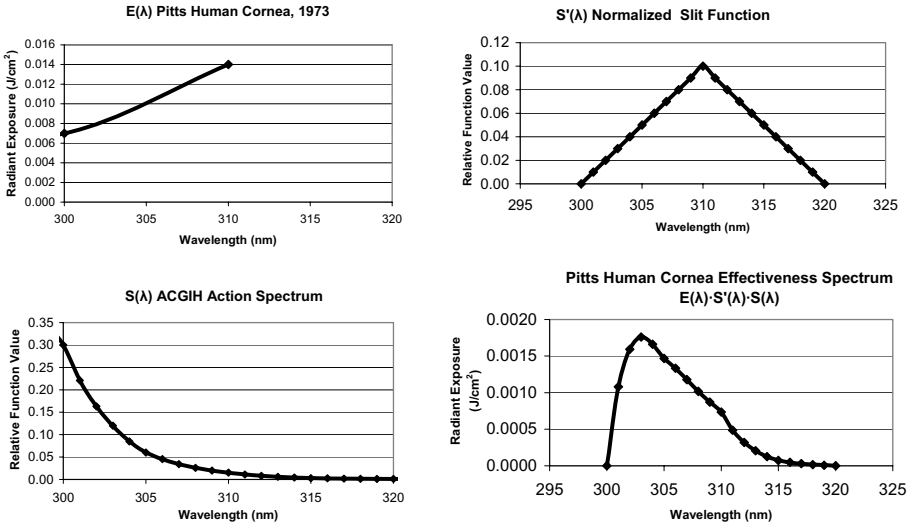

Figure 5. The upper left panel is the radiant exposure threshold at 310 nm as determined by Pitts' 1973 experimental data. The upper right panel is the normalized slit function; the lower left panel is the S(λ) action spectrum. When the slit function is weighted by the experimental data and the action spectrum, the effective wavelength shifts as shown in the lower right panel.

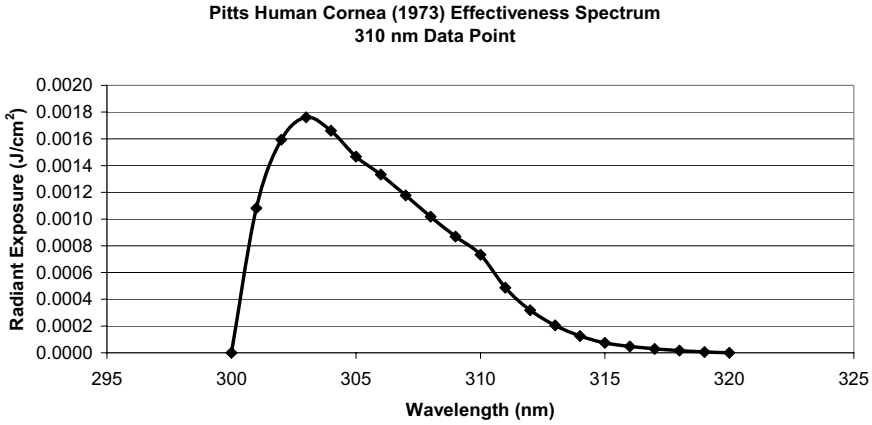

Figure 6. The weighted slit function for the Pitts' human cornea 310 nm data point. The most effective wavelength is 303 nm.

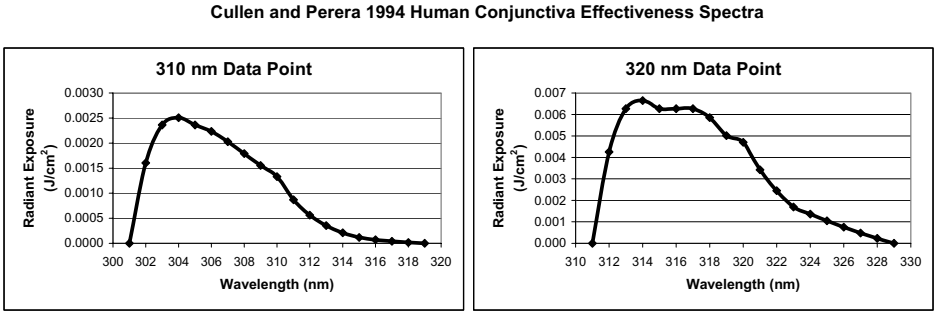

Figure 7. The weighted slit functions for Cullen's and Perera's human conjunctiva data. The left panel shows the 310 nm data point, with its most effective wavelength at 304 nm; the right panel shows the 320 nm data point with its most effective wavelength at 314 nm.

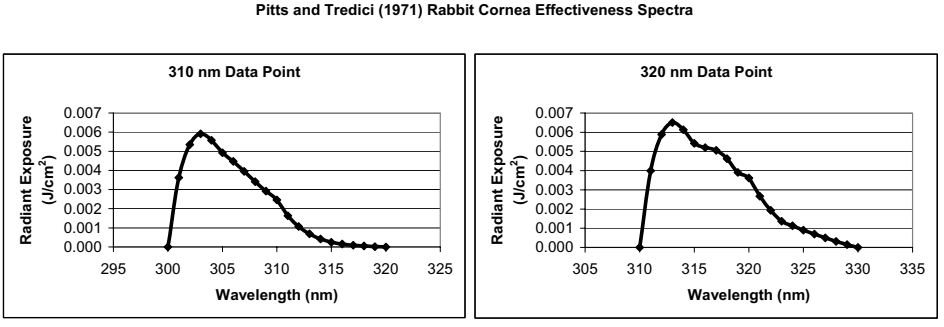

Figure 8. The weighted slit functions for Pitts' and Tredici's rabbit cornea data. The left panel shows the 310 nm data point, with its most effective wavelength at 303 nm; the right panel shows the 320 nm data point with its most effective wavelength at 313 nm.

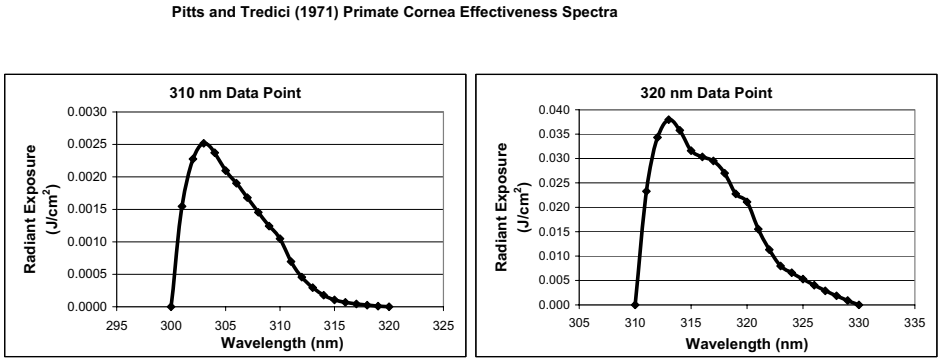

Figure 9. The weighted slit functions for the primate cornea data of Pitts and Tredici. The left panel shows the 310 nm data point, with its most effective wavelength at 303 nm; the right panel shows the 320 nm data point with its most effective wavelength at 313 nm.

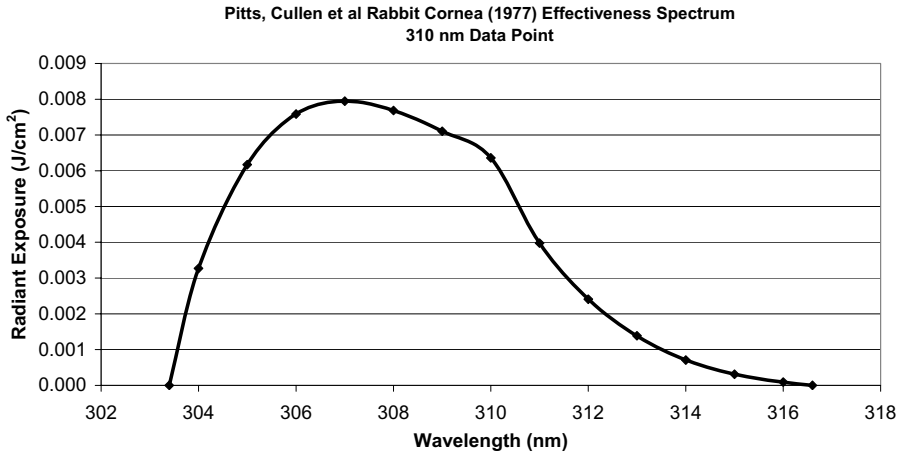

Figure 10. The weighted slit functions for the Pitts, Cullen, et al. rabbit cornea [11] 310 nm data point. The most effective wavelength is 307 nm. This data point was obtained with a smaller bandpass (6.6 nm FWHM assumed) than the others, thus the shift in wavelength is less pronounced.

It is difficult to arrive at the "true" effective wavelength for proper plotting of the data points of the action spectra. No monochromator really achieves a perfect, triangular slit function, but instead there is a "skirt" at the base of the triangle. For example, if it is assumed for the Pitts human cornea 310 nm data point that at 300 nm the slit function had at least a 1% value, the effective wavelength shifts noticeably to the shorter wavelengths, because the S(λ) value at 300 nm is 20 times more effective than at 310 nm.

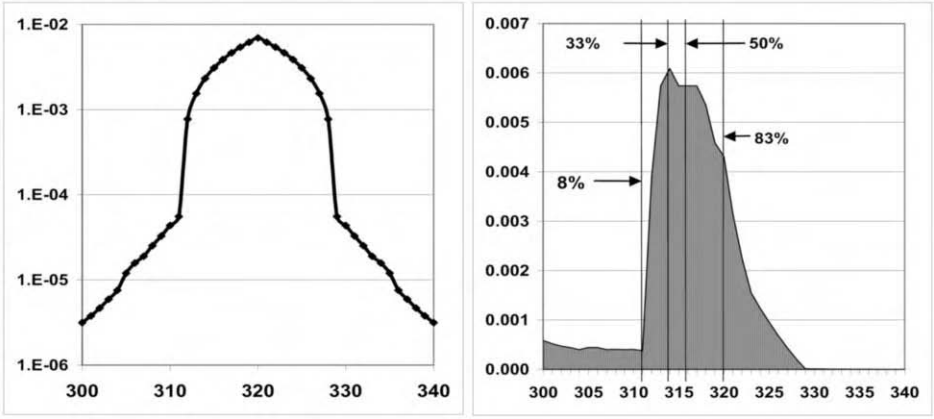

Figure 11. Slit function (left) and Effectiveness Spectrum (right) for 320 nm Cullen and Perera [12] data point. The effects of stray light are shown in each. The effectiveness spectrum shows that 8% of the effective dose comes from short-wavelength stray light that should be excluded by the monochromator. Thirty-three percent of the effective dose comes from the peak wavelength (314 nm) and shorter wavelength radiation, as opposed to 27%, which was calculated for the "perfect" monochromator. Half the effective dose is present from wavelengths at 316 nm and shorter; and 83% from 320 nm and shorter wavelength radiation.

In an effort to show the impact of monochromator bandwidth on threshold data, the effectiveness spectra were recalculated, assuming the bandwidths specified in the literature were not FWHM values, but full bandwidth values at the base. In other words, the slit functions considered here are half as wide as the slit functions described earlier. The exception was the Cullen and Perera data, which clearly specified the FWHM bandwidths. These narrower bandwidths result in much less pronounced shifts in the effective wavelength.

5. Conclusions

When determining action spectra using broadband UV sources and monochromators, a bandwidth (FWHM) of 4 nm or less will yield more accurate results than a larger bandwidth. The most effective dose will come from the wavelength at the center of the monochromator, even in the rapidly-changing 300-320 nm region. However, the shorter wavelengths (i.e., those before the center wavelength) will still contribute more to the effective dose than the longer wavelengths. A tunable UV laser is probably the most accurate way to determine the spectral effectiveness of each individual wavelength. It is therefore important that at least two, if not more laser photokeratitis thresholds be determined with laser wavelengths between 300 and 320. Such an experiment would put to rest any concerns about the uncertainty of the current guidelines for the eye.

References

[1] CIE, 1987.
[2] CIE, 2001.

[3] Diffey B., "Variation of erythema with monochromator bandwidth". *Arch Dermatol*, vol. 111, p.p. 1070-1071, 1975.
[4] ICNIRP Statement. Guidelines on UV radiation exposure limits. Health Phys, vol. 71(6), p.p. 978, 1996.
[5] Sliney D.H., "Photobiological action spectra—limits on resolution". In: "Measurements of Optical Radiation Hazards", Rüdiger Matthes and David Sliney, Editors, Geneva, CIE and ICNIRP, p.p. 41-47, 1998.
[6] Sliney D.H. and Wolbarsht M., "Safety with lasers and other optical sources". New York, Plenum Press, p.p. 445-450, 1980.
[7] Young S. and Diffey B., "Influence of monochromator bandwidth on the erythema action spectrum in the UV-B region". *Photodermatology*, vol. 2, p.p. 383-387, 1985.
[8] Kostkowski H.J., "Reliable Spectroradiometry". La Plata, MD, Spectroradiometry Consulting, pp 89-120, 1997.
[9] Pitts D.G. and Tredici T.J., "The effects of ultraviolet on the eye". *Am. Ind. Hygiene Assoc. J.*, vol. 32(4), p.p. 235-246, 1971.
[10] Pitts D.G., "The ocular ultraviolet action spectrum and protection criteria". *Health Phys*., vol. 25(6), p.p. 559-566, 1973.
[11] Pitts D.G., Cullen A.P., Hacker P.D. and Parr W.H., "Ocular ultraviolet effects from 295 nm to 400 nm in the rabbit eye". Cincinnati, OH: U.S. Department of Health, Education, and Welfare; p.p. 77–170, 1977.
[12] Cullen A.P. and Perera S.C., "Sunlight and human conjunctival action spectrum". In: "Ultraviolet Radiation Hazards", David H. Sliney, Michael Belkin, M.D., Editors, Proc SPIE 2134B, pp 24-30, 1994.
[13] ACGIH, "Threshold limit values for chemical substances and physical agents and biological exposure indices". Cincinnati, ACGIH, p.p. 155-158, 2001.
[14] ICNIRP, 1992.
[15] INIRC/IRPA. Proposed change to the IRPA 1985 guidelines on limits of exposure to ultraviolet radiation. Health Phys, vol. 56(6), p.p. 971-972, 1989.
[16] Sliney D.H., "The merits of an envelope action spectrum for ultraviolet radiation exposure criteria". *Am. Ind. Hygiene Assoc. J.*, vol. 33(10), p.p. 644-653, 1972.
[17] Peak M.J., Peak J.G., Moehring M.P. and Webb R.B., "Ultraviolet action spectra for DNA dimmer induction, lethality, and mutagenesis in *Escherichia coli* with emphasis on the UVB region". *Photochemistry and Photobiology*, vol. 40(5), p.p. 613-620, 1984.
[18] Kurtin W.E. and Zuclich J.A., "Action spectrum for oxygen-dependent near-ultraviolet induced corneal damage". *Photochemistry and Photobiology*, vol. 27, p.p. 329-333, 1978.
[19] Zuclich J.A. and Taboada J., "Ocular hazard from UV laser exhibiting self-mode-locking". *Applied Optics*, vol. 17(10), p.p. 1482-1484, 1978.

Cell Biology and Instrumentation: UV Radiation, Nitric Oxide and Cell Death in Plants
Y. Blume et al. (Eds.)
IOS Press, 2006

Ultraviolet Spectroradiometry for Environmental Biology

Brian G. GARDINER
British Antarctic Survey
Madingley Road, Cambridge CB3 0ET, UK

Abstract. Solar ultraviolet radiation is a significant factor in environmental biology. It can be measured spectrally by a spectroradiometer, or non-spectrally by a broadband radiometer. The characteristics of these instruments determine the reliability and suitability of the results. The radiation data should be accompanied by detailed documentation on the calibration and operating procedures, sufficient to assure the data user that the measurements are accurate enough for the intended purpose. A description of the observing site and conditions should also be supplied, so that the user can determine whether the observing conditions meet the requirements of the environmental investigations.

Introduction

The purpose of this document is to set out the factors that should be taken into account when making use of measurements of solar ultraviolet radiation as an adjunct to investigations of biological effects in the environment [1-3].

We are concerned here with absolute spectroradiometry, *not* differential spectroscopy. In differential (optical absorption) spectroscopy, the aim is to determine the concentration of a substance by measuring the fractional change in the radiation due to absorption by the substance. It is therefore only necessary to know the *ratio* of the intensities with and without the substance in the optical path. If the instrument remains stable during the measurement, it is possible to detect small changes in the ratio and therefore provide a sensitive determination of the concentration. Subsequent changes in the source of the radiation, or in the response of the instrument, are not critical to the accuracy of the measurements, as they do not generally affect the ratio. In differential spectroscopy it is not necessary to know the absolute intensity of the radiation.

1. Spectroradiometry

In spectroradiometry, on the other hand, the aim is to determine the absolute amount of radiation falling on the sensor. If the response of the instrument changes from one day to the next, the accuracy will suffer accordingly. Spectroradiometry therefore depends critically on calibration and operational techniques. In practice, the quality of spectroradiometric data is rather variable, and the user needs to be sure that the accuracy of the measurements is sufficient for the intended purpose [1].

Even when the measurements are of high quality, they are never as accurate as those of other environmental parameters. For example, the Earth's magnetic field can be measured to an accuracy of 1 part in 10^5 with an instrument costing $10,000, barometric pressure to 1 part in 10^4 for $1,000, and the time of day can be determined to better than 1

in 10^5 for $10, but solar ultraviolet spectral irradiance can only be measured to about 1 part in 10^1, even with an instrument costing $100,000.

It is a costly and time-consuming task to obtain reliable spectral measurements of the solar ultraviolet irradiance. Nevertheless, it is vital to have spectrally resolved measurements for a full understanding of environmental radiation effects, as every photobiological process depends on the wavelength of the incident radiation.

2. Instrumentation

2.1 Broadband Radiometers

Despite the requirement for spectrally resolved measurements, a great deal of environmental UV data is obtained from so-called broadband radiometers, which reduce the whole spectrum to one integrated value. These have the advantage that they are generally more compact (and less expensive) than spectroradiometers, so that they can be deployed in experimental locations where a larger instrument would be impractical. However, each broadband instrument has a characteristic spectral response, which is not generally the same as the action spectrum of the biological (or other) process under investigation. For example, many broadband instruments are designed to mimic the erythemal response of human skin. There is no harm in using broadband radiometers provided that the investigator understands their limitations and can relate the results to the requirements of the experiment, but their calibration ultimately derives from comparison with a spectroradiometer and a determination of their spectral response.

2.2 Spectroradiometers

To obtain information about the relative importance of different wavelengths in the biological system under investigation, measurements must be obtained from spectroradiometers. We therefore now consider the main distinguishing features of these instruments [1].

A spectroradiometer may be designed to scan from one end of its spectral range to the other, in regular steps, or it may be constructed to record the whole spectrum at once. As it can take several minutes for a scanning instrument to complete a scan, it is tempting to favour the instantaneous method on the grounds of speed. In environmental work in the open air, this has the advantage that the cloud conditions are the same for the whole spectrum, whereas the cloud cover could change during a long scan. However, the instantaneous method records the radiation by projecting the spectrum on to an array of sensors (a diode array or similar solid-state device) so that each individual sensor collects a small slice of the spectrum.

There are typically about 1000 sensors packed into a small rectangle with an area of the order of a square centimetre. This method has several disadvantages. Apart from the inherent difficulty of calibrating the sensitivity of an array of sensors, and ensuring that the same wavelengths always fall on the same sensors, the diode-array system imposes a serious constraint on the optical design of the instrument: it can generally use only a single monochromator. By contrast, the scanning spectroradiometers can use either a single or a double monochromator. We therefore now consider the merits of single and double monochromators.

2.2.1 Single Monochromator

The aim of any spectrometer is to select photons from a small slice of the spectrum, and record them in isolation. It is important to exclude photons from the rest of the spectrum. In modern instruments this is usually achieved by means of a finely-ruled diffraction grating, which sends each wavelength in a different direction. The incident (white) light passes through the entrance slit of the instrument and is made to fall on the diffraction grating. The optical arrangement (mirrors, prisms, lenses, or even the curvature of the grating itself) then forms a focused image of the entrance slit on the exit surface. A spectrum therefore appears on the exit surface, as the focused image of the entrance slit for each wavelength is slightly displaced from the next. This is a single monochromator. In a diode-array instrument, the diode array is placed on the exit surface. In a scanning instrument, the exit slit is placed there, and the grating is slowly rotated so that each wavelength in turn falls on the exit slit. Photons passing through the exit slit are then recorded by a sensor such as a photomultiplier.

This works well for visible light. Unfortunately, at the shorter wavelengths in the ultraviolet there are so few photons that they are completely outnumbered by visible photons. No grating is perfect, and no instrument is completely free of internal scattering surfaces, so some visible photons will always end up on the exit surface. This stray light is a serious problem in the UVB region of the spectrum (280 nm to 315 nm). Although it could in principle be alleviated by the judicious use of filters to absorb the visible light, the stability and calibration of such filters merely introduce additional sources of measurement error. They are generally more trouble than they are worth. The answer to the problem of stray light is the double monochromator.

2.2.2 Double Monochromator

In the double monochromator, the exit slit of the first monochromator becomes the entrance slit of the second. The two monochromators are usually of identical design, and are cleverly positioned to minimise the effect of stray light. The second grating is rotated in step with the first. The general principle is that a visible photon may succeed in entering the second monochromator, and may even fall on the second grating, but it will then be directed away from the final exit slit. The consequent reduction in stray light allows measurements down to the shortest ultraviolet wavelengths encountered in solar radiation at the surface of the Earth.

2.2.3 Spectral Resolution

In principle, the spectroradiometer selects a single wavelength, but in practice the radiation falling on the exit slit (or on one sensor of a diode array) is a weighted sum of the incident radiation, mostly in a small interval of the spectrum. This weighting is often referred to as the slit function, and is typically triangular in shape, with weak wings due to imperfections in the optical system. The full width at half maximum (FWHM) of the slit function is a measure of the spectral resolution of the instrument, and is usually a fraction of a nanometre in the finest spectroradiometers and a few nm in the coarsest. If the FWHM of the slit function exceeds about 1.0 nm, measurements in the UVB region become progressively more misleading as shorter wavelengths are examined, because the incident solar radiation is such a steep function of wavelength that the exit slit is dominated by the longer end of the selected wavelength interval. The choice of spectral resolution therefore

depends on the nature of the proposed work. A finer resolution might be necessary if the action spectrum of a relevant biological effect was dominated by the shortest UVB wavelengths.

2.2.4 Directional Response

On the outer part of the instrument, the entrance optics serve to gather radiation from the environment and direct it into the spectrometer. Some care is required to ensure that radiation from different directions is gathered in the correct relative proportions, and the user needs to consider whether to record irradiance, actinic flux, or something else such as directional radiance.

2.2.4.1 Irradiance

For general purposes it is usual to record the irradiance on a horizontal surface (sometimes called global solar irradiance). This represents the energy passing through a square metre of horizontal surface per second, and therefore gives much less weight to radiation from a source near the horizon, such as the setting Sun. This is ideal for studying the energy budget of a horizontal snowfield or an agricultural crop with horizontal leaves, and is generally satisfactory for most processes that are confined to the surface of the Earth and have no special or critical directionality. The irradiance is usually obtained by deploying a translucent diffuser (a plane or domed receiving surface made from ground quartz or Teflon) or an integrating sphere (a hollow sphere painted white on the inside, with small entrance and exit apertures). When recording irradiance at an experimental site, it might be thought appropriate to tilt the receiver in a particular direction, for example if the site is on the slope of a hill, or if the plants turn towards the Sun. Some instruments are constructed with an optical fibre to transmit the radiation from the receiving surface to the spectrometer, which makes it possible to point the receiver in any desired direction.

2.2.4.2 Other Directional Responses

The term actinic flux refers to a scheme in which radiation sources are given equal weight irrespective of their direction, and is usually obtained by deploying a translucent sphere or its equivalent. The user needs to consider whether this is appropriate, as it includes not only the direct radiation from the low Sun, but also the radiation reflected upwards and sideways from the ground and buildings. It is often used when studying atmospheric photochemistry, as chemical reactions in the free atmosphere do not mind where their photons come from. It is also possible to construct a receiver that gathers radiation from one direction only, in a narrow cone, in order to explore the directional radiance of the incident radiation. However, this requires a high-specification instrument, as there is very little radiation available from such a restricted field of view. In most cases, therefore, biological studies in the environment will be conducted with instruments recording the global solar irradiance. This is true not only of ultraviolet and visible spectroradiometers but also of broadband radiometers.

3. Calibration

3.1 Wavelength

The wavelength calibration of UV spectroradiometers is important, but relatively straightforward, and can be achieved by reference to known spectral lines from mercury or

other discharge lamps, or by direct comparison of the measured solar radiation with known features in the spectrum of the Sun. Regular checks should be made until the temporal behaviour of the wavelength calibration is well established.

3.2 Broadband Irradiance

Much more difficult is the irradiance calibration. In the case of a broadband instrument, the calibration should be traceable to a direct comparison with a spectroradiometer. The measurement results from a broadband radiometer are generally expressed in weighted $W\ m^{-2}$, where the weighting function is the action spectrum of the effect that the instrument is designed to mimic. As the spectral response of the instrument will generally differ somewhat from the action spectrum, the calibration will usually have been adjusted to be appropriate for 'average' or 'typical' conditions, for example with the Sun neither high nor low in the sky, medium cloud cover, low surface albedo, and an arbitrary value for the atmospheric ozone amount. The further the actual conditions are from the typical values, the greater the error in the calibration. In addition, the broadband calibration will suffer from any errors in the spectroradiometer from which it was derived, and may also drift with time. The calibration of spectroradiometers is therefore rather important [2,3].

3.3 Spectral Irradiance

In order to calibrate a spectroradiometer it is necessary to obtain a radiation source whose spectral output has already been determined with reference to fundamental physical standards. This usually means a lamp with a certificated calibration showing its spectral irradiance in $W\ m^{-2}\ nm^{-1}$ at a fixed distance from the lamp. The lamp and the spectroradiometer are then placed in a darkened room, and the spectral radiation from the lamp is recorded by the instrument throughout the required range of wavelengths. Success depends on careful attention to the experimental conditions. The distance from lamp to instrument, typically 50 cm, must be accurately measured from the plane on the lamp holder specified in the lamp certificate to the receiving plane on the instrument. The lamp must be in the specified orientation and its current must be kept constant and measured to better than 1 part in 1000. All extraneous reflections from the walls, the bench and the equipment must be eliminated by the use of matt black paint, black velvet cloth, and black screens and baffles. Repeated spectral scans are required, on the day of the calibration and at regular intervals thereafter, until the stability and reproducibility of the spectroradiometer calibration have been established. Furthermore, in practice it is necessary to maintain a family of lamps, and monitor their behaviour relative to each other, so as to detect a faulty lamp, or one that is deteriorating. The stable lifetime of these lamps can be as short as 50 hours of burn time, at which point recalibration of the lamp is required. Finally, the experimenter must take precautions against fire, especially when using the typical 1 kW lamps, and against eye and skin damage, as the lamps usually have a quartz envelope and therefore emit significant UVC radiation (less than 280 nm), which is particularly harmful.

4. Quality Assurance

4.1 Documentation

As the reliability of spectral irradiance measurements depends critically on the quality of the calibration and maintenance procedures, the operators of the spectroradiometers should supply sufficient technical information to convince the user that the measured data are

accurate enough for the intended purpose [2,3]. This information should describe the calibration system and the procedures for operational measurements in the environment. The calibration description should include the number of lamps (at least three and preferably more), their types and details, traceability, and statistical information on their stability throughout the period of interest. If the lamp certificates are not from a national standards laboratory, they should at least be directly traceable to one and the traceability should be fully documented, including the serial numbers of the lamps and the dates and serial numbers of the calibrations from which the certificated calibrations were derived. There should be information about the frequency of calibrations, the lifetime of the lamps, and the repeatability and stability of the resulting spectroradiometer calibrations.

4.2 Intercomparison

An additional source of quality assurance is available if the spectroradiometer has been tested in an international blind intercomparison, where the errors and deficiencies of calibrations and operating procedures are systematically exposed and examined. However, the reports of such intercomparisons should not be regarded as a substitute for careful and regular calibration at the observing site. As the accurate measurement of solar radiation is particularly difficult, the data user should also be guided by the thoroughness of the procedural descriptions, the consistency of the results, and the professionalism of the documentation. This applies also to the description of the observing site, which we now consider.

5. Measurement Site

When ultraviolet radiation data are required for environmental investigations, the measurements will have been recorded either at a regular observing station in the region, or at the actual site of the investigations. When the measurements are at the investigation site, the user can examine the observational conditions and ensure that the measurements are relevant to the proposed experiments. It may even be possible to control the radiation measurements and configure them to suit the purpose, for example by specifying the spectral range, the frequency of observation, the exact location of the instrument, and the orientation of the receiver.

If, on the other hand, the data are obtained from a regular observing site such as a meteorological station or environmental institute, the conditions are out of the user's control, and it is necessary to determine whether the measurements are suitable. Provided that the station is in the same weather region, and that the latitude and altitude are similar, the results are likely to be of use, but for detailed work it may be necessary to take into account the local behaviour of the cloud cover on the days in question. Climatological data from regular observing sites will generally refer to irradiance on a horizontal surface.

5.1 Site Information

Whether the data are recorded locally or not, the accompanying information should include a description of the horizon as seen from the radiometer, listing the angular elevation and the azimuth (direction) of each significant obstruction such as buildings and mountains. There should also be a general description of the site and its surroundings including the nature of the surface, so that its albedo (reflectivity) can be estimated. This is useful if the measurements are subsequently used in model calculations to fill in gaps in the available data.

In general, the documentation of the site and the observing conditions can be just as useful as the calibration information, especially if the observers have been careful to annotate the data with details of the little daily technical difficulties that so often lead to unreliable results.

6. Conclusion

When measurements of ultraviolet spectral irradiance are required for environmental biology, the data user should not accept the data at face value, but ensure that they are supported by adequate explanatory documentation. The user should be satisfied that the radiation data are appropriate in type and quality for the intended purpose, and in particular that the calibration and operational observing procedures have been correctly performed. The suitability of the observing site should also be examined.

References

[1] Gardiner B.G., "Spectroradiometer calibration methods and techniques", in Zerefos, C.S. and Bais, A.F. (eds.), Solar Ultraviolet Radiation. Modelling, Measurements and Effects, NATO ASI Series I: Global Environmental Change, vol. 52, Springer Verlag, p.p 119-132, 1997.

[2] Webb A.R., Gardiner B.G., Martin T.J., Leszczynski K., Metzdorf J. and Mohnen V.A., "Guidelines for site quality control of UV monitoring", WMO/GAW Rep. 126, World Meteorological Organization, Geneva, WMO TD No. 884, 39 p., 1998.

[3] Webb A.R., Gardiner B.G., Leszczynski K., Mohnen V., Johnston P., Harrison N. and Bigelow D.S., "Quality assurance in monitoring solar ultraviolet radiation: the state of the art", WMO/GAW Rep. 146, World Meteorological Organization, Geneva, WMO TD No. 1180, 35 pp., 2003.

Cell Biology and Instrumentation: UV Radiation, Nitric Oxide and Cell Death in Plants
Y. Blume et al. (Eds.)
IOS Press, 2006

Ambient Levels of UV Radiation

Mario BLUMTHALER
Division for Biomedical Physics, Innsbruck Medical University
Müllerstr. 44, A-6020 Innsbruck, Austria

Abstract. The intensity of solar UV radiation at the Earth's surface is highly variable. The most important parameters for cloudless conditions are in the sequence of their significance: solar zenith angle, total ozone content of the atmosphere, amount and type of aerosols, albedo of the surrounding and altitude above sea level. Based on measurements, the effects of these parameters are discussed individually. Furthermore, clouds usually attenuate the irradiance, only in exceptional cases they can lead to an increase over short time periods. The attenuation by clouds is less strong for UV radiation compared with radiation from the whole spectral range.

Introduction

The ambient levels of solar UV radiation at the Earth's surface play an important role for the whole biosphere, because UV radiation can trigger a large number of effects on living organisms. Furthermore, solar UV radiation is important for photochemistry in the lower troposphere, as several chemical reactions are driven by the absorption of UV radiation. UV radiation also interacts with materials usually leading to changes in the molecular structure. All these effects are a consequence of the relatively high photon energy of UV radiation due to the short wavelengths. In contrast, the absolute amount of energy of solar UV radiation at the Earth's surface is relatively small, compared with the total energy emitted from the sun and received at the Earth.

The absolute level of the UV radiation depends on the intensity of the sun as the source, on astronomical and geographical parameters, on the characteristics of the Earth's atmosphere and on the local conditions of the ground in the surrounding of the measurement station.

The spectrum of solar radiation is primarily defined by the emission from the sun, which is close to an emission of a black body with a temperature of about 5800° Kelvin. When the radiation is passing through the outer part of the solar atmosphere it gets the high fine structure due to absorption by the molecules of the gas. These so called "Fraunhofer lines" appear in all measurements of the solar spectrum, and the smaller the used bandwidth the higher structure of the absorption lines can be observed. This extraterrestrial solar spectrum at the top of the Earth's atmosphere is further modulated in the annual course by the changing difference between sun and Earth. This leads to a variation of the intensity of all wavelengths by about ±3.5% with the maximal value on about 3 January and the minimal one on about 5 July.

Within the Earth's atmosphere, absorption and scattering processes modify the extraterrestrial spectrum. As a consequence of the scattering processes the radiation is

separated in a direct and a diffuse component, and this separation is strongly dependent on wavelength.

The direct component is reduced by extinction processes (scattering and absorption) in the atmosphere and can be described with the extinction law of Beer

$$I = I_0 * \exp(-\Sigma_i(m_i * \tau_i))$$

I_0 is the intensity outside the atmosphere, I is the intensity at the surface, m denotes the air mass, which is the length of the path of the direct beam through the atmosphere relative to the vertical path length. For the assumption of a plane-parallel atmosphere m depends on the solar zenith angle (SZA) with m=1/cos(SZA), which is a good approximation to the real situation for SZA<85°. Finally, τ is the extinction coefficient. The index i indicates the different scattering and absorption processes. In the UV range the most important processes are scattering on molecules (Raleigh scattering), absorption by gases and scattering and absorption by aerosols and clouds. The most important absorbing gas is ozone, which absorbs strongly below 300 nm (Hartley region) and more weakly up to about 330 nm (Huggins band). Further atmospheric gases which absorb in the UV range are nitrogen dioxide and sulphur dioxide, which can be significant in polluted urban environments. Scattering on molecules depends strongly on wavelength (proportional to λ^{-4}), whereas scattering on aerosols only weakly depends on wavelength (about proportional to $\lambda^{-1.3}$). Scattering on water droplets in clouds is almost independent on wavelength in the UV range.

The usual measurement quantity for solar radiation is "irradiance", which is the energy per time and wavelength interval through a horizontal surface. Therefore the unit is $Wm^{-2}nm^{-1}$. The combined diffuse and direct irradiance on a horizontal surface is called global irradiance. The share of diffuse irradiance on global irradiance increases with decreasing wavelength and with increasing SZA and further increases with higher amounts of scattering aerosols. As a consequence, in the UV range more than half of global irradiance can be diffuse.

In the following sections the variability of ambient levels of solar global irradiance is discussed based on measurements, which are carried out with spectroradiometric and broadband UV measurements under a large variety of environmental conditions and which allow deriving quantitative estimates of the effects of the influencing parameters. In general, such information could be retrieved also from radiative transfer calculations, but the variability of the input parameters has to be estimated from actual measurements. Therefore, radiative transfer model calculations are a helpful tool, but they cannot replace actual measurements. Most of the broadband measurements of solar UV radiation presented here are carried out with detectors which simulate the human erythema action spectrum [1] and which indicate therefore directly the erythemally-effective irradiance (G_{ER}). For the discussion of the effects of the various parameters on solar UV radiation, these measurements of G_{ER} can be interpreted as representative for the UVB range (280 nm to 315 nm), although a small contribution of the UVA range (315 nm to 400 nm) is included in these measurements.

1. UV Radiation under Cloudless Skies

The systematic discussion of the various parameters, which affect solar UV radiation, needs to exclude cloudiness in the first step. Then the most important parameter determining ambient UV levels is the solar zenith angle. In the UVB range the second important parameter is the total ozone content of the atmosphere. In urban environments with local air pollution the amount of aerosols is the next most important parameter. The reflectivity of

the ground (albedo) becomes a further important parameter, if the terrain is covered by snow. Finally, the altitude above sea level has a great influence, where usually several other parameters are interacting at the same time. The following detailed discussion of these parameters will show the quantitative effect of each of these parameters individually.

1.1. Effect of Solar Zenith Angle

According to Beer's law (see introduction) an increasing air mass as a consequence of increasing SZA will reduce the direct component of global irradiance. This becomes evident in the diurnal course of UV radiation as well as in the seasonal course, when the SZA is smaller at noon time in summer compared to winter. Furthermore, from this a latitudinal gradient arises, because smaller SZA at noon time occur when going from the pole towards the equator.

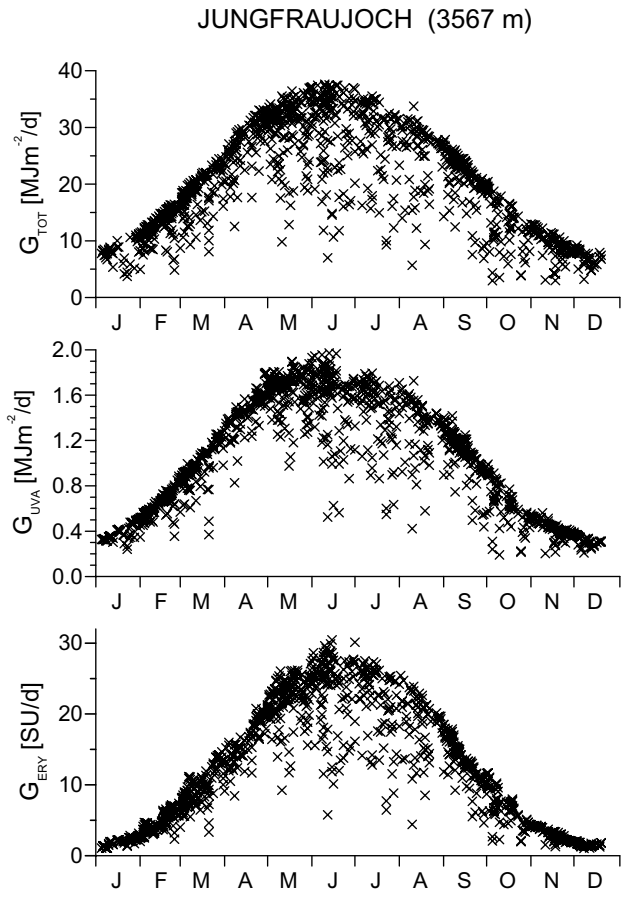

Figure 1. Seasonal course of daily totals of total global irradiance (G_{TOT}), global UVA (G_{UVA}) and erythemal UV irradiance (G_{ERY}) at the High Mountain Station Jungfraujoch (Switzerland).

In the UVB range the dependence on SZA is stronger pronounced than in the longer wavelength ranges. This is caused by the strongly increasing absorption in the ozone layer with increasing path length of the photons passing through the atmosphere. This can be seen clearly in the seasonal course of daily totals of the irradiance in different wavelength ranges (Fig. 1). There the course of the envelope, which represents maximal values due to minimal cloudiness, is much steeper for the UVB range compared to UVA and total global irradiance (300 – 3000 nm). The ratio of maximal values in summer relative to winter is about 18 for the UVB range and 5 for total global irradiance. For the same reason also the daily course of UVB irradiance is much steeper than for irradiance of longer wavelength ranges.

1.2. Effect of Ozone

A higher amount of total ozone in the atmosphere leads to lower values of UVB irradiance due to the strong absorption of ozone in the UVB range. The shorter the wavelength the stronger is the effect of ozone. For example, at 300 nm a decrease of ozone by 1% gives an increase in irradiance by 10% (at 60° SZA). The relation between irradiance I (monochromatic or broadband) and total ozone content O can be approximated by a power law

$$I \sim O^{-RAF}$$

The exponent RAF is called radiation amplification factor. This name comes from a linearization of the above mentioned power law for small variations, where

$$\Delta I/I = - \Delta O/O * RAF$$

This means that the percentage change in irradiance equals the percentage change in ozone times the RAF.

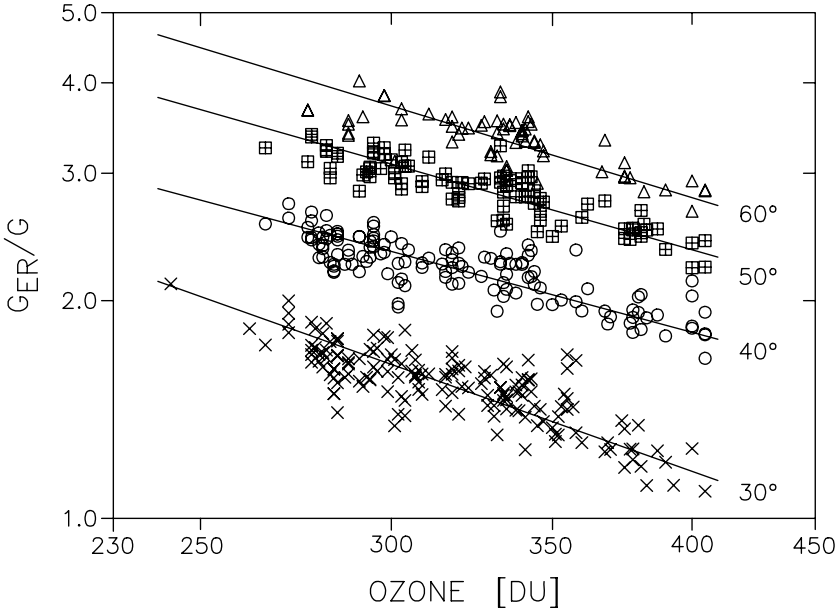

Figure 2. Relation between ozone and the ratio of erythemally weighted UV irradiance over total global irradiance for various solar elevations. From [2].

This relation can be verified with measurements under clear sky conditions at fixed SZA [2]. Measurements at the High Alpine mountain station Jungfraujoch (3576 m above sea level, Switzerland) are only marginally influenced by aerosols, and the effect of varying albedo is minimized by analysing the ratio G_{ER}/G. This shows clearly the relation following the power law, when in a log-log plot the relation becomes linear with the RAF as the slope of the linear regression line (Fig. 2). These measurements give a value for the RAF of 1.1, which is in very good agreement with model calculations using radiative transfer models. This means that a reduction of ozone by 1% will result in an increase of erythemally weighted UV irradiance by 1.1%.

1.3. Effect of Aerosols

Aerosols in the atmosphere can scatter or absorb UV radiation, depending on their chemical composition. In most cases the absorbing component is of the order of 1-10% of the whole extinction (absorption plus scattering), only when aerosols originate from great fires the absorbing component might be higher. As a consequence of the scattering component of aerosols the diffuse irradiance is increased and the direct irradiance is decreased. The quantitative amount of these effects depends on the amount and type of aerosols, on their size distribution and on the vertical distribution in the atmosphere. Aerosol extinction depends only slightly on wavelength with higher values at shorter wavelengths. As an example for the variable attenuation effect of aerosols on erythemally weighted irradiance in Fig. 3 the attenuation relative to an aerosol free situation is shown for measurements at a campaign near Athens, Greece, in summer 1996 [3]. For many days the attenuation is in the order of 5 to 15%, but on some days (depending on the local wind direction) the attenuation can reach values up to 30 and 35%, relative to an aerosol free atmosphere. It is interesting to mention that during the 20 days of this campaign the variability of aerosols had a greater effect on erythemally weighted irradiance than the variability of ozone.

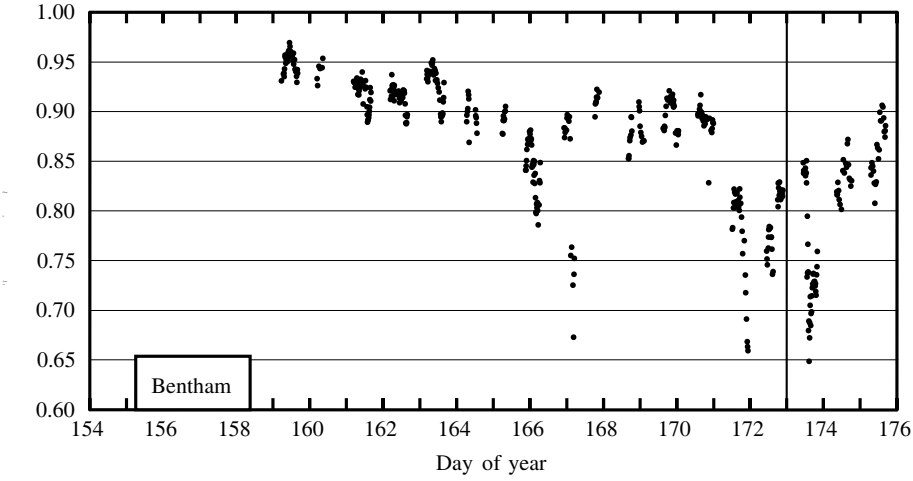

Figure 3. Attenuation of erythemally weighted irradiance relative to aerosol free conditions for a measurement campaign near Athens, Greece, in summer 1996. From [3].

A special influence of aerosols on UV radiation can be found if a layer of aerosols is formed in the lower stratosphere, usually as a consequence of very strong volcanic

eruptions. Model calculations show that under this condition the UV irradiance at 290 nm may increase by up to 45%, whereas at 300 nm a decrease of 5% would be expected [4].

1.4. Effect of Albedo

The albedo of the ground (ratio between diffuse reflected radiation and incoming radiation) enlarges the diffuse irradiance due to multiple reflections between the ground and the atmosphere. The value of the albedo of various surfaces is shown in Figure 4 in dependence on wavelength, determined from own spectral measurements. All snow-free surfaces show a relatively small albedo in the UV range, the smallest values are found for green grassland, where the albedo in the UV range is less than 1%. In contrast, high values are found for snow-covered terrain, where values higher than 90% can be measured.

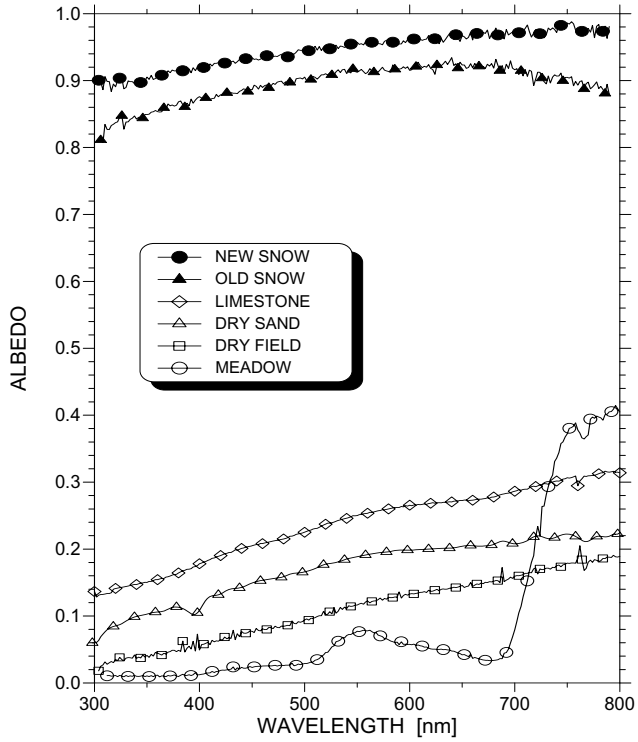

Figure 4. Spectral albedo of various surfaces, from measurements of the author.

The consequence of different albedo on global irradiance can be estimated from model calculations. For this, cloud free conditions are assumed. In general, a more pronounced effect of albedo is to be expected for cloudy situations, because in this case a higher amount of photons reflected from the ground to the atmosphere is reflected back towards the ground. For high mountain conditions, the result of the model calculations is shown in Fig. 5, which gives the amplification factor for global irradiance for an increase in ground albedo by 0.1 in dependence on wavelength. The results are slightly different for

different values of the reference albedo, but the general feature is always a maximal amplification effect for wavelengths around 320 nm and significantly smaller effects at 500 nm. The reason for this spectral behaviour is the increasing amount of diffuse irradiance with decreasing wavelength. The decrease of the amplification at wavelengths below 320 nm is a consequence of absorption by ozone and the strongly increasing ozone absorption coefficient at these wavelengths, because the multiple reflections between ground and atmosphere increase the pathlength of the photons and consequently increases the absorption.

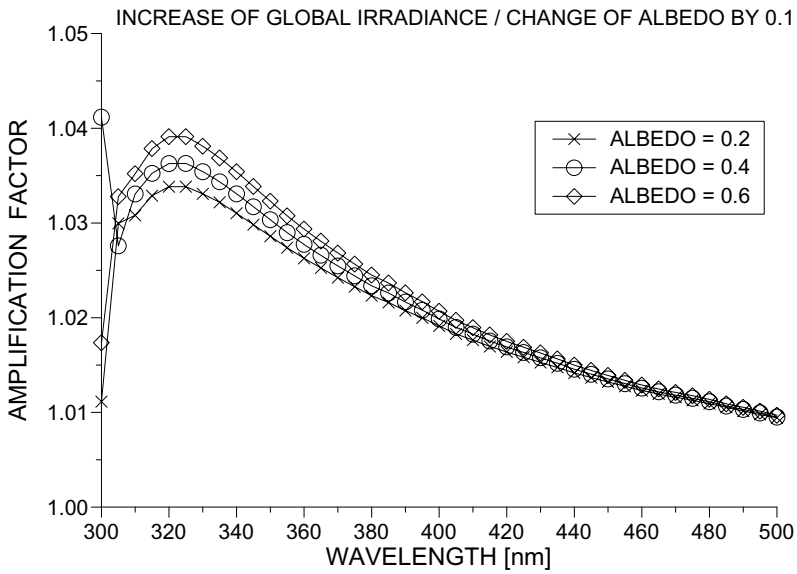

Figure 5. Increase of spectral global irradiance due to an increase of albedo by 0.1 for albedo values of 0.2, 0.4 and 0.6.

The results for albedo effects showed so far assume that the ground has an unlimited extension and that the albedo is homogeneous over the terrain. However, in practise the terrain is inhomogeneous and in that case the more complex three-dimensional radiative transfer calculations are necessary [5]. In comparison with the one-dimensional radiative transfer calculations an 'effective' albedo can be defined, which describes the reflection of a given inhomogeneous terrain by an area-averaged single albedo value [6]. Model calculations have shown that the radius of significance, where the albedo has still an influence on global irradiance, extends up to 30 km [7]. Measurements in high mountain areas with partly snow covered terrain have shown values for effective albedo between 0.7 and 0.4 as a consequence of complex distribution of snow covered and snow free surfaces.

1.5. Effect of Altitude

The increase of global irradiance with altitude is called 'altitude effect', and it is expressed as percentage increase for an increase in altitude by 1000 m. This increase of irradiance is mainly a consequence of the smaller irradiated air mass at higher altitudes. Therefore the altitude effect depends on wavelength, with higher values at shorter wavelengths due to stronger scattering at shorter wavelengths. Further important influencing parameters are the

optical characteristics of the air layer between the two altitudes, mainly the amount of aerosols and the amount of tropospheric ozone in this layer. The higher these two quantities are, the more reduced is the irradiance at the lower station and therefore the higher is the altitude effect. Additionally, the altitude effect can be increased, if at higher altitudes the terrain is snow covered. From all these influencing parameters it is clear that for the altitude effect not one single number can be given, but that it is necessary to describe it with a certain range of values in dependence on wavelength.

Examples for measurements of the altitude effect show this large range of variability. In the Chilean Andes, Piazena [8] found about 8% in the UVA and 9% in the UVB, Zaratti [9] found about 7% for erythemally weighted irradiance in Bolivia. In the Alps usually higher values were measured, as a consequence of higher amounts of aerosols and tropospheric ozone in the lowest layers of the atmosphere. An example is shown in Fig. 6 for measurements near Garmisch-Partenkirchen, Germany, where the spectral dependence was derived from simultaneous spectroradiometric measurements at different altitudes [10]. The given standard deviation shows the variability during this measurement campaign. Average values for the altitude effect in the UVA range are about 10% and for erythemally weighted irradiance about 15-20%. If in addition the surrounding of the mountain station is covered by snow and the station at low altitude is snow free, then the altitude effect might by further increased by 5-10%.

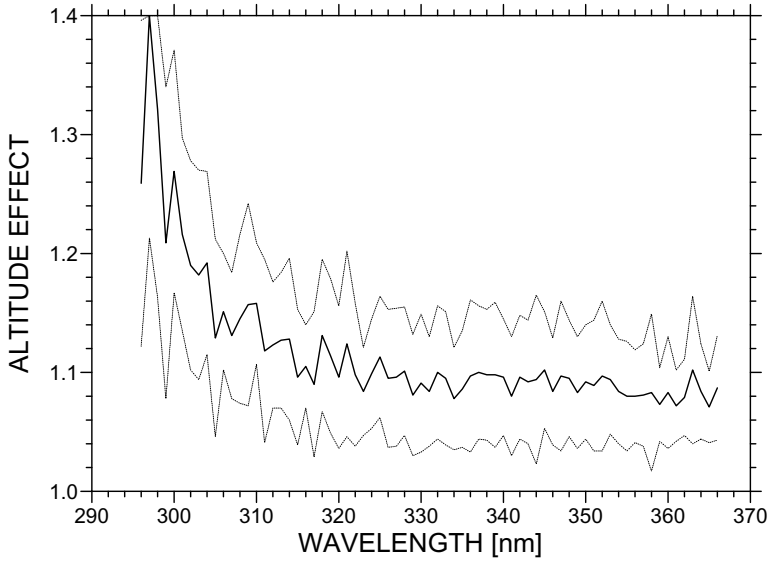

Figure 6. Increase of spectral global irradiance with altitude, average (solid line) and range of variation (dashed lines). From [10].

2. Effect of Clouds

In general, clouds attenuate the level of global irradiance at the Earth's surface, but this reduction can vary within a broad range. It depends on the optical depths of the cloud and if the clouds occult the sun itself. In some special cases it happens that global irradiance at the ground is enhanced by cloudiness [11], if bright clouds are close to the sun but do not occult

the sun itself. Due to reflections from the sides of the clouds an enhancement of 10-20% may occur for short time periods.

Due to the large variability of clouds a great number of measurements under different situations of cloudiness are necessary to determine the influence of clouds on global irradiance. Such an analysis could be carried out from long-term measurements at Jungfraujoch, Switzerland [12]. The different wavelength ranges were measured simultaneously and the data were normalised to the respective values under cloudless conditions. Cloudiness was estimated in tenths of the sky, covered by clouds (Fig. 7, left). The reduction for complete cloudiness (10/10 of the sky covered by clouds) reaches values up to 50% for this high altitude station, whereas at sea level average values of reduction up to 75% were measured [13]. Although the scattering process by clouds is only slightly dependent on wavelength, the effect of clouds on global irradiance is significantly dependent on clouds (Fig. 7, right). The ratio between erythemally weighted irradiance and UVA irradiance is almost constant with cloudiness, whereas the ratios of both ranges of UV irradiance over total global irradiance depend strongly on cloudiness. This means that under complete cloud cover erythemally weighted irradiance is about 40% less attenuated than total irradiance. The reason for this is the higher diffuse component of UV irradiance compared with total irradiance, and that diffuse irradiance is much less attenuated by clouds than direct irradiance.

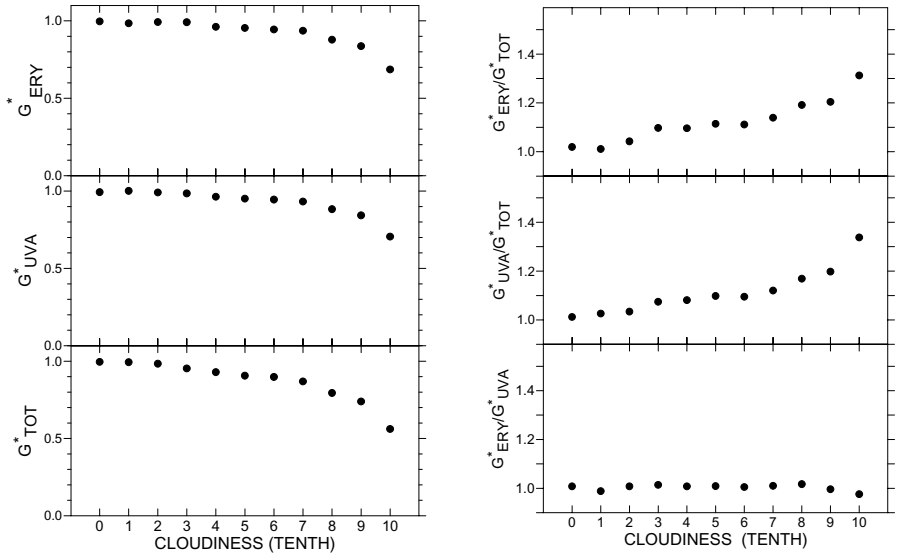

Figure 7. Left: attenuation by cloudiness of global irradiance (G^*_{TOT}), global UVA (G^*_{UVA}) and erythemal UV irradiance (G^*_{ERY}) at the High Mountain Station Jungfraujoch (Switzerland). The radiation fluxes are normalized to cloudless conditions. Right: ratios of the normalized radiation fluxes in dependence on cloudiness. Adapted from [12].

References

[1] McKinlay A.F. and Diffey B.L., "A reference action spectrum for ultraviolet induced erythema in human skin", *CIE Journal* vol. 6, p.p. 17-22, 1987.

[2] Blumthaler M., Salzgeber M. and Ambach W., "Ozone and ultraviolet-B irradiances: experimental determination of the radiation amplification factor", *Photochem. Photobiol.* vol. 61, p.p. 159-162, 1995.

[3] Kylling A., Bais A.F., Blumthaler M., Schreder J. and Zerefos C.S., "The effect of aerosols on solar UV irradiances during the PAUR campaign", *J. Geophys. Res.* vol. 103, p.p. 26051-26060, 1998.

[4] Michelangeli D.V., Allen M., Yung Y., Shia R., Crisp D. and Eluszkiweicz J., "Enhancement of atmospheric radiation by an aerosol layer", *J. Geophys. Res.*, vol. 97, p.p. 865-874, 1992.

[5] Kylling, A., Dahlback A. and Mayer B., "The effect of clouds and surface albedo on UV irradiances at a high latitude site", *Geophys. Res. Lett.* vol. 27, p.p. 1411-1414, 2000.

[6] Weihs P., Lenoble J., Blumthaler M., Martin T., Seckmeyer G., Philipona R., De la Casinieri A., Sergent C., Gröbner J., Cabot T.and others, "Modeling the effect on an inhomogeneous surface albedo on incident UV radiation in mountainous terrain: determination of an effective surface albedo", *Geophys. Res. Let.* vol. 28, p.p. 3111-3114, 2001.

[7] Degunther, M. and Meerkötter R., "Influence of Inhomogeneous Surface Albedo on UV Irradiance - Effect of a Stratus Cloud", *J. Geophys. Res.*, vol. 109, p.p. 22755-22761, 2000.

[8] Piazena H., "The effect of altitude upon the solar UV-B and UV-A irradiance in the tropical Chilean Andes", *Solar Energy* vol. 57, p.p. 133-140, 1996.

[9] Zarattit, F., Forno R., Fuentes J. and Andrade M., "Erythemally weighted UV variations at two high.-altitude stations", *J. Geophys. Res.* vol. 108(D9), ACH5_1-6, 2003.

[10] Blumthaler M., Webb A.R., Seckmeyer G., Bais A.F., Huber M. and Mayer B., "Simultaneous Spectroradiometry: A Study of Solar UV Irradiance at Two Altitudes", *Geophys. Res. Let.* vol. 21, p.p. 2805-2808, 1994.

[11] Cede A., Blumthaler M., Luccini E., Piacentini R. and Nunez L., "Effects of clouds on erythemal and total irradiance as derived from data of the Argentine network", *Geophys. Res. Lett.* vol. 29, p.p. 761-764, 2002.

[12] Blumthaler M., Ambach W. and Salzgeber M., "Effects of cloudiness on global and diffuse UV irradiance in a high-mountain area", *Theor. Appl. Climatol.* vol. 50, p.p. 23-30, 1994.

[13] Josefsson, W. and Landelius T., "Effect of clouds on UV irradiance: As estimated from cloud amount, cloud type, precipitation, global radiation and sunshine duration", *J. Geophys. Res.* vol. 105, p.p. 4927-4935, 2000.

Cell Biology and Instrumentation: UV Radiation, Nitric Oxide and Cell Death in Plants
Y. Blume et al. (Eds.)
IOS Press, 2006

DSCOVR, the First Deep Space Earth and Solar Observatory

Francisco P. J. VALERO[1], Jay HERMAN[2]
[1] *Scripps Institution of Oceanography, University of California, San Diego, 9500 Gilman Dr, La Jolla, California 92093-0242, USA*
[2] *NASA/Goddard Space Flight Center Code 916 Greenbelt, MD 20771 USA*

Abstract. Earth observations from satellites located in deep space offer the exciting opportunity to look at the Earth in a bulk thermodynamic sense, particularly as an open system exchanging radiative energy with the Sun and space, in a way never done before – "the Earth as a whole planet", astronomers would say. This is a fundamental scientific goal with very appealing prospects for Earth sciences. Climate research requires stable, accurate, long-term observations made with adequate spatial and temporal resolution in a synoptic context. From deep-space vantage points we can, with a single spacecraft, sample the outgoing energy from virtually an entire hemisphere of Earth at once with high temporal and spatial resolution. Measured spectral radiances will be transformed into data products (e.g., ozone; aerosols; cloud fraction, thickness, optical depth, and height; sulfur dioxide; precipitable water vapor; volcanic ash; and UV irradiance). At present this is only partially possible by combining data from low Earth orbit and geostationary orbit satellites into an asynoptic composite of hundreds of thousands of pixels - rather like assembling an enormous jigsaw puzzle. Another advantage of the deep-space perspective is that, because of the integral view of the planet's hemispheres, the observations will simultaneously overlap the observations of every LEO and GEO satellite in existence, making possible a unique synergy with great potential benefits for the Earth sciences.

Introduction

As early as 1960, [1] proposed L-1, the neutral gravity point between the Earth and the Sun, as an ideal deep space location for Earth and solar observations. DSCOVR will be the first Earth-observing mission to L-1. From this stable vantage point, the satellite will have a continuous view of the entire sunlit face of the rotating Earth 1.5 million km away. Named for the sailor on Columbus's voyage who first spotted the New World, DSCOVR is an exploratory mission to investigate the scientific and technological advantages of L-1 for Earth observation. The L-1 perspective provides a global, all-day view from sunrise to sunset, where daily climatological phenomenon will unfold in clear view of DSCOVR's instrumentation. This allows continuous measurements over large areas for long periods of time – an impossible scenario for Low Earth Orbit (LEO) and Geosynchronous Earth Orbit (GEO) satellites. Hourly variations in the atmosphere will be clearly observed simultaneously from sunrise to sunset [2].

Global climatic studies focus heavily on determining the interaction of incoming solar radiation with clouds and other constituents of the Earth's atmosphere. DSCOVR hosts three scientific instruments that will make a broad set of measurements in this field, some unique to this mission, others collaborative with data from other sources, and some complementary

to previous work. Taken as a whole, this data will make significant advances in completing the "patchwork mosaic" of geographically and time-of-day restricted measurements collected by other observing platforms. The planned retrievals are similar to those possible from LEO and GEO, but with the unique added value of combining high-time resolution and synoptic view (daytime only).

Differences exist between a LEO view of the Earth, requiring 45 minutes (50 min. for AVHRR) to cover ~ 1/14th of the planet, and the DSCOVR synoptic view of the sunlit hemisphere. DSCOVR will build synoptic ozone maps using three spectral channels in less than 1 minute of total exposure time (Figs. 1, 2).

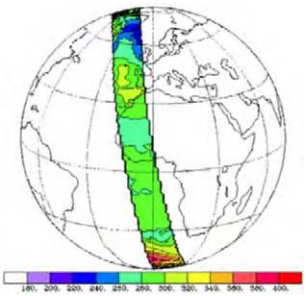

Figure 1. Data around Noon Only (TOMS)
Takes 24 hrs to build a hemisphere map

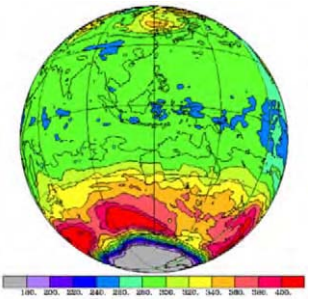

Figure 2. Continuous Data from Sunrise to Sunset
Nearly instantaneous DSCOVR view (less than 1 min.)

DSCOVR will provide a global synoptic (i.e. simultaneous over the entire sunlit face of the globe) view of water vapor, aerosols, column ozone, upper troposphere winds, stratospheric wave structures and circulation, cloud amount and properties, albedos, and aerosols, plus accurate broadband measurements of the Earth's reflected and emitted radiation from 0.2 to 100 μm. This comprehensive and synoptic view of the Earth will enable us to test and develop our understanding of the climate system through the use of Global Climate Models (GCM). Since GCM's are naturally synoptic, DSCOVR will provide the only consistent data sets for use with a GCM. The quantities retrieved from the DSCOVR measurements (data products) will be used to address a variety of scientific problems and generate new applications.

DSCOVR hosts three new instruments: the Scripps-Earth Polychromatic Imaging Camera (EPIC) 10-channel telescope-spectroradiometer, the Scripps-NIST Advanced Radiometer (NISTAR) four-channel radiometer (three absolute cavities plus one photo-diode), and the Goddard Space Flight Center (GSFC) PlasMag solar weather magnetometer, electron spectrometer, and Faraday cup. With this instrumentation, DSCOVR will obtain entirely new observations of the Earth's atmosphere and surface, its radiation balance, and the Earth's space environment. The GSFC SMEX-Lite, a small, highly capable spacecraft, will support the instruments in orbit and provide DSCOVR's maneuvering and data transmission capabilities.

1. Experimental

1.1 Vantage Point

Multispectral imagery and broadband radiometry from a deep space Lagrange-1 orbit (L-1) offer an exciting opportunity to look at the Earth in a bulk thermodynamic sense, particularly as an open system exchanging radiative energy with the Sun and space (See Fig.3.). "The Earth as a planet" astronomers would say, as opposed to the "pixelated" Earth. This is a fundamental scientific goal with very appealing prospects for Earth sciences. The location at L-1 is also ideal to monitor the Sun and study solar weather.

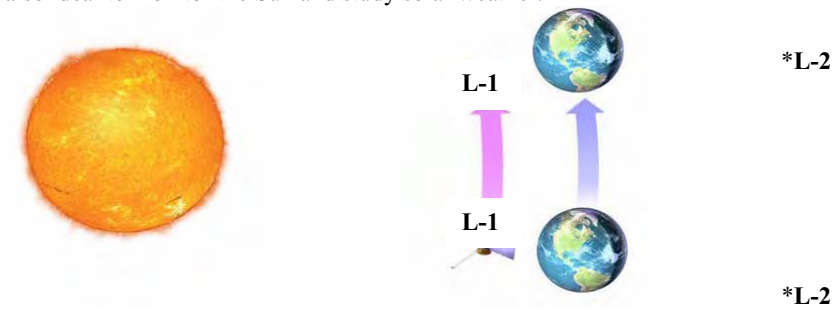

Figure 3. At L-1 and at L-2, the sum of the gravitational fields of the Earth and the Sun results in a net gravitational field equal to that at Earth. Therefore, a spacecraft at L-1 or L-2 must orbit the Sun with the same period as does the Earth.

DSCOVR will have a *continuous (from sunrise to sunset)* and *simultaneous* view of the sunlit face of the Earth as it rotates beneath the spacecraft. This alone gives the DSCOVR observatory a capability never available from any other spacecraft or Earth observing platform in the past. Spectral images and radiometric measurements will obtain important atmospheric environmental data (e.g., ozone, UV-irradiance at the Earth's surface, water vapor, aerosols, cloud height, etc.) and information related to the Earth's energy balance. DSCOVR measurements will have the advantage of synoptic context, high temporal and spatial resolution, and accurate in-flight lunar calibrations. Except for the period immediately after launch, DSCOVR will observe from near the retro-reflection position, thus gaining a unique piece of the Earth's energy-balance data and increased sensitivity to changes on the Earth's surface.

In this document we describe the questions that can be addressed by the DSCOVR data. We also demonstrate the value of deep-space observatories for acquiring important data not available from Earth orbiting spacecraft or surface measurements. A few key points emphasizing the unique features of the spacecraft's L-1 view of the Earth will be presented here.

1.2 Science Payload and Retrieved Quantities

The scientific payload is composed of the following instruments:

Scripps-EPIC is a 10-channel spectroradiometer (ultraviolet, visible, and near infrared) that uses a 30 cm telescope and a state of the art detector array (near infrared, visible, and ultraviolet sensitive 2048x2048 CCD) to achieve high sensitivity and spatial resolution.

EPIC will send back Earth-reflected radiances that will be transformed into data products (e.g., ozone; aerosols; cloud fraction, thickness, optical depth, and height; sulfur dioxide; precipitable water vapor; volcanic ash; and UV irradiance [3-14] every hour for the entire globe at 8-14 km surface resolution. EPIC will provide hourly observations from sunrise to sunset for the entire globe, instead of just once per day (as with TOMS, MODIS, SeaWifs, etc.), and will collect monthly measurements and images of the lunar surface in 10 wavelengths (317.5 to 905 nm) for calibration. General view of Scripps-EPIC on the DSCOVR Spacecraft is presented in Fig.4.

Figure 4. Scripps-EPIC on the DSCOVR Spacecraft.

Scripps-NISTAR (Fig.5) is a greatly improved, advanced technology version of the radiometer systems currently used to monitor total solar irradiance and the radiation reflected and emitted by the Earth. It consists of 4 radiometric channels (3 highly accurate and sensitive self-calibrating absolute cavities and 1 photo-diode) that will continuously measure the total UV, visible, and IR radiances (0.2 to 100 μm) reflected or emitted from the sunlit face of the Earth. DSCOVR's location at the L-1 observing position, rather than in Earth orbit, will permit long integration times, since no scanning will be required. A radiometric accuracy of 0.1% is expected, a 10-fold improvement in accuracy over Earth-orbiting satellite data. These will be the only measurements of the entire Earth's reflected and emitted radiation at the retro-reflection angles. As such, NISTAR will provide important missing data not obtainable by any Earth-orbiting satellite. NISTAR radiances will be used for: *a)* estimating the albedo for the Earth-atmosphere system, *b)* evaluating estimates of the Earth radiation budget (ERB) from other monitoring systems like CERES, *c)* validating the mean

radiance fields that can be directly computed from GCMs, *d)* evaluating the theoretical ratios of near-infrared to total reflectance, which are of intrinsic interest spacecrafto the vegetation, cloud and snow/ice communities, and *e*) attempting to use the thermal infrared as integrative measures of global change.

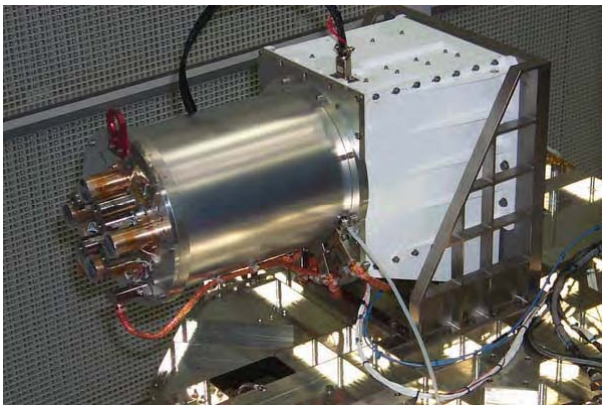

Figure 5. Scripps NISTAR on the DSCOVR. GSFC

PlasMag instrument suite is a comprehensive science and space-weather package that includes a fluxgate vector magnetometer, not present on SOHO, a Faraday Cup solar wind positive ion detector and a top-hat electron electrostatic analyzer (Fig.6) [13,14]. This instrument cluster provides high time resolution measurements in real time and represents the next generation of upstream solar wind monitors intended to provide continuity of measurements started by IMP 8, WIND, SOHO and ACE.

The PlasMag Faraday Cup (Fig.7) will provide very high time resolution (0.5 second) solar wind bulk properties in three dimensions, which coupled with magnetic field data (20 vectors/second), will allow the investigation of solar wind waves and turbulence at unprecedented time resolution. This, in turn, will allow new insights into the basic plasma properties: the process of turbulent cascade and the rate of reconnection. Both topics are critical in understanding the nature of coronal heating.

The electron electrostatic analyzer will allow the continual observation of the 3D-electron distribution function for various solar wind conditions. Special attention will be given to the supra-thermal component or "strahl" that follows the interplanetary field lines very closely and provides the closest link to the formation of the solar wind in the upper corona. It provides a way of identifying large magnetic loops that are still connected at both ends to the solar corona.

Since the departure of WIND from L1, ACE is currently the only satellite providing upstream magnetic field measurements. Since ACE has entered the fifth year of its five-year design life, it is important that DSCOVR be at L-1 before the ACE mission ends, to allow for cross calibration of the solar instruments, to augment solar wind early warning, and to

eventually replace ACE. The DSCOVR PlasMag fluxgate magnetometer will provide crucial continuity of observation of this important interplanetary solar wind parameter. The magnetic field measurements will allow, among other things, the connection of the photospheric magnetic sector structure to 1 AU heliospheric current sheet observations.

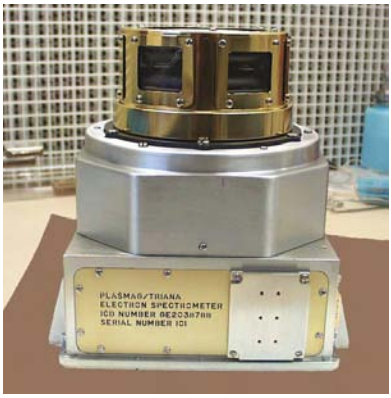

Figure 6. PlasMag Electron Electrostatic Analyzer

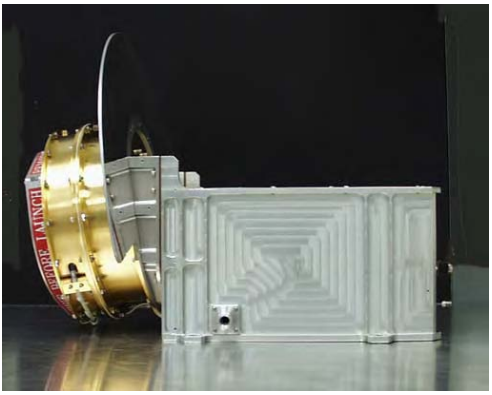

Figure 7. PlasMag Faraday Cup

All DSCOVR PlasMag observations will be part of a coordinated effort, involving multiple satellites, to investigate the large-scale structure of such transients as CMEs/Magnetic Clouds, interplanetary shocks and discontinuities and high-speed stream interfaces. Specifically, the likely operational time period of DSCOVR will enable the PlasMag observations to provide 1 AU measurements connecting the "Living with a Star" solar and heliospheric elements to the geospace components, hence providing a crucial link in the chain of events connecting solar activity to geomagnetic disturbances. The DSCOVR PlasMag data set will also form part of the ISTP database [15-17].

1.3 Data Dissemination

All data from the DSCOVR instruments will be made available to the science team and to the general scientific community within hours after reception at the DSCOVR Science and Operations Center (TSOC), located on the Scripps/UCSD campus. Long-term archive of the Scripps-EPIC and Scripps-NISTAR processed science data will be at the Goddard Distributed Active Archive Center. Raw spacecraft and science data will be archived at the UCSD Supercomputer Center. PlasMag solar weather data will be forwarded within minutes of acquisition to the National Oceanic and Atmospheric Administration (NOAA) for use in generating space weather forecasts and advisories.

2. Science Objectives in Brief

2.1 Earth's Atmosphere and Surface with EPIC

DSCOVR will be the first observatory to determine the daily cycles in total ozone, aerosols, and column water vapor at high temporal and spatial resolution. Ten global spectral images of the sunlit side of the Earth will be acquired within a 5-minute period every hour, providing spatial resolution from 8 km at nadir to 14 km near the Earth's limb.

With DSCOVR, ozone anomalies arising from a variety of sources can be tracked with much improved accuracy, and related to their meteorological environment (see Fig.8). This new knowledge should greatly enhance our basic understanding of ozone processing in the atmosphere and permit more accurate modeling and prediction of ozone variations. The ozone data, in combination with data-assimilation modeling, will significantly improve the study of wave motions, including gravity waves, in the stratosphere. Other dynamical processes, including the polar vortex structure, near-tropopause circulations, and jet stream winds can be observed. Arctic ozone depletion events can also be detected, allowing timely assessment of their ecological threats through enhanced UV radiation. Finally, the hourly DSCOVR ozone, cloud, and aerosol data can be used to compute surface UV irradiance so that exposures and health risks can be more accurately determined.

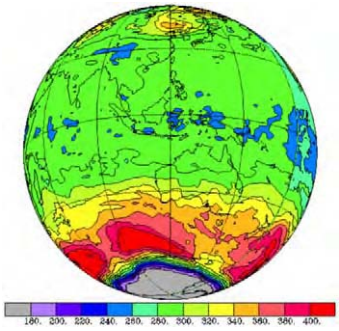

Figure 8. TOMS data was used to simulate this global ozone map (in Dobson units), showing the nearly instantaneous view that will be seen from DSCOVR during the southern hemisphere spring. DSCOVR's orbit around the L1 point will be optimized for seeing southern Polar Regions.
Actual DSCOVR views will have higher spatial and time resolutions and will not be limited to near local noon. A strong gradient of column ozone is seen at the edge of the polar vortex. Variations in column ozone around the vortex are associated with planetary waves.

Aerosols will be monitored hourly using combinations of UV and visible wavelengths. The new combination of wavelengths allows determination of optical depth, single scattering albedo, and particle size. Previous use of visible wavelengths for aerosols was limited to water or forest backgrounds. This new information, provided at high spatial and temporal resolution, will be extremely useful for understanding and modeling the processes that disperse and deplete aerosols, allowing for better assessment and prediction of their chemical, cloud, and radiative impacts. Detection of aerosols in the Arctic Basin, where anthropogenic haze (Arctic Haze) is a significant factor, can permit a more accurate determination of the aerosol impact in this extremely sensitive part of the world. The ability to detect aerosols each hour at high spatial resolution will be exploited to provide timely warnings of volcanic ash events and visibility anomalies (smoke and dust plumes) to the air transportation industry (through the FAA), the US Park Service, and the EPA.

EPIC data will also be used to develop valuable new information about cloud, water vapor, and surface properties. Since LEO and GEO satellites are being used to develop comprehensive climatologies of cloud properties at high spatial and temporal resolution, the unique viewing geometry of EPIC can be exploited in conjunction with these other satellites to determine cloud phase and particle shape. Cloud particle habit (shape) is an assumed parameter in current retrieval methods and in mesoscale models and GCMs. Retrieval of this parameter on a global basis will reduce the uncertainties in cloud and radiation modeling as well as in the retrievals of cloud particle size and ice water path. Reflectance measurements over all Earth surfaces on an hourly basis will be used to derive atmospheric total or precipitable column water vapor, complementing similar estimates from infrared retrievals of upper tropospheric water vapor column. The near retro-reflection geometry of the EPIC view will allow determination of anisotropic reflectance properties of various types of vegetation and to improve characterization of canopy structure and plant condition. Diurnal variations of surface spectral albedo will also be derived to provide more accurate models for radiation calculations in GCMs and other atmospheric models.

DSCOVR is a valuable platform for multi-angle remote sensing because its EPIC images can be collocated with those from any Earth orbiting satellite with close temporal and spatial tolerances. Although only one multi-angle application has been noted, it is expected that the ease of matching EPIC and other satellite data will be an extremely valuable resource for remote sensing and climate modeling, especially in the area of validation. Conversely, other satellite and ground-based measurements taken at sparse temporal or spatial resolution will serve to verify DSCOVR's hourly retrievals.

DSCOVR's use of the "far side" of the Moon as a calibration reference will aid in assessing the calibration of other satellite sensors through matching of co-angled collocated pixels. It is expected that DSCOVR's data will be used to characterize the spectral response of the lunar surface.

The global, high-resolution monitoring of the Earth with EPIC's unique spectral complement will be valuable for scientific field missions. With DSCOVR, phenomena such as aerosol plumes that were only detectable with once-per-day satellite observations can be compared in the field each hour. Mission guidance can be provided for aircraft observations of aerosol plumes or ozone changes. Thus, large-scale context can be characterized more accurately, providing more information to mission planners to allow them to enhance both the efficiency and value of scientific field missions.

2.2 Earth's Radiation and Climate with NISTAR

The thermal infrared radiances measured by NISTAR will provide broadband observations that can serve as a global index of the Earth's climate. The data can be interpreted in terms of the effective emitting temperature of the planet and thus, NISTAR can act as a kind of global thermometer. The observed seasonal and inter-annual variability could be compared with simulated signals from climate models to assess the significance of any observed short or long-term fluctuations.

When combined with the EPIC imagery and retrievals of cloud properties, the NISTAR short-wave radiances will produce estimates of the global albedo. The derived albedo values, or the original radiance data, can serve to evaluate the radiation calculations in global climate models, GCMs. The NISTAR short-wave and long-wave radiances will also be used to estimate errors in the albedos and long-wave fluxes derived from interpolations of

sparsely sampled LEO data, the more conventional technique for measuring the Earth radiation balance.

The NISTAR spectral complement will also provide new data to confirm or negate previous estimates of the ratio of near-infrared (NIR) to visible (VIS) albedos. The NIR/VIS ratios have been used extensively to quantify differences between measured and modeled cloud radiative properties. It will provide a globally integrated test of the episodic but highly time- and space-localized findings of discrepant NIR/VIS cloud albedo ratios [18]

Because the near-infrared channel is sensitive to vegetation and snow/ice cover in addition to clouds, the NIR/VIS ratio is an attractively simple and fundamental analysis tool for studying global change, and DSCOVR has the perfect vantage point to begin using that tool. (No current or planned LEO or GEO Earth radiation budget satellites have a broadband near-infrared channel, although CERES is planning to add one in the post-2003 timeframe, which should serve as a nice complement to that on DSCOVR.)

A modeling infrastructure will be developed based upon existing efforts at NCAR, participating NASA laboratories, and other institutions. This modeling infrastructure will be used to simulate the NISTAR signals and EPIC spectral imagery. Because of DSCOVR's simple viewing geometry and relatively simple data processing requirements compared to LEO satellites, scientists and students will be able to study a wide variety of phenomena without many of the complexities usually associated with remote sensing. Because of the lunar calibration for EPIC and absolute calibration for NISTAR, the scientific community would be able to focus on geophysical applications of a stable, high-accuracy data set. This could have important repercussions both for remote sensing and climate.

2.3 Solar Wind and Space Weather with PlasMag

The three PlasMag instruments (Faraday cup, magnetometer, and electron analyzer) will obtain 3-dimensional measurements of the velocity distribution functions of protons, helium ions, and electrons, and continuous measurements of the interplanetary magnetic field. Because DSCOVR is a fixed orientation spacecraft (not spin stabilized), the PlasMag instruments will remain oriented toward the sun, permitting the solar wind ions and electrons to strike the Faraday cup continuously. Thus, PlasMag will produce data that are easier to interpret, and will be capable of collecting data at higher rates than current solar wind observatories.

The data collected by PlasMag will provide early warning of solar events that may cause damage to power generation, communications, and other satellites. The PlasMag suite of instruments will provide a 1-hour warning to the appropriate agencies that safeguard electrical equipment on Earth and satellites in Earth orbit. Present plans include routinely providing the data to NOAA with typically only a 5-minute data processing delay from detection of an event at the DSCOVR spacecraft position to the time that it is delivered. Monitoring of the solar weather has become a mandatory function of government due to the growth of civilian and military satellite communications. PlasMag will add to, or replace, the first generation space-weather monitors, such as WIND, IMP-8, and ACE. ACE, the most recently launched, is concentrated upon solar wind isotopic composition, rather than particulars of the solar wind flow. As mentioned earlier, but worth stressing, ACE has entered the fifth year of its five-year design life. Thus, PlasMag will provide an essential augmentation and enhancement of present solar wind observations and will eventually be the only satellite between the Earth and the Sun and capable of providing early warning of solar events.

The PlasMag magnetometer, Faraday cup, and an electron spectrometer will analyze the solar wind and the local space environment to derive proton and electron densities, temperatures, and vector bulk velocities, and vector magnetic field data at 1-second resolution. Full 3D electron distribution functions, proton to alpha ratios, and 1msec magnetic field data with power spectrum will be generated. Using PlasMag data, researchers plan to investigate the mechanism by which small-scale fluctuations dissipate in plasmas. Other areas of research that DSCOVR is particularly suited to investigate include magnetic holes, very narrow regions in the interplanetary medium through which magnetic field strength decreases abruptly to nearly zero. Tangential discontinuities, in which the magnetic field has no component normal to the discontinuity surface, will also be investigated, taking advantage of DSCOVR's high-time resolution plasma and magnetometer data. Finally, the high-time resolution plasma and magnetic field instruments onboard DSCOVR will open a window into the inner structures of weak- and slow-interplanetary shocks, which should lead to a better understanding of their formation and dissipation mechanisms.

Correlation of data from the PlasMag with that from other spacecraft near L-1 would allow the detailed study of the non-radial solar wind fluctuations. This study was begun with earlier spacecraft such as the Explorers, IMP, and ISEE, but with DSCOVR, new opportunities would become available. PlasMag solar wind measurements could be correlated with those from other spacecraft at a variety of positions away from L-1, providing multiple baselines. These measurements would help to determine the symmetry of the fluctuations in the wind that in turn determine the way in which energetic particles propagate in the heliosphere. This basic understanding is central to determining how solar events affect the Earth and its near-space environment, and thus is important for determining the effects of solar activity on spacecraft and manned space flights.

3 Conclusions

From its location in deep space, DSCOVR will view the Earth in a different way – as an entire planet rather than a patchwork of regions of interest. It will uniquely acquire synoptic (all regions in the sunlit side seen simultaneously) sunrise to sunset, high time resolution data for most points on Earth using state of the art, highly accurate, in flight calibrated instruments.

DSCOVR will collect information on the climate system combining atmospheric dynamics, cloud physics, aerosols, radiation and surface remote sensing.

Ozone measurements will be used to study upper atmosphere circulation using ozone as a tracer. This is uniquely possible for DSCOVR because it has the necessary synoptic view and temporal and spatial resolutions to allow the description and study of dynamic processes in the upper atmosphere.

Surface ultraviolet exposure estimates will be enhanced by the continuous daylight view; surface remote sensing (including the oceans and vegetation canopies) will be made possible by DSCOVR's location at L-1.

Measurements of solar wind magnetic field and plasma (density, velocity, temperature) will provide data to study turbulence and solar corona heating and the slow solar wind. Solar wind events will be "seen" by DSCOVR approximately 50 minutes before reaching the Earth's magnetosphere— providing enough time to issue warnings to protect sensitive systems (satellites, etc).

Another contribution of DSCOVR will be as a synergistic link between Earth observing satellites by correlating simultaneous multi-satellite observations, by comparing calibrations, and by helping to build a unified Earth Observations network with the Moon as a calibration reference (DSCOVR will have the Moon in plain view).

The DSCOVR views of our world will be used as a teaching tool that will inspire the quest for knowledge, a quest that we will support with public and elementary to higher education outreach, teacher training and research opportunities for undergraduate and graduate students.

DSCOVR may well be the first Deep Space "climate satellite" and has the potential to prove the unique usefulness of deep space observation points such as L-1 or L-2, for Earth Sciences.

References

[1] Farquhar R.W. "The flight of ISEE-3/1CE: Origins, mission history, and a legacy", *J. Astronautical Sciences*, 2001, vol. 49 (1), pp. 23-73.
[2] National Academy of Sciences (USA), Space Studies Board Annual report 2000, Chapter 4, pp.93-108.
[3] Saunders, R. W. and Kriebel, K. T., "An improved method for detecting clear sky and cloudy radiances from AVHRR data", *International Journal of Remote Sensing*, 1988, vol. 9, pp.123-150.
[4] Wylie, D. P. and W. P. Menzel, "Two Years of Global Cirrus Cloud Statistics using VAS", *Journal of Climate,* 1989, vol. 2, pp.380-392.
[5] Gao, B.C., Goetz, A.F.H., and W.J. Wiscombe, "Cirrus cloud detection from Airborne Imaging Spectrometer Data using the 1.38 micron water vapor band", *J. Geophys. Ltr.,1993,* vol. *20*, pp. 301-304.
[6] Ou. S. C., Liou, K. N., Gooch, W. M., and Y. Takano, "Remote sensing of cirrus cloud parameters using AVHRR 3.7 and 10.9 mm channels", *Applied Optics,* 1993, vol. 32, pp.2171-2180.
[7] Wylie, D. P., Menzel, W. P., Woolf, H. M., and K. I. Strabala, "Four Years of Global Cirrus Statistics using HIRS", *Journal of Climate*, 1994, vol. 7, pp.1972-1986.
[8] Menzel, P. and K. Strabala, "Cloud Top Properties and Cloud Phase Algorithm Theoretical Basis Document", NASA MODIS Program, 1997.
[9] Wilheit, T. T. and K. D. Hutchison, "Water Vapor Profile Retrievals using Passive Microwave Data Constrained by Infrared-Based Cloud Information", *International Journal of Remote Sensing*, 1997, vol. 18, pp.3263-3278
[10] Wilheit, T. T. and K. D. Hutchison, "Cloud Base Height Retrieval from DMSP Microwave Data and a priori Cloud Top Temperatures", in.: *Proceedings of 9th AMS Conference on Satellite Meteorology and Oceanography,* 1998, pp 244-245.
[11] Watzin J. "Observations from over a decade of experience in developing faster, better, cheaper missions for the NASA Small Explorer Program", *Acta Astronautica,* 2001, vol. 48 (5-12), pp.853-858,
[12] Krotkov N, Herman J, Bhartia PK, et al., "Version 2 total ozone mapping spectrometer ultraviolet algorithm: problems and enhancements", *Optical Engineering,* 2002, vol. 41 (12), pp. 3028-3039.
[13] Aellig MR, Lazarus AJ, Kasper JC, et al., "Rapid measurements of solar wind ions with the Triana PlasMag Faraday Cup", *Astrophysics and Space Science*, 2001, vol. 277 (1-2), pp. 305-307.
[14] Halem M, Kouatchou J, Norris P, et al. "Cloud field assimilation using simulated Triana satellite-data", *Advances in Space research,* 2002, vol. 30 (11), pp. 2447-2454.
[15] Coakley J. A., and F. P. Bretherton, "Cloud cover from high-resolution scanner data: detecting and allowing for partially filled fields of view", *J. Geophy. Res.,* 1982, vol. 87, pp.4917-4932.
[16] Baran, A. J., Watts, P. D., and P. N. Francis, "Retrieval of Cirrus Microphysical and Bulk Properties using Radiance Data from the Along Track Scanning Radiometer (ASTR-2) ", in: *Proceedings of 9th AMS Conference on Satellite Meteorology and Oceanography*, 1998, pp 218-221.
[17] Chepfer H, Minnis P, Young D, et al., "Estimation of cirrus cloud effective ice crystal shapes using visible reflectances from dual-satellite measurements", *J. Geophys. Res.* 2002, vol. 107 (D23), Art. No. 4730.
[18] Valero F.P.J. "Triana provides flexibility", *Aviation week and Space technology,* 2002, vol. 156 (23), p. 6.

Cell Biology and Instrumentation: UV Radiation, Nitric Oxide and Cell Death in Plants
Y. Blume et al. (Eds.)
IOS Press, 2006

Retrieval of the Transmitted UV Irradiance from Reflected Data

I.N. Melnikova
Research Center for Ecological Safety, Russian Academy of Science
Korpusnaya Str., 18, 197110, St.Petersburg, Russia

Abstract. The main consequence of the ozone depletion, which is apparent over much of the globe several yeas ago, is the increase of the biologically damaging UV irradiance at the ground level. Data for the airborne spectral observations of upward irradiance at the upper level (~5 km) and downward irradiance at the down level (~500m) are compared for finding the empirical dependence between them. Radiation experiments aver different surfaces (sand, water, snow) and in different conditions (clear or cloudy sky) are considered

Introduction

In the previous publications it was shown that the UV irradiance is also affected by aerosols and the effects of bulk values of ozone and aerosol on the downward and upward radiances were compared [1,2,3,4]. Since the biologically damaging UV irradiance could be expected to increase in the future [5,6], efforts have been made to create a global network of UV monitoring. Because the UV irradiances have to be registered with high accuracy, spectral measurements of UV are expensive and tedious and therefore are restricted to a few locations. Direct calculations of the radiative transfer [7] can provide UV levels for the locations where measurements are not available, but the question of how exact the UV irradiances can be delivered by model calculations, having been discussed in a number of papers, is still open [1,8]. The retrieval of optical properties of the atmosphere from reflected data of UV and following calculation transmitted irradiance near surface with radiative transfer methods [9,10]. Certainly this way is complicated and results are ambiguous.

The aim of this study is, being out of frames of model calculations, to assess the possibility of solving the problem of retrieval the UV ground levels with the use of UV radiances measured at the top of the atmosphere by satellites. Here we are not interesting in the optical properties of the atmosphere. It seems to be reasonable for the approximate estimation of ground UV irradiance because both the reflected and transmitted irradiance form the same atmospheric column and incident solar flux. The set of airborne radiative observations presented in the book [11], is used here for finding the empirical links between the reflected and transmitted irradiance.

1. Observational data

Airborne observations of spectral solar radiances and irradiances have been accomplished during 1983-1985 with using the measuring complex of the instruments [12]. The measuring part of the complex was provided with K-3 spectrometer [13]. It was a diffractive-mirror

spectrometer with the grating of 600 lines per mm as a dispersing element. The operating spectral range of the instrument was 330–978 nm. Only the spectral interval 330-470 nm is considered here. Details of data processing and uncertainty estimation are presented in the book [11]. The Table 1 presents data of 22 experiments in the clear sky and 10 experiments in cloudy sky conditions, which are used here. Flights were accomplished above the Kara-Kum Desert with the sand surface (11 experiments), above the Ladoga Lake with the water surface (7 experiments), and above the Ladoga Lake with the snow surface (4 experiments) in the clear atmosphere. We also consider here the observations in the case of the overcast cloudiness over different surfaces, which were accomplished during 1970th.

It is safe to suppose that the transmitted and reflected irradiances are formed not only by solar incident flux and atmospheric properties but also by surface albedo. To illustrate the spectral dependence of the surface albedo, we consider empirical approximation of this dependence for sand, water, and snow. The examples of the surface albedo spectral dependence are presented in Fig. 1 for sand and water surface. Results of all mentioned experiments are included. It is clear that the power-series fit for the spectral albedo leads to expression for the sand surface:

$$A(\lambda) = -1.3\lambda^2 + 2.2\lambda - 0.5 \quad ,$$

and in the case of the water surface – the expression with the inverse signs:

$$A(\lambda) = 0.3\lambda^2 - 0.5\lambda + 0.2 \quad .$$

The surface albedo for fresh snow demonstrates no spectral variations and the value is about: $A(\lambda)$ =const=0.95. Nevertheless if the snow and ice intermingle with water, the surface albedo perceives certain features specific for the water surface but with linear spectral dependence. In cloudy conditions all the features of the albedo spectral dependence preserve.

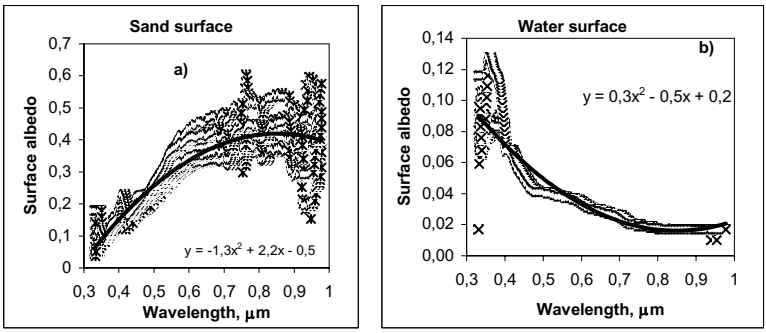

Figure 1. Spectral dependence of the surface albedo a) – for sand surface and b) – for water surface.

Fig 2 illustrates the relation between transmitted and reflected irradiances $F^{\downarrow}=rF^{\uparrow}$ for two experiments. Points in the figure correspond to one spectral series in UV-ranges. It should be emphasized that for the experiments above the snow surface and in a cloudy atmosphere the unique coefficient r within 330-970 nm spectral ranges is revealed. It should be noted that there is no linear relation between the reflected and transmitted irradiance in

relative units of the incident solar flux. That is to say that solar flux governs both the transmitted and reflected irradiance mostly.

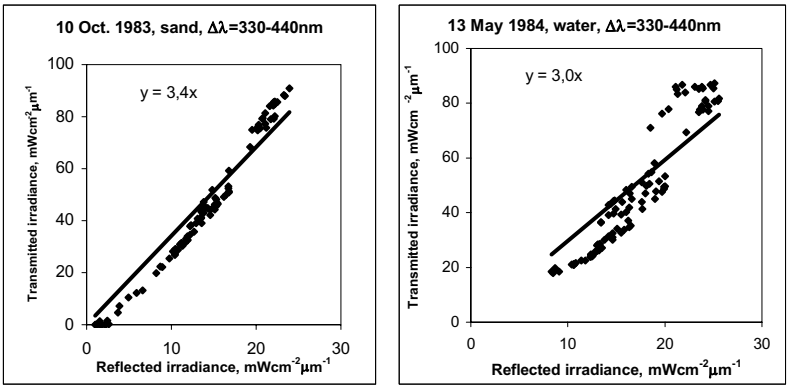

Figure 2. Relations between the reflected and transmitted irradiance in the cases of the sand and water surface derived from the observational data of UV spectral range

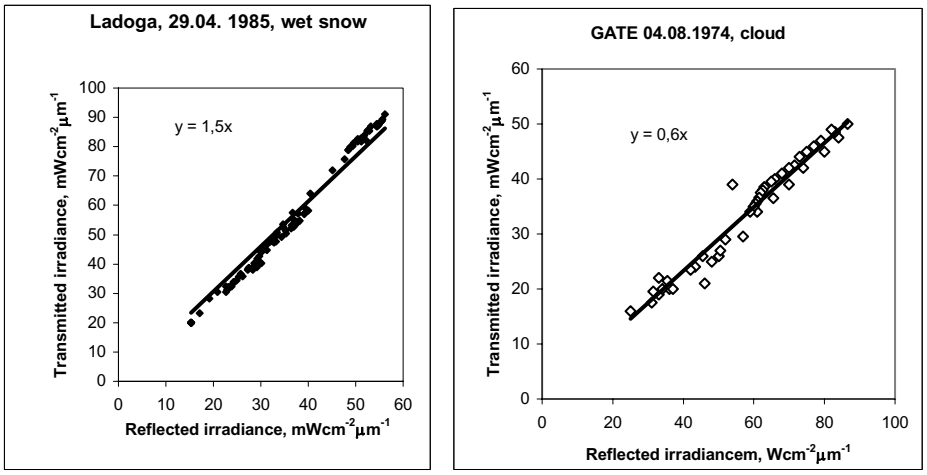

Figure 3. Relations between the reflected and transmitted irradiance in the cases of the snow surface and in cloudy atmosphere delivered from the observation data of 330-970 nm spectral range

The result of averaging is shown in Fig 3 for sand, water, and snow surfaces and for the cloudy condition. It is clear that the relation $F^{\downarrow}=3.4F^{\uparrow}$ can be accepted for both sand and water surfaces in the UV ranges. In intermediate cases of surface reflection is thought the same relation to occur. In the case of snow surface the relation can be estimated as $F^{\downarrow}=1.5F^{\uparrow}$.

In the cloudy condition the kind of the surface is not significant also. The relation between the reflected and transmitted irradiances looks as $F^{\downarrow}=0.5F^{\uparrow}$. If the UV danger at the ground level is considered it will be more correct to accept the maximal values of the

Sand surface, The Kara-Kum Desert				
Date	Surface albedo	r	θ_0, grad	$\mu_0=\cos\theta_0$
09.10.83	$-1.4\lambda^2+2.5\lambda-0.6$	3.1	51	0.629
10.10.83	$-0.9\lambda^2+1.8\lambda-0.5$	3.4	51	0.629
11.10.83	$-0.8\lambda^2+1.9\lambda-0.4$	3.1	51	0.629
12.10.83	$-1.4\lambda^2+2.5\lambda-0.6$	2.5	51	0.629
13.10.83	$-0.9\lambda^2+1.8\lambda-0.4$	2.8	51	0.629
14.10.83	$-1.1\lambda^2+2.1\lambda-0.5$	3.0	51	0.629
16.10.83	$-1.2\lambda^2+2.4\lambda-0.6$	2.8	51	0.629
19.10.84	$-1.6\lambda^2+2.5\lambda-0.6$	2.2	51	0.629
23.10.84	$-1.3\lambda^2+2.0\lambda-0.4$	2.3	51	0.629
24.10.84	$-2.0\lambda^2+2.9\lambda-0.7$	2.1	51	0.629
26.10.84	$-1.8\lambda^2+2.8\lambda-0.7$	2.6	51	0.629
Average value	$-1.3\lambda^2+2.2\lambda-0.6$	2.7		
Maximum value	$-0.9\lambda^2+1.8\lambda-0.5$	3.4	51	0.629
Water surface, The Ladoga Lake				
13.05.84	$0.2\lambda^2-0.4\lambda+0.2$	3.0	43	0.731
14.05.84	$0.3\lambda^2-0.5\lambda+0.2$	3.0	43	0.731
15.05.84	$0.3\lambda^2-0.5\lambda+0.2$	2.7	43	0.731
16.05.84	$0.2\lambda^2-0.3\lambda+0.2$	3.5	43	0.731
17.05.84	$0.3\lambda^2-0.4\lambda+0.2$	2.1	43	0.731
18.05.84	$0.5\lambda^2-0.7\lambda+0.3$	1.9	42	0.743
30.09.72	$0.01\lambda^2-0.1\lambda+0.1$	3.1	74	0.276
Average value	$0.3\lambda^2-0.5\lambda+0.2$	2.7		
Maximum value	$0.2\lambda^2-0.3\lambda+0.2$	3.5	43	0.731
Snow surface, The Ladoga Lake				
26.03.84	0.95	0.9	59	0.515
14.04.85	0.95	0.6	55	0.574
28.04.85	$-0.4\lambda+0.85$ (wet snow)	1.4	48	0.669
29.04.85	$-0.3\lambda+0.65$ (wet snow)	1.5	48	0.669
Average value	0.9	1.2		
Maximal value	0.95	1.5	48	0.669
Overcast cloudiness				
24.09.72	$1.8\lambda^2-1.9\lambda+0.8$ water	0.2	64	0.440
10.04.71	$0.2\lambda^2-0.3\lambda+0.2$ water	0.6	35	0.819
05.10.72	$0.1\lambda^2-0.2\lambda+0.1$ water	0.3	52	0.616
05.12.72	$-0.1\lambda^2+0.3\lambda$ ground	0.4	64	0.438
12.07.74	$0.4\lambda^2-0.6\lambda+0.3$ water	0.4	16	0.961
04.08.74	$0.2\lambda^2-0.3\lambda+0.2$ water	0.6	17	0.956
01.10.72	$0.007\lambda+0.35$ ice+water	0.6	74	0.276
29.05.76	0.8 snow	0.5	61	0.483
30.05.76	$-0.1\lambda+0.1$ ice+water	0.8	61	0.483
20.04.85	$-0.5\lambda+0.9$ wet snow	1.0	50	0.647
Average value		0.5		
Maximal value		1.0	50	0.647

Table 1. Radiative airborne experiments

coefficient r= 3.5 for the sand and water surfaces, 1.5 for the snow surface, and 0.6 for the cloudy atmosphere according to Table 1.

2. Conclusion

The estimation of the transmitted irradiance from observed reflected values is of most practical interest while employing UV-irradiance at the ground level. It is appropriate to estimate only the link between transmitted and reflected irradiances with disregarding properties of the atmosphere. The very simple relation is revealed for different surfaces and atmospheric conditions. The relation between transmitted and reflected irradiances is proportional with the coefficient close to k=2.0 in the clear atmosphere, to k=3.0 in the dusty atmosphere, to k=0.5 in the cloudy atmosphere over a water surface, and to k=1.0 in the cloudy atmosphere. Certainly it is not a strict calculation but a practical estimation allowing a real-time processing.

References

[1] Varotsos C., "The southern hemisphere ozone hole split in 2002". *Environmental Science and Pollution Research*, vol. 9, p.p. 375-376, 2002.
[2] Varotsos C., "What is the Lesson from the Unprecedented Event over Antarctica in 2002?" *Environmental Science & Pollution Research*, vol. 10, p.p. 80-81, 2003.
[3] Stamnes K., S.C.Tsay, W. Wiscombe, and K. Jayaweera, "Numerically stable algorithm for discrete ordinate method radiative transfer in multiple scattering emitting layered media", *Appl.Opt.,* vol. 27, p.p. 2502-2509, 1988.
[4] Zeng J., R.McKenzie, K.Stamnes, M.Wineland and J.Rosen, "Measured UV spectra compared with discrete ordinate method simulations". *J.Geoph.Res.,* vol. 99, p.p. No. D11, 23019-23030, 1994.
[5] Kondratyev K.Ya. and C. Varotsos, "Atmospheric Ozone Variability, "Implications for Climate Change, Human Health and Ecosystems", Springer-Praxis, Chichester, UK, 2000.
[6] Varotsos C., "Solar ultraviolet-radiation and total ozone, as derived from satellite and ground-based instrumentation". *Geophysical Research Letters*, vol. 21, p.p. 1787-1790, 1994.
[7] Forster P.M. de F., K.P. Shine, and A.R. Webb, "Modeling ultraviolet radiation at the Earth's surface. Part II, p.p. Model and instrument comparison". *J.Appl.Meteorol,* vol. 34, p.p. 2426-2439, 1995.
[8] Schwander H., P. Koepke and A. Ruggaber, "Uncertainties in modeled UV irradiances due to limited accuracy and availability of input data". *J.Geoph.Res.,* vol. 102, p.p. No. D8, 9419-9429, 1997.
[9] Pinker R.T. and I. Laszlo, "On the coupling of satellite algorithms with ground truth". *J. Atmos. Ocean Techn*., vol. 8, p.p. 96-107, 1991.
[10] Pinker R.T. and I. Laszlo, "Modelling surface solar irradiance for satellite applications on a global scale". *J. Appl. Meteor.*, vol. 31, p.p. 194-211, 1992.
[11] Melnikova I. and A. Vasilyev, "Short-wave solar radiation in the Earth atmosphere. Calculation. Observation. Interpretation.", Springer-Verlag GmbH&Co.KG, Heidelberg, 2004.
[12] Vasilyev O.B., Grishechkin V.S., Kovalenko A.P. et al., "Spectral information – measuring system for airborne and ground study of the shortwave radiation field in the atmosphere" (in Russian). In, p.p. Complex remote lakes monitoring. Leningrad, Nauka, p.p. 225–228, 1987.
[13] Mikhailov V.V. and V.P. Voytov, "An improved model of universal spectrometer for investigation of short-wave radiation field in the atmosphere" (in Russian). In, p.p. *Problems of Atmospheric Physics.* Leningrad University Press, Leningrad, vol. 6, p.p. 175–181, 1969.

Cell Biology and Instrumentation: UV Radiation, Nitric Oxide and Cell Death in Plants
Y. Blume et al. (Eds.)
IOS Press, 2006

Solar UV as Environmental Factor: Measurements and Model

Claudio RAFANELLI, Andrea ANAV, Ivo DI MENNO, Massimo DI MENNO
C. N. R. - Institute of Atmospheric Sciences and Climate - Section of Rome
Via del Fosso del Cavaliere, 100, Rome, Italy

Abstract. The solar UV radiation flux reaching the Earth is one of important factors to evaluate the planetary energy balance. The UV flux (200 – 400 nm) at the top of atmosphere is about 8% of the total flux from the Sun. But the amount of UV measured at ground level is lower, this because the UV, crossing the atmosphere, undergoes both strong spectral absorption and diffusion. The spectral part 200 – 280 is practically negligible at ground.
The normal irradiance, and the radiation on a horizontal surface, as global spectral irradiance is expressed by vertical component of direct radiation and the diffused one. They are obtained by instruments calibrated in physical units, or evaluated by models.
The work shows the problems linked to a correct understanding and interpretation of solar UV data sampled at ground, several practical and theoretical problems of measurement are shown. In particular, the comparison among different sites or instruments is analyzed, and the effects due to O_3 level, albedo and cloudiness are discerned. The impact of clouds and their position respect to the Sun on the observation carried out both by spectral and broad-band instruments are also examined by models.

Introduction

The UV flux (200 – 400 nm) at the top of atmosphere is about 8% of the total flux from the Sun [1]. But the amount of UV measured at ground level is lower, this because the UV undergoes both strong spectral absorption and diffusion crossing the atmosphere. The spectral part 200 – 280 nm is practically negligible at ground [2]. Then, the right evaluation of the irradiance at ground is the base for every application in environmental field. For this reason the measurement of irradiance in the open needs some close examination due to inherent nature of phenomena.

The effects of the environmental factors existing, in the same places but in different seasons or between different places, during the time of measure and the instrumental characteristics can modify the results and to have consequences on the comparison of data. So, the information about environmental conditions and instrumental characteristics must be part of the radiometric datum [3].

The well known large classes of spectral or broad-band equipments to measure irradiance or effective irradiance (the irradiance weighed by an action spectrum) has individual specifications, and it is necessary to know several information and to follow some rules to be sure of compare the resulting data in right way.

Besides, a relative new third class of instruments is in the middle of the previous classes. The multi-channel radiometers are instruments having several filters (generally 4 or 7) with wide, semi-large or narrow pass-band windows to divide the spectrum in parts [4]. By analytical models they evaluate the irradiance or other atmospheric parameters, like

the ozone content, in very fast way and cheaply [5,6]. For these instruments it is necessary pay attention to the precision of each band-pass filters and to reliability of retrieval models [7]. But the calibration is essential for all 3 classes, especially for measurements in cloudy conditions [8].

The work shows the problems linked to a correct understanding and interpretation of solar UV data sampled at ground, several practical and theoretical problems of measurement are shown too. In particular, the comparison between different sites or instruments is analyzed, and the effects due to O_3 level, albedo and cloudiness are discerned. The impact of clouds and their position respect to the Sun on the observation carried out both by spectral and broad-band instruments are also examined by models.

1. Measurements

The intercomparison of the results of measuring campaigns is based on the statement that the physical quantities obtained by instruments are right. But for the solar UV measurements this declaration is applicable only if beside the instrumental data other information are known. The environmental factors play a fundamental role on the right reconstruction of the physical datum in a place.

In this paper, among environmental factors, the effects due to a correct positioning, with clear horizon (sky-line), and those linked to the geographical position (latitude, longitude and altitude) are assumed as well-known [9]. The solar radiation data needs also of time reference, and UTC is the most common.

As known, the physical principle on which the solar instruments are based, to measure the normal irradiance, is the conversion of photons in electrical signals proportional to the solar flux. To select the UV band, a set of filters, realizing the pass-band filters, is inserted into the optical path. Of course these filters have some characteristics: central wavelength, shape of the band and band-width. Due to the manufacturing process the characteristics are specific for each piece. Different manufacturers can produce instruments having nominally in the same UV band, different windowing [10]. As known wavelengths on the right part of the solar spectrum has a very large amount of irradiance then the comparison between radiometers having different band-width or different shape of the window, are incorrect if not recomputed for the same band width and this is not always known or possible. For a correct comparison of data and to avoid the above disadvantage the use of the same class of instrument produced by the same manufacturer is recommended [11, 12].

The calibration theory is based on the statement that the electric signal output is proportional to integral of the flux into the characteristic band of the instrument. So, in the world, the calibration set up is performed in clear sky condition. That is in a sky situation of isotropy for scattering, but any information does not given about aerosol optical dept, ozone content etc. during the test. The presence of the various aerosol amount and different aerosol size distribution can modify the relative irradiance between wavelengths, especially at different solar zenith angle (SZA), Fig. 1. The ozone content modifies the irradiance increasing the available environmental dose, Fig. 2. So, having modified the integral of the flux, the calibration constants obtained during the calibration set up produce, for a broad-band or multi-channel instrument, different outputs when used in different atmospheric conditions.

For a right evaluation of irradiance should be necessary perform long campaign of measurement with different atmospheric conditions and recalibrate the instrument for each situation [13]. Of course this is a technique applicable in an observatory or in a network. Impossible for short campaign, so this possible effect must bear in mind.

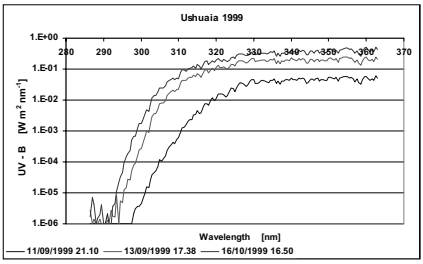

Figure 1. 1- UV–B spectra in Ushuaia (Argentina) during APE GAIA project
SZA : 82.5° (Sep. 11); 60.3 (Sep. 13); 46.3 (Oct. 16)

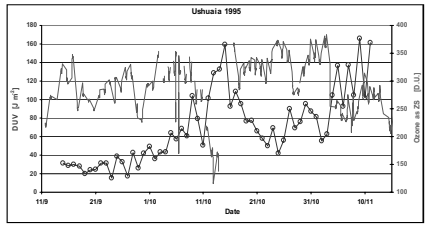

Figure 2. - Ushuaia (Argentina) during ozone hole season. Daily DUV trend (circle) and Ozone total content (solid line, as ZS) by Brewer spectrophotometer

But the most important reason of wrong comparison in the radiometric campaign is the presence of clouds in the sky. Those, with their different types, presence of ice or snow inside, height and more important with their position referred to the Sun modify in very strong way the irradiance at ground, Fig. 3. In general they behave like a grey filter, so the cloudy conditions are very important information of the radiometric datum. Actually to take pictures of sky automatic equipments based on digital cameras are developing. In Fig. 4 a-b, a picture and the software result of a Total-sky Camera (TSC) developed by the author are shown [14]. Where these facilities are not available some analytical techniques can be applied to evaluate the cloudiness [15], and in some cases the kind of the clouds [16], can be used [17].

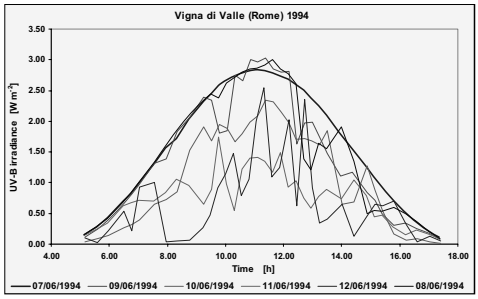

Figure 3. - Dose rate trends in clear sky day, 07 June, and with various levels of cloudiness (by Brewer spectrophotometer)

Of course with these models there are some uncertain attribution (20 % about) of covering and type. Moreover it is not possible define the relative position to the Sun. This is important because some time, the relative irradiance between wavelengths is modified, Fig. 5 a-b and Fig. 6, then the integral into the filter band is modified respect to the calibration values.

To avoid all these problems linked to the calibration, only instruments with very narrow band, < 2 nm, are useful, i.e. spectroradiometers or narrow-band multi-channel radiometers [4,18]. In this case it is possible to assume negligible any variation of irradiance respect to the calibration, inside the band window.

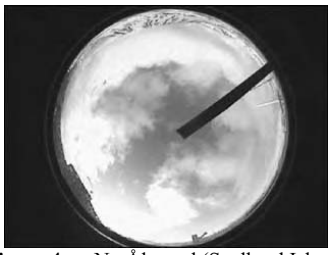

Figure 4a. - Ny Ålesund (Svalbard Island, Norway). June 14, 2002 21:30 UTC
Image of the sky by the TSC automatic camera

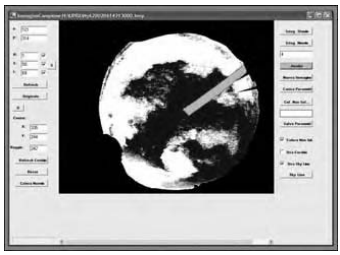

Figure 4b - Screen capture of the TSC software output.
Evaluated 4 octas.

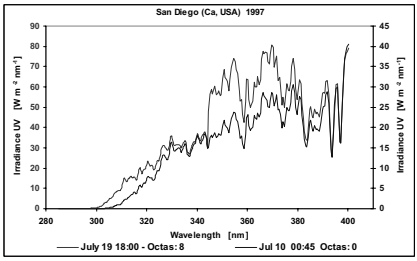

Figure 5a. - Comparison of spectral irradiance UV (285 – 400 nm) sampled by SUV 100 spectroradiometer

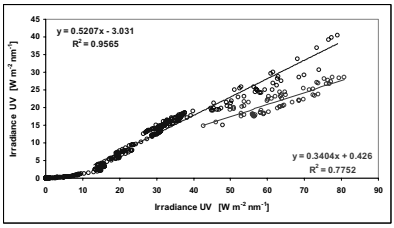

Figure 5b. - Scatter plot of same data of 5a.
In evidence the interval 345-375 nm

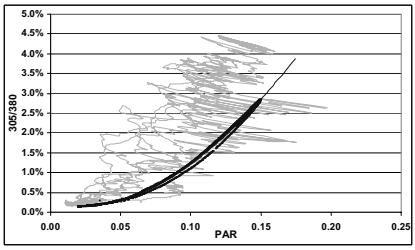

Figure 6. - The 305/380 ratio vs. PAR [µE sec-1] by GUV multichannel radiometer in TNB (Antarctica). The blue line is the path in a blue sky period. The pink dots are the ratios during cloudy days.
Regression curve:
y = -1.67 x3 + 1.95 x2 - 0.080 x + 0.0023; r2 = 0.997

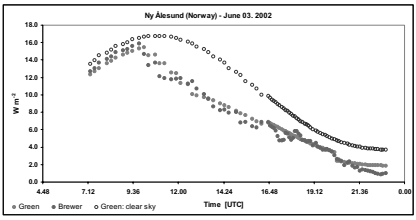

Figure 7. - Comparison between Green model (evaluating CF by TSC pictures) and Brewer spectrophotometer dose rate.
Scatter plot parameters:
y = 1.0249x - 0.4085 - R2 = 0.9818
In black the Green model with CF = 0

2. **Models**

2.1 Theoretical bases

The irradiance of a single wavelength, I_λ, of the global spectral irradiance on a horizontal surface is expressed by [19]:

$$I_\lambda = D_\lambda + d_\lambda \quad (1)$$

Where $\underline{D}$ is the irradiance of direct radiation and $\underline{d}$ is the diffused one. The first term of the (1) is the Lambert and Beer law:

$$D_\lambda = D_\lambda^* \, e^{(-k_\lambda m)} \cos\theta \quad (2)$$

where $k_\lambda m = \Sigma_i (k_{\lambda i} m_i)$ is the total optical extinction (function both of the optical mass m_i and the attenuation coefficient $k_{\lambda i}$ of each atmospheric component), θ is the solar zenith angle (SZA); D_λ^* is the extraterrestrial irradiance. For short period this can be considered as constant, but for a right evaluation of the (2) it is necessary an update due to Earth relative position and solar activity [2]. While the diffuse radiation is explained by:

$$d_\lambda = (d_{r\lambda} + d_{a\lambda}) \bullet (1-\rho_\lambda)\text{-}1 + d_{n\lambda} [(\rho_\lambda)/(1-\rho_\lambda)] \cos\theta \quad (3)$$

where $d_{r\lambda}$ is the Rayleigh scattering radiation; $d_{a\lambda}$ is the radiation diffused by the aerosols; $\rho_\lambda = \rho_{r\lambda} \bullet \rho'_{a\lambda}$ is the reflectance due both to Rayleigh, $\rho_{r\lambda}$, and to aerosol, $\rho'_{a\lambda}$; and $d_{n\lambda}$ is the irradiance due to multiple reflections produced by the albedo. The coefficients $\underline{\rho}$ and $\underline{k}$ are set assuming isotropic conditions and blue sky. Each addend of (1), sampling separately the direct and diffuse radiation at ground, add up 50% to the total irradiance. So, only good knowledge of the atmospheric effects produced by each term of (3) allows a good reconstruction of the spectrum at ground.

2.2 Spectral radiative transfer models

Many spectral radiative transfer models are available, for instance LOTRAN (release LOTRAN-7), STAR, TUV, etc. But each of them needs information about some parameters. The most important are: aerosols characteristics, air density profile, air humidity, air temperature profile, clouds situation, nitrogen dioxide profile, ozone vertical profile, sulphur dioxide profile and surface albedo. This information normally is not available in the place of measurement. So are replaced with climatological data, not always representative of the real situation. Among them, the presence of clouds modifies the isotropic condition of the sky, the base of scattering theory. So it is necessary to implement an algorithm to evaluate the effects on irradiance of cloud's coverage. In general, a simple factor (CF) is inserted in the models. It acts as a grey filter attenuating the irradiance in proportion to the coverage (in octas, or tents). This procedure, of course, provides for the same attenuation in each wavelength and do not take account of differential absorption due to presence of water as droplets, snow or ice, inside the cloud, Fig. 6. Additionally, the clouds are considered as total coverage and it is no possible to define the height or type of clouds; moreover the position related to the Sun is not supplied too.

To avoid these effects it is necessary to substitute the CF with a function having parameterized the whole sky situation. The problem is under study [20,21]. In an Arctic campaign, 2002, a long series of cloudiness was monitored. In Fig. 7 the output of a model, the Green model [22], depicts the good correlation with the irradiance by a

spectroradiometer Brewer, using the appropriate CF existing during the measure and evaluated by the TSC software. The relative position to the Sun is just under study by the authors.

2.3 Models for multichannel radiometers

The multichannel radiometers, as told above, allow to evaluate some atmospheric constituent as total ozone content or aerosol optical depth. This is obtained applying best fit models for the irradiance values measured by each filter. Of course some ancillary information or preliminary mini-campaign for tuning the model are a necessary consequence [6]. The results are good as much as the ancillary information are representative of the real situation during the measurement.

A new model to obtain irradiance dose rate is the WL4UV [5]. It evaluates the irradiance into the range 280 - 400 nm having 2% of accuracy. This is useful for every environmental studies or biological impact analysis of the UV [23].

It computes the dose rate evaluating the straight line crossing spectral irradiance at each filter of radiometer and integrating into the UV range. It does not need any ancillary information; and the model is useful also to evaluate the effective dose rate applying a proper effective spectrum. Of course the results are good as much as the filters are narrow band filters.

3. Conclusions

The solar irradiance monitoring and more the inter-seasonal comparison or studies between sites far each other need attentions due to inherent nature of the involved phenomena. The radiometric data require ancillary information; without them the use is restricted or invalidated. Consequently, the irradiance is a cluster of data, easily managed by computer. Particular attention must be placed with radiometric sampling during cloudy day, because the instrumental response could be not representative. Therefore, the manager of radiometric instruments cannot be a simple operator but he would be skilled on instrumental characteristics and involved in the physics of the phenomena. Consequently, the operator must be rightly trained and inserted at right level in a working staff.

Acknowledgements
The authors thank the NATO-ARW for inviting. They thank also the PNRA, the Italian Antarctic Program, for funding the researches and the activities. Last but not the least they thanks all Argentinean staff to manage the PNRA instruments in Antarctica. UV data of SUV 100 from San Diego, Ca - USA, was provided by the NSF UV Monitoring Network, operated by Biospherical Instruments Inc. under a contract from the United States National Science Foundation's Office of Polar Programs via Raytheon Polar Services Company.

References

[1] Badosa J. and van Weele M., “Effects of aerosols on UV-index”. KNMI Sci. Report, 2002, WR 2002-07.
[2] Zerefos C.S., K. Toutpali, B.R. Bojkov, D.S. Balis, B. Rognerund and S.A. Isaksen, “Solar activity-total column ozone relationships, Observations and model studied with heterogeneous chemistry”. *J. Geoph. Res.*, 12 D1, p.p. 1561-1559, 1997.
[3] Rafanelli C., “Effects on environmental factors on solar UV measurements”. *Radiation Protection Dosimetry*, vol. 97 n° 4, p.p. 423-428, 2001.

[4] Petkov B., V. Vitale, C. Tomasi, S. Scaglione, D. Flori, R. Santaguida, "Ultraviolet radiometer for measuring the global UV solar radiation reaching the earth surface". *Proc. National Meeting on PNRA Technology*, 14÷16 May, Frascati (Roma), Italy, 2003.

[5] Anav A., C. Rafanelli, I. Di Menno and M. Di Menno, "An algorithm to evaluate solar irradiance and effective dose rates using spectral UV irradiance at four selected wavelengths". *Radiation Protection Dosimetry*, vol. 111 n° 3, p.p. 239-250, 2004.

[6] Dalhback A., "Measurements of biologically effective UV doses, total ozone abundances, and cloud effects with multichannel, moderate bandwidth filter". *Applied optics*, vol. 35, n°33, p.p. 6514-6521, 1996.

[7] Di Menno, M.L. Moriconi, M. Di Menno, G.R. Casaleand and A.M. Siani, "Spectral ultraviolet measurements by a multichannel monitor and a Brewer spectrophotometer, a field study". *Radiation Protection Dosimetry*, vol. 102 n°3, p.p. 259-263, 2002.

[8] Rafanelli C., A. Anav, L. Ciattaglia, I. Di Menno, M. Di Menno, R. Iturraspe, J. Araujo, H. Ochoaand and H. Rodriguez, "The cloud effects on UV irradiance modeled in Antarctica - 5",° *Simposio Argentino y I° Latinoamericano sobre Investigaciones Antarticas.* 2004, Aug. 30 - Sept. 3, Buenos Aires, Argentina, 2004.

[9] WMO, "Guide to meteorological instruments and methods of observation. WMO, n° 8, Geneva, Switzerland, 1996.

[10] Anav A., M.L. Moriconi, S. Giannoccolo and M. Di Menno, "Field measurements of global UV-B radiation, a comparison between a broad-band radiometer and a Brewer spectrophotometer". *Il Nuovo Cimento*, vol. 19 C n° 4, p.p. 505-516, 1996.

[11] Hicks, B. B., J. J. DeLuisi, and D. R. Matt, "The NOAA Integrated Surface Irradiance Study (ISIS) - a new surface radiaton monitoring program". *Bulletin of the American Meteorological Society*, vol. 77, p.p. 2857-2864, 1996.

[12] Weatherhead, E. C., G. C. Tiao, G. C. Reinsel, J. E. Frederick, J. J. DeLuisi, D. C. Choi, and W.Tam, "Analysis of long-term behavior of ultraviolet radiation measured by Robertson- Berger meters at 14 sites in the United States". *Journal of Geophysical Research*, vol. 102, p.p. 8737-8754, 1997.

[13] Casale G, J. Groebner, private communication, 2004.

[14] Rafanelli C., A. Anav and I. Di Menno, "Cloud effect on solar UV-B irradiance at ground, a campaign in Arctic region". *Proceedings LXXXVIII Congresso Nazionale Società Italiana di Fisica*, Alghero, Italy, Sep. 26 - Oct. 01, 2002.

[15] Kasten F. and G. Czeplack, "Solar and terrestrial radiation dependent on the amount and type of cloud". *Solar energy,* vol. 24, p.p. 177-189, 1980.

[16] Duchon C. and M.S. O'Malley, "Estimating cloud type from pyranometer observation". *J. Appl. Meteor*, vol. 38, p.p. 132-141, 1999.

[17] Nardino M., A. Lupi, V. Vitale, T. Georgiadis, F. Calzolai, F. Evangelisti, C. Tomasi, D. Bortoli and G. Trivellane, "Clouds effects on the radiattive bilance terms at Terra Nova Bay". *Conf. Proc. Vol. 80, "Italian Reasearch on Antarcic Atmospheric"*, M. Colacino Ed., SIF, Bologna, 2002.

[18] Kaifel A.K., J. Kaptur, O. Routter, M. Wohlfart, P. Koepke, H. Schwander, U. Feister, R. Grewe, M. Koehl and F. Brucker, "UV-Sprafimo, A new UV spectroradiometer on filter model basis". *Proceeding of Optical Science and Technology*, 2003, 3÷8 Aug., San Diego, Ca, USA, 2003.

[19] Iqbal M., "An Introduction on Solar Radiation. Academic Press, chapter 6th, 1983.

[20] Shields J.E., R.W. Johnson, M. Karr, A. Burden and J. Backer, "Whole-sky imagers for UV research programs. *Proceeding of Optical Science and Technology*, 2003, 3÷8 Aug., San Diego, Ca, USA, 2003.

[21] Rafanelli C., A. Anav, I. Di Menno, M. Di Menno and G.R. Casale, "UV solar irradiance with cloudiness at high latitudes; a comparison between radiometer GUV 511 and model's output". *Proc. of SPIE, Ultraviolet ground. and space-based. Measurements, models and effects III,* vol. 5156, p.p. 372-383, 2003.

[22] Green A. E. S., "The penetration of ultraviolet radiation to the ground". *Physiol. Plant*, vol. 58, pp. 351-359, 1983.

[23] Bianciotto O.A., L.B. Pinedo, N.A. San Roman, A.Y. Blessio and M.B. Collantes, "The effect of natural UV-B radiation on a perennial Salicornia salt-marsh in Bahia San Sebastian, Tierra del Fuego, Argentina, a 3-year field study". *Journal of Photochemistry and Photobiology B, Biology*, vol. 70 n° 3, p.p. 177-185 (9), 2003.

Cell Biology and Instrumentation: UV Radiation, Nitric Oxide and Cell Death in Plants
Y. Blume et al. (Eds.)
IOS Press, 2006

Reconstruction of the UV-Time Series Weighted for the Plant Action Spectrum Based on the UV and Total Ozone Data Collected at Belsk, Poland, in the Period 1992-2003

Piotr SOBOLEWSKI, Janusz KRZYŚCIN
Institute of Geophysics, Polish Academy of Sciences, Warsaw, Poland

Abstract. The UV observations weighted for the plant action spectrum are rather limited. The activities in the UV ground-based measurements mainly focused on the human erythemal effects. Our objective is to find the long-term variations in the UV radiation weighted by the plant effects using the data (erythemal UV irradiance and total ozone measurements) collected at in the period of 1992-2003. The transfer function from the erythemal weighted UV radiation to the UV radiation convolved with the plant action spectrum is constructed using total ozone observations (from the Brewer spectrophotometer) and UV spectral and UV erythemal data (from the Brewer spectrophotometer and the broadband UV biometer SL 501 for the erythemal effects) taken during the intercomparison campaign of the spectrophotometers in Warsaw, May 2004. The long-term variations in the reconstructed data are discussed concerning the impact of total ozone and cloudiness fluctuations on the UV radiation for the period of 1992-2003 (Belsk [52N,21E], Poland).

Introduction.

The ultraviolet radiation (UVR) reaching the ground is only a small portion of the radiation (~ 8%) received from the Sun but decisive for the Earth ecosystem. Increased interest in the variations of the surface level of UVR since late 1980s stemmed from anticipated positive UV trend over the extratropical regions related to the observed total ozone decline there (e.g. [1]). Solar UV is known to have adverse effects on the biosphere, including terrestrial and aquatic ecosystems as well as public health e.g. sunburn, snow blindness, skin cancer, cataracts, suppression of immune system, etc. It is well documented that increased release of man-made halogen compounds is responsible for the severe depletion of the ozone layer over the midlatitudes, including Europe, during past 2-3 decades [2]. High levels of UVR were observed (e.g., [3,4]) being a result of the changes in the atmosphere transparency due to superposition of the ozone and cloud/aerosols effects on transmission of the solar radiation. Increasing danger of excessive UVR possesses a multidisciplinary aspect comprising various areas of medicine (e.g. skin cancer), agrobiology (e.g. plants sensitivity to UVR), and fishery (e.g. codfish eggs mortality). However, for years, continuous measurements of UVR reaching the Earth's surface have been focused on effects causing redness of human (Caucasian type) skin, because it was possible to construct [5] an

instrument (Robertson-Berger biometer) having spectral sensitivity close to that of the human erythema.

Long-term time series of the UV measurements weighted by action spectra other than that describing reddening of human skin (erythema spectrum) are not available. Thus, the objective of this work is to reconstruct such time series (for example using an action spectrum for higher plants) based on available data, i.e., total ozone and the erythemally weighted UV from standard observations by the Dobson or Brewer spectrophotometer and UV biometers, respectively.

1. Spectra reconstruction.

We reconstruct a transfer function from erythemal irradiance to the irradiance weighted by

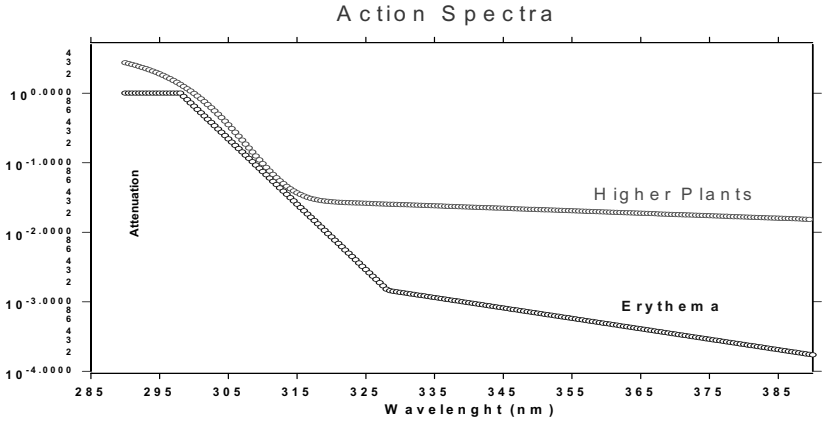

Figure 1. The erythema action spectrum (CIE) and the action spectrum for higher plants

higher plant action spectrum. Figure 1 shows the erythema action spectrum [6] and that for higher plants [7]. The procedure described here may be used also for any other spectra.

We calculated the weighted irradiance using the UV spectra (with 0.5nm resolution) measured by the Brewer spectrophotometer during the period of May-June 2004. The spectrophotometer was located at the Institute of Geophysics, Polish Academy of Sciences , Warsaw (on a roof of building ~20 m above the ground). An example of the Brewer Spectrum is shown in Figure 2.

The UV spectral irradiances weighted by the erythema and the higher plants action spectrum are presented in Figure 3. It should be noted the Brewer measures the 290-325 nm spectra, the 325-400 nm part of the spectrum is retrieved from the **SHICrivm** software tool (http://www. rivm.nl/shicrivm) developed by the Dutch National Institute of Public Health and Environmental Protection in Bilthoven within the program of European Data Base for UV Climatology and Evaluation (EDUCE), sponsored by the European Commission under the Fifth Framework Program. Both spectra are integrated over the 290-400 nm range to obtain the weighted irradiances in W/m^2.

The higher-plant-weighted irradiances are regressed on the erythema irradiance, total ozone, and solar zenith angle. Below, you may find an output (within asterisk lines) from the S+ software (stepwise multivariate regression accounting for the interactions between the explaining variables that selects most important variables) is presented.

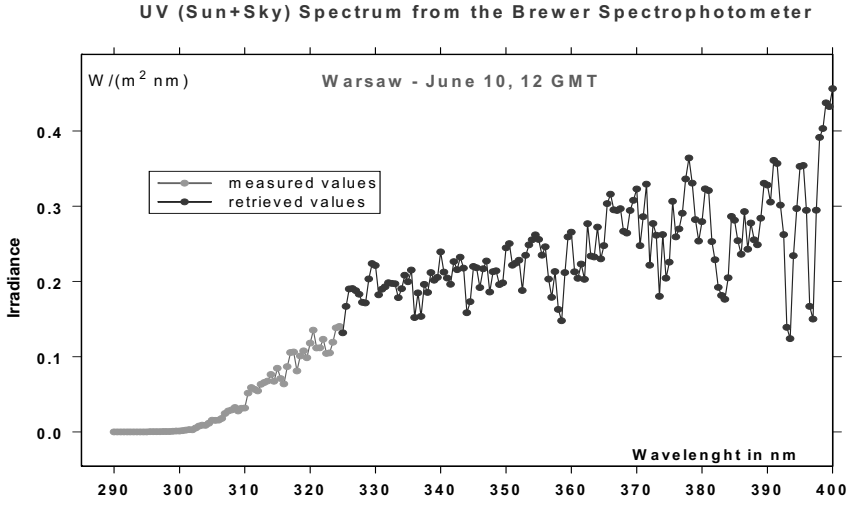

Figure 2. An example of the Brewer Spectrum

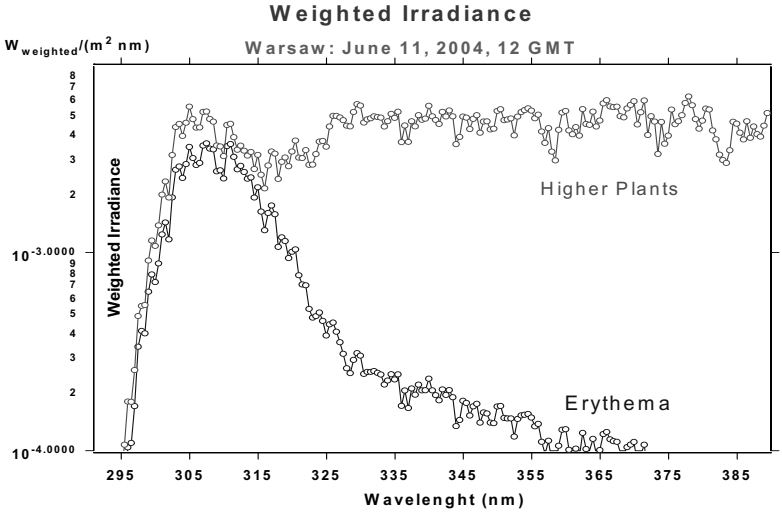

Figure 3. The UV irradiance weighted by the erythema and the higher plants action spectrum

A comparison between the modeled and measured the plant-weighted irradiances is presented in Figure 4 and both the time series are drawn for a 2-day period in variable cloudiness conditions (Figure 5). Note that 98.5% of the variance is explained by the model. Here the following notation is applied:

V2 - UV irradiance weighted by the higher plants action spectrum
V3 - UV irradiance weighted by the erythema action spectrum
V4 - Solar Zenith Angle
V5 - Total Ozone from the Brewer Spectrophotometer.

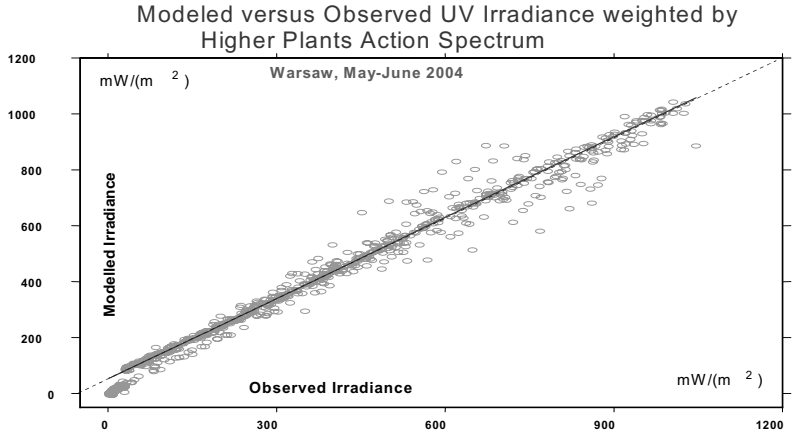

Figure 4. A comparison between the modeled and measured the plants weighted

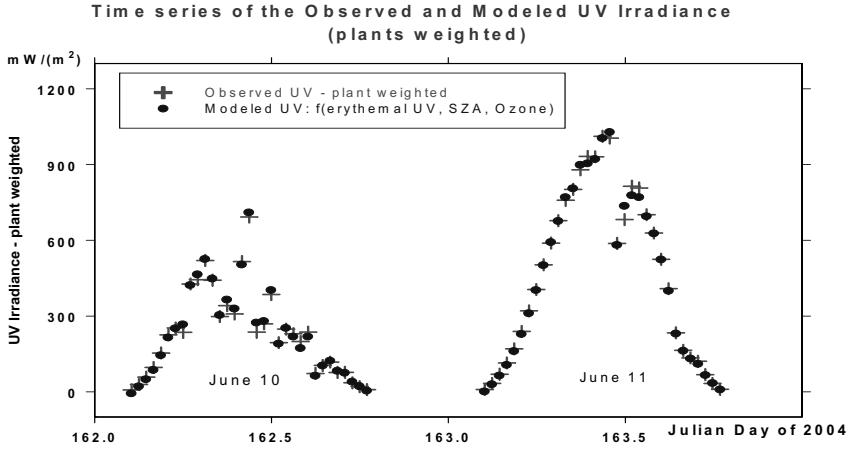

Figure 5. Both time series drawn for 2-day period with variable cloudiness

```
*********************************************************
Call: lm(formula = V2 ~ V3 + V4 + V5 + V3^2 + V4^2 + V3^3 + V4^3 + V5^3 +
V3:V4:V5,
        data = modelplant, na.action = na.omit)
Residuals:
   Min    1Q Median    3Q   Max
 -195.4 -7.34 0.2601 7.345 219.3

Coefficients:
                Value        Std. Error   t value      Pr(>|t|)
(Intercept)     161.2101     171.5553     0.9397       0.3477
         V3       3.2632       0.8033      4.0624       0.0001
         V4     -30.0937       4.3295     -6.9509       0.0000
         V5       1.5251       0.6173      2.4705       0.0137
    I(V3^2)     -0.0162       0.0062     -2.6099       0.0092
    I(V4^2)      0.5152       0.0675      7.6304       0.0000
    I(V3^3)      0.0001       0.0000      3.0981       0.0020
    I(V4^3)  -   0.0028       0.0003     -8.0102       0.0000
    I(V5^3)      0.0000       0.0000     -2.3622       0.0184
  V3:V4:V5       0.0004       0.0000     11.6143       0.0000

Residual standard error: 34.73 on 811 degrees of freedom
Multiple R-Squared: 0.9854
F-statistic: 6085 on 9 and 811 degrees of freedom, the p-value is 0.

*********************************************************
```

The model has been run using following input values: 5-min averages of the erythemal UV dose rate daily course measured by SL 501 A biometer with 1-min resolution and daily mean total ozone values from the Dobson spectrophotometer for the period of 1993-2003. Figure 6 shows the retrieved time series of the monthly fractional deviations of the UV radiation weighted by the plant action spectrum superposed on the smoothed (by a LOWESS lowpass filter) values calculated from the SL biometer measurements. The increase (~ 10%) of the plant-weighted UV irradiances in recent years should be noted, being approximately two times greater than that of the erythemally weighted UV irradiances. Figure 7 illustrates the corresponding seasonal profiles (the 1993-2003 average of the monthly mean doses) of weighted irradiances together with its monthly standard deviations. Much larger values for the plant-weighted irradiance are a result of strong and long UV-A tail (see also Figure 3).

Conclusion

Reasonable reconstruction of the UV irradiance weighted by the higher plants action spectrum is possible if the erythemal UV irradiance and total ozone data are available. The erythemal irradiance is measured for many European sites (5 in Poland) by various broadband instruments. Thus, for many stations possessing also the total ozone data (ground-based or from satellite observations) we can calculate the UV irradiance weighted by various biological effects.

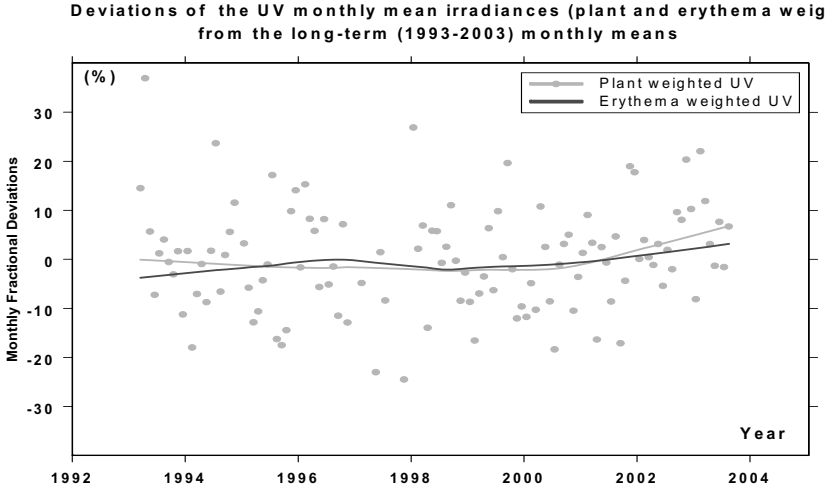

Figure 6. The retrieved time series of the monthly fractional deviations of the UV radiation weighted by the plant action spectrum

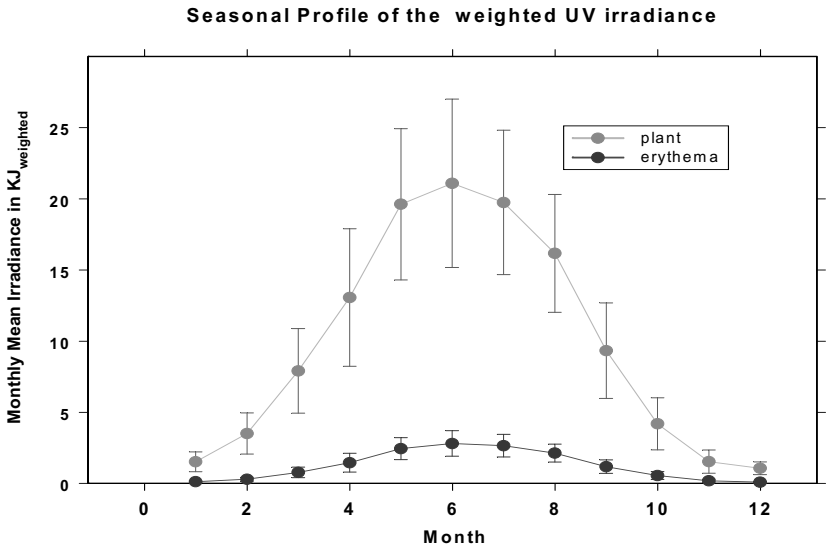

Figure 7. The seasonal profiles (1993-2003) of the monthly mean UV doses.

Acknowledgements

The study has been partially supported by the State Committee for Scientific Research, Poland, and by the State Inspectorate for Environmental Protection, Poland, under contract

561/2003/WN0/MN-PO-BD/D. It constitutes a contribution of the Institute of Geophysics, Polish Academy of Sciences to the COST-726 action

References

[1] Madronich, S., "Implications of recent total atmospheric ozone measurements for biologically active ultraviolet radiation reaching the Earth's surface", *Geophys. Res. Lett.*, vol. 19, pp.37-40, 1992.
[2] World Meteorological Organization (WMO), "Scientific Assessment of Ozone Depletion: 2002". Global Ozone Research and Monitoring Project, Report No. 47, Geneva, 2003.
[3] Blumthaler, M. and W. Ambach, "Indication of increasing solar ultraviolet-B radiation flux in Alpine regions", *Science,* vol. 248**,** pp. 206- 208, 1990.
[4] Kerr, J.B. and C.T. McElroy, "Evidence for Large Upward Trends of Ultraviolet-B radiation Linked to Ozone Depletion", *Science,* vol. 262**,** pp. 1032-1034, 1993.
[5] Berger, D. "The sunburning ultraviolet meter: design and performance". *Photochem. Photobiol.***,** vol. 24, p.p. 587-593, 1976.
[6] CIE (International Commission on Illumination) Research Note, "A reference action spectrum for ultraviolet induced erythema in human skin"*, CIE J.***,** vol. 6, p.p. 17-22, 1987.
[7] Flint, S.D. and M. M. Caldwell, "A biological spectral weighting function for ozone depletion research with higher plants", *Physiologia Plantarum*, vol. 117, pp. 137–144, 2003.

Cell Biology and Instrumentation: UV Radiation, Nitric Oxide and Cell Death in Plants
Y. Blume et al. (Eds.)
IOS Press, 2006

Detector of the Ultraviolet Radiation for Biologically Active Ranges of Solar Radiation on the Bases of ZnSe Semiconductor

[1)]Leonid GAL'CHINETSKII, Volodymyr MAHNIY, Volodymyr RYZHIKOV, Volodymyr SEMINOZHENKO, Nikolai STARZHINSKIY,
[2)]Jong-Kyung KIM,
[3)]Yong-Kyun KIM, Woo-Gyo LEE
[1)] *STC "Institute for Single Crystals", Kharkov, Ukraine*
[2)] *iTRS, Hanyang University, Seoul, Korea*
[3)] *KAERI, Daejeon, Korea*

Abstract. ZnSe(Te) crystals can be used as components of "semiconductor-metal" structures with Schottky barrier that are photosensitive in the UV range. Basing on the n- ZnSe(Te,O)-Ni structures in combination with filters, selective photodetectors have been developed for UVA and UVB ranges, which were used in development of small-sized household and professional instruments.

Introduction

Solar UV radiation is one of the most powerful factors affecting human health (see the reviews [1] and references therein). The International Commission on Radiation (CIE) has defined, judging from the photobiological point of view, the following specific ranges of UV solar radiation: from 315 to 400 nm (UVA), from 280 to 315 nm (UVB) and from 100 to 280 nm (UVC). Radiation in the UVB range is partially absorbed by the stratosphere ozone layer, while the UVC radiation is absorbed almost completely. Due to its ability to destroy DNA and other biological macromolecules, the UVB region is generally associated with a skin cancer. This radiation causes formation of the cataract, affects the immune system of humans and animals, and even leads to the extinction of certain kinds of plants.

It is quite clear that potential risk related to UV solar radiation factors should be adequately estimated. For this purpose, convenient and reliable methods are required for measurements of UV radiation parameters and their monitoring.

By the present time, several types of UV radiation meters have been developed (see reviews [2,3] and references therein).

First of all, one should mention broadband spectral instruments used to measure the total energy of UV radiation. Thus, in Robertson-Berger broadband meters, the spectral curve of the photoelectric sensitivity is close to the biological effective spectrum of UV radiation for erythema [4] (the Diffey curve). However, the use of such instruments is limited, because different biological processes have different effective spectra.

Secondly, there are laboratory stationary spectroradiometers, which can scan the entire UV spectrum in detail. The spectral data are weighted with respect to the effective

spectrum for any biological process.

Thirdly, there are biological dosimeters, e.g., a solar dosimeter based on DNA [5], which directly determines the spectral density of the light energy falling onto the measurement surface with respect to the spectral density of photobiological efficiency.

Next, there are dosimeters based on calibrated sets of photochromic materials, which allow reconstruction of the real solar spectrum in UVA and UVB ranges [6].

Finally, in the recent years, instruments have been developed that measure UV radiation parameters in certain narrow spectral bands cut out by light filters [6]. In the best meters of this type, UV radiation is being filtered using interference light filters [7]. Calculation of biologically active doses is carried out using the model solar spectrum at different polar angles and effective biological spectrum for erythema [4].

A disadvantage of all these types of UV radiation meters is that they are either large-sized stationary installations or "passive" instruments that measure the absorbed dose not accounting for dynamics of the spectral-energy parameters of UV radiation.

The existing portable UV meters, as a rule, do not account for the so-called "cosine factor" – a qualitative coefficient describing variation of the instrument readings as a function of the light incidence angle for a concrete design of the photoreceiver.

Therefore, to meet the most important practical requirements, two types of UV solar radiation meters are to be developed:

- a small-sized inexpensive "household" instrument, which would give an adequate response to UVA and UVB radiation, allowing to evaluate hazardous factors in the real time mode. Such an instrument will found broad application in health resorts, at agricultural work sites etc, allowing one to reduce the risk of UV radiation-induced illnesses;
- a portable professional instrument, which would make it possible to determine both spectral-energy parameters of biologically active UV radiation in the real time mode and the integral dose of absorbed radiation in the given time period. Such an instrument is necessary for development of new efficient protection methods against hazardous factors of UV solar radiation.

STC "Institute for Single Crystals" has developed and produced experimental UV meters of both the types, using original detectors based on zinc selenide crystals as UV radiation receivers.

1. Detector

Unique possibilities of purposive variation of properties offered by isovalently doped AIIBVI compounds, and, in particular, by ZnSe(Te) scintillation crystal [8,9], have opened the way for their broad application in radiation instruments – detectors of α-, β-, X-ray, and γ-radiation [9]. The scintillation crystal ZnSe(Te) is characterized by its combination of characteristics making it the optimum choice for "scintillator-photodiode" detectors. The most important parameters of ZnSe(Te) crystals are presented in Table 1 in comparison with CsI(Tl).

It is clearly seen that ZnSe(Te) is obviously superior in such qualities of primary importance as conversion efficiency and absolute light output, afterglow, spectral matching, and hygroscopicity. In addition, the absorption depth in CsI(Tl) at energies below 40 keV is less than 0.25 mm. This means that negative influence of the surface layer upon scintillation parameters is negligible with ZnSe(Te), but it is significant with thinner CsI(Tl) samples. Thus, advantages of ZnSe(Te) in comparison with CsI(Tl) as scintillator for low-energy detector arrays are clear and undeniable.

Among advantages of ZnSe(Te), one should also note its high radiation stability (not less than 10^7 rad) and high upper limit of working temperature (up to 100^{o}C). All these

show that ZnSe(Te) is the most promising material for "scintillator-photodiode" detectors of radiation in the range of up to 40-60 keV.

Parameter	Scintillator material		
	CsI(Tl)	ZnSe(Te)	
		"fast"	"slow"
Melting temperature, K	894	1773-1793	1773-1793
Density ρ, g/cm^3	4.51	5.42	5.42
Effective atomic number, Z	54	33	33
Hygroscopicity	low	no	no
Emission maximum, λ_{max}, nm	550	610	640
Afterglow, δ (after 6 ms), %	0.1-5.0	<0.05	<0.05
Attenuation coefficient of intrinsic radiation (λ_{max} = 610-640 nm), α, cm^{-1}	<0.05	0.05-0.2	0.05-0.2
Light yield with PD with respect to CsI(TI) at 1 mm thickness, E_x = 60 keV, %	100	up to ~110	up to ~140
Decay time, τ, μs	1	1-3	30-70
Maximum value of the spectral matching factor K_u	0.77	0.9	0.92
Refraction coefficient, n	1.79	2.61	2.59
Light yield, photons/MeV-γ	5.5-10^4	up to 6·10^4	up to 7.5·10^4
Depth of 90 % absorption X-ray (40 keV), mm	<0.25	0.65	0.65

Table 1. Principal parameters of scintillators ZnSe(Te).

Recent studies have shown that ZnSe(Te) crystals can be also used as components of "semiconductor-metal" structures with Schottky barrier that are photosensitive in the UV range [10-12]. Though many different types of UV detectors are known (e.g., based on GaAs, InP, Si, GaN, SiC, etc.), most of them have serious disadvantages – either highly complex way of production, or low sensitivity, poor reproducibility, low radiation stability, or the spectral sensitivity range not meeting the requirements of specific applications [13]. As problems of detection and quantitative evaluation of UV radiation effects upon materials and biological objects has been attractive more and more attention, development and studies of new types of UV detectors is of undeniable interest. In this paper, we describe properties of photoreceivers with the "metal-semiconductor" junction fabricated on the basis of n-type ZnSe crystals, and we also report our studies on how their properties are affected by bias voltage, temperature, substrate doping level, etc.

As substrates, we used zinc selenide crystals doped with Te and O. Concentration of free electrons n_0 ($n_0 = 10^{12} – 10^{18}$ cm^{-3}) was determined both by the activator concentration and thermodynamic parameters of thermal pre-treatment of the crystals in Zn vapor [14]. These dopants create donor levels in ZnSe crystals, with activation energy of $E_a < 0.05$ eV [9,14]. Semi-transparent barrier contacts were made of nickel and are characterized by high and uniform transmission in the UV range [11,12]. Ohmic indium contacts were applied onto the opposite side of the substrate. Effective area of the photoreceivers was 0.01-0.1 cm^2.

The height of the Schottky barrier φ_0 for Ni-ZnSe depends upon the doping level of the substrate and increases from 1.2 to 2.0 eV when the concentration n_0 is reduced from 10^{17} to 10^{15} cm^{-3} [11,12]. The photosensitivity spectrum of the photoreceivers at the bias voltage $U_S = 0$ V is a broad band in the 0.20-0.47 μm region (Fig.1). Typical values of the monochromatic current sensitivity S_λ at λ_{max} = 0.42-0.44 μm are 0.1-0.15 A/W, which corresponds to quantum efficiency of 0.3-0.4 electron/quantum. The dynamic linearity range of the ampere-watt characteristic is not less than six orders of magnitude.

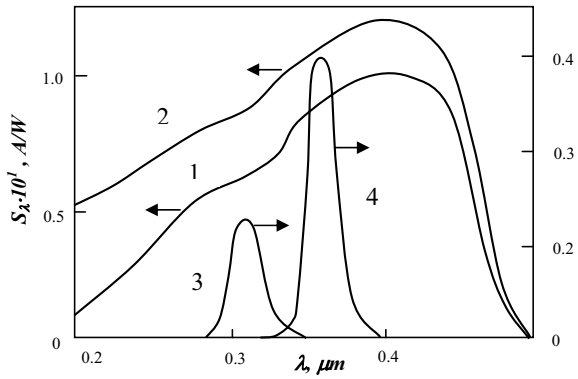

Figure 1. Photosensitivity S_λ spectra of the structure n-ZnSe(Te) – Ni at U_s=0 V (1) and 6 V (2) and T=300 K, and photosensitivity ranges of the photoreceivers with light filters in UVA (4) and UVB (3) ranges.

Our studies on effects of the preparation technology and other factors upon the output parameters of the photoreceivers with Schottky barrier have shown the following. At 230-350 K their sensitivity at $\lambda \leq 0.4$ μm varies not more than by 0.1%/K, and the temperature shift of the long-wave edge of the photosensitivity spectrum is about $7 \cdot 10^{-4}$ eV/K, being close to the temperature variation coefficients for φ_0 and E_g [11,12].

As it is seen from Fig.1, the photosensitivity spectrum of ZnSe-based Schottky diodes covers all biologically relevant ranges – UVA, UVB, UVC, - and remains "blind" at $\lambda > 480$ nm, which makes the task of development of UV filters much easier. Basing on the n-ZnSe(Te,O)-Ni structures in combination with filters made of optical glass, selective photodetectors have been developed for UVA and UVB ranges, which were used in development of small-sized household and professional instruments.

As the most dangerous for human health is the UVB range, special attention was paid to achieve a similarity between the transmission spectrum of the UVB filter and the spectral density D_λ of photobiological efficiency: $D_\lambda = E_\lambda K_\lambda$, where E_λ is the spectral density of the standard solar radiation, and K_λ is the standard biological action spectrum for erythema (the Differ curve, approved by CIE in 1987, see Fig 2, 3).

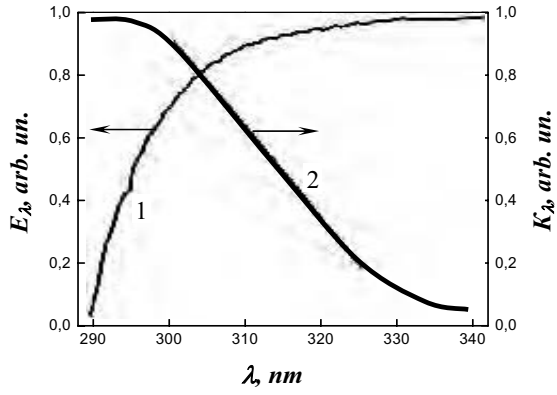

Figure 2. Wavelength dependence of the spectral density of the standard solar radiation E_λ and the standard biological action spectrum for erythema K_λ.

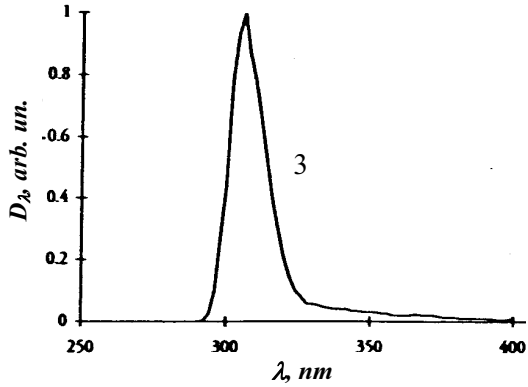

Figure 3. Wavelength dependence of the spectral density of photobiological efficiency D_λ.

In this case, the photodetector measures the photobiological efficiency (F) of UV radiation in the wavelength range from λ_1 to λ_2:

$$F = \int_{\lambda 1}^{\lambda_2} D_\lambda d\lambda.$$

2. Household UV radiation dose meter

The instrument is designed for measurement of UVA and UVB radiation in W/m^2 units. Among the advantages of the instrument, there are its small size, high sensitivity in the range of UV radiation biological activity, and low energy consumption. The instrument comprises a UV radiation detector based on ZnSe, an analog-to-digit converter (ADC) in the form of a KR572PV5 chip, and a liquid crystal indicator (LCI).

The detector is designed for converting the UV radiation intensity into electric current. As shown above, its current sensitivity (S_λ) is monochromatic at wavelengths 310-360 nm (about 0.02 A/W), and its internal resistance is high. Accounting for these peculiar features, we used a stage circuit ensuring amplification of the detector current and its conversion into voltage. Specifically, we used a current amplifier based on an integral micro-power operation amplifier with. From the amplifier output, the signal is fed to the ADC, which converts it to a digital code displayed by LCD. The instrument uses a 3½ digit indicator directly conjugated with ADC. The instrument has two measurement ranges: 0-10 W/m^2 and 0-100 W/m^2. The instrument receives power from a galvanic battery of 9 V nominal voltage, the consumed current is 0.7 mA, time of continuous operation – 20 days. Overall dimensions of the instrument: 100x70x15 mm, weight – not more than 100 g.

To weaken the influence of the cosine factor, the specially made Teflon diffusor was placed before the detector, which ensured, in addition, almost full independence of the readings upon azimuth values.

Effective biological spectrum for the erytheme, weighted with respect to the standard solar spectrum, is close to the transmission spectrum of light filters designed for UVB region. Because of this, the developed household dosimeter with a Teflon diffusor allows measurements of the solar_protection factor SPF – the ratio of photobiological

efficiency of UV radiation in the wavelength range from λ_1 to λ_2 without a protecting material to the same photobiological efficiency after transmission of the solar light through the protective material:

$$SPF = \frac{\int_{\lambda_1}^{\lambda_2} D_\lambda}{\int_{\lambda_1}^{\lambda_2} D_\lambda T_\lambda} d\lambda ,$$

where T_λ is transmission of the solar radiation protective material at the wavelength λ.

Thus, the proposed instrument can be also used to measure of protective properties of various materials (tissues, cremes, etc.) in UVA and UVB ranges.

3. Professional UV radiation meter

The professional UV radiation meter has been developed on the basis of modern microelectronics. It is designed for measurement of intensity and integral dose of UV radiation in UVA and UVB spectral ranges. The instrument allows one to carry out routine measurements of UV radiation dose, information storage during a pre-set time period and its transfer to an external computer using an appropriate interface, and ensures sound indication when the pre-set UV radiation dose threshold is reached in each of its channels.

The UV radiation meter comprises: two detectors of UV radiation with sensitivity spectra corresponding to UVA and UVB spectral ranges; two identical converting amplifiers-converters; a two-channel ADC, microcontroller, memory unit, control board, indicator device, voltage transformer, and an interface for connection with a computer.

The information display device (specifically, an intellectual two-line LCI) indicates the values of intensity and accumulated UV radiation dose simultaneously through two channels, in standard measurement units (W/m^2 and J/m^2, respectively), and it also indicates the operation mode. For power supply, 3 V voltage is used, and the consumed current is ~20 mA.

It would be interesting to broaden functional possibilities of the professional UV radiation meter. Recently, an assumption has been made that experimentally observed changes in diffuse reflection coefficient [15] and absorption coefficient [16] of human skin under UV irradiation are due to functioning of protection mechanisms against unfavorable effects of irradiation. In this connection, it is proposed to equip the developed professional instrument with an integrating photometric Ulbricht sphere (see Fig.4), which could be used for measurement of transmission and reflection coefficients of light-scattering objects, as well as (using a multi-filter system and calibrated detectors) for determination of spectral dependences of these coefficients by means of special computer processing [17]. The use of the Ulbricht sphere will also allow a more precise determination of SPF for different materials.

It follows from the theory of multiple reflections inside the Ulbricht sphere that illumination of the internal surface of the sphere is equal at all points and is expressed as

$$E = \left(\frac{F}{4\pi R^2} \times \frac{\rho}{1-\rho}\right),$$

where F is the light flux entering the sphere, R is radius of the sphere, and ρ is reflection

coefficient of the surface of the sphere. To obtain high values of E, ρ should be sufficiently high. Therefore, internal surface of the sphere is covered with a layer of $BaSO_4$, for which the diffuse reflection coefficient is more than 95% in the UV range.

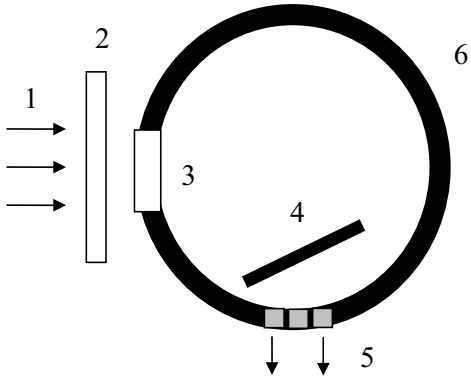

Figure 4. Scheme of the integrating sphere:
1 – source of UV radiation;
2 – tissue, crème, etc. (for measurement of SPF);
3 – teflon window (a diffusor of special shape);
4 – shielding from directUV rays;
5 – set of UV detectors with light filters;
6 – the integrating sphere.

It would be also interesting to consider the use in a professional dosimeter of the Ulbricht sphere with multi-filter detectors for computer reconstruction of the entire biologically active solar UV spectrum basing on several experimental points. Taking this information into consideration will allow, in turn, more precise determination of SPF. Presently, the sphere and the computer software for reconstruction of the spectrum are in the course of development.

References

[1] Longstreth J., de Gruijl F.R., Kripke M.L., Abseck S., Arnold F., Slaper H.J., Velders G., Takizawa Y., van der Leun J.C., "Health risks". *J. Photochemistry and Photobiology, B: Biology*, 998, vol. 46, 1-3, p.p. 20-39, 1998.

[2] Driscoll M.H., "Dosimetry methods for UV radiation". *Protection Dosimetry*, vol.72, 3-4, p.p. 217-223, 1997.

[3] Bais A.F., "Spectral solar UV measurements within SESAME". *In: Advances in Solar Ultraviolet Spectroradiometry* (ed. A. R. Webb), Luxembourg, EC, p.p. 173-182, 1997.

[4] McKinlay A.F. and Diffey B.L. "A reference action spectrum for ultraviolet induced erythema in human skin". *CIE-Journal*.vol. 6, 1, p.p. 17-22, 1987.

[5] Ishigaki Y., Takayama A., Yamashita S. and Nikaido O., "Development and characterization of a DNA solar dosimeter". *J. Photochemistry and Photobiology, B: Biology*, vol. 50, 2-3, p.p. 184 – 188, 1999.

[6] Parisi A.V., Wong J.C.F. and Moore G.I. "Assessment of the exposure to biologically effective UV radiation using dosimetric technique to evaluate the solar spectrum", *Phys. Med. Biol*., vol. 42, 1, p.p. 77-88, 1997.

[7] Richards D.L., Davies R.E. and Boone J.L., **"**A selective Pt-CdS photodiode to monitor erythemal flux*". J. Photochemistry and Photobiology, B: Biology*, vol. 47, 1, p.p. 22-30, 1998.

[8] Ryzhikov V.D., Silin V.I. and Starzhinskiy N.G., "A new ZnSe(Te) scintillator: luminescence mechanism*". Nucl. Traces Radiat. Meas*., vol. 2, 1, p.p. 53-55, 1993.

[9] Atroschenko L.V., Burachas S.F., Gal'chinetskii L.P. etc., "Crystals of scintillators and detectors on their base". Kyiv, Naukova dumka, 1998.

[10] Baranuk V.S., Mahniy V.P., Melnik V.V. and Ryzhikov V.D., "Detectors of ionizing and ultraviolet radiation on the basis of broad-band compounds A2B6". In: *Abstract Booklet of the First International Conference on Material Science of Chalcogenide and Diamond-Structure Semiconductors*, vol.1, Chernivtsi, p. 22, 1994.
[11] Mahniy V.P. and Melnik V.V., "Photoelectric properties of contacts Ni-ZnSe". *Semiconductors,* vol. 29, 8. p.p. 1468-1472, 1995.
[12] Mahniy V.P., "UV photoreceivers on the basis of zinc selenide". *Technical Physics*, vol.68, 9, p.p. 123-125, 1998.
[13] Rogalski A. and Razeghi M., "Semiconductor ultraviolet photodetectors". *J. Appl. Phys.,* vol. 79, 10, p.p.7433-7473, 1996.
[14] Ryzhikov V.D., "Scintillation crystals of semiconductor compounds $A^{II}B^{VI}$", Moscow, NIITEHIM, 1989.
[15] Cader A. and Jankowski J., "Reflection of ultraviolet radiation from different skin types". *Health Physics*, vol. 74, 2, 1998
[16] De Gruijl F.R. "Health effects from solar ultraviolet radiation". *Radiation Protection Dosimetry*, vol. 72, 3-4, p.p. 177-196, 1997.
[17] Malahov B.A. "The use of filters for measurement of spectral characteristics of low-intensity light sources". *Pribory teh. eksperiment*., 2, p.p. 172-173, 1983.

Cell Biology and Instrumentation: UV Radiation, Nitric Oxide and Cell Death in Plants
Y. Blume et al. (Eds.)
IOS Press, 2006

UV and VIS Radiation Meters for Environmental Monitoring

[1)] Petro SMERTENKO, Vitaliy KOSTYLYOV, Ivan KUSHNEROV,
Olexandra SHMYRYEVA, Eduard MANOILOV,
[2)] Mykola BRYCHENKO, Valeriy KRUGLOV, Anatoliy MARYENKO,
Rostislav STOLYARENKO,
[3)] Yaroslav BLUME
[4)] Don J. DURZAN
[1)] V.Lashkaryov Institute of Semiconductor Physics, Department of Optoelectronics, National Academy of Sciences of Ukraine, 45 Prospect Nauki, Kyiv, 03028 Ukraine
[2)] S. Korolyov MERYDIAN JSC, 8, I. Lepse blvd, Kyiv, 03680 Ukraine
[3)] Institute of Cell Biology and Genetic Engineering, Cell Genetics Department, National Academy of Sciences of Ukraine, 112 Zabolotnogo Str., 03207 Kyiv, Ukraine
[4)] Department of Plant Sciences, MS 6, University of California, One Shields Ave. Davis, CA 95616-8587, USA

Abstract. New UV meters and software have been developed and manufactured for environmental monitoring in the Ukraine. The multifunctional meters offer low cost and provide one and four channels for biological, meteorological and medical applications. The main specifications, advantages, and design features of each device developed is presented.

Introduction

UV irradiation is one of the environment factors that has either a favorable or unfavorable dose-dependent effect on living organisms [1-10]. Exceeding the UV irradiation dose is harmful and even pathological. In humans and animals UV-irradiation deficiency leads to vitamin imbalance, a decrease in immune protection [11-16]. Many an examples exist why it is necessary to carry out the UV monitoring [17-23].

Control of the optical energy irradiation and dose in wide spectral ranges (UV to NIR, including visible radiation) is important to determine the separate actions of UV, photosynthesis, and thermal effects of the radiation. Control also enables the estimation of complex influence of optical radiation on biological objects and their surroundings [24-29]. In all cases, it is necessary to have simple and accurate measuring devices.

In the world-wide market there are many different devices. These comprise radiometers of UV radiation, flux meters, radiometers of IR radiation, and others (Fig.1.) [30-32]. Their high costs are prohibitive for common applications in Ukraine. Therefore one of our main criteria for the development and manufacture of the photometers was their cost characteristic with the highest possible design unification in the monitoring system [33].

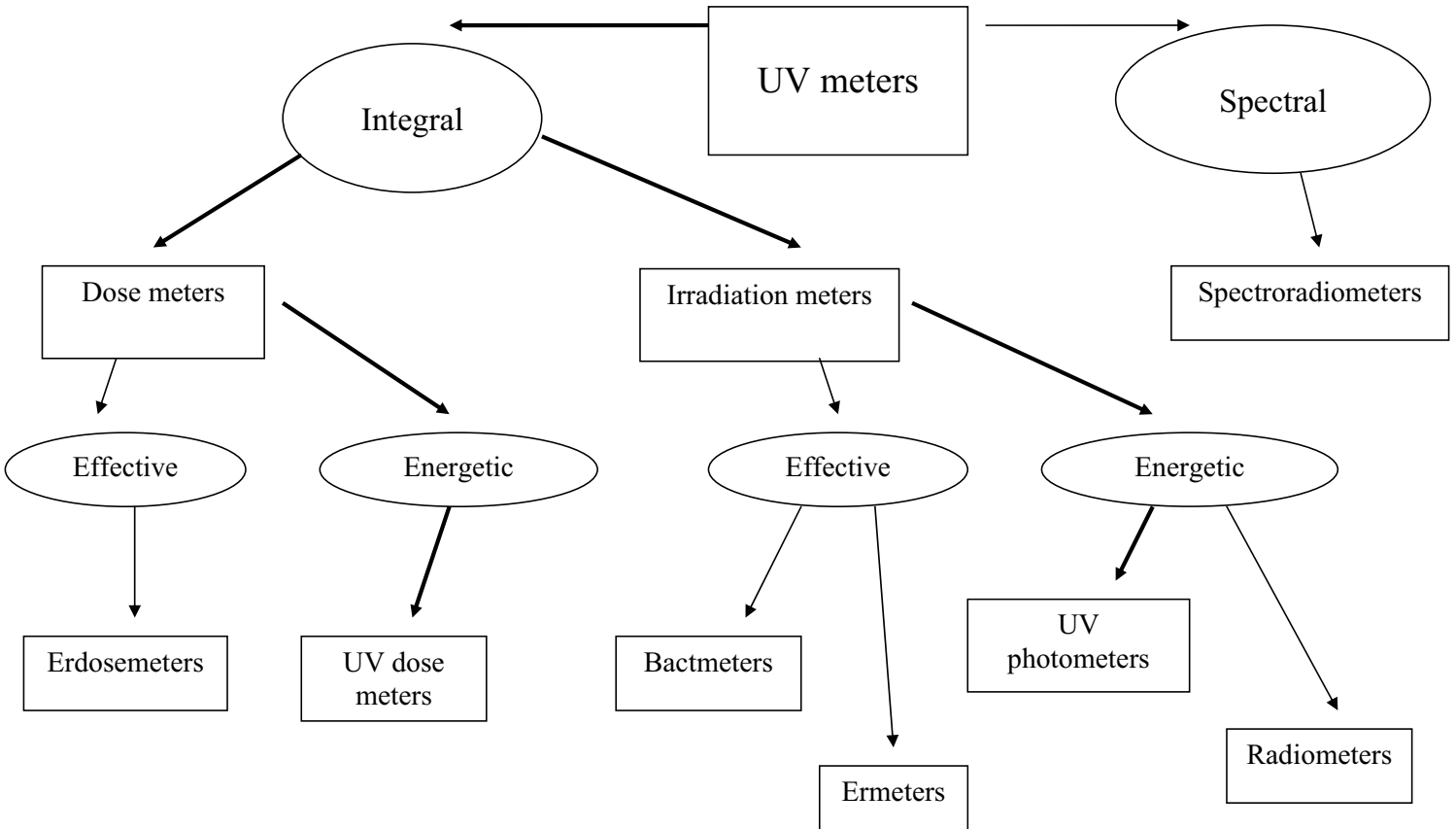

Figure 1. A proposed classification of UV meters [30]. Bold arrows show the types of devices developed for the Ukraine.

1. Optical energy irradiation and dose meters (OIM and DM)

To develop OIM and DM and yet retain their low cost, the filter broadband was redesigned. Classification of the optical devices for measurements of UV radiation is presented in Fig. 1. [33]. The ermeter measures erythema, the device for quantifying the electromagnetic energy to control the degree of erythema. It was calibrated in erythema units. The erdosemeter determines the erythermal dose by optical measurement. It was calibrated in units of erythema doses. The bactmeter is used to evaluate the bacteriological action of UV radiation. It used for to measure disinfection, sterilization or sanitization by UV radiation. These devices measure either irradiance or dose. The devices for measuring of irradiance and dose are divided into those that measure energy values or effective values. We selected the best way to measure energy values (bold arrows in Fig.1.).

Their main advantages are:

- easy to use;
- broad distribution possible;
- response function similar to biological weighting function;
- low cost.

The main disadvantages concern the high demands for instrument calibration for:

- wavelength coverage;
- sensitivity;
- long-time stability;
- temperature stabilization;
- data logger capacity.

These instruments can monitor, collect and store information. This requires linkage with a personal computer (PC) for portability and long-term automated operation for accurate measurements and simplicity of use. These specifications were successfully introduced for two kinds of devices: portable one-channel FEO-M, and professional four-channel FEO-P photometers.

Both kinds were designed as unified selective photodetectors to provide measurements in different ranges of spectrum (spectral types UVA, UVB, UVAB, vis etc). They were also modified to meet a variety of end uses and complexity of measurement tasks.

The portable photometer of optical energy irradiation and dose FEO-M (Fig.2.) is a simple one-channel portable small current (up to 3 мА) meter. It was designed from the simple and relatively cheap microelectronic elements – microcontroller of type PIC16F628 and ADC of type AD7822, which increases its desirable functionality for:

- measuring of optical energy irradiance;
- automatic identification of the working photodetector;
- automatic calculation of optical irradiance and dose of irradiation;
- control of time of radiant dose exposure;
- measuring of ambient temperature in the point of measurements;
- digital indication of optical irradiance, dose, time of exposure and detector temperature;
- interface transmission of data to PC for the next visualization and processing.

The professional photometer of optical energy irradiation and dose FEO-P (Fig.3.) is the device that measures information. It has a 4-channel microprocessor block for measurements. Data are displayed on the LCD panel. Automatic turning of the limits of measurements ensures desirable multifunctionality of the device for:

- measuring of optical energy irradiance;
- automatic identification of the working photodetector;
- automatic calculation of optical irradiance and dose of irradiation;

- control of time of radiant dose exposure;
- measuring of ambient temperature in the point of measurements;
- setting of limits of radiant dose or time of exposure in each optical channel;
- digital indication of irradiance, dose, temperature, time of exposure, limits of radiant dose and exposure time;
- sound signalization about exceeding of set limits;
- storage of information in nonvolatile memory;
- interface transmission of data to PC for the next visualization and treatment according to procedure.

Figure 2. Portable photometer FEO-M

Figure 3. Professional photometer FEO-P

The device has 4 independent input measuring channels that transform signals into the digital values by 24-bit ADC of type ADS1240. The digital filter and pre-amplifier with 128-stage turning of the amplification coefficient allows us to increase significantly the dynamic range of measurements to 10^8. In contrast, with FEO-M, a more powerful microcontroller of type PIC16F877 (20 MHz, 8k x 14 – FLESH ROM) provides wider functionalities. The functional possibilities and technical characteristics of devices are shown in Table 1.

In comparison with portable photometer FEO-M, the professional photometer FEO-P has the following advantages:

- multichannel work from the 4 photodetectors simultaneously;
- large dynamic range of measurements - due to utilization of more powerful microscheme of ADC with 24-bit and build-up programming 128-time pre-amplification;
- big volume of programming memory up to 4 times (8 kilowords)
- high speed of program execution up to 20 times – due to utilization of more powerful microcontroller PIC16F877;
- graphic display of 128x64 pixels instead of LCD indicator of 4 numbers;
- extended control with the use of keyboard;

- registration of IR trends - due to utilization of microscheme of permanent memory 500 Kbytes, sufficient to remember of dozen measurements;
- build-up sound indicator of programming limit values of the exposure dose in each channel.

Table 1. Technical characteristics of fabricated photometric devices (without photodetectors)

Parameters	**FEO-M**	**FEO-P**
Number of measuring channels	1	4
Range of measurement of optical energy irradiation E, W/m^2	$5x10^{-2}...10^4$	$10^{-3}...10^4$
Limit of the irradiation measuring error dE, %	±3	±1
Range of measurement of the exposure dose D, kJ/m^2	$5x10^{-2}...10^4$	$10^{-3}...10^4$
Limits of the dose measuring error dD, %	±4	±1
Range of measurement of the exposure time T, min	$1 ... 6\ 10^3$	$3.3\ 10^{-2}... 6\ 10^5$
Limit of the exposure time measuring error dT, %	0,01	0,01
Range of measurement of the temperature, ^oC	- 9 ...+60	- 9...+60
Limit of the temperature measuring error dt, %	±0.5	±0.5
Power supply current I_c, mA - with the illumination	2 -	30 300
Range of work temperatures, ^oC	-10 ...+50	-10...+50
Interface with PC Transmission speed, bod	RS232 9600	RS232 9600
Operational time in autonomous CW mode, h	100 – 250	

2. Unified photodetector for the photometers of optical energy irradiation and dose FEO-M and FEO-P.

The unified selective photodetector (FD) is a constituent part of the photometers FEO-M and FEO-P. FD transforms directly the irradiation into electrical signals. The change of the photodetector changes the sensitivity of the photodetector. The photodetector presents the photosensitive element with the selective optical filter.

FD uses an identifier which identifies the photodetector by the spectral range and the limits of measurements. This takes into account the spectral characteristics and corrects for the temperature dependence. It can utilize photodetectors of different types. The identifier's input limits measurements to 1000, 300, 100, 30, 10, 3, 1 or 0.3 W/m2. This represents a coefficient of transformation provided by the amplifier with the following spectral characteristics: (B type) 280-315 nm, (A-type) 315-400 нм, (AB-type) 280-400 nm and (V-type) 400-760 nm.

The photodetector (PD) has the following components:

- optical filters that can transmit optical radiation in the given range;
- photosensitive sensor that can transforms the light flux into the electrical signal;
- circuit board where pre-amplifier and identifier are situated;
- connector for connection between photodetector and microcontroller for data processing.

The glass optical filters and photosensors are united into the photoreceiver that has a single case marked by the corresponding types (A, B, C, V, IR). If necessary, interference filters can be used.

PD includes the selective photodiode, which transform the optical radiation into the electrical current, the identifier of the detector type (D1 – DS18S20), and the scheme of normalization of the output signals (D2 – ADS8551AR). We recognized the need to regulate the transformation coefficient to adjust of the photodetector and photometer. The

identifier (microscheme) has a unique number (48 bits), a temperature sensor (accuracy $\pm 0{,}5^0$C), and a permanent memory (16 bit) for writing the values of the coefficient of transformation and the type of spectral characteristics. The photodetector is recognized by the photometer, and determines the type and the data necessary for pre-programming corrections and measurements.

The normalization of the signal is executed as an amplifier-transformer I/U on a precise operational amplifier. The latter has very low (20 pA) input current and bias (5 μV) with a small temperature drift (0.03 μV/^{o}C). This allows the user to select the coefficient of transformation ($k_o = U_{out}/I_{in}$) in a very wide range (roughly – by changing of the resistance nominal R1 in the limits of 1.0...1000 kΩ, and precisely, in 1.5 steps – by the potentiometer R2). The necessary coefficient of transformation k_o is determined from the formula $k_o = Un_{out} / E_{max} \cdot S_i$, where Un_{out} is output voltage of the transformer. This is equal to maximal input voltage of ADC (2.5 V as for FEO-M and for FEO-P); E_{max} is the limit of optical energy irradiation, W/m^2; S_i is integral sensitivity of the phototransformer, μA/Wm^{-2}. Thus, for example, during the measurement of the energy irradiation in the field of UV-B from the natural sun (E_{max}= 10 W/m^2) by the photodetector with sensitivity S_i = 1 μA/Wm^{-2}, it is necessary to set a transformation coefficient k_o = 0.25 V/μA (R_{oc} = 0.25 MΩ).

For the photodiode we used a Si special diode [33, 34]. Its reproducibility is shown on Fig. 4. The spectral characteristics of PD in UV and visible ranges are shown on Figs. 5.6., respectively.

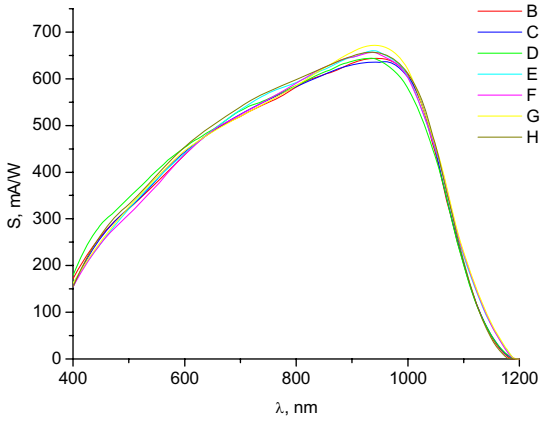

Figure 4. Dispersion of spectral sensitivity curves for 7 experimental samples of the Si pgotodiodes [34].

There are photodiodes on the base with other materials [36-40]. The GaN and diamond photodiodes may be used in UV meters to blend with the visible range, but they are currently too expensive for use in our devices.

3. Development of the software for monitoring of UV irradiation

For UV irradiation monitoring, the EMMStation program has been developed. It allows collecting, storing and processing the data got from photometer FEO-M/FEO-P.

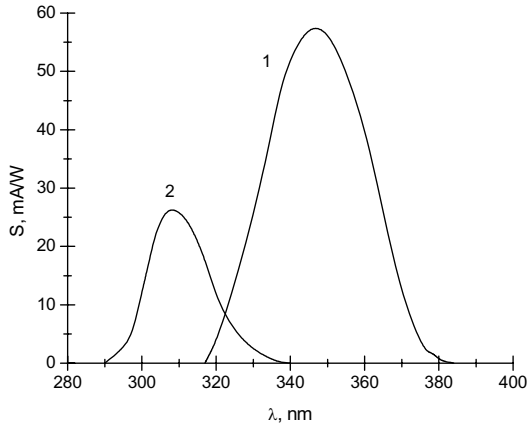

Figure 5. Spectral sensitivity of photosensor in UV ranges:1 – UVA, 2 – UVB.

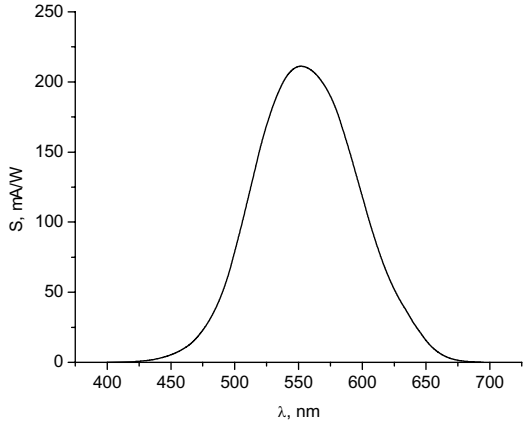

Figure 6. Spectral sensitivity of PD in visible range

EMMStation include the following components for:

- interaction with FEO-M/FEO-P (data collection and operation);
- database support, using BDE driver (Borland Database Engine) and operating the database in Paradox format;
- generation and forming of alarm messages ;
- a mail agent for sending alarm messages through the SMTP mail server;
- an adjustment wizard for the mail agent and parameters of dispatch.

EMMStation allows:

- inspecting and collecting the data from FEO-M/FEO-P;

- storing observed data in the database with possibility of their graphics visualization on each of measuring channels selected by the user and in a selected range of a time;
- exporting observed data from the database to a text file and to import from a text file to the database;
- carrying out a control of integrity and clearing (restoring) of the database;
- inspecting the generation and creation of alarm messages and sending these through a SMTP mail server on the given users addresses.

Depending on specific tasks (object of visualization, range and errors of measurements, spatial and temporal resolution, station site, and IOM/DM situation), we can:

- select different modes of observation with necessary parameters of monitoring;
- offer appropriate methods of diagnostics with necessary characteristics of sensitivity and selectivity;
- develop advanced algorithms of signal registration;
- processing and represent data;
- entered the optimum configuration for the monitoring equipment.

Further improvements will yield more informative methods of monitoring and sensing of the optical irradiation and dose of biological active atmospheric radiation from the sun and the sky.

4. Conclusions

The cost-effective portable FEO-M and professional FEO-P photometers provide precise measurements of optical energy irradiation in different spectral ranges. The devices have a high accuracy on a real time-scale, and control the irradiation dose. Alarm protection occurs during the accumulation of doses in spectral ranges used for common monitoring.

These instruments have a unique combination of functions.

The portable photometer FEO-M offers:

- measuring of optical energy irradiance;
- automatic identification of the working photodetector;
- automatic calculation of optical irradiance and dose of irradiation;
- control of time of radiant dose exposure;
- measuring of ambient temperature in the point of measurements;
- digital indication of optical irradiance, dose, time of exposure and detector temperature;
- interface transmission of data to PC for the next visualization and processing.

The professional photometer FEO-M provides:

- measuring of optical energy irradiance;
- automatic identification of the working photodetector;
- automatic calculation of optical irradiance and dose of irradiation;
- control of time of radiant dose exposure;
- measuring of ambient temperature in the point of measurements;
- setting of limits of radiant dose or time of exposure in each optical channel;
- digital indication of irradiance, dose, temperature, time of exposure, limits of radiant dose and exposure time;
- sound signalization about exceeding of set limits;
- storage of information in nonvolatile memory;
- transmission of data to personal computer for the next visualization.

The operation of these devices and their software was tested in some centres of ozone and UV irradiation. This includes the Ukrainian Hydrometeorological Research Institute (Kyiv city) and the sunniest zone in Ukraine (Crimea). The Crimea Geophysical Observatory (Kurortnoe town) was involved in this activity.

Acknowledgments
This work was done in the frame of STCU project #1556.

References

[1] Cline M.G. and Salisbury F.B., "Effect of UV radiation on leaves of higher plants". *Rad. Bot*., vol. 6, N2, p.p.151, 1966.
[2] Caldwell M.M., Teramura A.N. and Tevini M, "The changing solar ultraviolet climate and the ecological consequences for higher plants", *Trends in Ecol. and Evol*., vol. 4, p.p.363-367, 1989.
[3] Diffey B.L., "Solar ultraviolet radiation effects on biological systems", *Physics in Medicine and Biology*, vol. 36, p.p.299-328, 1991.
[4] Jenkins G.I., Christie J.M., Fuglevand G., Long J.C., and Jackson J., "Plant responses to UV and blue light: biochemical and genetic approaches", *Plant Sci*., vol. 112, p.p.117-138, 1995.
[5] Sampson B.I. and Cane J.H., "Impact of enhanced ultraviolet-B radiation on flower, pollen, and nectar production", *American Journal of Botany*, vol. 86, p.p.108-114, 1999.
[6] Barnes J. D., Paul N.D., Percy K.E., Broadbent P.P., McLaughlin C.K. and Wellbum A.R., "Effects of UV-B radiation on wax biosynthesis", In: Air Pollutants and the Leaf Cuticle . K.E. Percy, J.N. Cape, R. Jagels, and C. Simpson, eds., NATO ASI Series G, vol. 36. Heidelberg: Springer-Verlag, p.p.194-204, 1994.
[7] Garssen J., Goettsch W., de Cruize F., Slob W. and Van Loveren H., "*Risk assessment of UVB effects on resistance to infectious diseases*", Photochem. Photobiol., vol. 64, p.p.269-294, 1996.
[8] Sampson B.I. and Cane J.H., "Impact of enhanced ultraviolet-B radiation on flower, pollen, and nectar production", *American Journal of Botany*, vol. 86, p.p.108-114, 1999.
[9] Jansen M.A.K., Gaba V. and Greenberg B.M. "Higher plants and UV-B radiation: balancing damage, repair and acclimation". *Trends in Plant Sci*., vol. 3, p.p.131-135, 1998.
[10] Kondratyev K.Ya. and Varatsos C.A., "Atmospheric Ozone Variability: Implications for Climate Change", Human Health and Ecosystems. Springer, Chichester, 2000.
[11] McKinlay A.F. and Diffey B.L., "A reference action spectrum for ultraviolet induced erythema in human skin". *CIE Jornal*, vol. 6, p.p.17-22, 1987.
[12] Azizi E., Lusky A., Kushelevsky A.P. and Schewach-Millet M., "Skin type, hair colour, and freckles are predictors of decreased minimal erythema ultraviolet radiation dose". *J. Am. Acad. Dermatol.*, vol. 19, p.p.32-40, 1988.
[13] Environmental Health Criteria 160: Ultraviolet radiation.-Gewneva: WHO, 353 p.p., 1994.
[14] De Gruijl F.R. and van der Leun J.C. "Estimate of the wavelength dependency of ultraviolet carcinogenesis in humans and its relevance to the risk assessment of a stratospheric ozone depletion". *Health Physics*, vol. 67, p.p.317-323, 1994.
[15] Kimlin M.G., Parisi A.V., Wong J.C.F., "The whole human body distribution of solar erythemal ltraviolet radiation". *Proceedings of First Internet Conference on Photochemistry & Photobiology*, 1997.
[16] Parisi A., Wong J., "Actinic ultraviolet exposures to humans assessed with a dosimetric technique". *International Journal of Environmental Health Research*., vol. 9, p.p.277-284, 1999.
[17] Kerr J.B. and McElroy C.T., "Evidence for large upward trends of ultraviolet radiation linked to ozone depletion", *Science*, vol. 262, p.p.1032-1034, 1993.
[18] World Meteorological Organization, Scientific Assessment of Ozone Depletion: 1994 Global Ozone Research and Monitoring Project, Report #37, 1994.
[19] Michaels P.J., Singer S.F. and Knappenberger P.C., "Analyzing Ultraviolet-B Radiation: Is There a Trend?", *Science*, vol. 264, p.p.1341, 1994.
[20] Zerefos C.S., Bias A.F., Meleti C. and Ziomas I.C., "A note on the recent increase of solar UV-B radiation over northern middle latitudes", *Geophys. Res*. Lett., vol. 22, p.p.1245, 1995.
[21] Madronich S., McKenzie R.L., Caldwell M.M. and Bjom L.O., "Changes in ultraviolet radiation reaching the earth's surface", *Ambio*, vol. 24, p.p.143-164, 1995.
[22 Herman J.R., Bhartia P.K., Ziemke J., Ahmad Z. and Larko D., "UV-B increases (1979-1992) from decreases in total ozone", *Geophys. Res. Lett*., vol. 23, p.p.2117-2120, 1996.

[23] Bigelow D.S., Slusser J.R., Beaubien A.F. and Gibson J. H., "The USDA Ultraviolet Radiation Monitoring Program", *Bull. Amer. Met. Soc*., vol. 79, p.p.601-619, 1998.
[24] Weatherhead E.C., Tiao G.C., Reinsel G.C., Frederick J.E., DeLuisi J.J., Choi D.S. and Tam W.K., "Analysis of long-term behavior of ultraviolet radiation measured by Robinson-Berger meters at 14 sites in the United States", *J. Geophys. Res*., vol. 102, p.p.8737-8754, 1997.
[25] Long C., Miller A.J., Lee H.-T., Wild J. D., Przywarty R. C. and Hufford D., "Ultraviolet index forecasts issued by the National Weather Service", Bull. Amer. Met. Soc., vol. 77, p.p.729-748, 1997.
[26] Ozone Data for the World, Canad.Atmos.Envir.Servol., Downsview-Ontario, WMO, 1963-2000.
[27] Climate Change 2001. The Scientific Basis. Report UNEP/WMO, 2002.
[28] Proceedings of Annual Assembly of European Geophysical Society. EGS Office, Brussels, 1990-2004.
[29] NASA TOMS ozone data Web page: http://hyperion.gsfc.nasa.gov/Data_services/
[30] "Ultraviolet measuring devices". Coordination Center of CEH member states and SFRU on "Investigation in the are of biological physics", Pushchino, 1977, 84 p.p.
[31] KIPP&ZONEN, www.kippzonen.com.
[32] Brewer, http://breweruv.com.
[33] Kruglov V.V., Odinets G.S., Stolyarenko R.D., Maistrenko A.S., Smertenko P.S., Naumov V.V., Belyavskii A.V., Meknik A.S. and Hairy Sh., "Novel UV meters for UV monitoring system", in: *IRS 2000: Current Problems in Atmospheric Radiation,* A. Deepak Publishing, Hampton, Virginia, p.p.877-881, 2001.
[34] Gorbach T.Ya., Smertenko P.S., Svechnikov S.V., Bondarenko V.P., Ciach R. and Kuzma M., "SEM Observation, Photoconductivity Investigation and I-V Study of Si Structures with Patterned Morphology for Solar Irradiance Detection", *Solar Energy Materials & Solar Cells*, vol. 72, p.p.525-52, 2002.
[35] Ciach R., Dotsenko Yu.P., Naumov V.V., Shmyryeva A.N. and Smertenko P.S., "Injection Technique for Study of Solar Cells Test Structures", *Solar Energy Materials & Solar Cell*s, vol. 76/4, p.p. 613–624, 2003.
[36] Razeghi M. and Rogalski A., "Semiconductor Ultraviolet Detectors", *J. Appl. Phys*., vol. 79, p.p.7433-7473, 1996.
[37] Hamamatsu. Opto-semiconductors condensed catalog, 1999.
[38] Lansley S.P., Gaudin O., Whitfield M.D., McKeag R.D., Rizvi N. an d Jackman R.B., "Diamond deep UV photodetectors: reducing charge decay times for 1-kHz operation", *Diamond and Related Materials*, vol. 9, 2, p.p. 195-200, 2000.
[39] Badila M., Brezeanu G., Millan J., Godignon P., Locatelli M.L., Chante J.P., Lebedev A., Lungu P., Dinca G., Banu V. and Banoiu G., "Lift-off technology for SiC UV detectors", *Diamond and Related Materials*, vol. 9, 3-6, p.p. 994-997, 2000.
[40] Sukach G.A., Smertenko P.S., Shepel L.G., Ciach R. and Kuzma M., "Selective Photodetectors on the Base of GaAlAs/GaAs, GaP/GaAs, GaN/GaInN Heterostructures", *Solid State Electronics*, vol. 47, p.p.583-587, 2003.

This page intentionally left blank

EFFECTS OF UV RADIATION

This page intentionally left blank

Cell Biology and Instrumentation: UV Radiation, Nitric Oxide and Cell Death in Plants
Y. Blume et al. (Eds.)
IOS Press, 2006

Maintenance of the Plant Genome under Natural Light

Anne BRITT and Kevin CULLIGAN
Section of Plant Biology, University of California, Davis, California 95616

Abstract: Solar UV interacts with and alters a number of cellular components. Among these, DNA is perhaps the most critical and irreplaceable target. The majority of UV-induced damage takes the form of pyrimidine dimers. These lesions act both as blocks to the progression of both replicative DNA polymerases and the RNA polymerase holoenzyme. Expression of "dimer bypass" DNA polymerases may also lead to permanent changes (mutations) in DNA sequence, by inserting potentially incorrect bases opposite the lesion. Thus the excision or reversal of UV-induced damage is important both in the soma, as it is required for the maintenance of gene expression, and in the 'germline', where error-free repair pathways maintain genomic integrity. The basic mechanisms of photoreactivation and excision repair of UV-induced dimers are well understood in plants, although we would like to learn more about the tissue-specificity and environmental regulation of these important UV-protective mechanisms. Field experiments suggest that repair of UV-induced dimers is not essential to the survival of *Arabidopsis* plants, nor is the expression of the sinapic acid esters that act as natural sunscreens. However, plants that are defective in both repair and sunscreen production die within hours of exposure to natural light.

Progression through the cell cycle in the presence of unrepaired DNA damage products leads to a progressive deterioration of the genome. During S phase, persisting lesions are either miscopied or produce daughter strand gaps opposite dimers, which are difficult to repair in an error-free manner. For this reason, cells respond to persisting DNA damage by arresting the cell cycle in order to provide time prior to the initiation of S phase (G1/S arrest), the continuation of S phase (intra-S arrest) or progression into M (G2/M arrest). These DNA damage-induced cell cycle "checkpoints" are now being characterized in plants. Given the homologies between plant and mammalian damage checkpoint genes, it is likely that many aspects of cell cycle regulation by UV-induced damage are shared between plants and animals.

One UV-induced mammalian response to persisting DNA damage is the induction of programmed cell death. This actively induced apoptosis and necrosis of damaged cells leads to the inflammation observed in sunburn. The induction of cell death has two beneficial effects: the resulting bursts of radicals are thought to further stimulate the repair response of neighboring cells, and the suicide of damaged cells precludes their possible progression into cancer. Plant cells can also be killed by very high doses of UV light, in what might be a programmed response (as the genomic "laddering" characteristic of programmed cell death occurs), but it is not clear that such a response occurs under natural light. Given plants natural resistance to the lethal effects of cancer, it is possible that plants differ from mammals in this aspect of UV-response, and lack a sensitive apoptotic response to DNA damage.

Introduction

Although the stratospheric ozone layer significantly reduces UV flux at ground level, it is not, in and of itself, sufficient to reduce incident UV radiation to nonlethal levels. All living things protect themselves from solar UV-B and UV-A (320-400 nm) radiation via the production of

UV-absorbing pigments and the expression of DNA repair mechanisms designed to remove the UV-induced damage.

In the absence of effective DNA repair mechanisms, sunlight is lethal to man. This is dramatically illustrated by the hypersensitivity of patients afflicted with Xeroderma pigmentosum (XP), a heritable defect in repair of DNA damage. These patients lack the ability to perform nucleotide excision repair (described further below) a process that, in placental mammals, provides the only mechanism for the repair of UV-induced pyrimidine dimers [1]. Even indirect sunlight can induce massive sunburn in XP patients. In the absence of environmental UV, the symptoms of XP are more subtle indicating that although nucleotide excision repair is a general, nonspecific repair pathway that can remove a variety of lesions, sunlight is by far our most significant exogenous source of DNA damage.

Plants are obliged to live in the presence of sunlight. They protect themselves from UV though a variety of means. They shield meristematic tissues from light, annually dispose of photosynthetic tissues, produce UV-absorbing agents, and express a variety of DNA repair mechanisms, some specialized for the repair of UV-induced lesions. This review will focus on the mechanisms by which plants protect their genomes via the repair of UV-induced damage. DNA-damage-induced cell cycle checkpoints certainly also play an important role in maintenance of the genome, and may be involved in UV resistance. This review will also briefly cover what little we know about damage-induced cell cycle checkpoint mechanisms in plants.

1. Induction of DNA damage by UV

While UV radiation induces, to some degree, oxidatively damaged and crosslinked lesions, the predominant class of lesions induced is the pyrimidine dimer. Cyclobutane pyrimidine dimers make up the bulk of the damage (about 75% of damaged bases), with the pyrimidine (6-4)pyrimidinone dimers making up the rest. Both classes of dimers act as blocks to transcription and DNA replication. However, both classes of dimers are premutagenic lesions; although normal replicative polymerases will not progress beyond these lesions, all organisms possess specialized polymerases that can, with greatly reduced accuracy, polymerize past a dimer. These “lesion bypass” polymerases are required to complete the replication of a damaged template, but their reduced accuracy sometimes results in the formation of point mutations. Thus cells need to repair UV-induced dimers for two reasons: to restore transcription, and to restore error-free DNA replication. Although mutagenesis is certainly an important consequence of the induction of DNA damage, the effects on transcription are probably more critical to the survival of the organism. Even nonreplicating, terminally differentiated cells (such as the cells of a mature leaf) need to clear dimers away from the path of RNA polymerase.

2. Penetration of solar UV-B into plant tissue

Proteins and nucleic acids are very effective absorbers of UV and thus, while acting as targets for UV-induced damage, the epidermis can shield deeper cell layers from UV. In addition, plants produce UV- and visible-light-absorbing pigments that are highly expressed in epidermal cells. Some of these pigments (in *Arabidopsis*, the sinapic acid esters [2]) play a significant role in reducing the damaging effects of solar UV [3-6]. The degree to which

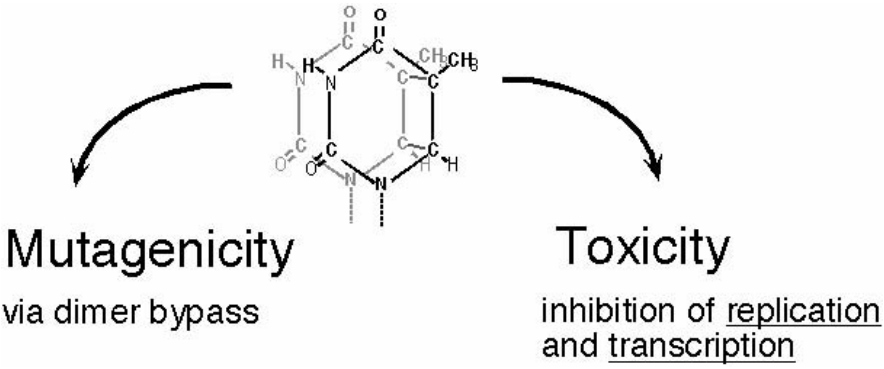

Figure 1. UV-induced DNA damage presents a challenge both to the viability of the plant (through inhibition of transcription) and to its genetic stability.

epidermal pigments (and cuticular waxes) protect the cells of the leaf mesophyll varies widely between species. Virtually no biologically effective UV-B penetrates through the epidermis of the needles of a wide variety of pines [7]. In contrast, the epidermis of many herbaceous species is not as effective an absorber of UV, with as much as 40% of the incident UV penetrating to the cells of the mesophyll [8]. Expression of UV-absorbing pigments is induced by environmental UV-B. Plants also alter their development in many ways in response to UV (reviewed in [9]); some of these responses may enhance UV resistance, while others may be symptoms of stress. Some flavonoid pigments (for instance anthocyanins), may play multiple roles in stress reduction, acting not only as UV absorbing agents [10] and antioxidants [11], but also as absorbers of visible light. This shading effect may act to protect tissues from the damaging effects of photoinhibition during the assembly of the photosynthetic apparatus in emerging leaves and during its disassembly in senescing leaves [12].

In most cases, reproductive (meristematic) tissues are tucked away and shielded from UV at least until flowering, at which point the pollen grains, but not the ova, are exposed as they emerge from the anther and make their way to the stigma. Thus it is not clear whether UV exposure during the growth of the plant contributes to the mutational load of the 'germline'. Recent studies, assaying recombination between tandem repeats, suggest that physiologically relevant exposures to UV-B can induce 'germline' mutations of this type in plants, and the full extent of solar UV-B's contribution to "spontaneous" mutation rates has yet to be established [13-15]. However, the causal links between the UV treatment and the recombination events observed remain unclear; the same types of mutations can be induced by other stresses, such as viral infection [16]. If UV-B does contribute significantly to the mutational load in the 'germline', the effect would likely be seen on a population and/or generational scale. For example, mismatch-repair defective *Arabidopsis* lines accumulate point mutations and small insertion/deletions, but are phenotypically normal within the first few generations [17]. In later generations, however, the overall fitness of the population begins to decline; a higher incidence of phenotypic abnormalities and extinctions are observed, suggesting the population is less fit. Nonetheless, the possible effects of solar UV on the long-term genetic stability of plants, and

any roles for DNA repair or damage tolerance pathways in reducing this effect, remains an open question.

3. Repair of UV-induced DNA damage I: Photoreactivation

There is no natural environment in which plants are exposed to ultraviolet radiation without also being exposed to visible light. It has long been observed that most organisms exhibit enhanced resistance to UV if subsequently exposed to visible light. This phenomenon, termed "photoreactivation" is due to the presence of a light-dependent pathway for the reversal of pyrimidine dimers. While most DNA damage products are repaired via a variety of "remove and replace" excision repair mechanisms, pyrimidine dimers are one of the few lesions that are both common and consequential enough to merit a specialized pathway for their direct reversal, through the action of photolyases.

Photolyases specifically bind to either CPDs or 6-4 dimers, but not both, as the structures of the lesions are very different. *Arabidopsis* expresses both 6-4 and CPD-specific photolyases, and one would assume that most plants possess both classes of photolyase. All photolyases are monomeric and carry 2 chromophores. A flavin cofactor (FADH-) acts as a transient electron donor to reverse the crosslink between the bases. A second chromophore acts as an antenna pigment to excite the electron donor. This antenna pigment is methenyltetrahydrofolate or 8-deazaflavin, depending on the species and enzyme, and it largely determines the action spectrum of the enzyme. Photolyases bind their cognate lesions even in the absence of light, but once a photon (in the UV-A to blue range) is absorbed, the lesion is reversed and the enzyme dissociates from the DNA [18].

Some plant photolyases are regulated by visible light, and by UV-B. *Arabidopsis* CPD photolyase activity is only detected when plants have been exposed to visible light prior to, as well as during, the period of repair [19]. This is because the transcription of the gene is regulated by white light (and by UV-B) [20-22]. However, the gene is not simply induced by light; high-level expression of both the protein and the mRNA seem to require day/night cycling. Continuous exposure to white light results in a gradual decrease in protein level over a period of several hours [21]. Similar effects, suggestive of diurnal regulation, have been observed in cucumber [23]. This induction of photolyase activity at dawn, and subsequent decrease in expression later in the day, makes sense in terms of optimizing expression in relation to UV flux. On the other hand, the 6-4 photolyase is constitutively expressed; it isn't clear why both proteins would not be regulated in the same way. The mechanism regulating expression of photolyase is still poorly understood, but a recessive UV-resistant mutant of *Arabidopsis*, *uvi1*, has been identified that does not require prior exposure to light to express the CPD photolyase [22]. This mutant appears to be upregulated for a variety of UV repair pathways, as it also exhibits an enhanced rate of dark repair of 6-4 products (see nucleotide excision repair, below). In Chlamydomonas, a second gene (*PHR1*) in addition to the CPD photolyase gene itself (*PHR2*) is required for full activity of the CPD photolyase protein [24]. Although the *PHR1* gene might represent a post-translational regulatory step, at present it appears to be a protein cofactor required for maximal CPD binding activity of the Chlamydomonas photolyase.

Work in the *Arabidopsis* seedling, in rice, and in alfalfa indicates that photoreactivation greatly enhances the rate of removal of dimers. Although in the absence of photoreactivating (blue/near UV) light dimers are slowly eliminated from bulk DNA (and 6-4 products are generally observed to be repaired more quickly than CPDs), the half life of both CPDs and 6-4

products is greatly reduced by blue light [19,25-28]. Plants grown in the presence of photoreactivating radiation will eliminate the majority of both 6-4 products and CPDs within hours, or in some cases minutes, of their induction.

The plant genomes are divided into three membrane-bound compartments, the nucleus, the plastid, and mitochondrion. The PHR2 CPD photolyase of Chlamydomonas includes a plastid targeting sequence, and is required for the repair of both the plastid and nuclear genomes. In contrast, the *Arabidopsis* and cucumber CPD photolyases lack predicted organellar targeting sequences. Whether the organellar genomes of higher plants are subject to photoreactivation is a matter of debate; although sequence-specific analysis of CPD photoreactivation in *Arabidopsis* seedlings indicated no significant photoreactivation of the organellar genomes [19], analysis of bulk DNA repair in expanding leaves, as well as the continued replication of organellar DNAs in this organ, suggests that organellar DNAs might be subject to photoreactivation [25].

4. Repair of UV-induced DNA damage II: Nucleotide excision repair

Most types of DNA damage cannot be directly reversed, but are instead excised, and the resulting gap filled using the undamaged strand as a template, resulting in error-free repair. A variety of lesion-specific glycosylases have evolved that recognize commonly occurring oxidized or alkylated bases and so initiate “base excision repair” [29]. An additional mechanism, termed nucleotide excision repair (NER), recognizes, with varying efficiencies, a wide variety of damage products. In organisms such as Humans that lack photolyase activity, NER is a critical pathway for repair of UV-induced damage. As mentioned above, in Xeroderma pigmentosum patients defective in NER, exposure to sunlight results in hospitalization, and skin cancers appear at an early age.

Plants, in contrast, possess very efficient photolyases, capable of reversing dimers within minutes to hours of their induction. However, plants also possess a nucleotide excision repair (NER) pathway that is capable of excising dimers, particularly 6-4 photoproducts. Genetic and genomic analysis indicates that the plant NER pathway is homologous to that of mammals and fungi and unrelated to the bacterial system [30-35]. However, continued classical genetic analysis has unearthed at least one additional factor required for NER in Chlamydomonas; a homolog of this gene, *rex1* is also found in higher plants, fungi, and mammals [36]. The NER pathway, illustrated in Figure 2, involves damage recognition, unwinding of the damaged DNA, binding of two distinct endonucleases to the 5’ and 3’ ends of the damaged strand, incision, removal of the damaged oligonucleotide, resynthesis using the undamaged strand as a template, and finally ligation of the resulting contiguous 5’ and 3’ ends. The coordinate actions of perhaps a dozen proteins are required to recognize damage and complete the excision step. In mammals, fungi, and bacteria, NER is at once promoted and complicated by the presence of a stalled RNA polymerase at the lesion. RNA polymerase clearly plays a role in damage recognition (damage on the transcribed strand of a transcribed region is repaired more efficiently than damage on the untranscribed strand or a nontranscribed region) [37,38], but additional protein factors are required to either push the polymerase away from the lesion or, alternatively, target it for proteolysis (to make way for repair or lesion bypass proteins) [39,40]. Transcription-coupled repair has not yet been demonstrated to take place in plants, but given its presence in bacteria, fungi, and mammals, it is quite likely that it occurs in plants too.

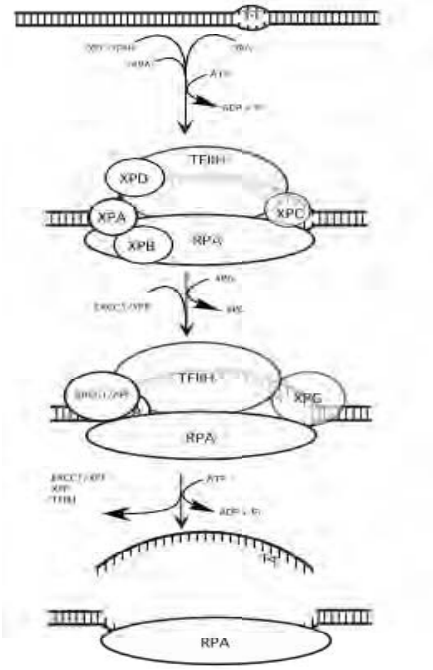

Figure 2. Nucleotide excision repair. Damage recognition and excision by NER requires the coordinated actions of approximately a dozen proteins. Damage products are bound by XPA, XPC, RPA, and TFIIH. The XPB and XPD helicases of TFIIH then act to create a "repair bubble". Guided by RPA, the 5' (ERCC1/XPF) and 3' XPG endonucleases nick the damaged strand. The damaged oligonucleotide and repair factors are removed. Finally (not shown) DNA polymerases delta/alpha accurately copy the undamaged strand and DNA ligase seals the remaining nick. In transcription-coupled repair, primary recognition is via RNA polymerase II, and does not require XPC.

The significance of NER in the repair of UV-induced damage is unclear. It is possible that NER, even in the presence of photoreactivation, plays a role in the removal of transcription-blocking dimers or of other UV-induced lesions, as at least some NER-defective mutants do exhibit a UV-sensitive phenotype even in the presence of photoreactivating light [41]. Whether NER plays any role in limiting UV-induced mutagenesis in plants remains to be determined.

5. "Damage tolerance": the repair of daughter strand gaps

Replicative polymerases are fastidious enzymes, refusing to polymerize past a noninformational lesion like a pyrimidine dimer. Stalled replication forks in turn induce cell cycle checkpoints, arresting progression through the cell cycle, and so blocking both cell division and, perhaps, the endoreduplicative cycle. In mammals prolonged arrest can result in the induction of cell death, and sunburn is a manifestation of the collective suicide of skin cells

undergoing this response to UV irradiation [42]. In haploid cells (such as yeast) permanent arrest is the genetic equivalent of death. For this reason irradiated yeast and bacteria will first respond to damage by inducing repair, and if, for some reason, repair is not completed, they will proceed into a secondary "damage tolerance" phase in which stalled DNA polymerases will be rolled back or removed from sites of damage, and a second set of more specialized and less precise polymerases upregulated to perform "dimer bypass"; the polymerization of DNA past a damaged site [43]. While all bypass polymerases, operating on damaged substrates, are less accurate than normal replicative polymerases operating on undamaged substrates, some, such as the Y-family polymerase pol eta (Rad30 in yeast, XPV in mammals) still correctly interpret many commonly encountered lesions, and thus are loosely termed "error-free" bypass polymerases [44]. Pol eta enables cells to complete DNA synthesis in spite of the persistence of DNA damage, in a relatively risk-free manner. This permits haploid cells to survive at the expense of a small risk of mutation. Loss of pol eta, in yeast, results in enhanced UV-induced mutagenesis at the UV-induced mutagenesis hotspots TC and CC, indicating that this protein acts to protect yeast from the mutagenic effects of UV [44]. XPV, the human pol eta, plays a very important role in resistance to UV-induced mutagenesis in humans [45], generally bypassing pyrimidine dimers correctly. Loss of XPV results in hypersensitivity to both the induction of sunburn (as cells actively induce death in response to persisting stalled replicative polymerases) and the induction of skin cancer (as far more error-prone polymerases step into the breach generated by the loss of pol eta), and through the induction of recombinational repair [46]).

In contrast, the Y-family polymerase encoded by the umuC and umuD genes of *E. coli* is actually *required* for UV-induced mutagenesis; defects in this gene result in the near-complete loss of UV-induced mutagenesis, but this comes at the expense of a slight increase in sensitivity to the lethal effects of UV [47]. Presumably UmuC/D is employed by *E. coli* as part of a last ditch effort to restore DNA replication at those sites (such as dimers opposite daughter strand gaps) that cannot be repaired in an error-free fashion.

The B-family error-prone polymerase zeta (whose subunits are Rev3 and Rev7 in yeast) extends mismatched primers (including those generated by other bypass polymerases) and is required for >98% of UV-induced mutagenesis in yeast [48]. *Arabidopsis* mutants defective in *atrev3* exhibit hypersensitivity to both the lethal effects of UV and its effects on DNA replication. UV-hypersensitivity was observed in the dark and under photoreactivating conditions, as well as hypersensitivity to the crosslinking agent mitomycin C, suggesting a role in the tolerance and/or repair of closely opposed or crosslinked lesions. These types of lesions cannot be directly repaired by NER, as there is no undamaged strand available to act as a template for repair replication [26].

6. Cell cycle responses to UV-induced DNA damage

UV doesn't induce mutations directly. It is the process of DNA replication, and the error-prone nature of replication past dimers, that generates mutations. In addition, replication blocks generated by dimers can induce the formation of daughter-strand gaps, and a second round of replication at these gaps can produce double-strand breaks, leading to translocations, and/or deletions. Therefore, an efficient cellular response to DNA damage requires more than just the induction of DNA repair. Cells arrest cell cycle progression in response to damage, single stranded gaps, and replication blocks, delaying entry into S-phase or mitosis. These genome-surveillance mechanisms, known as cell-cycle "checkpoints", permit the cell to repair its DNA

before progression through the cell cycle makes a bad situation worse. Although the term checkpoint suggests a particular point of inhibition, such as the transition from G1 to S-phase, a damage-induced "checkpoint" may also initiate at any point during the cell cycle at which DNA replication and/or integrity is monitored. These responses have been well characterized in yeast and mammalian systems, and are proving to be conserved in plants.

Multiple cell-cycle checkpoints can be activated throughout the process of DNA replication, including the initiation of DNA replication (G1/S), within S-phase, and at the end of DNA replication at the G2/M boundary. In many cases, these responses are activated via the same core molecular mechanisms, although the effect on cell cycle arrest and the downstream molecular players involved can be quite different, depending on the phase on the cell cycle.

Ideally, before initiating DNA replication, a cell would repair UV-induced damage generated during G1, thereby restoring the template for DNA replication. Persistence of UV-induced photoproducts could lead to the stalling of the replication fork, followed by replication restart downstream of the lesion, resulting in a daughter-strand gap. A damage product opposite a gap is no longer a substrate for excision repair, and a repair option has been lost. However, although yeast and mammalian cells do exhibit cell cycle responses to UV-irradiation in G1, there is no direct evidence that this is in response to DNA damage [49], and it is often unclear whether this arrest (measured as the delay of onset of S phase) is actually occurring at the G1/S boundary (i.e., in response to stalled replication forks rather than to UV-induced damage or repair intermediates) rather than being a true, intra-G1, response to the presence of dimers or their repair intermediates.

As cells initiate DNA replication, the replication machinery itself acts as a scanning mechanism for replication blocking agents. Stalling of a replication fork, the resulting persistence of single stranded DNA, generates a signal that globally inhibits replication origin firing, inducing both inhibition of further replication and the repair of disrupted replication forks through recombinational mechanisms [50]. This constitutes an "intra-S checkpoint". The persistence of ssDNA also blocks progression into M phase (S/M arrest), as can damage induced during G2 (G2/M arrest). Repair of these gaps prior to M phase is advantageous as there is the option for homologous recombinational repair with the fully aligned sister chromatid. Failure to repair gaps at this stage in the cell cycle will inevitably lead to either the formation of double-strand breaks or the filling of the gap by a possibly error-prone bypass polymerase. All of these responses share a requirement for the PI 3-kinase-like protein kinases ATM and ATR (and, in vertebrates, DNA PKcs) [51]. Because the functions of ATM and DNA-PKcs are to some extent DSB-specific, we will focus our discussion here on damage/replication block recognition and signal transduction by ATR [52].

Studies of the gene products involved in DNA damage-induced checkpoints in yeast or mammalian systems show that they are highly conserved in structure and function. In response to UV-induced DNA damage, the ATR-Chk1-Cdc25 pathway is primarily active, with ATR playing a central, regulatory role (Figure 3). ATR (also called MEC1 in *S. cerevisiae* and Rad3 in *S. pombe*) is a protein kinase that bridges sensing of DNA damage to downstream direct effectors of cell cycle control [50,53,54]. DNA damage is generally sensed through specific recognition of RPA-bound single-stranded DNA (ssDNA), which accumulates if replication forks are blocked, or during DNA-repair processing of damaged DNA. At least two molecular pathways are involved; one includes a PCNA-like complex of proteins called the 9-1-1 complex (for Rad9, Hus1, and Rad1), the Rad17-RFC complex, RPA (replication protein A which binds ssDNA) and ATRIP (ATR Interacting Protein), while the other consists of a more direct interaction of RPA, ATR and ATRIP with ssDNA or damaged DNA [50]). These protein interactions promote the recruitment of checkpoint signaling machinery, including ATR, into

an active state. Once active, ATR phosphorylates the protein kinase Chk1 leading to a cascade of downstream events that specifically regulate the cell cycle. For example, G2-phase phosphorylation of Chk1 leads to the inhibitory phosphorylation of cdc25. This form of cdc25 is unable to activate the mitotic promoting cyclinB/cdc2 kinase, thus blocking progression into mitosis [50,55].

In plants, the study of cell-cycle checkpoints in response to DNA damage has lagged behind that of yeast and animals, but recent progress has established the existence of such checkpoints and some of the players involved in the signal transduction pathway have been identified. Growth responses suggestive of damage-dependent cell-cycle arrest were first observed in plants as the arrest of growth following gamma-irradiation of plant seeds [56,57]. These "gamma plantlets", grown from irradiated seeds, were healthy and responded normally to environmental stimuli, but didn't produce postembryonic leaves. This suggested a regulatory effect specifically affecting dividing cells, rather than a direct toxic effect. Recent studies of *Arabidopsis* mutants defective in DNA ligase IV, which is involved in repairing DNA double

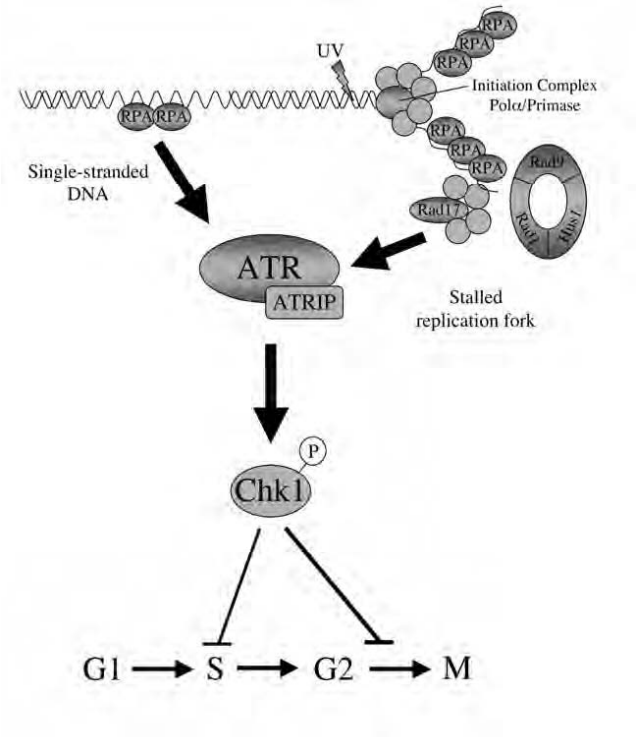

Figure 3. General overview of UV-induced cell-cycle check-point activation mechanisms. The protein kinase ATR plays a central role by bridging the sensing of ssDNA (left pathway) or stalled replication forks (right pathway) to downstream effectors of cell cycle progression. Not all of the molecular players are shown for simplicity. Phosphorylation by ATR-ATRIP of Chk1 leads to activation of direct regulators of cell cycle progression at the G1/S transition, S-phase progression, or the G2/M transition (adapted from [50]).

strand breaks, display a more pronounced gamma-plantlet effect versus wild-type plants [35, 58]. These mutants form gamma plantlets at lower doses of gamma irradiation than do wild-type plants, suggesting that the gamma arrest response is induced by persisting DNA damage (in this case double strand breaks) rather than through direct detection of radiation, or by damage to some other cellular component.

The isolation of an *Arabidopsis* mutant (termed "*sog*" for "*suppressor of gamma plantlet*") specifically defective in cell-cycle response to IR-induced DNA damage [59] indicates that this DNA damage-induced inhibition of cell-cycle progression in plants is indeed a programmed response to damage, rather than a direct effect of a compromised genome. As would be expected, although *sog* mutants are resistant to the inhibitory growth-effects of persisting IR-induced DNA damage, they are hypersensitive to its mutagenic effects.

Genes involved in damage-induced cell-cycle checkpoint pathways have also been isolated through reverse-genetic approaches. *Arabidopsis* encodes an ortholog of ATR, and recent studies have shown that this gene, like its yeast and animal counterparts, is required for G2 arrest in response to replication inhibitors [60]. Plants defective in ATR were hypersensitive to UV-B light, as measured by root growth. Furthermore, while wild-type root meristem cells displayed arrest in G2 in response to aphidicolin [60] and UV-B light (Culligan and Britt, unpublished), the *atr* mutant plants were defective in this arrest. This indicates that ATR's function as a detector of replication blocks has been conserved in plants. However, while *ATR* is an essential gene in mammals, it is not essential for plants. *atr* null homozygotes exhibit normal growth rate and full fertility [60].

Other mutants in orthologs of the ATR-dependent pathway have been described in *Arabidopsis*, such as Rad9 (of the 9-1-1 complex), Rad17 (involved in recognition of DNA damage [61]), ATM (Ataxia Telangiectasia Mutated, a paralog and functional partner of ATR) [62] and BRCA1 (breast cancer susceptibility [63]). Specific DNA damage-induced effects on the cell cycle have not yet been described in these mutants, but their DNA damaging agent hypersensitivity suggests that their role in these processes may be conserved.

Finally, plants, and other organisms, exhibit responses to UV that are unrelated to the induction of DNA damage. These may be triggered by UV receptors (analogous to other wavelength dependent developmental responses in plants) or they may be induced by damage to other cellular components.

7. Do plants exhibit an apoptotic response to DNA damage?

A further response to UV-light DNA damage in animal cells is p53-dependent programmed cell death. Plants, like fungi, lack a p53 homolog, and probably also lack the sensitive apoptotic response to UV. Given that fact that plants cannot be killed by cancer (as, even in long-lived plants, cancers cannot metastasize), there is probably no adaptive role for such a phenomenon in plants. However, very high, non-physiological doses of UV-C have been shown to induce an apoptotic-like response in *Arabidopsis* leaves, including characteristic DNA-laddering and Caspase-like activities [64,65]. In *Arabidopsis* plants defective in ATR, the replication-blocking agent aphidicolin induces an apoptotic-like response, in which the nuclei of meristematic cells first become condensed and then are lost entirely [60]. Both of these lines of evidence, particularly the laddering observed by Danon et al., suggest that a programmed cell death response to DNA damage may exist in plants. However, induction of this type of cell death in plants may require very high levels DNA damage, as DNA-repair defective mutants in *Arabidopsis*, even when challenged with exogenous DNA-damaging

agents, do not show obvious signs of apoptosis [35,66]. The response observed in the two studies cited above may represent an ordered disassembly of a hopelessly compromised cell, rather than the selective elimination of perfectly viable, but possibly precancerous, cells observed in mammals.

8. Functional significance of DNA repair in terms of plant growth

Much progress has been made in the last 15 years in understanding plant DNA repair and damage tolerance mechanisms. Given the existence of plants defective in specific repair or tolerance pathways, it should be possible to determine the relevance of these pathways to resistance to solar UV. Humans defective in nucleotide excision repair cannot survive continued exposure to sunlight. Can plants with similar defects survive under natural conditions? Are both NER and photoreactivation important contributors to survival? What about dimer bypass? Does UV-B-induced mutagenesis in the 'germline' contribute the plant population's long-term fitness? Some of these questions have been addressed in the laboratory; all of the abovementioned mechanisms contribute to UV resistance, but their relevance to growth in the field remains unclear. Plants are exquisitely sensitive to the spectral balance of light, particularly as it affects UV resistance [9,67], and it is very difficult (and expensive) to reproduce natural light balances in the growth chamber. In addition, many researchers use unnaturally intense and short-term exposures to UV to address issues of sensitivity. Given current interest in the effects of ozone depletion, it is important to understand how plants tolerate their constant exposure to UV and how adaptable they might be to elevations in ambient UV-B. If the results of these experiments are to be relevant to plant growth under natural conditions, they must be performed either in the field (with UV-absorbing filters, or carefully monitored supplemental lighting, or through changes in UV ratios generated by changes in elevation) or under very carefully controlled and monitored artificial lighting. Experiments testing the effects of natural UV on plant growth have been performed out of doors (under UV-B transparent vs. UV-B opaque filters) and results often, but by no means always, suggest that ambient UV-B does have a small but measurable effect on, for example, crop yield [3,68-71].

Results of the single "ambient UV" field study on repair defective *Arabidopsis* plants suggested that the effects of deficiencies in photoreactivation, nucleotide excision repair, or both processes were surprisingly slight [71]. In dramatic contrast to NER-defective mammals, repair defective *Arabidopsis* lines exhibited only a slightly enhanced sensitivity to solar UV-B. The effects of the *tt5* mutation, which eliminates production of flavonoid pigments, were slightly more impressive. Plants defective in *both* sunscreen biosynthesis *and* DNA repair were strikingly sensitive to solar UV-B, with obvious effects within a day of exposure to unfiltered sunlight [71]. Thus the difference between Humans and *Arabidopsis* in terms of the importance of DNA repair in resistance to the effects of ambient UV-B might be ascribed to the synthesis, in *Arabidopsis*, of very effective natural sunscreens. However, it might also be due to the fact that plants do not actively induce cell death in response to biologically relevant levels of DNA damage.

References

[1] Cleaver, J.E., "Xeroderma pigmentosum, The first of the cellular caretakers". *Trends in Biochemical Sciences*, vol. 26, 6, p.p. 398-401, 2001.

[2] Landry, L.G., C.C.S. Chapple, and R.L. Last, "*Arabidopsis* mutants lacking phenolic sunscreens exhibit enhanced ultraviolet-B injury and oxidative damage". *Plant Physiol*., vol. 109, 4, p.p. 1159-1166, 1995.

[3] Fiscus, E.L., et al., "Growth of *Arabidopsis* flavonoid mutants under solar radiation and UV filters". *Envir. & Exper. Bot.,* vol. 41, p.p. 231-245, 1999.

[4] Bieza, K. and R. Lois, "An *Arabidopsis* mutant tolerant to lethal ultraviolet-B levels shows constitutively elevated accumulation of flavonoids and other phenolics". *Plant Physiology*, vol. 126, 3, p.p. 1105-1115, 2001.

[5] Alenius, C.M., T.C. Vogelmann, and J.F. Bornman, "A three-dimensional representation of the relationship between penetration of u.v.-B radiation and u.v.-screening pigments in leaves of Brassica napus". *New Phytologist*, vol. 131, 3, p.p. 297-302, 1995.

[6] Reuber, S., J.F. Bornman, and G. Weissenboeck, "A flavonoid mutant of barley (Hordeum vulgare L.) exhibits increased sensitivity to UV-B radiation in the primary leaf. Plant". *Cell & Environment*, vol. 19, 5, p.p. 593-601, 1996.

[7] Turunen, M.T., T.C. Vogelmann, and W.K. Smith, "UV screening in lodgepole pine (Pinus contorta ssp.p. latifolia) cotyledons and needles". *International Journal of Plant Sciences*, vol. 160, 2, p.p. 315-320, 1999.

[8] Day, T.A., T.C. Vogelmann, and E. DeLucia, "Are some plant life forms more effective than others in screeening out ultraviolet-B radiation?". *Oecologia*, vol. 92, p.p. 513-519, 1992.

[9] Rozema, J., et al., "UV-B as an environmental factor in plant life, stress and regulation". *Trends Ecol. & Evol*., vol. 12, 1, p.p. 22-28, 1997.

[10] Casati, P.P. and V. Walbot, "Gene expression profiling in response to ultraviolet radiation in maize genotypes with varying flavonoid content". *Plant Physiol*., vol. 132, p.p. 1739-1754, 2003.

[11] Gould, K., J. McKelvie, and K. Markham, "Do anthocyanins function as antioxidants in leaves?". *Plant Cell Environ*., vol. 25, p.p 1261-1269, 2002.

[12] Feild, T., D. Lee, and N. Holbrook, "Why leaves turn red in the autumn. The role of anthocyanins in senescing leaves of Red-Osier Dogwood". *Plant Physiol.*, VOL. 127, p.p. 566-574, 2001.

[13] Walbot, V., "UV-B damage amplified by transposons in maize". *Nature*, vol. 397, p.p. 398-399, 1999.

[14] Ries, G., et al., "Elevated UV-B radiation reduces genome stability in plants". *Nature,* vol. 406, p.p. 98-101, 2000.

[15] Ries, G., et al., "UV-damage-mediated induction of homologous recombination in *Arabidopsis* is dependent on photosynthetically active radiation". *Proc. Natl. Acad. Sci., USA*, vol. 97, 24, p.p. 13425-13429, 2000.

[16] Kovalchuk, I., et al., "Pathogen-induced systemic plant signal triggers DNA rearrangements". *Nature*, vol. 423, p.p. 760-762, 2003.

[17] Hoffman, P.P.D., et al., "Rapid accumulation of mutations during seed-to-seed propagation of mismatch repair defective *Arabidopsis*". *Genes & Devel*., vol. 18, 21, p.p. 2627-2685, 2004.

[18] Sancar, A., "Structure and function of DNA photolyase". *Biochem*., vol. 33, 1, p.p. 2-9, 1994.

[19] Chen, J.-J., D. Mitchell, and A.B. Britt, "A light-dependent pathway for the elimination of UV-induced pyrimidine (6-4) pyrimidinone photoproducts in *Arabidopsis* thaliana". *Plant Cell*, vol. 6, 9, p.p. 1311-1317, 1994.

[20] Ahmad, M., et al., "An enzyme similar to animal type II photolyases mediates photoreactivation in *Arabidopsis*". *Plant Cell*, vol. 9, 2, p.p. 199-207, 1997.

[21] Waterworth, W.M., et al., "Characterization of Arabidopsis photolyase enzymes and analysis of their role in protection from ultraviolet radiation". J. *Exper. Bot*., vol. 53, p.p. 1005-1015, 2002.

[22] Tanaka, A., et al., "An ultraviolet-B-resistant mutant with enhanced DNA repair in Arabidopsis". *Plant Physiol*., vol. 129, p.p. 64-71, 2002.

[23] Takahashi, S., et al., "Diurnal change of cucumber CPD photolyase gene (CsPHR) expression and its physiological role in growth under UV-B radiation". *Plant Cell Physiol*., vol. 43, p.p. 342-349, 2002.

[24] Petersen, J.L. and G.D. Small, "A gene required for the novel activation of a class II DNA photolyase in Chlamydomonas". *Nucl. Acids Res*., vol. 29, 21, p.p. 4472-4481, 2001.

[25] Draper, C.K. and J.B. Hays, "Replication of chloroplast, mitochondrial and nuclear DNA during growth of unirradiated and UVB-irradiated Arabidopsis leaves". *Plant Journal*, vol. 23, 2, p.p. 255-265, 2000.

[26] Sakamoto, A., et al., "Disruption of the AtRev3 gene causes hypersensitivity to UV-B light and gamma rays in Arabidopsis, implication of the presence of a translesion synthesis mechanism in plants". *Plant Cell*, vol. 15, 9, p.p. 2042-2057, 2003.

[27] Kang, H.-S., J. Hidema, and T. Kumagai, "Effects of light environment during culture on UV-induced cyclobutyl pyrimidine dimers and their photorepair in rice (Oryza sativa L.)". *Photochemistry and Photobiology*, vol. 68, 1, p.p. 71-77, 1998.
[28] Quaite, F.E., et al., "DNA damage levels determine cyclobutyl pyrimidine dimer repair mechanisms in alfalfa seedlings". *Plant Cell*, vol. 6, 11, p.p. 1635-1641, 1994.
[29] Britt, A., "Repair of damaged bases, in The Arabidopsis Book". C. Somerville and E. Meyerowitz, Editors. 2002, American Society of Plant Biologists, Rockville, MD, 2002.
[30] Liu, Z., et al., "Repair of UV damage in plants by nucleotide excision repair, Arabidopsis UVH1 DNA repair gene is a homolog of Saccharomyces cerevisiae Rad1". *Plant J.*,vol. 21, 6, p.p. 519-528, 2000.
[31] Fidantsef, A., D. Mitchell, and A. Britt, "The Arabidopsis UVH1 gene is a homolog of the yeast repair endonuclease RAD1". *Plant Physiol*., vol. 124, p.p. 579-586, 2000.
[32] Liu, Z., J.D. Hall, and D.W. Mount, "Arabidopsis UVH3 gene is a homolog of the Saccharomyces cerevisiae RAD2 and human XPG DNA repair genes". *Plant Journal*, vol. 26, 3, p.p. 329-338, 2001.
[33] "Arabidopsis Genome, I., Analysis of the genome sequence of the flowering plant Arabidopsis thaliana". *Nature*, vol. 408, p.p. 796-815, 2000.
[34] Kunz, B., et al., "Plant genes implicated in nucleotide excision repair or translesion synthesis, in Recent Research Development in DNA Repair and Mutagenesis". M. Ruiz-Rubio, E. Alejandre-Duran, and T. Roldan-Arjona, Editors. Research Signposts Publications, Trivandrum, India. p.p. 111-139, 2002.
[35] Hefner, E.A., S.B. Preuss, and A.B. Britt, "Arabidopsis mutants sensitive to gamma radiation include the homolog of the human repair gene ERCC1". *J. Exp. Bot.*, vol. 54, 383, p.p. 669-680, 2003.
[36] Cenkci, B., J. Petersen, and G. Small, "Rex1, a novel gene required for DNA repair". *J. Biol. Chem*., vol. 278, p.p. 22574-22577, 2003.
[37] Bohr, V.A., et al., "DNA repair in an active gene, removal of pyrimidine dimers from the DHFR gene of CHO cells is much more efficient than in the genome overall". *Cell*, vol. 40, p.p. 359-369, 1985.
[38] Mellon, I., G. Spivak, and P.P.C. Hanawalt, "Selective removal of transcription-blocking DNA damage from the transcribed strand of the mammalian DHFR gene". *Cell*, vol. 51, p.p. 241-249, 1987.
[39] van den Boom, V., G.J. Jaspers Nicolaas, and W. Vermeulen, "When machines get stuck, Obstructed RNA polymerase II, Displacement, degradation or suicide". *Bioessays*, vol. 24, 9, p.p. 780-784, 2002.
[40] Woudstra, E.C., et al., "A Rad26-Def1 complex coordinates repair and RNA pol II proteolysis in response to DNA damage". *Nature*, vol. 415(6874), p.p. 929-933, 2002.
[41] Harlow, G.R., et al., "Isolation of Uvh1, an Arabidopsis Mutant Hypersensitive to Ultraviolet Light and Ionizing Radiation". *Plant Cell*, vol. 6, 2, p.p. 227-235, 1994.
[42] Guzman, E., J. Langowski, and L. Owen-Schaub, "Mad dogs, Englishmen and apoptosis, the role of cell death in UV-induced skin cancer". *Apoptosis*, vol. 8, p.p. 315-325, 2003.
[43] Goodman, M.F., ed. "Error-prone repair DNA polymerases in prokaryotes and eukaryotes". Annual Review of Biochemistry, ed. C.C.K. Richardson, Roger; Raetz, Christian R. H.; Thorner, Jeremy W. Vol. 71. 2002, Annual Reviews, Palo Alto, CA. 17-50, 2002.
[44] Yu, S.-L., et al., "Requirement of DNA plymerase eta for error-free bypass of UV-induced CC and TC photoproducts. Molec". *Cell. Biology*, vol. 21, 1, p.p. 185-188, 2001.
[45] Stary, A., et al., "Role of DNA polymerase eta in the UV mutation spectrum in human cells". *J. Biol. Chem*., vol. 278, 21, p.p. 18767-18775, 2003.
[46] Limoli, C.L., et al., "UV-induced replication arrest in the xeroderma pigmentosum variant leads to DNA double-strand breaks, gamma-H2AX formation, and Mre11 relocalization". *Proc. Natl. Acad. of Sci., USA*, vol. 99, 1, p.p. 233-238, 2002.
[47] Bagg, A., C.J. Kenyon, and G.C. Walker, "Inducibility of a gene product required for UV and chemical mutagenesis". *Proc. Natl. Acad. Sci. USA*, vol. 78, 9, p.p. 5749-5753, 1981.
[48] Lawrence, C. and R. Christensen, "UV mutagenesis in radiation-sensitive strains of yeast. III. rev3 mutant strains". *Genetics*, vol. 82, p.p. 207-232, 1976.
[49] Nilssen, E., et al., "Intra-G1 arrest in response to UV irradiation in fission yeast". *Proc. Natl Acad. Sci., USA,* vol. 100, 19, p.p. 10758-10763, 2003.
[50] Sancar, A., et al., "Molecular mechanisms of mammalian DNA repair and the DNA damage checkpoints. *Ann. Rev. Biochem*., vol. 73, p.p. 39-85, 2004.
[51] Abraham, R., "PI 3-kinase related kinases, "big" players in stress-induced signaling pathways". *DNA Repair*, vol. 3, p.p. 883-887, 2004.
[52] Shechter, D., V. Constanzo, and J. Gautier, "Regulation of DNA replication by ATR, signaling in response to DNA intermediates. *DNA Repair*, vol. 3, p.p. 901-908, 2004.

[53] Abraham, R., "Cell cycle checkpoint signaling through the ATM and ATR kinases. *Genes & Devel*., vol. 15, 17, p.p. 2177-2196. 2001.
[54] Melo, J. and D. Toczyski, "*A unified* view of the DNA-damage checkpoint". *Curr. Opin. Cell Biol*., vol. 14, 2, p.p. 237-245, 2002.
[55] O'Connell, M., N. Walworth, and A. Carr, "The G2 phase DNA damage checkpoint". *Cell Biol*, vol. 10, 7, p.p. 296-303, 2000.
[56] Haber, A.H. and D.E. Foard, "Anatomical analysis of wheat growing without cell division". *Am. J. Botany*, vol. 48, p.p. 438-446, 1961.
[57] Haber, A.H., W.L. Carrier, and D.E. Foard, "Metabolic Studies of Gamma-Irradiated Wheat Growing Without Cell Division". *Amer. J. Bot*., vol. 48, 6, p.p. 431-446, 1961.
[58] Friesner, J.D. and A.B. Britt, "Ku80- and DNA ligase IV-deficient plants are sensitive to ionizing radiation and defective in T-DNA integration". *Plant J*., vol. 34, p.p. 427-440, 2003.
[59] Preuss, S.B. and A.B. Britt, "A DNA damage induced cell cycle checkpoint in *Arabidopsis* ". *Genetics*, vol. 164, p.p. 323-334, 2003.
[60] Culligan, K.M., A. Tissier, and A.B. Britt, "ATR regulates a G2-phase cell-cycle checkpoint in *Arabidopsis thaliana*". *Plant Cell*, vol. 16, p.p. 1091-1104, 2004.
[61] Heitzeberg, F., et al., "The Rad17 homologue of *Arabidopsis* is involved in the regulation of DNA damage repair and homologous recombination". *Plant J*., vol.. 38, 6, p.p. 954-968, 2004.
[62] Garcia, V., et al., "AtATM is essential for meiosis and the somatic response to DNA damage in plants". *Plant Cell*, vol. 15, p.p. 119-132, 2003.
[63] Lafarge, S. and M. Montane, "Characterization of the *Arabidopsis thaliana* ortholog of the human breast cancer susceptibility gene 1,AtBRCA1, strongly induced by X-rays". *Nucl. Acids Res*., vol. 31, 4, p.p. 1148-1155, 2003.
[64] Danon, A. and P.P. Gallois, "UV-C radiation induces apoptotic-like changes in *Arabidopsis thaliana*". *FEBS Letters*, vol. 437, 1-2, p.p. 131-136, 1998.
[65] Danon, A., et al., "Ultraviolet-C overexposure induces programmed cell death in *Arabidopsis*, which is mediated by caspase-like activities and which can be suppressed by caspase inhibitors, p35 and Defender against Apoptotic Death". *J. Biol. Chem*., vol. 279, 1, p.p. 779-787, 2004.
[66] Riha, K., et al., "Telomere length deregulation and enhanced sensitivity to genotoxic stress in *Arabidopsis* mutants deficient in Ku70". *EMBO J*., vol. 21, 11, p.p. 2819-2826, 2002.
[67] Fiscus, E.L. and F.L. Booker, "Is increased UV-B a threat to crop photosynthesis and productivity?". *Photosyn. Res*., vol. 43, p.p. 81-92, 1995.
[68] Olszyk, D., et al., "UV-B effects on crops, Response of the irrigated rice ecosystem". *Journal of Plant Physiology*, vol. 148, 1-2, p.p. 26-34, 1996.
[69] Pal, M., et al., "Exclusion of UV-B radiation from normal solar spectrum on the growth of mung bean and maize". *Agriculture Ecosystems & Environment*, vol.61, 1, p.p. 29-34, 1997.
[70] Yuan, L., et al., "Intraspecific responses in crop growth and yield of 20 soybean cultivars to enhanced ultraviolet-B radiation under field conditions". *Field Crops Research*, vol.78, 1, p.p. 1-8, 2002.
[71] Britt, A. and E. Fiscus, "Response of *Arabidopsis* DNA repair defective mutants to solar radiation". *Physiol. Plant*., vol. 118, p.p. 183-192, 2003.

Cell Biology and Instrumentation: UV Radiation, Nitric Oxide and Cell Death in Plants
Y. Blume et al. (Eds.)
IOS Press, 2006

UV-Induced DS(SS)-DNA Damage: Optical and Electrical Recognition

Alina VELIGURA[1]., Michael KHULER[2], Wolfgang FRITZSCHE[3], Peter SCHARFF[2], Karl RISCH[2], Peter LYTVYN[4], Alexandr GORCHINSKYY[1], Eugenia BUZANEVA[1]

[1] *National Taras Shevshenko University of Kyiv, Radiophysics Department, The Scientific and Training Center "Physical and Chemical Material Science" of this University and NASU; 64, Vladimirskaya Str., 01033, Kiev, Ukraine*

[2] *Technische Universitat Ilmenau, Institut fur Physik / FG Chemie, Postfach 100565, 986884 Ilmenau, Germany*

[3] *Institute for Physical High Technology, PF 100239, D-07702 Jena, Germany*

[4] *Institute of Semiconductor Physics of National Academy of Sciences of Ukraine, Prospect Nauki 45, Kyiv, 03028, Ukraine.*

Abstract

This paper deals with UV-induced ds (ss)-DNA damage, placed in buffer solution and in wet, dry absorbed layer, using optical spectroscopy and conductivity methods. Mechanisms of UV induced ds (ss)-DNA damage are accounted of photochemical reactions of cyclobutane-pyrimidine dimer and (4-6) adduct formation. These models are based on: decreasing absorption intensity with maxima at 252 nm for ds-DNA and 256 nm for ss-DNA water solutions, and long-wave shifting of absorption maximum (252 nm) for ds-DNA water solution. The absorption spectral range of $235 < \lambda < 252$ nm is defined by absorption on T and A bases. Photoluminescence spectra of wet ds-DNA layer have maxima at 432,440 and 454, 463 nm before and after UV irradiation of 337 nm and 365 nm for one hour respectively.

The photochemical reactions appear by decreasing dry absorbed ds-DNA molecular layer with networks conductivity under periodically switched UV irradiation. As a result the conductivity decreases after the first radiation reflecting the reducing of pyrimidine bases (that formed dimers) and the contribution to ds-DNA conductivity. The increasing of conductivity after UV irradiation could be caused by a particular reparation of ds-DNA under applied voltage of 1 V. But it's important to develop methods for the further ability to direct possible photochemical reactions in ds (ss)-DNA.

1. Introduction

The main targets for UV irradiation in biological cells are DNA molecules [1]. Damaging photochemical reactions in DNA caused by UV irradiation are important for studies in cell biology. DNA in this report deals with double-stranded (ds) and single-stranded (ss) DNA.

1.1 Known mechanisms of UV induced DNA damage in cells

Based on the review of photochemical reactions in cells caused by UV irradiation [2] we chose photochemical reactions that occur in buffer solutions. When excited by UV light the nucleotide bases begin to take part in photochemical reactions of cyclobutane-pyrimidine dimer and (4-6) adduct formation.

The reactions of cyclobutane-pyrimidine dimers formation are represented in Fig. 1. They comprise 70-80 % of all UV-induced photochemical reactions. They could be reversed in cells in the presence of UV light and enzyme photolyase. Dimers form between two adjacent pyrimidines. Fig. 1 shows the thymine- thymine dimer and thymine-cytosine dimer.

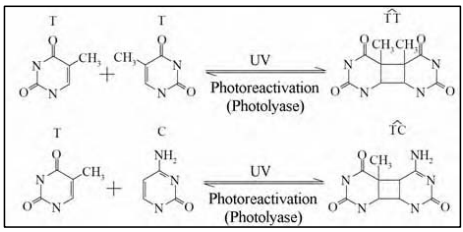

Figure 1. Formation of cyclobutane-pyrimidine dimers in DNA sites under UV irradiation. T-thymine, C- cytosine are marked.

The photochemical reaction of (4-6) adducts formation caused by a wavelength at 254 nm is represented in Fig. 2. The (6-4) products are formed at 5'-T-C-3', 5'-C-C-3', 5'-T-T-3' but not at 5'-C-T-3' sites in DNA molecule. The (6-4) products under illumination at 312 nm can transform into isomers that are not reversed and become more toxic for the cell.

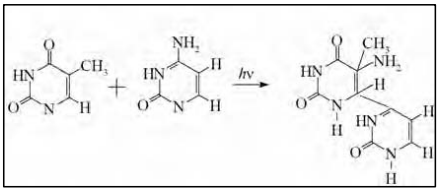

Figure 2. Formation of (6-4) adducts in DNA sites under UV irradiation (254 nm).

1.2 Absorption DNA spectrum in the range 200 - 300 nm

Characteristic two absorption bands are evident in ds-DNA water solution (Fig. 3a). They have a maxima at 208 and 256 nm caused by π-π^* transition of the nucleotide bases. Computer simulation of the absorption spectra of separate bases are shown in Fig. 3b [3].

These spectra represent an essential contribution to absorption maximum of DNA molecule (Fig. 3a) caused by electronic transition of thymine and adenine bases. Changes in bases (for example, dimers formation) could then lead to the changes in absorption intensity and shifting of absorption maxima (208, 256 nm).

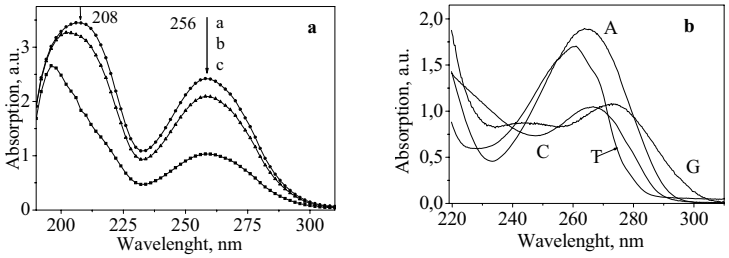

Figure 3. a) Absorption spectra of ds-DNA polymerized molecules in water solution with various ratios between DNA and water: a- 1:1, b- 1:40, c-1:50. Absorption maxima are 208 and 256 nm, correspondingly.
b)Absorption spectra of separated nucleoside bases: A-adenine, T-thymine, C- cytosine, G- guanine obtained by computer simulation.

1.3. Photoluminescence of ds-DNA molecule

For a DNA molecule the optical transitions correspond to the electron transition between energy levels of the various single bases (Fig. 3), i.e. intra-base excitations. The band gap respects the energy difference between the top of the HOMO band and the bottom of the LUMO band, which are corresponding to different bases [4].

Now we can analyze the photoluminescence spectra of DNA polymerized molecules in the layer and determine HOMO – LUMO transition [5]. Using this value we predict the types of IV characteristics of the structures with ds-DNA molecules as metal, semiconductor, and insulator [3].

1.4. Charge transport in DNA

One way to detect DNA damage and its configuration involves the investigation of DNA film conductivity in wet and dry samples. Since direct investigation of UV-induced electronic process in DNA in cells requires complicated equipment [2], mostly research is made using DNA extracted from cells or synthesized DNA molecules with fixed length and known base sequences [4, 6-8].

The choice of conductivity measurements as a sensitive method for the detecting could be based on a models of ds-DNA as a “one-dimensional electronic material” [3, 9, 10]. The π-electron overlap between the base pairs within the double helix implies that the stacked base pairs might be a one-dimensional pathway for electronic charge transport. In classical DNA structure, the bases within the double helix are oriented perpendicular to the axis of the helix and parallel to each other with separation distance of 0.34 nm along the axis of the helix [6].

The observation of 1D conductivity in ds-DNA requires aligned DNA helixes and sufficient π-electron overlap. Oriented films of a ds-DNA-surfactant complex satisfy both these criteria. The aligned double helixes separated by 4.1 nm with face to face base pair stacking and base separated by 0.34 nm [6].

The film hydration drives the base pairs into planar stacking with relatively strong π-electron overlap along the axis (wet DNA). There is relatively little information in the literature concerned specifically with the direct observation of base-pair stacking dynamics driven by water content in film [11]. The results of X-ray diffraction study of base-pair

stacking in aligned films of DNA- surfactant complex are obtained [6]. The base-pair spacing within the DNA helix are 0.41 nm when the sample is dried in air at 50% relative humidity and 0.34 nm in aqueous environment at room temperature. Dehydration of DNA (dry DNA) causes the bases to rotate from planar to edge stacking with correspondingly poor π-electron overlap.

When DNA film is not aligned (for example, DNA polymerized molecules form network [12]) the conductivity is defined by morphology of absorbed DNA molecules on a substrate (single- or multilayer films), DNA molecule conformation (wet or dry DNA) and nucleoside bases set in synthesized DNA. For such DNA layers it's necessary to account additional pathway of charge transport, for example, transport with including of barriers between adjacent molecules [3, 13]. Then contribution of charge transport on one-dimensional pathway through base stacking in single molecules could be only the part of general current film.

Besides carrying out of these wet DNA film conductivity measurements it's important to take in account the electrolysis of a buffer solution and a deposition of ions on metal contacts [14].

From 1.1, 1.2, 1.3 analyses we can assume that UV induced bases excitations and cyclobutane- pyrimidine dimer and (4-6) adducts formation in DNA molecules can leads to the changes in π-orbitals overlapping and therefore ones can be observed in changes of DNA conductivity.

On the base of analyzes in 1.1 -1.4, with the aim to reveal UV induced damage in DNA molecules, in contrast to earlier listed investigations, we studied absorbed wet ds-DNA polymerized molecules layer from networks on mica surface, using DNA polymerized molecules in pure buffer solution, and dry layer from ordered networks with added SiO_2 spheres (4.5 nm in size) [15]. These layers were dried in air (70% relative humidity) under visible light.

This study by optical spectroscopy, photoluminescence, conductivity gives the evidence that UV induced changes in ds(ss)-DNA molecules in buffer solutions and wet, dry layers are photochemical reactions with cyclobutane- pyrimidine dimer and (4-6) adducts formation and repair in applied electrical field.

2. Experimental

In experiments we used 2 mM plant ds-DNA polymerized molecules (Eris, France [11]) that were dissolved in 3 mM NaOH buffer and 2 mM ss-DNA with 15 oligonucleotides bases: 3' – CCA CCG CTG CTG AGG – 5', length 5.4 nm, wide 1 nm (Jena BioScience, Germany) were dissolved in 100 mM carbonate/bicarbonate buffer [7].We prepared ds-DNA polymerized molecules water solutions dissolving 0.1 ml of DNA in buffer solution in 1, 40, 50 ml of water showed a pH of 7.4 (the volume ratios are 1:1, 1:40, 1:50, correspondingly) and ss-DNA water solution dissolving 1 ml of DNA in buffer solution in 5 ml of water showed pH of 7.4. The solutions in quartz cuvvettes were irradiated by UV (λ = 200-400 nm) during 5-90 min with the light power 10^{20} photon/(cm^2 s).

Absorption spectra of ds (ss)-DNA solutions were recorded with a Jasco V-570 double beam spectrometer in quartz cuvettes (1 and 0.5 sm wide, respectively) in the range of 200-300 nm at T=293 K.

Photoluminescence and absorption spectra of ds-DNA polymerized molecules in tris HCl buffer (0.5 M Tris base, pH 7.6); before and after UV irradiation at 60 min (337 nm) and 90 min (200-400 nm), respectively were recorded. The solutions in quartz cuvettes were irradiated

for 60 min by impulse N^+ laser (λ = 337 nm) and 365 nm wavelength separated from mercurial lamp illumination by a filter. The laser provided impulses with a frequency at 100 Hz, long time of impulse 10 ns, power 1.3 kW, and a light-illuminated square 3 mm in diameter. Emission spectra of ds-DNA solutions were recorded with KSV-23 spectrometer with vacuum photo detector FEU- 100(300-700 nm) having the resolution 2A/mm at T=293 K. The time of recording of every spectrum was 2 min.

To obtain absorbed ds-DNA layers the prepared solution (1:50) was dropped on the insulator surface and dried in air (70% relative humidity) under visible light for 10 min. A dry layer was formed from ds-DNA with added SiO_2 spheres (4.5 nm in size) [15] with aim to absorb bonded water molecules from ds- DNA. SiO_2 spheres with a surface modified by CH chains with NH_2 end groups were used.

AFM images were studied to the characterize the morphology of the absorbed ds-DNA as a wet and dry layer on mica surface. AFM images were obtained by Digital Instruments Nanoscope IIIa. The measurements were performed at ambient condition in tapping mode to increase sensitive and resolution and to decrease the contact force between sample surface and AFM tips during surface topography measurements. The scanning was taken by a 100 μm G-scanner using an etched silicon tip with a nominal radius of curvature 10 nm [16].

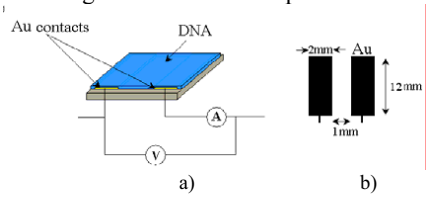

Figure 4. a- Scheme of measurements of current and voltage in Au strip-DNA-Au strip structure; b- Configuration and sizes of Au strips.

Conductivity measurements were taken for the absorbed ds-DNA layer between and on two golden strips on the insulator as shown in Fig. 4. For the wet-absorbed ds-DNA layer the measurements were carried out after 10 min. of layer preparation, and for the dry layer – after 24 h drying in the air in dark at room temperature. A typical value of the current through the layer was nanoamperes.

The current through the Au-DNA-Au structure as a function of applied voltage during 30 s was measured before and during UV irradiation. The dependence of current through the structure under fixed voltage 1 V (conductivity under fixed voltage) on the time for the periodical switched UV irradiation was investigated. Measurements were carried out on automatic complex equipment in our Lab [3].

3. Results and discussions

3.1. Recognition of UV induced changes in ds(ss)-DNA absorption and photoluminescence spectra

For the comparison of UV irradiation influence on different types of DNA sequences the experiments used ds(ss)-DNA molecules in water solutions (Figs 5,7).

3.1.1 Absorption spectra of different concentration of ds-DNA molecules in water solution. Influence of UV irradiation on ds-DNA molecule absorption

Two absorption bands with maxima at 208, 204, 196 and only at 256 nm based on π-π^* transition of nucleotide bases (Fig. 3a) are observed for different concentrations of ds-DNA molecules in water solutions. Volume ratios were ds-DNA:H_2O 1:1, 1:40, 1:50, correspondingly. A weak shift of the absorption maximum was seen at 208 nm (8 nm) with the ds-DNA molecules and decreasing concentration in water. This was caused by ds-DNA hydration in water [3]. The absorption intensity at these maxima and at others wavelengths (190-300 nm) was reduced with the decreased concentration of ds-DNA molecules in water.

Absorption spectrum of ds-DNA molecules in tris-HCl buffer (the volume ratios 1:10) in Fig. 5a has two wide absorption bands with maxima at 218 and 252 nm. Then this experiment confirms the influence of ds-DNA environment in solution on absorption spectrum, especially at band with maximum 218 nm that is sensitive to ds-DNA molecules hydration in water.

To minimize the ds-DNA molecules hydration in water we chose a tris-HCl buffer: the intensities of both maxima are comparable and the wavelength distance between them is 34 nm in comparison with water solutions 48, 52, 54 nm (1:1, 1:40, 1:50). To search for UV-induced changes in ds-DNA in water we selected ds-DNA molecules in tris-HCl buffer solution.

The influence of UV irradiation on ds-DNA absorption spectra from Fig. 5a, curves a-f revealed that the shapes of absorption curves b-e at range 235-280 nm changed. The absorption band had a maximum at 252 nm and the absorption intensity of left shoulder at $\lambda < 252$ nm reduced more essentially than for the right shoulder. The position of absorption maxima shifts from 252 to 256 nm). Changes of band shape with absorption maximum at 218 nm were caused by changes in absorption intensity of right shoulder. The saturation of changes in the absorption spectra – curve e and f are identical. This result is illustrated by dependence of ds-DNA absorption intensity (for wavelengths 252 nm) on UV-radiation time (Fig. 6 curve a). The absorption intensity doesn't change after 60, 80 min.

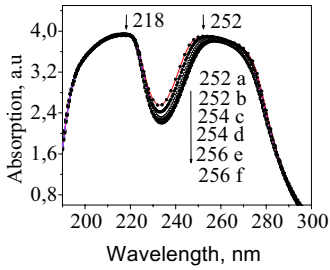

Figure 5. Absorption spectra of ds-DNA molecules in water solution before (a) and after UV irradiation: b, c, d, e, f during 15, 30, 45, 60, 90 min correspondingly

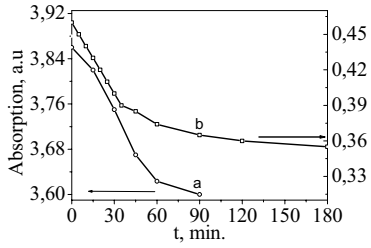

Figure 6. Absorption intensity of:
a – ds-DNA molecules at 252 nm;
b – ss-DNA molecules at 256 nm versus UV irradiation time.

Comparison of observed UV-induced shifts and intensity of ds- DNA absorption maxima with positions and intensity of nucleotide bases absorption maxima is shown in Fig. 3b. The changes of absorption intensity in the range of $235 < \lambda < 252$ nm corresponds to absorption on thymine base. Decreasing thymine's contribution to ds-DNA absorption spectrum with a long-wave shift (maximum at 252 nm nearest to the maximum) corresponded

to the adenine base. We assume that these shifts and decreasing of absorption intensity was caused by reducing nucleotide bases (T and C) number in ds-DNA sequences with the formation of cyclobutane-pyrimidine dimers and/or (4-6) adduct formation. Absorption intensity doesn't change after 60, 90 min (Fig. 6*).* We assume that this represent the time of UV- induced reactions .

On the other hand, the band in short wavelengths ($\lambda < 235$ nm) with a maximum at 218 nm is not sensitive to UV irradiation. We assume that this confirms that UV irradiation influences only the nucleotide bases.

We compared the absorption (Fig. 5a) and photoluminescence spectra (Fig. 9) of ds-DNA molecules in tris-HCl buffer solution before and after UV irradiation of 60 min (200-400 nm) and 60 min (337 nm), respectively. We observed that the absorption and photoluminescence spectra are well separated (Fig.10). The positions of the sub-bands in absorption spectra are at 253 (4.9), 265 (4.7), 274 (4.5), 285 nm (4.3 eV) and 251 (4.9), 269 (4.6), 274 nm (4.5 eV) in Fig. 7 a b, correspondingly. Comparison of spectra before and after UV irradiation revealed: a main electronic transition at 253 nm (4.9 eV) that determines the maximum absorption of DNA molecules before irradiation remains, but the value of absorption decreases over 1.5 a.u.. The transition at 265 nm (4.7 eV) shifts to 269 nm (4.6 eV), and the transition at 274 nm (4.5 eV) doesn't change. The transition at 285 nm (4.3 eV) did not appear after irradiation. The transition shift at 265 nm (4.7 eV) to 269 nm (4.6 eV) is caused by the thymine bases (Fig. 2b) that took part in photochemical reaction (Fig. 1, 2). The absence of transition at 285 nm (4.3 eV) after irradiation also confirms our results.

Photochemical reactions in the nucleotide base pairs with the formation of dimers and/or (4-6) adducts led to the change of electronic levels of the DNA molecule. This was revealed in absorption spectra (Fig. 5):

- absorption maximum at 265 nm (4.7 eV) shifts to 269 nm (4.6 eV) – this caused by additional absorption on formed dimers;
- maximum at 285 nm (4.3 eV) is absent – absorption on cytosine base becomes minimal: we assume that cytosine was used in dimer formation.

3.1.2. Absorption spectra of ss-DNA molecules in water solution. Influence of UV irradiation on ss-DNA molecule absorption

In ss-DNA absorption spectra two bands are seen with maxima are at 200 and 256 nm (Fig. 7). Differences between these absorption spectra and ds-DNA molecules spectra (Fig. 5) appear in another shape of the band with maxima over 252, 256 nm: the shoulder with maxima at 269 nm. This corresponds to the absorption of guanine, thymine bases, which number more then adenine, cytosine base number in ss-DNA (Fig. 3), is good seen.

The intensity of absorption spectra of the band with maximum at 256 nm decreases with the time of UV irradiation, but the shape of curves doesn't change. However, the weak long wave shift of left shoulder at $\lambda < 256$ nm is observed. Differences between these absorption

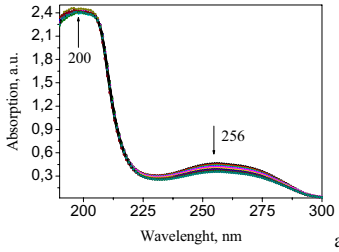

Figure 7. Absorption spectra of ss-DNA molecules in water solution in the range 190-300 nm before and during UV irradiation

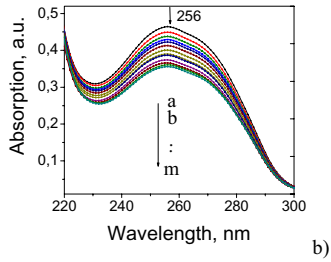

Figure 8. Absorption spectra of ss-DNA molecules in water solution in the range 190-300 nm before and during UV irradiation

spectra and ds-DNA molecules spectra, and also their UV-induced behaviour could be explained by another nucleotide bases set in ss-DNA. In this nucleotide bases set, for each ss-DNA molecule we have only 2 pairs of adjacent T and C that can form cyclobutane-pyrimidine dimer and/or (4-6) adducts (Fig. 1,2). Thus the shift of absorption maxima isn't observed and the shape of absorption band doesn't change sufficiently as and for ds-DNA.

The dependence of ds-DNA absorption intensity (for wavelengths 252 nm) on UV radiation time is represented in Fig. 6b. Almost all changes in absorption take place during first 30 min of UV radiation. In comparison with ds-DNA, this could be caused by smaller number of adjacent T and C in ss-DNA bases sequence.

The band in short wavelengths ($\lambda < 235$ nm) with maximum at 220 nm is not sensitive to UV irradiation as for ds-DNA. Our results prove that UV effect in DNA becomes apparent in excitation of nucleoside bases (absorption maxima is 235-280 nm), and photochemical reaction in DNA chains. The sensitivity of optical recognition of UV-induced DNA damage depends on nucleotide bases set in DNA molecules.

3.1.3. Photoluminescence of ds-DNA molecule

Photoluminescence and absorption spectra of ds-DNA molecules in tris-HCl buffer solution, before and after UV irradiation at 60 min (337 nm) and 60 min (200-400 nm), respectively, (Fig. 9, Fig.10 a, b) revealed the following:

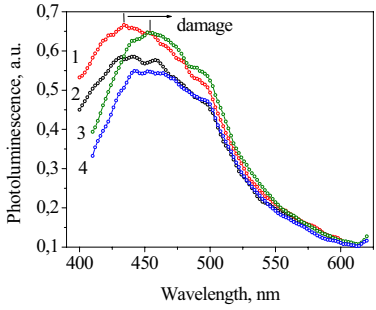

Figure 9. Photoluminescence spectra of ds-DNA polymerized molecules in tris-HCl buffer, recording with excitation λ = 337 nm (curve 1) without UV irradiation, and after UV irradiation at λ = 337 nm during 60 min (curve 2), and for next measurements (curves 3,4) with excitation λ = 365 nm before (curve 3) and after UV irradiation at λ = 365 nm during 60 min (curve 4).

These ds-DNA molecules emit light across the visible range spectrum which is broad. PL spectra ranges from 400 (3.10) to 600 nm (2.06 eV) (Fig. 9). The PL spectral ranges with these wavelengths were obtained for ds-DNA polymerized molecules in network layer absorbed on a nanostructured Si surface [5] with the intensive PL peak at 2.8 – 2.9 eV.

As seen from Fig. 1, UV induced changes in PL spectra are:

- decrease of the intensity of emission at 400-600 nm range (less decreasing of one is at 520 – 600 nm range);
- weak increase of intensity of emission at 450-500 nm range after beginning UV irradiation λ = 337 nm during 60 min and next recording of these spectra;
- narrowing of PL bands after UV irradiation because of moving the left edges of spectra to longer wavelengths range;
- the change of PL spectra shape at 400-520 nm range with more observable maxima appearance (Fig. 10).
-

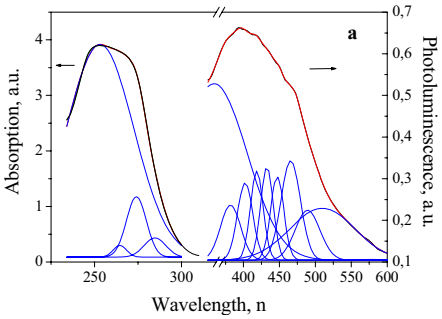

Figure 10. Photoluminescence and absorption spectra of ds-DNA molecules in tris-HCl buffer;
a – before;
b– after UV irradiation at 60 min (λ = 337 nm) and 60 min (200-400 nm), respectively. The PL was measured under impulse N^+ laser excitation (λ = 337 nm) at T= 273 K.

The UV-induced changes in PL spectra the decomposition of the photoluminescence and absorption spectra, before and after UV irradiation are shown in Fig. 10. The summation curve contains overlays on the experimentally measured spectra. Residuals are scarcely evident.

These ds-DNA polymerized molecules have the absorption and emission spectra well separated (Fig. 9). The absorption of emitted light is now week (these spectra are similar to the semiconductors polymer [17]). They have strong absorption coefficients (Fig. 3). Intensive emission is now possible through participation of electronic states corresponding to molecular orbital systems in the nucleotide base pairs [3], and sides of the ladder having a periodic structure with alternating sugar and phosphate groups [4]. Note that a part of electron levels that determine PL spectrum can correspond the formation of DNA molecular networks (Fig. 11).

From the summarized emission sub-bands for PL spectra (Fig. 10 a,b) we detected UV induced shifts of maxima positions in sub-bands (440→ 442, 454→456, 467→470 nm) forming with maxima at 437 and 452 nm (Fig. 10), and stimulating the shift of maximum at 437 → 452 nm. In Fig. 10 it's marked as damage. The destruction of sub-band with maximum at 466 nm (2.66 eV) after UV irradiation (Fig. 9, curves 3,4) was also seen.

The quantitative estimation of UV-induced changes of electronic state density can be determined from the conductivity of ds-DNA polymerized molecules in the network layer.

3.2. Recognition of UV induced damage and repair in dry and wet ds-DNA polymerized molecules in network layers from conductivity measurements.

3.2.1. Morphology of absorbed ds-DNA polymer on mica surface

Fig. 11a, b, shows the AFM images of adsorbed ds-DNA polymerized molecules in wet and dry DNA layers on a mica surface have different morphology.

The evaporation of water molecules from absorbed wet ds- DNA molecules (Fig. 11a) leads to the formation of cell-network (with average diameters from 0.4 to 1 μm). the molecules interweave with each other (Image of relief in Fig. 11). Inside the cell-network the separated ds-DNA molecules are rolled up into balls (with height from 0.5nm to 6 nm; and from 20 to 50 nm wide).

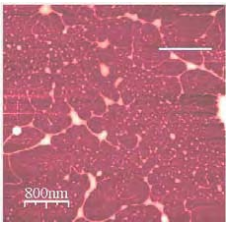

a)

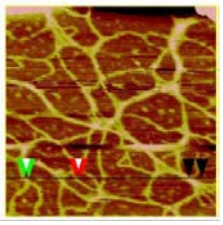

b)

Figure 11. a - AFM image of absorbed wet ds-DNA on mica surface. On a scale 4×4 μm. b - AFM image of absorbed mixture of dry ds-DNA and modified silicon on mica surface. On a scale 1×1 μm

To change the wet DNA conformation into a dry conformation, the modified SiO_2 nanoparticles were mixed with ds-DNA water solution (Fig. 11b). The absorption of water by the nanoparticles was confirmed from IR transmission spectra of the mixture. This leads to the self organization of regular networks (with cells diameters from 0.15 to 0.5 μm) around of bioactive silica nanoparticles.

The size of cells formed by DNA networks was controlled through quantity and size of silica nanoparticles without special attachment of the ds-DNA and silica nanoparticles to the mica surface. Thus DNA conformation determines the morphology of the sample. Both these factors can influence on measured conductivity.

3.2.3. Changes of dry and wet ds-DNA conductivity under periodical UV irradiation

I-V characteristics of Au- DNA-Au structures are nonlinear or near to linear if ds-DNA molecular network layers are wet or dry [3,5]. These characteristics are also nonlinear and asymmetrical for the structures with ds-DNA molecular network dried by silica spheres [15]. It's important to note that IV characteristics with values current higher 1 nA and lower 10^{-2} nA in Au strip-DNA-Au strip structure (Fig. 4) are typical for ds-DNA molecular network cells formed by ds-DNA in wisps, and by separated ds-DNA molecules, respectively (Fig. 11).

The current through the structure Au-DNA-Au (Fig. 4) under fixed voltage 1V (conductivity) versus of the time for the periodical switched UV irradiation is represented in Fig. 12 a, b. Results are different for wet and dry ds-DNA molecular network layers. For the structures with ds-DNA molecular network added dried by silica spheres including the value of

current was small (10^{-2} nA) and the similar dependence to curve in Fig. 12b were observed under bigger voltages. We do not discuss this here.

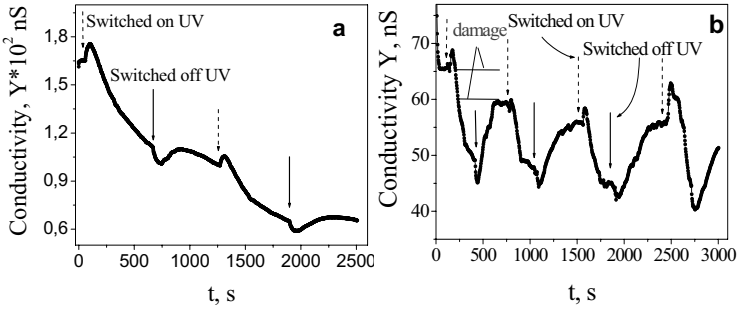

Figure 12. Typical time dependence of conductivity through the structures Au- DNA-Au under periodical UV radiation for ds-DNA molecular network layers: a – wet and b – dry.

For Au– wet DNA-Au structure with conductivity decreasing during time (Fig. 12a) the influence of periodical UV irradiation is weak. After UV was switched on for 10 min, decreasing conductivity was observed. When the UV was switched off, the conductivity value weak enhances, but the effect of applied voltage is bigger then UV irradiation influence. This leads to the main decrease of conductivity that was determined by electrolytic current from the buffer solution [7,13]. A small opposite UV-induced effect is observed in a few seconds just after each switching on or off UV irradiation. Therefore, interpretation of conductivity behaviour of Au– wet DNA-Au structure as probe for UV induced DNA damage is difficult.

The same experiment for dry ds-DNA molecular networks was carried out (Fig. 12b). In this case the electrolytic current component from buffer solution is minimized in the structure Au– dry DNA-Au. The UV radiation influence on conductivity could be easily observed. After 10 min of UV irradiation the conductivity decreases on 11.4-15 nS. The values of conductivity changes ΔY of Au- dry DNA-Au structure for different UV irradiation times are: 1st time – 15.20; 2nd time – 11.42; 3rd time – 12 nS. This is explained by the photochemical reactions that take place with nucleotide bases. The electronic structure of ds-DNA molecule changes were confirmed by results from the optical absorption and PL. The π-overlapping decreases was confirmed from observed conductivity changes.

After UV irradiation time of $\tau \approx 6$ min the saturation effect of conductivity changes is observed. In conditions of chosen UV induced DNA damage the value of conductivity change characterizes the number of nucleotide bases in DNA helix that transformed.

When UV irradiation is switched off the conductivity rises, but doesn't approach to its initial value before irradiation. The reversibility of UV induced conductivity changes in our opinion is caused by the reversibility of photochemical reactions in ds-DNA helix under applied voltage. No full reconstruction to conductivity after first UV irradiation time indicates that some photochemical reactions can lead to mutagenic changes in ds-DNA helix. The process of damage/repair is shown in the time dependence of conductivity in Fig. 12b.

4. Conclusion

This study shows that UV-induced changes in ds(ss)-DNA molecules in buffer solutions and dry layers are photochemical reactions that form cyclobutane-pyrimidine dimers and (4-6) adducts, and are repaired in an applied electrical field. Optical spectroscopy and measurements of conductivity time dependence together can be used as a sensitive method for the detecting early changes in ds-DNA structure in buffer solutions, and in dry layers exposed to damaging UV.

Acknowledgments

We are thankful to the chemist Carmen Siegmund and Dr. V. Gurin for useful discussions and recommendations on analysis of experimental results. A. Veligura is grateful to the DAAD, Germany for providing the Leonard –Euler Scholarship to carry out of this research work.

References

[1] J.Courcelle, D.J. Crowley and P.C. Hanavalt, Recovery of DNA Replication in UV-Irradiated Escherichia coli Requires both Excision Repair and RecF Protein Function*, Journal of Bacteriology*, p.p 916-922. 1999.

[2]. R.P. Sinha and D.-P. Hader, UV-induced DNA damage and repair: a review*, Photochem. Photobiol. Sci*, vol. 1, p.p 225-236, 2002.

[3]. E. Buzaneva, A. Gorchinskiy, P. Scharff, K. Risch, A. Nassiopoulou, C. Tsamis, Yu. Prilutsyy, O. Ivanuta, A. Zhugayevych, D. Kolomiyets and others, DNA, DNA/Metal Nanoparticles, DNA/Nanocarbon and Macrocyclic Metal Complex/Fullerene Molecular Building Blocks for Nanosystems: Electronics and Sensing // In Book *Frontiers of multifunctional integrated nanosystems*, Eds: Eugenia Buzaneva and Peter Scharff, NATO Science Series, II-Mathematics, Physics and Chemistry, vol.64, Kluwer Akademic Publishers, Dordrecht, Netherland, p.p. 251-276, 2004.

[4] E. Helgren, A. Omerzu, G. Gruner, D. Mihailovic, R. Podgornic and H. Grimm, Electrons on the duplex helix: optical experiments on native DNA*, Physical Review Letters*, January 20, 2003.

[5] E. Buzaneva, A.Gorchynskyy, G. Popova, A. Karlash, Y.Shtogun, K.Yakovkin, D.Zherebetskiy, O.Matyshevska, Yu. Prylutskyy, P. Scharff, Nanotechnology of DNA/nano – Si and DNA/carbon nanotubes/nano – Si chips, // In Book *Frontiers of Multifunctional Nanosystems*, Ed. E.Buzaneva and P.Scharff, NATO Science Series, Mathematics, Physics and Chemistry, vol. 57, Kluwer Academic Publishers, Dordrecht, p.p. 191–212, 2002.

[6] C.Y.D. Moses and A.J. Heeger, Base –pair stacking in oriented films of DNA-Surfactant Complex*, Advanced Materials*, vol. 15, p.p. 1364-1367, 2003.

[7] A. Csaki, P. Kaplanek, R. Moller and W. Fritzsche, The optical detection of individual DNA-conjugated gold nanoparticle labels after metal enhancement, *Nanotechnology,* vol. 14, p.p. 1262-1268, 2003.

[8] J.M. Kuhler, T.H Kirner, J. Wagner, R. Muller and W. Fritzsche, Nanopartical Reactions on Chip // In Book *Frontiers of multifunctional integrated nanosystems*, Eds: Eugenia Buzaneva and Peter Scharff, NATO Science Series, II-Mathematics, Physics and Chemistry – vol. 64, Kluwer Akademic Publishers, Dordrecht, p.p. 114-123, 2004.

[9] P.G. Schouten, Z. M. Warman, M.P. de Haas, M.A. Fox and H.L. Pan, (1991), *Nature,* vol. 353, p.p. 736-740, 1991.

[10]. Z.G. Yu and X and Song , Variable Range Hopping and Electrical Conductivity along the DNA Double Helix*, Phys. Rev. Lett*. vol. 86, p. 6018, 2001.

[11] K. Tanaka and Y. Okahata, *Am. Chem. Soc*., vol. 118, p.p. 1079-1089, 1996**.**

[12] E.V.Buzaneva, A.Karlash, K.Yakovkin, Ya. Shtogun, S.Putselyk, D.P.Zherebeskyy, A.Gorchinskiy, G.Popova, S.Prilutska, O.Matyshevska and others, DNA nanotechnology of carbon nanotube cells: physico-chemical models of self-organization and properties, Materials Science and Engineering C19, p.p. 41-45, 2002.

[13] Danny Porath, Gianaurelio Cuniberti and Rosa Di Felice, Charge transport in DNA-based Devises, *Topics in Current Chemistry,* 2004.
www-mcg.unir.de/pubs/reprints/2004_TCC_237_183.pdf.
[14] A. Rakitin, P. Aich, C. Papadopoulos, Yu. Kobzar, A. Vedeneev, J.S. Lee and J.M. Xu, Metallic conduction through engineered DNA: DNA nanoelectronic building blocks*, Phys. Rev. Letters*, vol. 86, № 16, p.p. 3670-3673, 2001.
[15] A. Veligura and A. Gorchinskiy**,** The changes of the polymerized DNA conductivity induced by the UV irradiation and addition of silicon nanoparticles , *Bulletin of the University of Kiev*, Series: Physics & Mathematics*,* vol. 4, p.p. 300-306, 2003.
[16] E. Gromozova, P. Lytvyn and V. Podgorsky, Peculiarities of Th. Terrestris spores surface ultrastructure investigated by AFM // In Book *Frontiers of Multifunctional Nanosystems*, Ed. E.Buzaneva and P.Scharff, NATO Science Series, Mathematics, Physics and Chemistry, vol.57. Kluwer Academic Publishers, Dordrecht, p.p. 341-347, 2002.
[17] I.D.W. Samuel and G.A. Turnbull, Polymer lasers: recent advances, *Materials today*, p.p. 28-35, 2004.

Cell Biology and Instrumentation: UV Radiation, Nitric Oxide and Cell Death in Plants
Y. Blume et al. (Eds.)
IOS Press, 2006

Caspase-like Activities and Programmed Cell Death Induced by UV in *Arabidopsis*

Rui HE, Vitalie I. ROTARI, Laurent BONNEAU[2] and Patrick GALLOIS[1]
Faculty of Life Sciences, University of Manchester, 3.614 Stopford Building, Oxford road, Manchester M13 9PT, UK
[2]*Université de Bourgogne, Laboratoire de Phytobiologie Cellulaire, UPRES 469, Faculté des Sciences Mirande, BP 47870, 21078 Dijon Cedex, France*

[1]Author to whom correspondence should be addressed (Tel: + 44 161 275 3922; Fax +44 161 275 3938; E-mail: patrick.gallois@manchester.ac.uk)

Abstract. UV radiation damage DNA and can trigger Apoptosis in animal cells. Using *A. thaliana* we have shown that UV radiation can induce apoptotic-like changes at the cellular level and that an UV experimental system was relevant to the study of Programmed Cell Death (PCD) in plants. UV induction of PCD requires light and a protease cleaving the caspase substrate Asp-Glu-Val-Asp (DEVDase activity) is induced within 30 minutes and peaks at one hour. This DEVDase appears related to animal caspases at the biochemical level, being insensitive to broad-range cysteine protease inhibitors. In addition, caspase1, caspase-3 inhibitors and the pancaspase inhibitor p35 were able to suppress DNA fragmentation and cell death. These results suggest that UV radiation induce a PCD in plants that is apoptotic-like. This pathway appears however to have differences when compare to the animal pathway. In particular, there is no convincing evidence that plant cell activates PCD in response to DNA damage.

Introduction

It is now clear that plants, animals and several branches of unicellular eukaryotes are using Programmed Cell Death (PCD) for defence or development mechanisms [1]. This argues for a common ancestral apoptotic system in eukaryotes. Despite this, plants seem to have evolved their own pathways to cope with plant specific features. Some cellular aspects are conserved in animals and plants such as DNA laddering, protoplast shrinkage, chromatin condensation, and others are not such as apoptotic bodies. Light dependency is another example of some forms of plant PCD. How light is required for activating cell death or for its execution is not yet clear. At the molecular level, very few conserved sequences have been identified [2].

1. Programmed cell death in plants

A very important goal is to determine which molecular components may be used in the execution of PCD in plants, which have been conserved during evolution and which are plant specific. PCD is involved in some plant pathogen interactions [3] and in normal developmental processes during the plant life cycle. For example, it plays a role in the germination of seeds, the differentiation of the tracheary elements, reproduction, flower senescence [4], and senescence [5]. Apart from the aspect of understanding eukaryotic evolution, studying PCD in plants has biotechnology applications: e.g. in the development of novel durable pathogen resistance in plants to reduce pesticide usage, for the increased

production of high added value compounds in plant cell cultures, in extended shelf-life of fresh products and in improving both food processing procedures and the quality of food and feed products.

2. Caspase-like activities in plants mediate PCD

Table1 shows up to six caspase-like activities have been detected in plants. In animals, caspases are specifically activated during PCD. In particular, caspases initiate cell death by degrading several proteins essential for cell integrity (e.g. poly (ADP-ribose) polymerase (PARP), lamins, gelsolin). Caspase activities can be measured using fluorogenic peptide substrates and can be blocked by the same peptide substrates coupled to an aldehyde. Caspase-like activities have been detected and measured in plant PCD induced during the Hypersensitive Response (HR) [6] or after a heat shock of suspension cells [7]. In support for a role of these caspase-like activities in plant PCD, experiments in tobacco showed that during PCD induced by menadione in protoplasts, caspase inhibitors could block the induction of a DNA ladder and of PARP cleavage [8]. Caspase inhibitors (Ac-DEVD-CHO or Ac-YVAD-CHO) have also been shown to block PCD after pathogen induction [6]. Thomas and Franklin-Tong ([9] showed that a caspase3-like (DEVDase) is required for PCD triggered by self-incompatibility in *Papaver* pollen. Expression of P35, a pancaspase inhibitor, has been reported to reduce the onset of apoptosis in embryonic callus in maize [10]. This protein specifically inhibits caspases in insects, nematodes and humans by blocking their active site [11, 12].

Table 1. Caspase-like activities detected in plants

Activity	Species	Reference
Caspase-1-like YVADase	Tobacco	del Pozo and Lam, (1998)
	Barley	Korthout et al., (2000)
	Arabidopsis thaliana	Danon et al., (2004)
	Picea glauca	He and Kermode, (2003)
	Tobacco (BY2)	Mlejnek and Procházka, (2002)
Caspase-3-like DEVDase	Barley	Korthout et al., (2000)
	Arabidopsis thaliana	Danon et al., (2004)
	Picea glauca	He and Kermode, (2003)
	Tobacco (BY2)	Mlejnek and Procházka, (2002)
	Avena sativa	Coffeen and Wolpert, (2004)
	Tobacco (BY2)	Tian et al., (2000)
	Norway spruce	Bozhkov et al., (2004), Suarez et al., (2004)
	Papaver	Thomas and Franklin-Tong, (2004)
Caspase-6-like VEIDase	*Arabidopsis thaliana*	Rotari and Gallois, (2005)
	Norway spruce	Bozhkov et al., (2004)
Caspase-8-like (saspase) IETDase	*Arabidopsis thaliana*	Rotari and Gallois, unpublished
	Avena sativa	Coffeen and Wolpert, (2004)
Saspase VKMDase	*Avena sativa*	Coffeen and Wolpert ,(2004)
TATDase	Tobacco Xanthi,	Chichkova et al., (2004)

More recently, it was shown that transgenic tomato plants bearing the p35 gene were protected against AAL-toxin-induced death and pathogen infection, confirming that p35 can suppress PCD in plants [13]. We have shown that both synthetic caspase inhibitors and p35 block PCD induced by UV radiation in *A. thaliana* [14]. These results provide convincing arguments to suggest that caspase-like activities in plants mediate cellular changes that are observed after induction of PCD. In addition, the inhibitory effect of various inhibitors suggests that there are several different activities/proteases required for the PCD process.

3. Metacaspases do not have DEVDase activity

Sequencing of the *Arabidopsis* genome is now complete, and has revealed that four hundred and eighty eight proteases are encoded [15]. However, none of these are obvious caspase homologues. It has been proposed that plant metacaspases are homologous and functionally equivalent to animal caspases [16].

Metacaspases are a family of nine genes in *Arabidopsis*, [17]. Like caspases, the metacaspases are cysteine proteases that contain a cysteine/histidine catalytic diad. In addition, caspases contain two conserved regions, which form the p20 and p10 subunits. These regions can be cleaved either by another caspase or by autoprocessing, and then form the active caspase heterotetramer with a second caspase dimer. Similar p20 and p10-like regions have been identified in metacaspases.

The metacaspases can be classified into two groups. Type I metacaspases (Atmc1-3) possess a proline rich pro-domain with a zinc finger motif, and have short linker sequence between p20 and p10-like subunits. Type II metacaspases (Atmc4-9) do not have a pro-domain, and have a much longer linker sequence. Initial studies by Madeo et al. ([18] and Suarez et al. ([19] suggested that metacaspases had a caspase 6-like activity (VEIDase). However, the evidence presented was indirect and metacaspases could in fact activate the VEIDase without having this activity themselves.

Expression of metacaspases as recombinant proteins in *E.coli* have demonstrated that metacaspase 9 requires cysteine-dependent autocatalytic processing for activation, however unlike caspases which show specificity towards aspartate at the P1 cleavage site on a target, metacaspases 1, 4, 5 and 9 showed arginine/lysine specificity [17, 20].

In our work using antibodies against AtMTC4, 6 and 8, western analysis of caspase-like purified fractions showed no cross reaction, suggesting that these metacaspases were absent from the fractions studied [21]. In addition, the detected size using biotinylated substrates does not match the predicted size of the metacaspase full size protein or sub-units, although post-translational modifications might account for that. These evidences suggest that the metacaspases are not responsible for the caspase-like activity in plants, although not all have been studied. In conclusion, cloning metacaspases is not an alternative to caspase-like activity purification.

4. Known proteases with caspase-like activity

There are three proteases identified in plants so far that display a bona-fide caspase-like activity. [22] have purified and characterised 2 serine proteases associated with PCD in *Avena sativa* that exhibit a caspase 6-like activity (VKMDase). The Hara-Nishimura lab has shown that the protease VPE- has a caspase-1 activity (YVADase) [23, 24]. No isolated protease has so far shown a clear DEVDase activity.

5. UV overexposure induces apoptotic-like changes in *Arabidopsis*

We have shown that a UV-C stress induces apoptotic-like changes in *Arabidopsis* seedlings and protoplasts. These include detection of a DNA ladder, changes in nucleus morphology (crescent shape) and nucleus fragmentation. In protoplasts, DNA fragmentation was detected using the TUNEL reaction and correlated with the onset of cell death measured using a vital dye [14]. UV-C radiation has often been used to study various physiologically relevant responses to DNA damage, and in particular, it has been shown to induce apoptosis in animal cells [25]. UV radiation can damage many aspects of plant processes at the physiological and DNA level [26] and our study showed that this cellular damage can trigger a PCD in response [27].

We have recently published [14] that UV induction of PCD requires light. Light is also required for the induction of cell death in a number of lesion mimic mutants in *Arabidopsis* lsd1 [28] acd11 [29],or in maize, lls1 [30] Light is also required for PCD induced by the mycotoxin fumonisin B1 [31]. We published as well that the pancaspase inhibitor p35 was able to suppress DNA fragmentation and cell death measured using Evans blue. To go into more details, we showed that a caspase-1 inhibitor (YVAD) and a caspase-3 inhibitor (DEVD) could suppress PCD. These results suggested that a protease cleaving the substrate Tyr-Val-Ala-Asp (YVADase activity) and a protease cleaving the substrate Asp-Glu-Val-Asp (DEVDase activity) are possibly mediating DNA fragmentation during plant PCD induced by UV overexposure.

These findings confirm that UV-induced cell death is a form of PCD [14].

The caspase activities detected could have been due to a non-specific cleavage of caspase substrates by cysteine-proteases such as papain or legumain. Cysteine proteases of the papain family are associated with PCD induced using H202 in soybean cells [32] and are also induced in tracheary element differentiation in *Zinnia elegans* [33]. Legumain, another family of cysteine proteases, are expressed in senescent tissue of *A. thaliana* [34]. In addition, legumain can cleave the caspase-1 substrate Ac-YVAD-AMC [35]. Results from the Hara-Nishimura lab suggest that the YVDase could be a VPE (Vacuolar Processing Enzyme of the legumain family) [23]. In our experimental system, we have evidence that the DEVDase activity detected is not due to unspecific substrate cleavage by legumain or papain because the latter activities are down regulated after UV treatment and by contrast, the DEVDase is up regulated. Moreover, E64 inhibits the papain activity but not the DEVDase detected. Legumain or papain can also be separated from DEVDase using purification steps. Finally, leupeptin, pepstatin and E64 do not inhibit animal caspase and do not inhibit the DEVDase activity in our assay. The DEVDase therefore behaves biochemically as an animal caspase (Rotari and Gallois unpublished).

Although we observed a correlation between caspase-1 or caspase-3 activities and DNA fragmentation in *Arabidopsis*, the process involved may not mirror what happens during animal apoptosis but correspond to some alternative pathway to be discovered.

6. Characterisation of caspase-like activities

The data above were a good starting point for caspase-like activity purification in plants. There are three main activities that we can now detect: VEIDase/IETDase, YVADase and DEVDase. We characterised these activities in various assay buffers, for their pH optimum stability in increasing salt concentration and inhibition using various inhibitors. Several chromatographic techniques in various combinations were tested for binding of caspase-like activities. We have now designed protocols to purify these activities that we can separate

using different chromatographic media. The purifications were followed in the fractions by activity assays as well as by western analysis using affinity labelling with biotinylated caspase inhibitors. ECL detection showed there are 3 to 4 band that interacted with biotin-VAD-fmk and biotin-DEVD-fmk. The most advance purification is the one for the DEVDase. Remarkably, there is an increase in specific DEVDase activity after two purification steps. This could be due either to its activation during purification, as in the case of caspase-1 [36], or to the removal of an endogenous inhibitor during purification.

7. A metacaspase type II correlates with PCD induced by UV

Using RT-PCR and gene specific primers, we analysed the transcription of the 9 metacaspases (AtMTC1 to 9) that are present in the *Arabidopsis* genome. The most striking result was that one transcript level was increased 120 fold after induction of PCD using UV-C. We carried out yeast complementation experiments that showed that *Arabidopsis* Type II metacaspases could complement a yeast metacaspase (YCA1) KO and restore PCD upon addition of H2O2. This shows a conservation of metacaspase function between yeast and plants. Our current hypothesis is that metacaspases are part of a network comprising proteases with canonical caspase activities.

8. Conclusion

DNA damage induced by UV can trigger apoptosis in animal cells. The DNA damage caused by UV radiation is detected by specific proteins and depending of the outcome of repair the cell make the decision either to resume division or to trigger self-destruction via an apoptotic pathway. P53 is an extensively characterised protein that is a key to the decision to live or die. P53 can trigger death by modifying the balance of two mammalian apoptosis regulators: Bcl2 and Bax [37]. Using *A. thaliana,* we have shown that UV radiation can induce apoptotic-like changes at the cellular level and that an UV experimental system was relevant to the study of Programmed Cell Death (PCD) in plants.

The sequence of the genome of *Arabidopsis* reveals however that P53, Bcl2 and Bax are absent, suggesting that those genes are metazoan 'inventions'. A convergent point between UV-induced cell death in animal and plants is that in plants a protease cleaving the caspase substrate Asp-Glu-Val-Asp (DEVDase activity) is induced within 30 minutes and peaks at one hour. This DEVDase appears related to animal caspases at the biochemical level, being insensitive to broad-range cysteine protease inhibitors. In addition, caspase1, caspase-3 inhibitors and the pancaspase inhibitor p35 were able to suppress DNA fragmentation and cell death. These results suggest that UV radiation induce a PCD in plants that is apoptotic-like. This pathway appears however to have differences when compare to the animal pathway. In particular, UV induction of PCD requires light. We can measure that UV induces DNA damage in our experimental system. However so far the DNA repair mutants tested did not show evidence that a DNA damage pathway is implicated.

References

[1] Ameisen JC, *On the origin, evolution, and nature of programmed cell death: a timeline of four billion years.* Cell Death and Diff, 2002. **9**: p. 367 ± 393.

[2] Danon, A. and P. Gallois, *UV-C radiation induces apoptotic-like changes in Arabidopsis thaliana.* FEBS Lett., 1998. **437**: p. 131-136.

[3] Lam, E., D. Pontier, and O. del Pozo, *Die and let live - programmed cell death in plants.* Curr Opin Plant Biol, 1999. **2**(6): p. 502-7.
[4] Pennell, R.I. and C. Lamb, *Programmed cell death in plants.* Plant Cell, 1997. **9**: p. 1157-1168.
[5] Delorme, V.G., et al., *A matrix metalloproteinase gene is expressed at the boundary of senescence and programmed cell death in cucumber.* Plant Physiol, 2000. **123**(3): p. 917-27.
[6] del Pozo, O. and E. Lam, *Caspases and programmed cell death in the hypersensitive response of plants to pathogens.* Cur Biol, 1998. **8**: p. 1129-1132.
[7] Tian, R.-H., et al., *Involvement of poly(ADP-ribose) polymerase and activation of caspase-3-like protease in heat shock-induced apoptosis in tobacco suspension cells.* FEBS Lett, 2000. **474**: p. 11-15.
[8] Sun, Y., et al., *Cytochrome c release and caspase activation during menadione-induced apoptosis in plants.* FEBS Lett., 1999. **462**: p. 317-321.
[9] Thomas, S.G. and V.E. Franklin-Tong, *Self-incompatibility triggers programmed cell death in Papaver pollen.* Nature, 2004. **429**(6989): p. 305-9.
[10] Hansen, G., *Evidence for Agrobacterium-induced apoptosis in maize cells.* Mol Plant-Microbe Interact, 2000. **13**: p. 649-657.
[11] Bump, N.J., et al., *Inhibition of ICE family proteases by baculovirus antiapoptotic protein p35.* Science, 1995. **269**: p. 1885-1888.
[12] Bertin, J., et al., *Apoptotic Suppression by Baculovirus P35 Involves Cleavage by and Inhibition of a Virus-Induced CED-3/ICE-Like Protease.* J. of Virology, 1996. **70**: p. 6251-6259.
[13] Lincoln, J.E., et al., *Expression of the antiapoptotic baculovirus p35 gene in tomato blocks programmed cell death and provide broad-spectrum resistance to disease.* Proc Natl Acad Sci USA, 2002. **99**: p. 15217-15221.
[14] Danon, A., et al., *Ultraviolet-C overexposure induces programmed cell death in Arabidopsis, which is mediated by caspase-like activities and which can be suppressed by caspase inhibitors, p35 and Defender against Apoptotic Death.* J Biol Chem, 2004. **279**: p. 779-787.
[15] van der Hoorn, R.A. and J.D. Jones, *The plant proteolytic machinery and its role in defence.* Curr Opin Plant Biol, 2004. **7**(4): p. 400-7.
[16] Uren, A., et al., *Identification of paracaspases and metacaspases: two ancient families of caspase-like proteins, one of which plays a key role in MALT lymphoma.* Mol Cell., 2000. **6**: p. 961-7.
[17] Vercammen, D., et al., *Type II metacaspases Atmc4 and Atmc9 of Arabidopsis thaliana cleave substrates after arginine and lysine.* J Biol Chem, 2004. **279**(44): p. 45329-36. Epub 2004 Aug 23.
[18] Madeo, F., et al., *A caspase-related protease regulates apoptosis in yeast.* Mol Cell, 2002. **9**: p. 911-917.
[19] Suarez, M.F., et al., *Metacaspase-dependent programmed cell death is essential for plant embryogenesis.* Curr Biol, 2004. **14**: p. R339-R340.
[20] Watanabe, N. and E. Lam, *Recent advances in the study of caspase-like proteases and Bax inhibitor-1 in plants: their possible roles as regulators of programmed cell death.* Mol Plant Path, 2004. **5**: p. 65-70.
[21] Rotari, V.I., R. He, and P. Gallois, *Death by proteases in plants: whodunit.* Physiol. Plant., 2005. **123**(4): p. 376-385.
[22] Coffeen, W.C. and T.J. Wolpert, *Purification and characterization of serine proteases that exhibit caspase-like activity and are associated with programmed cell death in Avena sativa.* Plant Cell, 2004. **16**: p. 857-873.
[23] Hatsugai, N., et al., *A Plant Vacuolar Protease, VPE, Mediates Virus-Induced Hypersensitive Cell Death.* Science, 2004. **305**(5685): p. 855-858.
[24] Nakaune, S., et al., *A Vacuolar Processing Enzyme, {delta}VPE, Is Involved in Seed Coat Formation at the Early Stage of Seed Development.* Plant Cell, 2005. **17**(3): p. 876-87.
[25] Kulms, D. and T. Schwarz, *Molecular mechanisms of UV-induced apoptosis.* Photodermatol Photoimmunol Photomed, 2000. **16**(5): p. 195-201.
[26] Jansen, M., V. Gaba, and B. Greenberg, *Higher plants and UV-B radiation: balancing damage, repair and acclimation.* Trends Plant Sci., 1998. **3**: p. 131–135.
[27] Danon, A. and P. Gallois, *UV-C radiation induces apoptotic-like changes in Arabidopsis thaliana.* FEBS Letters, 1998. **437**: p. 131-136.
[28] Rusterucci, C., et al., *The disease resistance signaling components EDS1 and PAD4 are essential regulators of the cell death pathway controlled by LSD1 in Arabidopsis.* Plant Cell, 2001. **13**(10): p. 2211-24.
[29] Brodersen, P., et al., *Knockout of Arabidopsis accelerated-cell-death11 encoding a sphingosine transfer protein causes activation of programmed cell death and defense.* Genes Dev, 2002. **16**(4): p. 490-502.
[30] Gray, J., et al., *Light-Dependent Death of Maize lls1 Cells Is Mediated by Mature Chloroplasts.* Plant Physiol, 2002. **130**(4): p. 1894-907.

[31] Asai, T., et al., *Fumonisin B1-induced cell death in arabidopsis protoplasts requires jasmonate-, ethylene-, and salicylate-dependent signaling pathways.* Plant Cell, 2000. **12**(10): p. 1823-36.
[32] Solomon, M., et al., *The involvement of cysteine proteases and protease inhibitor genes in the regulation of programmed cell death in plants.* Plant Cell, 1999. **11**: p. 431-443.
[33] Minami, A. and H. Fukuda, *Transient and specific expression of a cysteine endopeptidase associated with autolysis during differentiation of Zinnia mesophyll cells into tracheary elements.* Plant Cell Physiol, 1995. **36**: p. 1599-1606.
[34] Kinoshita, T., et al., *Vacuolar processing enzyme is up-regulated in the lytic vacuoles of vegetative tissues during senescence and under various stress conditions.* Plant J, 1999. **19**: p. 43-53.
[35] Rotari, V.I., P.M. Dando, and A.J. Barrett, *Legumain forms from plants and animals differ in their specificity.* Biol Chem, 2001. **382**: p. 953-959.
[36] Thornberry, N.A., *Interleukin-1 beta converting enzyme.* Methods Enzymol, 1994. **244**: p. 615-31.
[37] Zamzami, N. and G. Kroemer, *p53 in apoptosis control: an introduction.* Biochem Biophys Res Commun, 2005. **331**(3): p. 685-7.

Cell Biology and Instrumentation: UV Radiation, Nitric Oxide and Cell Death in Plants
Y. Blume et al. (Eds.)
IOS Press, 2006

Plant Phenolic Metabolites as Antioxidants and Mutagenesis Inhibitors

Adam MATKOWSKI
Dept Pharmaceutical Biology and Botany, Medical University in Wroclaw
Al. Jana Kochanowskiego 10, 51-601 Wrocław, Poland

Abstract. Plant secondary metabolites are involved in versatile functions on different levels in the plant organism. One of the roles is scavenging of free radicals and the protection against excess oxidation caused by UV irradiation, chemical oxidants or pathogen attack or other kinds of stress. Involved are phenolic compounds from different classes such as numerous phenol carboxylic acids, hydroxylated flavonoids such as flavones, flavonols, anthocyanins, procyanidins and isoflavonoids. Many of these substances have been isolated from plant species possessing valuable and intensively studied medicinal properties.

For assessment of the free radical scavenging and antioxidant capacity of phenolic complexes in plants the chemical *in vitro* (cell free) tests can be used for their relative simplicity and sometimes reasonable cost. Here, we will report the application of several antioxidant and anti-free radical spectrophotometric assays for testing the antioxidant abilities of some rarely studied plant species containing different classes of polyphenols. In addition, the antimutagenic bacterial assays were used to examine the in vivo genoprotective activity of these compounds against chemical mutagens. Among the investigated compounds there are lipophilic flavones from *Scutellaria baicalensis* and Iridaceae-type isoflavonoids from *Belamcanda chinensis*. Phenolic acids, procyanidins and flavonols containing Lamiaceae species such as *Leonurus cardiaca*, *Lamium sp*., *Stachys betonica*, *Marrubium vulgaris*, *Galeopsis tetrahit* have been also studied to comprise wider spectrum of different types of polyphenols. The antimutagenic activity of the extracted phenol complexes and isolated compounds correlates with free radical scavenging. In the Ames bacterial assays the direct mutagenesis by chemical mutagens can be distinguished from the mutagenesis induced by activation of pro-mutagen with cytochrome P-450 enzymatic microsomal fractions. Free radical scavenging by the low molecular weight compounds can play an important role as the last line of defense against oxidative damage of the cells for they are more stable than enzymatic antioxidant apparatus and can be easily accumulated in stress conditions (e.g. deposited in the cell wall or the vacuole). Superoxide scavenging can protect the cells against the production of deleterious peroxynitrite upon reaction of the relatively harmless superoxide with an important signaling molecule - nitric oxide. The *in planta* function of the antioxidant and antigenotoxic compounds should be further explored in order to obtain the complete insight into their role in protecting the plant cell.

1. Plant Phenolic Compounds

Plants make and accumulate a variety of phenolic secondary metabolites. Phenolics can be generally described as the compounds consisting at least one aromatic C-6 ring substituted with one or more hydroxyl moieties. Although the phenolic structure is widespread among the compounds from various chemical groups and metabolic pathways, such as amino acids or isoprenoids, plant phenolics (or polyphenols) are typically referred to as the compounds

that can be derived from cinnamic or benzoic acid (which themselves are of course not included in this group).

Plant phenolics include an immense variety of chemical structures that can be customarily divided into several main groups , p.p. free phenols, phenolic acids (phenol carboxylic acids), coumarins, phenol alcohols, aldehydes, flavonoids, stilbenes, xanthones, tannins, lignans and lignin. Other metabolites can also contain phenolic groups and these include sterols, quinones (in hydroquinone form), cannabinoids, alkaloids. Most phenolic compounds can be glycosylated with a variety of sugars and their derivatives. Each of the mentioned groups can be closely interrelated in the complex metabolic networks sharing common intermediates and biosynthetic enzymes as well as similar functions in the plant. The knowledge of the function of different groups of phenolics in general as well as of particular compounds has been intensively accumulating for decades but is still not complete. Below we list the proven or putative functions of different types of phenolic compounds in plants , p.p.

1.1. Pigmentation

Colors of different organs can be brought about by polyphenols belonging to flavonoids (anthocyanins, aurones, flavones, chalcones) or xanthones. These compounds give a variety of colors to flowers for attracting pollinators. The colors by anthocyanins can range from pink or red through mauve to dark purple and blue. The blue colored flowers usually contain complexes of anthocyanins, flavones and metal ions [1]. The ultraviolet absorbing colorless flavonoids are also found in white flowers where they serve as guides for pollinating *Hymenoptera* [2]. Many reddish or purple fruits are also pigmented by anthocyanins. That is also thought to attract animals that help to disseminate the propagules.

1.2. Interspecific communication.

The symbiotic non-plant organisms use flavonoid signals for recognition of the host-plant as for instance in rhizobia infection in legumes. Here, the Nod factor in different rhizobia strains can be activated by isoflavonoids or the flavone luteolin [3]. In ectomycorrhiza, the mycobiont is attracted by the rhizospheric exudates containing rutin [4]. Allelopathy is another example of the interaction in which the phenolic compounds are involved. Phenolic acids inhibit germination, root development and mineral uptake [5] and epicatechin released by the roots of *Centaurea maculosa* inhibits growth and germination of other species [6]. In allelopathy, the complex mixtures of phenolic and non-phenolic compounds such as abscisic acid or other isoprenoids are likely to act synergistically, because usually the inhibitory concentration of each compound, especially phenolic, is less likely to be available in nature [7, 8].

1.3. Defense and resistance

Phenolics can play a role in both plant immune response signaling and as direct anti-pathogen chemicals. The benzoic acid derivative – salicylic acid (SA) is a recognized signaling molecule in stress responses including pathogen attack [9, 10]. Phytoalexins are antipathogen molecules produced in plants either constitutively or in response to the infection. Upon treatment with a biotic elicitor, the phenolic biosynthesis is intensively upregulated and their composition is frequently modified [11]. The typical anti-microbial compounds are isoflavonoids, especially pterocarpans, a stilbene – resveratrol, but also a number or other polyphenols, described abundantly in the phytopharmacological literature

[1, 12, 13]. Antifeedant properties towards herbivore insects and mammals are attributed to tannins and flavonol glycosides [1].

1.4. Structural

Lignins which are polymerized phenols derived from such compounds as coniferyl or sinapyl alcohols reinforce the cell walls in woody plants. Phenolic acids bound to the cell walls are also involved in regulation of developmental processes such as embryo maturation [14]. The ability of phenols to cross-linking the cell wall polymers contributes also to strengthening of the tissues and organs. The accumulation of phenols, also in oxidized forms, as well as their deposition in cell walls is associated with the senescence and cell death and has been considered a big obstacle in plant tissue culture.

1.5. Hormonal regulation

Flavonoids can also serve as the regulators of auxin action. Data available from developmental, biochemical and genetic studies suggest the role of endogenous polar auxin transport inhibitors performed by flavonols [15, 16]. In *Arabidopsis thaliana* mutants lacking the activity of flavonoid biosynthesis enzymes, the phenotypes suggesting the increased auxin transport are observed that can be reversed by feeding with appropriate precursors. The aforementioned flavonols can displace the synthetic auxin efflux inhibitor NPA (1-*N*-naphtylphtalmic acid) from the membrane binding sites, therefore indicating the mode of their action in retention of auxins in the plant cell [16]. During rhizobia nodulation in white clover, the flavonoids turned up to regulate the auxin breakdown by peroxidase and 7,4'-dihydroxyflavone inhibited, while an isoflavone formononetin accelerated peroxidase activity [17].

1.6. UV and excessive light – shield

Hydroxylated aromatic compounds absorb strongly the UV radiation of different wavelengths depending on their structure. This ability is employed by the plants for the protection of inner tissues against excessive irradiation. Phenolics contained in the cuticle can screen the leaves from incident UV and possibly also convert some energy to visible light as a result of UV excited fluorescence. However, the real significance of the fluorescence in utilization of the excessive UV is uncertain. Similarly, the UV absorbing compounds associated with the epidermal cell walls contribute to the protection of internal tissues. The induction of secondary metabolites by UV irradiation has been reported many times [18-22] and for a number of species including the model plant *Arabidopsis thaliana. Arabidopsis* mutants deficient in phenolic acids and flavonoids are oversensitive to UV-B. The deficiency in flavonols caused sensitivity to high doses of UV, whereas the mutants lacking both flavonols and phenolic acids were highly damaged by lower intensity irradiation [23]. The interspecific variation in the protection strategies with respect to UV absorbing phenolics has been shown in three *Vaccinium* species [24]. The deciduous *V. myrtillus* and evergreen *V. vitis-idaea* differed in the absorption spectrum and in the reaction to UV irradiation. In the deciduous species the soluble phenolics were predominant, distributed more uniformly in the leaf tissues, whereas in the evergreen species, the phenolics were bound to the cell wall and located mainly in the epidermal layer. In the third species *V. uliginosum*, which has seasonal, but more robust foliage and similar to *V. vitis-idaea* leaf anatomy, the response was intermediate. The differential adaptation can reflect the complementary mechanisms in UV protection, i.e. shielding of the sensitive inner layers from penetration of the radiation or prevention of UV-induced

damage inside the cells. The latter strategy might be plausible in deciduous plant enabling more flexible mobilization and utilization of soluble compounds season after season. The UV absorbing compounds inside the living cell would be less important as irradiation screen, but can act efficiently against the damage of the genetic material or photosynthetic apparatus resulting from the overproduction of ROS. With respect to the UV protection, the typical for most plants, diversity of phenolic compounds can be an important for adaptation since every compounds can have slightly different spectrum of absorption. For example, the estrification of flavonoids by cinnamic acid, enhances the absorbance in the UV-B region (280-320nm) compared to the unsubstituted individual compounds [25].

1.7. Antioxidant

Free radical scavenging and antioxidant properties of plant phenols are perhaps the most evident and intensively studied [1, 26, 27]. Given the proven importance of dietary polyphenols and botanical medicines for human health, the existence enormous literature on that topic is obvious. However, the antioxidant properties of these compounds are at the same time least clear with respect to the actual function in the plant organism [28]. This discrepancy is even more upsetting for the plant biology, when thinking of green plants as of the major source of atmospheric oxygen.

The huge amount of data has been collected from food chemistry and pharmacology studies on different aspects of antioxidative activity of polyphenols. In mammals, including humans, these compounds play an important role in the prevention of a variety of diseases, he etiology of which can be related to the disruption of redox and free radical homoeostasis in the organism. It has been confirmed by animal, clinical and epidemiological studies that such phenolics as resveratrol, proanthocyanidins, rosmarinic acid, and many other can efficiently prevent or slow the development of atherosclerosis, coronary disease or cancer [29, 30]. The antioxidant action of the phenolics can be exerted through various mechanisms. It can be direct scavenging of the ROS, such as peroxides and superoxide anion radical, hydroxyl or peroxyl radicals. Flavones, resveratrol and hydroxycinnamic acids are also known to inhibit the prooxidant or ROS generating enzymes such as myeloperoxidase (MPO), lipoxygenases, different hepatic P450 cytochromes or xanthine oxidase [26, 31, 32]. The antiimflammatory properties of many flavonoids [33], besides the direct ROS scavenging, is also attributed to their ability to inhibit such enzymes as iNOS and COX-2. Another confirmed property of some polyphenols, especially certain flavonoids, is the ability to chelate transition metal ions [26, 27, 34, 35]. This mechanism can either interfere with the reactivity of chelated ions or facilitate direct quenching the radicals created in a Fenton type reaction as a result of the proximity to the reaction site, or both [26]. Involvement of interaction of phenolics with metal ions in the inhibition of metal-based oxidases such as P450 is also possible. Some phenolics are oxidized by interaction with a oxidizing agents, therefore playing a role of “sacrificial antioxidants” [14, 26].

The relative importance of a particular mechanism depends on the conditions of the reaction. Such differences have been observed in lipid peroxidation inhibition by polyphenols [35]. In NADPH-dependent peroxidation the inhibition was positively correlated with the chelation ability, contrary to the Fenton-type reaction induced peroxidation. In the latter case, the inhibition was ascribed to the quenching of lipid free radicals. The Cu^{2+} chelation also appeared to be responsible for inhibition of copper-induced LDL peroxidation [34]

The structure-activity relationship of antioxidant polyphenols has been reported [34, 36-40]. The hydroxylation pattern of phenolics is of great importance for the antioxidant capacity, but also significant are other substitutions. The *ortho*-dihydroxyl configuration of

the aromatic rings is postulated to be essential for high antioxidant capacity in phenolic acids and flavonoids [39, 40]. The glycosylation usually decreases antioxidance, but due to the higher hydrophilicity of glycosides, their availability in aqueous environment might be better, whereas in lipophilic conditions the aglycones act more efficiently. Analogously, the methylation of –OH groups reduces their hydrogen donation ability, but can facilitate the interaction with lipid membranes, thereby enhancing their protective activity. The estrification with additional phenolic molecules increases the antioxidant power as for instance in catechin – gallic acid esters (gallotannins), which are among the most potent antioxidants, much more active than an individual flavanol or hydroxybenzoic acid molecule. Among phenolic acids, the cinnamic acid derivatives are stronger antioxidants than hydroxybenzoic acids. This is attributed to lower prooxidant impact of the carboxylate group onto the phenolic ring [39].

The physiological function of plant phenolics for antioxidant defense of plant themselves is less known. It is assumed from the in vitro and animal systems that the role of phenolics as antioxidants in plants should be at least as important as in human diet. Indirect indication of their function is the known fact of phenolic biosynthesis stimulation upon ROS generating stress [9, 10, 41] such as UV irradiation, hypoxia, xenobiotics, osmotic and thermal stress. The diverse functions of plant phenols can be spatially or temporally regulated, as exemplified by the differences in UV defenses. [24]. The experiments with *Scutellaria baicalensis* cell cultures have shown that ROS can induce the rapid changes in glycosides/aglycones ratio [42]. When the cells are treated with H_2O_3 the flavone glucuronide – baicalin was hydrolyzed to its aglycone – baicalein, which is a very potent lipophilic antioxidant. The glycosylation/hydrolysis mechanism can therefore function as means of maintaining the fast and sustainable delivery of antioxidant flavonoids from constitutive reserve when needed, simultaneously preventing uncontrolled activity. Not to forget is also the supposed importance of the prooxidant face of phenolics [43], that may be involved in cell signaling and toxicity to pathogenes or herbivores.

Phenolic systems are likely to act in concert with other endogenous antioxidant mechanisms such as ROS deactivating enzymes or other antioxidants like tocopherols, carotenoids, thiols (GSH) and ascorbate. Recently, [28] it has been found out that oxidized phenolic compounds are recycled by ascorbate and enzymatic ascorbate regeneration system. These findings suggest the fundamental role of phenols in maintaining the redox homoeostasis in plants.

2. Oxidative stress, free radicals, mutagenesis and defense

2.1. What are free radicals and ROS

Free radical is an independently existing unit (atom or molecule) with an unpaired electron. Free radicals in biological systems are frequently very reactive and short lived [26, 44]. They are involved in many essential metabolic processes but can also have deleterious effects on the integrity of the cell structure and physiology. Most biologically relevant free

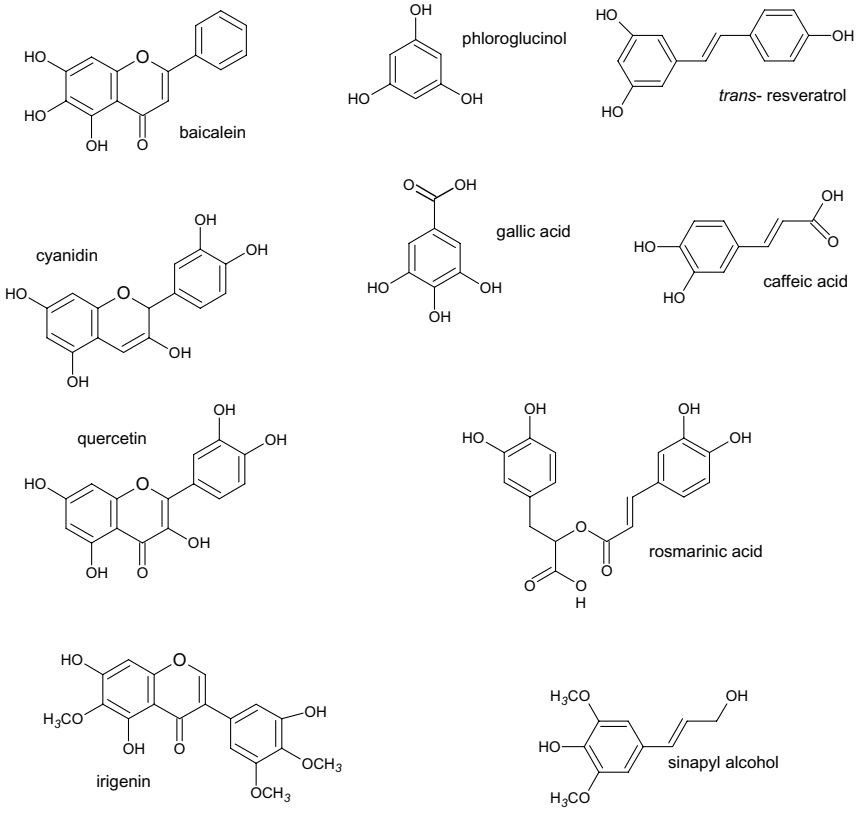

Fig. 1. Examples of phenolic compounds from plants

radicals are oxygen centered and therefore are included in Reactive Oxygen Species (ROS). It has to borne in mind that not all ROS, like H_2O_2, singlet oxygen or HOCl, are free radicals. Some important radicals are also S, N, or C – centered and some very reactive molecules such as nitric oxide (a free radical) or peroxynitrite (non-radical) are also termed Reactive Nitrogen Species (RNS).

2.2 How are the free radicals and ROS formed?

Free radical reactions involve an initiation, when the radical is created from non-radical molecules, propagation, when a radical interacts with non-radical resulting in the occurrence of an unpaired electron in another molecule and the termination - a reaction between the radical species breaking the propagation chain.

Free radicals are normally formed and found in the living organism as the important components or by-products of many crucial metabolic pathways, such as electron transport chains in mitochondria and chloroplasts or immune responses. They can be also derived from external sources and as a result of stress. In aerobic conditions, molecular oxygen is a primary source of some ROS , p.p. singlet oxygen, superoxide anion radical ($O_2^{\bullet-}$). Singlet

oxygen is generated by photodynamic reactions after illumination of such compounds as chlorophyll, furanocoumarins or hypericin. Water molecule can also yield ROS upon homolytic fission caused by ionizing irradiation. In this reaction, a highly oxidizing hydroxyl radical is formed. However, in vivo generation of free radicals is often caused by enzymatic reactions or is catalyzed by transition metal ions. $O_2^{\bullet-}$ is produced by several enzymes, e.g , p.p. xanthine oxidase, nitric oxide synthase, by mitochodrial electron transport chain and by P450 oxidases. $O_2^{\bullet-}$ is subsequently enzymatically or spontaneously dismutated to H_2O_2, which in turn can be converted to water by peroxidases or catalases, or can interact with metal ions, thereby generating hydroxyl radical in Fenton-type reactions. UV irradiation of H_2O_2 can also yield $OH^{\bullet}$ by homolytic fission. Thus, there is a number of diverse sources of free radicals and ROS in vivo, that have to be considered in the methodology of antioxidant research.

2.3. Redox balance, oxidative stress and effects of free radical reactions

Despite existence in mostly highly oxidizing environment, aerobic organisms maintain the balanced redox state according to the actual needs of each level of organization, even in a particular cellular compartment. However, different kinds of stress can transiently disrupt this balance leading to the overproduction of oxidizing agents (oxidative stress). In plants, many environmental factors can increase the ROS levels, which in moderate amounts serve to stress signaling and adaptation purposes, but can be damaging after prolonged exposure of the stressed cells [45]. These include abiotic factors – excessive UV and visible illumination, elevated or reduced temperature, excessive ozone in the atmosphere, water deficiency, oxygen deprivation, pollution and herbicide treatment. When subjected to infection or herbivory plants also release ROS [10, 46].

The reactive molecules formed during the stress response interact with each other as well as they can directly attack other cellular compounds. These reactions are usually complex and still some of the processes possible in vivo remain incompletely described. The ROS interactions in different organisms and in vitro are intensively studied and have been also reviewed recently [10, 41, 46]. Here, only the few basic examples will be mentioned to provide a general overview of the multifaceted consequences of oxidative damage. The relatively less harmful $O_2^{\bullet-}$ reacts with nitric oxide giving the very reactive peroxynitrite. In lower pH, the superoxide anion changes to its uncharged form, hydroperoxyl radical, a more reactive species capable of crossing cell membranes. Dismutation of $O_2^{\bullet-}$ results in hydrogen peroxide, which in turn can initiate the oxidation/reduction cycle of transition metals, such as Fenton reaction with ferrous ions. The product of these reactions, $OH^{\bullet}$ is one of the most reactive (oxidizing) species found in biological systems. Superoxide anion itself can also accelerate the Fenton-type reactions by reducing the metal ions [26, 47].

Among the molecular targets of $OH^{\bullet}$ are most vital biomolecules such as nucleic acids, proteins and membrane lipids. The DNA damage can contribute to the accumulation of mutations and cell death. Lipid peroxidation is one of the most studied aspects of oxidative activity of free radicals. It is also a normal metabolic process important for biosynthesis of signaling molecules and proceeds either enzymatically or non-enzymatically, but both routes differ in the product spectra and their functions [41, 48]. A free radical, such as $OH^{\bullet}$ reacts with polyunsaturated fatty acids (PUFA) by abstracting the hydrogen atom from methylene group. The carbon-centered radicals undergo the propagation by reacting with oxygen that begins chain reaction during which highly reactive peroxyl radicals which in turn can further oxidize PUFA and form lipid peroxides. In the presence of transition metal ions, lipid peroxides react in a similar way to H_2O_2 producing alkoxyl radicals capable of initiating a new chain reaction. In fact, the end

products of lipid peroxidation are much more diverse and include also epoxides, conjugated dienes, cyclic peroxides, various ketones, aldehydes such as malondialdehyde (MDA) and hydrocarbons. The intermediate lipid radicals can also attack other molecules such as membrane proteins or nucleic acids.

2.4. What is an antioxidant?

Living organisms have developed sophisticated methods of protection against the oxidative injury. Antioxidants are important part of the protective networks. An antioxidant can be defined as any substance capable of delaying or preventing oxidation of a substrate, when present in low concentration compared to the oxidizable substrate [26, 44]. The antioxidant can be recycled in the cell by reduction of the oxidation products.

Another possibility is that antioxidants are irreversibly damaged by oxidation, but the products are less harmful or can be further metabolized or removed from the cell, then the compounds are "sacrificial antioxidants" [26].

There are several antioxidant defense systems. The strategy of first line of defense is to eliminate the less dangerous ROS – $O_2^{\bullet-}$ and H_2O_2 that would give rise to hydroxyl radical and to prevent their reaction with iron, copper and other transition metal ions by firm binding the metals.

The enzymatic antioxidant apparatus is quite well described in different organisms, also in plants [41, 49]. The main components are three enzymes directly eradicating ROS. Superoxide dismutase (SOD) catalyzes dismutation of $O_2^{\bullet-}$ to H_2O_2. Hydrogen peroxide is then decomposed by catalase to give H_2O and O_2 or removed by peroxidase which uses it to oxidize another substrate. SOD is an ubiquitous group of enzymes containing different transition metals in its active center. There are ZnCu, Mn, Fe and Ni based SOD, the first three being more common, and the NiSOD reported only in few microorganisms [26]. SOD is usually sensitive to stress and its activity can either increase or decrease, leading to adaptation or exacerbation of oxidative stress, respectively. The catalase and peroxidase activities are essential for controlling the H_2O_2 levels. The peroxidases are dependent on provision of reducing substrate such as glutathione (GSH) or ascorbate. The reducing substrate can be subsequently regenerated by a set of GSH and ascorbate reductases in the Halliwell-Asada cycle using NADPH for reducing GSSG and dehydroascorbates [26, 41]. An important function of peroxidases is the ability to reduce the lipid hydroperoxides. By this means, they can serve as the second line of defense, breaking one step in propagation of lipid peroxidation [26, 41, 48].

Besides the ROS controlling enzymes, there is a number of lower molecular mass compounds that serve this purpose either occasionally or as a principal task. The role of these small molecules (for simplicity, they will be referred to as just "antioxidants") is dual, they can prevent oxidation by reacting with the oxidizing agents, e.g. scavenging of oxygen radicals or chelation of metals and, on the other hand, they can interfere with propagation of intermediate free radicals, terminating the chain reaction. The reactions of antioxidants are usually less specific than the enzymatic ones, which makes them more universal. The advantage of low molecular mass compounds is their relative spatial or temporal independence on protein synthesis, they can be also easily mobilized and their diversity enables acting in concert for better protection from a variety of harmful intermediates of free radical reactions.

The important feature of antioxidants is their lipophilicity or hydrophilicity which determines their potential site of activity. The lipophilic compounds are likely to protect membrane PUFA and easily cross the membranes, the hydrophilic can effectively act in aqueous environment where most of ROS are formed. GSH and ascorbate are the compounds which apart from being crucial substrates for peroxidases, are also effective

ROS scavengers. Other abundant antioxidants are the lipophilic tocopherols and carotenoids (carotenes and xanthophylls). Phytic acid (*myo*-inositol-hexaphosphate) binds tightly transition metal ions, making them less available to catalyze Fenton-type reactions. And last but not least, the aforementioned phenolics, which can be either lipophilic or hydrophilic depending on the structure.

3. How to measure the antioxidant capacity of plant metabolites?

There are different approaches possible to assess the antioxidant properties [26, 44, 50]. One possibility is to separate and quantify all compounds that may contribute to that activity. One minus here is that individual compounds are not necessarily identical in their efficiency and that the knowledge on synergies and antagonisms would be lacking. Another disadvantage, especially in the studies where the multifactorial interactions with the environment are investigated, is the complex analytical methodology and sometimes costly instrumentation needed. The latter is likely to improve with continuing development of fast and affordable phytochemical techniques.

A reasonable and economical approach is to initially assess the total antioxidant capacity of given object by as many as possible different means, bringing information on the mechanisms involved in antioxidation. Here, some limitations also exist, the lack of detailed information of the contribution of particular components of the system to the assayed properties is one of the most important. In any of the known techniques there are tendencies to preferentially assay the activity of some compounds [26, 36, 44]. Therefore, use of several different methods is highly recommended to avoid this drawback. The bioactivity guided fractionation/separation is very helpful in ascribing the particular activity to an individual compound or fraction and in studying possible synergism or antagonism between individual components or fractions.

This approach is commonly used in pharmacological studies for application in human medicine and standardization of herbal drugs as well as in food science [50-53]. Combination of these approaches will yield valuable data for experimental studies on the role of each compound or group of compounds in the alleviation of oxidative stress in plants.

As it has been in many other fields of plant research (including the $NO^{\bullet}$ studies), the in vitro methods for antioxidant testing have been developed for biomedical, human physiology and nutrition science purposes. Below we present different assays of total antioxidant capacity, discuss their applications to assess certain mechanisms of antioxidation with respect to phenolic compounds and give some case examples from our studies on the antioxidant phenolics from medicinal plants. Besides, we will describe a simple bacterial assay for testing the potential protective role of phenolics in inhibition of mutagenesis, and discuss the likely involvement of antioxidant properties in that.

3.1 Different assays

Some methods are based on the direct observation of free radical scavenging by an antioxidant. One can use either stable free radicals, that are not found in vivo, but are convenient to use, or more biologically relevant ROS but they can give less reliable and comparable measurements. The decreasing concentration of the molecules with unpaired electrons can be directly detected by means of the Electron Spin (Paramagnetic) Resonance [51, 54, 55] . The advantage of using ESR is the possible insight into the detailed mechanism of the antioxidant/free radical interaction and tracing of potential intermediate radical products. However, this technique requires quite expensive instrumentation and an

experienced researcher who properly interprets the spectra. Moreover, some naturally occurring radicals can only be detected by use of spin trapping [26, 51].

Alternatively, the photometric or fluorimetric approaches can be used when the free radical is colored itself, or can react with another compound giving colored product.

3.1.1. The assays using ABTS cation radical

These routine assays are based on the change of absorbance of the relatively stable 2,2'-azino-bis-3-ethylbenzothiazoline-6-sulfonic acid ($ABTS^{\bullet}$) radical cation obtained in vitro by oxidation of the non-radical ABTS substrate [56, 57]. As oxidizing agents, different chemicals have been reported such as metmyoglobin/H_2O_2, MnO_2 or sodium persulfate. The oxidized cation radical form is green in aqueous solutions and scavenging converts it to the colorless product. Absorbance peaks at 417, 645, 734, and 815 nm are present, but the loss of absorbance at 734 nm is usually monitored and referred to the standard antioxidant Trolox (5,7,8-tetramethylchroman-2-carboxylic acid). The results are expressed as Trolox Equivalent Antioxidant Capacity (TEAC). This assay has been also used for studying the antioxidant reaction kinetics with respect to flavonoid B-ring chemistry [58] as well as for determination of antioxidants production in callus cultures of hawthorn [59]. There are also commercially available kits for determination of TAS (total antioxidant status) by Randox Labs.

3.1.2. $DPPH^{\bullet}$ reduction assay

1,1-diphenyl-2-picrylhydrazyl is a stable free radical deep purple in color with a maximum absorbance of 515-520 nm. This radical can be also directly monitored by ESR. It is only slightly soluble in water, but dissolves well in alcohols or DMSO. Therefore it is suitable for lipophilic antioxidants, but can be also used for the more hydrophilic ones when assayed in hydroalcoholic solutions (e.g. 80% ethanol). Upon reaction with a scavenger the solution is discolored and the absorbance loss can be used for quantitative assessment of the scavenging power expressed either as a percentage in a given concentration of an antioxidant or preferably as EC_{50}. The absorbance has been proved to be linearly correlated to molarity, thus the results from different studies are easier to compare [60, 61]. The kinetic measurement can also help to distinguish between fast and slow antioxidants. The $DPPH^{\bullet}$ staining can be also used in connection with Thin Layer Chromatography for screening of antioxidant compounds in complex mixtures. By comparison to other TLC detection techniques (e.g. polyphenol specific), the free radical scavenging capacity of each separated and identified compound can be assessed [62].

3.1.3. Superoxide scavenging assay

In these assays the superoxide anion radical reacts with the detecting reagent to produce pigments measured spectrophotometrically. The superoxide can be conveniently generated in vitro by X/XOD reaction [44, 51, 63] The most common reagent used to detect $O_2^{\bullet-}$ is NBT (nitroblue tetrazolium) that as a result of the reduction by $O_2^{\bullet-}$ produces blue formazan pigment. The antioxidant can compete with an indicator for the $O_2^{\bullet-}$, decreasing the absorbance at 560 nm. The kinetics can be assessed using known constants of $O_2^{\bullet-}$ reaction with color reagents. SOD can be used as standard (positive control). Importance of appropriate controls eliminating the direct interactions of the sample with the indicators or the $O_2^{\bullet-}$ source must be borne in mind. The $O_2^{\bullet-}$ can be also detected with cytochrome-*c* [44] and nitrite method [64] but phenolic compounds can directly reduce cytochrome-*c*, making the inhibition evaluation inaccurate[44].

3.1.4. TRAP (total radical trapping antioxidant parameter)

TRAP assay measures the scavenging of peroxyl radicals derived from decomposition of donor compounds such as AAPH (2,2'-azobis(2-amidinopropane) dihydrochloride) or AMVN (2,2'-azobis(2,4-dimethylvaleronitrile)). The incubation with antioxidants extends the lag phase before onset of substrate peroxidation measured by monitoring the O_2 uptake and the activity is compared to that of a standard antioxidant, usually Trolox. Alternatively, peroxyl radicals can be detected directly by luminol-enhanced chemiluminescence [26].

3.1.5. Other ROS/RNS

There are also possibilities to assess the influence of antioxidants on other radicals found in vivo such as hydrogen peroxide, $NO^{\bullet}$, peroxynitrite or hypochlorite. For example, nitric oxide can be satisfactorily detected and measured using $NO^{\bullet}$-specific fluorescent dyes (DAF-2 or DAR 4M) [65]. However there are so far no reports on using this approach to investigate the interactions of phenolic antioxidants with $NO^{\bullet}$. H_2O_2 scavenging can be assessed by inhibition of phenol red staining [40] and HOCl scavenging by the ability to protect α-antiproteinase against inactivation [44].

3.1.6. Reducing power towards the transition metals

Antioxidants can reduce transition metal ions that can be detected spectrophotometrically after forming colored products.

In the FRAP (ferric reducing antioxidant power) assay ferric iron (Fe III) can be reduced to the Fe(II), that forms colored complex with TPTZ (2,4,6-tripyridyl-*S*-triazine) absorbing at 593 nm. One should always take into account that the reduction of ferric to ferrous ions may also accelerate the $OH^{\bullet}$ production in the presence of H_2O_2, therefore exerting rather pro-oxidant than antioxidant influence. Therefore, the results from this assay can sometimes give different antioxidant activity trends than others [66, 67]. However, due to the relative simplicity FRAP has been used in combination with further assays to show the antioxidant power of phenolic compounds, for example in tissue cultures [59] or induced by wounding [68].

Another method uses the reduction of Mo(VI) to Mo (V) by the analyte and the formation of a green-blue phosphomolybdenum complex [69]. The phosphomolybdenum assay can be used for both hydrophilic and lipohilic antioxidants. The reducing power can be expressed as Trolox or ascorbic acid equivalents or referred to other strong antioxidants. The technique has proven very reliable and reproducible, and is remarkably inexpensive. The reaction mixture contains 600 mM sulfuric acid, 28 mM sodium phoshate (tribasic) and 4 mM ammonium molybdate. After incubation at an appropriate temperature, the absorbance is recorded at 695 nm an compared to the absorbance of a standard antioxidant. Although very simple and efficient, the method has one major weakness, namely the unverified relevance to *in vivo* conditions. Contrary to Fe, Cu, Cr or Mn ions, Mo has not been demonstrated to contribute to the oxidative stress, even though some important enzymes as xanthine oxidases contain Mo in their active center. This method, still not very widely used, has been implemented for determination of tocopherols and antioxidant capacity of different plant extracts and phenolic compounds [70, 71].

Yet another approach to learn about the oxidation decreasing ability of plant phenols is to study the chelation of transition metals. The UV spectra of polyphenols

change upon binding the metal cations and can be restored by addition of a stronger chelator like EDTA or DTPA (diethyltriamine penta-acetic acid) [34].

3.2. Assays based on the prevention of substrate oxidation

Another group of assays shows the ability of antioxidants to inhibit the oxidation reactions to some extent imitating the natural conditions. The intermediate or end products of oxidation are measured either directly or by formation of colored complexes. The oxidation is started by various methods, such as thermal treatment, air incubation, Fenton type reactions, microsomal enzymatic systems, artificial peroxyl radical donors, radio- and photolysis etc. [26, 44]

The substrates for oxidation such as lipids, proteins, nucleic acids, can be in form of native structures, cell membranes, microsomes, mitochondria or plastids. Alternatively, for more accuracy, the pure diagnostic compounds can be used

3.2.1. Lipid based assays

Various lipids such as pure PUFA (linoleic acid), PUFA esters (methyl linoleate), LDL (low density lipoproteins) or membrane lipids and liposomes can be the substrate for oxidation [52, 72].

One possibility of assessing the intensity of peroxidation is looking directly at the products, such as conjugated dienes. Inhibition of conjugated diene formation can be measured at 234 nm [72, 73]. This method however, has limited suitability in case of phenolic antioxidants, absorption of which frequently overlaps this wavelength [26, 44].

3.2.2. Ferric thiocyanate method

It is based on reaction of the coloring agent – ferric thiocyanate with lipid hydroperoxides formed during air incubation [74] or transition metal ion induced oxidation of linoleic acid [73]. The change of absorbance at 500nm is monitored and the flattening of the absorbance curve indicates the prevention of PUFA oxidation by the sample.

3.2.3. Carotene bleaching inhibition [38, 54]

ß-carotene bleaching method measures the ability of an antioxidant to reduce the decline of ß-carotene during the coupled oxidation of a polyunsaturated fatty acid (e.g. linoleic acid) and ß-carotene, initiated by heat. The absorbance is monitored at 450 nm and compared to appropriate controls. The oxidation can be also initiated by incubation with transition metal ion containing mixtures capable of generating $OH^{\bullet}$.

3.2.4. TBARS assay

Another common technique for evaluating lipid peroxidation is based on thiobarbituric acid (TBA), which reacts with malondialdehyde (MDA). The reddish product of this reaction – TBARS (TBA reacting substance) is quantified by absorbance at 532 nm.

TBARS assay is also used with deoxyribose as a substrate subjected to the oxidation by hydroxyl radical [75]. $OH^{\bullet}$ is generated usually by different iron ion/ascorbate/H_2O_2 systems. The role of different mechanisms in total antioxidant activity can be frequently deduced from the $OH^{\bullet}$/TBARS based assays and sometimes also pro-oxidant properties in certain conditions. The mechanisms can involve interference with $OH^{\bullet}$ formation, for

example by chelation of metals, removal of $OH^{\bullet}$ radical or chain breaking of free radical propagation [26, 34, 35, 50].

TBARS is also one of the few methods applied in plant physiology for estimation of endogenous lipid peroxidation level imposed by the stress treatments [48, 76]

3.3.3. Protein based assay – ORAC [77]

Oxygen-radical absorbance capacity assay (ORAC) uses the in vitro generated peroxyl radical derived from AAPH (2,2'-azobis(2-amidinopropane) dihydrochloride that damages the fluorescent protein ß-phycoerythrin and the decrease of the fluorescence can be competitively inhibited by a radical scavenger [77]. This assay and its improved modifications have been popularly employed in human plasma studies and in determination of antioxidant ability in foodstuffs including phenolic compounds of fruits [78]. The antioxidant capacity is expressed as Trolox equivalents.

4. Investigation of antimutagenic properties

Mutagenesis is thought to be one of the injurious consequences of oxidative stress [29, 30, 50]. To reveal the relationship between antioxidance and antimutagenicity, the described above antioxidant assays can be complemented by simple tests showing the inhibitory influence of phenolics towards induced mutations in bacterial cells. Several tests have been developed, each having its drawbacks and advantages [26]. Some of the widely used bacterial systems are *Salmonella* based Ames test and *umu* test and *E. coli* based assays [79, 80]. *Salmonella typhimurium* mutant strains provide a convenient object to investigate different types mutagenesis and its inhibition [81]. A set of standard strains have been developed that enables testing several aspects of mutagenicity such as direct chemical mutagenesis, mutagenesis by chemicals needing metabolic activation by microsomal oxidizing enzymes like P450 and oxidizing agents-induced mutations. Each tester strain contains a different type of mutation in the histidine operon as well as additional mutations that increase their susceptibility to various mutagens. The general idea behind the Ames system is that the standard mutant strains, unable to grow on the histidine depleted media are induced to reverse-mutations above the spontaneous level. The more surviving colonies (called revertants) is observed, the more back-mutations must have occurred. Most of that histidine-requiring mutants have G-C pairs at the site for reversion, and one TA102 is based on the A-T base pair. Initially, the assay was designed to screen for mutagenic activity of environmental xenobiotics as potential carcinogens. By using standard diagnostic mutagens, it has been adapted for antimutagenicity studies of various factors, including plant polyphenols [71, 79, 82].

The detailed procedures are thoroughly described in the technical papers by Ames and co-workers [81, 83, 84]. In testing the inhibition of indirect mutagens, pro-mutagens have to be activated by the pre-incubation with the microsomal S9 fraction from rat liver pre-stimulated with PCB such as Aroclor. The microsomal P450 type enzymes convert the inactive precursor into the mutagen. In the direct mutagenic tests, the S9 fraction is omitted, and the mutagen is added to the incubation medium.

Various standard strains are intended for preferential use with certain diagnostic mutagens that give the best response. For example TA98 with 2-AF (2-aminofluorene), TA100 for NQNO (4-nitroquinoline-*N*-oxide) and sodium azide whereas TA102 for oxidative mutagenicity. Direct mutagenesis and its inhibition is tested with NQNO or sodium azide while the indirect with 2-AF or B(a)P (benzo-*a*-pyrene) and for the TA102

oxidation-induced mutations , p.p. hydrogen peroxide, UV irradiation, photoactivated coumarins, and hydroperoxides are used. [83].

5. Study examples

5.1. Case study I. – lipophilic flavones in extracts from Scutellaria baicalensis [53]

Baikal skullcap is a medicinal plant originating in China and Siberia and cultivated in the Far East for pharmaceutical uses. The roots accumulate unusually high amounts (10-15% dw) of lipophilic flavones and glucuronides such as baicalein (BE, 5,6,7-trihydroxyflavone) (Fig. 1.) and its glucuronide baicalin (BI) as well as the flavone wogonin (5,7-dihydroxy-8-methoxyflavone, WO) and the 7-O-glucuronide (wogonoside - WG). Unlike most other flavonoids, these of Baikal skullcap have unsubstituted B-ring, hence the hydrophobic character of the aglycons. The hydroalcoholic extracts from the *S. baicalensis* roots containing a rich flavone fraction are highly antioxidant and antiradical as revealed by many *in vitro* and *in vivo* assays [85, 86]. Among the four main flavones, baicalein was the most efficient $DPPH^{\bullet}$ scavenger with EC_{50} of 8 µg/mL. In Ames test, the activity guided separation revealed that purified baicalein fraction is the most efficient inhibitor of both directly (by NQNO) and indirectly (by 2-AF) induced mutations in strains TA98 and TA100. The inhibition rates of direct mutagenesis were following:

Strain TA98 , p.p. BE - 93%, WO - 41%, BI - 47%, WG – no activity;

Strain TA100 , p.p. BE - 62%, WO - 57%, BI - 72%, WG – no activity;

The suppression of mutations induced by metabolized 2-AF was higher for all four flavones:

Strain TA98 , p.p. BE – 99%, WO – 95%, BI – 64%, WG – 79%;

Strain TA100 , p.p. BE – 100%, WO – 100%, BI – 94%, WG – 85%;

In the 2-AF mutatgenesis the aglycons BE and WO are markedly more efficient as antimutagens. In the NQNO-induced mutagenesis, baicalein and baicalin are more active. Baicalein, which is also the strongest antioxidant, can play the important role in securing the roots of *S. baicalensis* against oxidative stress an genotoxicity. It can be quickly mobilized from less potent baicalin by the endogenous ß-glucuronidases [42]. The lipophilic character of the B-ring will be beneficial for protecting the membrane lipids, whereas the hydroxylation of the A-ring carbons suffices for powerful antioxidant activity. However, the biological significance of the baicalin/baicalein and wogonin/wogonoside relationships in this and other skullcaps has not been fully understood.

5.2. Case study II. – various phenolics in extracts from selected European Lamiaceae. [87]

Plant from the Lamiaceae family are usually rich in polyphenols. Many popular herbs and spices from this family (rosemary, thyme, sage, marjoram, oregano, basil) are known as potent dietary antioxidants thanks to the presence of various phenolic acids, flavonoids and tannins [88]. Rosmarinic acid (Fig.1.) is a good example of the thoroughly studied antioxidant phenolic acid [89]. For our study, we chose several less investigated medicinal plants from Central Europe, containing various types of phenolics together with other metabolites responsible for their therapeutic value. Antioxidant activity was tested with three different assays and related to the total polyphenol and flavonoid amount in the hydroalcoholic extracts. In the DPPH assay the anti-free radical EC_{50} was following in an ascending order (from highest to lowest activity) , p.p. *Leonurus cardiaca* > *Lamium album* (flowers) >> *Lamium purpureum* (flowers) > *Marrubium vulgare* > *Galeopsis tetrahit* > *Stachys betonica*.

The difference in the speed (kinetics) of reaction with the free radical was also observed. The decrease in $DPPH^{\bullet}$ absorbance was almost immediate in case of *Lamium* flowers and in *Leonurus* leaves but in *Galeopsis* and *Marrubium* the same maximum scavenging percentage have not been reached till 40^{th} minute of incubation. The differences in composition of "quick" and "slow" antioxidants probably accounts for these differences.

Remarkably, in the second assay, the phosphomolybdenum reduction test, the tendency was different , p.p. *Stachys betonica >> Lamium album > Lamium purpureum > Marrubium vulgare > Leonurus cardiaca > Galeopsis tetrahit*

In Fe^{2+}/ascorbic acid-induced linoleic acid peroxidation, the inhibition was less variable between each species, ranging at 200µg/mL between 60% and 77%. The sequence from the strongest to the weakest antioxidant in TBARS assay was following , p.p. *Marrubium vulgare > Stachys betonica > Lamium purpureum > Lamium album.> Leonurus cardiaca > Galeopsis tetrahit.*

Interestingly, the differences in the total amount of phenolic compounds were rather insignificant (between 13.2% and 19.9% gallic acid equivalents) in comparison to the antioxidant activities and no clear correlation could be found between them. On the other hand, different classes of phenolic compounds dominate in each species as indicated by the overall flavonoid content (*Leonurus* - 6% and *Stachys* – 8% whereas *Marrubium* – 19% and *Lamium* 32 - 41% quercetin equivalents), but without correlation to the antioxidance, either.

A noteworthy finding is an outstanding and rapid antioxidant reactivity of *Lamium* flowers, presumably resulting from high concentration of flavonols. Flowers are usually exposed to environmental impacts and are therefore especially prone to oxidative damage from UV radiation or ozone pollution. The antioxidant protection of reproductive structures provided by constitutive phenolics would add to their well established role as pollinator attracting pigments and co-pigments.

These preliminary results suggest a great complexity of the involved mechanisms that can vary even among the related species. The research is being continued to clarify the contribution of different classes of phenolics to the antioxidant protection in each of the studied species by means of activity guided fractionation and by testing the ability for inhibition of oxidant-induced mutations in the *Salmonella* TA102 strain. The above Lamiaceae species could also provide a useful objects for research on antioxidant defense strategies, alongside with model plants.

5.3. Case study III. – isoflavonoids in extracts from Belamcanda chinensis [90]

Isoflavonoids are found primarily in two angiosperm families – Fabaceae and Iridaceae. The isoflavonoids in such model legumes as soybean or *Medicago sp*. are intensively studied and their genetics and biosynthesis is relatively well described [91]. In contrast, little is known about the biosynthesis and exact biological function of Iridaceae isoflavones, usually differently substituted than those of legumes. We have been investigating the plant from Iridaceae - *Belamcanda chinensis*. The antioxidant and antimutagenic activities of isoflavonoid rich fractions extracted from roots and rhizomes were analyzed using four antioxidant assays and the Ames test. The main isoflavonoids found in this plant are irigenin (Fig.1.), tectorigenin, and the corresponding glucosides iridin and tectoridin as well as a number of minor isoflavonoids [92].

The strong free radical scavenging capacity has been observed in the $DPPH^{\bullet}$ assay, whereas only moderate in $ABTS^{\bullet+}$ based TEAC test. This in agreement with the relatively less polar character of the main isoflavonoids due to the partial methylation of hydroxyl groups (see the structure on Fig.1). The isoflavonoids constitute over 16% of the extracted dry mass, with tectorigenin and irigenin as major compounds.

The antioxidant ability has been also tested with lipid peroxidation inhibition assay. Linoleic acid (LA) was used as a substrate oxidized by the hydroxyl radical generated via Fe^{2+}/ascorbate system and the peroxidation products determined as TBARS. The peroxidation of LA was reduced by from 45% to 97% depending on the concentration of the extract in the test sample and EC_{50} was 45µg/mL. In the Ames test, both direct and indirect mutagenesis was inhibited by 82.7% and 94.4% respectively. The effective concentration range was similar to that of *Scutellaria baicalensis* flavones. The higher rate of mutagenicity reduction for metabolized mutagens suggests some contribution of the P450 inhibition to the overall antimutagenic activity of Belamcanda isoflavones.

The actual biological role of these particular isoflavonoids in Iridaceae is yet to be discovered, but similarly to the Fabaceae, they could serve as phytoalexins, antioxidants and maybe also signaling molecules of unknown function. Future work on the bioactivity guided fractionation is required for the isolation and characterization of individual isoflavonoids from *Belamcanda chinensis* and to determine the mechanisms involved in their antioxidant and antimutagenic effects.

References

[1] Harborne J.B. and Williams C.A., "Advances in flavonoid research since 1992". *Phytochemistry*, vol. 55, p.p. 481-504, 2000.

[2] Halbwirth H., Wurst F., Forkmann G. and Stich K., "Biosynthesis of yellow flower pigments belonging to flavonoids and related compounds". *Recent Advances in Phytochemistry*, vol. 1, p.p. 35-49, 2000.

[3] Mirabela R., Franssen H. and Bisseling T., "LCO signalling in the interaction between rhizobia and legumes". In: Scheel D, Wasternack C (eds.) "Plant Signal Transduction" Frontiers in Molecular Biology", Oxford University Press, Oxford, New York, pp. 250-271, 2001.

[4] Martin F., Duplessis S., Ditengou F.A., Lagrange H., Voiblet C. and Lapeyrie F., "Rhizospheric signals and early molecular events in the ectomycorrhizal symbiosis". In: Scheel D, Wasternack C (eds.) "Plant Signal Transduction" Frontiers in Molecular Biology, Oxford University Press, Oxford, New York, pp. 272-288, 2001.

[5] Politycka B., "Phenolics and the activities of phenylalanine-ammonia lyase, phenol ß-glucosyltransferase and ß-glucosidase in cucumber roots as affected by phenolic allelochemicals". *Acta Physiol Plant*, vol. 20, p.p. 405-410, 1998.

[6] Bais H.P., Vepachedu R., Gilroy S., Callaway R.M. and Vivanco J.M., "Allelopathy and exotic plant invasion: from molecules and genes to species interactions". *Science*, vol. 301, p.p. 1377-1380, 2003.

[7] Inderjit, Duke S.O., "Ecophysiological aspects of allelopathy". *Planta*, vol. 217, p.p. 529-539, 2003.

[8] Kato-Noguchi H., "Allelopathic substance in rice root exudates: Rediscovery of momilactone B as an allelochemical". *J. Plant Physiol*., vol. 161, p.p. 271-276, 2004.

[9] Ananieva E.A., Christov K.N. and Popova L.P., "Exogenous treatment with salicylic acid leads to increased antioxidant capacity in leaves of barley plants exposed to paraquat". *J. Plant Physiol*., vol. 161, p.p. 319-328, 2004.

[10] Delledonne M., Zeier J., Marocco A. and Lamb C., "Signal interactions between nitric oxide and reactive oxygen intermediates in the plant hypersensitive disease resistance response". *Proc. Natl. Acad. Sci. USA*, vol. 98, p.p. 13454–13459, 2001.

[11] Gómez-Vásquez R., Day R., Buschmann H., Randles S., Beeching J.R. and Cooper R.M., "Phenylpropanoids, Phenylalanine Ammonia Lyase and peroxidases in elicitor-challenged cassava (*Manihot esculenta*) suspension cells and leaves". *Ann. Bot*., vol. 94, p.p. 87-97, 2004.

[12] Ahmad I. and Beg A.Z., "Antimicrobial and phytochemical studies on 45 Indian medicinal plants against multi-drug resistant human pathogens". *J. Ethnopharmacology*, vol. 74, p.p. 113-123, 2001.

[13] Rauha J.P., Remes S., Heinonen M., Hopia A., Kahkonen M., Kujala T., Pihlaja K., Vuorela H. and Vuorela P., "Antimicrobial effects of Finnish plant extracts containing flavonoids and other phenolic compounds". *Int. J. Food Microbiol*., vol. 56, p.p. 3-12, 2000.

[14] Cvikrova M., Mala J., Eder J., Hrubcova M. and Vagner M., "Abscisic acid, polyamines and phenolic acids in sessile oak somatic embryos in relation to their conversion potential". *Plant Physiol. Biochem*., vol. 36, p.p. 247-255, 1998.

[15] Brown D.E., Rashotte A.M., Murphy A.S., Normanly J., Tague B.W., Peer W.A., Taiz L., Muday G.K., "Flavonoids act as negative regulators of auxin transport in vivo in *Arabidopsis*". *Plant Physiol*., vol. 126, p.p. 524-535, 2001.
[16] Murphy A., Peer W.A. and Taiz L., "Regulation of auxin transport by aminopeptidases and endogenous flavonoids". *Planta*, vol. 211, p.p. 315-324, 2000.
[17] Mathesius U., "Flavonoids induced in cells undergoing nodule organogenesis in white clover are regulators of auxin breakdown by peroxidase". *J. Exp. Bot*., vol. 52, p.p. 419-426, 2001.
[18] Bonomelli A., Mercier L., Franchel K., Baillieul F., Benizri E. and Mauro M.C., "Response of grapevine defenses to UV-C exposure". *Am. J. Enol. Viticult*., vol. 55, p.p. 51-59, 2004.
[19] Schmitz-Eiberger M. and Noga G., "UV-B radiation influence on antioxidative components in *Phaseolus vulgaris* leaves". *J. Appl. Bot. – Angew. Bot*., vol. 75, p.p. 210-215, 2001.
[20] Schmitz-Hoerner R. and Weissenböck G., "Contribution of phenolic compounds to the UV-B screening capacity of developing barley primary leaves in relation to DNA damage and repair under elevated UV-B levels". *Phytochemistry*, vol. 64, p.p. 243-255, 2003.
[21] Tegelberg R., Aphalo P.J. and Julkunen-Tiitto R., "Effects of long-term, elevated ultraviolet-B radiation on phytochemicals in the bark of silver birch (*Betula pendula*)". *Tree Physiol*., vol. 22, p.p. 1257-1263, 2002.
[22] Warren J.M., Bassman J.H., Fellman J.K., Mattinson D.S. and Eigenbrode S., "Ultraviolet-B radiation alters phenolic salicylate and flavonoid composition of *Populus trichocarpa* leaves". *Tree Physiol*., vol. 23, p.p. 527-535, 2003.
[23] Li J., Ou-Lee T-M., Raba R., Amundson R.G. and Last R.L., "Arabidopsis flavonoid mutants are hypersensitive to UV-B irradiation". *Plant Cell*, vol. 5, p.p. 171-179, 1993.
[24] Semerdjieva S.I., Sheffield E., Phoenix G.K., Gwynn-Jones D., Callaghan T.V. and Johnson G.N., "Contrasting strategies for UV-B screening in sub-Arctic dwarf shrubs". *Plant Cell Environ*., vol. 26, p.p. 957-964, 2003.
[25] Stochmal A. and Oleszek W., "Acylation of flavones with hydroxycinnamic acids – an alfalfa (*Medicago sativa*) case". In: 4th International Symposium on Chromatography of Natural Products, Lublin, Poland, p. 1953, 2004.
[26] Halliwell B. and Gutteridge J.M.C., "Free Radicals in Biology and Medicine". Oxford University Press, Oxford, pp. 936, 1999.
[27] Heim K.E., Tagliaferro A.R. and Bobilya D.J., "Flavonoid antioxidants , p.p. chemistry, metabolism and structure-activity relationships". *J. Nutr. Biochem*., vol. 13, p.p. 572-584, 2003.
[28] Sakihama Y., Cohen M.F., Grace S.C. and Yamasaki H., "Plant phenolic antioxidant and prooxidant activities , p.p. phenolics-induced oxidative damage mediated by metals in plants". *Toxicology*, vol. 177, p.p. 67-80, 2002.
[29] Ames B.N., Shigenaga M.K., Hagen T.M., "Oxidants, antioxidants and the degenerative diseases of aging". *Proc. Natl. Acad. Sci*.USA, vol. 90, p.p. 7915-7922, 1993.
[30] Surh Y.J. and Ferguson L.R., "Dietary and medicinal antimutagens and anticarcinogens , p.p. molecular mechanisms and chemopreventive potential – highlights of a symposium". *Mutat. Res*., vol. 523-524, p.p. 1-8, 2003.
[31] Mikstacka R., Gnojkowski J. and Baer-Dubowska W., "Effect of natural phenols on the catalytic activity of cytochrome P450 2E1". *Acta Biochim. Pol*., vol. 49, p.p. 917-925, 2002.
[32] Schewe T. and Sies H., "Flavonoids as protectants against prooxidant enzymes" Research Monographs, Institut für Physiologische Chemie 1, Heinrich-Heine-Universität Düsseldorf, http://www.uni-duesseldorf.de/WWW/MedFak/PhysiolChem/index.html.
[33] Zielińska M., Kostrzewa A., Ignatowicz E. and Budzianowski J., "The flavonoids, quercetin and isorhamnetin 3-O-acylglucosides diminish neutrophil oxidative metabolism and lipid peroxidation". *Acta Biochim. Pol*., vol. 48 , p.p. 183–189, 2001.
[34] Brown J.E., Khodr H., Hider R.C. and Rice-Evans C.A., "Structural dependence of flavonoid interactions with Cu2+ ions , p.p. implications for their antioxidant properties". *Biochem. J*., vol. 330, p.p. 1173-1178, 1998.
[35] Ozgova S., Hermanek J. and Gut I., "Different antioxidant effects of polyphenols on lipid peroxidation and hydroxyl radicals in the NADPH-, Fe-ascorbate- and Fe-microsomal systems". *Biochem. Pharmacol*., vol. 66, p.p. 1127–1137, 2003.
[36] Arts M.J.T.J., Dallinga J.S., Voss H.P., Haenen G.R.M.M. and Bast A., "A critical appraisal of the use of the antioxidant capacity (TEAC) assay in defining optimal antioxidant structures". *Food Chem*., vol. 80, p.p. 409-414, 2003.
[37] Chen Z.Y., Chan W.P., Ho K.Y., Fung K.P. and Wang J., "Antioxidant activity of natural flavonoids is governed by number and location of their aromatic hydroxyl groups". *Chem. Phys. Lipids*, vol. 79, p.p. 157-163, 1996.
[38] Fukumoto L.R. and Mazza G., "Assessing antioxidant and prooxidant activities of phenolic compounds." *J. Agric. Food Chem*., vol. 48, p.p. 3597-3604, 2000.

[39] Rice-Evans C.A., Miller N. and Paganga G., "Structure-antioxidant activity relationships of flavonoids and phenolic acids." *Free Radical Biol. Med*., vol. 20, p.p. 933-956, 1996.
[40] Sroka Z. and Cisowski W., "Hydrogen peroxide scavenging, antioxidant and anti-radical activity of some phenolic acids." *Food Chem. Toxicol*., vol. 41, p.p. 753-758, 2003.
[41] Blokhina O., Virolainen E. and Fagerstedt K.V., "Antioxidants, oxidative damage and oxygen deprivation stress: a review". *Ann. Bot*., vol. 91, p.p. 179-194, 2003.
[42] Morimoto S., Tateishi N., Matsuda T., Tanaka H., Taura F., Furuya N., Matsuyama N. and Shoyama Y., "Novel hydrogen peroxide metabolism in suspension cells of *Scutellaria baicalensis* Georgi*." J. Biol. Chem*., vol. 273, p.p. 12606-12611, 1998.
[43] Galati G. and O'Brien P.J., "Potential toxicity of flavonoids and other dietary phenolics , p.p. significance for their chemopreventive and anticancer properties". *Free Radical Biol. Med*., vol. 37, p.p. 287-303, 2004.
[44] Halliwell B., "Antioxidant characterization. methodology and mechanism". *Biochem. Pharmacol*., vol. 49, p.p. 1341-1348, 1995.
[45] Mahalingam R. and Fedoroff N., "Stress response, cell death and signalling , p.p. the many faces of reactive oxygen species". *Physiol. Plant*, vol. 119, p.p. 56-68, 2003.
[46] Vranova E., Van Breusegem, Dat J., Belles-Boix E. and Inze D., "The role of active oxygen species in plant signal transduction". In: Scheel D, Wasternack C (eds.) "Plant Signal Transduction" Frontiers in Molecular Biology, Oxford University Press, Oxford, New York. p.p. 45-73, 2001.
[47] Winterbourn C.C. and Kettle A.J., "Radical-radical reactions of superoxide , p.p. a potential route to toxicity." *Biochem. Biophys. Res. Commun*., vol. 305, p.p. 729-736, 2003.
[48] Spiteller G., "The relationship between changes in the cell wall, lipid peroxidation, proliferation, senescence and cell death". *Physiol. Plant*, vol. 119, p.p. 5-18, 2003.
[49] Grene-Alscher R., Erturk N. and Heath L.S., "Role of superoxide dismutases (SODs) in controlling oxidative stress in plants". *J. Exp. Bot*., vol. 53, p.p. 1331-1341, 2002.
[50] Arouma O.I., "Methodological considerations for characterizing potential antioxidant actions of bioactive components in plant foods". *Mutat. Res*., vol. 523-524, p.p. 9-20, 2003.
[51] Ohsugi M., Fan W., Hase K., Xiong Q., Tezuka Y., Komatsu K., Namba T., Saitoh T., Tazawa K. and Kadota S., "Active-oxygen scavenging activity of traditional nourishing-tonic herbal medicines and active constituents of *Rhodiola sacra*". *J. Ethnopharmacology*, vol. 67, p.p. 111-119, 1999.
[52] Velazquez E., Tournier H.A., Mordujovich de Buschiazzo P., Saavedra G. and Schinella G.R., "Antioxidant activity of Paraguayan plant extracts". *Fitoterapia*, vol. 74, p.p. 91-97, 2003.
[53] Woźniak D., Lamer-Zarawska E. and Matkowski A., "Antimutagenic and antiradical properties of flavones from the oots of *Scutellaria baicalensis* Georgi". *Food/Nahrung*, vol. 48, p.p. 9-12, 2004.
[54] Amarowicz R., Pegg R.B., Rahimi-Moghaddam P., Barl B. and Weil J.A., "Free-radical scavenging capacity and antioxidant activity of selected plant species from the Canadian prairies". *Food Chem*., vol. 84, p.p. 551-562, 2004.
[55] Ellnain-Wojtaszek M., Kruczyński Z. and Kasprzak J., "Investigation of the free radical scavenging activity of *Ginkgo biloba* L. leaves". *Fitoterapia*, vol. 74, p.p. 1-6, 2003.
[56] Bartosz G. and Bartosz M., "Antioxidant activity , p.p. what do we measure?". *Acta Biochim. Pol*., vol. 46, p.p. 23-29, 1999.
[57] Re R., Pellegrini N., Proteggente A., Pannala A., Yang M. and Rice-Evans C., "Antioxidant activity applying an improved ABTS radical cation decolorization assay". *Free Radical Biol. Med*., vol. 26, p.p. 1231-1237, 1999.
[58] Pannala S.A., Chan T.S., O'Brien P.J. and Rice-Evans C.A., "Flavonoid B-ring chemistry and antioxidant activity , p.p. fast reaction kinetics". *Biochem. Biophys. Res. Commun*., vol. 282, p.p. 1161-1168, 2001.
[59] Bahorun T., Aumjaud E., Ramphul H., Rycha M., Luximon-Ramma A., Trotin F. and Arouma O.I., "Phenolic constituents and antioxidant capacities of *Crataegus monogyna* (Hawthorn) callus extract" *Nahrung/Food*, vol. 47, p.p. 191-198, 2003.
[60] Brand-Williams W., Cuvelier M.E. and Berset C., "Use of a free radical method to evaluate antioxidant activity". *Lebensm.-Wiss. Technol*., vol. 28, p.p. 25-30, 1995.
[61] Molyneux P., "The use of the stable free radical diphenylpicrylhydrazyl (DPPH) for estimating antioxidant activity". *Songklanakarin J. Science Technol*., vol. 26, p.p. 211-219, 2004.
[62] Soler-Rivas C., Espin J.C. and Wichers H.J., "An easy and fast test to compare total free radical scavenger capacity of foodstuffs". *Phytochem. Anal*., vol. 11, p.p. 330-338, 2000.
[63] Choi C.W., Kim S.C., Hwang S.S., Choi B.K., Ahn H.J., Lee M.Y., Park S.H. and Kim S.K., "Antioxidant activity and free radical scavenging capacity between Korean medicinal plants and flavonoids by assay-guided comparison". *Plant Sci*., vol. 163, p.p. 1161-1168, 2002.
[64] Fukuda T., Ito H. and Yoshida T., "Antioxidative polyphenols from walnuts (*Juglans regia* L.)". *Phytochemistry*, vol. 63, p.p. 795-801, 2003.

[65] Matkowski A. and Durzan D.J., "Early somatic embryogenesis and in vivo imaging of the nitric oxide bursts in long term cultures of *Araucaria angustifolia*, a recalcitrant tropical conifer". *Vitro Cell Dev. Biol. PL*, vol. 40, p.p. 53A, 2004.
[66] Ou B., Huang D., Hampsch-Woodill M., Flanagan J.A., Deemer E.K., "Analysis of antioxidant activities of common vegetables employing oxygen radical absorbance capacity (ORAC) and ferric reducing antioxidant power (FRAP) assays: a comparative study". *J. Agric. Food Chem*., vol. 50, p.p. 3122-3128, 2002.
[67] Schlesier K., Harwat M., Bohm V. and Bitsch R., "Assessment of antioxidant activity by using different in vitro methods". *Free Radical Res*., vol. 36, p.p. 177-187, 2002.
[68] Kang H.M. and Saltveit M.E., "Antioxidant capacity of lettuce leaf tissue increases after wounding". *J. Agric. Food Chem.*, vol. 50, p.p. 7536-7541, 2002.
[69] Prieto P., Pineda M. and Aquilar M., "Spectrophotometric quantitation of antioxidant capacity through the formation of phosphomolybdenum complex: specific application to the determination of vitamin E". *Anal. Biochem*., vol. 269, p.p. 337-341, 1999.
[70] Lu Y. and Foo L.Y., "Antioxidant activities of polyphenols from sage (*Salvia officinalis*)". *Food Chem*., vol. 75, p.p. 197-202, 2001.
[71] Negi P.S., Jayaprakasha G.K. and Jena B.S., "Antioxidant and antimutagenic activities of pomegranate peel extracts". *Food Chem*., vol. 80, p.p. 393-397, 2003.
[72] Kähkönen M.P., Hopia A.I., Vuorela H.J., Rauha J.P., Pihlaja K., Kujala T.S. and Heinonen M., "Antioxidant activity of plant extracts containing phenolic compounds". *J. Agric. Food Chem*., vol. 47, p.p. 3954-3962, 1999.
[73] Lavelli V., Peri C. and Rizzolo A., "Antioxidant activity of tomato products as studied by model reactions using xanthine oxidase, myeloperoxidase, and copper-induced lipid peroxidation". *J. Agric. Food Chem*., vol. 48, p.p. 1442-1448, 2000.
[74] El-Ghorab A.H., El-Massry K.F., Marx F. and Fadel H.M., "Antioxidant activity of Egyptian *Eucalyptus camaldulensis var. brevirostris* leaf extracts". *Nahrung/Food*, vol. 47, p.p. 41-45, 2003.
[75] Sabu M.C. and Kuttan R., "Anti-diabetic activity of medicinal plants and its relationship with their antioxidant property". *J. Ethnopharmacol*., vol. 81, p.p. 155-160, 2002.
[76] Hodges D.M., DeLong J.M., Forney C.F. and Prange R.K., "Improving the thiobarbituric acid-reactive-substances assay for estimating lipid peroxidation in plant tissues containing anthocyanin and other interfering compounds". *Planta*, vol. 207, p.p. 604-611, 1999.
[77] Cao G., Alesiodagger H.M. and Cutler R.G., "Oxygen-radical absorbance capacity assay for antioxidants". *Free Radical Biol. Med*., vol. 14, p.p. 303-311, 1993.
[78] Zheng W. and Wang S.Y., "Oxygen radical absorbing capacity of phenolics in blueberries, cranberiies, chokeberries, and lingonberries". *J. Agric. Food Chemistry*, vol. 51, p.p. 502-509, 2003.
[79] Miyazawa M., Sakano K., Nakamura S. and Kosaka H., "Antimutagenic activity of isoflavone from *Pueraria lobata*". *J. Agric. Food Chem*., vol. 49, p.p. 336-341, 2001.
[80] Simić D., Vuković-Gacić B. and Knezević-Vukcević J., "Detection of natural bioantimutagens and their mechanisms of action with bacterial assay-system.". *Mutat. Res*., vol. 402, p.p. 51-57, 1998.
[81] Ames B.N., McCann J. and Yamasaki E., "Methods for detecting carcinogens and mutagens with the Salmonella/mammalian microsome mutagenicity test". *Mutat. Res*., vol. 31, p.p. 347-364, 1975.
[82] Shaughnessy D.T., Setzer R.W. and DeMarini D.M., "The antimutagenic effect of vanillin and cinnamaldehyde on spontaneous mutation in *Salmonella* TA104 is due to a reduction in mutations at GC but not AT sites". *Mutat. Res*., vol. 480-481, p.p. 55-69, 2001.
[83] Levin D.E., Hollstein M., Christman M.F., Schwiers E.A. and Ames B.N., "A new *Salmonella* tester strain (TA102) with A-T base pairs at the site of mutation detects oxidative mutagens*". Proc. Natl. Acad. Sci. USA*, *vol*. 79, p.p. 7445-7449, 1982.
[84] Maron D. and Ames B.N., "Revised methods for the Salmonella mutagenicity test". *Mutat. Res*., vol. 113, p.p. 173-215, 1983.
[85] Gao Z., Huang K., Yang X. and Xu H., "Free radical scavenging and antioxidant activities of flavonoids extracted from the radix of *Scutellaria baicalensis* Georgi". *Biochim. Biophys. Acta*, vol. 1472, p.p. 643-650, 1999.
[86] Yokazawa T., Dong E., Liu Z.W. and Shimizu M., "Antioxidative activity of flavones and flavonols in vitro". *Phytother. Res*., vol. 11, 446-449, 1997.
[87] Piotrowska M, "Antioxidant activity of some Central European medicinal plants from the Lamiaceae" MSc Thesis under supervision of A. Matkowski, Dept Pharmaceutical Biology and Botany, Medical University in Wrocław, Poland, 2004.
[88] Zgórka G. and Głowniak K., "Variation of free phenolic acids in medicinal plants belonging to the *Lamiaceae* family". *J. Pharm. Biomed. Anal*., vol. 26, p.p. 79-87, 2001.
[89] Petersen M. and Simmonds M.S., "Rosmarinic acid". *Phytochemistry*, vol. 62, p.p. 121-125, 2003.
[90] Woźniak D., Lamer-Zarawska E., Oszmiański J. and Matkowski A., "Antioxidant and antimutagenic activities of extract from *Belamcanda chinensis* (L.) DC." submitted

[91] Dixon R.A. and Steele C.L., "Flavonoids and isoflavonoids - a gold mine for metabolic engineering". *Trends Plant Sci*., vol. 4, p.p. 394-400, 1999.
[92] Yamaki M., Kato T., Kashihara M. and Takagi S., "Isoflavones of *Belamcanda chinensis*". *Planta Med*., vol. 56, p.p. 335, 1990.

Cell Biology and Instrumentation: UV Radiation, Nitric Oxide and Cell Death in Plants
Y. Blume et al. (Eds.)
IOS Press, 2006

New Approach to a Radiation Amplification Factor

[1)]P.Smertenko, [2)]V.Stepanov, [2)]C.Ol'khovik and [2)]D.J.Durzan
[1)] *V.Lashkaryov Institute of Semiconductor Physics, Department of Optoelectronics, National Academy of Sciences of Ukraine, 45 Prospect Nauki, Kyiv, 03028 Ukraine*
[2)] *Department of Plant Science, University of California, One Shields Ave. Davis, CA 95616 USA*

Abstract. The radiation amplification factor (RAF) and its dimensionless sensitivity provide a useful and general mathematical base. Dimensionless sensitivity (α) is represented by the formula $\alpha = d(lgy)/d(lgx)$. With such definition the ranges of constancy of the $\alpha(V)$ dependency correspond to the power behaviour ($y \sim x^{\alpha}$). Processing of data by this approach permits us to compare different physical values. Use of the exponent RAF offers greater possibilities for comparing the effects and mechanisms of UV radiation.

Introduction

One important factor for the estimation of climate change is the Radiation Amplification Factor (RAF) defined as the percentage increase in the biologically active UV irradiance, or exposure (UV_{bio}) that would result from 1 % decrease in the column amount of atmospheric ozone [1-4]. UV_{bio} is defined as the area under the spectral overlap function,

$$UV_{bio} = \int F(\lambda)\, B(\lambda)\, d\lambda \qquad (1)$$

where $F(\lambda)$ is the spectral irradiance, $B(\lambda)$ is the action spectrum for a particular biological effect, and the integral is carried out over all UV wavelengths.

Spectral sensitivity functions (action spectra) have been determined in laboratory and in field studies for a number of biological endpoints. Action spectra enable the estimation of the effect of simultaneously changing radiation at different wavelengths by different amounts, as happens when ozone reductions occur.

As was noted earlier [3] the RAF can be used only to estimate effects of small ozone changes, e.g., of a few percent, because the relationship between ozone and UV_{bio} becomes non-linear for larger ozone changes (*cf.* Blumthaler, this volume). For action spectra that decease approximately exponentially with increasing wavelength over 300-330 nm, UV_{bio} will scale with larger ozone changes according to a power relationship

$$UV_{bio} \sim (Ozone)^{[-RAF]} \qquad (2)$$

From the considerable experimental and theoretical data collected up to now models for the effects of UV on different objects both alive and dead are possible [e.g., 4-8]. This includes a mathematical tool for the analysis of fine behaviour with integral characteristics using a differential approach with dimensionless sensitivity [e.g., 9-19].

In this report we this work we review and illustrate the use of the differential approach for the investigation and interpretation of UV data.

2. Mathematical base

Let's rewrite the equation (2) in the form

$$U = AO^{\alpha} \tag{3}$$

where U is UV_{bio}, A is the proportional coefficient, O is column amount of atmospheric ozone and $\alpha(O)$ is (-)RAF. After logarithmation and differentiation of equation (3) we have

$$\lg U = \lg A + \alpha(O) \cdot \lg O; \tag{4}$$

$$\frac{dU}{U} = \alpha(O) \cdot \left(\frac{dO}{O} \right); \tag{5}$$

$$\alpha(O) = \frac{dU/U}{dO/O}; \tag{6}$$

In other words RAF is the ratio of relative changes of UV_{bio} and the ozone column. We can say also that RAF is differential slope α of UV_{bio} to the ozone column relationship in log-log scale.

In differential approach the slope of $\alpha(O)$ is introduced just as (6) in the form:

$$\gamma(O) = \frac{d\alpha/\alpha}{dO/O}; \tag{7}$$

In case the value $\alpha(O)$ determines the power behaviour (3), the value $\gamma(O)$ determines the exponent behaviour

$$U = B \exp\{O^{\gamma}\}; \tag{8}$$

where B is the proportional coefficient.

This approach was effectively used for the investigation of diverse values such as: current voltage characteristics [20-24], temperature characteristics [10, 25], reaction kinetics [26], colloid transport [14], images [27-28], reliability of metabolic and physiological models [29]. The main peculiarity of this approach is its dimensionless property. This enables us to compare diverse values having different physical meanings.

3. Analysis of experimental data.

In principle, it is necessary to obtain dependence $U=f(O)$ (6, 8). The ranges of α =const and γ=const characterize the UV effect. For example, in [5] the RAFs were used to compare a number of different known effects (Table 1).

A detailed and comparative analysis of dimensionless RAF values (from the point of view of dimensionless nature) can give the following results:

1) A very strong UV effect (RAF>2) can be observed in DNA-dependent processes: inhibition of growth of cress seedlings in plant, (6-4) photoproduct formation, HTV-1 activation, cyclobutane-pyrimidine dimer formation

2) A relatively strong influence and superlinear dependence of RAF (1.4<RAF<2) is observed for: generalized DNA damage, skin erythema, photocarcinogenesis, melanoma in fish, mutagenicity and fibroblast killing, cyclobutane-pyrimidine dimer formation, occupational exposure limits, membrane-bound K+-stimulated ATPase inactivation, isoflavonoid formation in bean, inhibition of motility (*Euglena gracilis*), tropospheric photolysis $O_3+hn\text{-}O(D')+O_2$.

Effect	RAF		Reference
	January 290DU	July 305DU	
Skin			
Erythema Reference	1.1	1.2	A.F.McKinlay and B.L.Diffey, 1987
Skin cancer in SKH-1 hairless mice (Utrecht)	1.5	1.4	F.R.deGruijl et al., 1993
SKH-1 corrected for human skin transmission	1.2	1.1	F.R.deGruijl and van der Leun, 1994
Elastosis	1.1	1.2	L.H.Kligman, R.M.Sayre, 1991
Photocarcinogenesis, skin edema	1.6	1.5	C.A.Cole et al., 1986
Photocarcinogenesis (based on STSL)	1.5	1.4	G.Kelfkens et al., 1990
Photocarcinogenesis (based on PTR)	1.6	1.5	G. Kelfkens et al., 1990
Melanogenesis	1.7	1.6	J.A.Parrish et al., 1982
Erythema	1.7	1.7	J.A.Parrish et al., 1982
Melanoma in fish	0.1	0.1	R.B.Setlow et al., 1993
DNA Related			
Generalized DNA damage	2.0	1.9	R.B.Setlow, 1974
Mutagenicity and fibroblast killing	[1.7] 2.2	[2.7] 2.0	F.Zohlzer, J.Kiefer,1984; M.J.Peak et al., 1984
Fibroblast killing	0.3	0.6	S.M.Keyse e al., 1993
Cyclobutane Pyrimidine Dinier formation	[2.0] 2.4	[2.1] 2.3	G.I.Chan et al., 1986
(6-4) photoproduct formation	[2.3] 2.7	[2.3] 2.5	G.I.Chan et al., 1986
HTV-1 activation	[0.1] 4.4	[0-1] 3.3	B.Stein et al., 1989
Eyes			
Damage to cornea	1.2	1.1	D.J.Pitts et al., 1977
Damage to lens (cataract)	0.8	0.7	D.J.Pitts et al., 1977
Other effects on animal cells			
Occupational exposure limit	1.4	1.5	ACGIH, 1992
Immune suppression	[0.4] 1.0	[0.4] 0.8	E.C.DeFabo, F.P.Noonan, 1983
Cell mortality in Chinese hamster	1.3	1.2	H.Banrud et al., 1993
Substrate binding in Chinese hamster	0.4	0.4	H.Banrud et al., 1993
Membrane damage			
Glycine leakage from *E. Coli*	0.2	0.2	Sharma and Jagger, 1979
Alanine leakage from *E. Coli*	0.4	0.4	Sharma and Jagger, 1979
Membrane bound K+-stimulated ATPase interaction.	[0.3] 2.1	[0-3] 1.6	C.W.Imbrie, T.M.Murphy, 1982
Plants			
Generalized plant spectrum	2.0	1.6	M.M.Caldwell et al., 1986
Inhibition of growth of cress seedlings	[3.6] 2.8	3.0	Steinmetz and E.Wellmann, 1986
Isoflavonoid formation in bean	[0.1] 2.7	[0.1] 2.3	E.Wellmann, 1985
Inhibition of phytochrome induced anthocyanin synthesis in mustard	1.5	1.4	E.Wellmann, 1985
Anthocyanin formation in maize	0.2	0.2	Beggs and Wellmann, 1985
Anthocyanin fonnation in sorghum	1.0	0.9	Yatsuhashi et al., 1982
Photosynthetic electron transport	0.2	0.1	L.W.Jones, B.Kok, 1966
Overall photosynthesis in leaf of *Rumex Patientia*	0.2	0.3	R.D.Rundel, 1983
DNA damage in alfalfa	0.5	0.6	F.E.Quaite et al., 1992
	RAF		

Effect	January 290DU	July 305DU	Reference
Phytoplankton			
Inhibition of motility *(Euglena gracilis)*	1.9	1.5	D.-P.Hahder, R.C.Worrest, 1991
Inhibition of photosynthesis *(Phaeodactylum sp.)*	0.2	0.2	J.J.Cullen et al., 1992
Inhibition of photosynthesis *(Prorocentrum micans*	0.3	0.4	J.J.Cullen et al., 1992
Inhibition of photosynthesis, in Antarctic community	0.8	0.8	N.P.Boucher, B.B.Prezelin, 1994
Inhibition of photosynthesis *(Nodular ia spumigena* cyanobacteria	0.2	0.2	D.-P.Hahder et al., 1994
Tropospheric photolysis			
$O_3 + h\nu \rightarrow O(^1D) + O_2$	2.1	1.8	W.P. de More et al., 1997
$O_3 + h\nu \rightarrow O(^3P) + O_2$	0.1	0.1	W.P. de More et al., 1997
$H_2O_2 + h\nu \rightarrow OH + OH$	0.4	0.4	W.P. de More et al., 1997
$HNO_3 + h\nu \rightarrow OH + NO_2$	1.1	1.0	W.P. de More et al., 1997
$NO_2 + h\nu \rightarrow O(^3P) + NO$	0.0	0.0	W.P. de More et al., 1997
$HCHO + h\nu \rightarrow H + CHO$	0.5	0.5	W.P. de More et al., 1997
$HCHO + h\nu \rightarrow H_2 + CO$	0.2	0.2	W.P. de More et al., 1997
Aqueous photochemistry			
CO production (Suwannee River)	0.3	0.3	R.Valentine, R.G.Zepp, 1993
COS production (Gulf of Mexico)	0.2	0.2	R.G.Zepp, M.O.Andreae, 1994
COS production (North Sea)	0.6	0.6	R.G.Zepp, M.O.Andreae, 1994
Photodegradation of nitrate ions	1.1	1.0	R.G.Zepp et al., 1987
Photodegradation of HCHO (Biscayne Bay)	1.3	1.1	R.L.Kieber et al., 19990
Photoproduction of H_2O_2 in freshwater	0.1	0.1	W.J.Cooper et al., 1988
Materials damage			
Yellowness induction in polyvinyl chloride	0.2	0.2	A.L.Andrady et al., 1989
Yellowness induction in polycarbonate	0.4	0.4	A.L.Andrady et al., 1991

Table 1. Radiation Amplification Factors (RAFs) at 30°N.

3) A linear dependence (0.9 <RAF< 1.1) was found for: SKH-1 corrected for human skin transformation, elastosis, damage to cornea, immune suppression, tropospheric photolysis $HNO_3+hn\text{-}OH+HNO_2$, photodegradation of nitrate ions, photodegradation of *HCHO* (Biscayne Bay).

4) A sublinear dependence (0.4<RAF<0.6) is character for: fibroblast killing, substrate binding in Chinese hamster, DNA damage in Alfalfa, tropospheric photolysis $H_2O_2+hn\text{-}OH+OH$, $HCHO+hn\text{-}H+CHO$, yellowness induction in polycarbonate.

5) A weak dependence (RAF<0.2) was found for: melanoma in fish, photosynthetic electron transport, inhibition in photosynthesis (*Phaoedactylum sp*.), tropospheric photolysis $O_3+hn\text{-}O(3P)+O_2$, $HCHO+hn\text{-}H_2+CO$, photoproduction of H_2O_2 in freshwater.

The most influential effect was HIV-1activation with a RAF = 4.4.

4. Conclusion

The dimensionless analysis of RAF for different biological objects allows us to compare and distinguish between different mechanisms having diverse values and different physical meanings over a wide range of experimental conditions.

5. Acknowledgments

This work was done in the frame of STCU project #1556.

References

[1] Kerr J.B. and McElroy C.T., "Evidence for large upward trends of ultraviolet radiation linked to ozone depletion", *Science*, vol. 262, p.p.1032-1034, 1993.

[2] Michaels P.J., Singer S.F., and Knappenberger P.C., "Analyzing Ultraviolet-B Radiation: Is There a Trend?". *Science,* vol. 264, p.1341, 1994.

[3] Madronich S., "The radiation equation". *Nature,* vol. 377, p. 682, 1995.

[4] Madronich S., McKenzie R.L., Caldwell M.M, and Bjom L.O., "Changes in ultraviolet radiation reaching the Earth's surface", *Ambio*, vol. 24, 143-164, 1995.

[5] Madronich S., McKenzie R.L., Bjom L.O., Caldwell M.M., "Changes in biologically active ultraviolet radiation reaching the Earth's surface", *J. Photochem. Photobiol, B: Biology*, vol. 46, pp.5-19, 1998.

[6] Caldwell M.M., Teramura A.N., and Tevini M.,"The changing solar ultraviolet climate and the ecological consequences for higher plants", *Trends in Ecol. and Evol.,* vol. 4, p.363-367, 1989.

[7] Bomman J.F., and Teramura A.N., "Effects of ultraviolet-B radiation on terrestrial plants", In Environmental UV Photobiology. A.R, Young et al., eds., New York: Plenum Press, p.427-471, 1993.

[8] Blair I. Sampson and James H. Cane, "Impact of enhanced ultraviolet-B radiation on flower, pollen, and nectar production", *American Journal of Botany,* vol. 86, p.108-114, 1999.

[9] Hjeldnes E.I., Bretvik S.K., Skoglund K.A. and Hylen S., "An experimental study of oil contamination spreading in sand", *Geotechnical Engineering. Norwegian University of Science and Technology (NTNU), Trondheim, Norway. Bulletin*, vol. 32, 16 p, 1995.

[10] Wataru Ootani, Yutaka Ito, Keiji Nishigaki, Yasuhiro Kishimoto, Makoto Minowa, Youiti Ootuka, "Sensitive germanium thermistors for cryogenic thermal detector of Tokyo dark matter search programme", *Journal-ref: Nucl. Instr. and Meth*. A 372, pp.534-538, 1996.

[11] Smertenko P.S., Ivanov A.M., Svechnikov S.V., "Verification method for integral values meters", *Russia patent* 2059260, G 01 R 35/04, 1996.

[12] Gorokhovski V. and Hosseinipour E. Zia, "Dimensionless Sensitivity Analysis of Subsurface flow and Transport Models"*, Environmental & Engineering Geoscience Journal*, vol. 3, pp.269-274, 1997.

[13] Smertenko P.S. et al., "Dimensionless Sensitivity as a Base for Modelling of Thermometric Characteristics of Thermodiode Sensors", *In Book of Abstracts, 5th International Workshop Thermal investigations of ICs and Systems (THERMINIC'99)*, Rome, 1999.

[14] Ning Sun, Ne-Zheng Sun, Menachem Elimelech, and Joseph N. Ryan, "Sensitivity analysis and parameter identifiability for colloid transport in geometrically heterogeneous porous media", *Water Resourses Research*, vol. 37, pp.209-222, 2001.

[15] Michael C. Kohn , "Use of Sensitivity Analysis to Assess Reliability of Metabolic and Physiological Models", *Risk Analysis*, vol. 22, pp. 623-631, 2002.

[16] Frey H.Ch., Patil S.R., "Identification and Review of Sensitivity Analysis Methods", *Risk Analysis*, vol. 22, pp. 553-578, 2002.

[17] www.lakeshore.com

[18] Smertenko P.S. et al., "Injection Technique for Study of Solar Cells Test Structures", *Solar Energy Materials & Solar Cells,* vol. 76/4, pp.613–624, 2003.

[19] Smertenko P., Fenenko L., Brehmer L., Schrader S., "Differential approach to study integral characteristics in polymer films", *Advances in Colloid and Interface Science,* 2005.

[20] Pfister J.C. "Note on the interpretation of space-charge limited currents with traps", *phys. stat. sol.(a)*, vol. 24, p.p. K15-K17. 1974.

[21] Manfredotti C., De Blasi C., Galassini S., Micocci G., Ruggiero L., Tepore A. "Analysis of SCLC curves by a new direct method". *phys. stat. sol.(a)*, vol. 36, p.p. 569-577, 1976.

[22] Nespurek S., Sworakowski J. "A differential method of analysis of steady-state space-charge-limited currents on extention". - *phys. stat. sol.(a)*, vol. 49, p.p.K149-K152, 1978.

[23] Smertenko et.al., "Evolution of the current-voltage characteristics of photoluminescing porous silicon during chemical etching", *Semiconductors*, vol. 31, p.p. 1221-1224, 1997.

[24] Mikhelashvili V. et al., "On the extraction of linear and nonlinear physical parameters in nonideal diodes". *J. Appl. Phys*., 1999, vol. 85(9), p.p. 6873-6894, 1999.

[25] Temperature Measurement and Control, Lake Shore, USA,1997.

[26] P. A. Frantsuzov, O. A. Igoshin, E. B. Krissinel, "Differential approach to the memory-function reaction kinetics", *Chemical Physics Letters*, vol. 317 (3-4), p.p. 481-489, 2000.

[27] S. Omori, Y. Nihei, E. Rotenberg, J.D. Denlinger, S.D. Kevan, B.P. Tonner, M.A. Van Hove and C.S. Fadley, "Imaging of Cu(001) Atoms by a New Differential Approach to Photoelectron Holography", *J. El. Spectrosc. Rel. Phen*., vol. 114-116**,** p.p. 455-460, 2001.

[28] S. Omori, Y. Nihei, E. Rotenberg, J.D. Denlinger, S.D. Kevan, B.P. Tonner, M.A. Van Hove and C.S. Fadley, "Differential Photoelectron Holography: A New Approach for Three-Dimensional Atomic Imaging", *Phys. Rev. Lett*., vol. 88, p.p. 1-4, 2002.

[29] Michael C. Kohn , Use of Sensitivity Analysis to Assess Reliability of Metabolic and Physiological Models*, Risk Analysis*, 2002, vol. 22(3), p.p. 623-631, 2002.

Cell Biology and Instrumentation: UV Radiation, Nitric Oxide and Cell Death in Plants
Y. Blume et al. (Eds.)
IOS Press, 2006

Effects of the Radiation on Some Aquatic Primary Producers

Liviu-Daniel GALATCHI
Ovidius University of Constanta, Department of Ecology and Environmental Protection, Bd. Mamaia, 124, 900527 Constanta– 3, Romania

Abstract: Ultraviolet B radiations increase the activity of the pure hydrolase (alpha amylase, E.C.3.2.1.1.) and Merck peroxidase (E.C.1.11.1.7.), by means of free radicals generated from synthetic polymers walls of the experimental tubes. The activation is higher in UV-B than in UV-A. UV-B and UV-A increase the intensity determined on nude alga *Tetraselmis suecica*, on exponential phase of cultivated bacteria *Escherichia coli* O_{157}, *Acinetobacter calcoaceticus*, and on total germs, after the short time of exposure in the thermo-stated conditions, the cell structure destruction by means of free radicals of activated hydrolases.

The nude alga *Tetraselmis suecica* is more resistant and store starch and lipids. It has the skill to convert the energy of radiations in the chemical energy of synthesis products. Creating a thick inhomogeneous sub-silique, under which a new silique appears, encysts some individuals of *Tetraselmis suecica.* Other cells increase their glucide (intra-plastids starch granules) and lipid reserves of provisions (oleosoma appear in the central part of the cell and affect the tillacoide lamellar structure; plasto-globules appear as well).

Cultivated bacteria on poor specific media have a small development in 300 – 800 nm. If the bacteria are cultivated on reach media, which absorb UV (Martin medium) they are developed by n^3 rule, instead n^2 in the first stage, after irradiations of bacteria culture bottle (transmittance 235 – 800 nm).

Introduction

B ultraviolet radiations UV-B (280 – 320 nm) and A ultraviolet radiations UV-A (320 – 400 nm) activate the enzymatic reactions following a well known mechanism, which relates at the catalytic action of UV radiations on some chemical reactions. The mechanism is frequently used by the preparative organic chemistry (chlorination, polymerisation of some polymers).

The energetic content of certain chemical links is in close connection with the potential energy delivered by the solar radiations (visible and UV). The presence of such chemical links in a chemical grouping (R) of an enzymatic substrate (S) determines the instability of the group (R) as a result of sun exposure.

The enzymatic reactions are inactivated by radiations with different wave lengths, depending on the nature of the chemical group (R), causing thus disastrous effects on living organisms [1-3].

The ultraviolet radiations are sources of free radicals that can cause important modifications to the proteins: conformational modifications, fragmentations of the polypeptides catenae, chemical modifications of the constituent amino acids. In addition, the free radicals can alter the proteins and indirectly initiate the peroxydation of lipids. The products resulted through the decomposition of lipidic peroxides (malonic aldehyde, 4-hydroxynonenal) can irreversibly block the groups $–NH_2$ and –SH from the proteic

structures. In the case of enzymes, these modifications can determine the loss of catalytic activity. According to Nechifor and Mester [4], the ultraviolet radiations and the copper acetate, as sources of free radicals, determine a significant diminishment of the activity of G6PDH and catalase in homogenised *Saccharomyces cerevisiae*. The inactivation is proportional to the degree of peroxydation of lipids determined through the measuring of the concentration of reactive substances the tiobarbituric acid (TBARS).

1. Material and Methods

Two kinds of experiments have been performed:

- the determination of the action of UV-B radiations on the enzymatic reactions;
- action of UV-B, UV-A and visible natural solar radiations.

1.1. Determination of the Action of UV-B Radiations on the Enzymatic Reactions

The determination of the action of UV-B radiations on the enzymatic reactions was effected with crystallized enzymes (alpha amylase – pancreatic – lyophylised 320 IU $\cdot$ mg^{-1} Merck, E.C.3.2.1.1. with Zulkowsky starch substrate), and peroxydase E.C.1.11.1.7. with substrate – ascorbic acid + H_2O_2 + benzidine.

The work method was according to Biochemica Merck [5] for the alpha amylase and Brad [6] for the peroxydase. The reagents were introduced into quartz test tubes (transmittance: 200-800 nm), made of synthetic transparent polymers (transmittance: 280 - 800 nm) and of glass (transmittance: 300 - 800 nm). The reactions were effected at ambient temperature, using the same time of reaction under the influence of laboratory light (with open windows).

The alpha amylase activity was measured by dosing the products of reaction with the colour reagent on a base of 3-5 dinitrosalicylic acid. The activity of the peroxydase was determined chronometrically.

1.2. Action of UV-B, UV-A and Visible Natural Solar Radiations

The action of UV-B, UV-A and visible natural solar radiations (90 - 110 k lux), intensified ten times with a metallic parabolic mirror (diameter 1.9 m; focal distance 0.89), has been experimented on: nude algae *Tetraselmis suecica* (culture in exponential phase), on marine invertebrates: *Mytilus galloprovincialis* (partially uncovered mantle), *Pilumnus hirtellus* (eggs in pre-hatching phase), the *Cyprinus carpio* three months old offspring, as well as on certain bacteria isolated from the marine environment: *Escherichia coli* O_{157}, *Acinetobacter calcoaceticus*, and total embryos (culture in exponential phase on marine environment + sterilized water 1:10).

The biologic material was introduced in an aquarium with double quartz walls. In between the double walls there was introduced a solution of Penicillin G 0.4% that allowed UV-B, UV-A and visible (265 - 800 nm) radiations pass through. The living organisms were exposed to radiations for ten minutes while the temperature was maintained constant. Afterwards the electron microscopic analysis of the tissues on a Tesla microscope, or bacteria count, was made.

2. Results and Discussions

The alpha pancreatic amylase is strongly influenced by the quality of the light filtrated through the reaction vessels at the Zulkowsky starch hydrolysis. At 23 ^{0}C and 18,000 lux, the enzymatic activities expressed in IU (mg maltose · min^{-1} · protein grams^{-1}) were 10.22 (quartz), 40.80 (polymers), 24.33 (glass). The peroxydase (50 micro g · sample^{-1}) developed the benzidine bluish colour at 16,000 lux after 4'11'' in transparent polymer test tubes and after 7'53'' in glass test tubes.

The effects of the UV-B solar radiations (intensified ten times) on the aquatic organisms, in the experimental conditions mentioned above, induces in aquatic organisms destructive processes at sub-cellular level that are incompatible with life.

2.1. Effects of the UV-B Solar Radiations on the Nude Alga Tetraselmis suecica

This alga displays an increased resistance to light irradiation because it has the ability to convert the radiation energy into the chemical energy of synthesis products.

The nude alga *Tetraselmis suecica* has certain representatives that isolate themselves in a cyst by forming a very thick non-homogenous subtecal layer under which a new pod appears. Other cells amplify their sugar deposits (grains of intraplastidial starch) and lipid deposits (big lipidic drops – oleosoms -, appear in the central part of the cell that disturbs the tilacoidal lamellar structure; and also appear numerous plastoglobes) (figure 1 and 2).

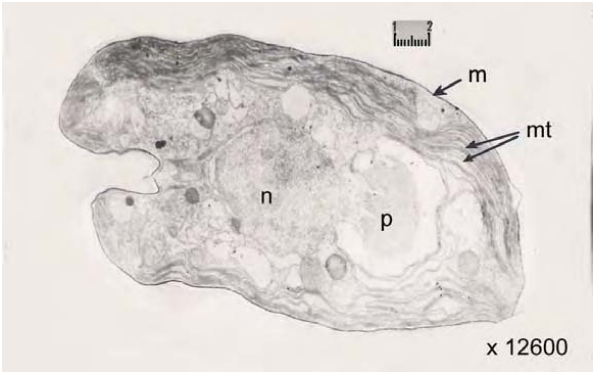

Figure 1. Nude prasinophyte alga *Tetraselmis suecica* - the normal aspect, 12,600 times amplified (m = membrane, n = nucleus, p = pyrenoid, mt = tilacoidal membrane)

2.2. Effects of the UV-B Radiations on Aquatic Environment Bacteria

As about the effect of UV-B radiations on aquatic environment bacteria, by placing in water from 0.5 to 0.5 meters until four meters deep, cultures of *Escherichia coli* O_{157} (isolated in aquatic environment) $22 \cdot 10^6 \cdot ml^{-1}$, introduced in semitransparent, UVB pervious (235 - 800 nm) 1.5 l bottles, it is observed that within thirty-five days the culture has had the greatest development at 0.5 meters deep after eight days ($75 \cdot 10^6 \cdot ml^{-1}$). Then, at this depth the number of germs decreased gradually reaching the number $5 \cdot 10^8 \cdot ml^{-1}$in the thirty-fifth day. The same dynamic but with smaller values was recorded on the samples placed deeper. As

an example, the number of germs in the eighth day decreased with the depth, the numbers recorded being: $75 \cdot 10^9 \cdot ml^{-1}$ (0.5 m); $37 \cdot 10^9 \cdot ml^{-1}$ (2 m) and $7 \cdot 10^7 \cdot ml^{-1}$ (4 m).

The sample kept day and night on the outside in closed bottles and exposed to the effect of environmental factors had a similar evolution but two size orders bigger: $22 \cdot 10^6 \cdot ml^{-1}$ (starting moment); $23 \cdot 10^8 \cdot ml^{-1}$ (48 hours); $178 \cdot 10^{11} \cdot ml^{-1}$ (8 days); $170 \cdot 10^{11} \cdot ml^{-1}$ (13 days); $1.2 \cdot 10^8 \cdot ml^{-1}$ (35 days).

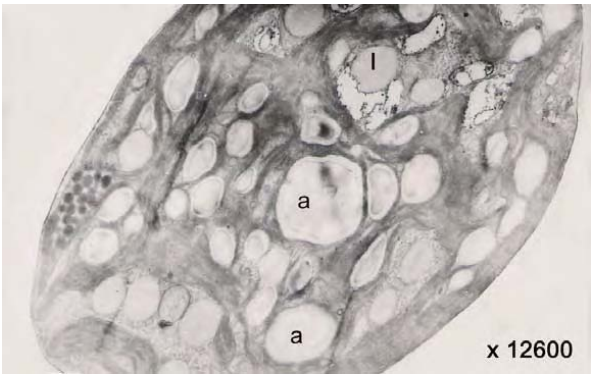

Figure 2. Nude prasinophyte alga *Tetraselmis suecica* - the 10' sun amplified light post-irradiation aspect (265 – 800 nm), 12,600 times amplified (a = starch, l = lipid)

The *Escherichia coli* witness kept in the laboratory in the dark (in a cardboard box) had an evolution similar to the sample kept on the terrace (as size order), but slightly diminished: $22 \cdot 10^6 \cdot ml^{-1}$ (starting moment); $15 \cdot 10^9 \cdot ml^{-1}$ (48 hours); $63 \cdot 10^{11} \cdot ml^{-1}$ (8 days); $73 \cdot 10^{11} \cdot ml^{-1}l$ (13 days); $12.5 \cdot 10^8 \cdot ml^{-1}$ (35 days).

In another experimental sample pure cultures of germs isolated from the seawater were separately exposed: *Acinetobacter calcoaceticus*, *Escherichia coli* O_{157}, and cultures of total germs from the seawater, in the focus of the parabolic mirror that intensified the solar radiations 10 times. The system was provided with a cooling device, so that the temperature variations should be in the limit of diurnal thermic oscillations.

It is observed that 10 minutes, 22 minutes, 30 minutes or 35 minutes exposure periods, alternated with periods of refrigerator keeping (4 – 8 ^{0}C) for days, determines the following phenomena in the cultures on Martin environment:

a) The number of germs triples after 10 minutes of exposure to the parabolic mirror in the first 8 days of observation. Then the effect diminishes with the aging of the culture up to 35 days.
b) The number of germs remains constant on the duration of refrigerator keeping.

3 samples of sediment and 3 samples of water were drawn in June 2004 from the following points, in Romania:

1. Mamaia Park – seawall (bathing area);
2. Mamaia Bay – Pescarie (spilling area from a pipe belonging to the water-filtering station Constanta);
3. Tabacarie Lake (very polluted with domestic waste products).

Five media of specific culture were used for aerobic heterotrophs, *Salmonella sp.*, anaerobic flora, aerobic and anaerobic cellulozolytics.

The inseminations were effected in a double copy (sample – exposed to the influence of the UVB and visible radiations and witness –, kept in the laboratory) in Petri boxes made of plastic that are pervious to 300 - 800 nm radiations.

Both the witness samples and the samples exposed to direct solar radiation influence, without being protected against the rise of environmental temperature, for 3 hours (8 - 11 a.m.), had 10^{14} - 10^{20} germs·ml^{-1}.

Within each sample, after a 3-hour-exposure to the solar radiation, the number of germs diminished from 3 times (water from Mamaia Bay – Pescarie) to 33 times (Tabacarie Lake sediments). In the case of the cellulozolytic germs the diminishment after exposure was 2.14 times (sediments from Mamaia Bay – Pescarie), up to 76.2 times (water from Mamaia Bay – Pescarie).

16 ml of the following mixture were introduced into Plexiglas Petri boxes (diameter 8.5 cm): 135 ml of seawater disinfected through sterilization, plus 150 ml fresh seawater. At certain time intervals, samples were drawn and the germs were counted using the dilution method (4 samples average). The dynamic of the total number of germs from the seawater exposed to the influence of radiations (300 - 800 nm), intensified 10 times compared to the natural environment, has the following development in the first 180 minutes: starting moment → 63 germs · 10; 15 minutes → 38 germs · 10; 30 minutes → 10 germs · 10; 60 minutes → 23 germs · 10; 90 minutes →12 germs · 10; 120 minutes → 2 germs · 10; 150 minutes → 6 germs · 10; 180 minutes → 5 germs · 10. It is observed that after 2.5 hours of irradiation with intensified light a second maximum of thermophilic bacteria develops.

3. Concluding Remarks

In vitro, in conditions of natural light, it has been established that the starch hydrolysis by the pure alpha amylase and the activity of the Merck peroxydase are strongly influenced by the light spectrum and that the enzymes are activated in the presence of the free radicals generated by the walls of the vessels made from synthetic polymers, in which the measurements were effected (transmittance 280 - 800 nm).

The ultraviolet radiations are absorbed in the walls of the glass vessels (transmittance 300 - 800 nm) and the enzymatic activities determined in them were: 24.33 IU (alpha amylase) and 7'53'' · peroxidase^{-1} · the time for the appearance of the benzidine blue colour.

The synthetic polymer vessels (transmittance 280 – 800 nm) are generators of free radicals under the influence of UV B radiations.

The free radicals activated the enzymes and the numbers recorded were bigger than the ones determined in the glass vessels, respectively 40.80 IU (alpha amylase) and 4'11'' (peroxydase).

All spectrum radiations pass trough quartz vessels (transmittance 200 - 800 nm), and the enzymes studied were inhibited: 10.22 IU (alpha amylase) and more than 10' for peroxydase.

The rise of UV-B and visible solar radiations (265 - 800 nm) up to 10 times comparing the natural fund, from the determination moment, induces the production of free radicals *in vivo* as a consequence of oxidative stress [1]. At the same time, the hydrolyses activate themselves by "pulverising" the sub-cellular structures in various tissues and organs of marine organisms, irreversibly altering the physiological and biochemical processes.

The nude algae prasinophyte *Tetraselmis suecica*, which lives in the superficial layer of the seawater, has an increased resistance to the influence of the natural solar radiations (265 - 800 nm), 10 times amplified. After a 10-minute-exposure it manages to transform the energy of the radiations absorbed in the energy of the reserve products stored as starch and lipid grains.

The bacteria from water and sediments in marine environment or in fresh water lakes are inhibited if cultivated in specific liquid poor media. In rich culture media (Martin environment diluted 1:10 with seawater), which absorb the UV radiations, the bacteria develop by the rule n^3 instead of n^2.

References

[1] R.Olinescu, "Peroxidarea in chimie, biologie, medicina", Editura Stiintifica si Enciclopedica, Bucharest, Romania, p. 61, 1992.
[2] S.C.O.P.E., a, "Effects of Increased Ultraviolet Radiation on Biological Systems – report", UNEP, Budapest, Hungary, p.1-40, 2002.
[3] S.C.O.P.E., b, "Effects of Increased Ultraviolet Radiation on Biological Systems – report", UNEP, Tamariglio (Sassari), Sardinia, Italy, p.1-47, 2002.
[4] M. Nechifor, R. Mester, "Efectul radicalilor liberi asupra activitatii enzimelor sistemului antioxidant", Buletinul SNBC, Bucharest, Romania, p. 170, 2004.
[5] Biochemica Merck, p.6, 1988.
[6] I. Brad, G. Marinescu, E. Glodeanu, "Chimie si biochimie vegetala – lucrari practice", Editura Reprografia Universitatii Craiova, Romania, p. 80, 1998.

NITRIC OXIDE AND PLANT STRESS

This page intentionally left blank

Cell Biology and Instrumentation: UV Radiation, Nitric Oxide and Cell Death in Plants
Y. Blume et al. (Eds.)
IOS Press, 2006

Signals from Reactive Oxygen Species

Robert FLUHR
Plant Sciences, Weizmann Institute of Science, Rehovot Israel, 76100

Abstract. Reactive oxygen species can arise from normal metabolic activity such as organelle-based electron transport or be intermediates in signal transduction pathways activated by plant respiratory burst oxidase homologs (*Rboh*). Divergent stress including temperature drought and UV-B exposure yield overlapping transcriptome response profiles whose origin can be traced to the use of reactive oxygen signaling intermediates. However, ROS signaling is ubiquitous and contributes in pathways controlled by hormones and developmental cues as well. Scavenging systems and NO are likely to temper its signaling properties and help contribute to the specificity of particular responses.

Introduction

Reactive oxygen species (ROS) have long been considered the waste products of imperfect metabolic activity and the unavoidable consequence of biological systems that operate in an oxidizing atmosphere. When the mitochondrial terminal oxidases, cytochrome *c* oxidase or the alternative oxidase, react with oxygen, four electrons are transferred to oxygen one at a time and water is the product. However, frequently (1 to 5% of all aerobic reactions) oxygen can react with other electron transport components. In this case, the result is a one electron transfer to form the superoxide anion $O_2^{\cdot -}$. The anion is a free radical initiator and through a variety of reactions, superoxide leads to the formation of hydrogen peroxide, an oxidizing agent or to the formation of ROS intermediates such as the hydroxy radical by interaction with iron, and these in turn can cause cellular damage in various ways including protein modification, breakage of unsaturated fatty acids or reactions with DNA. The superoxide radical can also directly serve as a nucleophile deprotonating alcohols or causing the hydrolysis of esters.

At the cellular level this source of ROS is controlled by constitutive and inducible scavenging systems. A central component of this control, superoxide dismutase, accelerates the rapid spontaneous dismutation which transforms the superoxide molecule to the peroxide. Hydrogen peroxide, can then be scavenged by catalase or peroxidase i.e. a process that returns the errant electrons of ROS to water and oxygen. In addition to the 'natural' metabolic production of ROS and its containment, recent work has pointed to the use of ROS as key signals in coordinating the plants ongoing physiological responses and its normal development. Thus, against the background flux of ROS turnover the cell has an embedded a fine-tuned signaling system that utilizes regulated ROS production and scavenging systems to implement controlled pulses of cellular information. As ROS is ubiquitous the question of how its modulation can be informative is not trivial. The discussion here addresses the potential cellular sources of ROS signal, their role in the induction of cellular response and interactions with NO in the use of ROS as a signaling medium.

1. Oxidative stress an example of organelle dysfunction

During normal metabolism ROS output is a quantitative product of ROS released from oxidative metabolic activity and ROS released from signaling components balanced by cellular scavenging capability. ROS overproduction that saturates and depletes scavenging capability will shift the redox milieu. If the local magnitude of this shift is sufficient, it can effect reactive groups e.g. cysteine moieties in proteins that could introduce activity modifications or undermine the integrity of membrane components. A cell can reach a state of oxidative stress by chloroplast or mitochondria dysfunction arising from environmental insult that turns the organelles into controlled or uncontrolled ROS generators. For example, under normal light flux the amount of superoxides produced is rapidly scavenged, however, under conditions of carbon skeleton limitations unutilized reducing power can lead to changes in the electromotive membrane state stimulating production of ROS. Similarly, under conditions of high light, the saturation of the photosystem capacity can result in photochemical breakdown that release ROS. Environmental conditions that perturb mitochondrial membranes such as cold or heat-treatment will also increase the intermediate drain of electron flow into alternative substrates to yield superoxides. In all these cases, subsequent disturbance in redox equilibriums will then be interpreted as an oxidative stress signal.

1.1 Commonalities in organelle-generated oxidative stress response

Hydrogen peroxide, a major product of ROS metabolism irrespective of its cellular source is rapidly diffused and is highly permeable making it well poised to serve as a signal molecule. Illustrating this point is the fact that ROS resulting from a singlet oxygen source that was released in a particular cell could propagate a diffusible extracellular hydrogen peroxide signal [1,2]. Transcriptome analysis can be used as a basis for comparing oxidative stress signals and differentiate between an apoplastic source, or an organelle source of ROS. Apoplastic sources of oxidative stress were simulated by the addition of exogenous hydrogen peroxide to *Arabidopsis* cells. Among the affected up-regulated genes are those that belong to cell rescue (ROS scavenging) and cell defense responses such as heat-shock proteins, phytoalexin biosynthetic genes, and senescence-related transcripts. The down-regulated genes were transcripts for the photosynthetic apparatus [3]. These same transcripts were shown to be inducible by wilt or UV treatment that also simulate oxidative stress. Chloroplast sources for ROS were established in tobacco discs subjected to oxidative stress by application of light-dependent ROS-generating methyl-viologen. In that case, the up-regulated genes included anti-oxidant genes, PR proteins, phytoalexin biosynthetic genes and genes of oxylipin metabolism. While many down regulated genes were related to photosynthesis [4]. The inhibition of photosynthesis may reflect the cellular need to minimize ROS production. A mitochondrial source of ROS was achieved by the inhibition of mitochondrial electron transport with antimycin A that was also shown to generate a significant increase in cellular ROS. Transcripts that were induced by antimycin treatment included PR proteins, GST, ethylene biosynthesis and senescence-related genes. The same genes were also induced by direct application of hydrogen peroxide or salicylic acid [5]. In this case, the activation of Aox1 that encodes mitochondrial alternative oxidase may partially offset the potential of ROS release by this organelle. We conclude that despite differences tissues used or plant species involved the transcriptome picture of oxidative stress from disparate ROS sources show a degree of commonality.

2. ROS signal and cell death

Oxidative stress can culminate in cell death either by rapid necrosis or a special type of programmed cell death. In animal cells, the mitochondria play an important role in triggering programmed cell death in response to diverse stimuli. A key step in this process is the opening of mitochondrial permeability transition pores, which allows for the release of apoptosis-inducing factor and the translocation of cytochrome c into the cytosol [6]. Tiwari et al.[7] showed that cytochrome c leakage occurs from *Arabidopsis* mitochondria after treatment of cells with a superoxide generator. Similarly, stimulation of stress-related transcripts by antimycin A, hydrogen peroxide and SA was blocked by the addition of an inhibitor of pore transition, bongkrekic acid [5]. The results suggest similarities in mitochondrial-based oxidative stress-induced PCD in plant cells and apoptosis of animal cells.

As noted above, chloroplasts-based ROS generation can lead to similar transcriptome programs as that found for mitochondria-based ROS generation. In this case it is likely that the 2 organelles can also interact via ROS cross-talk. Thus, the failure to dissipate photosynthetic-derived ROS will cause ROS products such as hydrogen peroxide to permeate the cell and affect the function of mitochondria. In this way, chloroplast dysfunction will contribute indirectly to PCD. Rapid and irreversible destruction of the chloroplast and tissue can also occur by addition of photosynthetic inhibitors. For example addition of norflurazon represses photo-protective carotenoid accumulation by inhibition of phytoene desaturase. Without carotenoids, chloroplasts rapidly destruct as a function of light intensity leading to necrosis. Thus, dependent on the intensity of ROS necrosis or a PCD signal may be channeled via the mitochondria but can be initiated from different sources.

2.1 Commonalities in ROS and NO-dependent pathways

Superoxide can rapidly react with NO to form the peroxynitrite ($ONOO^-$) a known mediator of cellular injury. This reaction occurs in a near diffusion-limited rate i.e. it can be more rapid than the SOD catalyzed removal of the superoxide. In soybean suspension cultures hydrogen peroxide formed by the dismutation of superoxide can function with NO to trigger plant hypersensitive response [8]. In this case, an unexpected balance between NO and hydrogen peroxide was found necessary for hypersensitive response whereas the direct application of the peroxynitrite was ineffective. In this cell system superoxide by combining with NO could serve to down-regulate the ability of NO to interact with hydrogen peroxide.

As NO and ROS appear to be interrelated it is of interest to examine their influence on cellular transcription profiles. The transcriptome profiles generated by direct NO treatment featured disease related transcripts, genes for alternative oxidase, ethylene biosynthesis, an ethylene responsive element, and GST [9,10]. In a cursory comparison, a subset of these transcripts are similar to transcripts that appear during antimycin treatment that effects mitochondria [5]. The result is not surprising as treatment of carrot cells with NO donors caused depletion of cytochrome C from mitochondria and induction of alternative oxidase activity [11]. These results are consistent with the effect on mitochondria functionality as one direct mode of action of NO.

3. Non-organelle sources of ROS: Rboh

In plants, enhanced O_2^{-} generation can be observed in microsomes prepared from pathogen-challenged leaf material [12]. Diphenylene iodonium (DPI), a non-specific suicide substrate inhibitor of the neutrophil NADPH oxidase and other flavin-containing enzymes [13], blocks the plant oxidative burst [12]. The kinetics and defense functions of ROS during activation of mammalian neutrophils have served as a model for similar processes in plants. While homology to the neutrophil core $gp91^{phox}$ was the basis for molecular cloning of plant respiratory burst oxidase homologs (*Rboh*) in *Arabidopsis* [14,15], the additional plasma membrane proteins and cytosolic regulatory proteins are not present in the plant genome. Plant *Rboh* define transcripts encoding a protein of about 105-112 kD size and have a cytosolic N-terminus domain containing calcium binding EF hand motifs and also a degree of similarity to the human RanGTPase-activating protein [14,16]. Direct activation of plant Rboh by calcium may be important for rapid stimulation of the oxidative burst during the hypersensitive response and plant Rboh unlike the mammalian $gp91^{phox}$ complex is active in the absence of additional cytosolic components [17]. Novel human family member, NOX5, is most homologous to the plant Rboh and contains the $gp91^{phox}$ core cytochrome as well as N-terminus EF hand motifs [18].

The gp91phox homologues *AtrbohD, F,* from *Arabidopsis, NtrbohD* from *Nicotiana tabacum* and *NbrbohA, B* from *Nicotiana benthamiana* were shown to be required for ROS accumulation in the leaf and plant defense responses [16,19-21]. The rapid ROS bursts associated with Rboh could serve as direct pathogen protective agents due to their toxicity, or their ability to propagate defense signals.

3.1. ROS signals generated by Rboh

The wounding response in tomato is thought to progress through the release of systemin (an 18 aa wound signal) in the wounded leaf, subsequent activation of early-response signal relay genes such as polygalacturonase, allene oxide synthase and lipoxygenase, and synthesis of a long-distance signal jasmonic acid (JA). A second wave of gene induction follows involving synthesis of proteinase inhibitor (PIN) and other defense polypeptides [22,23]. The wound-induced increase in H_2O_2 levels is JA-dependent and DPI sensitive, suggesting that a NADPH-like oxidase activity is required for the activation of wound/systemin-responsive genes [24,25]. Antisense plants with down-regulated Rboh activity showed the requirement of Rboh for expression of certain wound response genes, while other wound-responsive genes were regulated in a Rboh-independent manner [26]. Unexpectedly, the down-regulation of *Rboh* expression resulted in a highly branched phenotype and a phenotypic switch in the tomato growth habit from indeterminate to determinate growth. The reproductive organs and fruit displayed fasciation. The reduced Rboh levels shifted cellular redox metabolism as measured by hydrogen peroxide production. Surprisingly, ectopic expression of flower specific-homeotic genes was detected in the leaves. The results imply that multiple developmental functions are controlled by Rboh.

An early event in root hair formation is the specific recruitment of Rop GTPases to the site that will form root hair bulges [27,28]. Rop GTPases were fond to activate mammalian NADPH oxidase and in plants to be important in cell death [29] or differentiation [30] that involve hydrogen peroxide production. The *Arabidopsis RbohC* deficient mutants were defective in Ca^{2+} uptake and displayed short root hairs on stunted roots [20]. The results suggest that ROS produced by this *Rboh* species regulates plant cell expansion and is a downstream recipient of Rop GTPase activity.

3.2 Rboh source of ROS and UV-B responses

UV-B radiation can stimulate the plant pathogenesis state in a ROS dependent manner [31]. An interesting convergence was noted between *Nicotiana longiflora* transcriptome response to insect feeding and UV-B radiation [32]. Prominent similarities were down-regulation of several photosynthesis-related genes, and up-regulation of genes involved in oxylipin biosynthesis and a WRKY transcription factor. The remarkable similarity of UV-B transcriptome reponse to wound responses may indicate that common signaling mechanisms are involved. Activation of a Rboh-like activity was shown in *Arabidopsis* treated with UV-B radiation but not in leaves treated with ozone [33]. In maize lines, UV-B increased expression of defense, salt, and oxidative stress related genes including Rboh, whereas as shown in other cases of oxidative stress, photosynthesis-associated genes were down-regulated [34]. At the molecular level the application of systemin or various oligosaccharide elicitors as well as UV-B treatment stimulated overlapping sets of MAP-kinases [35]. Taken together, the result may indicate a common stimulatory mechanism which utilizes Rboh-dependent ROS production.

3.3 Rboh and NO pathways interact

Rboh-mediated H_2O_2 synthesis has been implicated in ABA-induced signaling processes in *Arabidopsis* [36] and likely in maize [37]. The *Arabidopsis* genes *AtrbohD* and *AtrbohF* function in ROS-dependent ABA signaling for stomatal closure [38]. Interestingly, both jasmonic acid and ABA promote stomatal closure via hydrogen peroxide production. This production is preceded by alkalization of the cytoplasm [39]. The sequence of events in hormone-induced stomatal closure is thus hormone-dependent activation of a phosphorylation/calcium pathway followed by alkanization, Rboh activation and activation of K^+ efflux. How this sequence proceeds at the molecular level is not known. The *Arabidopsis Atnos1* gene, implicated in plant nitric oxide synthesis, was found to be essential for ABA-induced stomatal closure [40], implicating a dual superoxide and NO signal for ABA signaling. Other evidence implies a role for nitrate reductase in NO dependent stomatal closure [41]. This finding is particularly intriguing as in mammalian vascular regulation there is a resultant loss of NO bioactivity upon reaction with superoxides or potentiation via the formation of nitrosylated thiols [42]. In the signaling systems for both defense and guard cell closure promoted by ROS, NO species have been implicated in playing a decisive role in signaling. Will this prove to be a paradigm for ROS signaling in other pathways?

References

[1] Allan A.C. and Fluhr R., "Two distinct sources of elicited reactive oxygen species in tobacco epidermal cells". *Plant Cell*, vol. 9, p.p. 1559-1572, 1997.

[2] Allan A.C., Lapidot M., Culver J.N. and Fluhr R., "An early tobacco mosaic virus-induced oxidative burst in tobacco indicates extracellular perception of the virus coat protein". *Plant Physiol.*, vol. 126, p.p. 97-108, 2001.

[3] Desikan R., Mackerness S.A.H., Hancock J.T. and Neil, S.J., "Regulation of the *Arabidopsis* transcriptome by oxidative stress". *Plant Physiol.*, vol. 127, p.p. 159-172, 2001.

[4] Vranova E., Atichartpongkul S., Villarroel R., Van Montagu M., Inze D. and Van Camp W., "Comprehensive analysis of gene expression in Nicotiana tabacum leaves acclimated to oxidative stress". *Proc. Natl. Acad. Sci. USA,* vol 99, p.p. 10870-10875, 2002.

[5] Maxwell D.P., Nickels R. and McIntosh L., "Evidence of mitochondrial involvement in the transduction of signals required for the induction of genes associated with pathogen attack and senescence". *Plant J.*, vol. 29, p.p. 269-279, 2002.

[6] Desagher S. and Martinou J.C., "Mitochondria as the central control point of apoptosis". *Trends Cell Biol.*, vol. 10, p.p. 369-377, 2000.
[7] Tiwari B.S., Belenghi B. and Levine A., "Oxidative stress increased respiration and generation of reactive oxygen species, resulting in ATP depletion, opening of mitochondrial permeability transition, and programmed cell death". *Plant Physiol.*, vol. 128, p.p. 1271-1281, 2002.
[8] Delledonne M., Zeier J., Marocco A. and Lamb C., "Signal interactions between nitric oxide and reactive oxygen intermediates in the plant hypersensitive disease resistance response". *Proc. Natl. Acad. Sci. USA,* vol. 98, p.p. 13454-13459, 2001.
[9] Polverari A., Molesini B., Pezzotti M., Buonaurio R., Marte M. and Delledonne M., "Nitric oxide-mediated transcriptional changes in *Arabidopsis thaliana*". *Mol. Plant Microbe In.*, vol. 16, p.p. 1094-1105, 2003.
[10] Parani M., Rudrabhatla S., Myers R., Weirich H., Smith B., Leaman D.W. and Goldman S.L., "Microarray analysis of nitric oxide responsive transcripts in *Arabidopsis". Plant Biotech. J.*, vol. 2, p.p. 359-366, 2004.
[11] Zottini M., Formentin E., Scattolin M., Carimi F., Lo Schiavo F. and Terzi M., Nitric oxide affects plant mitochondrial functionality in vivo. *Febs Lett*, vol. 515, p.p. 75-78, 2002.
[12] Doke N. and Ohashi Y., "Involvement of an O-2-Generating System in the Induction of Necrotic Lesions on Tobacco-Leaves Infected with Tobacco Mosaic-Virus". *Physiol. Mol. Plant P.*, vol. 32, p.p. 163-175, 1988.
[13] Cross A.R. and Jones O.T., "The effect of the inhibitor diphenylene iodonium on the superoxide-generating system of neutrophils. Specific labelling of a component polypeptide of the oxidase". *Biochem. J.*, vol. 237, p.p. 111-116, 1986.
[14] Keller T., Damude H.G., Werner D., Doerner P., Dixon R.A. and Lamb C., "A plant homolog of the neutrophil NADPH oxidase gp91phox subunit gene encodes a plasma membrane protein with Ca2+ binding motifs. *Plant Cell*, vol. 10, p.p. 255-266, 1998.
[15] Torres M.A., Onouchi H., Hamada S., Machida C., Hammond-Kosack K.E. and Jones J.D.G., "Six *Arabidopsis thaliana* homologues of the human respiratory burst oxidase (gp91(phox))". *Plant J.*, vol. 14, p.p. 365-370, 1998.
[16] Simon-Plas F., Elmayan T. and Blein J.P., "The plasma membrane oxidase NtrbohD is responsible for AOS production in elicited tobacco cells". *Plant J.*, vol. 31, p.p. 137-147, 2002.
[17] Sagi M. and Fluhr R., "Superoxide production by plant homologues of the gp91(phox) NADPH oxidase. Modulation of activity by calcium and by tobacco mosaic virus infection". *Plant Physiol.*, vol. 126, p.p. 1281-1290, 2001.
[18] Banfi B., Molnar G., Maturana A., Steger K., Hegedus B., Demaurex N. and Krause K.H., "A Ca2+-activated NADPH oxidase in testis, spleen, and lymph nodes". *J. Biol. Chem.*, vol. 276, p.p. 37594-37601, 2001.
[19] Torres M.A., Dangl J.L. and Jones J.D.G., "*Arabidopsis* gp91(phox) homologues AtrbohD and AtrbohF are required for accumulation of reactive oxygen intermediates in the plant defense response". *Proc. Natl. Acad. Sci. USA,* vol. 99, p.p. 517-522, 2002.
[20] Foreman J., Demidchik V., Bothwell J.H., Mylona P., Miedema H., Torres M.A., Linstead P., Costa S., Brownlee C., Jones J.D. et al., "Reactive oxygen species produced by NADPH oxidase regulate plant cell growth". *Nature*, vol. 422, p.p. 442-446, 2003.
[21] Yoshioka H., Numata N., Nakajima K., Katou S., Kawakita K., Rowland O., Jones J.D. and Doke N., "Nicotiana benthamiana gp91phox homologs NbrbohA and NbrbohB participate in H2O2 accumulation and resistance to Phytophthora infestans". *Plant Cell*, vol. 15, p.p. 706-718, 2003.
[22] Ryan C.A., "The systemin signaling pathway: differential activation of plant defensive genes". *Biochem. Biophys. Acta*, vol. 1477, p.p. 112-121, 2000.
[23] Lee G.I. and Howe G.A., "The tomato mutant spr1 is defective in systemin perception and the production of a systemic wound signal for defense gene expression". *Plant J.*, vol. 33, p.p. 567-576, 2003.
[24] Orozco-Cardenas M. and Ryan C.A., "Hydrogen peroxide is generated systemically in plant leaves by wounding and systemin via the octadecanoid pathway". *Proc. Natl. Acad. Sci. USA*, vol. 96, p.p. 6553-6557, 1999.
[25] Orozco-Cardenas M.L., Narvaez-Vasquez J. and Ryan C.A., "Hydrogen peroxide acts as a second messenger for the induction of defense genes in tomato plants in response to wounding, systemin, and methyl jasmonate". *Plant Cell*, vol. 13, p.p. 179-191, 2001.
[26] Sagi M., Davydov O., Orazova S., Yesbergenova Z., Ophir R., Stratmann J.W. and Fluhr R., "Plant respiratory burst oxidase homologs impinge on wound responsiveness and development in Lycopersicon esculentum". *Plant Cell*, vol. 16, p.p. 616-628, 2004.
[27] Molendijk A.J., Bischoff F., Rajendrakumar C.S.V., Friml J., Braun M., Gilroy S. and Palme K., "*Arabidopsis thaliana* Rop GTPases are localized to tips of root hairs and control polar growth". *EMBO J.*, vol. 20, p.p. 2779-2788, 2001.

[28] Jones M.A., Shen J.J., Fu Y., Li H., Yang Z.B. and Grierson C.S., "The *Arabidopsis* Rop2 GTPase is a positive regulator of both root hair initiation and tip growth". *Plant Cell*, vol. 14, p.p. 763-776, 2002.
[29] Kawasaki T., Henmi K., Ono E., Hatakeyama S., Iwano M., Satoh H. and Shimamoto K., "The small GTP-binding protein Rac is a regulator of cell death in plants". *Proc. Natl. Acad. Sci. USA,* vol. 96, p.p. 10922-10926, 1999.
[30] Potikha T.S., Collins C.C., Johnson D.I., Delmer D.P. and Levine A., "The involvement of hydrogen peroxide in the differentiation of secondary walls in cotton fibers". *Plant*, vol. 119, p.p. 849-858, 1999.
[31] Green R. and Fluhr R., "UV-B-Induced PR-1 Accumulation Is Mediated by Active Oxygen Species". *Plant Cell*, vol. 7, p.p. 203-212, 1995.
[32] Izaguirre M.M., Scopel A.L., Baldwin I.T. and Ballare C.L., "Convergent responses to stress. Solar ultraviolet-B radiation and Manduca sexta herbivory elicit overlapping transcriptional responses in field-grown plants of Nicotiana longiflora". *Plant Physiol.*, vol. 132, p.p. 1755-1767, 2003.
[33] Rao M.V., Paliyath C. and Ormrod D.P., "Ultraviolet-B- and ozone-induced biochemical changes in antioxidant enzymes of *Arabidopsis thaliana*". *Plant Physiol.*, vol. 110, p.p. 125-136, 1996.
[34] Casati P. and Walbot V., "Gene expression profiling in response to ultraviolet radiation in maize genotypes with varying flavonoid content". *Plant Physiol.*, vol. 132, p.p. 1739-1754, 2003.
[35] Holley S.R., Yalamanchili R.D., Moura D.S., Ryan C.A. and Stratmann J.W., "Convergence of signaling pathways induced by systemin, oligosaccharide elicitors, and ultraviolet-B radiation at the level of mitogen-activated protein kinases in Lycopersicon peruvianum suspension-cultured cells". *Plant Physiol.*, vol. 132, p.p. 1728-1738, 2003.
[36] Pei Z.M., Murata Y., Benning G., Thomine S., Klusener B., Allen G.J., Grill E. and Schroeder J.I., "Calcium channels activated by hydrogen peroxide mediate abscisic acid signalling in guard cells". *Nature*, vol. 406, p.p. 731-734, 2000.
[37] Jiang M. and Zhang J., "Cross-talk between calcium and reactive oxygen species originated from NADPH oxidase in abscisic acid-induced antioxidant defence in leaves of maize seedlings". *Plant Cell Environ.*, vol. 26, p.p. 929-939, 2003.
[38] Kwak J.M., Mori I.C., Pei Z.M., Leonhardt N., Torres M.A., Dangl J.L., Bloom R.E., Bodde S., Jones J.D.G. and Schroeder J.I., "NADPH oxidase AtrbohD and AtrbohF genes function in ROS-dependent ABA signaling in *Arabidopsis*". *EMBO J.*, vol. 22, p.p. 2623-2633, 2003.
[39] Suhita D., Raghavendra A.S., Kwak J.M. and Vavasseur A., "Cytoplasmic alkalization precedes reactive oxygen species production during methyl jasmonate- and abscisic acid-induced stomatal closure". *Plant Physiol.*, vol. 134, p.p. 1536-1545, 2004.
[40] Guo F.Q., Okamoto M. and Crawford N.M., "Identification of a plant nitric oxide synthase gene involved in hormonal signaling". *Science*, vol. 302, p.p. 100-103, 2003.
[41] Desikan R., Griffiths R., Hancock J. and Neill S., "A new role for an old enzyme: nitrate reductase-mediated nitric oxide generation is required for abscisic acid-induced stomatal closure in *Arabidopsis thaliana*". *Proc. Natl. Acad. Sci. U S A,* vol. 99, p.p. 16314-16318, 2002.
[42] Wolin M.S., "Interactions of oxidants with vascular signaling systems". *Arterioscler Thromb Vasc Biol.*, vol. 20, p.p. 1430-1442, 2000.

Cell Biology and Instrumentation: UV Radiation, Nitric Oxide and Cell Death in Plants
Y. Blume et al. (Eds.)
IOS Press, 2006

Nitric Oxide Functions in the Plant Hypersensitive Disease Resistance Response

Matteo DE STEFANO, Alberto FERRARINI, Massimo DELLEDONNE
Dipartimento Scientifico e Tecnologico, Università degli Studi di Verona, Strada le Grazie 15, 37134 Verona, Italy, e-mail: massimo.delledonne@univr.it

Abstract. Nitric oxide (NO) is a highly reactive molecule that rapidly diffuses and permeates cell membranes. In animals, NO is implicated in a number of diverse physiological processes such as neurotransmission, vascular smooth muscle relaxation, and platelet inhibition. It may have beneficial effects, for example as a messenger in immune responses, but it's also potentially toxic when the antioxidant system is weak and an excess of reactive oxygen species (ROS) accumulates. During the last few years NO has been detected also in several plant species, and the increasing number of reports on its function in plants have implicated NO as an important effector of growth, development, and defense. The innate immune system of organisms as diverse as vertebrates, invertebrates, and plants shows several characteristics similar with respect to involvement of NO. In the mammalian immune system, NO cooperates with ROS to induce apoptosis of tumor cells and macrophage killing of bacteria. In plants a similar mechanism has evolved to prevent tissue invasion by pathogens. The rapid accumulation of ROS and NO through the activation of enzyme systems similar to neutrophil NADPH oxidase and nitric oxide synthase (NOS) is one of the earliest events in the resistance response. Both NO and ROS are necessary to trigger host cell death in order to delimit the infected zone and avoid the multiplication and spread of the pathogen. NO and ROS are also components of highly amplified and integrated defense system that triggers the local expression of resistance genes. NO also functions independently of ROS in the induction of various defense genes including pathogenesis-related proteins and enzymes of phenylpropanoid metabolism involved in the production of lignin, antibiotics and the secondary signal salicylic acid. NO signaling functions depend on its reactivity and ROS are key modulators of NO in triggering cell death, although through mechanisms different from those commonly observed in animals.

Introduction

Plants exhibit a wide array of both passive and active defense strategies against pathogen attack. The preformed physical barriers (e.g. the cuticle and cell wall) and biochemical defenses (e.g. antimicrobial toxins) often are not sufficient to avoid spread of infection. In fact, after recognition of the invading pathogen, plants activate a very effective arsenal of inducible defense responses (the hypersensitive reaction, HR) characterized by hypersensitive cell death, tissue reinforcement and production of anti-microbial metabolites [1-3]. The rapid recognition of pathogen infection is supported by a sophisticated surveillance system capable of distinguishing between self-generate signals and those emitted by the pathogens [4] and is followed by establishment of a systemic acquired resistance (SAR), a salicylic acid dependent long lasting immunity against a broad spectrum of pathogens [5].

The HR requires active host protein synthesis and is kept under tight genetic control being activated only if the plant detects a prospective invader [6]. In this way plant cells

autonomously maintain constant vigilance against pathogen by expressing large arrays of '*R*-genes' (R, resistance). *R* genes encode putative receptors that respond to the product of '*Avr*-genes' (Avr, avirulence) which are expressed by a pathogen during infection. This gene-for-gene interaction results from either direct or indirect interaction between the *R* gene and *Avr* gene products depending on *R-Avr* gene pair [1]. *R*-gene-mediated activation of HR triggers a number of rapid cellular responses, including perturbations in ion fluxes and in the pattern of protein phosphorylation, which precede the accumulation of reactive oxygen species (ROS) and nitric oxide (NO) [7,8]. These initial responses are followed by the production of phytoalexins, transcriptional activation of defense genes and hypersensitive cell death, a form of programmed cell death with some regulatory and mechanistic features characteristic of apoptosis in animal cells, like membrane dysfunction, vacuolization of the cytoplasm, chromatin condensation and endonucleolytic cleavage of DNA [9,10]. The interplay between ROS and NO contributes to the establishment of the HR and to augmentation of defense responses [11] (Figure 1). Downstream events are inhibited by some blockers for Ca^{2+} channels and anion channels, suggesting that the initial ion fluxes are crucial for the induction of defense responses [12].

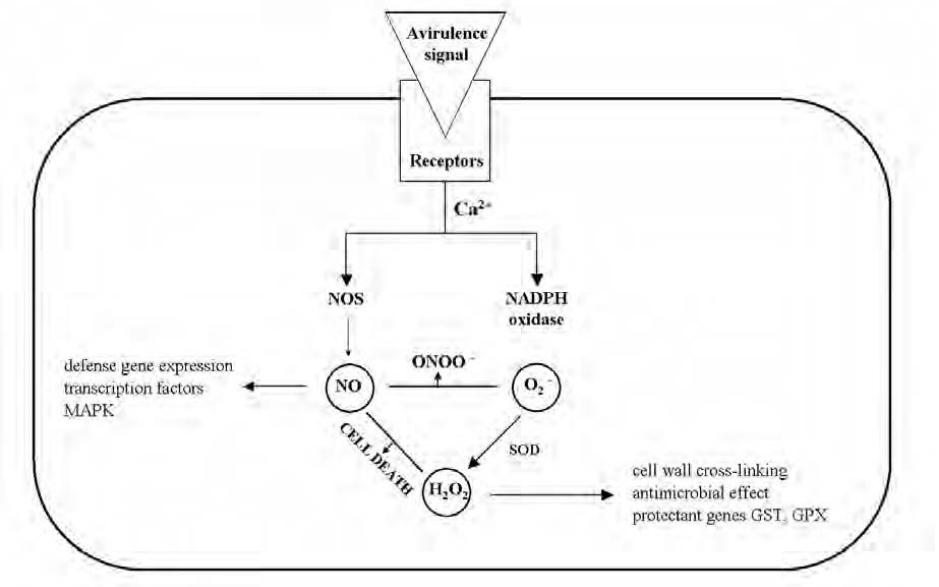

Figure 1. NO-mediated activation of defense response. NO, nitric oxide; NOS, nitric oxide synthase; $ONOO^-$peroxynitrite; H_2O_2, hydrogen peroxide; O_2^- superoxide; GPX, glutathione peroxidase; GST, glutathione S-transferase; SOD, superoxide dismutase; MAPK, mitogen-activated protein kinase.

1. ROS production and signaling

One of the most rapid defense responses following pathogen recognition is the so-called oxidative burst, a rapid accumulation of superoxide (O_2^-) and hydrogen peroxide (H_2O_2) at the site of attempted invasion [13]. There are a number of potential sources of ROS in plants. Many pharmacological, immunological and molecular studies strongly support the idea that the primary source of ROS in plant cells is an O_2^- generating membrane-bound NADPH oxidase [14,15]. The enzymatic complex of NADPH oxidase found in mammalian

neutrophils consists of two plasma membrane proteins and several cytosolic regulatory proteins that traslocate to the plasma membrane to form the active complex after stimulation [16]. In plants, NADPH oxidase is analogous to the mammalian counterpart and has an N-terminal extension, which contains two Ca^{2+} binding elongation factor (EF) hands [15]. These findings support the hypothesis that plant plasma membrane contains an enzyme closely related to the neutrophil NADPH oxidase and reveal direct activation by Ca^{2+} ions. Other enzymatic ROS sources have been characterized: extracellular enzymes such as amine, diamine, and poliamine oxidases have been implicated as possible sources of ROS following pathogen recognition [13]. The major source of ROS in French bean cells treated with an elicitor from *Collectothricum lindemuthianum* appears to be dependent on an extracellular peroxidase [17,18]. Finally, intracellular sources of ROS are chloroplasts, mitochondria, plasma membrane and peroxisomes [13,19-21].

Several roles in plant defense have been proposed for ROS. H_2O_2 can be directly toxic to pathogens and it contributes to structural reinforcement of plant cell walls, either by cross-linking various hydroxyproline and proline-rich glycoproteins to the polysaccharide matrix or by increasing the rate of lignin polymer formation by way of peroxidase enzyme activity, both of which would make the plant cell wall more resistant to microbial penetration and enzymatic degradation [22,23]. The deployment of antioxidant enzymes or scavengers has been shown to blunt the development of cell death during a number of incompatible plant-pathogen interactions. Moreover, the inhibition of endogenous antioxidant mechanisms using specific and non-specific pharmacological agents, which increased the concentration of ROS, resulted in elevated levels of host cell death [9].

ROS generated via the oxidative burst have been proposed to play a central role in the development of host cell death during the HR [24] and to influence the expression of a large number of genes by two main ways: through the oxidation of components of signaling pathways that subsequently activate transcription factors, or through the oxidation of redox-sensitive transcription factors [25]. ROS can activate protein kinase cascades (MAPK) resulting in indirect activation of transcription regulators [26]. As increases in cytosolic Ca^{2+} is a common, early response to H_2O_2, it is likely that activation of Ca^{2+} dependent protein kinases and phosphatases is also an early step, with some enzymes potentially mediating downstream signaling components such as other protein kinases/phosphatases and other effector proteins [27].

2. NO production and signaling

The broad chemistry of NO involves an interplay between three species differing in their physical properties and chemical reactivity: the nitrosonium cation (NO^+), the radical ($NO^\cdot$) and nitroxyl anion (NO^-). This highly reactive molecule rapidly diffuses and permeates the cell membrane and can modulate intercellular signaling through regulation of redox centers in proteins whose regulation is based on a reduced/oxidized switch [28, 29]. In plants, NO production is well documented in response to infection with bacterial, viral and fungal pathogens [35, 36, 37] and after treatments with elicitors lipopolysaccharides (LPS) extracted from plant and animal pathogens [34]. NO is produced through non-enzymatic and enzymatic routes. The former routes include nitrite/ascorbate interaction or the light mediated conversion of NO_2 to NO via carotenoids [30]. The latter routes of NO synthesis include the reduction of nitrite by nitrate reductase (NR) [31] and conversion of arginine to citrulline by nitric oxide synthase (NOS) [32]. In contrast to animals that possess three different isoforms of NOS (inducible, neuronal and endothelial) [33] the only plant gene encoding a NOS is AtNOS1 from *A. thaliana* [32]. AtNOS1 does not share sequence

identity with animal NOS and display a flavin-, heme-, and tetrahydrobiopterin-independent NOS activity and appears to be constitutively expressed [34]. Recently, AtNOS1 mutant *A. thaliana* plants were shown to be more susceptible to virulent *Pseudomonas syringae* and display a much more severe development of disease symptoms and enhanced bacterial growth compared to wild-type [34].

The mobile nature of NO and its chemical reactivity with various cellular targets means that downstream effects of NO may be directly induced by interaction with various cellular components, like ion channels or proteins that modulate gene expression, or indirectly following interaction with signaling proteins such as protein kinase [29]. In mammals, one of the most important targets of NO is guanylate cyclase (GC). NO interacts with the heme prosthetic group of this enzyme, leading to its activation and results in increased generation of intracellular cyclic GMP (cGMP) [38]. Administration of NO donors or recombinant mammalian NOS to tobacco plants or suspension cells triggers expression of defense related genes phenylalanine ammonia lyase (*PAL*) and pathogenesis related protein PR-1 [35]. *PAL* gene expression is also induced by exogenous application of cGMP, suggesting that the NO/cGMP-dependent signaling pathway present in animals may also exist in plants [35]. However, the partial suppression of *PAL* induction in tobacco plants by inhibitors of NO-inducible GC suggests the existence of both cGMP-dependent and independent pathways [39]. Although the involvement of cGMP in several plant signal transduction pathways has been demonstrated, it remains to be determined whether or not NO is the physiological activator of plant GC [40].

In mammals, another molecule that serves as second messenger for NO signaling is cyclic ADP ribose (cADPR) [33]. In plants, cADPR is known to be involved in the abscissic acid signaling pathway in tomato and *Arabidopsis* [41]. In addition, cADPR has been found to elicit Ca^{2+} release in *Vicia faba* from vacuoles, and induce *PAL* and *PR-1* expression in tobacco. This induction can be blocked by a cADPR-gated Ca^{2+} channel inhibitor [39] and by a cADPR antagonist [42]. Since expression of *PR-1* and *PAL* genes is amplified when cGMP and cADPR are added simultaneously, these second messengers appear to act synergistically.

NO has been shown to activate protein kinases (PKs) in *Arabidopsis* and tobacco [36,43]. Two MAPKs have been recently found to function as early positive regulators in plant defense. The tobacco SIPK (SA-induced protein kinase) and WIPK (wounding-induced protein kinase) are activated upon different stimuli including biotic and abiotic stresses [43]. SIPK is typically induced by SA and by H_2O_2 [44] and shows SA-mediated NO inducibility [43], while WIPK is not induced by either SA or NO. The NtMEK2 kinase represents an upstream link between SIPK and WIPK as it can specifically activate both kinases [44]. A number of other kinases, and kinase kinases, have been identified that might constitute a complex signaling network leading to resistance, which may at least partially overlap other responses to a number of different stresses [45].

3. NO and ROS cooperation in the HR

One of the earliest events of the HR is the rapid accumulation of ROS and NO [43,46]. The reaction between NO and O_2^- produces $ONOO^-$ [47] a highly reactive oxidant molecule which then interacts with many molecular components and may modulate downstream signaling [48]. In mammals, $ONOO^-$ induces apoptosis and is cytotoxic by causing oxidative tissue damage [49]. In plants $ONOO^-$ does not appear to be an essential intermediate of NO-induced cell death [50]. However, $ONOO^-$ induce *PR-1* accumulation in tobacco leaves [39] and protein nitration leading to changes in the redox state of the cell [50]. Since the formation of O_2^- and NO is an inevitable event in plant cells [51] the

continuous formation of $ONOO^-$ can be postulated. Consequently, plant cells may have developed specific mechanisms to overcome the toxicity of $ONOO^-$, and they may have adopted different NO/ROS signals for triggering cell death during HR. In the so-called balance model [50] the fluctuation in O_2^- levels is the key indicator of redox stresses in uninfected cells and the sensor integrating NO and H_2O_2 coactivation of pathogen-induced hypersensitive cell death in the infected tissue. The relative rates of H_2O_2 production by a SOD mediated dismutation of O_2^- and the generation of $ONOO^-$ determines the balance beetwen NO and H_2O_2 required for the activation of the cell death program [52]. How NO and ROS actually kill is still unclear. In animal, NO cooperates with ROS to induce DNA fragmentation and cell lysis in murine lymphoma, hepatoma and endothelial cells but these two molecules don't appear to be directly involved in killing [53, 54]. *In vitro* studies have suggested that reaction of NO with H_2O_2 produces singlet oxygen or hydroxyl radicals in both the gaseous and liquid phase [55]. However, it is now well accepted that NO-induced cell death is an active process in which proteases play a crucial role. Cystatine-sensitive protease have been found to be critical regulators for cell death in a soybean model system [56, 57]. In addition, Ac-YVAD-CMK, an irreversible inhibitor of mammalian caspase-1, a class of cysteine proteases involved in apoptosis, was shown to block NO induced cell death [36].

4. Conclusion

Although several hypotheses still await experimental demonstration, it is now clear that NO is an important component of plant defense systems. Much evidence supports the view that NO plays a key role in disease resistance responses. Moreover, the recent identification of a plant NOS will lead to the characterization and manipulation of mechanisms modulating NO signaling. Thus, the understanding of NO signaling functions at the biochemical, cellular and molecular levels will soon make it possible to discern several important physiological and pathological processes in plants, as already demonstrated in mammals.

References

[1] McDowell J. M. and Woffenden B. J., "Plant disease resistance genes: recent insights and potential applications". *Trends Biotechnol*, vol. 21, p.p. 178-183, 2003.
[2] Dangl J.L., Dietrich R.A. and Richberg M.H., "Death don't have mercy: cell death programs in plant-microbe interactions". *Plant Cell*, vol. 8, p.p. 1793-1807, 1996.
[3] Hammond-Kosack K.E. and Jones J.D.G., "Resistance gene dependent plant defense responses". *Plant Cell*, vol. 8, p.p. 1773-1791, 1996.
[4] Holub E.B., "The arms race is ancient history in *Arabidopsis*, the wildflower". *Nat Rev Genet*, vol. 2, p.p. 516-527, 2001.
[5] Ryals J.A., Neuenschwander U.H., Willits M.G., Molina A., Steiner H.Y. and Hunt M.D., "Systemic acquired resistance". *Plant Cell*, vol. 8, p.p. 1809-1819, 1996.
[6] Baker B., Zambryski P., Staskawicz B. and Dinesh-Kumar S.P., "Signalling in plant–microbe interactions". *Science*, vol. 276, p.p. 726-733, 1997.
[7] McDowell J.M. and Dangl J.L., "Signal transduction in the plant immune response". *Trends Biochem Sci,* vol 25, p.p. 79-82, 2000.
[8] Cohn J., Sessa G. and Martin G.B., "Innate immunity in plants". *Curr Opin Immunol*, vol. 13, p.p. 55-62, 2001.
[9] Levine A., Tenhaken R., Dixon R. and Lamb C., "H_2O_2 from the oxidative burst orchestrates the plant hypersensitive disease resistance response". *Cell*, vol. 79, p.p. 583-593, 1994.
[10] Gilchrist D. G., "Programmed cell death in plant disease: the purpose and promise of cellular suicide". *Annu Rev Phytopathol.*, vol. 36, p.p. 393-414, 1998.

[11] Blume B., Nürnberger T., Nass N., Scheel D., "Receptor-mediated increase in cytoplasmic free calcium required for activation of pathogen defense in parsley". *Plant Cell*, vol. 12, p.p. 1425-1440, 2000.
[12] Wendehenne D., Lamotte O., Frachisse J.M., Barbier-Brygoo H. and Pugin A., "Nitrate efflux is an essential component of the cryptogein signaling pathway leading to defence responses and hypersensitive cell death in tobacco". *Plant Cell*, vol. 14, p.p. 1937-1951, 2002.
[13] Grant J.J. and Loake G.J., "Role of reactive oxygen intermediates and cognate redox signaling in disease resistance". *Plant Physiol*, vol. 124, p.p. 21-29, 2000.
[14] Groom Q. J., Torres M.A., Fordham-Skelton A.P., Hammond-Kosack K.E., Robinson N.J. and Jones J.D., "rbohA, a rice homologue of the mammalian gp91phox respiratory burst oxidase gene". *Plant J*., vol. 10, p.p. 515-522, 1996.
[15] Keller T., Damude H.G., Werner D., Doerner P., Dixon R.A. and Lamb C., "A plant homolog of the neutrophil NADPH oxidase gp91phox subunit gene encodes a plasma membrane protein with Ca^{2+} binding motifs". *Plant Cell*, vol. 10, p.p. 255-266, 1998.
[16] Yoshioka H., Numata N., Nakajima K., Katou S., Kawakita K., Rowland O., Jones J.D. and Doke, N., "*Nicotiana benthamiana* gp91phox homologs NbrbohA and NbrbohB participate in H_2O_2 accumulation and resistance to *Phytophthora infestans*". *Plant Cell*, vol. 15, p.p. 706-718, 2003.
[17] Bolwell C. J. and Wojtaszek P., "Mechanisms for the generation of reactive oxygen species in plant defences, p.p. a broad perspective". *Physiol Mol Plant Pathol*, vol. 51, p.p. 347-366, 1997.
[18] McLusky S.R., Bennett M.H., Beale M.H., Lewis M.J., Gaskin P. and Mansfield J.W., "Cell wall alterations and localized accumulation of feruloyl-3 '-methoxytyramine in onion epidermis at sites of attempted penetration by *Botrytis allii* are associated with actin polarisation, peroxidase activity and suppression of flavonoid biosynthesis". *Plant J*., vol. 17, p.p. 523-534, 1999.
[19] Asada K., "The water-water cycle in chloroplasts, p.p. scavenging of active oxygens and dissipation of excess photons". *Annu. Rev. Plant Physiol. Plant Mol. Biol*., vol. 50, p.p. 601-639, 1999.
[20] Scheel D., "Oxidative burst and the role of reactive oxygen species in plant–pathogen interactions". In: Inze D, Van Montagu M (eds) "Oxidative Stress in Plants", Taylor & Francis, NewYork, 137-153, 2002.
[21] del Rio L.A., Corpas F.J., Sandalio L.M., Palma J.M., Gomez M. and Barroso J.B., "Reactive oxygen species, antioxidant systems and nitric oxide in peroxisomes". *J. Exp. Bot*., vol.53, p.p. 1255-1272, 2002.
[22] Brisson L.F., Tenhaken R. and Lamb C.J., "Function of oxidative cross-linking of cell wall structural proteins in plant disease resistance". *Plant Cell*, vol. 6, p.p. 1703-1712, 1994.
[23] Ros Barcelò A., "Lignification in plant cell walls". *Int. Rev. Cytol*., vol. 176, p.p. 87-132, 1997.
[24] Tenhaken R., Levine A., Brisson L.F., Dixon R.A. and Lamb, C., "Function of the oxidative burst in hypersensitive disease resistance". *Proc. Natl. Acad. Sci. USA*, vol. 92, p.p. 4158-4163, 1995.
[25] Laloi C., Apel K. and Danon A., "Reactive oxygen signalling: the latest news". *Curr. Opin. Plant Biol*., vol. 7, p.p. 323-328, 2004.
[26] Desikan R., Clarke A., Hancock J.T. and Neill S.J., "H_2O_2 activates a MAP kinase-like enzyme in *Arabidopsis thaliana* suspension cultures". J. Exp. Bot., vol. 50, p.p. 1863-1866, 1999.
[27] Neill S., Desikan R. and Hancock J., "Hydrogen peroxide signalling". *Curr. Opin. Plant. Biol*., vol. 5, p.p. 388-395, 2002.
[28] Stamler J.S., "Redox signaling, p.p. nitrosylation and related targets interactions of nitric oxide". *Cell*, vol. 78, p.p. 931-936, 1994.
[29] Neill S.J., Desikan R. and Hancock J.T., "Nitric oxide signalling in plants". *New Phytol*., vol. 159, p.p. 11-35, 2003.
[30] Delledonne M., Xia Y., Dixon R.A. and Lamb C., "Nitric oxide functions as a signal in plant disease resistance". *Nature*, vol. 394, p.p. 585-588, 1998.
[30] Cooney R.V., Harwood P.J., Custer L.J. and Franke A.A., "Light-mediated conversion of nitrogen dioxide to nitric oxide by carotenoids". *Environ. Health Perspect*., vol. 102, p.p. 460-462, 1994.
[31] Rockel P., Strube F., Rockel A., Wildt J. and Kaiser W.M., "Regulation of nitric oxide (NO) production by plant nitrate reductase in vivo and in vitro". *J. Exp. Bot*., vol. 53, p.p. 103-110, 2002.
[32] Guo F.Q., Okamoto M. and Crawford N.M., "Identification of a plant nitric oxide synthase gene involved in hormonal signaling". *Science*, vol. 302, p.p. 100-103, 2003.
[33] Wendehenne D., Pugin A., Klessig D.F. and Durner J., "Nitric oxide, p.p. comparative synthesis and signaling in animal and plant cells". *Trends Plant. Sci*., vol. 6, p.p. 177-183, 2001.
[34] Zeidler D., Zahringer U., Gerber I., Dubery I., Hartung T., Bors W., Hutzler P. and Durner, J., "Innate immunity in *Arabidopsis thaliana*, p.p. Lipopolysaccharides activates nitric oxide synthase (NOS) and induce defense genes". *Proc. Natl. Acad. Sci. USA*, vol. 101, p.p. 15811-15816, 2004).
[35] Durner J., Wendehenne D. and Klessig D.F., „Defense gene induction in tobacco by nitric oxide, cyclic GMP and cyclic ADP-ribose". *Proc. Natl. Acad. Sci. USA,* vol. 95, p.p. 10328-10333, 1998.
[36] Clarke A., Desikan R., Hurst R.D., Hancock J.T. and Neill, S.J., "NO way back, p.p. nitric oxide and programmed cell death in *Arabidopsis thaliana* suspension cultures". *Plant J*., vol. 24, p.p. 667-677, 2000.

[37] Tada Y., Mori T., Shinogi T., Yao N., Takahashi S., Betsuyaku S., Sakamoto M., Park P., Nakayashiki H. and Tosa Y., "Nitric oxide and reactive oxygen species do not elicit hypersensitive cell death but induce apoptosis in the adjacent cells during the defense response of oat". *Mol. Plant. Microbe. Interact*., vol. 17, p.p. 245-253, 2004.
[38] Wendehenne D., Durner J. and Klessig D.F., "Nitric oxide, p.p. a new player in plant signalling and defence responses". *Curr. Opin. Plant Biol*., vol. 7, p.p. 449-455, 2004.
[39] Durner J. and Klessig D.F., "Nitric oxide as a signal in plants". *Curr. Opin. Plant. Biol*., vol. 2, p.p. 369-374, 1999.
[40] Delledonne M., Polverari A. and Murgia I., "The functions of nitric oxide-mediated signaling and changes in gene expression during the hypersensitive response". *Antioxid. Redox Sign*., vol. 5, p.p. 33-41, 2003.
[41] Sánchez J.P., Duque P.& C. and Nam-Hai, « ABA activates ADPR cyclase and cADPR induces a subset of ABA-responsive genes in *Arabidopsis*". *Plant J*., vol. 38, p.p. 381-395, 2004.
[42] Klessig D.F., Durner J., Noad R., Navarre D.A., Wendehenne D., Kumar D., et al., „Nitric oxide and salicylic acid signaling in plant defense". *Proc. Natl. Acad. Sci. USA*, vol. 97, p.p. 8849-8855, 2000
[43] Kumar D.and Klessig D.F., „Differential induction of tobacco MAP kinases by the defence signals nitric oxide, salicylic acid, ethylene and jasmonic acid". *Mol. Plant Microbe Interact*., vol. 13, p.p. 347-351, 2000.
[44] Yang K.Y., Liu Y. and Zhang S., "Activation of a mitogenactivated protein kinase pathway is involved in disease resistance in tobacco". *Proc. Natl. Acad. Sci. USA,* vol. 98, p.p. 741-746, 2001.
[45] Nurnberger T. and Scheel D., "Signal transmission in the plant immune response", *Trends Plant Sci*., vol. 6, p.p. 372-379, 2001.
[46] Lamb C. and Dixon R.A., "The oxidative burst in plant disease resistance". *Ann. Rev. Plant Physiol. Plant Mol. Biol*., vol. 48, p.p. 251-275, 1997.
[47] Koppenol W. H., Moreno J. J., Pryor W. A., Ischiropoulos H. and Beckman J.S., "Peroxynitrite, a cloaked oxidant formed by nitric oxide and superoxide". *Chem. Res. Toxicol*., vol. 5, p.p. 834-842, 1992.
[48] Beckman J.S., Beckman T.W., Chen J., Marshall P.A. and Freeman, B.A., "Apparent hydroxyl radical production by peroxynitrite, p.p. implications for endothelial injury from nitric oxide and superoxide". *Proc. Natl. Acad. Sci. USA*, vol. 87, p.p. 1620-1624, 1990.
[49] Lin K.T., Xue J.Y., Nomen M., Spur B. and Wong P.Y., "Peroxynitrite induced apoptosis in HL-60 cells". *J. Biol. Chem*., vol. 270, p.p. 16487-16490, 1995.
[50] Delledonne M., Zeier J., Marocco A. and Lamb C., "Signal interactions between nitric oxide and reactive oxygen intermediates in the plant hypersensitive disease resistance response". *Proc. Natl. Acad. Sci. USA*, vol. 98, p.p. 13454-13459, 2001.
[51] Romero-Puertas M.C. and Delledonne M., "Nitric oxide signaling in plant-pathogens interaction". *IUBMB Life*, vol. 55, p.p. 579-583, 2003.
[52] Delledonne M., Murgia I., Ederle D., Sbicego P.F., Biondani A., Polverari A. and Lamb C., "Reactive oxygen intermediates modulate nitric oxide signaling in the plant hypersensitive disease resistance response". *Plant Physiol. Biochem*., vol. 40, p.p. 605-610, 2002.
[53] Farias-Eisner R., Chaudhuri G., Aeberhard E. and Fukuto J. M., "The chemistry and tumoricidal activity of nitric oxide/hydrogen peroxyde and the implications to cell resistance/susceptibility". *J. Biol. Chem*., vol. 271, p.p. 6144-6151, 1996.
[54] Filep J.G., Lapierre C., Lachance S. and Chan J. S., "Nitric oxide cooperates with hydrogen peroxyde in inducing DNA fragmentation and cell lysis in murine lymphoma cells". *Biochem. J*., vol. 321, p.p. 897-901, 1997.
[55] Noronha-Dutra A.A., Epperlein M.M. and Woolf, N., "Reaction of nitric oxide with hydrogen peroxide to produce potentially cytotoxic singlet oxygen as a model for nitric oxide-mediated killing". *FEBS Lett.,* vol. 321, p.p. 59-62, 1993.
[56] Solomon M., Belenghi B., Delledonne M., Menachem E. and Levine A., "The involvement of cysteine proteases and protease inhibitor genes in the regulation of programmed cell death in plants". *Plant Cell*, vol. 11, p.p. 431-444, 1999.
[57] Belenghi B., Acconcia F., Trovato M., Perazzolli M., Bocedi A., Polticelli F., Ascensi P. and Delledonne M., "AtCYS1, a cystatin from *Arabidopsis thaliana*, suppresses hypersensitive cell death". *Eur J. Biochem.*, vol. 270, p.p. 1-12, 2003.

Cell Biology and Instrumentation: UV Radiation, Nitric Oxide and Cell Death in Plants
Y. Blume et al. (Eds.)
IOS Press, 2006

Nitric Oxide in Cell Damage and Protection

Steven NEILL, Jo BRIGHT, Radhika DESIKAN, Judy HARRISON, Tanya SCHLEICHER and John HANCOCK
Centre for Research in Plant Science, Genomics Research Institute, University of the West of England, Bristol, Coldharbour Lane, Bristol BS16 1QY, UK

Abstract. The key research questions must be directed to the effects of UV on NO generation and action in plants. Research programmes will require methods to assess accurately NO emissions from leaves and to determine NO concentrations in cells and sub-cellular microdomains; the use of mutants and transgenic plants altered in NO synthetic and scavenging capacities; analyses of the molecular and biochemical events required for activation of PCD by NO and UV; and the development of techniques to monitor simultaneously cell death, NO and ROS generation in the field during exposure to UV.

Introduction

Less than ten years ago, the impact on plant biology of the gaseous free radical gas nitric oxide ($NO^{\cdot}$) related only to its toxic effects as a component of NO_x, released into the atmosphere as an air pollutant during the combustion of fossil fuels. It is now clear that NO is a multi-faceted and versatile endogenous signalling molecule with an importance in many if not all aspects of plant growth and development. At least two enzymatic sources of NO in plants have been characterised and mechanisms that serve to scavenge NO have also been identified. Downstream signalling responses to NO include generation and action of the second messenger molecules calcium, cyclic GMP and cyclic ADPR, protein phosphorylation, protein nitrosylation and specific effects on gene expression. NO also interacts directly with Reactive Oxygen Species (ROS) and with components of ROS-activated signalling pathways. NO and ROS play key roles in an orchestra of plant defence responses. Rapid generation of NO and ROS following pathogen or elicitor challenge mediates a multitude of metabolic and transcriptional alterations including Programmed Cell Death (PCD).

However, it is important to note that in some cases the actions of NO can be cytoprotective rather than toxic, potentially via antioxidant effects of NO, and prevention of NO synthesis or action can delay or inhibit PCD. In addition to the roles of NO and ROS in biotic stress responses, NO and ROS generation also occurs in response to various abiotic stresses, including UV radiation which itself can induce PCD. Recent data suggest that NO mediates some UV responses and that UV radiation can also stimulate the release of NO_x from leaves.

Key research questions to be addressed must be directed to the effects of UV on NO generation and action in plants. Research programmes will require methods to assess accurately NO emissions from leaves and other organs and to determine NO concentrations in cells and sub-cellular microdomains; the use of mutants and transgenic plants altered in NO synthetic and scavenging capacities; analyses of the molecular and biochemical events required for activation of PCD by NO and UV; and the development of techniques to

monitor simultaneously cell death, NO and ROS generation in the field during exposure to UV.

1. What is NO and what does it do?

Less than ten years ago, the impact on plant biology of the gaseous free radical gas NO related only to its toxic effects as a component of NO_x, released into the atmosphere as an air pollutant during the combustion of fossil fuels [1]. It is now clear that NO is a multi-faceted and versatile endogenous signalling molecule with an importance in many if not all aspects of plant growth and development. Plant NO research began in earnest when it was found that pathogen challenge induced NO generation and that NO participated in pathogen-induced cell death [2, 3]. Thus NO synthesis and action can determine various 'life-or-death' situations in plants. However, its actions and effects are much more widespread, as they also contribute to a plant's 'quality of life'. This is because, in addition to effects at the stress margins, NO also regulates various processes at the centre of normal plant biology that include seed germination, root initiation, gravitropism, leaf development, nutrition and stomatal closure in response to abscisic acid. Moreover, as would be expected for a molecule that mediates key signalling processes, it interacts with other signals such as ROS, salicylic acid and jasmonic acid [4-6].

2. How is NO made and removed?

Plants contain an array of NO-generating capabilities for which the full molecular and physiological details have not yet been deciphered [5,6]. Animal cells generate NO via nitric oxide synthase (NOS), a group of related enzymes that convert L-arginine to L-citrulline and NO. Although plant NOS activity has often been described, no structurally related enzymes have yet been found. However, a unique plant NOS enzyme, AtNOS1, has recently been characterised. AtNOS1 was cloned from *Arabidopsis*, based on sequence similarity to a snail protein implicated in NO synthesis [7] and although AtNOS1 uses L-arginine as a substrate its sequence differs to that of animal NOS. Importantly, plant cells can also produce NO via the enzyme nitrate reductase (NR), catalysing NO synthesis from nitrite [4-6,8], as shown in transgenic tobacco plants with permanently active NR which emit greatly elevated amounts of NO [9]. Genetic and biochemical data indicate that AtNOS1 and NR have biological functions during hormonal signalling [7,10]. There are also other less well-characterised potential NO sources in plants, including a plasma membrane enzyme generating NO from nitrite [11], non-enzymatic synthesis [12], xanthine oxidoreductase and NOS-like activities that remain to be isolated [5]**.** Clearly, more research is required to determine the contributions and interactions of these potential sources of NO (Figure 1).

Because NO induces a diverse range of biological effects that include cell death, it might be expected that plants possess mechanisms to detoxify NO. Recent data have shown that plant non-symbiotic haemoglobins may well perform this function. Plant haemoglobins are induced by hypoxic stress [13], a stress that also induces substantially elevated rates of NO generation [14,15]. Over- or under-expression of a barley haemoglobin in alfalfa root cultures [14] or maize suspension cultures [16] reduced or increased NO levels respectively and expression of an alfalfa haemoglobin in tobacco altered plant responses to NO treatment or pathogen challenge [17]. Metallothioneins, recently shown to function as ROS scavengers in plants [18], may also possess NO-scavenging capacity. NO can also react with the small tripeptide glutathione to form S-nitrosoglutathione (GSNO). GSNO can be

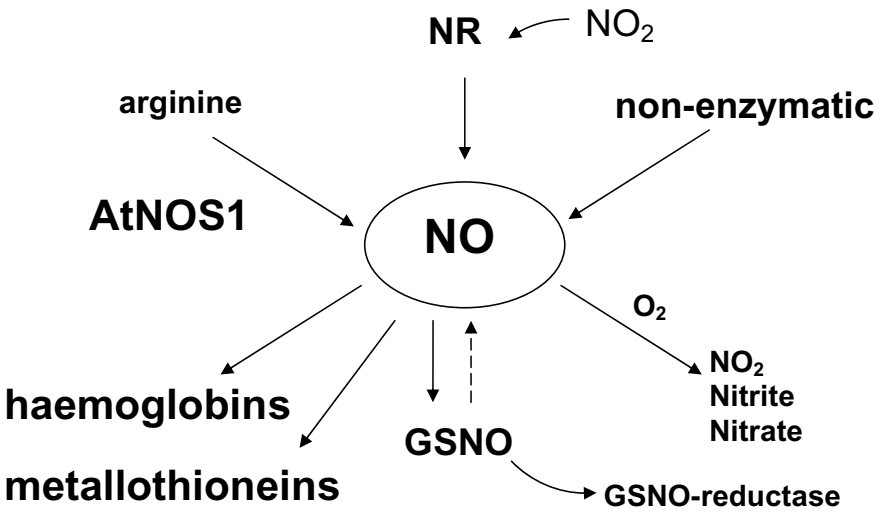

Figure 1. NO biosynthesis and removal. Generation of NO can occur from arginine via NOS, from nitrite via NR, through other enzymatic sources or non-enzymatically. NO can be removed by reaction with haemoglobins and metallothioneins, via S-nitrosylation of glutathione to form S-nitroglutathione or by reaction with oxygen to form nitrogen dioxide, which degrades to nitrite and nitrate.

metabolised, thereby removing NO, or it could act as a source of NO within plants, potentially at a site distant from its point of generation [see 5] (Figure 1).

3. Why might NO be relevant to UV responses?

Various abiotic and biotic stresses, including exposure to higher than normal amounts of UV radiation, result in oxidative stress, altered patterns of gene expression and cell death. Because several of these stresses also cause increased NO production, with NO having both positive and negative effects on cell survival, it is quite possible that UV effects also involve NO signalling.

3.1. NO, biotic and abiotic stress

NO plays a key role in defence responses during plant-pathogen interactions. NO is strongly involved in important mechanisms induced by pathogen recognition, that lead to the repulsion of potentially invasive bacteria and fungi. These responses include the expression of 'defence-related genes', encoding products that contribute to disease resistance, for example anti-microbial proteins or enzymes that catalyse the biosynthesis of anti-microbial phytoalexins, and the Hypersensitive Response, a form of PCD localised to the points of infection. PCD is a genetically determined, metabolically directed cellular process resulting in cell suicide – cells die because of activation of intrinsic signalling and execution processes rather than by necrosis induced by other forms of damage. There are several different types of PCD, activated by a range of signals, in plants [19]. Localised cell death during the HR limits pathogen spread by restricting nutrient supply and acting as a focus for anti-microbial chemical activities. NO is rapidly generated in response to challenge by pathogens [2,3,20,21] or elicitors [22-27], chemical signals released during

plant-pathogen interactions that are recognised by host plant cells and that induce a range of defence responses. Although there is some controversy over the exact role of NO [28], it is clearly an important one, as exogenous NO can induce hypersensitive cell death or PCD and expression of defence-related genes, and removal of NO via genetic or chemical means impairs disease resistance and pathogen-induced HR [2,5,6,17,29,30].

Increasing data indicate that NO might also be generated in response to some abiotic environmental stresses [see 5]. Although the effects of dehydration (drought stress) remain to be resolved, with both increases and decreases in NO emission from pea [31] and *Arabidopsis* [32] being described, drought stress resulted in increased NOS activity in wheat seedlings and ABA accumulation was inhibited by NOS inhibitors [33]. Moreover, both osmotic and salinity stress can induce rapid NO generation [34]. NO induces stomatal closure and has been shown to be an essential component of the guard cell signalling network initiated by ABA and resulting in stomatal closure [35-37]. If NO is removed or its synthesis prevented then stomatal closure in response to ABA is impaired [7,10,37]. Recently, the requirement for NO in salicylic acid-induced stomatal closure in *Vicia faba* has been reported [38]. Heat stress also increases NO production [34], whilst mechanical stress/wounding may or not increase NO levels, perhaps depending on the species or cell type [34,39-43].

3.2. NO, cell death and Reactive Oxygen Species

Another key feature of plant defence responses is the 'oxidative burst' during which ROS such as the superoxide anion, (O_2^-) and hydrogen peroxide (H_2O_2) are rapidly generated in response to the same stimuli as is NO. ROS are well-established mediators of defence responses and contribute to the initiation of the HR and pathogen-induced PCD. An oxidative burst and elevated ROS generation also occur in response to various abiotic stresses, either via perturbation of metabolism by the stress or mediated by specific ROS-generating enzymes such as NADPH oxidase that are also activated by pathogen signals [44]. Such abiotic stresses include extremes of temperature, wounding, UV irradiation, anoxia and air pollutants such as ozone. Cell death, potentially programmed (the molecular and biochemical details remain to be fully elucidated), is also induced by these stresses. Increasingly, it appears that NO and ROS interact in response to various stimuli that induce cell death, such that *either* cell survival *or* PCD is the outcome.

PCD in plants probably shares some conserved aspects with PCD in animal cells but also possesses plant-specific features [45]. Nuclear DNA degradation and chromatin condensation are often associated with PCD and disrupted mitochondrial function may well be an early component of PCD induced by several stimuli. Altered mitochondrial membrane permeability results in release of cytcohrome c to the cytoplasm. In animal cells, cytochrome c release then leads to the activation of a proteolytic cascade involving various caspases, cysteine proteases with aspartate-specific cleavage activity that cleave numerous cellular proteins, ultimately bringing about cell death [45]. No true caspases have been identified in plants but (mammalian) caspase inhibitors do inhibit PCD in plant cells and plant proteases with some caspase-like properties, such as metacaspases, legumains and subtilisin-like serine proteases, may be functionally equivalent to caspases [46].

Toxic effects of NO as an air pollutant were first observed many years ago [see 1]. These effects were assumed to represent necrosis induced by NO but it may be that at least some of the toxic effects of NO are due to its ability to participate in the activation and spread of PCD. Exogenous NO can induce cell death that has features characteristic of PCD, including chromatin condensation, increased caspase activity and inhibition by caspase inhibitors, and disrupted mitochondrial function. NO induces PCD in cell cultures of *Arabidopsis* [20], carrot [47] *Citrus sinensis* [48] and *Taxus* [43]. In carrot and *Citrus*,

NO treatment induced cytochrome c release [47] and altered mitochondrial membrane permeability respectively [48]. Respiration was inhibited by NO via inhibition of the cytochrome oxidase pathway. However, NO can also activate the alternative oxidase (AOX) pathway for respiration and induce expression of the alternative oxidase [47,49,50]. Such induction of the AOX pathway may represent a 'survival response', perhaps partly preventing excess ROS generation [51], and inhibition of AOX resulted in increased NO sensitivity and cell death [49]. Moreover, NO generation and action are components of PCD induced by bacterial or viral challenge [2,17], elicitors [25,27,39,52], mechanical stress [42] and hypoxia [14]: enhanced NO generation and release have been assayed by various means and inhibition of NO synthesis or scavenging of NO, either via chemicals such as cPTIO or via transgenic expression of haemoglobins, retards cell death. NO treatment can alter the expression of genes whose products may have a role in the regulation of PCD or that are involved in protective responses. These include genes often induced during plant responses to pathogens, as well as those encoding enzymes of oxidative stress responses and scavenging of toxic compounds such as glutathione transferases, signalling proteins and transcription factors [29,32,49].

Other experiments have demonstrated the toxic effects of nitrosative stress. Transgenic plants with reduced nitrite reductase activity had over 10-fold the nitrite content and NO emissions were increased over 100-fold higher, and such plants displayed drastically reduced growth and development when cultured on nitrate [53]. The nitrite reductase-deficient plants had much higher levels of protein tyrosine nitration, suggesting that nitrite toxicity is due, at least in part, to increased generation of NO (and thus peroxynitrite; see below) and protein nitrosation. Whether the toxic effects were mediated by an intrinsic cell death pathway activated in response to the excessive protein nitrosation, or due to impaired cell functioning via inactivation of essential proteins is not known. In alfalfa root cultures exposed to hypoxic conditions growth was reduced considerably and NO emission increased greatly [14]. Moreover, hypoxic stress resulted in cellular disintegration characteristic of cell death. Cell death was reduced or increased under hypoxic conditions in cell lines over- or under-expressing haemoglobin, correlating well with reduced or increased rates of NO release in these transgenic cultures [14]. Again, the mechanism of cell death has yet to be elucidated but other data indicate that hypoxia-induced cell death in roots is indeed programmed [13].

Much evidence indicates that ROS also initiate cell death during various stresses [44]. Given that NO and ROS such as O_2^- and H_2O_2 (O_2^- dismutates to H_2O_2) are both generated in response to biotic and some abiotic stimuli it is not surprising to find interactions between these two signals. As described above, both NO and ROS can induce cell death, but in fact it may well be that it is actually the relative amounts of NO, O_2^- and H_2O_2 that determine whether PCD results. NO and O_2^- react to form peroxynitrite, $ONOO^-$. Peroxynitrite can react with proteins to form nitrosated tyrosine groups [4]. In animal cells peroxynitrite may be a key PCD-inducing factor, but appears not to be as toxic to plant cells. In soybean cells, neither NO nor peroxynitrite induced PCD [54]. However, PCD induced by NO was greatly enhanced in the presence of H_2O_2. Thus it was suggested that the balance of ROS and NO is critical, such that if O_2^- was scavenged by excess NO or NO by excess O_2^- , then insufficient H_2O_2 or NO would be present to activate PCD; if, on the other hand, an appropriate balance of H_2O_2 and NO was generated then PCD would be the result [53]. Cell death induced in *Arabidopsis* plants by infiltration of the NO-generating compound sodium nitroprusside was reduced in plants over-expressing a thylakoid ROS-scavenging ascorbate peroxidase enzyme, again suggesting interactions between ROS and NO [55]. Other studies have also reported that PCD induced by H_2O_2 and NO together is much greater than that induced by either alone [20,24,56], but the biochemical explanation remains to be resolved.

Interactions between NO and ROS, in which NO has protective as opposed to toxic properties, related to its antioxidant characteristics, have been described in both animal and plant systems [57]. H_2O_2 can react with redox active metals such as iron in the Fenton reaction to generate the highly reactive and short lived hydroxyl radical $OH^{\cdot}$ that can oxidise a wide range of biomolecules. Protective effects of NO linked to its ability to directly scavenge superoxide (and hence reduce H_2O_2 formation and thus prevent the Fenton reaction) and thereby reduce subsequent oxidative damage have been reported for situations where excess ROS arise through photoxidative stress, exposure to methylviologen herbicides and fungal infection in potato [58,59], exposure of lupin roots to the heavy metals lead and cadmium [60] and gibberellin treatment of barley aleurone [61]. A recent report highlights interactions between superoxide and NO *in vivo* [62]. Basal rates of NO release from leaves of *Vicia faba* and *Arabidopsis* of *ca*. 1 $nmolg^{-1}h^{-1}$ were assayed using EPR (electron paramagnetic resonance) spectroscopy. When corrections were applied to account for the removal of free NO by endogenous superoxide, substantial increases in NO were detected, implying that under normal situations much of the NO generated by cells does actually react with superoxide, presumably to form peroxynitrite [62]. These data suggest that peroxynitrite is a ubiquitous metabolite in plant cells, that could be formed at relatively high rates when NO and superoxide are generated rapidly, for example, under high light or drought stress, or in response to pathogen challenge. It may be that peroxynitrite is intrinsically less toxic to plant cells than it is to animal cells (as suggested by the data in [54]), although when NO is made in great excess, protein nitrosation (presumably via peroxynitrite) is associated with reduced growth [53]. In addition, plants might contain peroxynitrite-scavenging properties, a topic that may be worthy of further research.

NO affects iron homeostasis by increasing transcript abundance of ferritins, iron storage proteins [50, 55, 63]. Endogenous nitrosylated iron complexes have also been detected by EPR, suggesting that such complexes might contribute to the bioavailability of iron within cells [62]. Exogenous NO can relieve the symptoms of iron deficiency [4], implying that NO effects on iron homeostasis might be beneficial because generation of destructive $OH^{\cdot}$ radicals is minimised whilst at the same time iron is made available for cellular metabolism. It is likely that NO also interacts with endogenous factors during senescence and various effects on senescence and generation of ethylene, a hormone often associated with senescence, have been reported [see 4,5].

Clearly, the effects of NO can be either toxic (mainly via PCD) or protective, perhaps via direct interaction with ROS or via activation of antioxidant systems, through effects on iron availability, via the expression of 'defensive-genes' and via effects on tissue water potential through stomatal closure.

In some situations NO does activate cell death, but NO might represent only one of a group of signals whose co-ordinated effects bring about cell death. For example, NO might interact with ROS or other signals activated by pathogens or abiotic stress to initiate a 'full PCD programme'. As each specific signal (e.g. fungal hypha, bacterium, elicitor, drought, UV etc) may activate a specific and unique spectrum of intracellular responses (that of course probably overlaps with that induced by other discrete signals), it might be expected that the effects of NO will differ according to the specific signalling scenario. Moreover, different cell types, or even the same cells in different developmental or physiological states, are also likely to respond differently to NO. For example, NO is undoubtedly associated with stomatal closure in response to ABA [37] and with IAA-induced rooting [4]. Yet in these cells NO does not activate PCD as it does in other situations. Perhaps the 'co-effectors' required to work in concert with NO are not active in these cells, hence no cell death (except at unusually high NO concentrations]. The large-scale transcriptomic analyses demonstrating that the expression of numerous, different, and

in many cases unknown, genes is altered in response to NO [29,49,50] indicate that there are likely to be several cellular pathways activated or repressed by NO. Thus it is likely that the key factors determining the effects of NO relate to where (i.e. which tissues, cells and intracellular locations), when, how much and how rapidly NO is made, and to how the NO interacts with other toxic and signalling factors such as ROS, ethylene, salicylic acid, ABA and jasmonate.

4. NO signalling

Reversible protein phosphorylation and elevations in cytosolic calcium are central components of signal transduction in eukaryotic cells, including NO signalling in plants. Addition or removal of phosphate groups to proteins results in conformational changes that in turn alter the activity and sometimes location of the substrate protein. Cytosolic calcium concentrations are usually maintained below 200 nM via active export from the cell or sequestration into intracellular vesicles of the endoplasmic reticulum (ER) or vacuole. Various stimuli elevate cytosolic calcium, often in discrete intracellular domains, via activation and opening of calcium-permeable ion channels in the plasma membrane or ER and tonoplast. Calcium ions bind to calcium-binding proteins such as calmodulin, which can then interact with and activate calmodulin-binding protein kinases (PKs), or bind directly to PKs, protein phosphatases (PPs) and other proteins that possess integral calcium-binding domains. NO activates PKs in *Arabidopsis* and tobacco that are probably part of a mitogen-activated protein kinase (MAPK) system [see 5,6]. MAPK signalling modules are highly conserved in all eukaryotes and consist of a three-kinase cascade. MAPKs (serine/threonine PKs) are activated via dual phosphorylation by a MAPK kinase (MAPKK) on a conserved T-X-Y motif; after activation MAPKs are often observed to migrate to the nucleus where they phosphorylate transcription factors and thereby alter the spectrum of gene expression. In turn, MAPKKs are activated by serine phosphorylation via a MAPKK kinase (MAPKKK). The action of PPs is also involved in NO signalling, as the stomata of ABA-insensitive mutants altered in PP2C signalling are also NO-insensitive [10]. NO-modulated calcium signalling has been demonstrated for both guard cells and suspension cultures [see 4,5,25,34]; activation of calcium channels is likely to involve generation and action of the second messengers cyclic GMP and cyclic ADP ribose (cADPR), cADPR synthesis potentially being dependent on cGMP action [4-6]. cADPR activates intracellular calcium channels and cGMP is likely to activate ion channels and protein kinases, although classical cGMP-dependent PKs have not been identified in plants. Both stomatal closure and cell death induced by NO are inhibited by prevention of cyclic GMP and cADPR signalling [see 5,6]. NO may also affect protein activities directly via S-nitrosylation of reactive thiol groups. S-nitrosylation would result in changes in conformation and thus activity. As described above, NO can modulate the expression of many genes. No NO-responsive regulatory DNA sequences and cognate transcription factors have yet been identified; altered activities of transcription factors may be effected by direct interaction with NO or via activation of signalling cascades that results in, for example, phosphorylation of transcription factors.

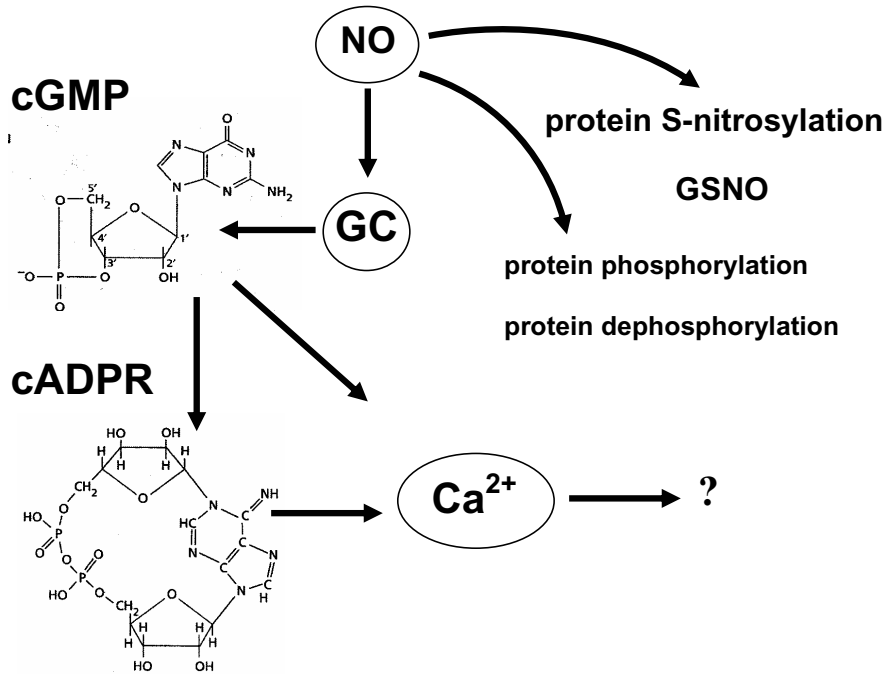

Figure 2. NO signalling

NO signalling in plants involves protein kinases and protein phosphatases. The production of the second messengers cyclic GMP (cGMP) and cyclic ADP ribose (cADPR) also occurs downstream of NO, probably activating protein kinases and inducing intracellular calcium mobilization. NO may also directly alter the activity of proteins by S-nitrosylation of thiol groups.

5. What role might NO have in the responses of plants to excess UV irradiation?

Plant responses to elevated UV include synthesis of potentially UV-protective pigment molecules, expression of a sub-section of the suite of 'defence-related genes', generation of ROS, and cell death with characteristics of PCD [64,65]. It is expected that some of these responses may be adaptive, for example, increased concentrations of UV-absorbing molecules would have an obvious benefit, as would synthesis of antioxidant enzymes that could reduce the intracellular content of potentially toxic ROS. Others may not have any apparent protective effect, for example, activation of genes often associated with defence responses, or with PCD. Such responses may arise due to the generation during UV exposure of signalling (and potentially toxic) molecules such as ROS, and potentially NO, that induce a spectrum of effects that are not wholly appropriate in all stress situations. Moreover, as some responses to UV may well be adaptive, such that plants acclimate to increased exposure to UV, it is likely that plant responses to UV differ, depending not only on the intensity of UV radiation but also on whether exposure is acute or chronic and whether or not there has been any acclimation.

Given that that some UV responses are similar to those induced by NO and that NO and ROS interact closely, it is likely that NO too will feature in plant UV responses. In

Arabidopsis, expression of *CHS*, encoding chalcone synthase, a key enzyme of flavonoid synthesis thought to be important in UV-protection, is induced by exposure to UV-B [65]. Pharmacological data indicated that such induction was mediated by NO: UV-induced *CHS* expression was reduced by pre-treatment with an NO scavenger or with a NOS inhibitor and *CHS* expression was induced by two NO donors. More recent data utilising plant:bacteria interactions in which NO levels were reduced by expression of bacterial nitric oxide dioxygenase also indicate that UV-induction of *CHS* expression is mediated by NO [30]. UV-B radiation induced NO generation in the green alga *Chlorella pyrenoidosa* and UV-induced chlorophyll loss was reduced by addition of exogenous NO (via sodium nitroprusside) [66]. NO donors also protected potato leaves against UV-induced oxidative injury [67]. UV-B increased NOS activity and NO release in maize mesocotyls [68]. Moreover, during exposure to UV-B, exogenous NO effects on growth inhibition were similar to those of a ROS scavenger, suggesting again that NO has both signalling and antioxidant roles depending on the relative concentrations of NO and ROS [68]. It has been shown recently that UV radiation induces the emission of NO_x from shoots of *Pinus sylvestris* [69], thus raising the real possibility that exposure to UV does indeed influence NO production. Again, the timing and amounts of NO generated are likely to determine the cellular effects.

Interestingly, UV-B does appear to influence stomatal movement, a process profoundly affected by NO, although the reported effects are somewhat confusing. For example, pea, *Commelina* and oilseed rape plants grown under UV-B had lower stomatal conductances than control plants, and UV-irradiation of previously unexposed plants also induced stomatal closure [70]. However, other workers have shown that UV-B at low fluence rates induces stomatal opening in *V. faba* [71], or that UV-B at high fluence can either open or close *V. faba* stomata [72]. More recent work [73] has provided evidence for a separate UV-B photoreceptor in *V. faba* guard cells and shown that green light inhibits UV-B-induced opening. Given that UV-B can stimulate ROS (and potentially NO) generation, it is likely that UV effects on stomata are determined by complex interactions involving UV fluence rate and the amount of visible light in addition to a range of other factors.

6. Experimental approaches to determine the involvement of NO in plant responses to UV radiation

Experimental approaches to determine the role(s) of NO will require:

- methods to assess accurately NO emissions from leaves and localised regions of plants. Various methods to assay NO have been used, including real-time intracellular imaging using fluorescent dyes, chemiluminescence, spectrometric assays, NO electrodes, EPR spectroscopy, photoacoustic laser spectroscopy and mass spectrometry [4,5,15,21,62,74]. It will be important to determine emissions and intracellular concentrations of other nitric oxides, such as NO_2, the other component of NO_x in fossil fuel emissions and N_2O, both of which can be made by plants and released from soils [75,76]. Re-evaluation of the effects of NO_2 and N_2O along with those of NO may also be informative – for example, NO_x in smoke is able to stimulate seed germination [77]. A thorough analysis of peroxynitrite and its effects on plants may also be informative.
- determination of NO concentrations and biosynthetic routes at the sub-cellular level within cells and in specific compartments and microdomains, including interactions with other signalling components.

- use of mutants and transgenic plants altered in the synthesis of, and responses to, NO, to demonstrate any requirement for NO synthesis and action and to assess the source(s) of NO.
- transgenic plants altered in NO scavenging capacity.
- pharmacological and genetic experiments to assess the requirement for NO and downstream signalling, using chemical and genetic manipulation of NO synthesis and responses.
- large-scale transcriptomic, proteomic and metabolomic analyses of the effects of UV and NO.
- biochemical and molecular analyses of the processes of cell death induced by UV.
- techniques to assess simultaneously PCD and the generation of signal molecules such as ROS that can interact and co-act with NO.
- development of large-scale imaging systems to monitor PCD, NO and ROS generation in the field in response to UV radiation.
- interactions of NO, UV and other stresses and stimuli e.g. NO_x, pathogens, drought, cold stress.
- Assessments of NO_x contributions from other components of the ecosystem.

7. Conclusion

NO is a multi-faceted and versatile endogenous signalling molecule in plants with an importance that probably stretches to most if not all aspects of plant growth and development. At least three enzymatic sources of NO in plants have been identified in addition to mechanisms that scavenge NO. Downstream signalling responses to NO include generation and action of the second messenger molecules calcium, cyclic GMP and cyclic ADPR, protein phosphorylation, protein nitrosylation and specific effects on gene expression. NO signalling interacts with that activated by Reactive Oxygen Species (ROS). Both ROS and NO are generated rapidly following challenge by pathogens or elicitors and represent key members of an orchestra of defence responses that includes numerous metabolic and transcriptional changes in addition to Programmed Cell Death (PCD). NO can induce and influence PCD and inhibition of NO synthesis or action delays or inhibits PCD. However, NO can also interact directly and indirectly with ROS, and in some cases NO actions may be cytoprotective rather than cytotoxic. ROS generation is stimulated by various abiotic as well as biotic stresses, including UV–irradiation that itself induces PCD. Recent data indicate that NO can also be produced in response to abiotic stress, and that UB irradiation might stimulate release of NO_x from plant leaves.

Acknowledgements

Research in the authors' laboratory is supported by BBSRC, Defra and The Royal Society.

References

[1] Mansfield T.A., "Nitrogen oxides: old problems and new challenges". In: "Air Pollution and Plant Life", 2nd ed. JNB Bell and M Treshow, eds. John Wiley and Sons Ltd, Chichester, UK, 2002.
[2] Delledonne M., Xia Y., Dixon R.A. and Lamb C., "Nitric oxide functions as a signal in plant disease resistance". *Nature*, vol. 394, p.p.585-588, 1998.
[3] Durner J., Wendehenne D. and Klessig D.F., "Defense gene induction in tobacco by nitric oxide, cyclic GMP and cyclic ADP-ribose". *Proc. Natl. Acad. Sci. USA*, vol. 95, p.p. 10328-10333, 1998.

[4] Lamattina L., Garcia-Mata C., Graziano M. and Pagnussat G., "Nitric oxide: the versatility of an extensive signal molecule". *Annu. Rev. Plant. Biol*., vol. 54, p.p. 109-136, 2003.
[5] Neill S.J., Desikan R. and Hancock J.T., "Nitric oxide signalling in plants". *New Phytologist*, vol. 159, p.p. 11-35, 2003.
[6] Wendehenne D., Durner J. and Klessig D.F., „Nitric oxide: a new player in plant signalling and defence responses". *Curr. Opin. Plant Biol*., vol. 7, p.p. 1-7, 2004.
[7] Guo F.-Q., Okamoto M. and Crawford N.M., "Identification of a plant nitric oxide synthase gene involved in hormonal signalling". *Science*, vol. 302, p.p. 100-103, 2003.
[8] Yamamoto A., Katou S., Yoshioka H., Doke N. and Kawakita H., "Nitrate reductase, a nitric oxide-producing enzyme: induction by pathogen signals". *J. Gen. Pathol*., vol. 69, p.p. 218-229, 2003.
[9] Lea U.S., Ten Hoopen T., Provan F., Kaiser W.M., Meyer C. and Lillo C., "Mutation of the regulatory phosphorylation site of tobacco nitrate reductase results in high nitrite excretion and NO emission from leaf and root tissue". *Planta*, vol. 219, p.p. 59-65, 2004.
[10] Desikan R., Griffiths R., Hancock J. and Neill S., "A new role for an old enzyme: nitrate reductase-mediated nitric oxide generation is required for abscisic acid-induced stomatal closure in *Arabidopsis thaliana*". Proc. Natl. Acad. Sci. USA, vol. 99, p.p. 16314-16318, 2002.
[11] Stohr C., Strube F., Marx G., Ullrich W.R. and Rockel P., "A plasma membrane-bound-enzyme of tobacco roots catalyses the formation of nitric oxide from nitrite". *Planta*, vol. 212, p.p. 835-841, 2001.
[12] Bethke P.C., Badger M.R. and Jones R.L., "Apoplastic synthesis of nitric oxide by plant tissues". *Plant Cell*, vol. 16, p.p. 332-341, 2004.
[13] Dordas C., Rivoal J. and Hill R.D., "Plant haemoglobins, nitric oxide and hypoxic stress". *Ann. Bot*., vol. 91, p.p. 173-178, 2003.
[14] Dordas C., Hasinoff B.B., Igamberdiev A.U., Manac'h N., Rivoal J. and Hill R.D., "Expression of a stress-induced hemoglobin affects NO levels produced by alfalfa root cultures under hypoxic stress". *Plant J*., vol. 35, p.p. 763-770, 2003.
[15] Rockel P., Strube F., Rockel A., Wildt J. and Kaiser W.M., "Regulation of nitric oxide (NO) production by plant nitrate reductase *in vivo* and *in vitro*". *J. Exp. Bot*., vol. 53, p.p. 103-110, 2002.
[16] Dordas C., Hasinoff B.B., Rivoal J. and Hill R.D., "Class-1 hemoglobins, nitrate and NO levels in anoxic maize cell-suspension cultures". *Planta*, vol. 219, p.p. 66-72, 2004.
[17] Seregelyes C., Barna B., Hennig J., Konopka D., Pasternak T.P., Lukacs N., Feher A., Horvath G.V. and Dudits D., "Phytoglobins can interfere with nitric oxide functions during plant growth and pathogenic responses: a transgenic approach". *Plant Sci*., vol. 165, p.p. 541-550, 2003.
[18] Wong H.L., Sakamoto T., Kawasaki T., Umemura K. and Shimamoto K., "Down-regulation of metallothionein, a Reactive Oxygen Scavenger, by the small GTPase OsRac1 in rice". *Plant Physiol*., vol. 135, p.p. 1447-1456, 2004.
[19] Gray J., ed., "Programmed Cell Death in Plants". Blackwell Publishing, Oxford, UK, 2004.
[20] Clarke A., Desikan R., Hurst R.D., Hancock J.T. and Neill S.J., "NO way back: nitric oxide and programmed cell death in *Arabidopsis thaliana* suspension cultures". *Plant J*., vol. 24, p.p. 667-677, 2000.
[21] Mur L.A.J., Santosa I.E., Laarhoven L-J.J., Harren F. and Smith A.R., "A new partner in the *danse macabre*: the role of nitric oxide in the hypersensitive response". *Bulg. J. Plant Phys. (Special Issue*), p.p. 110-123, 2003.
[22] Foissner I., Wendehenne D., Langebartels C. and Durner J., „*In vivo* imaging of an elicitor-induced oxidative burst in tobacco". *Plant J*., vol. 23, p.p. 817-824, 2000.
[23] Hu X., Neill S.J., Cai W. and Tang Z., "Nitric oxide mediates elicitor-induced saponin synthesis in cell cultures of *Panax ginseng*". *Func. Plant Biol*., vol. 30, p.p. 901-907, 2003.
[24] Hu X., Neill S.J., Cai W. and Tang Z., "NO-mediated hypersensitive responses of rice suspension cultures induced by incompatible elicitor". *Chinese Sci. Bull.*, vol. 48, p.p. 358-363, 2003.
[25] Lamotte O., Gould K., Lecourieux D., Sequeira-Legrand A., Lebrun-Garcia A., Durner J., Pugin A. and Wendehenne D., "Analysis of nitric oxide signalling functions in tobacco cells challenged by the elicitor cryptogein". *Plant Physiol*., vol. 135, p.p. 516-529, 2004.
[26] Modolo L.V., Cunha F.Q., Braga M.R., Salgao I., "Nitric oxide synthase-mediated phytoalexin accumulation in soybean cotyledons in response to the *Diaporthe phaseolorum* f.sp. *meridionalis* elicitor". *Plant Phys*., vol. 130, p.p. 1288-1297, 2002.
[27] Yamamoto A., Katou S., Yoshioka H., Doke N. and Kawakita H., "Involvement of nitric oxide generation in hypersensitive cell death induced by elicitin in tobacco cell suspension culture*". J. Gen. Pathol*., vol. 70, p.p. 85-92, 2004.
[28] Zhang C., Czymmek K.J. and Shapiro A.D., "Nitric oxide does not trigger early programmed cell death events but may contribute to cell-to-cell signalling governing progression of the *Arabidopsis* hypersensitive response". *Mol. Plant-Microbe Interact*., vol. 16, p.p. 962-972, 2003.
[29] Polverari A., Molesini B., Pezzotti M., Buonaurio R., Marte M. and Delledonne M., "Nitric oxide-mediated transcriptional changes in *Arabidopsis thaliana*". *Mol. Plant-Microbe Interact*., vol. 16, p.p. 1094-1105, 2003.

[30] Zeier J., Delledonne M., Mishina T., Severi E., Sonoda M. and Lamb C., "Genetic elicidation of nitric oxide signalling in incompatible plant-pathogen interactions". *Plant Physiol*., vol. 136, p.p. 2875-2886, 2004.
[31] Lesham Y.Y. and Haramaty E., "The characterisation and contrasting effects of the nitric oxide free radical in vegetative stress and senescence of *Pisum sativum* Linn. Foliage". *J. Plant Phys*., vol. 148, p.p. 258-263, 1996.
[32] Magalhaes J.R., Monte D.C. and Durzan D., "Nitric oxide and ethylene emission in *Arabidopsis thaliana*". *Phys. Mol. Biol. Plants*, vol. 6, p.p. 117-127, 2000.
[33] Zhao Z., Chen G. and Zhang C., "Interaction between reactive oxygen species and nitric oxide in drought-induced abscisic acid synthesis in root tips of wheat seedlings". *Aust. J. Plant Physiol*., vol. 28, p.p. 1055-1061, 2001.
[34] Gould K.S, Lamotte O., Klinguer A., Pugin A. and Wendehenne D., "Nitric oxide production in tobacco leaf cells: a generalized stress response?" *Plant, Cell and Environ*, p.p. 1851-1862, 2003.
[35] Garcia-Mata C., Lamattina L., "Nitric oxide induces stomatal closure and enhances the plant adaptive plant responses against drought stress". *Plant Physiol*., vol. 126, p.p. 1196-1204, 2001.
[36] Garcia-Mata C., Lamattina L., "Nitric oxide and abscisic acid cross-talk in guard cells". *Plant Physiol*., vol. 128, p.p. 790-792, 2002.
[37] Neill S.J., Desikan R., Clarke A. and Hancock J.T., "Nitric oxide is a novel component of abscisic acid signalling in stomatal guard cells". *Plant Physiol*., vol. 128, p.p. 13-16, 2002.
[38] Xin L., Zhang S. and Chenghou L., "Involvement of nitric oxide in the signal transduction of salicylic acid regulating stomatal movement". *Chinese Sci. Bull*., vol. 48, p.p. 449-452, 2003.
[39] Huang X., Stettmaier K., Michel C., Hutzler P., Mueller M.J. and Durner J., "Nitric oxide is induced by wounding and influences jasmonic acid signalling in *Arabidopsis thaliana*". *Planta*, vol. 218, p.p. 938-946, 2004.
[40] Jih P-J., Chen Y-C. and Jeng S-T., "Involvement of hydrogen peroxide and nitric oxide in expression of the ipomoelin gene from sweet potato". *Plant Physiol*., vol. 132, p.p. 381-389, 2003.
[41] Orozco-Cardenas M.L. and Ryan C.A., "Nitric oxide negatively modulates wound signalling in tomato plants". *Plant Physiol*., vol. 130, p.p. 487-493, 2002.
[42] Pedroso M.C., Magalhaes J.R. and Durzan D., "A nitric oxide burst precedes apoptosis in angiosperm and gymnosperm callus cells and foliar tissues". *J. Exp. Bot*., vol. 51, p.p. 1027-1036, 2000.
[43] Pedroso M.C., Magalhaes J.R. and Durzan D., "Nitric oxide induces cell death in *Taxus* cells". *Plant Sci*., vol. 157, p.p. 173-180, 2000.
[44] Neill S.J., Desikan R. and Hancock J.T., "Hydrogen peroxide signalling". *Curr. Opin. Plant Biol*., vol. 5, p.p. 388-395, 2002.
[45] Hoebericht F.A. and Woltering E.J., "Multiple mediators of plant programmed cell death: interplay of conserved cell death mechanisms and plant-specific regulators". *BioEssays*, vol. 25, p.p. 47-57, 2002.
[46] Woltering E.J., "Death proteases come alive". *Trends Plant Sci., (in press)*.
[47] Zottini M., Formentin E., Scattolin M., Carimi F., Lo Schiavo F. and Terzi M., Nitric oxide affects plant mitochondrial functionality in vivo". *FEBS Lett*., vol. 515, p.p. 75-78, 2002.
[48] Saviani E.E., Orsi C.H., Oliveira J.F., Pinto-Maglio C.A. and Salgado L., "Participation of the mitochondrial permeability transition pore in nitric oxide-induced plant cell death". *FEBS Lett*., vol. 510, p.p. 135-140, 2002.
[49] Huang X., von Rad U. and Durner J., "Nitric oxide induces transcriptional activation of the nitric oxide-tolerant alternative oxidase in *Arabidopsis* suspension cells". *Planta*, vol. 215, p.p. 914-923, 2002.
[50] Parani M., Rudrabhatla S., Myers R., Weirich H., Smith B., Leaman D.W. and Goldman S.L., "Microarray analysis of nitric oxide responsive transcripts in *Arabidopsis*". *Plant Biotech. J*., vol. 2, p.p. 359-366, 2002.
[51] Yamasaki H., Shimoji H., Oshiro Y. and Sakihama Y., "Inhibitory effects of nitric oxide on oxidative phoshorylation in plant mitochondria". *Nitric Oxide: Biol. and Chem*., vol. 5, p.p. 261-270, 2001.
[52] Krause M. and Durner J., "Harpin inactivates mitochondria in *Arabidopsis* suspension cells*". Mol. Plant-Microbe Interact*., vol. 17, p.p. 131-139, 2004.
[53] Morot-Gaudry-Talarmain Y., Rockel P., Moureaux T., Quillere I., Leydecker M.T., Kaiser W.M. and Morot-Gaudry J.F., "Nitrite accumulation and nitric oxide emission in relation to cellular signalling and nitrite reductase in antisense tobacco". *Planta*, vol. 215, p.p. 708-715, 2002.
[54] Delledonne M., Zeier J., Marocco A. and Lamb C., "Signal interactions between nitric oxide and reactive oxygen intermediates in the plant hypersensitive disease resistance response". *Proc. Natl. Acad. Sci. USA*, vol. 98, p.p. 13454-13459, 2001.
[55] Murgia I., Taranton D., Vannini C., Bracale M., Carrivieri S. and Soave C., "*Arabidopsis thaliana* plants overexpressing thylakoidal ascorbate peroxidase show increased resistance to paraquat-induced photooxidative stress and to nitric oxide-induced cell death". *Plant J*., vol. 38, p.p. 940-953, 2004.

[56] de Pinto M.C., Tommasi F. and de Gara L., "Changes in the antioxidant systems as part of the signalling pathway responsible for the programmed cell death activated by nitric oxide and reactive oxygen species in Bright-Yellow 2 cells". *Plant Physiol*, vol. 130, p.p. 698-708, 2002.
[57] Wink D.A., Cook J.A., Pacelli, Liebmann J., Krishna M.C. and Mitchell J.B., "Nitric oxide (NO) protects against cellular damage by reactive oxygen species". *Toxicol. Lett*., vol. 82/83, p.p. 221-226, 1995.
[58] Beligni M.V. and Lamattina L., "Nitric oxide interferes with plant photo-oxidative stress by detoxifying reactive oxygen species". *Plant, Cell and Env*., vol. 25, p.p. 737-748, 2002.
[59] Beligni M.V. and Lamattina L., "Nitric oxide counteracts cytotoxic processes mediated by reactive oxyen species in plant tissues". *Planta*, vol. 208, p.p. 337-344, 1999.
[60] Kopyra M. and Gwozdz E.A., "Nitric oxide stimulates seed germination and counteracts the inhibitory effects of heavy metals and salinity on root growth of *Lupinus luteus*". *Plant Physiology and Biochemistry*, vol. 41, p.p. 1017-1024, 2003.
[61] Beligni M.V., Fath A., Bethke P.C., Lamattina L. and Jones L., "Nitric oxide acts as an antioxidant and delays programmed cell death in barley aleurone layers". *Plant Physiol*., vol. 129, p.p. 1642-1650, 2002.
[62] Vanin A.F., Svistunenkov D.A., Mikoyan V.D., Serezhenkov V.A., Fryer M.J., Baker N.R. and Cooper C.R., "Endogenous superoxide production and the nitrite/nitrate ratio control the concentration of bioavailable free nitric oxide in leaves". *J. Biol. Chem*., vol. 279, p.p. 24100-24107, 2004.
[63] Murgia I., Delledonne M. and Soave C., "Nitric oxide mediates iron-induced ferritin accumulation in *Arabidopsis*". *Plant J*., vol. 30, p.p. 521-528, 2002.
[64] Danon A., Rotari V.I., Gordon A., Mailhac N. and Gallois P., "Ultraviolet-C overexposure induces programmed cell death in Arabidopsis, which is mediated by caspase-like activities and which can be suppressed by caspase inhibitors, p35 and Defender against Apoptotic Death". *J. Biol. Chem.,* vol. 279, p.p. 779-787, 2004.
[65] Mackerness S.A-H., John C.F., Jordan B. and Thomas B., "Early signalling components in ultraviolet-B responses: distinct roles for reactive oxygen species and nitric oxide". *FEBS Lett*., vol. 489, p.p. 237-242., 2001.
[66] Chen K., Feng H., Zhang M. and Wang X., "Nitric oxide alleviates oxidative damage in the green alga *Chlorella pyrenoidosa* caused by UV-B radiation". *Folia Microbiologica*, vol. 48, p.p. 389-393, 2003.
[67] Beligni M.V. and Lamattina L., "Nitric oxide in plants: the history is just beginning. *Plant Cell and Env*., vol. 24, p.p. 267-278, 2001.
[68] Zhang M., Lizhe A., Feng H., Chen T., Chen K., Liu Y., Tang H., Chang J. and Wang X., "The cascade mechanisms of nitric oxide as a second messenger of ultraviolet B in inhibiting mesocotyl elongations". *Photochemistry and Photobiology*, vol. 77, p.p. 219-225, 2003.
[69] Hari P., Raivonen M., Vesala T., Munger J.W., Pilegaard K. and Kulmala M., "Ultraviolet light and leaf emission of NO_x". *Nature*, vol. 422, p. 134, 2003.
[70] Nogues S., Allen D.J., Morison J.I.L. and Baker N.R., "Characterisation of stomatal closure caused by ultraviolet-B radiation". *Plant Physiol*., vol. 121, p.p. 489-496, 1999.
[71] Eisinger W., Swartz T.E., Bogomolni R. and Taiz L., „The ultraviolet action spectrum for stomatal opening in broad bean". *Plant Phys*., vol. 122, p.p. 99-106, 2000.
[72] Jansen M.A.K. and van den Noort R.E., "Ultraviolet-B radiation induces complex alterations in stomatal behaviour". *Physiologia Plantarum*, vol. 110, p.p. 189-194, 2000.
[73] Eisinger W., Bogomolni R. and Taiz L., "Interactions between a blue-green reversible photoreceptor and a separate UV-B photoreceptor in stomatal guard cells". *Am. J. Bot*., vol. 90, p.p. 1560-1566, 2003.
[74] Conrath U., Amoroso G., Kohle H. and Sultemeyer D.F., "Non-invasive online detection of nitric oxide from plants and some other organisms by mass spectrometry". *Plant J*., vol. 38, p.p. 1015-1022, 2004.
[75] Bremner J.M., "Sources of nitrous oxide in soils". *Nut. Cyc. in Ecosystems*, vol. 49, p.p. 7-16, 1997.
[76] Davidson E.A. and Kingerlee W., "A global inventory of nitric oxide emissions from soils*". Nut Cyc in Ecosystems*, vol. 48, p.p. 37-50, 1997.
[77] Keeley J.E. and Fotheringham C.J., "Trace gas emission and smoke-induced seed germination". *Science*, vol. 276, p.p. 1248-1250, 1997.

Cell Biology and Instrumentation: UV Radiation, Nitric Oxide and Cell Death in Plants
Y. Blume et al. (Eds.)
IOS Press, 2006

NO Signaling Functions in the Biotic and Abiotic Stress Responses

David WENDEHENNE[1], Kevin GOULD[2], Olivier LAMOTTE[1], Elodie VANDELLE[1], David LECOURIEUX[3], Cécile COURTOIS[1], Laurent BARNAVON[1], Marc BENTÉJAC[1], Alain PUGIN[1]

[1] *UMR INRA 1088/CNRS 5184/Université de Bourgogne, Plante-Microbe-Environnement, 17 rue Sully, BP 86510, Dijon 21065 Cedex, France*

[2] *Plant Sciences Group, School of Biological Sciences, University of Auckland, Private Bag 92019, Auckland, New Zealand*

[3] *UMR CNRS 6161, Laboratoire de Transport des Assimilats, UFR Sciences-Bâtiment Botanique, 40 avenue de Recteur Pineau, Poitiers 86022 Cedex, France*

Abstract. In the late 1990s, NO became an increasingly popular target of investigation in plants. As in mammals, NO fulfils a broad spectrum of signaling functions in pathophysiological processes in plants. Here, we summerize studies published in recent years that provide novel insights into the signaling functions of NO produced by plant cells exposed to abiotic stresses and biotic stress (pathogen-derived elicitors). Particularly, we report that NO emerges as a key messenger governing the overall control of Ca^{2+} homeostasis. Although the precise signaling functions of NO are poorly understood, its capacity to modulate Ca^{2+} homeostasis provides an extraordinary and remarkably effective way of conveying information.

Introduction

Over the past two decades, it has been recognized that nitric oxide (NO) plays important roles in diverse mammalian physiological processes. NO impinges on almost all areas of biology, including the regulation of blood vessels, immunological defense against invading organisms, apoptosis and neurotransmission. The production of NO is primarily catalysed by nitric oxide synthase (NOS) that converts L-arginine to L-citrulline and NO [1]. Because of its high reactivity, NO synthesis is under tight and complex control. Nitric oxide regulates physiological processes by modulating the activity of proteins principally by nitrosylation, a process referring to the binding of NO to a transition metal centre or cysteine residues [2]. Nitrosylation is a reversible, post-translational modification that plays a central role in NO-mediated signaling. An important class of proteins that constitutes key targets of NO is that of Ca^{2+} channels including cardiac and skeletal ryanodine receptors (RYR), voltage-gated Ca^{2+} channels, store-operated Ca^{2+} channels, cyclic nucleotide-gated Ca^{2+} channels, the N-methyl-D-aspartate receptor and the inositol triphosphate receptor (IP_3R). NO modulates these channels directly by nitrosylation, but also indirectly *via* the second messenger cyclic GMP (cGMP) and/or cyclic ADP ribose (cADPR), a direct triggering molecule for RYR-mediated Ca^{2+} release [2,3]. Therefore, NO, which may be produced intracellularly or may originate from neighbouring cells, emerges as a key messenger governing the overall control of Ca^{2+} homeostasis [3].

In the late 1990s, NO also became an increasingly popular target of investigation in plants. As in mammals, NO fulfils a broad spectrum of signaling functions in (patho)physiological processes in plants [4-6]. Furthermore, two enzymes capable of

producing NO in plants have been recently identified , p.p nitrate reductase [7] and AtNOS1 [8], a NOS-like enzyme showing sequence identity with a protein implicated in NO synthesis in the snail *Helix pomatia*. This review summarizes studies published in recent years that provide novel insights into the signaling functions of NO produced by plant cells exposed to abiotic stresses and biotic stress (pathogen-derived elicitors). It focuses particularly on the cross-talk operating between NO and Ca^{2+}.

1. Nitric oxide signaling activities in response to abiotic and abiotic stressors

Analysis of the involvement of NO in plant immune responses is a fruitful area of research. Such studies have not only enhanced our understanding of the role of NO in plant defense, they also serve to illustrate the potential benefits of using plant-pathogen interactions as a model to investigate NO signaling. Over the past few years, we have studied the functions of NO in plant cells challenged with elicitors of defense responses. Two elicitors have been used primarily, p.p cryptogein, a 10 kDa elicitor produced by the oomycete *Phytophthora cryptogea* [9], and endopolygalacturonase (BcPG1) purified from the culture filtrates of *Botrytis Cinerea* [10].

Upon application to tobacco, cryptogein causes a hypersensitive-like response (HR), elicits the accumulation of transcripts encoded by defense-related genes and induces acquired systemic resistance (SAR) to diverse pathogens [9]. Using tobacco cell suspensions, it has been possible to characterize early events implicated as transduction components in the cryptogein induction of defense responses. These include cryptogein-binding to high affinity binding sites in the plasma membrane [11], ion channel-mediated changes in plasma membrane permeability [12], intracellular Ca^{2+} release through activation of RYR- and IP_3-R-like receptors [13], increase of nuclear free Ca^{2+} concentration (D Lecourieux, personal communication, 2004), modulation of protein kinases including mitogen activated protein kinases (MAPK) [14], production of NADPH oxidase-dependent reactive oxygen species (ROS) [15] and disruption of the microtubular cytoskeleton [16]. Cryptogein-induced elevation of cytosolic free Ca^{2+} concentration is required for the elicitor-triggered early and late reactions including phytoalexin synthesis and cell death [13].

Using the NO sensitive fluorophore 4,5-diaminofluorescein diacetate (DAF-2DA), we reported the real-time imaging of NO production in epidermal tobacco cells treated with cryptogein [17]. After elicitation with the elicitor, the earliest burst of NO was in the chloroplasts, where NO production occurred within 3 minutes. The level of fluorescence increased with time, and after 6 minutes NO was also found along the plasma membrane, in the nucleus and most probably in peroxisomes. In mammals, NO-dependent responses are governed by the subcellular compartment of NO production and by the frequency/duration of its synthesis [1,2]. Therefore, because the extent and timing of NO synthesis observed in response to cryptogein seems tightly regulated, we would anticipate that NO operates over a spatial and temporal range both for specificity of targeting and for propagation of the elicitor signal.

To investigate the signaling events that mediate NO production, and to analyse NO signaling activities in the cryptogein transduction pathway, a spectrofluorometric assay using DAF-2DA was developed to follow NO production in tobacco cultured cells. As observed in tobacco epidermal tissue, cryptogein induced a fast and transient NO production in tobacco cell suspensions [18]. This production was completely suppressed in the presence of the NO scavenger cPTIO, and was reduced by 55 to 85% by mammalian NOS inhibitors. By contrast, inhibitors of NR had no effect on cryptogein-induced NO production. Interestingly, the NO burst was also sensitive to carboxymethoxylamine and aminoacetonitrile, two inhibitors of the

variant of the P protein of glycine decarboxylase complex (iNOS), an enzyme originally reported as being a plant NOS enzyme [19]. These inhibitors also suppressed NO production induced by other elicitors of defense responses in tobacco, grapevine and *Arabidopsis* suspension cells (unpublished data). Although we can not give a conclusive answer, we suggest that the inhibitory effect of these compounds is caused by their ability to act on plant NOS or on proteins acting upstream of NOS.

Calcium signals are thought to play an important role in the tobacco cells response to cryptogein [12-16]. To investigate whether NO was active in this process, the recombinant aequorin technology was used. Aequorin is a photoprotein from *Aequora victoria* which undergoes a conformational change and emits luminescence when occupied by Ca^{2+} [20]. Using transgenic *Nicotiana plumbaginifolia* cell suspensions that constitutively express aequorin in the cytosol, it was shown that cryptogein triggers a first increase of cytosolic free Ca^{2+} concentration ($[Ca^{2+}]_{cyt}$) resulting from an influx of extracellular Ca^{2+} and Ca^{2+} release from internal stores [13]. This first Ca^{2+} peak was followed immediately by a second, sustained $[Ca^{2+}]_{cyt}$ mainly due to the influx of extracellular Ca^{2+}. When cryptogein-triggered NO production was suppressed by cPTIO or inhibitors of mammalian NOS, the intensity of the first $[Ca^{2+}]_{cyt}$ increase was reduced by almost 50% whereas the second $[Ca^{2+}]_{cyt}$ peak was unaffected [18]. Because similar pharmacological treatments did not affect cryptogein-induced entry of extracellular Ca^{2+} (as measured by quantifying uptake of extracellular $^{45}Ca^{2+}$), we assumed that NO participates in the elevation of cryptogein-mediated $[Ca^{2+}]_{cyt}$ through the mobilization of Ca^{2+} from intracellular stores. We also examined whether NO has any role in initiating the increase of nuclear free Ca^{2+} concentration ($[Ca^{2+}]_{nuc}$) observed in cryptogein-treated cells. Result from this study indicates that NO generation did not lead to the rise of nuclear free Ca^{2+}.

The ability of endogenous NO to promote Ca^{2+} changes has been also analysed in grapevine suspension cells treated with BcPG1 (E Vandelle, personal communication, 2004). This elicitor mediates a rapid NO production, which is sensitive to mammalian NOS inhibitors and strictly dependent on extracellular Ca^{2+} influx. Here too, NO appears to contribute to the elicitor-induced $[Ca^{2+}]_{cyt}$ elevation by promoting the release of Ca^{2+} from intracellular Ca^{2+} stores into the cytosol. Moreover, surprisingly, when the BcPG1-triggered NO burst was suppressed, the elicitor-induced influx of extracellular Ca^{2+} was clearly increased, indicating that NO also negatively regulates Ca^{2+} entry. The physiological significance of this inhibition remains unknown. From what is known of the NO-dependent transduction mechanisms in animals [2], we postulate that this inhibition in plants could constitute a negative feedback loop which assists the cells to reduce extracellular Ca^{2+} influx and therefore regulates Ca^{2+}-dependent processes including NO synthesis and NO-derived deleterious effects.

To expand our understanding of NO signaling, its putative involvement in cryptogein-induced defense gene expression was investigated. The selected genes included those that encode pathogenesis-related (PR) proteins, glutathione-S-transferase (GST), lipoxygenase 1 (LOX), the ethylene-forming enzyme cEFE-26, a low-molecular-mass heat-shock protein (TLHS-1), the hypersensitive-related proteins hsr515 and hsr203J, sesquiterpene cyclase, phenylalanine ammonia-lyase and SAR 8.2, a small highly basic protein of unknown function expressed during the HR and SAR. Amongst these genes, only *cEFE-26* and *TLHS-1* transcripts were shown to accumulate under regulatory control by NO, suggesting that NO might contribute to ethylene and HSP synthesis [18]. Accordingly, the levels of both mRNAs were elevated in tobacco cells that had been treated with NO donors (O Lamotte, personal communication, 2004). In plants, low-molecular-mass heat-shock protein (sHsps) are synthesised rapidly in response to a wide range of environmental stressors, including heat, cold, drought and salinity. These proteins are thought to play an important role in the

acquisition of stress tolerance by binding and stabilizing denatured proteins, facilitating their refolding by Hsp70/Hsp100 complexes [21]. Furthermore, in mammals, sHsps are known to be involved in cellular functions such as apoptosis by regulating cellular redox state. However, the involvement of TLHS-1 as regulator of NO-induced stress response remains to be established. In contrast to cryptogein, NO produced in response to BcPG1 was shown to alter the expression of genes associated with phytoalexins synthesis, namely *PAL* and *VST1* encoding stilbene synthase (E Vandelle, personal communication, 2004). Therefore, NO may confer to grapevine cells a selective advantage against *Botrytis Cinerea* by contributing to phytoalexin synthesis. In support of this hypothesis, NO released by NO donors was shown to activate phytoalexin accumulation in potato tuber tissue and soybean cotyledon [22, 23].

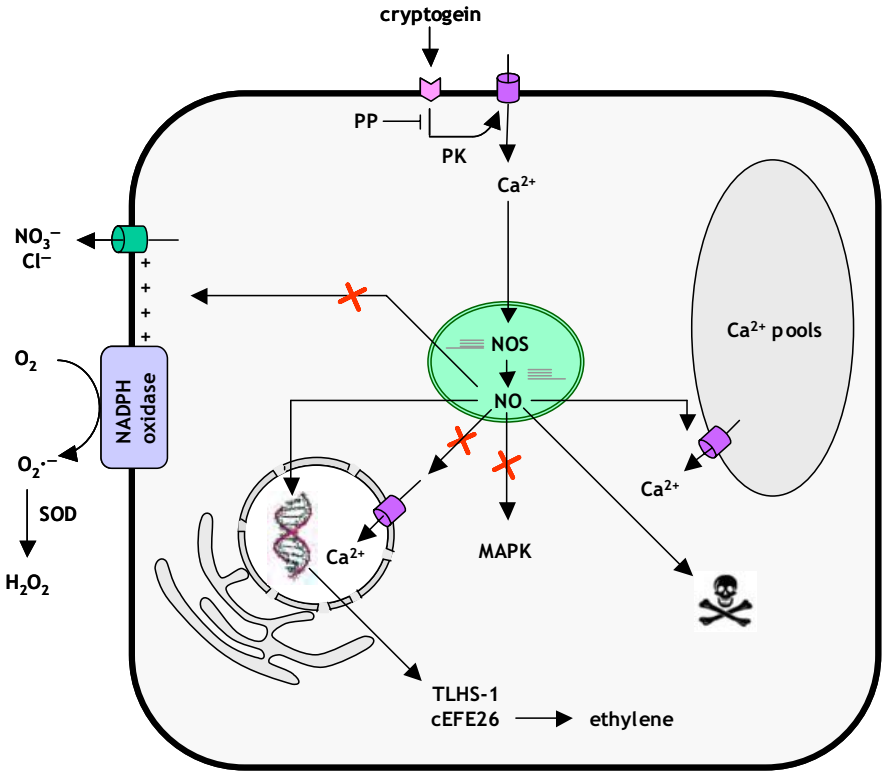

Figure 1. Figure Caption , p.p Hypothetical model of NO functions in cryptogein signaling in tobacco cells. Cryptogein binding to high affinity binding sites is followed by protein kinase-mediated phosphorylation events leading to a large and sustained Ca^{2+} influx. Both protein phosphorylation and Ca^{2+} influx are required for NOS-dependent NO synthesis which may occur in plastids. Once produced, NO activates intracellular Ca^{2+} permeable channels contributing to the elevation of cytosolic but not nuclear free Ca^{2+} concentrations. Furthermore, NO production is an upstream step in the elicitor transduction pathway leading to cell death and *TLHS-1* and *cEFE-26* transcripts accumulation. In contrast to its function in BcPG1 signaling (see text for details), NO produced in response to cryptogein does not regulate ROS synthesis. In addition, MAPK, anion channels activation and the subsequent plasma membrane depolarisation are NO-independent processes. All the cryptogein cascade seems negatively regulated by at least one phosphatase. PK, p.p protein kinase, PP, p.p protein phosphatase, SOD, p.p superoxide dismutase.

In animals, superoxide collaborates with NO *via* the formation of peroxynitrite ($ONOO^-$) to induce apoptosis and execute invading pathogens. In plants, the NO and ROS burst observed in response to elicitors and avirulent pathogens are usually synchronized, suggesting a concerted action of both compounds. Accordingly, NO was shown to act synergistically with ROS to promote cell death in soybean cells [24]. Interestingly, HR seems to be activated when NO interacts with H_2O_2 generated from superoxide by superoxide dismutase, rather than with superoxide per se [25]. Similarly, in our own investigations we identified NO but not $ONOO^-$ as an effective inducer of cryptogein-triggered HR [18]. In our model system, however, HR seems to occur independently of H_2O_2, because the inhibition of NADPH oxidase had no effect on the elicitor-mediated cell death [12,16]. Because the overall time course of NO and ROS are almost identical in elicitor-treated cells, it is also conceivable that NO might regulate ROS production and *vice versa* in particular contexts. Supporting this hypothesis, BcPG1-induced H_2O_2 production in grapevine cells was shown to be tightly dependent on NO. The question of whether NO produced in response to BcPG1 (in)directly activates NADPH oxidase, or whether it inhibits H_2O_2 scavenging enzyme as suggested by Clark *et al*. [26] will require further investigation.

Our data, along with those from other studies, highlight the crucial role of NO in protecting plants against pathogens by promoting Ca^{2+} mobilization, ROS synthesis, defense- and stress-related gene expression and HR (Figure 1). This concept was recently confirmed at the genetic level by Zeidler *et al*. [27] who reported that *Atnos1* mutant plants showed dramatic susceptibility to the pathogen *Pseudomonas syringae* pv. tomato DC3000. Besides pathogen attack, abiotic stressors, such as drought, salinity and extreme temperature are serious threats to agriculture. In the recent years, a significant amount of work has gone into investigating NO synthesis and functions in plants exposed to abiotic stressors. For example, it was shown both in tobacco leaf peels and tobacco suspension cells that high temperature, osmotic stress, or salinity, generate a rapid and significant surge in NO levels [28]. In contrast, light stress and mechanical injury had no apparent effect on NO production in tobacco and/or tomato [28, 29]. Thus, although NO synthesis can be triggered by several, disparate abiotic stressors, it cannot be considered a universal plant stress response.

Experiments using NO donors suggest that NO may exert beneficial effect on stress tolerance. For instance, it was shown that NO released by sodium nitropruside (SNP) enhanced the tolerance of wheat seedlings to drought stress [30]. A key question which remains mostly unresolved is how NO contributes to plant adaptation to abiotic stress ? As commonly suggested, by scavenging the superoxide radicals commonly produced by plants challenged by abiotic stressors, NO would prevent superoxide-induced deleterious effects such as the formation of the highly toxic hydroxyl radicals. It is also reasonable to expect that NO synthesized by plant cells in response to abiotic stressors encodes and conveys information leading to stress tolerance. Supporting this hypothesis, recent evidence shows that NO participate in the elevation of $[Ca^{2+}]_{cyt}$ triggered by hyperosmotic stress in tobacco cell suspensions [28]. Exploring these pathways will undoubtedly aid our understanding of plants acquired stress tolerance.

2. The NO/Ca^{2+} cross-talk

The hypothesis that NO might play a key role in controlling free Ca^{2+} mobilization in plant cells was first postulated by Durner *et al*. [31] and Klessig *et al*. [32]. Both studies provided pharmacological arguments suggesting the occurrence of a NO/cGMP/cADPR/Ca^{2+} signaling cascade in plant cells. The results discussed here confirm this tight interaction between the

Ca^{2+} and the NO signaling systems. A similar NO/Ca^{2+} connection has also been found to be active in abscisic acid signaling leading to stomatal closure [33].

Recently, the role of NO in controlling Ca^{2+} homeostasis was investigated more thoroughly. Its has been shown that NO, released by the sulphur-free NO donor DEA-NONOate, elicits within minutes a transient influx of extracellular Ca^{2+} and a synchronized increase of $[Ca^{2+}]_{cyt}$ in aequorin-transformed tobacco cells [18]. As predicted from a pharmacological study, the channels responsible for NO-induced $[Ca^{2+}]_{cyt}$ elevation include voltage-dependent Ca^{2+} channels of the plasma membrane and intracellular Ca^{2+} channels sensitive to RYR and IP_3R inhibitors. This observation paralleled the situation encountered in animal cells in which almost all the molecules involved in the control of Ca^{2+} homeostasis seem to be modulated by NO [3]. By contrast, NO released by the donor did not induce nuclear free Ca^{2+} changes in tobacco cell suspensions (D Lecourieux, personal communication, 2004). Therefore, the modulation by NO of intracellular Ca^{2+}-permeable channels leading to an enrichment of the nuclear free Ca^{2+} concentration seems unlikely. However, caution in the interpretation of these data needs to be exerted. Indeed, a main problem facing experiments based on NO donors is the access of NO to its targets. For example, it is possible that NO entering the cells was metabolised before acting on the nucleus Ca^{2+} homeostasis. Furthermore, NO might not be sufficient to activate the mechanisms involved in the increase of nuclear free Ca^{2+} concentration.

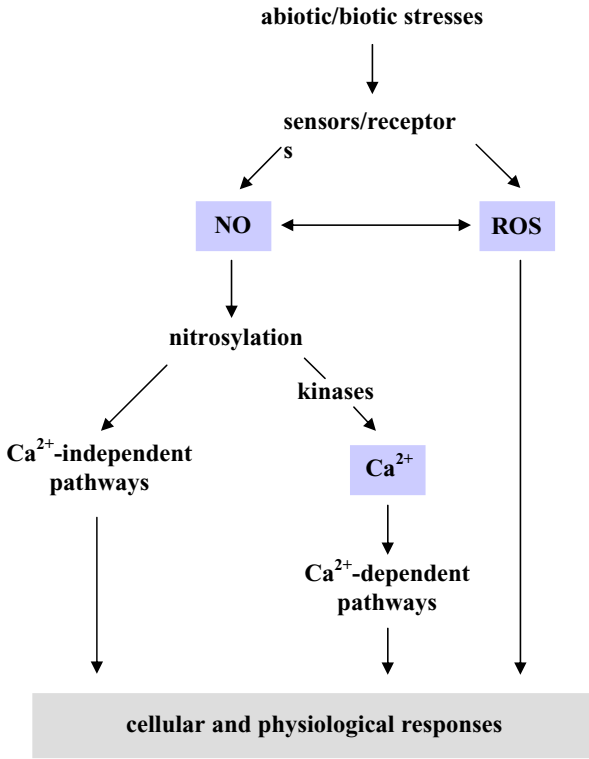

Figure 2. Schematic description of NO involvement in biotic/abiotic transduction pathways

Recent evidence from our laboratory suggest that NO mediates $[Ca^{2+}]_{cyt}$ through multiple mechanisms (O Lamotte, C Courtois, personal communication, 2004) . First, the elevation of $[Ca^{2+}]_{cyt}$ triggered by NO in aequorin-transformed tobacco cells was diminished by dithiothreitol, a reducing agent capable of denitrosylation nitrosothiol groups [34]. This inhibitory effect suggests that NO might partly act by S-nitrosylation or oxidation of cysteine residues. Second, we obtained evidence that NO operates on Ca^{2+} mobilization through phosphorylation-dependent processes, suggesting that the NO signal converges into protein kinases pathways. Accordingly, we demonstrated that NO can induce within minutes the activation of two protein kinases, a serine/threonine protein kinase and a MAPK. Whether both protein kinases are involved in NO signaling leading to Ca^{2+} mobilization is currently unknown. Third, 8-bromo-cADPR, a selective agonist of cADPR-mediated Ca^{2+} release, suppressed the Ca^{2+}-mobilizing action of NO, confirming the existence of a NO/cADPR/Ca^{2+} signaling cascade in plant cells. Finally, NO treatment depolarised the plasma membrane of tobacco cells, most probably through the inhibition of outward-rectifying K^+ channels as recently reported by Sokolovski and Blatt [35]. This depolarisation may in turn activate voltage-dependent Ca^{2+} channels of the plasma membrane.

3. Conclusion

Plants express adaptive response to allow them to confer tolerance to environmental stresses and ensure survival. NO function is signal transduction pathways during this response (Figure 2). Although the precise signaling functions of NO are poorly understood, its capacity to modulate Ca^{2+} homeostasis provides an extraordinary and remarkably effective way of conveying information. Little is known about the signaling consequence of the NO/Ca^{2+} crosstalk but it is likely that modulation of the expression of stress-related gene may occur. Elucidating the role of NO in plant response to stressors will also require the identification of nitrosylated proteins. A recent novel strategy has been reported for the identification of such proteins [36] and within the next few years, numbers of them will become available. The challenge will be to understand their functions and to determine the extent to which nitrosylation influences plant cell response to environmental and infection stresses.

Acknowledgements

Work in our laboratory was supported by the Institut National de la Recherche Agronomique (SPE, grant number 1088-01a), the Ministère de la Jeunesse, de l'Education Nationale et de la Recherche, the Conseil Régional de Bourgogne, and the Bureau Interprofessionnel des Vins de Bourgogne.

References

[1] Kone B.C., Kuncewicz T., Zhang W., Yu Z-Y., “Protein interactions with nitric oxide synthases: controlling the right time, the right place, and the right amount of nitric oxide”. *Am. J. Renal. Physiol.* 2003, vol. 285 , p.p 178-190.

[2] Stamler J.S., Lamas S., Fang F.C., “Nitrosylation: the prototypic redox-based signalling mechanism”. *Cell*, vol. 106 , p.p 675-683, 2001.

[3] Clementi E., "Role of nitric oxide and its intracellular signalling pathways in the control of Ca^{2+} homeostasis". *Biochem. Pharmacol*, vol. 55 , p.p 713-718<. 1998.
[4] Desikan R., Cheung M.K., Bright J., Henson D., Hancock J.T. and Neill S.J., "ABA, hydrogen peroxide and nitric oxide signalling in stomatal guard cells". *J. Exp. Bot.*, vol. 55 , p.p 205-212, 2004.
[5] Romero-Puertas M.C., Perazzolli M., Zago E.D. and Delledonne M., „Nitric oxide signalling functions in plant-pathogen interactions". *Cell Microbiol.*, vol. 6 , p.p 795-803, 2004.
[6] Wendehenne D., Durner J., Klessig D.F., "Nitric oxide: a new player in plant signalling and defence responses". *Curr. Opin. Plant Biol.*, vol. 7 , p.p 449-455, 2004.
[7] Yamasaki H. and Sakihama Y., "Simultaneous production of nitric oxide and peroxynitrite by plant nitrate reductase: *in vitro* evidence for the NR-dependent formation of active nitrogen species". *FEBS Lett.*, vol. 468 , p.p 89-92, 2000.
[8] Guo FQ, Okamoto M, Crawford NM, "Identification of a plant nitric oxide synthase gene involved in hormonal signaling. *Science* 2003, vol. 302 , p.p 100-103.
[9] Ricci P., "Induction of the hypersensitive response and systemic acquired resistance by fungal proteins: the case of elicitins". In: *Plant-Microbe Interactions*, *Vol. 3* (Edited by Stacey, G, Keen NT). Chapman and Hall, New York, p.p. 53-75, 1997.
[10] Poinssot B., Vandelle E., Bentejac M., Adrian M., Levis C., Brygoo Y., Garin J., Sicilia F., Coutos-Thevenot P. and Pugin A., "The endopolygalacturonase 1 from *Botrytis cinerea* activates grapevine defense reactions unrelated to its enzymatic activity". *Mol Plant Microbe Interact*, vol. 16 , p.p 553-64, 2003.
[11] Bourque S., Binet M.N., Ponchet M., Pugin A. and Lebrun Garcia A., "Characterization of the cryptogein binding sites on plant plasma membranes". *J. Biol. Chem.*, vol. 274 , p.p 34699-34705, 1999.
[12] Wendehenne D., Lamotte O., Frachisse J.M., Barbier-Brygoo H. and Pugin A., "Nitrate efflux is an essential component of the cryptogein signaling pathway leading to defense responses and hypersensitive cell death in tobacco". *Plant Cell*, vol. 14 , p.p 1937-1951, 2002.
[13] Lecourieux D., Mazars C., Pauly N., Ranjeva R. and Pugin A, "Analysis and effects of cytosolic free calcium increases in response to elicitors in *Nicotiana plumbaginifolia* cells". *Plant Cell*, vol.14, p.p 2627-2641, 2002.
[14] Lebrun-Garcia A., Ouaked F., Chiltz A. and Pugin A, "Activation of MAPK homologues by elicitors in tobacco cells". *Plant J.*, vol.15 , p.p 773-781, 1998.
[15] Pugin A., Frachisse J.M., Tavernier E., Bligny R., Gout E., Douce R. and Guern J., "Early events induced by the elicitor cryptogein in tobacco cells: involvement of a plasma membrane NADPH oxidase and activation of glycolysis and pentose phosphate pathway". *Plant Cell*, vol.9 , p.p 2077-2091, 1997.
[16] Binet M.N., Humbert C., Lecourieux D., Vantard M. and Pugin A, "Disruption of microtubular cytoskeleton induced by cryptogein, an elicitor of hypersensitive response in tobacco cells". *Plant Physiol.*, vol. 125 , p.p 564-572, 2001.
[17] Foissner I., Wendehenne D., Langebartels C. and Durner J., "*In vivo* imaging of an elicitor-induced nitric oxide burst in tobacco". *Plant J.*, vol. 23 , p.p 817-824, 2000.
[18] Lamotte O., Gould K., Lecourieux D., Sequeira-Legrand A., Lebrun-Garcia A., Durner J., Pugin A and Wendehenne D., "Analysis of nitric oxide signaling functions in tobacco cells challenged by the elicitor cryptogein". *Plant Physiol*, vol. 135 , p.p 516-529, 2004.
[19] Chandok M.R., Ytterberg A.J., van Wijk K.J. and Klessig D.F., "The pathogen-inducible nitric oxide synthase (iNOS) in plants is a variant of the P protein of the glycine decarboxylase complex". *Cell*, vol. 113 , p.p 469-482, 2003.
[20] Price A.H., Taylor A., Ripley S.J., Griffiths A., Trewavas A.J., Knight M.R., "Oxidative signals in tobacco increase cytosolic calcium". *Plant Cell*, vol. 6 , p.p 1301-1310, 1994.
[21] Wang W., Vinocur B., Shoseyov O. and Altman A., "Role of plant heat-shock proteins and molecular chaperones in the abiotic stress response". *Trends Plant Sci.*, vol. 9 , p.p 244-252, 2004.
[22] Modolo L.V., Cunha F.Q., Brage M.R. and Salgado I., "Nitric oxide synthase-mediated phytoalexin accumulation in soybean cotyledons in response to the *Diaporthe phaseolorum* f.sp. *meridionalis* elicitor". *Plant Physiol.*, vol. 130 , p.p 1288-1297, 2002.
[23] Noritake T., Kaxakita K., Doke N., "Nitric oxide induces phytoalexin accumulation in potato tuber tissues". *Plant Cell Physiol.*, vol. 37 , p.p 113-116, 1996.
[24] Delledonne M., Xia Y., Dixon R.A. and Lamb C., « Nitric oxide functions as signal in plant disease". *Nature*, vol. 394 , p.p 585-588, 1998.
[25] Delledonne M., Zeier J., Marocco A. and Lamb C., "Signal interactions between nitric oxide and reactive oxygen intermediates in the plant hypersensitive disease resistance response". *Proc. Natl. Acad. Sci. USA*, vol. 98 , p.p 13454-13459, 2001.
[26] Clark D., Durner J., Navarre D.A. and Klessig D.F., "Nitric oxide inhibition of tobacco catalase and ascorbate peroxidase". *Mol. Plant Microbe Interact.*, vol. 13 , p.p 1380-1384, 2000.

[27] Zeidler D., Zahringer U., Gerber I., Dubery I., Hartung T., Bors W., "Hutzler Pand Durner J, "Innate immunity in *Arabidopsis thaliana*: lipopolysaccharides activate nitric oxide synthase (NOS) and induce defense genes". *Proc. Natl. Acad. Sci. USA*, vol. 101 , p.p 15811-15816, 2004.
[28] Gould K.S., Lamotte O., Klinguer A., Pugin A. and Wendehenne D., "Nitric oxide production in tobacco leaf cells, p.p a generalized stress response?" *Plant Cell Environ.*, vol. 26 , p.p 1851–1862, 2003.
[29] Orozco-Cardenas M.L. and Ryan C.A., "Nitric oxide negatively modulates wound signaling in tomato plants". *Plant Physiol.*, vol. 130 , p.p 487-493, 2002.
[30] Garcia-Mata C. and Lamattina L., "Nitric oxide induces stomatal closure and enhances the adaptive plant responses against drought stress". *Plant Physiol.*, vol. 126 , p.p 1196-1204, 2001.
[31] Durner J., Wendehenne D. and Klessig DF, "Defense genes induction in tobacco by nitric oxide, cyclic GMP and cyclic ADP ribose". *Proc. Natl. Acad. Sci. USA*, vol. 95 , p.p 10328-10333, 1998.
[32] Klessig D.F., Durner J., Noad R., Navarre D.A., Wendehenne D., Kumar D., Zhou J.M., Shah J., Zhang S., Kachroo P. and other, "Nitric oxide and salicylic acid signaling in plant defense.. *Proc. Natl. Acad. Sci. USA*, vol. 97 , p.p 8849-8855, 2000.
[33] Garcia-Mata C., Gay R., Sokolovski S., Hills A. and Lamattina Land Blatt M.R., "Nitric oxide regulates K^+ and Cl^- channels in guard cells through a subset of abscisic acid-evoked signaling pathways". *Proc. Natl. Acad. Sci. USA*, vol. 100 , p.p 11116-11121, 2003.
[34] Hart J.D., Dulhunty A.F., "Nitric oxide activates or inhibits skeletal muscle ryanodine receptors depending on its concentration, membrane potential and ligand binding". *J. Membr. Biol.*, 173 , p.p 227-236, 2000.
[35] Sokolovski S., Blatt M.R., "Nitric Oxide Block of Outward-Rectifying K^+ Channels indicates Direct Control By Protein Nitrosylation In Guard Cells". *Plant Physiol*., vol. 136, 2004, in press.
[36] Jaffrey S.R., Erdjument-Bromage H., Ferris C.D., Tempst P and Snyder SH, "Protein S-nitrosylation: a physiological signal for neuronal nitric oxide". *Nat. Cell Biol.*, vol. 3 , p.p 193-197, 2001.

Cell Biology and Instrumentation: UV Radiation, Nitric Oxide and Cell Death in Plants
Y. Blume et al. (Eds.)
IOS Press, 2006

Effect of Nitric Oxide on Concentration of Cytosolic Free Ca^{2+} in Transgenic *Arabidopsis thaliana* Plants Under Oxidative Stress

Ekaterina V. KOLESNEVA, Lyudmila V. DUBOVSKAYA, Igor D. VOLOTOVSKI
Institute of Biophysics and Cell Engineering, National Academy of Sciences of Belarus, Academicheskaya Str. 27, 220072, Minsk, Belarus

Abstract. Nitric oxide (NO) is a very important molecule taking part in various signaling pathways in plants including plant responses to different stress conditions. In this work we have investigated the effect of NO on the cytosolic free calcium concentration ($[Ca^{2+}]_{cyt}$) under oxidative stress induced by hydrogen peroxide. Using seedlings of transformed *Arabidopsis thaliana* expressing Ca^{2+}-reporter apoaequorin in cytosol, we have shown that H_2O_2 influences $[Ca^{2+}]_{cyt}$ in a dose-depended manner and induces two peaks of calcium-dependent chemiluminescence measured in plant seedlings. The NO donors sodium nitroprusside (SNP) and (±)-E-2-[(E)-Hydroxyimino]-6-methoxy-4-methyl-5-nitro-3-hexenamide (NOR-1) alone led to a transient increase in $[Ca^{2+}]_{cyt}$, but simultaneously reduced the amplitude of the first peak of H_2O_2–induced $[Ca^{2+}]_{cyt}$ increase by 42%. The nitric oxide synthase (NOS) and nitrate reductase (NR) inhibitor analysis showed that the production of NO, participating in H_2O_2-induced Ca^{2+}-response, occurred due to NOS-like plant enzyme to be sensitive to oxidative stress. In summary, our data indicate that NO is likely to have a protective effect under oxidative stress and reduced a calcium increase induced by reactive oxygen species like hydrogen peroxide.

Introduction

Plants are frequently subjected to different stresses and contain various defence mechanisms to survive under these conditions. It is shown that NO can function to mitigate the effects of stressors in diverse plant species [1].

Many plants are believed to produce substantial amounts of NO in their natural environments [2]. The possibility exists that NO production occurs under natural conditions as a generalized stress response [3]. Two interrelated mechanisms by which NO might abate stress have been proposed. Firstly, NO might function as an antioxidant, directly scavenging the reactive oxygen species (ROS) that are generated by most of stressors. NO can interact rapidly with superoxide radical to form peroxynitrite [4]. Although peroxynitrite and its protonated form ONOOH are themselves oxidizing agents, they are considered to be less toxic than peroxides and may therefore minimize cell damage [5].

Secondly, NO may function as a signalling molecule in the cascade of events leading to gene expression [6]. The chemical properties of NO (small molecule, short life time, absence of charge, and high diffusivity) suggest that it would be an ideal inter- and intramolecular signalling molecule in plant stress responses [7].

Plants are considered to be subjected to oxidative stress when ROS are produced in uncontrollable toxic amounts. Generation of superoxides, hydrogen peroxide, hydroxyl radicals and other free radicals can result from the involvement of oxygen in normal

respiratory processes and the production of oxygen during photosynthesis [8]. The protective mechanisms against oxidative damage are operating with the involvement of enzymes (superoxide dismutase, catalases and peroxidases), and free radical scavengers (carotenoids, ascorbate, tocopherols, oxidized and reduced glutathione, GSSG and GSH, respectively) [9]. In animal cells the ratio of GSH to GSSG is crucial for cell reaction. The GSH/GSSG ratio influences cytosolic calcium homeostasis resulting from oxidative changes in sensitive thiols of Ca^{2+} - ATPases [10]. NO can activate guanylyl cyclase which in turn can influence cytosolic calcium homeostasis. The oxidative damage can result from such processes as pathogen infections, drought and other stresses, herbicide treatment, *etc.*

Beligni and Lamattina have found that NO interferes with plant photo-oxidative stress induced by bipyridinium herbicide diquat [11]. They demonstrated that two NO donors, SNP and S-nitroso-N-acetylpenicillamine (SNAP), strongly reduced the lipid peroxidation and the protein loss caused by the application to potato leaf pieces or isolated chloroplasts of high doses of diquat. NO donors also protect the RNA against oxidative damage. Their results have provided the evidence that NO is a potent antioxidant in plants and that its action may, at least in part, be explained by its ability to directly scavenge ROS. NO was demonstrated to confer a water-deficit tolerance to both detached wheat leaves and wheat seedlings under a drought stress condition. NO availability to induce stomatal closure also may play a role [12]. NO was supposed to act as an antioxidant and protect membranes and lipoproteins from oxidation either directly by inactivating ROS such as lipid hydroxyl radical, or indirectly by inhibiting lipoxygenase activity [13, 14].

Plants are often challenged by potential pathogens. The activation of plant defence responses is initiated through the recognition of microorganisms-derived molecules called elicitors, which trigger rapid defence responses *via* complex signal transduction pathways [15]. Lamotte *et al.* investigated the signalling events that mediate NO production, and analyzed NO signalling activities in the cryptogein transduction pathway [16]. They found that cryptogein production in tobacco cell suspensions was sensitive to NOS inhibitors and may be catalyzed by the recently identified pathogen-inducible plant NOS – variant P. NO was shown to participate in cryptogein-mediated elevation of cytosolic free calcium through the mobilization of Ca^{2+} from intracellular stores. The NO donor diethylamine NONOate promoted an increase in cytosolic free calcium concentration, which was sensitive to intracellular Ca^{2+} channel inhibitors. The demonstration that NO is involved in the mobilization of intracellular Ca^{2+} establishes Ca^{2+} channels as putative NO targets in plant signal transduction mechanisms. Thus, their data indicated that NO was involved in the signal transduction processes leading to cryptogein-induced defense responses.

NO also plays a key role in plant disease resistance. For example, in soybean cell suspensions inoculated with *Pseudomonas syringae,* NO increased in parallel with other ROS and potentiated the induction of hypersensitive response and programmed cell death. At the same time, NO functioned independently of other ROS to induce genes for the synthesis of protective natural products. Moreover, the authors have found that the inhibitors of NO synthesis compromised the hypersensitive disease-resistance response of *Arabidopsis* leaves to *P. syringae*, promoting disease and bacterial growth [17]. NO was also shown to delay the onset of GA-induced PSD of barley aleurone cells. However, the mechanism by which NO caused its protective effect in plant systems is still unclear [13, 18].

High doses of chemical and physical stimuli, including the oxidative stress, might induce transient increases in the concentration of cytosolic free Ca^{2+} ($[Ca^{2+}]_{cyt}$). Ca^{2+} influx into the cytosol can occur because of the opening of Ca^{2+} channels with Ca^{2+} entering the cell down a concentration gradient or can be released from internal Ca^{2+} stores, such as vacuoles, Golgi apparatus, mitochondria and others [19, 20]. Price *et al.* showed that the treatment of tobacco seedlings transformed to express apoaequorin with hydrogen peroxide

resulted in transient burst of calcium-dependent luminescence, at that H_2O_2 provoked the release of Ca^{2+} predominantly from internal sources [21]. In contrast, in work of Lecourieux *et al.* $[Ca^{2+}]_{cyt}$ increase that followed H_2O_2 addition in tobacco cell suspensions resulted mainly from extracellular Ca^{2+}-influx [22].

As NO was shown to be involved in intracellular Ca^{2+}-mobilization [16] and to participate in stress defense responses we proposed that NO might play an important role in ROS-induced Ca^{2+}-response. Therefore, the aim of our work was to study the influence of exogenous NO on increase of $[Ca^{2+}]_{cyt}$ during H_2O_2-induced oxidative stress being measured using *Arabidopsis thaliana* seedlings transformed to express apoaequorin.

1. Materials and methods

1.1. Plant material

8-day-old transgenic *Arabidopsis thaliana* seedlings expressing apoaequorin were grown at 22°C in Petri dishes under the condition when 15 hr polychromatic white light (30 $w \times m^{-2}$) was alternated with 9 hr continuous dark. The seeds of transgenic *Arabidopsis thaliana* were kindly provided by Prof. Mark R. Knight (Department of Plant Sciences, University of Oxford, UK).

1.2. Aequorin reconstitution and $[Ca^{2+}]_{cyt}$ measurement

The *Arabidopsis thaliana* seedlings were incubated in 5 μM coelenterazine for 6 hours in the dark to reconstitute the aequorin. Chemiluminescence measurements were performed with a digital chemiluminometer (model PCHL-01, Biopribor, Moscow, Russia) equipped with a PEU-84 photomultiplier and chart recorder. At the end of the experiment, residual functional aequorin ($I_{lum\ max}$) was quantified by adding an equal volume of 1.8 M $CaCl_2$/EtOH (40%) (v/v).

The peak-value of the stimuli-induced $[Ca^{2+}]_{cyt}$ transient was calculated as described by Cobbold P.H. and Rink T.J. (1987) [23] with some modifications to take into account the specific isoform used and the experimental temperature:

$$pCa = 0.332588(-\log k) + 5.5593,$$
$$k = I_{lum} / I_{lum\ max}$$

1.3. Hydrogen peroxide treatment

After the aequorin reconstitution, the seedlings were floated in 100 μl of distilled water in a cuvette in the luminometer, and background readings were taken until the luminescence had been stabilized from touch stimulation (generally 1 to 2 min). Hydrogen peroxide was added from a syringe through a luminometer port. The intensity of luminescence was recorded every 10 sec during at least 40 min with continuous traces being made on a chart recorder attached to the luminometer.

1.4. NO donors and NO scavenger studies

When NO donors were used, the seedlings containing reconstituted aequorin were floated in solution of donor for 30 min. After this time, the seedlings were washed in distilled water before stimulation with hydrogen peroxide.

Before the hydrogen peroxide treatment, NO scavengers carboxy-PTIO and methylene blue were added to the seedlings alone or together with a donor solution after the aequorin reconstitution.

1.5. Inhibitor treatments

NOS inhibitor TRIM and NR inhibitor NaN_3 were added to seedlings containing reconstituted aequorin for 30 min ageing. After this time, the seedlings were washed in distilled water before a hydrogen peroxide treatment.

1.6. Data analysis

Where indicated, values were expressed as means ± SD of at least five independent experiments. A value of $P < 0.05$ was considered as significant for mean differences.

2. Results

2.1. Hydrogen peroxide increases $[Ca^{2+}]_{cyt}$ in Arabidopsis thaliana seedlings

Hydrogen peroxide appeared to influence $[Ca^{2+}]_{cyt}$ in a dose-depended manner and induced two peaks of calcium-dependent chemiluminescence of *Arabidopsis* seedlings (Fig. 1, A).

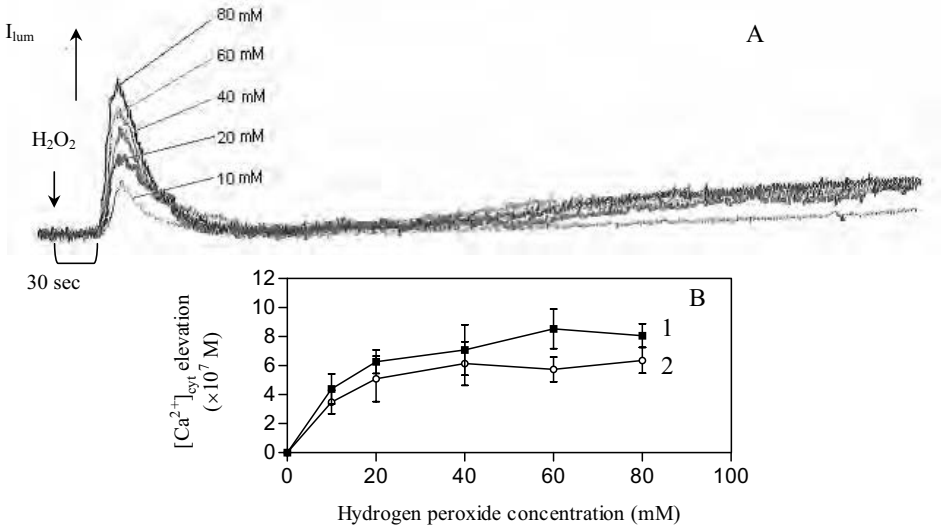

Figure 1. Effect of hydrogen peroxide on $[Ca^{2+}]_{cyt}$ in transgenic *Arabidopsis thaliana* seedlings. A – effect of H_2O_2 on Ca^{2+}-dependent chemiluminescence. B – elevation of $[Ca^{2+}]_{cyt}$. The first peak (1) was registered in 20-40 sec and the second one (2) – in 20 min after hydrogen peroxide treatment.

When the samples were placed in a chemiluminometer and H_2O_2 was added, a single spike of calcium-dependent chemiluminescence was observed followed by the second sustained Ca^{2+}-elevation. This specific cytosolic calcium signature followed a lag-phase of 20 – 40 sec, peaked after 1 min and returned to a background level in 1.5 – 2 min, and the second $[Ca^{2+}]_{cyt}$ increase had a lag-phase of 5 – 10 min reaching maximum after 19 min and lasted at least for 30 min without reaching the basal level (Fig. 1, B). At saturating

H_2O_2-concentration of 40 mM the $[Ca^{2+}]_{cyt}$ elevations peaked at 0,707±0,174 μM and 0,614±0,150 μM.

2.2. Exogenous NO influences $[Ca^{2+}]_{cyt}$ during oxidative stress induced by hydrogen peroxide treatment

To test the hypothesis that NO may mobilize Ca^{2+} in plants, we investigated first the ability of exogenously applied NO donors to affect $[Ca^{2+}]_{cyt}$ in *Arabidopsis thaliana* seedlings. The treatment of seedlings with 5 mM NO donor SNP led to a transient increase in $[Ca^{2+}]_{cyt}$ after lag-phase of 2 min with maximum at 0,739±0,070 μM lasting for 1 min (Fig. 2, A). The magnitude of Ca^{2+}-responses was dependent on the SNP concentration (Fig. 2, B).

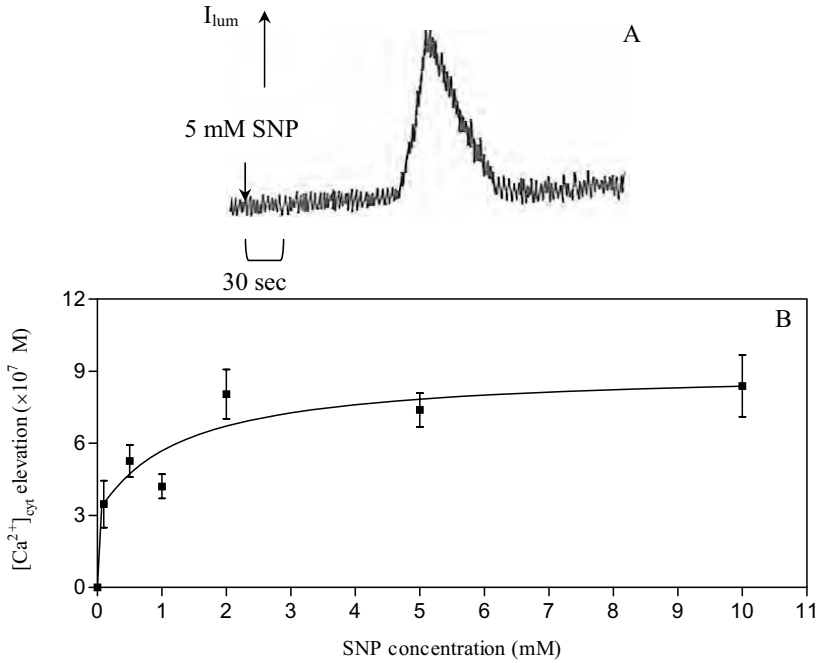

Figure 2. Effect of SNP on $[Ca^{2+}]_{cyt}$ in transgenic *Arabidopsis thaliana* seedlings. A – effect of 5mM SNP on Ca^{2+}-dependent chemiluminescence in transgenic *Arabidopsis thaliana* seedlings. B – elevation of $[Ca^{2+}]_{cyt}$.

At the same time, the pretreatment of samples with 5 mM SNP prior to hydrogen peroxide did reduced the first peak of $[Ca^{2+}]_{cyt}$ by 42%, whereas the second elevation was not modified (Fig. 3). Thus, NO probably influences the first elevation in $[Ca^{2+}]_{cyt}$ during the H_2O_2-mediated signalling. The second one is likely to originate from a source insensitive to NO.

5 mM NO donor NOR-1 influenced Ca^{2+}-response in a similar manner by triggering a transient Ca^{2+} increase reaching 0,682±0,166 μM. Pre-treatment of seedlings with 5 mM NOR-1 before the addition of 40 mM H_2O_2 reduced the first peak of $[Ca^{2+}]_{cyt}$ by 12 % (data not shown).

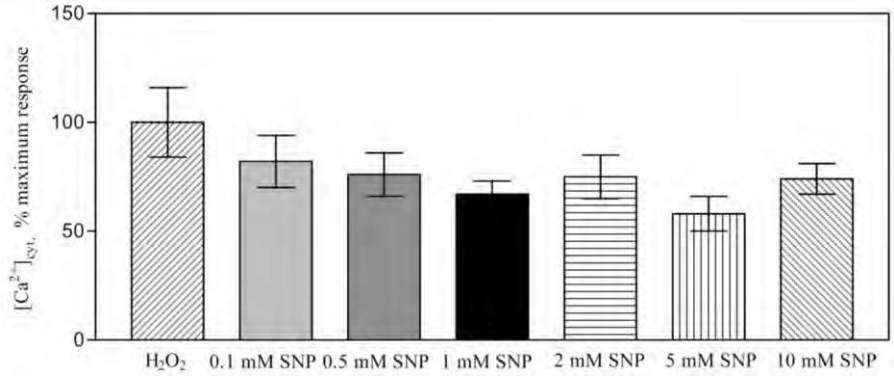

Figure 3. Effect of SNP on $[Ca^{2+}]_{cyt}$ during oxidative stress induced by 40 mM H_2O_2 in transgenic *Arabidopsis thaliana* seedlings. Ca^{2+} variation was evaluated as a percentage of the maximum $[Ca^{2+}]_{cyt}$ increase induced by 40 mM H_2O_2.

In order to correlate the above effects with NO release from donor solutions, the NO scavengers such as carboxy-PTIO and methylene blue were used.

In the same kind of experiment, carboxy-PTIO was added with SNP and NOR-1 together. NO donor-induced Ca^{2+} - increase was completely suppressed by 5 mM carboxy-PTIO confirming NO involvement in this process.

The effects of SNP- and NOR-1 on $[Ca^{2+}]_{cyt}$ elevation during oxidative stress were arrested in the presence of carboxy-PTIO (Fig. 4). The same effects were obtained using methylene blue, another NO scavenger. These data are an evidence of NO participating in the $[Ca^{2+}]_{cyt}$ increase that is induced by H_2O_2.

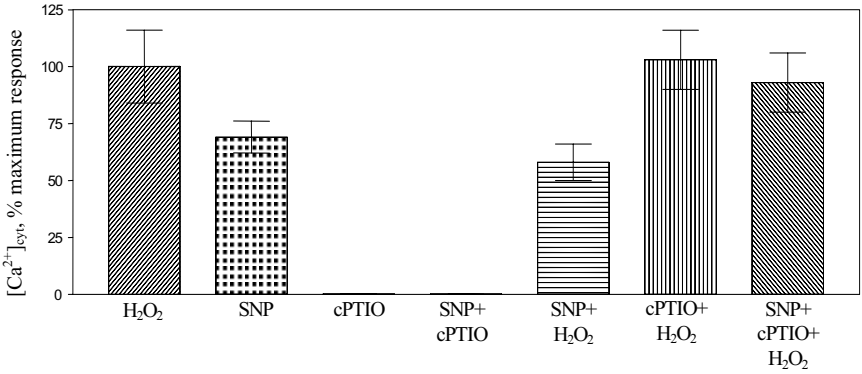

Figure 4. Effects of 5 mM SNP and 5 mM cPTIO on transient peak of $[Ca^{2+}]_{cyt}$ elevation in transgenic *Arabidopsis thaliana* seedlings in response to oxidative stress induced by 40 mM hydrogen peroxide. Ca^{2+} variation was evaluated as a percentage of the maximum $[Ca^{2+}]_{cyt}$ increase induced by 40 mM H_2O_2.

2.3 The influence of NOS and NR inhibitors on $[Ca^{2+}]_{cyt}$ during oxidative stress

To evaluate a possible effect of NOS inhibitors on the increase in $[Ca^{2+}]_{cyt}$ under oxidative stress, the seedlings were pretreated with TRIM, a common NOS inhibitor. Pretreatment of seedlings with 5 mM TRIM before the addition of 40 mM H_2O_2 increased magnitude of the

first peak of $[Ca^{2+}]_{cyt}$ by two times (Fig. 5). The lag-phase was diminished to 5-10 sec and the maximum was reached after 20 sec.

To analyse the possible contribution of NR to NO production under oxidative stress induced by H_2O_2, we studied the effect of sodium azide (NaN_3), a potent inhibitor of NR on $[Ca^{2+}]_{cyt}$ [11]. Fig. 5 shows that the increase in $[Ca^{2+}]_{cyt}$ in the seedlings under oxidative stress conditions was insensitive to the treatment with NaN_3, suggesting that NR is not involved in NO synthesis during the H_2O_2-induced oxidative stress.

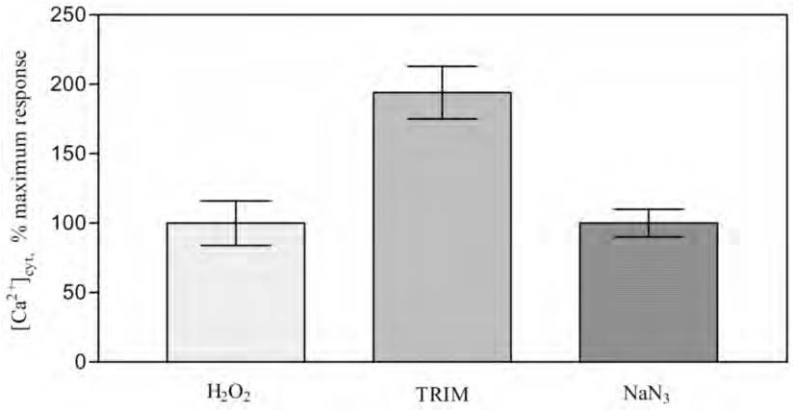

Figure 5. Effects of 5 mM TRIM and 50 μM NaN_3 on transient peak of $[Ca^{2+}]_{cyt}$ elevation in transgenic *Arabidopsis thaliana* seedlings in response to oxidative stress induced by 40 mM hydrogen peroxide. Ca^{2+} variation was evaluated as a percentage of the maximum $[Ca^{2+}]_{cyt}$ increase induced by 40 mM H_2O_2.

3. Discussion

In the present study, we investigated the enzymatic source of NO and analysed its role in the increase of $[Ca^{2+}]_{cyt}$ induced by H_2O_2-treatment using *Arabidopsis thaliana* seedlings.

In our experiments we studied the influence of exogenous hydrogen peroxide on increase in $[Ca^{2+}]_{cyt}$ in transgenic *Arabidopsis thaliana* seedlings expressing apoaequorin. Today, a Ca^{2+}-dependent chemiluminescence of the photoprotein aequorin is extensively used to report changes in intracellular calcium levels in animal and plant cells [24]. The use of this method enabled us to report $[Ca^{2+}]_{cyt}$ changes in whole *Arabidopsis thaliana* seedlings.

The results described in this study suggest that oxidative stress in the form of the hydrogen peroxide treatment causes an increase in $[Ca^{2+}]_{cyt}$. The treatment of *Arabidopsis thaliana* seedlings with hydrogen peroxide was shown to result in two peaks in $[Ca^{2+}]_{cyt}$. H_2O_2 triggered the first transient increase in $[Ca^{2+}]_{cyt}$ after a lag-period. The lag-phase is probably necessary for the penetration of hydrogen peroxide inside the cell. Our data regarding the first $[Ca^{2+}]_{cyt}$ peak are similar to those obtained by Price A.H. *et al.*, which describe a role of calcium in plant responses to oxidative stress in tobacco [21]. It is essential to note that our data about the second peak in the calcium increase are in accordance with the data obtained by Lecourieux *et al.* for tobacco cell suspensions treated by elicitor cryptogein. The authors suggested that the second sustained Ca^{2+}-increase in the cryptogein signalling was caused by H_2O_2 [22].

In animal cells NO evoked changes in levels of $[Ca^{2+}]_{cyt}$ in response to a number of stimuli. To investigate the ability of NO to influence $[Ca^{2+}]_{cyt}$ in H_2O_2-signaling the effects

of NO donors were examined. The treatments of *Arabidopsis thaliana* seedlings with NO donors SNP and NOR-1 resulted in rapid and transient increase of $[Ca^{2+}]_{cyt}$. This finding confirms the ability of NO to mobilize $[Ca^{2+}]_{cyt}$ in plants. Accordingly, Lamotte *et al.* obtained the similar results using tobacco cells expressing the apoaequorin in cytosol. They showed that NO donor diethylamine NONO-ate promoted an increase in $[Ca^{2+}]_{cyt}$ with the maximum of 2,2 μM in 10 min after the treatment [16].

At the same time, the pretreatment of samples with NO donors by SNP and NOR-1 prior to hydrogen peroxide reduced the first peak of $[Ca^{2+}]_{cyt}$ while the second elevation was not altered. In this case NO is likely to exert a protective function by detoxifying ROS resulted from the oxidative stress. The mechanisms of NO action are under discussion yet. For instance, Beligni and Lamattina have shown that the protective effect of NO during photo-oxidative stress can be originated from NO ability to directly scavenge ROS [11].

In order to define the role of endogenous NO in $[Ca^{2+}]_{cyt}$ responses induced by hydrogen peroxide the possible effect of NOS inhibitor TRIM has been studied. In mammals, NO is produced mainly by NOS. The evidence for mammalian-type NOS in plants has been increased in recent years. NOS-like activities as well as inhibition of NO-synthesis by inhibitors of animal NOS have been reported in plants. The pretreatment of seedlings with TRIM before the addition of H_2O_2 lead to increase of a magnitude of the first peak of $[Ca^{2+}]_{cyt}$ by two times, suggesting the involvement of a NOS-like enzyme.

In addition to NOS plant, NR can catalyse the NAD(P)H-dependent reduction of nitrite to NO [25]. But NR inhibitor NaN_3 did not influence H_2O_2-induced Ca^{2+}-response. Probably NO production during oxidative stress is NR-independent. In agreement with this hypothesis, the similar results were obtained by Lamotte *et al.* suggested that NR is not involved in NO synthesis observed in response to cryptogein [16].

In summary, the obtained results suggest that NO is unambiguously involved in the regulation of intracellular calcium concentration. It is likely to have a protective effect during oxidative stress by reducing the calcium increase induced by reactive oxygen species such as hydrogen peroxide.

References

[1] Leshem Y.Y. and Kuiper P.J.C., "Is there a GAS (general adaptation syndrome) response to various types of environmental stress?". *Biol. Plant.*, vol. 38, p.p. 1–18, 1996.

[2] Wildt J., Kley D., Rockel A. and Segschneider H.J., "Emission of NO from higher plant species". *J. Geophys. Res.,* vol. 102, p.p. 5919–5927, 1997.

[3] Magalhaes J.R., Pedroso M.C. and Durzan D.J., "Nitric oxide, apoptosis and plant stresses". *Physiol. Plant Mol. Biol.*, vol. 5, p.p. 115–125, 1999.

[4] Radi R., Beckman J.S., Bash K.M. and Freeman R.A., "Peroxynitrite induced membrane lipid peroxidation, p.p. cytotoxic potential of superoxide and nitric oxide". *Arch. Biochem. Biophys.*, vol. 228, p.p. 481–487, 1991.

[5] Wink D.A., Hanbauer I., Krishna M.C., DeGraff W., Gamson J. and Mitchell J.B., "Nitric oxide protects against cellular damage and cytotoxity from reactive oxygen species". *Proc. Natl. Acad. Sci. USA*, vol. 90, p.p. 9813–9817, 1993.

[6] Wendehenne D., Pugin A., Klessig D.F. and Durner J., "Nitric oxide: comparative synthesis and signaling in animal and plant cells". *Trends Plant Sci.*, vol. 6, p.p. 177–183, 2001.

[7] Foissner I., Wendehenne D., Langebartels C. and Durner J., "*In vivo* imaging of an elicitor-induced nitric oxide burst in tobacco". *Plant J.*, vol. 23, p.p. 817–824, 2000.

[8] Bowler C., Van Montagu M. and Inze D., "Superoxide dismutase and stress tolerance". *Annu. Rev. Plant Physiol. Plant Mol. Biol.*, vol. 43, p.p. 83–116, 1992.

[9] Halliwell B. and Gutteridge J.M.C., "Free radicals in biology and medicine". Oxford, UK, Oxford University Press.

[10] Nicoterra P., Kass G.E.N. and Orrenius S., "Calcium mediated mechanisms in chemically-induced cell death". *Annu. Rev. Pharmacol. Toxicol.*, vol. 32, p.p. 449–470, 1992.

[11] Beligni M.V. and Lamattina L., "Nitric oxide interferes with plant photo-oxidative stress by detoxifying

reactive oxygen species". *Plant Cell Environ*., vol. 25, p.p. 737–748, 2002.
[12] Beligni M.V. and Lamattina L., "Nitric oxide induces stomatal closure and enhances the adaptive plant responses against drought stress". *Plant Physiol.*, vol. 126, p.p. 1196–1204, 2001.
[13] Beligni M.V. and Lamattina L., "Is nitric oxide toxic or protective?" *Trends Plant Sci.*, vol. 4, p.p. 299–300, 1999.
[14] Beligni M.V., Fath A., Bethke P.C., Lamattina L. and Jones R.L., "Nitric oxide acts an antioxidant and delays programmed cell death in barley aleurone layers". *Plant Physiol.*, vol. 129, p.p. 1642–1650, 2002.
[15] Scheel D., "Resistance response physiology and signal transduction". *Curr. Opin. Plant. Biol.*, vol. 1, p.p. 305–310, 1998.
[16] Lamotte O., Gould K., Lecourieux D., Sequeira-Legrand A., Lebrun-Garsia A., Durner J., Pugin A. and Wendehenne D., "Analysis of nitric oxide signaling functions in tobacco cells challenged by the elicitor cryptogein". *Plant Physiol*., vol. 135, p.p. 516–529, 2004.
[17] Delledonne M., Xia Y., Dixon R.A. and Lamb C., "Nitric oxide functions as a signal in plant disease resistance". *Nature*, vol. 394, p.p. 585–588, 1998.
[18] Beligni M.V., Fath A., Bethke P.C., Lamattina L. and Jones R.L., "Nitric oxide acts an antioxidant and delays programmed cell death in barley aleurone layers". *Plant Physiol.*, vol. 129, p.p. 1642–1650, 2002.
[19] Gilroy S. and Trewavas A.J., "A decade of plant signals". *BioEssays*, vol. 16, p.p. 677–682, 1994.
[20] Rudd J.J. and Franklin-Tong E., "Unravelling response-specifity in Ca^{2+} signaling pathways in plant cells". *New Phytol.*, vol. 151, p.p. 7–33, 2001.
[21] Price A.H., Taylor A., Ripley S.J., Griffiths A., Trewavas A.J. and Knight M.R., "Oxidative signals in tobacco increase cytosolic calcium". *Plant Cell*, vol. 6, p.p. 1301–1310, 1996.
[22] Lecourieux D., Mazars C., Pauly N., Ranjeva R. and Pugin A., "Analysis and effects of cytosolic free calcium increases in response to elicitors in *Nicotiana plumbaginifolia* cells". *Plant Cell*, vol. 14, p.p. 2627–2641, 2002.
[23] Cobbold P.H. and Rink T.J., "Fluorescence and bioluminescence measurements of cytoplasmic free calcium". *Biochem. J*., vol. 248, p.p. 313–328, 1987.
[24] Knight H., Trewavas A.J. and Knight M.R., "Cold calcium signaling in Arabidopsis involves two cellular pools and change in calcium signature after acclimation". *Plant Cell*, vol. 8, p.p. 489–503, 1996.
[25] Yamasaki H., Nitrite-dependent nitric oxide production pathway: implications for involvement of active nitrogen species in photo-inhibition *in vivo*". *Philos. Trans. R. Soc. Lond.*, vol. 355, p.p. 1477–1488, 2000.

Cell Biology and Instrumentation: UV Radiation, Nitric Oxide and Cell Death in Plants
Y. Blume et al. (Eds.)
IOS Press, 2006

Nitric Oxide, Peroxidases and Programmed Cell Death in Plants

Maria Concetta DE PINTO and Laura DE GARA
Dipartimento di Biologia e Patologia Vegetale
Via E. Orabona 4, I-70125 Bari, Italy

Abstract Nitric oxide (NO) acts as intra- and inter-cellular signal in plant and animal cells. Recent findings point out that NO production is promoted in plants both by external and internal stimuli. The signalling pathways triggered by this reactive species also depend by cellular environmental conditions and by the presence of other reactive species. NO alters protein activity and/or structure, by directly interacting with thiol or heme groups or through pathways involving gene expression and/or protein synthesis. The NO effects on peroxidases (a super-family of heme–isoenzymes that play critical roles in both cell differentiation and defence responses), has been widely studied. NO is also a pivotal molecule in triggering programmed cell death (PCD) in plants. In this process NO, alone or in synergy with other molecules, affects different peroxidases acting at different levels of the signalling pathways leading to PCD. The relationship between NO and peroxidases involved in cell differentiation and in PCD is reviewed.

Introduction

Nitric oxide (NO) has been widely studied in animal cells for its roles as an intra- and inter-cellular messenger that modulates essential biological processes [1]. Several physio-pathological responses also are regulated by this short-lived, highly reactive gas and by its interaction with other reactive molecules [2]. In the last decade, an increasing body of data indicates that NO also affects plant development. It promotes root elongation and the formation of the shoot-born roots, replaces light in specific photo-morphogenetic processes, is involved in tuberization and gravitropism as well as affecting the senescence pattern of several plant organs [3 and references therein]. NO is also involved in adaptive or defence responses: from stomatal movement [4] to defence against oxidative stress [5, 6] and to phytoalexin synthesis [7]. Interestingly, cross-talk has been reported to occur between NO and the classical five classes of phyto-hormones [3]. In spite of the involvement of NO in such processes being clearly evident, the molecular mechanism through which NO acts is not yet clear. The study of NO effects is complicated by its complex redox chemistry: NO stability depends on its concentration, the redox state of the environment as well as the presence of transition metals and reactive oxygen species (ROS). Depending on these factors, NO has a cyto-protective role, acting as an antioxidant, or it activates the defence responses typically induced under oxidative stress, acting as a pro-oxidant molecule [3]. Moreover, the various NO generators, used for studying the effects of NO, produce different chemical species: the free radical gas ($NO\cdot$), the nitrosium cation (NO^+) or the nitroxyl anion (NO^-) and have different timing of NO production. Consistently, different NO donors have been reported to diversely affect the same metabolic process in both animal and plant cells [8, 9].

The discovery that biosynthetic pathways for NO production are active in plant cells further substantiates its regulatory role in plant metabolism (Table 1). The presence of different biosynthetic routes, the relevance of which varies in different conditions and/or tissues, increases the possibility of modulating NO production. Moreover, the activation of different pathways for NO production could respond to the requirement of synthesising different amounts of NO in order to trigger different physiological or defence responses.

Source of NO	Substrates	Comments	References
Nitric oxide synthase (NOS)	L-arginine; NADPH, oxygen	NO synthesis is the primary activity of the enzyme. The presence of NOS in plants is still under debate.	[11, 12, 13]
Nitrate reductase	NO_2^-; NAD(P)H	NO synthesis requires increased NO_2^- concentration (K_M 100 μM) and low NO_3^- concentration (Ki 50 μM)	[14, 15]
Xanthine oxido-reductase	Xanthine; NO_2^-	The production of NO versus O_2^- synthesis is regulated by O_2 tension. Depending on O_2 tension, peroxyinitrite can also be formed because of the contemporary production of NO and O_2^-.	[16]
Class III peroxidase	H_2O_2, hydroxyurea; N-hydrohyarginine, N-hydrohynitrosamine	Isoenzymes able to utilise specific nitrogen containing substrates as reductant.	[17, 18]
NO_2^- – NO oxido-reductase	NO_2^-, cytochrome C	NO synthesised by a plasma membrane enzymes with kinetic characteristics different from the soluble NO_2^- reductase	[19]
Ascorbate - dependent reduction	NO_2^-, ascorbate, acid environment	The NO_2^- reduction is irrelevant at pH above 4	[20]
light –dependent on enzymatic reduction	NO_2^-,carotenoids	NO synthesis requires acid pH (thylakoidal lumen as putative synthesis site)	[21]
NO_2 conversion to NO by unknown mechanism	NO_2, reducing polysaccharides	NO production has been observed in few species after *in vivo* treatment with NO_2	[22]

Table 1 Enzymatic and non-enzymatic reactions for NO production in plants
The cited references are not exhaustive, for a more detailed description of the pathways see [10]

Consistently, the different isoenzymes of nitric oxide synthase (NOS), characterized in animal cells, differ in their amount and timing of NO production. Endothelial NOS, which is involved in several physiological processes, produces low concentrations of NO over a relatively prolonged period. On the other hand, the inducible NOS generates high amounts of NO and its expression/activation is required for counteracting pathogens and for coordinating T cell response during immune reaction [23].

Much attention has been paid to the capability of NO to alter protein activity and/or structure. Indeed, the presence of thiol or heme groups makes proteins putative NO targets. In animal cells the formation of S-nitrosothiol groups, ferrous-nitrosyl-heme complexes, or the nitration of specific tyrosine residues are part of the signalling pathways triggered by NO [24]. A guanylyl cyclase isoenzyme of smooth muscle is activated by the NO binding to the heme group located in its regulatory domain and the consequent increase of cGMP concentration activates a cGMP-dependent protein kinase [24, 25]. Moreover, NO trans-

nitrolisation and oxidation of specific cysteine residues has been reported to induce conformational changes in trans-membrane calcium channel proteins in neuronal cells [1]. The activities of plant catalase and peroxidases, both heme-containing proteins as well as that of tobacco aconitase, a Rieske iron-sulphur containing protein, are strongly affected by the presence of NO. Furthermore, the impairment of these enzymes has been suggested as one of the mechanism through which NO could affect cell metabolism [26, 27, 28, 29].

1. NO and Peroxidases

Several peroxidase isoenzymes are involved in plant metabolism. They are hemo-proteins catalysing the mono-valent oxidation of different substrates with the concomitant reduction of hydrogen peroxide to water. Depending on their different catalytic properties and their structural relationships, plant peroxidases belong to one of the classes of the peroxidase super-family. Ascorbate peroxidases (APXs) belong to class I, which are ubiquitous in plants and algae, whereas their presence has only been reported in a few cases in other taxonomic groups (the protozoan *Trypanosoma cruzi* [30] and the bovine eye [31]). The APX isoenzymes are characterized by a relatively high specificity for ascorbate as physiological substrate, and are localized in several cellular compartments: chloroplasts [32], mitochondria [33, 34], microbodies [33, 35], cell wall [36] and cytosol [37, 38, 39, 40]. The so-called secretory peroxidases (POD) belong to class III. They are mostly glycoproteins localised in cell walls and vacuoles, and use a wide range of substrates, mainly phenolic molecules, as electron donors for reducing H_2O_2 [41]. From a functional point of view, APX and POD differ greatly, since, in spite of both reducing hydrogen peroxide to water, only APX is a H_2O_2 scavenger. PODs have many different functions in plant metabolism but they are correlated with the oxidation of the reducing substrates more than with H_2O_2 removal. Indeed, PODs utilise H_2O_2 for the oxidative polymerisation of lignin, the formation of cross links between the polysaccharides or proteins present in the cell wall matrix [42] and the oxidation of secondary metabolite precursors [43], even if specific POD isoenzymes could also be related to H_2O_2 level regulation [40].

As previously mentioned, NO affects peroxidase activity, forming a nitroso-ferrous ($Fe(II)NO^+$) complex that subtracts enzymatic intermediates from the catalytic cycle with a Ki in the micromolar range [26, 44]. NO also acts as a competitive inhibitor of POD [45], replacing the reducing substrate and making its activity fruitless, at least as far as the oxidation of the reducing substrate is concerned (Figure 1).

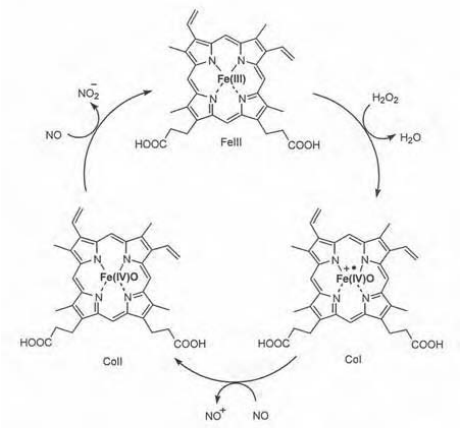

Figure 1. Competitive inhibition of NO on POD activity.

The peroxynitrite, generated in the reaction between nitric oxide and superoxide, is also a POD substrate. The reaction between peroxynitrite and the ferric form of the enzyme, directly produces compound II and the radical $NO_2^{\cdot}$. However, diversely from NO, peroxynitrite does not regenerate the ferric enzyme. The POD catalytic cycle can be completed in the presence of a phenolic electron donor. This suggests that the oxidation of a phenolic antioxidant, such as chlorogenic acid, could be coupled with peroxynitrite removal in the catalytic cycle of POD isoenzymes. In this way, PODs could prevent the oxidative damage induced by peroxynitrite [46].

Apart from being enzymes able to remove NO and its derivates, PODs are also involved in NO biosynthesis. Indeed, POD isoenzymes can oxidise nitrogen-containing molecules giving NO as a by-product of the reaction [47, 48].

A few data are also present in the literature on the effect of NO on APX. An inhibitory effect of NO on APX activity has been obtained by *in vitro* treatment of APX from tobacco leaves and tobacco BY-2 cells with different NO donors [27, de Pinto and De Gara unpublished results]. Such inhibition has been attributed to direct NO binding to the APX heme group. Intriguingly, during *in vivo* experiments performed by treating tobacco BY-2 cultured cells with SNP, a decrease in APX activity is not induced, but there is even a transient increase in its activity during the first hours after the treatment [49]. The different *in vivo* and *in vitro* effects of NO generators also underline that NO concentration and the microenvironment in which it acts are important parameters affecting the reactivity of this molecule.

2. Nitric oxide and Programmed Cell Death

Programmed cell death (PCD) is a genetically orchestrated process of cellular suicide activated by both endogenous stimuli and environmental stresses, both of biotic and abiotic nature. An increasing body of data indicates a central role for NO in the induction of PCD. In particular, the involvement of NO as a pivotal molecule has been extensively studied in the PCD induced by unfavourable environmental conditions. Treatment of cultured *Citrus* cells with NO donors induces cell death that shares similarities with PCD, including chromatin condensation and loss of mitochondrial membrane electrical potential [50].

A lot of data also provide evidence of a key role for NO in the induction of hypersensitive response (HR), a PCD process activated in plant tissues for defence against pathogen attacks [51]. An early event in the signalling pathway leading to HR, is the generation of reactive oxygen species (ROS), which causes an oxidative burst [52]. It has been demonstrated that NO acts synergistically with ROS to strengthen the induction of hypersensitive cell death in soybean and *Arabidopsis* cells [11, 53]. It has also been reported that the generation of ROS alone, at least within a certain range of concentrations, is not sufficient to induce PCD in soybean and tobacco cells. On the other hand, when NO is also produced, in such a concentration that alone does not affect cell viability, a typical PCD is triggered. This suggests that the co-presence of ROS and NO is able to activate metabolic pathways different from those activated by the single reactive species [49, 54]. Consistently, inhibitors of nitric oxide synthesis compromise the HR induced by *Pseudomonas syringae* in *Arabidopsis* leaves [11]. Moreover, tobacco plants, resistant to the infection of *Ralstonia solanacearum*, exhibit high levels of NOS activity. Whereas in plants treated with NOS inhibitors the onset of HR is delayed and, as a consequence, the defence capability weakened [55]. In the infection with tobacco mosaic virus of resistant, but not susceptible, tobacco plants enhanced NOS activity has also been demonstrated [12]. Furthermore, infection of tobacco leaves with virulent pathogens induces a level of

hypersensitive necrosis reduced in transgenic plants over-expressing the cDNA of alfalfa haemoglobin (a NO scavenger protein) compared with the not transformed plants [56].

It is well known that different abiotic stresses, such as ozone exposure, low and high temperatures, mechanical stresses etc., can induce PCD [57, 58, 59, 60]. Several kinds of these abiotic stresses seem to require NO as a pivotal molecule for triggering PCD. Indeed, the mechanical stress in leaves and callus of *Kalanchoe daigremontiana* and *Taxus brevifolia* caused by centrifugation induces NO production which is responsible for the activation of an apoptotic process, as shown by the analysis of the DNA ladder formation. The fact that a decrease in PCD efficiency occurs when cells or leaves are centrifuged in the presence of NMMA, an inhibitor of NOS, indicates that NO is directly or indirectly responsible for the occurrence of PCD [61]. In *Arabidopsis* plants, exposure to ozone induces NOS activity that precedes salicylic acid accumulation and cell death [62]. Alfalfa root cultures exposed to low oxygen tension produce NO and show cellular damage, which are characteristics of PCD. On the other hand, transgenic lines over-expressing haemoglobin have lower NO levels and, when subjected to the same treatment, do not show any cell structure damage [63]. Other abiotic stresses are also able to induce PCD, such as high temperatures, hyper-osmotic stress, and salinity generate a rapid and significant increase in NO levels [64]. Therefore, it is probable that NO production is a general event occurring during stress-induced PCD, even if more experimental evidence is still necessary to define a general correlation between stress-induced PCD and NO.

Recently the involvement of NO as a key factor regulating developmental processes has also been suggested. In particular, Ros Barcelò and his co-workers have demonstrated a tight correlation between NO production and vessel differentiation. In order to study the factors promoting activation of the procambial cells differentiation into vessel, they used both *Zinnia elegans* plantlets and cultured mesophyll cells, in which vessel differentiation had been activated by an opportune culture medium [65]. In the differentiating vascular bundle of *Z. elegans* stems, the histochemical localization of NO, performed by using the NO-fluorescent probe 4,5-diaminofluorescein diacetate, indicates that cells differentiating to both vessels and phloem fibres actively produce NO. A spatial NO gradient is also evident in the vascular bundle, with an inverse correlation between the levels of cell wall lignification (higher in the procambial derivatives located at the bundle periphery) and NO production (higher in the younger differentiating vessels). The production of NO in the vascular bundle also decreases along the stem, from the younger to the more differentiated zones [65]. Trans-differentiating *Z. elegans* mesophyll cells showed a temporal gradient of NO production with the highest production in the still living thin-walled cells, which are differentiating into tracheary elements, and undetectable levels in the tracheary elements, which have almost completed the differentiation process. Removal of NO from the cultured cells with the NO scavenger 2-phenyl-4,4,5,5-tetramethyl imidazoline-1-oxyl-3-oxide (PTIO) causes a reduction in PCD as well as in tracheary element formation [65]. Interestingly, both the procambial derivatives differentiating vessels or fibres and the trans-differentiating mesophyll cells also produce H_2O_2 [66], thus underlying that NO and ROS also act in synergy in developmentally-regulated PCD.

The complexity of NO action is also evident in PCD. In spite of a lot of data supporting an inducing effect of NO on this process, a few data show that NO can also act as an anti-apoptotic modulator, preventing cell death. NO donors delay gibberellin-induced PCD occurring in barley aleurone layers during germination. Such a delay effect is specifically due to NO, since it is blocked by the NO scavenger PTIO [67]. NO also markedly decreases ion leakage and the number of lesions, indicative of cell death, produced upon infection of potato leaves with *Phytophthora infestans* [5]. The delay of gibberellin-induced PCD as well as the prevention of *P. infestans* induced death could be due to the fact that, in these contexts, the NO antioxidant properties prevail over its

capability to activate other metabolic pathways, perhaps due to the absence of other signalling molecules. The antioxidant capability of NO hinders the increase in the levels of ROS required to activate PCD. As previously mentioned, NO has been proved to remove ROS and, as a consequence, it can protect plant tissues from oxidative stress conditions [4, 5].

3. Ascorbate Peroxidase and Nitric oxide in Programmed Cell Death

It has been reported that during PCD, APX is finely regulated. Tobacco leaves inoculated with tobacco mosaic virus (TMV), activate a typical HR aimed to counteract the TMV penetration. During the hypersensitive PCD the activity of APX is suppressed [68]. Consistently, tobacco plants, transformed with antisense technology, with reduced APX are hyper-responsive to TMV attacks [69]. The mechanism of APX regulation seems to be quite complex, as in the TMV infected plants an increase in the expression of the cytosolic APX isoenzyme has been reported, despite the remarkable reduction in its activity being clearly evident [68]. This suggests that the post-transcriptional regulation of cytosolic APX is part of the signalling pathway leading to hypersensitive PCD. In the tobacco BY-2 cells, in which PCD has been induced by heat shock, the suppression of cytosolic APX also occurs as an early step of the process [60]. In this case, the reduction of the activity precedes for several hours the decrease in the amount of APX mRNA induced by the heat shock. The kinetic analysis show a change in the enzyme properties. In control cells, the cytosolic APX has a sigmoidal dependence on ASC concentration, which is indicative of the presence of two ASC-binding sites, as it has been reported in the literature for the same isoenzymes purified from other sources [70]. In contrast, the APX of cells en route to PCD has an hyperbolic dependence on ASC concentration, which is typical of enzymes having only one substrate binding site. These results suggest that the decrease in the APX V_{MAX} arise not only from a decrease in the amount of the enzyme, but also from modification involving substrate – enzyme interaction [60].

As previously mentioned, the fact that APX is a hemeprotein makes it a putative NO target. However, when NO is *in vivo* generated it could also indirectly affect APX by activating different regulatory mechanisms. Indeed, in tobacco BY-2 cells the activity of APX is not affected by the generation of NO (which, alone, does not trigger any PCD, at least in the used concentrations). However, if H_2O_2 is also generated in the culture medium at concentrations which are completely ineffective when it is produced alone, a strong decrease in the activity and in the protein amount of APX precedes the occurrence of PCD [49]. The effect of NO plus H_2O_2 can not be simply attributed to the oxidative environment caused by the interaction between these two reactive species in the cells, because when PCD blockage occurs by treatment with protein synthesis and gene expression inhibitors, the suppression of APX is also reverted (Figure 2). The collected data suggests that the contemporary presence of different reactive chemical species (in this case NO and H_2O_2) induces metabolic responses that are quite different from those induced when only one reactive chemical species is generated.

Also, the effect of NO on APX was reported in *planta*. Treatment of *Arabidopsis* plants with the NO donor SNP induces a reduction of thylacoidal APX (tAPX) transcript accumulation and causes a partial reduction of tAPX enzymatic activity. Such decrease in the chloroplastic ROS scavenging capability determines damages in the leaves. Interestingly, SNP treatment induces a transcript accumulation of a cytosolic isoform of APX, even if the absence of information on the enzyme activity does not allow to verify whether other regulatory mechanism has also be activated (Murgia et al. 2004). *Arabidopsis* lines overexpressing the tAPX gene show reduced damages when treated with SNP instead

of control plants [71]. Consistently, the antisense reduction of tAPX in *Arabidopsis* plants enhances NO-induced cell death and makes the plant more sensitive to paraquat [72].

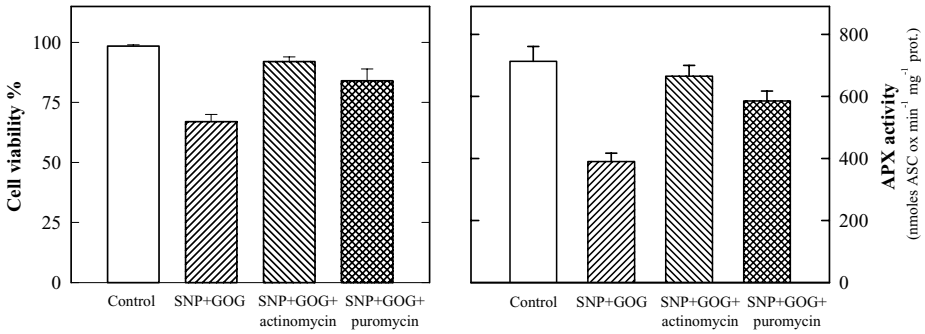

Figure 2. Effect of PCD inhibitors on the decrease in APX activity.
PCD has been induced by sodiumnitroprusside (SNP) and glucose oxidase-glucose (GOG) as reported in [49] and blocked by inhibitors of gene expression and protein synthesis (left panel). The inhibitors of PCD also determines a clear recovery of APX, despite of NO and H_2O_2 presence (right panel). The activity of APX has been assayed as reported in [49] after 5 h of treatment from the induction of PCD

Regulation of the different APX isoenzymes represents a critical point in the responses against oxidative stress. It is interesting to note that many data indicate that an increase in the ROS production, due both to abiotic and to biotic stresses which does not induce PCD, determines an increase in the expression/activity of specific APX isoenzymes or of global cellular APX activity [73, 74, 75, 76]. Since an increase of ROS production also occurs during PCD, it is intriguing to hypothesize that the different behavior of APX could actually occur, due to the activation of NO synthesis by those stimuli able to activate PCD. A long way must still be covered in order to substantiate this hypothesis, in which the use of the same experimental model submitted to different conditions able to activate PCD or to improve the antioxidant defenses will be very useful.

References

[1] Nelson E.J., Connolly J. and McArthur P., "Nitric oxide and S-nitrosylation: excitotoxic and cell signaling mechanism". *Biol. Cell*, vol. 95, p.p. 3-8, 2003.

[2] Chung H.T., Pae H.O., Choi B.M., Billiar T.R. and Kim Y.M., "Nitric oxide as a bioregulator of apoptosis". *Biochem. Bioph. Res. Co.*, vol. 282, p.p. 1075-1079, 2001.

[3] Lamattina L., Garcia-Mata C., Graziano M., and Pagnussat G., "Nitric oxide: the versatility of an extensive signal molecule". *Annu. Rev. Plant Biol.*, vol. 54, p.p. 109-136, 2003.

[4] Mata C.G. and Lamattina L., "Nitric oxide induces stomatal closure and enhances the adaptive plant responses against drought stress". *Plant Physiol.*, vol. 126, p.p. 1196-1204, 2001.

[5] Beligni M.V. and Lamattina L., "Nitric oxide counteract cytotoxic processes mediated by reactive oxygen species in plant tissues". *Planta*, vol. 208, p.p. 337-344, 1999.

[6] Hsu Y.T. and Kao C.H., "Cadmium toxicity is reduced by nitric oxide in rice leaves". *Plant Growth Reg.* , vol. 42, p.p. 227-238, 2004.

[7] Noritake T., Kawaikita K. and Doke N., "Nitric oxide induces phytoalexin accumulation in potato tuber tissues". *Plant Cell Physiol.*, vol. 37, p.p. 113-116, 1996.

[8] Wink D.A., Cook J.A., Pacelli R., DeGraff W., Gamson J., Liebmann J., Krishna M.A. and Mitchell J.B., "The effect of various nitric oxide-donor agents on hydrogen peroxide-mediated toxicity: a direct

correlation between nitric oxide formation and protection". *Arch. Biochem. Biophys.*, vol. 331, p.p. 241-248, 1996.

[9] Murgia I., de Pinto M.C., Delledonne M., Soave C. and De Gara L., "Comparative effects of various nitric oxide donors on ferritin regulation, programmed cell death, and cell redox state in plant cells". *J. Plant Physiol.*, vol. 161, p.p. 777-783, 2004.

[10] Neill S.J., Desikan R. and Hancock J.T., "Nitric oxide signalling in plants". *New Phytol.* 159, p.p. 11-35, 2003.

[11] Delledonne M., Xia Y., Dixon R.A. and Lamb C., "Nitric oxide functions as a signal in plant disease resistance". *Nature*, vol. 394, p.p. 585-588, 1998.

[12] Durner J., Wendehenne D. and Klessig D.F., "Defense gene induction in tobacco by nitric oxide, cyclic GMP, and cyclic ADP-ribose". *Proc. Natl. Acad. Sci. USA*, vol. 95, p.p. 10328-10333, 1998.

[13] Chandok M.R., Ytterberg A.J., van Wijk K.J. and Klessig D.F., "The pathogen-inducible nitric oxide synthase (iNOS) in plants is a variant of the P protein of the glycine decarboxylase complex". *Cell*, vol. 13, p.p. 469-482, 2003.

[14] Yamasaki H., Sakihama Y. and Takahashi S., "An alternative pathway for nitric oxide production in plants: new features of an old enzyme". *Trends Plant Sci.*, vol. 4, p.p. 128-129, 1999.

[15] Morot-Gaudry-Talarmain Y., Rockel P., Moureaux T., Quillere I., Leydecker M.T., Kaiser W.M. and Morot-Gaudry J.F., "Nitrite accumulation and nitric oxide emission in relation to cellular signaling in nitrite reductase antisense tobacco". *Planta*, vol. 215, p.p. 708-715, 2002.

[16] Harrison R., "Structure and function of xanthine oxidoreductase: Where are we now?". *Free Radical Biol. Med.*, vol. 33, p.p. 774-797, 2002.

[17] Boucher J.L., Genet A., Vadon S., Delaforge M. and Mansuy D., "Formation of nitrogen-oxides and citrulline upon oxidation of n-omega-hydroxy-l-arginine by hemeproteins". *Biochem. Bioph. Res. Co.*, vol. 184, p.p. 1158-1164, 1992.

[18] Huang J.M., Sommers E.M., Kim-Shapiro D.B. and King S.B., "Horseradish peroxidase catalyzed nitric oxide formation from hydroxyurea". *J. Am. Chem. Soc.*, vol. 124, p.p. 3473-3480, 2002.

[19] Stohr C., Strube F., Marx G., Ullrich W.R. and Rockel P., "A plasma membrane-bound enzyme of tobacco roots catalyses the formation of nitric oxide from nitrite". *Planta*, vol. 212, p.p. 835-841, 2001.

[20] Bethke P.C., Badger M.R. and Jones R.L. "Apoplastic synthesis of nitric oxide by plant tissues". P*lant Cell*, vol. 16, p.p. 332-341, 2004.

[21] Cooney R.V., Harwood P.J., Custer L.J. and Franke A.A., "Light-mediated conversion of nitrogen-dioxide to nitric-oxide by carotenoids". *Environ. Health Persp.*, vol. 102, p.p. 460-462, 1994.

[22] Nishimura H., Hayamizu T. and Yanagisawa Y., "Reduction of NO_2 to NO by Rush and other plants". *Environm. Sci. Technol*., vol. 20, p.p. 413-416, 1986.

[23] Crane B.R., Arvai A.S., Ghosh D.K., Wu C., Getzoff E.D., Stuehr D.J. and Tainer J.A., "Structure of nitric oxide synthase oxygenase dimer with pterin and substrate". *Science*, vol. 279, p.p. 2121–2125., 1998

[24] Hofmann F., Ammendola A. and Schlossmann J., "Rising behind NO: cGMP-dependent protein kinases". *J. Cell Sci*., vol. 113, p.p. 1671-1676, 2000.

[25] Lucas K.A., Pitari G.M., Kazerounian S., Ruiz-Stewart I., Park J., Schulz S., Chepenik K.P. and Waldman S.A., "Guanylyl cyclases and signalling by cyclic GMP". *Pharmacol. Rev.*, vol. 52, p.p. 375-414, 2000.

[26] Ferrer M.A. and Barcelo A.R., "Differential effects of nitric oxide on peroxidase and H_2O_2 production by the xylem of *Zinnia elegans*". *Plant Cell Environ.*, vol. 22, p.p. 891-897, 1999.

[27] Clark D., Durner J., Navarre D.A. and Klessig D.F., "Nitric oxide inhibition of tobacco catalase and ascorbate peroxidase". *Mol. Plant Microbe Interact.*, vol. 13, p.p. 1380-1384, 2000.

[28] Navarre D.A., Wendehenne D., Durner J., Noad R. and Klessig D.F., "Nitric oxide modulates the activity of tobacco aconitase". *Plant Physiol.*, vol. 122, p.p. 573-582, 2000.

[29] Ros Barcelò A. Pomar F., Ferrer M.A., Martinez P., Ballesta M.C. and Pedreno M.A., "In situ characterization of a NO-sensitive peroxidase in the lignifying xylem of *Zinnia elegans*". *Physiol Plant.*, vol. 114, p.p. 33-40, 2002.

[30] Boveris A.H., Sies H., Martino E.E., Decampo R., Turreus J.F. and Stoppani A.O.M., "Deficient metabolic utilization of hydrogen peroxide in *Trypanosoma cruzi*". *Biochem. J.*, vol. 188, p.p. 643-648, 1980.

[31] Wada N., Kinoshita S., Matsuo M., Amako K., Miyake C. and Asada K., "Purification and molecular properties of ascorbate peroxidase from bovine eye". *Biochem. Bioph. Res. Co.*, vol. 242, p.p. 256-261, 1998.

[32] Jespersen H.M., Kjaersgard I.V.H., Østergaard L. and Welinder K.G., "From sequence analysis of three novel ascorbate peroxidases from *Arabidopsis thaliana* to structure, function and evolution of seven types of ascorbate peroxidase". *Biochem. J.*, vol. 326, p.p. 305-310, 1997.

[33] Jiménez A., Hernández J.A., Pastori G., Del Rio L.A. and Sevilla F., "Role of the ascorbate-glutathione cycle of mitochondria and peroxisomes in the senescence of pea leaves". *Plant Physiol*., vol. 118, p.p. 1327-1335, 1998.

[34] De Leonardis S., Dipierro N. and Dipierro S., "Purification and characterization of an ascorbate peroxidase from potato tuber mitochondria". *Plant Physiol. Biochem.*, vol. 38, p.p. 773-779, 2000.

[35] Zhang H., Wang J., Nickel U., Allen R.D. and Goodman H.M., "Cloning and expression of an *Arabidopsis* gene encoding a putative peroxisomal ascorbate peroxidase". *Plant Mol. Biol.* 34, p.p. 967- 971, 1997.

[36] de Pinto M.C. and De Gara L., "Changes in the ascorbate metabolism of apoplastic and symplastic spaces are associated with cell differentiation". *J. Exp. Bot.*, vol. 55, p.p. 2559-2569, 2004.

[37] Kubo A., Saji H., Tanaka K. and Kondo N., "Genomic DNA structure of a gene encoding cytosolic ascorbate peroxidase from *Arabidopsis thaliana*". *FEBS Lett.*, vol. 315, p.p. 313 – 317, 1993.

[38] Shigeoka S., Ishikawa T., Tamoi M., Miyagawa Y., Takeda T., Yabuta Y. and Yoshimura K., "Regulation and function of ascorbate peroxidase isoenzymes". *J. Exp. Bot*., vol. 53, p.p. 1305-1319, 2002.

[39] De Gara L., "Ascorbate metabolism and plant growth – from germination to cell death". In: Asard H., May J., Smirnoff N. eds. Vitamin C: Its unction and biochemistry in animals and plants. Oxford: BIOS Scientific Publisher Ltd., p.p. 83-95. 2003.

[40] De Gara L., "Class III peroxidases and ascorbate metabolism in plants". *Phytochem. Rev*., vol. 3, p.p. 195-205. 2004.

[41] Ros Barcelò A., Pomar F., Lopez-Serrano M. and Pedreno M.A., "Peroxidase: a multifunctional enzyme in grapevines peroxidase: a multifunctional enzyme in grapevines". *Funct. Plant Biol.*, vol. 30, p.p. 577-591, 2003.

[42] Ros Barcelò A., "Lignification in plant cell walls". *Int. Rev. Cytol.*, vol. 176, p.p. 87-132, 1997.

[43] Sottomayor M. and Barcelò A.R. (2003) Peroxidase from Catharanthus roseus (L.) G. Don and the biosynthesis of alpha-3 ',4 '-anhydrovinblastine: a specific role for a multifunctional enzyme *Protoplasma*, vol. 222, p.p. 97-105.

[44] Ischiropoulos H., Nelson J., Duran D. and AlMehdi A., "Reactions of nitric oxide and peroxynitrite with organic molecules and ferrihorseradish peroxidase: Interference with the determination of hydrogen peroxide". *Free Radical Bio. Med.*, vol. 20, p.p. 373-381, 1996.

[45] Gabaldon C., "Produccion de oxido nitrico por el xilema de Zinnia elegans y su relacion con la muerte cellular programada y la lignificacion. PhD Thesis Universidad de Murcia, 2004.

[46] Grace S.C., Salgo M. and Prior W.A., "Scavenging of peroxynitrite by a phenolic peroxidase system prevents oxidative damage to DNA". *FEBS Lett.*, vol. 426, p.p. 24-28, 1998.

[47] Xian M., Li X., Tang X., Chen X., Zheng Z., Galligan J.J., Kreulen D.L. and Wang P.G., "N-hydroxy derivatives of guanidine based drugs as enzymatic NO donors". *Bioorg. Med. Chem. Lett.*, vol. 11, p.p. 2377-2380, 2001.

[48] Cai T., Xian M. and Wang P.G., "Electrochemical and peroxidase oxidation study of N'-hydroxiguanidine derivates as NO donors". *Bioorg. Med. Chem. Lett.*, vol. 12, p.p. 1507-1510, 2002.

[49] de Pinto M.C., Tomsasi F. and De Gara L., "Changes in the antioxidant systems as part of the signaling pathway responsible for the programmed cell death activated by nitric oxide and reactive oxygen species in tobacco bright-yellow 2 cells". *Plant Physiol.*, vol. 130, p.p. 698-708, 2002.

[50] Saviani E.E., Orsi C.H., Oliveira J.F.P., Pinto-Maglio C.A.F. and Salgado I., "Participation of the mitochondrial permeability transition pore in nitric oxide-induced plant cell death". *FEBS Lett.*, vol. 510, p.p. 136-140, 2002.

[51] De Gara L., de Pinto M.C. and Tommasi F., "The antioxidant systems vis-a-vis reactive oxygen species during plant-pathogen interaction". *Plant Physiol. Biochem.*, vol. 41, p.p. 863-870, 2003.

[52] Lamb C. and Dixon R.A., "The oxidative burst in plant disease resistance". *Annu. Rev. Plant Physiol. Plant Mol. Biol.*, vol. 48, p.p. 251-275, 1997.

[53] Clarke A., Desikan R., Hurst R.D., Hancock J.T. and Neill S.J., "NO way back: nitric oxide and programmed cell death in *Arabidopsis thaliana* suspension cultures". *Plant J.*, vol. 24, p.p. 667-677, 2000.

[54] Delledonne M., Zeier J., Marocco A. and Lamb C., "Signal interactions between nitric oxide and reactive oxygen intermediates in the plant hypersensitive disease resistance response". *Proc. Natl. Acad. Sci. USA*, vol. 98, p.p. 13454-13459, 2001.

[55] Huang J.S. and Knopp J.A., "Involvement of nitric oxide in *Ralstonia solanacearum*-induced hypersensitive reaction in tobacco". In: Prior P., Elphinstone J., Allen C., eds. Bacterial Wilt disease: molecular and ecological aspects. Berlin: INRA and Springer Editions, p.p. 218–224, 1998.

[56] Seregélyes C., Barna B., Hennig J., Konopka D., Pasternak T.P., Lukacs N., Fehér A., Horvath G.V. and Dudits D., "Phytoglobins can interfere with nitric oxide functions during plant growth and pathogenic responses: a transgenic approach". *Plant Sci*., vol. 165, p.p. 541-550, 2003.

[57] Langebartels C., Wohlgemuth H., Kschieschan S., Grun S. and Sandermann H., "Oxidative burst and cell death in ozone-exposed plants". *Plant Physiol. Bioch.*, vol. 40, p.p. 567-575, 2002.

[58] Koukalova B., Kovarik A., Fajkus J. and Siroky J., "Chromatin fragmentation associated with apoptotic changes in tobacco cells exposed to cold stress". *FEBS Lett.*, vol. 414, p.p. 289-292, 1997.

[59] McCabe P.F., Leaver C.J., "Programmed cell death in cell cultures". *Plant Mol. Biol.*, vol. 44, p.p. 359-368, 2000.

[60] Vacca R.A., de Pinto M.C., Valenti D., Passarella S., Marra E. and De Gara L., "Production of reactive oxygen species, alteration of cytosolic ascorbate peroxidase, and impairment of mitochondrial metabolism are early events in heat shock-induced programmed cell death in tobacco bright-yellow 2 cells". *Plant Physiol.*, vol. 134, p.p. 1100-1112, 2004.

[61] Pedroso M.C., Magalhaes J.R. and Durzan D., "A nitric oxide burst precedes apoptosis in angiosperm and gymnosperm callus cells and foliar tissues". *J. Exp. Bot.*, vol. 51, p.p. 1027-1036, 2000.

[62] Rao M.V. and Davis K.R., "The physiology of ozone induced cell death". *Planta*, vol. 213, p.p. 682-690. 2001.

[63] Dordas C., Hasinoff B.B., Igamberdiev A.U., Manac´h N., Rivoal J. and Hill R.D,. "Expression of a stress-induced haemoglobin affects NO levels produced by alfalfa root cultures under hypoxic stress". *Plant J.*, vol. 35, p.p. 763-770, 2003.

[64] Gould K., Lamotte O., Klinguer A., Pugin A. and Wendehenne D., "Nitric oxide production in tobacco leaf cells: a generalised stress response?". *Plant Cell Environ.*, vol. 26, p.p. 1851-1862, 2003.

[65] Gabaldon C., Ros L.V.G., Pedreno M.A. and Ros Barcelò A., "Nitric oxide production by the differentiating xylem of Zinnia elegans". *New Phytol.*, vol. 165, p.p. 121-130, 2005.

[66] Ros Barcelò A., "Xylem parenchyma cells deliver the H_2O_2 necessary for lignification in differentiating xylem vessels". *Planta*, vol. 220, p.p. 747–756, 2005.

[67] Beligni M.V., Fath A., Bethke PC., Lamattina L. and Jones R.L., "Nitric oxide acts as an antioxidant and delays programmed cell death in barley aleurone layers". *Plant Physiol.*, vol. 129, p.p. 1642-1650, 2002.

[68] Mittler R., Feng X. and Cohen M., "Post-transcriptional suppression of cytosolic ascorbate peroxidase expression during pathogen-induced programmed cell death in tobacco"{. *Plant Cell*, vol. 10, p.p. 461-473, 1998.

[69] Mittler R., Herr E.H., Orvar B.L., Van Camp W., Willekens H., Inzé D. and Ellis B.E., "Transgenic tobacco plants with reduced capability to detoxify reactive oxygen intermediates are hyperresponsive to pathogen infection". *Proc. Natl. Acad. Sci USA*, vol. 96, p.p. 14165-14170, 1999.

[70] Lad L., Mewies M. and Raven E.L., "Substrate binding and catalytic mechanism in ascorbate peroxidase: Evidence for two ascorbate binding sites". *Biochemistry*, vol. 41, p.p. 13774-13781, 2002.

[71] Murgia I., Tarantino D., Vannini C., Bracale M., Carravieri S. and Soave C., "*Arabidopsis thaliana* plants overexpressing thylakoidal ascorbate peroxidase show increased resistance to Paraquat-induced photooxidative stress and to nitric oxide-induced cell death". *Plant J.*, vol. 38, p.p. 940-953, 2004.

[72] Tarantino D., Vannini C., Bracale M., Campa M., Soave C. and Murgia I., "Antisense reduction of thylakoidal ascorbate peroxidase in *Arabidopsis* enhances Paraquat-induced photooxidative stress and Nitric Oxide-induced cell death. *Planta* In press. On line:DOI: 10.1007/s00425-005-1485-9, 2005.

[73] Di Cagno R., Guidi L., De Gara L. and Soldatini G.F., "Combined cadmium and ozone treatments affects photosynthesis and ascorbate-dependent defences in sunflower". *New Phytol.*, vol. 151, p.p. 627-636, 2001.

[74] Hernandez J.A., Ferrer M.A., Jimenez A., Barcelo A.R. and Sevilla F., "Antioxidant systems and $O_2(^{\cdot})$/H_2O_2 production in the apoplast of pea leaves. Its relation with salt-induced necrotic lesions in minor veins". *Plant Physiol.*, vol. 126, p.p. 817-831, 2001.

[75] Yoshimura K., Yabuta Y., Ishikawa T. and Shigeoka S., "Expression of spinach ascorbate peroxidase isoenzymes in response to oxidative stress". *Plant Physiol.*, vol. 123, p.p. 223-233, 2000.

[76] Mittler R., "Oxidative stress, antioxidants and stress tolerance". *Trends Plant Sci*., vol. 7, p.p. 405-410, 2002.

Cell Biology and Instrumentation: UV Radiation, Nitric Oxide and Cell Death in Plants
Y. Blume et al. (Eds.)
IOS Press, 2006

Plant Hemoglobins and Nitric Oxide in Acclimation to Hypoxic Stress

Christos DORDAS[1] and Robert D. HILL[2]
[1]*Laboratory of Agronomy, School of Agriculture, Aristotle University of Thessaloniki, 54124 Thessaloniki, Greece.*
[2]*Department of Plant Science, University of Manitoba, Winnipeg, MB R3T 2N2, Canada*

Abstract. Nitric oxide is a reactive gas involved in many biological processes of animals, plants and microbes. NO was found to be formed under hypoxia in plant tissues and it was demonstrated that NO reacts with class-1 plant hemoglobins. In this review we will discuss the recent findings about NO and its reaction with Hb in plants. Hb expression in plant tissue results in the maintenance of redox and energy status during hypoxic stress resulting in reduced production of ethanol and lactic acid. Hemoglobin acts as a NO-dioxygenase to convert NO back to nitrate consuming 2 ½ moles of NAD(P)H per mole of nitrate recycled during the reaction. The modulation of NO within the cell due to hemoglobin expression may influence root aerenchyma formation, a plant mechanism to avoid hypoxia.

Introduction

Nitric oxide (NO) is a molecule found in all biological systems (microorganisms, animals and plants). In animals it is involved in many biological processes, including the central nervous, cardiovascular and immune systems; in platelet inhibition and programmed cell death (apoptosis), in host responses to infection and many others [1-5]. Its biological significance was recognized by Science magazine in 1992 in designating it the "Molecule of the Year". Moreover, the Nobel Prize for Medicine in 1998 was awarded to three scientists who discovered that NO is a biological mediator produced by mammalian cells.

In spite of the recognition of the importance of NO in other biological systems, the significance of NO in plants has only been apparent for the last 6 years [6, 7]. Today, NO is believed to be involved in seed germination, root organogenesis, stomatal movement, senescence and programmed cell death (apoptosis), cell wall lignification, nodule metabolism, chlorophyll biosysnthesis, photophosphorylation, cytochrome c oxidase, alternative oxidase, catalase regulation, aconitase modulation, protein nitration, ferritin (iron homeostasis), hemoglobins, reactive oxygen species (ROS), GSH, hormone signal transduction, hypersensitive response, systemic acquired resistance, wounding, salinity, high temperature, drought, hypoxia [8]. In this review, we will discuss the recent findings concerning NO production under hypoxia and its reaction with plant class 1 hemoglobins. We will also discuss how NO is formed and its significance for the survival of plants in limited oxygen environments. Finally we will present a model to explain how NO and Hb interact in plants under hypoxic stress.

1. NO formation under hypoxia.

Nitric oxide was found to be produced in relatively large amounts in maize suspension cell

cultures and also in alfalfa roots cultures grown under hypoxic conditions [9-11]. The levels of NO, based on results for Hb-underexpressing maize cells, is about 0,4 nmol/g fresh weight/min [10]. This is lower than the 1.0-1.5 nmol/g fresh weight/min found upon bacterial treatment of *Arabidopsis* cell suspension cultures [12], but within the range where the NO effect on plant tissue might be similar. Since plant cell have the ability to scavenge amounts of NO as high as 4-5 μmol NO g^{-1} fresh weight min^{-1} [11], the measurements of NO formation *in situ* are probably an underestimation of the actual amount of NO that is produced by plant cells. An effective system to break down NO in plant tissue possible through its reaction with Hb has been postulated [13].

In plants there are two main pathways of NO formation. One is through nitric oxide synthase (NOS) and the other through nitrate reductase (NR). In animals and microorganisms NO synthase is the main source of NO formation. NOS catalyzes the oxygen and NADPH-dependent oxidation of L-arginine to NO and citrulline in a reaction requiring FAD, FMN, tetrahydrobiopterin (BH_4), calcium and calmodulin [14]. NO synthase (NOS) has been detected in plants [15, 16]. NO generation by NOS may be limited under hypoxic conditions by its requirement for oxygen and L-arginine. The NOS K_m for oxygen can, however, be as low as 5 μM [17]. Recently, a modified version of the P-protein of the glycine decarboxylase complex has been shown to have NO synthase activity [18]. However, the activity is low and possibly present only in green tissue, where glycine decarboxylase is abundant [19]. Another NO synthase involved in hormonal signaling has also been found which does not have any similarity to the mammalian isoform [20].

Nitrate reductase is another potential contributor to nitric oxide production [21], and is also activated during hypoxia [22]. Moreover nitrate was found to provide protection to a number of higher plants under hypoxia [23, 24]. Another advantage that nitrate reductase has compared with the NOS is that does not required oxygen for the reaction which consumes two moles of NAD(P)H per mole of NO formed. Another evidence that NO comes from NO_3^- and possibly through the nitrate reductase is the absence of NO production in hypoxic maize cell suspension cultures utilizing NH_4^+ in place of NO_3^- as the nitrogen source and the evidence that ^{15}NO is produced from $^{15}NO_3^-$ under the same conditions [10].

NO can also be formed in acidic and reducing environment by non-enzymatic reduction of nitrite to nitrous acid, which reacts with ascorbate producing dehydroascorbate and NO [25]. In aleurone layers, NO is formed non-enzymatically [26]. Furthermore, xanthine oxidoreductase (an enzyme located in peroxisomes) has been reported to produce NO [27].

Nitric oxide (NO) is an extremely reactive molecule, interacting with many biological molecules including hemoglobins. Plant class 1 hemoglobins are amongst this group [9-11]. In the following section, we will present the properties and chemistry of the plant hemoglobins to put in perspective the interaction of class 1 hemoglobins with NO and their function in metabolism to assist in the survival of plants under hypoxic environments.

2. Plant Hemoglobins

Hemoglobins are present in all organisms from animals to bacteria [28]. Currently, there are at least three distinct types of hemoglobins found in plants. These three types are the symbiotic, nonsymbiotic and truncated hemoglobins. Symbiotic hemoglobins (or leghemoglobins) are the most well known of the plant hemoglobins as they are the first hemoglobins found in plants. They are present mainly in nodules of plants capable of symbiotic nitrogen fixation. The function of the symbiotic hemoglobins is to regulate

oxygen supply to nitrogen-fixing bacteria [29]. The other type of hemoglobins, the nonsymbiotic hemoglobins, are not found in the nodules and also are not involved in symbiotic nitrogen fixation. They are found throughout the plant kingdom, and also in plants capable of symbiosis. Another difference between symbiotic hemoglobins and nonsymbiotic hemoglobins is that nonsymbiotic hemoglobins are experessed in almost all plant organs such as seed, root and stem tissue of both dicot and monocot plants [13, 30]. Recently it was found another type of hemoglobins the truncated hemoglobins which are probably found in all plant species and they share some of the characteristics and properties of the nonsymbiotic hemoglobins [31]. However the different origins, biochemistry and tertiary structure of the truncated plant hemoglobins indicates that these proteins may have separate cellular roles.

The nonsymbiotic hemoglobins are divided in two different classes the class 1 hemoglobins have very high affinity for oxygen and the class 2 hemoglobins have similar oxygen binding properties to symbiotic hemoglobins. Class 1 hemoglobins are induced by hypoxic stress, reduction in ATP and oversupply of some nutrients (NO_3^-) [13].

Class 1 hemoglobins are probably evolutionary predecessors of symbiotic hemoglobins together with the fact that they are found throughout the plant kingdom (more than 33 plant hemoglobins have been found in more than 20 species) suggests that stress-induced hemoglobins have most likely an important role in the metabolism of plants. Despite the fact that stress-induced hemoglobins are present throughout in the plant kingdom, their function is unknown.

3. Biochemistry of stress-induced hemoglobins

Hemoglobins have a heme domain and the ability to react with gases such as CO, O_2 and NO. The most well studied reaction of hemoglobin is with O_2. Different hemoglobins have different rate at which they bind and release oxygen, and this property is very important in defining its function in the cell. For the stress induced hemoglobins and especially the barley hemoglobin the kinetics of oxygen association is quite close with myoglobin and about an order of magnitude lower than that of leghemoglobin [32]. However the rate of release of oxygen from barley oxyhemoglobin is extremely slow, which means that the equilibrium dissociation constant of the complex is about 3 nM. This property (low dissociation constant) is very important in defining its cellular function as these hemoglobins will be remain oxygenated at very low oxygen concentration and will not be able to serve as an oxygen carrier, store or sensor [30].

Stress induced barley hemoglobin absorbs in the 400 nm region (Soret band) and also in the 500-600 nm region [32]. The spectral properties of the α and β region indicate that the preferred orientation of the ferrous and ferric forms is low spin 6-coordinate and not 5-coordinate. A molecule such as oxygen or NO will react with the 5-coordinate species of the hemoglobin which suggests that the rate of formation of the 5-coordinate form may be rate-limiting. From the kinetics of the reaction of Hb with oxygen agrees with this hypothesis [32].

In many systems such as animals and microorganisms the function of hemoglobin is closely related with the reaction and function with NO. In red blood cells hemoglobin reacts with NO forming NO complexes in the lung, following the complex is transported to distant capillaries where NO is released and causes the expansion of the capillaries through the activation of guanylate cyclase [5, 33, 35]. The expansion of the capillaries facilitates the oxygen delivery in the tissue. *Ascaris* is a parasitic intestinal nematode which has a hemoglobin with similar binding characteristics with barley stress induced hemoglobin. It has been proposed that *Ascaris* hemoglobin may function as a 'deoxygenase' reducing the

levels of oxygen (which is toxic for *Ascaris*) using the reaction with nitric oxide [36]. In microorganisma such as bacteria and yeast flavohemoglobin is found to act also as dioxygenases, which breaks down toxic NO to protect the organism from the toxic concentrations of NO [37]. All the above evidence that the function of Hb is closely related with the function of NO led us to study the formation of NO under hypoxic conditions and the interaction between NO and stress induced hemoglobins.

4. Mechanism of action of NO and plant hemoglobins in maintaining root growth under hypoxic stress

Plants that are exposed to hypoxic stress very rapidly lose a significant part of their ATP. In order to maintain the ATP synthesis they have to find an electron acceptor other than oxygen. Production of ethanol and lactic acid is one of the pathways to provide glycolytic substrate oxidation and ATP synthesis maintaining short term cell viability under hypoxic conditions. However there is evidence that stress-induced hemoglobin with high affinity for oxygen and nitric oxide is a second process regenerating NAD^+ through a reaction involving NO and Hb [9].

Plant hemoglobin was shown to react with NO *in vitro* [10]. Maize recombinant HbO_2 reacted with NO to form NO_3^- and HbFeIII. The characteristic signal for the complex was not evident in aerobic systems, even though hemoglobin is present. Furthermore, using either NO traps or an NO electrode, it was shown that significant amounts of NO are formed in hypoxic maize cells and in alfalfa root cultures during the first 24 hours of hypoxic treatment [9, 10, 13]. Transformed lines with reduced stress-induced hemoglobin expression produced greater amounts of NO than wild type or overexpressing-hemoglobin lines, suggesting that hemoglobin may be involved in turnover of the NO. It is possible from the above evidence that stress-induced hemoglobins function as dioxygenases, detoxifying NO produced during hypoxia.

Another important issue is why NO is formed under hypoxic conditions. One possibility is that NO is used as a product in a series of reactions to assist in the regeneration of NAD^+ to maintain glycolysis under hypoxic conditions, as an alternative to the use of alcohol dehydrogenase. In bacteria, nitrate has been shown to act as a terminal electron acceptor in the denitrification process in flooded soils and has been suggested to play a similar role in plants [38]. Moreover it has been suggested that stress-induced hemoglobins are implicated in regeneration of NAD^+ during hypoxia [9, 30]. The evidence for the implication of stress-induced hemoglobins on the regeneration of NAD^+ comes from that fact that alcohol dehydrogenase activity and CO_2 production are reduced under hypoxia in maize cells constitutively expressing barley hemoglobin (Sowa et al. 1998). Also lines overexpressing Hb maintain root growth under hypoxia and ATP levels and they have higher levels of NAD(P) [10, 11, 13]. Moreover stress-induced hemoglobin in *Arabidopsis* is induced in the presence of elevated nitrate [40] which indicates that the hemoglobin is used to modulate NO levels.

Figure 1 outlines a metabolic scheme showing how stress induced hemoglobin is induced and how NO is formed under hypoxia and also the reactions involving both NO and hemoglobin leading to the regeneration of NAD^+ under hypoxia in plant cells. Some aspects of the arguments favoring this scheme have been presented [41]. There are two known routes, nitric oxide synthase [15, 43, 44], and nitrate reductase [21, 45], for formation of NO in plants. While both pathways consume reduced pyridine nucleotide in the reactions, formation via nitrate reductase appears to be the more favoured route for the following reasons. Nitric oxide synthase consumes 1.5 moles of NADPH per mole of NO produced, but it also consumes 2 moles of oxygen in the process. Nitrate reductase

consumes 2 moles of NADH, without oxygen consumption, per mole of NO. Furthermore, nitrate reductase is activated upon exposure of plant roots to hypoxia [46] and nitrate assimilation during anoxia is blocked at the nitrite reductase step [47].

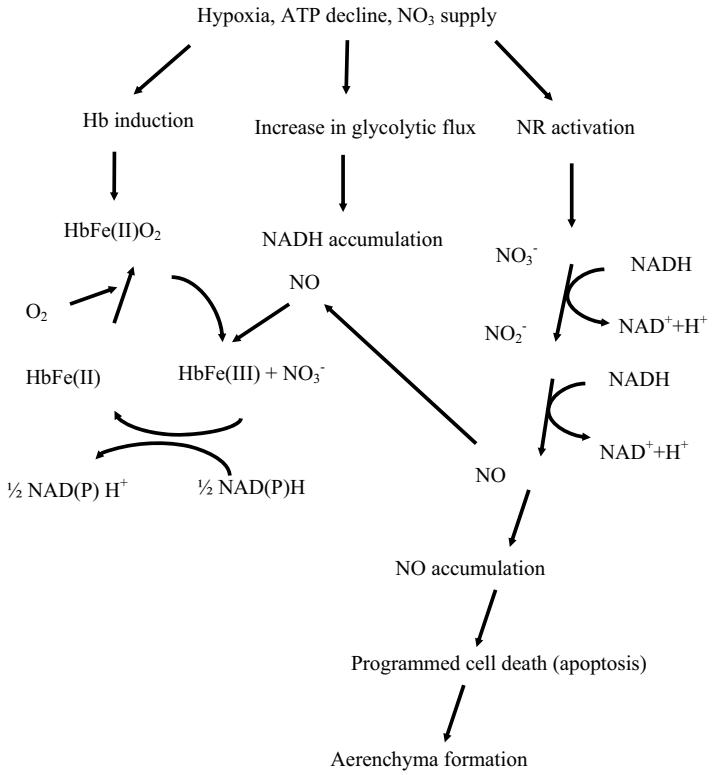

Figure 1. Suggested pathways by which nitric oxide formation and its interaction with hemoglobin may be involved in adaptation to hypoxic stress.

NO is highly reactive and toxic to the cells. In order for the cell to survive it is required to have a detoxification mechanism. The reaction of NO with hemoglobin is considered to be a major route for detoxification [48]. NO reacts rapidly with oxyhemoglobin forming nitrate and methemoglobin [Hb(Fe^{+3})] [49]. This route for metabolism of NO, with nitrate being recycled, would be advantageous to the hypoxic plant cell, exposed to conditions of prolonged soil waterlogging where nitrates would be severely depleted [50]. Following hemoglobins (Fe^{+3}) can be reduced to hemoglobins (Fe^{+2}) via NADH dependent reductases [51, 52]. An NADH-dependent reductase in hypoxic plant cells would provide an additional NAD^+ for glycolysis. Moreover NO and hemoglobins may be involved in other reactions than the metabolic regeneration of NAD^+ as bacterial flavohemoglobins oxidize NO to nitrate aerobically and reduce it to nitrous oxide anaerobically [52]. Flavohemoglobins, unlike hemoglobins, contain a ferredoxin-$NADP^+$ reductase-like domain in addition to a hemeprotein domain. Thus, any similar reactions of class 1 hemoglobins with NO would require interaction with some other protein in the cell

to convert methemoglobin formed to hemoglobin. Several proteins could serve this function, amongst them lipoamide dehydrogenase [41].

The levels of NO under low oxygen tension in the various cell cultures were inversely related to the hemoglobin content. NO reacts rapidly with oxyhemoglobin forming nitrate and methemoglobin [49], a reaction that also occurs with class 1 hemoglobins. We have evidence of an NO dioxygenase-like activity in alfalfa root cultures [11] that may be responsible for the catalysis of this reaction.

5. Nitric oxide and aerenchyma formation

The subject of NO in relation to plant biology is rapidly expanding and there are other areas relative to its involvement in plant anaerobiosis that warrant further investigation, in addition to its interactions with hemoglobins. One of these is the question of aerenchyma formation. Aerenchyma is the spaces, which are formed from selective cell death in the cortical area of the root, allowing the supply of air to the roots from the shoots. This is the major mechanism by which plants avoid hypoxic stress. Ethylene has been shown to be associated with aerenchyma formation in hypoxic maize roots [53-55]. This relationship has remained tenuous because the observation has been restricted to maize [56] and other stresses (eg N and P deficiency) can also cause aerenchyma formation. In some cases there is no need for an increase in ethylene production but only an increase in sensitivity to ethylene [57, 58]. NO is an attractive candidate for involvement in aerenchyma formation. Hypoxic alfalfa roots underexpressing Hb showed aerenchyma formation [9]. In contrast, alfalfa lines overexpressing Hb do not show formation of aerenchyma under hypoxic stress. Transgenic maize cell suspension cultures under-expressing class 1 hemoglobins produce up to six fold higher levels of ethylene than cells over-expressing the gene (Monac'h et al. 2005, Manuscript submitted). With the evidence in both maize and alfalfa systems that class 1 Hb modulates NO levels, this would suggest a relationship between NO and ethylene formation. Furthermore, if differential expression of class 1 Hb occurred in hypoxic root cells, it could be a possible explanation of why specific cells undergo programmed cell death during aerenchyma formation.

It is has been suggested that NO may interact with reactive oxygen species to produce peroxynitrite and directly kill plant pathogens [59]. There is an abundance of literature on NO and programmed cell death in many mammalian tissues. Depending on NO concentration and other factors, NO may either accelerate or inhibit apoptosis [60]. The effect may be either direct, through cell necrosis, or through regulatory pathways. It may also be selective in relation to the cells that do respond. A similar type of reaction could be responsible for selected cell death during aerenchyma formation in roots exposed to waterlogging [57]. NO, by its activation of guanylate cyclase, has pronounced effects on signal transduction pathways. Inhibitors of signal transduction pathways that have been linked to cGMP in mammalian cells [35] also effect aerenchyma formation in maize roots [58]. Similarly, NO has been implicated in programmed cell death of *Arabidopsis* cell suspension cultures through its action on signal transduction pathways involving guanylate cyclase [12].

6. Conclusions

Hemoglobin may be pivotal in the short term survival of plant root cells by regulating the levels of NO. Plant roots that express sufficient hemoglobin soon after exposure to hypoxic stress may modulate levels of NO, produced as a result of the stress, through reaction of the

NO with oxyhemoglobin. This would prevent the onset of cell death, maintaining ATP levels and energy charge, as has been observed in hypoxic maize cells overexpressing hemoglobin [39]. In primary roots, this may provide sufficient time for the plant to develop adventitious roots, needed for prolonged survival under hypoxia. In roots developing aerenchyma, hemoglobin expression or action may be cell selective, resulting in (programmed) death of some cells that underexpress the gene.

References

[1] Moncarda S., Palmer R.M.J. and Higgs E.A., "Nitric oxide: physiology, pathophysiology and pharamacology". *Pharmacol. Rev*., vol. 43, p.p. 109-142, 1991.
[2] Jeffrey S.R. and Snyder S.H., "Nitric oxide:. a neural messenger". *Ann. Rev. Cell Dev. Biol*., vol. 11, p.p. 417-440, 1995.
[3] Lloyd-Jones D.M. and Bloch K.D., "The vascular biology of nitric oxide and its role in atherogenesis". *Annu. Rev. Med*., vol. 47, p.p. 365-375, 1996.
[4] Wink D.A. and Mitchell J.B., "Chemical biology of nitric oxide, p.p. Insights into regulatory, cytotoxic, and cytoprotective mechanisms of nitric oxide". *Free Radical Bio. Med*., vol. 25 (4-5), p.p. 434-456, 1998).
[5] Ignarro L.J., "Haem-dependent activation of cytosolic guanylate cyclase by nitric oxide, p.p. a widespread signal transduction mechanism". *Biochem. Soc. Trans.*, vol. 20, p.p. 465-469, 1992.
[6] Delledonne M., Xia Y., Dixon R.A., Lamb C., Nitric oxide functions as a signal in plant disease resistance. *Nature*, vol. 394, p.p. 585-588, 1998.
[7] Durner J., Wendehenne D. and Klessig D.F., "Defense gene induction in tobacco by nitric oxide, cyclic GMP, and cyclic ADP-ribose". *Proc. Natl. Acad. Sci. USA*, vol. 95, p.p. 10328-10333, 1998.
[8] Del Rio L.A., Copras F.J. and Barroso J.B., "Nitric oxide and nitric oxide synthase activity in plants". *Phytochemistry*, vol. 65, p.p. 783-792, 2004.
[9] Dordas C., Hasinoff B., Igambrediev A.U., Manach N., Rivoal J. and Hill R.D., "Expression of a stress-induced hemoglobin affects NO levels produced by alfalfa under hypoxic stress". *Plant J*., vol. 35, p.p. 763-770, 2003.
[10] Dordas C., Hasinoff B., Manach N., Rivoal J. and Hill R.D., "Class-1 hemoglobins, nitrate and NO levels in anoxic maize cell-suspension cultures". *Planta*, vol. 219, p.p. 66-72, 2004.
[11] Igamberdiev A.U., Seregeyles C., Manac'h N. and Hill R.D., "NADH-dependent metabolism of nitric oxide in alfalfa root cultures expressing barley hemoglobin". *Planta*, vol. 219, p.p. 95-102, 2004.
[12] Clarke A., Desikan R., Hurst R.D., Hancock J.T. and Neill S.J., ЭNO way back, p.p. nitric oxide and programmed cell death in *Arabidopsis thaliana* suspension cultures". *Plant J*., vol. 24, p.p. 667-677, 2000.
[13] Dordas C., Rivoal J. and Hill R.D., "Plant haemoglobins, nitric oxide and hypoxic stress". *Ann. Bot*., vol. 91, p.p. 173-178, 2003.
[14] Alderton W.K., Cooper C.E., Knowles R.G., "Nitric oxide synthases: structure, function and inhibition". *Biochem J*., vol. 357, p.p. 593-615, 2001.
[15] Ribeiro E.A.Jr., Cunha F.Q., Tamashiro W.M. and Martins I.S., "Growth phase-dependent subcellular localization of nitric oxide synthase in maize cells". *FEBS Lett*., vol. 445, p.p. 283-286, 1999.
[16] Caro A. and Puntarulo S., "Nitric oxide generation by soybean embryonic axes. Possible effect on mitochondrial function". *Free Radical Res*., vol. 31, p.p. S205-S212 Suppl., 1999.
[17] Le Cras T.D. and McMurtry I.F., "Nitric oxide production in the hypoxic lung". *Am. J. Physiol. – Lung C*., vol. 280 (4), p.p. L575-L582, 2001.
[18] Butt Y.K.C., Lum J.H.K. and Lo S.C.L., "Proteomic identification of plant proteins probed by mammalian nitric oxide synthase antibodies". *Planta*, vol. 216 (5), p.p. 762-771, 2003.
[19] Chandok M.R., Ytterberg A.J., van Wijk K.J. and Klessig D.F., "The pathogen-inducible nitric oxide synthase (iNOS) in plants is a variant of the P protein of the glycine decarboxylase complex". *Cell*, vol. 113 (4), p.p. 469-482, 2003.
[20] Guo F.Q., Okamoto M. and Crawford N.M., "Identification of a plant nitric oxide synthase gene involved in hormonal signaling". *Science*, vol. 302 (5642), p.p. 100-103, 2003.
[21] Yamasaki H., Sakihama Y., "Simultaneous production of nitric oxide and peroxynitrite by plant nitrate reductase, p.p. in vitro evidence for the NR-dependent formation of active nitrogen species". *FEBS Lett*., vol. 468, p.p. 89-92, 2000.
[22] Glaab J. and Kaiser W.M., "Rapid modulation of nitrate reductase in pea roots". *Planta*, vol. 191 (2), p.p. 173-179, 1993.

[23] Arnon D.I., "Ammonium and nitrate nutrition of barley at different season in relation to hydrogen-ion conecnatrations, manganese, copper and oxygen supply". *Soil Sci*., vol. 44, p.p. 91-113, 1937.
[24] Fan T.W.N., Higashi R.M. and Lane A.N., "An in vitro1H and 31P NMR investigation of the effect of nitrate on hypoxic metabolism in maize roots". *Arch. Biochem. Biophys*., vol. 266, p.p. 592-606, 1988.
[25] Weitzberg E. and Lundberg J.O.N., "Nonenzymatic nitric oxide production in humans". *Nitric Oxide Biol*., Ch. 2 (1), p.p. 1-7, 1998.
[26] Bethke P.C., Badger M.R. and Jones R.L., "Apoplastic synthesis of nitric oxide by plant tissues". *Plant Cell*, vol. 16 (2), p.p. 332-341, 2004.
[27] Harrison R., "Structure and function of xanthine oxidoreductase: Where are we now? *Free Radical Bio. Med*., vol. 33 (6), p.p. 774-797, 2002.
[28] Wittenberg J.B. and Wittenberg B.A., "Mechanisms of cytoplasmic hemoglobin and myoglobin function". *Annu. Rev. Biophys. Biophys. Chem*., vol. 19, p.p. 217-241, 1990.
[29] Appleby C.A., ".The origin and functions of haemoglobin in plants". *Sci. Progress*, 76, p.p. 365-398, 1992.
[30] Hill R.D., "What are hemoglobins doing in plants? *Can. J. Bot*., vol. 76, p.p. 707-712, 1998.
[31] Watts R.A., Hunt P.W., Hvitved A.N., Hargrove M.S., Peacock W.J. and Dennis E.S., "A hemoglobin from plants homologous to truncated hemoglobins of microorganisms". *PNAS*, vol. 98, p.p. 10119-10124, 2001.
[32] Duff S.M.G., Wittenberg J.B. and Hill R.D., "Expression, purification, and properties of recombinant barley (*Hordeum* sp.) hemoglobin: Optical spectra and reactions with gaseous ligands". *J. Biol. Chem*., vol. 272, p.p. 16746-16752, 1997.
[33] Furchgott R.F., "The 1989 Ulf von Euler lecture. Studies on endothelium-dependent vasodilation and the endothelium-derived relaxing factor". *Acta Physiol. Scand*., vol. 139, p.p. 257-270, 1990.
[34] Ignarro L.J., "Nitric oxide as a unique signaling molecule in the vascular system: A historical overview". *J. Physiol. Pharmacol*., vol. 53 (4), p.p. 503-514, 2002.
[35] McDonald L.J. and Murad F., "Nitric oxide and cyclic GMP signaling". *Proc. Soc. Exp. Biol. Med*., vol. 211, p.p. 1-6, 1996.
[36] Minning D.M., Gow A.J., Bonaventura J., Braun R., Dewhirst M., Goldberg D.E. and Stamler J.S., "*Ascaris* haemoglobin is a nitric oxide-activated 'deoxygenase'". *Nature*, vol. 401, p.p. 497-502, 1999.
[37] Gardner P.R., Gardner A.M., Martin L.A., Salzman A.L., "Nitric oxide dioxygenase, p.p. an enzymic function for flavohemoglobin". *Proc. Natl. Acad. Sci. USA*, vol. 95, p.p. 10378-10383, 1998.
[38] Crawford R.M.M., "Metabolic adaptations to anoxia". In DD Hook, RMM Crawford, eds Plant life in anaerobic environments. Ann Arbor Science Publishers, Inc., Ann Arbor, pp 119-136, 1978.
[39] Sowa A., Duff S.M.G., Guy P.A. and Hill R.D., "Altering hemoglobin levels changes energy status in maize cells under hypoxia". *Proc. Natl. Acad. Sci. USA*, vol. 95, p.p. 10317-10321, 1998.
[40] Wang R., Guegler K., LaBrie S.T. and Crawford N.M., "Genomic analysis of a nutrient response in arabidopsis reveals diverse expression patterns and novel metabolic and potential regulatory genes induced by nitrate". *Plant Cell*, vol. 12, p.p. 1491-1510, 2000.
[41] Igamberdiev A.U. and Hill R.D., "Nitrate, NO and hemoglobin in plant adaptation to hypoxia, p.p. An alternative to classic fermentation pathways". *J. Exp. Bot*., vol. 55, p.p. 2473-2482, 2004.
[42] Igamberdiev A.U., Bykova N.V., Ens W. and Hill R.D., "Dihydrolipoamide dehydrogenase from porcine heart catalyzes NADH-dependent scavenging of nitric oxide". *FEBS Lett*., vol. 568 (1-3), p.p. 146-150, 2004.
[43] Barroso J.B., Corpas F.J., Carreras A., Sandalio L.M., Valderrama R., Palma J.M., Lupianez J.A. and del Rio L.A., "Localization of nitric-oxide synthase in plant peroxisomes". *J. Biol. Chem*., vol. 274, p.p. 36729-36733, 1999.
[44] Cueto M., Hernandez-Perera O., Martin R., Bentura M.L., Rodrigo J., Lamas S. and Golvano M.P., "Presence of nitric oxide synthase activity in roots and nodules of *Lupinus albus*". *FEBS Lett*., vol. 398, p.p. 159-164, 1996.
[45] Stöhr C., Strube F., Marx G., Ullrich W.R. and Rockel P., "A plasma membrane-bound enzyme of tobacco roots catalyses the formation of nitric oxide from nitrite". *Planta*, vol. 212, p.p. 835-841, 2001.
[46] Botrel A. and Kaiser W.M., "Nitrate reductase activation state in barley roots in relation to the energy and carbohydrate status". *Planta*, vol. 201, p.p. 496-501, 1997.
[47] Ferrari T.E. and Varner J.E., "Intact tissue assay for nitrite reductase in barley aleurone layers". *Plant Physiol*., vol. 47, p.p. 790-794, 1971.
[48] Wennmalm A., Benthin G., Petersson A.S., "Dependence of the metabolism of nitric oxide (NO) in healthy human whole blood on the oxygenation of its red cell haemoglobin". *Br. J. Pharmacol*., vol. 106, p.p. 507-508, 1992.
[49] Doyle M.P. and Hoekstra J.W., "Oxidation of nitrogen oxides by bound dioxygen in hemoproteins". *J. Inorg. Biochem*., vol. 14, p.p. 351-358, 1981.
[50] Tiedje J.M., Sexstone A.J., Myrold D.D. and Robinson J.A., "Denitrification, p.p. ecological niches, competition and survival". *Antonie van Leeuwenhoek*., vol. 48, p.p. 569-583, 1982.

[51] Jakob W., Webster D.A. and Kroneck P.M., "NADH-dependent methemoglobin reductase from the obligate aerobe *Vitreoscilla*, p.p. improved method of purification and reexamination of prosthetic groups". *Arch. Biochem. Biophys*., vol. 292, p.p. 29-33, 1992.
[52] Poole R.K. and Hughes M.N., "New functions for the ancient globin family, p.p. bacterial responses to nitric oxide and nitrosative stress". *Mol. Microbiol*., vol. 36, p.p. 775-783, 2000.
[53] Drew M.C., He C.J. and Morgan P.W., "Decreased ethylene biosynthesis, and induction of aerenchyma, by nitrogen- or phosphate-starvation in adventitious roots of *Zea mays* L". *Plant Physiol*., vol. 91, p.p. 266-271, 1989.
[54] Drew M.C., Cobb B.G., Johnson J.R., Andrews D., Morgan P.W., Jordan W. and He C.J., "Metabolic acclimation of root tips to oxygen deficiency". *Ann. Bot*., vol. 74, p.p. 281-286, 1994.
[55] He C.J., Morgan P.W. and Drew M.C., "Enhanced sensitivity to ethylene in nitrogen- or phosphate-starved roots of *Zea mays* L. during aerenchyma formation". *Plant Physiol*., vol. 98, p.p. 137-142, 1992.
[56] Jackson M.B., "Ethylene and responses of plants to soil waterlogging and submergence". *Ann. Rev. Plant Physiol*., 36, p.p. 145-174, 1985.
[57] Drew M.C., "Oxygen deficiency and root metabolism: injury and acclimation under hypoxia*". Ann. Rev. Plant Physiol. Plant Mol. Biol*., vol. 48, p.p. 223-250, 1997.
[58] Drew M.C., He I.I. and Morgan P.W., "Programmed cell death and aerenchyma formation in roots". *Trends Plant Sci*., vol. 5, p.p. 123-127, 2000.
[59] Durner J. and Klessig D.F., "Nitric oxide as a signal in plants". *Curr. Opin. Plant Biol*., vol. 2, p.p. 369-374, 1999.
[60] Kim P.K., Zamora R., Petrosko P. and Billiar T.R., "The regulatory role of nitric oxide in apoptosis*". Int. Immunopharmacol*., vol. 1, p.p. 1421-1441, 2001.

Cell Biology and Instrumentation: UV Radiation, Nitric Oxide and Cell Death in Plants
Y. Blume et al. (Eds.)
IOS Press, 2006

Nitric Oxide in Plants: the Cell Fate Regulator

Krisztina ÖTVÖS[1], Taras PASTERNAK[2], Pál MISKOLCZI[2], Attila SZŰCS[1], Dénes DUDITS[2] and Attila FEHÉR[1]
Laboratory of Functional Cell Biology (1) and Laboratory of Cell Division and Differentiation (2), Institute of Plant Biology, Biological Research Centre, Hungarian Academy of Sciences, Temesvári krt. 62., H-6726, Szeged, Hungary

Abstract. Mounting evidences support the hypothesis that nitric oxide (NO) serves as a signaling molecule in plant cells and participate in several signal transduction pathways. In this communication we report how NO can stimulate the activation of cell division and embryogenic cell formation in alfalfa leaf protoplast-derived cells in the presence of auxin. Based on our observations, it is hypothesized that NO is involved in the auxin-mediated activation but not in the progression of the plant cell division cycle.

Introduction

Understanding how plants grow and react to the environment is central to our attempt to realize basic mechanisms that drive biological processes as well as to create a rational approach to produce more or better quality food. Plants, as multicellular organisms, have developed highly sophisticated short and long-term adaptive mechanisms to the changing environment. Due to the simple fact that plants cannot alter their location in response to environmental changes, their development is highly flexible that results in a great variability of plant forms and growth that significantly influences productivity.

Depending on the concentration and type of the tissue where it is acting, nitric oxide (NO) can be considered either toxic or protective as well in animals as in plants [1, 2]. While some investigations consider NO as a stress-inducing agent, other reports emphasize its protective role as an activator of the plant defense system as well as a radical chain reaction breaker under oxidative stress conditions. In addition to its role in stress responses, NO has also been reported as an important signaling molecule during animal and plant development [3-5]. For an overview on NO biosynthesis, biology and signal transduction the reader may refer to two excellent recent summaries [6, 7].

The question to answer in this review is how nitric oxide (NO) - as a signaling molecule – can participate in the communication processes between the plant and its environment and how this remarkable molecule can be involved in the regulation of cell division and differentiation, the two major processes determining plant growth and development. The role of NO in apoptosis, a further important phenomenon in plant development, will be separately discussed in other chapters.

1. Nitric Oxide in Plants

Nitric oxide (NO) is a small, water and lipid soluble free radical and the first gas known to act as a biological messenger in animals. NO ultimately exerts its biological effects by reacting either directly or through other reactive nitrogen intermediates with a variety of targets such as heme groups, Fe-S or Zn-S clusters, sulfhydryl groups or various other chemical substrates [2, 8]. This diversity of potential targets is reflected in the large number of different systems that utilize NO as a mediator. In mammals, it is involved in diverse signal transduction pathways controlling smooth muscle tone, responses to infection, apoptosis, cell proliferation as well as fertilization [9-11].

Although plant genes coding for the homologues of animal nitric oxide synthase (NOS) enzymes could not be identified or isolated, NOS-like activity and NO accumulation have been reported in different plants species and organs [12]. Considering its possible functions in plants, NO has been shown to serve as a defence signal that induces various defense genes [13, 14]. Furthermore, NO was implicated in the adaptive plant response during drought stress [15] as well as in the regulation of plant growth and development under normal growth conditions [4, 16].

Recently, two different plant enzymes with significant biochemical, but not amino acid sequence, similarity to animal NOS proteins have been cloned by two different approaches [17, 18]. A variant form of the P protein of the plant glycine decarboxylase was purified based on its NO-producing activity in response to pathogen infection or elicitation [17]. An *Arabidopsis* mutant served to identify the *AtNOS1* gene and the product of it was also proved to catalyse NO production *in vitro* as well as *in vivo* [18]. Both enzymes have been shown to be sensitive against the inhibitors of animal NOS enzymes, such as arginine analogues, that verified the use of these compounds in plant cells to decrease endogenous NO production.

2. NO and the Regulation of Cell Division

The role of NO in coordinating plant defense against biotic and abiotic stresses is probably the best established [7, 13, 19]. However, there are accumulating pieces of experimental evidences that NO is also involved in the regulation of plant growth and development [6, 7]. Among others, NO can stimulate plant growth in general [7], root [20], hypocotyl [16] and mesocotyl elongation [21] and induce adventitious root development in various plant species [5, 22, 23]. These observations indicate that NO may, directly or indirectly, affect cell elongation and division, the two basic processes of plant morphogenesis. The interaction of NO-mediated signaling with the regulation of cell division and differentiation in mammalian cells is well established [5], but similar observations are largely missing in the case of plants. An exception is the role of NO in the regulation of apoptosis that has been clearly demonstrated in both type of eukaryotic organisms (for a recent review [24], and see also other chapters in this book).

Cell division is a vital process that requires ordered progression through well defined phases of the cell cycle. These cell cycle phases include an initial gap (G1), synthesis of DNA (S), a second gap (G2) and the final mitotic nuclear and cellular division (M) to result in two identical daughter cells. Our attention focuses on the G1 phase since it is the main phase where cells must decide whether they divide further or exit the cell cycle and differentiate. During G1, cells must integrate relevant signals before making decision to initiate DNA duplication, which implies commitment not only to S phase but also to completion of cell division. Although the molecular machinery regulating cell cycle progression is well known in plants,

our knowledge is scarce concerning the mechanisms by which growth regulators exerts their effects on the balance between cell proliferation and differentiation during plant development. Endogenous hormones such as auxin, abscisic acid, gibberellins and brassinosteroids as well as environmental factors all have been shown to regulate this progression [25].

Cyclin-dependent kinases (CDKs) - a special class of serine-threonine protein kinases which are functionally defined as requiring binding of a regulatory protein known as cyclin for activity - are the major regulators of the eukaryotic cell cycle, thus they are the main targets of phytohormone signals that control cell differentiation as well as proliferation. The activities of CDK-cyclin complexes are controlled by several complicated molecular mechanisms, including phosphorylation and protein-protein interactions, which result in oscillating CDK activity during the division cycle. These fluctuations trigger transitions between the different stages of the cell cycle (for review [25]). For example, in the G1 phase during cell division, D-type cyclins (CycD) interact with cyclin-dependent-kinase A (CDKA) regulating its kinase activity. The expression of genes coding for the CycD subunits is regulated by several growth factors such as auxin, cytokinin, gibberellin (GA), brassinosteroid (BR), abscisic acid (ABA) and sugars.

To get information about the possible role of NO during cell cycle activation and progression we used individual cell-wall-less plant cells, alfalfa leaf protoplasts, as *in vitro* experimental models. Due to the simplicity of the experimental manipulation, observation and molecular/cytological investigation of protoplast-derived cells, the system proved to be especially useful to study the earliest events associated with the activation of cell division and embryogenic development [26]. Although they are isolated via stressful procedures, experimental evidences demonstrate that properly handled protoplasts quickly recover in culture and respond to hormonal as well as stress signals as do intact plant cells [27].

We could manipulate cell division of the protoplast derived cells by supplying a source of NO (SNP), a NOS inhibitor (L-NMMA) or a NO scavenger (PTIO) to the culture medium [28]. SNP (only in a tight concentration range (1-10 μM)) could increase, while application of the NOS-inhibitor, L-NMMA, as well as the NO scavenger, PTIO, decreased the division rate of alfalfa leaf protoplast-derived cells. It was also indicated that either directly or indirectly NO affects the activity of the cell cycle machinery in the protoplast-derived cells as the activity of the cognate p34cdc2 kinase, Cdc2MsA/B (the CDK partner for CycD) was decreased and increased, in L-NMMA and SNP-treated cells, respectively. This observation was unexpected as the negative effect of environmental stresses on cell division and on the cell cycle machinery including core components such as cyclins and cyclin-dependent kinases (CDKs) is well documented in plants and in mammals as well [3, 29-31].

In animal cells, NO initiates a switch from proliferation to cytostasis during cellular differentiation and is considered as a regulator of the balance between cell proliferation and cell differentiation during development [10]. The acceleration of protoplast-derived cell division by NO - as a response to the 1-10 μM SNP treatment - might be a part of an adaptive strategy under stress conditions. This hypothesis is supported by the fact that the effect of L-NMMA was transient and depended on the time of application ([28] and Fig. 1). Protoplast-derived cells passing more than three days in culture become insensitive to the NO-synthesis inhibitor as cell cycle progression was concerned. In agreement, L-NMMA had no effect on cell cycle parameters of a continuously dividing suspension culture from the same ecotype.

The observations that neither dividing leaf protoplasts nor dividing suspension cultured cells are responsive to L-NMMA support a hypothesis that the activity of L-NMMA-sensitive plant enzymes is not required to sustain cell division activity in plant cells. It can be rather supposed that such activity(s) is needed for processes preceding the cell cycle entry of

dedifferentiating plant cells. Further studies are required to reveal the underlying processes and L-NMMA-sensitive enzymes that are involved in these pathways.

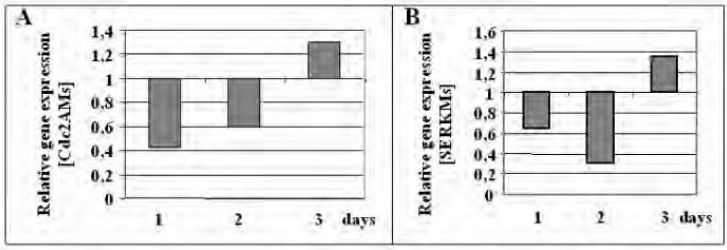

Figure 1. 10 mM L-NMMA transiently inhibits the expression of the Cdc2AMs cell cycle regulatory gene and the SERKMs embryogenic marker gene in alfalfa leaf protoplast cultures. Relative gene expressions were determined by the ABI PRISM 7000 Sequence Detection System and were normalised for actin gene expression as described in details elsewhere [24] in three replicates (the averages are shown; SDs for CT numbers were <0,2%).

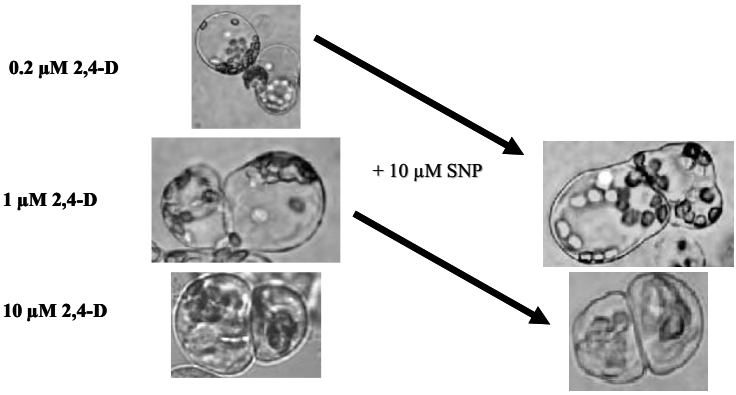

Figure 2. The NO donor SNP can alter auxin (2,4-D) sensitivity of alfalfa protoplast-derived cells. Application of 10 µM SNP to the culture medium results in a new morphology and division-type otherwise characteristic to cells grown in the presence of higher auxin (2,4-D) concentrations.

3. NO and Somatic Embryogenesis

Under appropriate *in vivo* or *in vitro* conditions, certain somatic plant cells have the capability to initiate embryogenic development (the process called, somatic embryogenesis) [26]. Somatic embryogenesis provides a unique experimental model to understand the molecular and cellular bases of developmental plasticity in plants. The influences of exogenously applied auxins, preferentially 2,4-dichlorophenoxyacetic acid (2,4-D), on the induction of somatic embryogenesis are well documented [32, 33]. It has been previously shown that leaf protoplast-derived cells can develop either to vacuolated, elongated cells or to small, isodiametric cells

with dense cytoplasm exhibiting embryogenic competence, depending on exogenous auxin concentration [33].

As it was discussed above, we were able to manipulate cell division by supplying a source of NO (SNP). Our further observations revealed that the application of 1-10 μM SNP resulted in the development of embryogenic-type cells already at low (1 μM) 2,4-D concentration (Fig. 2), while the NOS inhibitor L-NMMA delayed exogenous auxin concentration-dependent formation of embryogenic cell clusters in the presence of the inductive 10 μM 2,4-D concentration [28].

The high level expression of the *MtSERK1* gene and the further development of the cells under culture conditions allowing somatic embryo formation verified that NO (SNP) application could indeed alter the developmental pathway of the treated cells [28]. A transient inhibitory effect of L-NMMA on *SERKMs* expression could also be observed (Fig. 1B). The *SERKMs* gene is the alfalfa orthologue of the carrot and *Arabidopsis SERK* genes implicated in both somatic and zygotic embryogenesis, and used frequently as a gene expression marker of embryogenic competence [34].

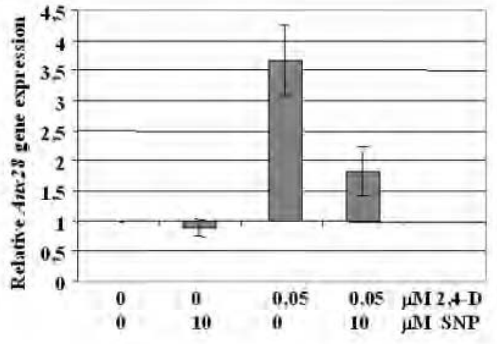

Figure 3. Relative expression of the *Aux28* auxin-regulated gene in alfalfa leaf protoplast cultures in response to 2,4-D and/or the NO-donor SNP. Relative gene expression was determined by the ABI PRISM 7000 Sequence Detection System and were normalised for actin gene expression as described in details elsewhere [24] in three independent experiments with three replicates each (the averages and SD are shown).

4. NO and Auxin

The altered response of protoplast-derived cells to exogenous auxin concentration in the presence of L-NMMA or SNP, and a further observation that in the absence of auxin SNP could not promote the division of protoplast-derived cells [28], may indicate that NO alters auxin sensitivity of the cells and/or is involved in the mediation of auxin action during these processes. However, our preliminary experiments could rather demonstrate a negative effect of NO on the expression of auxin-responsive genes (*Aux28 or IAA4*) (see Fig. 3). Auxin and NO have been suggested to share common steps in signal transduction pathways leading to root elongation [20] and adventitious root formation [5, 23, 35].

In cucumber explants, indoleacetic acid (IAA) treatment induced the level of endogenous NO in the region where the new root meristems developed. The effect of NO on IAA-induced root formation was shown to be dependent on intracellular cGMP levels,

although cGMP-independent pathways may also exist [5, 35]. The downstream events of the putative NO-dependent signaling cascade leading to mitotic activation by auxin in the root or in leaf protoplast-derived cells are unknown. Whether the same NO-affected signal transduction pathways operate during the formation of dividing, embryogenic cells from leaf protoplasts and adventious root meristem formation remains also a question to be answered.

5. Concluding Remarks

The life strategies of multicellular plant and animal species are fundamentally different. While active movement is characteristic of animal organisms, plants are sessile. This basic difference is reflected in the evolution of different approaches of short-term environmental adaptation by individuals. Animals respond to environmental signals or conditions by changes in their behavior, while plants accommodate environmental effects by altering metabolism and/or development. Developmental decisions of a plant are significantly influenced by environmental factors.

Striking examples of developmental plasticity of plants are provided by *in vitro* cultures where the differentiated fate of somatic plant cells can be easily altered. *In vitro* cultured plant cells de-differentiate and divide and develop into various organs or even into embryos depending on the culture conditions. Therefore it is obvious that environmental and hormonal signals control the regulation of cell division and differentiation more directly and with much more flexibility in plants as compared to animals.

Based on the above considerations it is not surprising that stress and developmental signaling in plants are closely linked and share similar signaling steps. It seems likely, for example, that NO, this multi-faceted molecule, has an essential role in determining the appropriate developmental pathway plant cells have to follow during normal plant development as well as in response to the continuously changing environment.

References

[1] Beligni M.V. and Lamattina L., *NitricOxide*, vol. 3, p.p. 199-208, 1999.
[2] Wink D.A. and Mitchell J.B., *Free Radical Biology and Medicine*, vol. 25, p.p. 434-456, 1998.
[3] Ishida A., Sasaguri T., Kosaka C., Nojima H. and Ogata J., *Journal of Biological Chemistry*, vol. 272, p.p. 10050-10057, 1997.
[4] Leshem Y.Y. and Pinchasov Y., *Journal of Experimental Botany*, vol. 51, p.p. 1471-1473, 2000.
[5] Pagnussat G.C., Lanteri M.L. and Lamattina L., *Plant Physiology*, vol. 132, p.p. 1241-1248, 2003.
[6] Lamattina L., Garcia-Mata C., Graziano M. and Pagnussat G., *Annual Reviews in Plant Biology*, vol. 54, p.p. 109-136, 2003.
[7] Neill S.J., Desikan R. and Hancock J.T., *New Phytologist*, vol. 159, p.p. 11-35, 2003.
[8] Cooper C.E., *Biochimica and Biophysica Acta-Bioenergetics*, vol. 1411, p.p. 290-309, 1999.
[9] Kuo R.K., Baxter G.T., Thompson S.H., Stricker S.A., Patton C., Bonaventura J. and Epel D., *Nature*, vol. 406, p.p. 633-636, 2000.
[10] Peunova N., Kuzin B., Roberts I., Okane C. and Enikolopov G., *Cold Spring Harbor Symposia on Quantitative Biology*, vol. 61, p.p. 417-426, 1996.
[11] Schmidt H.H. and Walter U., *Cell*, vol. 78, p.p. 919-925, 1994.
[12] Barroso J.B., Corpas F.J., Carreras A., Sandalio L.M., Valderrama R., Palma J.M., Lupianez J.A. and del Rio L.A., *Journal of Biological Chemistry*, vol. 274, p.p. 36729-36733, 1999.
[13] Delledonne M., Xia Y.J., Dixon R.A. and Lamb C., *Nature*, vol. 394, p.p. 585-588, 1998.
[14] Durner J. and Klessig D.F., *Current Opinion in Plant Biology*, vol. 2, p.p. 525-529, 1999.
[15] Mata C.G. and Lamattina L., *Plant Physiology*, vol. 126, p.p. 1196-1204, 2001.

[16] Beligni M.V. and Lamattina L., *Planta*, vol. 210, p.p. 215-221, 2000.
[17] Chandok M.R., Ytterberg A.J., van Wijk K.J. and Klessig D.F., *Cell*, vol. 113, p.p. 469-482, 2003.
[18] Guo F.Q., Okamoto M. and Crawford N.M., *Science*, vol. 302, p.p. 100-103, 2003.
[19] Gould K.S., Lamotte O., Klinguer A., Pugin A. and Wendehenne D., *Plant Cell and Environment*, vol. 26, p.p. 1851-1862, 2003.
[20] Gouvea C.M.C.P., Souza J.F. and Magelhaes M.I.S., *Plant Growth Regulation*, vol. 21, p.p. 183-187, 1997.
[21] Zhang M., An L., Feng H., Chen T., Chen K., Liu Y., Tang H., Chang J. and Wang X., *Photochemistry and Photobiology*, vol. 77, p.p. 219-225, 2003
[22] Correa-Aragunde N., Graziano M., and Lamattina L., *Planta*, vol. 218, p.p. 900-905, 2004.
[23] Pagnussat G.C., Simontacchi M., Puntarulo S. and Lamattina, L., *Plant Physiology*, vol. 129, p.p. 954-956, 2002.
[24] Hoeberichts F.A. and Woltering E.J., *Bioessays*, vol. 25, p.p. 47-57, 2003.
[25] Dewitte W. and Murray J.A.H., *Annual Reviews of Plant Biol*ogy, vol. 54, p.p. 235-264, 2003.
[26] Feher A., Pasternak T. P. and Dudits D., *Plant Cell Tissue and Organ Culture*, vol. 74, p.p. 201-228, 2003.
[27] Sheen J., *Plant Physiology*, vol. 127, p.p. 1466-1475, 2001.
[28] Ötvös K., Pasternak T.P., Miskolczi P., Szűcs A., Dudits D. and Fehér A., *Plant Journal* (submitted), 2004.
[29] Guo K., Andres V. and Walsh K., *Circulation*, vol. 97, p.p. 2066-2072, 1998.
[30] Schuppler U., He P.H., John P.C.L. and Munns R., *Plant Physiology*, vol. 117, p.p. 1528-1531, 1998.
[31] West G., Inze D. and Beemster G.T.S., *Plant Physiology*, vol. 135, p.p. 1050-1058, 2004.
[32] Dudits D., Bögre L. and Györgyey J., *Journal of Cell Science*, vol. 99, p.p. 475-484, 1991.
[33] Pasternak T., Prinsen E., Ayaydin F., Miskolczi P., Potters G., Asard H., Van Onckelen H., Dudits D. and Fehér A., *Plant Physiology*, vol. 129, p.p. 1807-1819, 2002.
[34] Baudino S., Hansen S., Brettschneider R., Hecht V.R.G., Dresselhaus T., Lorz H., Dumas C. and Rogowsky P.M., *Planta*, vol. 213, p.p. 1-10, 2001.
[35] Pagnussat G.C., Lanteri M.L., Lombardo M.C. and Lamattina L., *Plant Physiology*, vol. 135, p.p. 279-286, 2004.

Cell Biology and Instrumentation: UV Radiation, Nitric Oxide and Cell Death in Plants
Y. Blume et al. (Eds.)
IOS Press, 2006

Nitric Oxide, Cell Death and Increased Taxol Recovery

Don J. DURZAN
Department of Plant Sciences,MS 6. University of California,
One Shields Ave. Davis, CA 95616 USA
e-mail: djdurzan@ucdavis.edu

Abstract. Genes for plant nitric oxide synthase (NOS) now help explain how NO is produced from nitrate, nitrite, and/or L-arginine in the culture medium and in cells. Evidence is presented that under aseptic conditions; plant NOS activity, NO bursts, and cell death (apoptosis) are important factors in the recovery of taxol (paclitaxel) from cell suspensions of several *Taxus* sp. Cell-suspension responses to mechanical stresses, simulated microgravity, and hypergravity were dominated by NO bursts and cell death (apoptosis) and by the overproduction and release of free and bound taxol into the culture medium. The synthesis of the taxane ring in the chloroplasts and gravisensing amyloplasts, and the subsequent assembly of taxol and related taxane diterpenoids were visualized by immunocytochemical, laser confocal and scanning electron microscopy. Drug-producing cells and taxane-bearing materials in the culture medium were recovered using immunoparamagnetic beads. Bound taxol and taxanes were recovered from xylanase hydrolyates. Binding was associated with the expression of two proteins for 'touch' genes expressed under mechanical forces. Taxol recovery was increased by 64% by the use of a NO donor. NOS inhibition with guandino compounds, and the use of a NO trap, reduced taxol recovery and reduced taxane diterpenoid biosynthesis. This offered countermeasures to NO-mediated stress, and reduced apoptosis. In hypergravity, the taxol and taxanes released from cells by syneresis were recovered on hydrophobic PVDF (polyvinylidene fluoride) filters. Cyclodextrins added to the culture medium enhanced biomass yield and altered the solubility of taxanes to improve the recovery of taxol and taxanes.

Introduction

With NASA support this research aimed at evaluating early opportunities in Microgravity Sciences to commercialize space and to develop biotechnology facilities for the International Space Station [1]. The main task was to evaluate the production of taxol (generic name: paclitaxel) with cell suspensions in bioreactors designed for the Space Shuttle. Unexpectedly, this work led to the early demonstration of L-arginine-dependent nitric oxide (NO) bursts in mechanically and gravitationally stressed plant cells, to NO-dependent programmed cell death (apoptosis) (reviewed in [2]), and to a model describing how these factors contribute to increased taxol and taxane recovery from conifers.

Earlier, when intermediates of the Krebs-Henseleit or urea cycle (Figure 1) were fed to conifers, several substituted guanidino compounds were synthesized from uniformly labeled ^{14}C-L-arginine, and less so from UL-^{14}C-L-citrulline [3-7]. At that time, the functions of

substituted guanidines were either unknown or considered as respiratory inhibitors [8, 9]. Today, they are used as inhibitors of plant, animal and human NOSs. NOS substrates are L-arginine and oxygen. NOS products are L-citrulline and NO.

Since nitrite and nitrate reductases were known sources of NO, we obtained an *Arabidopsis* nitrate-reductase double mutant with the aim of finding out if cells could produce NO in the absence of nitrate, nitrite, and their reductases. With this mutant we reaffirmed that the source of NO was putative NOS activity [10]. The production of NO from L-arginine was blocked by D-arginine, and by the NOS inhibitor, N^G-monomethyl-L-arginine (L-NMMA) ensuring that NO was produced in the absence of any possible residual nitrate reductase activity. NOS-dependent NO production was inhibited by other guanidino compounds but not by D-arginine. Subsequently, the discovery by others of two plant NOS genes [11, 12] provided evidence that plant genomes encode for NOS. In our work, the substituted guanidines offered protection against mechanically induced stress and cell death (apoptosis).

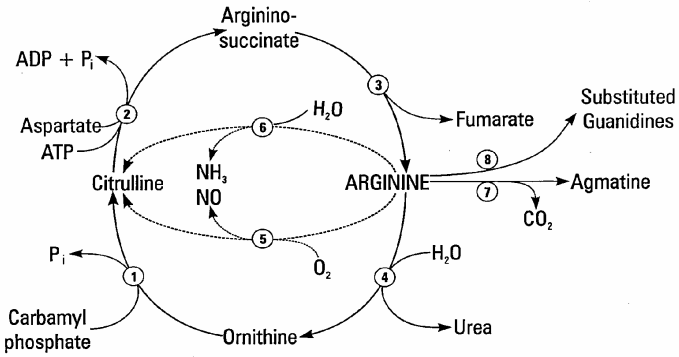

Figure. 1. The reactions of the Krebs-Henseleit (urea) cycle, a postulated citrulline-NO cycle, and the formation of guanidino compounds (substituted and unsubstituted). Enzymes: **1.** ornithine carbamoyl transferase, **2.** argininosuccinate synthetase, **3.** argininosuccinate lyase, **4.** arginase, **5.** nitric oxide synthase, **6.** arginine deiminase, **7.** arginine decarboxylase, **8.** numerous enzymes contributing to the formation of substituted guanidino compounds. Reactions 1 to 4 comprise the urea cycle. Reactions 2, 3, 5, may account for NOS activity in plants (citrulline-NO cycle, or arginine-citrulline cycle). Arginine deiminase was reported in chloroplasts but is mostly found in microorganisms. Reactions 7 and 8 comprise decarboxylation, oxidation, methylation, transamidination, phosphorylation, keeping the guanidino group intact or modify it by methylation, phosphorylation, etc. They remove L-arginine as a substrate from the urea cycle, and from reactions 5 and 6. Arginine represents and important branch point that links nitrate and ammonium nutrition to protein synthesis and turnover (not shown), to the urea cycle, to a postulated citrulline-NO cycle, and to the formation of guanidino compounds that are NOS inhibitors.

NO bursts are early stress responses even before the release of ethylene [13, 14]. High levels of NO are potentially harmful due to its reaction with superoxide forming peroxynitrite [1]. The latter has the potential to 'nitrate' phenols, and the tyrosine residues of cell regulatory

proteins. We now know that high levels of NO predispose apoptosis in angiosperms and gymnosperms [15-19]. Thiols, especially glutathione, react with NO to transport and translocate NO in signaling pathways involving guanylate cyclases [1, 20].

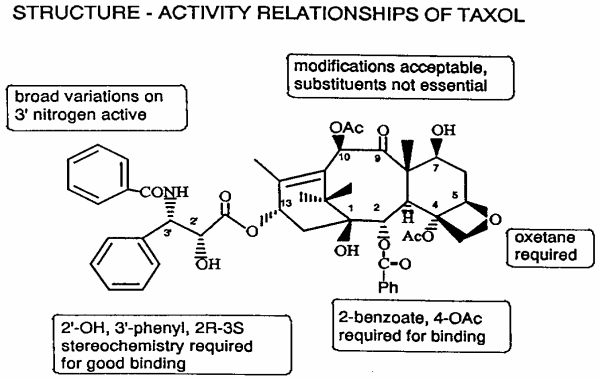

Figure 2. Taxol structure and the structural moieties required for binding to microtubules and anti-cancer activity. Color Plate 1 illustrates how antibodies specific for the *N*-benzoyl-3-phenylisoserine side-chain, the taxane ring, and taxol are processed during biosynthesis in egg cells. The overlap of both antibodies equates to the location of bound taxol shown in yellow. The taxane ring is synthesized in plastids. The *N*-benzyoyl-3-phenylisoserine side chain and the hydroxyl groups are added by the endoplasmic reticulum and Golgi stacks as the drug is transported to the plasmalemma and newly forming cell wall before release into the culture medium.

Taxol is an effective anti-cancer agent that was first isolated from the bark of *Taxus brevifolia* [21] (Figure 2). The bark of harvestable 100-year-old tree yields 0.017 % w/w taxol. Taxol binds to microtubules thereby offering a novel mechanism of blocking cell proliferation. In tumors, the binding of microtubules prevents daughter cells from replicating DNA and dividing. This contributes to the shrinkage of tumors and to the recovery of even a few terminally ill patients. By 1999, taxol became the best-selling anticancer drug in history. Commercial sales of were well over $ 1.5 billion [22, 23]. Over 350 different taxanes, with a wide range of physiological properties, occur in conifers [24, 25].

New models for taxol and taxane biosynthesis emerged [26-28] so that taxol biosynthesis could be followed at the subcellular level by immunocytochemistry, and by laser confocal and scanning electron microscopy [29-31]. The ability to bind microtubules suggested that taxol in conifer cells was compartmentalized or biosynthesized as a bound form [26, 32]. The use of NO donors, NOS substrates, products, inhibitors (substituted guanidines), and NO traps provided new opportunities to control the citrulline-NO cycle (Figure 1), apoptosis, and taxol production in unit gravity, simulated microgravity, and in hypergravity.

Haploid egg cells (oocytes) from female trees of *Taxus brevifolia* are easily screened without the effects of dominance, recessive, and epistatic interactions characteristic of diploid cells ([26], Color Plate 1.1 and 1.2). Lethal genes are directly expressed and removed by

apoptosis to make the population more uniform. Recessive adaptive mutations would be expressed to stabilize the cultures [33]. Diploid cell suspensions were established from needles of 3-year-old *T. brevifolia, T. cuspidata and T. media* from Zelenka Nursery (Grand Haven MI), and from seeds of *T. chinensis*.

1. Experimental Conditions

Taxus cell suspensions were maintained in darkness at 25 ± 2° C in a modified Gamborg's B5 medium [34]. Erlenmeyer flasks (125 ml, 60 rpm), 1 L nippled flasks on a clinostat (1 rpm), high-aspect rotating vessels (100 ml HARV 12.5 cm dia.) and rotating cylindrical culture vessels (100 ml RCCV 7.5 cm dia.) both at 10^{-2} x g (Synthecon, Houston, TX). The HARV and RCCV were used by NASA in early space shuttle experiments, and in a mini-payload integration center, designed as an in-flight laboratory [35].

Since weightlessness represents the condition where the acceleration of a cell is independent of its mass, true weightlessness is never achieved, even in the RCCV and HARV bioreactors that simulate 10^{-2} x g. The clinostat was a poor simulator of microgravity because its rotational motion generates centrifugal forces, particle oscillations with mass-dependent amplitudes of speed, and phase shifts, relative to the clinorotation [36]. The clinostat simulates 2 x 10^{-4} x g, but with significant convective mixing of the gaseous and liquid environment around cells. Cells on semi-solid medium, moist filter paper or on PVPF membranes in Petri dishes were placed in low-speed laboratory centrifuges set at 3x, 20, 24 and 150xg. The lift-off of the space shuttle imposes ca 3 x gravity. Null hypotheses and conclusions were supported by t-tests or by analysis of variance (ANOVA ± 5%).

2. NO Production is Controlled by NOS Substrates, Inhibitors and Traps

Ambient oxygen was used in all studies. NO released in, and from cells into the culture medium, was visualized with a fluorescent probe, *viz*. 4,5-diaminofluorescein diacetate (DAF-2DA). This probe is highly specific at high pH for NO [37]. A red diaminorhodamine probe [38] with greater stability, and not pH dependent, was also tested, but with few visual differences between the two probes. The DAF-2DA gave clearer green images.

The following experiment with *T. brevifolia* reports the effects of a NO donor, sodium nitroprusside (SNP), L-NMMA (NOS inhibitor), D-NMMA (control, a non inhibitor of NOS), and PTIO (2-(4-carboxyphenyl)-4,4,5,5-tetramethyl-imidazoline-1-oxyl-3-oxide, a stable radical scavenger for NO) on NO production. Heat-killed cells (1 g fresh wt) as a control did not produce NO. At unit gravity, 19% of the amyloplasts in live controls produced low levels of NO (Plate 1.3). Added 10^{-4} mM SNP quickly produced NO in > 98% of the cells. All cells centrifuged at 150 x g produced high levels of NO. NO production was reduced to 26% when cells were centrifuged with 0.5 mM L-NMMA. When D-NMMA was substituted for L-NMMA, 92% of the cells produced NO. NOS activity was not significantly blocked by D-NMMA. NO production was inhibited only by the levorotary NOS inhibitor. This is consistent with the enzyme specificity expected of plant NOS activity. The addition of PTIO trapped most of the NO so that levels of NO were below the live controls.

In cells treated with SNP, 3-nitrotyrosine was found in the free amino acid pool and in protein hydrolysates. SNP nitrated the tyrosine residues of cell proteins, which were turned over and released 3-nitrotyrosine into the free amino acid pool. At 10^{-4} M SNP, cell protein

contained 40 μM 3-nitrotyrosine/g dry weight (0.03% of the tyrosine residues were nitrated). The free amino acid fraction of cells contained 0.21 μM of 3-nitrotyrosine/g dry weight.The nitration of cell-regulatory proteins would block cell cycling, change the composition free amino acid pool, and predispose apoptosis.The percent free asparagine nearly doubled, while glutamine tripled to comprising 55 and 25% of the free amino acid pool, respectively. Now 80% of the soluble pool was dominated by amides at the expense of a corresponding percent drop in aspartate, glutamate, and alanine. Aspartate and glutamate N rather than providing N for arginine and NO biosynthesis now diverted their N to amides.

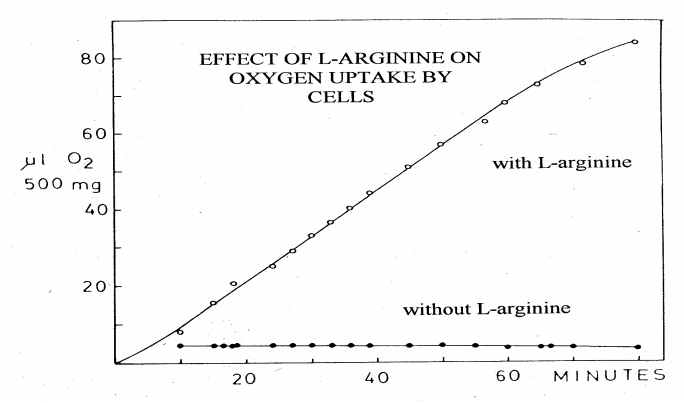

Figure 3. The addition of L-arginine to cells (500 mg fresh wt) at pH 6.2 consumes oxygen consistent with L-arginine and oxygen being substrates for nitric oxide synthase.

3. Naturally occurring guanidino compounds regulate plant NOS activity

A method for the determination of monosubstituted guanidines was developed and combined with an automated amino acid analyser designed for physiological fluids [39]. The Sakaguchi reagent, paper chromatography, and authentic chemical standards, were also used to compile lists of the yet unidentified naturally occurring guanidines in plants [8,9]. All are candidates as NOS inhibitors.

In conifers, the synthesis and accumulation of naturally occurring guanidines in the free amino acid pool is favored by supplying ammonium rather than nitrate [40]. The addition of L-arginine to cells under aseptic conditions consumes considerable oxgyen, the required substrate for NOS activy (Figure 3). Guanidines alter the generation of NADP, effect the citric acid cycle, and inhibit mitochondrial respiration [41].

Synthetic NOS inhibitors with a guanidino moiety, such as *S*-2-aminoethylisothiourea (AET or 2-mercaptoethyl guanidine), and bis-(2-guanidinoethyl) disulfide (GED) minimize the damage of DNA to ionizing radiation [42]. They have yet to be evaluated for a protective function against UV radiation damage. AET increases chlorophyll levels in *Phaseolus* [43]. Transamidination of the guanidino moiety accounts for the biosynthesis of most naturally occurring guanidines.

4. High Levels of NO Predispose Apoptosis

Apoptosis helps in remodeling tissues during developments and when plants respond to environmental changes. The connection between the intensity of NO bursts and apoptosis in gymnosperms and angiosperms was demonstrated by Pedroso *et al.* [19]. The TUNEL reaction distinguished morphologically and histochemically, apoptotic from nonapoptotic cells. Nuclei were counterstained with 1 μg/mL 4'-6-diamino-2-phenylindole dihydrochloride (DAPI). The TUNEL reaction uses the terminal deoxynucleotidyl transferase (TdT)-mediated dUTP labeling of the 3'OH ends of DNA generated by DNA nicking during the apoptosis [16,17]. Chloroplast DNA fragmentation was also detected *in situ* by the TUNEL method (Color Plate 1.8, 1.9).

NO formation, DNA fragmentation and cell death was observed using a Nikon (Tokyo, Japan) inverted microscope equipped with UV (excitation 360 nm; emission 420 nm) and FITC (excitation 450-490 nm; emission 520 nm) filters. Confocal images were obtained using Leitz Fluor 40x and 100x 1.3NA oil PL FLUOTAR objective lenses in a Leica TCS-NT confocal laser scanning microscope (Leica Lasertechnik GmbH, Heidelberg, Germany) equipped with Argon/Krypton and UV lasers (ex. spliter DD488/586), and Leica TCS-NT software (TCS-NT version 1.5.451). Serial confocal optical sections were taken at 1μm.

Untreated cell populations (controls) at unit gravity never showed more than 3% death. SNP added at 10^{-6}, 10^{-4}, and 10^{-2} M yielded 18, 33, and 76 % apoptosis, respectively. The centrifugation of cells (3 x g), centrifugation plus L-NMMA, and centrifugation plus D-NMMA gave 35, 9, and 32% apoptosis, respectively. NO released from SNP contributed to 3-nitrotyrosine formation, and to increased apoptosis. NO production and apoptosis were significantly reduced by the addition of the NOS inhibitor, L-NMMA.

5. Effects of Gravitational Forces on Growth, Taxol Biosynthesis and Recovery

A National Cancer Institute survey reported that our *T. brevifolia* genotype produced an 'average' solvent-extractable taxol content of 0.01% (w/w bark) compared to populations on the Pacific coast. Cells contained 0.05, 0.002, and 0.002 % taxol, cephalomannine, and baccatin III respectively. By 1995, it was already known that hypo- and hyper-gravity increased taxol and epicuticular wax biosynthesis in the Canadian yew (*T. canadensis*) [44]. Large-scale diploid tissue cultures were reported to yield up to 55 mg free taxol per liter per week [27].

Free baccatin III, taxol, and taxanes in cells and in the culture medium, or bound products released after xylanase activity, were measured with competitive inhibition enzyme-linked immunoassay (CIEIA) kits from Hawaii Biotechnology for anti-baccatin (TA-12), anti-taxol (TA 13), and anti-taxanes (TA 14) [26,29] (Figure 4). For samples larger than 10 g fresh biomass, the taxanes extracted were separated and determined using their absorption spectra during elution by HPLC with taxil columns (MetaChem Technologies Inc.). Cells were examined by laser confocal microscopy (Zeiss LSM 410 Invert Scan Microscope) for fluorescent double-labeling with FITC (green) and Cy3 (red) of the taxane ring (baccatin III) or the C-13 side chain. Co-location of the two antibodies (yellow) indicated the simultaneous occurrence of both moieties. Gold labeling was especially useful to identify products of biosynthesis in transport vesicles, the plasmalemma, cell walls, and in the culture medium.

Colloidal 40 nm gold-immunolabeled antibodies to taxanes, taxol, and baccatin III were visualized with 7 to 21 nM sensitivity, with and without gold backscatter [46], (Figure 5).

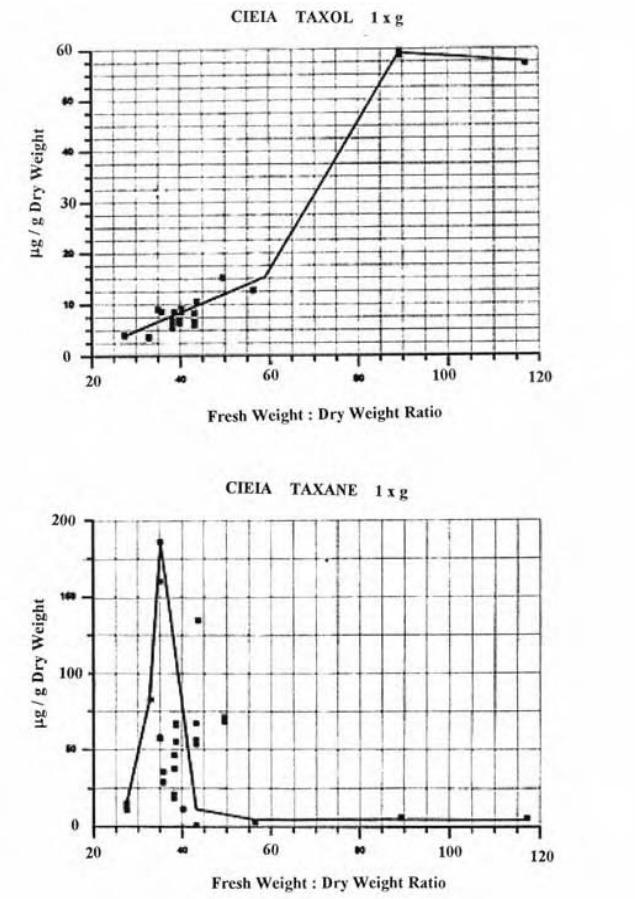

Figure 4a. Top. *T. cuspidata.* The recovery pattern for free taxol (µg/g dry wt) using competitive inhibition immunoassays at unit gravity, and as a function of the dry and fresh weigh ratio of biomass. Bottom. Taxanes in the same samples were recovered at much lower dry and fresh weight ratios.

With *T. cuspidata* in RCCV bioreactors and in 1 L nippled flasks after 3 wks (darkness at 24 ^{0}C), free taxol comprised 42 and 21 percent of the total taxanes (21 and 42 mg taxol/kg air-dry biomass weight), respectively. Centrifugation at 3 and 24 x g increased taxane content more than 500 fold but reduced taxol recovery from 42 to 7% of the total taxanes [30]. The

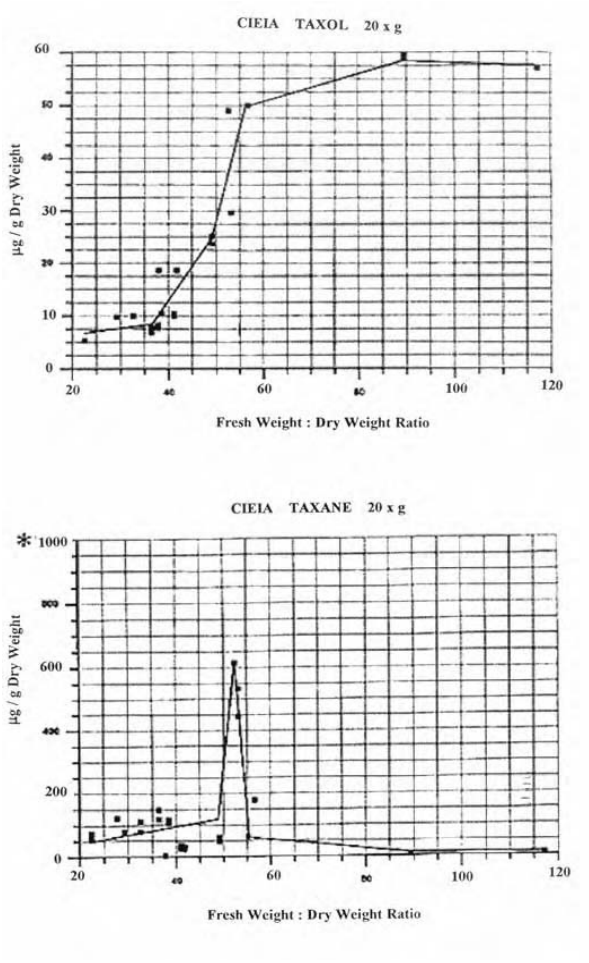

Figure 4b. Top. Centrifugation at 20xg increases the recovery of taxol at lower fresh and dry weight ratios. Bottom. Taxane recovery was markedly increased at higher fresh and dry weight ratios. Note the high scale for the y-axis.

recovery of taxol and taxanes at 1 and 20 x g as a function of the ratio of fresh weight to dry weight is shown in Figure 4. Taxol recoveries varied with biomass fresh and dry weight ratios. Taxane recovery at 20 x g was greatly increased at high fresh/dry weight ratios.

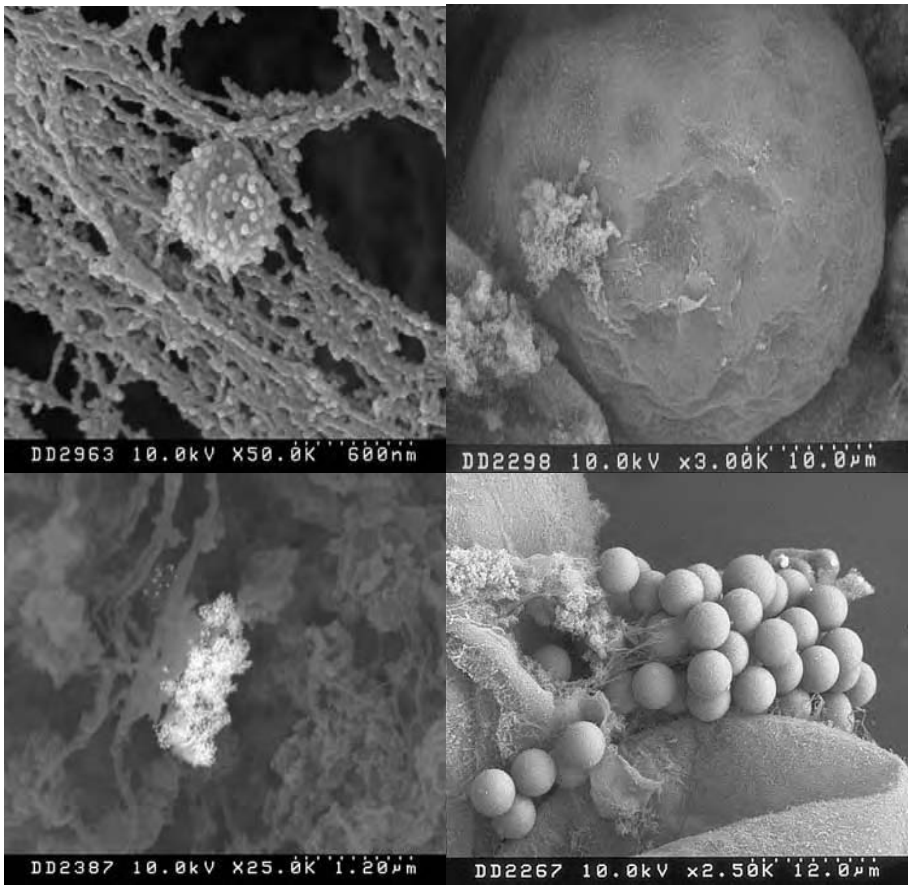

Figure 5. Left Top. *T. cuspidata*. Scanning electron microscopy (SEM) shows the combined colloidal-immunogold-antibody labeling of taxanes, taxol, and baccatin III (TA12, 13, 14). A surface gold-labeled vesicle is transported by motor proteins along cytoskeletal filaments within a cell. **Left Bottom**. A large vesicle, having more immunogold-labeled taxol, taxane, and baccatin III is highlighted by 'gold backscatter' SEM. Note the faint backscatter on the small vesicles with 8 or more gold beads to the left. **Top Right.** SEM image of the surface of a cell releasing bound taxane-bearing materials to the medium. **Bottom Right**. Labeled paramagnetic beads locate bound taxol and taxanes, and pull open and label the inside of the cell.

The tetracyclic diterpenoid ring of taxol is synthesized by cyclization of geranylgeranyl diphosphate to give taxa-4(5),11(12(-diene) in plastids and in light and darkness [28, *cf*. 45]. This basic ring structure gives rise to over 350 different taxanes (taxoids) [25]. One of these, baccatin III, provides the ring structure for the biosynthesis of taxol. Although the mechanism is not yet clear, taxol formation requires the addition of a C-13 side-chain originating from phenylalanine. Finishing structural changes for taxol and other taxanes involve modifications and hydroxylations in the endoplasmic reticulum and Golgi stacks (Plate 1.6).

Actin microfilaments, and microtubules, provide stability for cell shape, architecture, and for transport systems in cells responding to changing environments. Bound taxol precursors were processed by vesicles arising from plastid membranes. Drug-bearing vesicles were transported along cytoskeletal filaments to the plasmalemma, where taxol and taxanes were incorporated into newly forming cell walls (Figure 5, Color Plate l.7). The release of bound products into the culture medium occurs by exocytosis or secretion. Secretion was blocked by 7-dehydrobrevfeldin A (unpublished, *cf.* [47]). Products may also be discharged into the culture medium by 'osmocytosis' i.e., the deletion of parts of the plasma membrane [48] or by discharge of the surface materials.

The SEM of cell surfaces revealed several sites for the release of taxanes at the plasmalemma (Figure 5, top right). The number of sites was a function of how many amyloplasts and vesicles engaged in drug transport and release. In simulated microgravity, the flares of discharging materials changed the buoyancy and drag of suspended cells (Color Plate 1.6).

6. NOS activity Increases Free Taxol Recovery

In media lacking nitrate, NO production was associated directly with NOS activity. Reduced N was added (500 mg/L L-glutamine) to replace the nitrate and to provide N for arginine biosynthesis. Nitrate addition with or without L-arginine served as controls.

With *T. brevifolia* at unit gravity, cells exposed to the NO-donor SNP produced18 mg/Kg fresh weight of taxol after 10 d, (64% higher than the control without SNP). NO production was significantly and positively correlated with increased taxol yield. (unpublished studies by Drs H-C Dong and C. Pedroso). The number of cells showing NO production with SNP, was 86.7% higher than the control. The addition of the NOS inhibitor, L-NMMA (0.5 mM), reduced taxol recovery by 75% to 4.1 mg/Kg fresh weight, and NO production decreased by 87.3%.

In a separate study, the effects of SNP (10^{-4} mM), a nitrate reductase inhibitor (sodium tungstate, 1 mM), and L-NMMA were used to evaluate taxol recovery after 5 d. SNP added alone, or tungstate and SNP added together, accumulated taxol at 8.0 and 8.1 mg/Kg fresh weight. Nitrate reductase was not a significant contributor to NO and taxol production. The addition of L-NMMA alone, or with added tungstate, reduced taxol recovery to 2.1 and 2.0 mg/Kg fresh weight, respectively. This reaffirmed that NOS was the source of NO for enhancing taxol production. Taxol recovery was increased, albeit less effectively, by removing nutrients and starving *T. brevifolia* cells. It is possible that the calcium released during extended mechanical or gravitational stress, convectional mixing or starving, would activate the NOS genes and trigger apoptosis.

7. Recovery of Bound Taxol and Taxanes from Conifer Wood and Pulp

Touch genes (*TCH)* are expressed by plants in response to the gravitational and mechanical forces, and wind [50-52]. Expressed *TCH4* encodes a xyloglucan endotransglycosylase (XET) that modifies and strengthens the cell wall at xyloglucan sites. This can lead to tracheid and fiber formation in cells (Figure 6) [15, 17].

Covalently bound taxanes occur in the wood of conifers [26,32,49,53]. The 7-OH

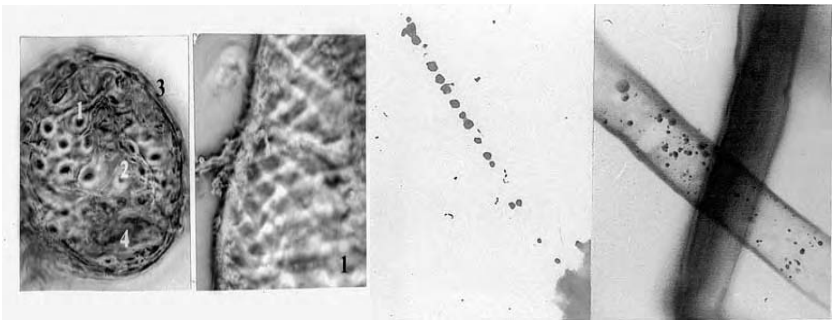

Figure 6. Left. *T. brevifolia*. Under strong mechanical forces, egg cells strengthen their cell walls with carbohydrates (iodine stained) from the amyloplasts (zones 1-4). Right. Differentiation continues as cells differentiate into tracheids. **Figure 7. Right.** Left. Norway spruce (*Picea abies* Karst.) untreated pulp contains bound taxanes (anti-taxane probe). Right. Bright-field image of the same fibers.

group of xyloglucan oligosaccharides in cells walls and wood link to the taxol ring forming 7-xylosyl derivatives of taxol and 10-deacetyltaxol. Xylanase treatment of wood fibers from *T. brevifolia* followed by HPLC (Taxil 5 μm MetaChem Technologies column, 66% methanol isocratic elution, 0.66 ml/min at 25 ^{0}C) yielded 10-deacetyl baccatin III, baccatin III, 10-deacetyl taxol, cephalomannine, taxol, and 7-epi-10-deacetyl taxol and a few unidentified taxanes. By comparison, the free taxanes recovered from RCCV and HARV bioreactors included many unidentified products, taxol, cephalomannine, baccatin III, and 10-deacetyl baccatin III.

Samples of enzymatically processed Norway spruce wood pulp were obtained from Finland, where enzymatic pulping is used in the environmental friendly manufacture of paper and other products. The pulp samples comprised xylanase-untreated (control) and treated (bleached) pulp. Treated pulp was prepared with a commercial xylanase (Ecopulp TX, Primalco, at 100 nkat xylanase/g dry pulp for 2 hours at pH 5). This xylanase was of commercial quality and not completely pure. Slight hydrolysis of other carbohydrates, e.g., glucomannan, cellulose, lignin, would occur. In this treatment, taxanes attached in cinnamoyl complexes would be broken when the xylanases released lignin.

The second treatment used purified xylanase (100 and 5000 nkat/g) from *Trichoderma reesei*. Treated and untreated pulp fibers were probed with antibodies for baccatin III, taxol and taxanes labeled with Alexa 488 for microscopic visualization with controls. These compounds were detected only in untreated pulp (Figure 7). Taxanes were not detected in xylanase-treated fibers even after 2 and 24 hour hydrolysis. The higher concentrations and times simply hydrolyzed more xylan residues. Yields were 0.7 ± 0.04 and 0.17 ± 0.04 μg/100 g of pulp for taxanes and taxol, respectively (CIEIA TA02 and TA04 analyses were provided by Hawaii Biotechnology).

Pulp mills are a major bulk source of conifer fibers, but the recovery of taxanes would require significant changes in enzymatic and nonenzymatic pulping methods. The economics and proof of this concept have not been worked out nor attempted.

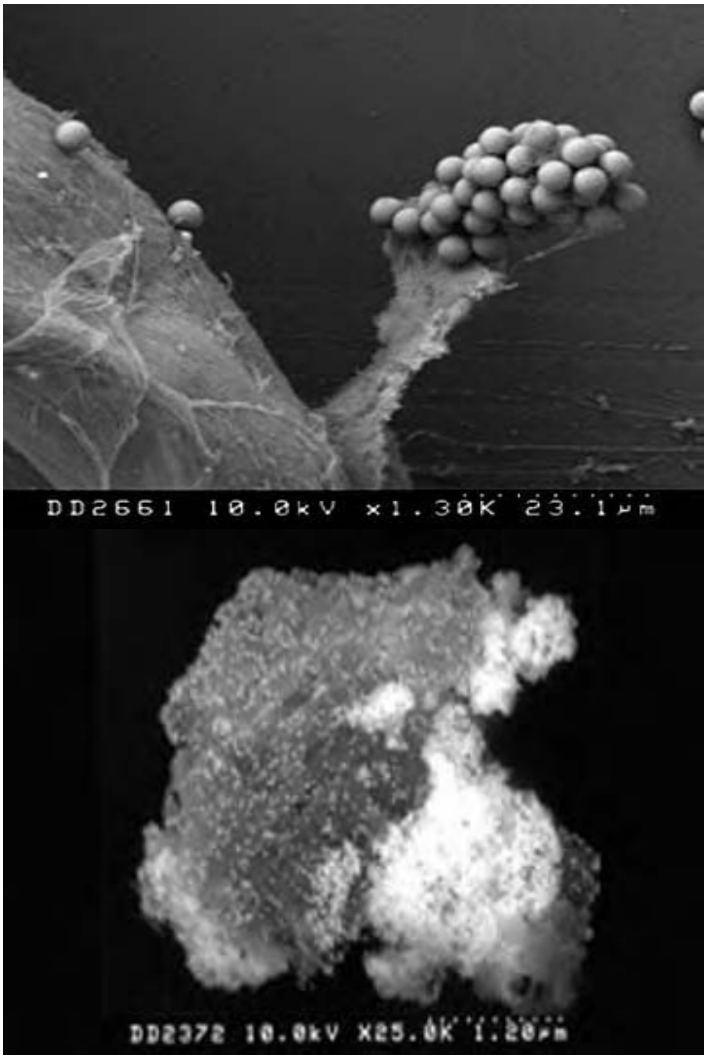

Figure 8. Top. *T. cuspidata.* Dynal paramagnetic beads, dia. of 4.5 microns, with anti-taxol bind to the surface material of a drug productive cell. Note the individual beads attached to fibers on the cell wall and inside the cell. **Bottom.** Collective baccatin III, taxol, and taxane labeling (immunogold, 40 nm dia.) of a plasmamembrane isolated from the culture medium reveals linear striations of gold leading to the densely labeled gold clusters. Limit of detection is ca. 7 nM.

8. Recovery of Drug-producing Cells and Cellular Materials

It would be an advantage to produce free and bound taxol and taxanes without depending on the need for live cultures. The cells and surface materials responsible for drug synthesis were

recovered by coated Dynal beads (M-450, 4.5 micron dia.). These are superparamagnetic, monodispersed, polymer beads with a hydrophobic surface. The beads were coated with sheep anti-mouse IgG molecules, and with anti-baccatin III, anti-taxol, and anti-taxane probes. A rare-earth cobalt magnet was used to collect the Dynal beads bound to the drug-containing cells, membranes, and fibers. Removal of the magnet freed and re-suspended the isolated cells and materials. This enriched the populations of drug-productive cells and cellular debris for further culture and study. After 10 d of culture, only ca. 6 % of the cells in suspension were recovered with taxol-labeled Dynal beads.

The recovery of bound products using Dynal beads offers materials that will be useful to collect and reveal the sequences of enzymes that are naturally responsible biosynthesis of taxol [53]. Membranes and cell materials may serve as cell-free preparations for the semi-synthesis of natural isomers, intermediates, and finished products having added structural specificity. This approach would benefit from a better understanding of taxol biosynthesis, rate-limiting enzymes, and the identification of the genes coding for the biosynthetic pathway.

The taxol on cells, membranes, and fibers was further located with 40 nm immunogold labeling. Labeling patterns revealed that the interdiffusion of polymers with taxol and taxanes occurred without significant intertanglement (Figure 8). The movement of a single flexible polymer in a newly forming cell wall or membrane seemed constrained by local obstacles, and to specific membrane and wall locations. The drug-bearing polymers formed by creeping, reptation [54], and possibly emerged further into the medium by percolation [55]. Their construction, assembly, and integration in membranes and cell walls may be usefully described by fractal reaction kinetics [56].

Cell wall enzymes involved in the distribution of polymers would include proton-ATPases, expansins, endoglucanases, pectinases, peroxidases, pectin esterases, and debranching enzymes. All bound and freed taxol, synthesized this way, even if chemically identical to authentic standards, must be tested for effectiveness in the appropriate assays and clinical trials.

9. Syneresis and Drug Recovery from Cells

A few cells of *T. brevifolia* somehow survived 150 x g continuously for three weeks in darkness without undergoing apoptosis or xylogenesis. The distribution of organelles inside cells was skewed to one side in a contracted cytoplasm. Cells near the bottom of the buckets survived on the factors or ‘necrohormones’ released by syneresis or from apoptotic cells. When the surviving live cells were plated back into unit gravity on fresh semisolid medium, callus was slowly regenerated after two or three months.

Exposures to 20 x g for 1h contracted the cytoplasm with a separation of liquids and materials from gels (syneresis). The liquids and materials containing taxol and taxanes released from cells were collected on hydrophobic PVDF (polyvinylidene fluoride) filters that supported the cells (Figure 9). Taxol recovery at 1 x g and 20 x g was ca. 3 and 24 µg/g dry weight, respectively. The greatest yields came from cells having the greatest fresh weight to dry weight ratio, rather than from those that were less vacuolated and more cytoplasmically dense.

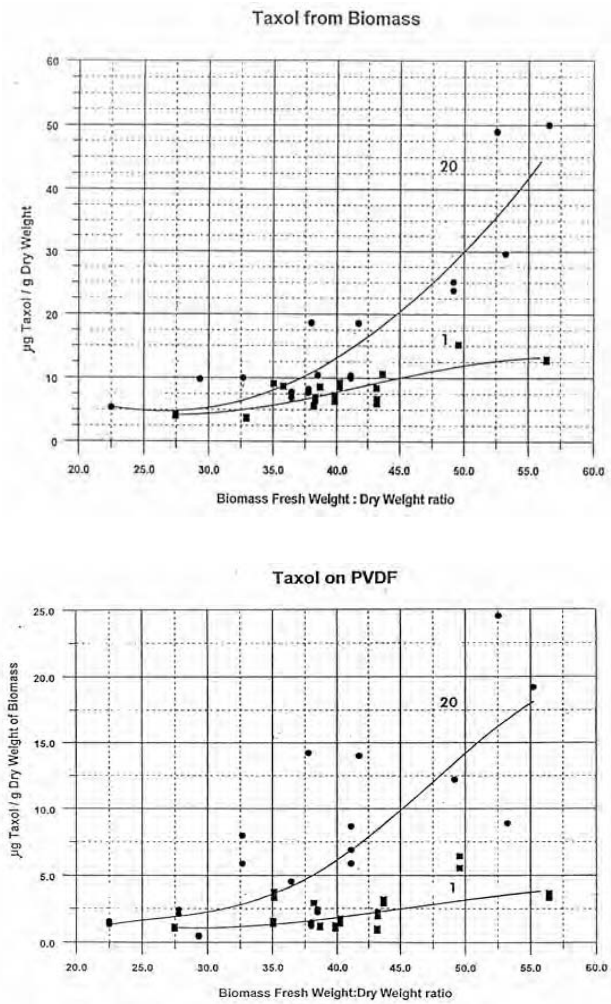

Figure 9. **Top**, *T. cuspidata*. Suspensions centrifuged at 20 x g for 1 hour produced more free taxol than at 1 x g but the recovery was a function of the fresh and dry weight ratio of cell populations. **Bottom**. Additional free taxol from cells at 1 and 20 x g were recovered on PVDF filters.

10. Opportunities and Challenges

The production of high-valued drugs using cell bioreactors has been historically disappointing [57, 58]. Taxol has recently been synthesized by Samyang Genex in small and large-scale balloon-type bubble bioreactors. Cell biomass was doubled by 12 d with a 30% inoculation density [59]. More than 70% of the cells remained viable at harvest. After 27d, the yield was 3

mg/L taxol and 74 mg/L total taxanes. Taxol produced in cell bioreactors in Korea is now marketed as Genexol®.

Regarding the prospects for metabolic engineering [61, 67], nitrate, L-arginine, NO release, guanidines, and apoptosis have yet to be tested as factors controlling taxol recovery on a large scale. Chlorsulfuron has value in reversibly maintaining cell cycling in the G1 phase for drug biosynthesis [61]. Biomass can first be scaled up and then G1 used for drug biosynthesis without the need to divert cellular energy and metabolites to replicate cells. Circadian genes that regulate the phasic and antiphasic expressions in the G1 of the cell cycle may also be involved

Cell-lines, suited to bioreactor conditions, remains an important factor in the adaptation of cells to aeration, nutrient feed, mechanical action, shear stress, gas circulation, etc., and to downstream processing [e.g. 61-65]. The long-term maintenance of stock cultures remains costly and a liability. While the use of drug-productive haploid or double-haploid cell lines may offer more long-term adaptive stability [66], the use of cell-free and enzymatic systems would provide more reliable control for drug biosynthesis

The US patent literature teaches us that cyclodextrins added to culture media are effective in isolating hydrophobic compounds such as taxol produced by cell cultures [68, 69]. Cyclodextrins are cyclic oligosaccharides, consisting of 6, 7, or 8 glucose units. Cyclodextrins introduced into culture medium increase *Taxus* cell biomass, improve development, and enhance drug recovery. Cyclodextrins alter the physico-chemical properties that determine taxane solubility in water or organic solvents.

Drug semisynthesis from extracted taxanes is now economically controlled by physical and chemical conditions. Three novel enzymes were discovered that convert taxanes into 10-deacetylbaccatin III (taxol without the C-13 side-chain and C-10 acetate), a precursor for taxol semisynthesis. The enzymes cleave the C-13 side chain, the C-10 acetate, and the C-7xylose from various xylosyl taxanes. The chemical coupling of 10-deacetylbaccatin III or baccatin III to the C-13 side chain of taxol offers a method to prepare taxol by semisynthesis using precursors extracted from natural sources [45].

A new drug, discodermolide, from an ocean sponge has dramatically enhanced the effectiveness of taxol [70]. When combined with taxol, the drug reduced the proliferation of lung-cancer cells in a lab setting by 41%. Administered alone, discodermolide reduced cancer-cell growth by 10%. Taxol alone reduced it by 16 percent. These drugs synergistically inhibited microtubule dynamics, mitosis, blocked cell cycle progression at G2-M, and enhanced apoptosis. This illustrates that much more work remains to be done. We are a long way from understanding the full potential of the wide range of natural products from *Taxus* sp., and how stresses imposed on cells control drug production in bioreactors.

Acknowledgements

This work was impossible without the support from NASA's Microgravity Grant No. 9-825. Special thanks go to Mr. Frank Ventimiglia, Dr. Cristina Pedroso and Dr. H-C Dong for the taxol, taxane, apoptosis, taxol and taxane assays. The author also thanks Dr. Maija Tenkanen at VTT Biotechnology and Food Research in Finland for supplying treated and untreated pulp samples. Dr. Dave Dorward at the National Institutes of Health, Rocky Mountain Laboratory, prepared the scanning electron micrographs.

References

[1] Durzan D.J. and Pedroso M.C., "Nitric Oxide and Reactive Nitrogen Oxide Species in Plants". *Biotechnology & Genetic Engineering Reviews,* vol. 19, p.p. 293-337, 2002.

[2] Leshem Y.Y., Occurrence, Function and Use of NO in Plants. Hingham:Kluwer Academic Publ. Dordrect, 180 pp, 2000.

[3] Durzan D.J., "Nitrogen metabolism of *Picea glauca*. I. Seasonal changes of free amino acids in buds, shoot apices and leaves, and the metabolism of uniformly labeled ^{14}C-L-arginine by buds during the onset of dormancy". *Canadian J. Botany, ,* vol. 46, p.p. 909-919, 1968a..

[4] Durzan D.J., "Nitrogen metabolism of *Picea glauca*. II. Diurnal changes of free amino acids, amides, and guanidino compounds in roots, buds, and leaves during the onset of dormancy of white spruce saplings". *Canadian J. Botany,* vol. 46, p.p. 921-928, 1968b.

[5] Durzan D.J., "Nitrogen metabolism of *Picea glauca*. III. Diurnal changes of amino acids, amides, protein, and chlorophyll in leaves of expanding buds". *Canadian J. Botany.* vol. 46, p.p. 929-937, 1968c.

[6] Durzan D.J., "Nitrogen metabolism of *Picea glauca*. IV. Metabolism of uniformly labelled ^{14}C-L-arginine, [carbamyl-^{14}C]-L-citrulline, and [1,2,3,4-^{14}C]-γ-guanidinobutyric acid during diurnal changes in the soluble and protein nitrogen associated with the onset of expansion of spruce buds". *Canadian J. Biochemisty, ,* vol. 47, p.p. 771-783. 1969a..

[7] Durzan D.J. and Chalupa V., "Growth and metabolism of cells and tissue of jack pine (*Pinus banksiana*). 5. Changes in free arginine and Sakaguchi-reactive compounds during callus growth and in germinating seedlings of similar genetic origin". *Canadian J. Botany, ,* vol. 54, p.p. 483-495, 1976.

[8] Durzan D.J. and Steward F.C., "Nitrogen metabolism", Chap. 2. In "Plant Physiology, an Advanced Treatise", F.C. Steward (ed.), Academic Press, Inc., New York, , vol. 8, p.p. 55-265, 1983.

[9] Bidwell R.G.S. and Durzan D.J,. "Some Recent Aspects of Nitrogen Metabolism". *In Historical and Recent Aspects of Plant Physiology: A Symposium Honoring F.C. Steward*, Cornell Univ. Press, College Agriculture and Life Science. p.p. 162-227, 1975.

[10] Garcês H, Durzan DJ, Pedroso MC. 2001. "Mechanical stress elicits nitric oxide formation and DNA fragmentation in *Arabidopsis thaliana*". *Annals of Botany,* vol. 87, p.p. 567-574, 2001.

[11] Guo F.-Q., Okamoto M. and Crawford N.M,. "Identification of a plant nitric oxide synthase gene involved in hormonal signaling". *Science,* vol. 302, p.p. 100-103, 2003.

[12] Chandok M.R., Ytterberg A.J., van Wijk K.J. and Klessig D.F., "The pathogen-inducible nitric oxide synthase (iNOS) in plants is a variant of the P protein of the glycine decarboxylase complex". *Cell ,* vol. 113, p.p. 469-482, 2003.

[13] Magalhaes J.R., Pedroso M.C. and Durzan, D.J., "Nitric oxide, apoptosis and plant stresses". *Physiology and Plant Molecular Biology,* vol. 5, p.p. 115-125, 1999.

[14] Magalhaes J.R., Monte D.C. and Durzan D.J., "Nitric oxide and ethylene emission in *Arabidopsis thaliana*". *Physiology and Plant Molecular Biology,* vol. 6, p.p. 117-127, 2000.

[15] Havel L. and Durzan D.J., "Apoptosis in plants". *Botanica Acta,* vol. 109, p.p. 268-277, 1996.

[16] Havel L. and Durzan D.J., "Apoptosis during diploid parthenogenesis and early somatic embryogenesis of Norway spruce". *International J. Plant Science,* vol. 157, p.p. 8-16, 1996b.

[17] Havel L., Scarano T. and Durzan D.J., "Xylogenesis in *Cupressus* callus involves apoptosis". *Advances in Horticultural Science.* vol. 11, p.p. 37-40, 1997.

[18] Pedroso M.C., Magalhaes J.R. and Durzan D.J., "A nitric oxide burst precedes apoptosis in an angiosperm and a gymnosperm". *J. Exptl Botany,* vol. 51, p.p. 1027-1036, 2000a.

[19] Pedroso M.C., Magalhaes J.R. and Durzan D.J., "Nitric oxide induces cell death in *Taxus* cells". *Plant Science,* vol. 157, p.p. 173-181, 2000b.

[20] Wendehenne D., Pugin A., Klessig D.F. and Durner J., "Nitric oxide: comparative synthesis and signaling in animal and plant cells". *Trends in Plant Science.* vol. 6, p.p. 177-183, 2002.

[21] Waini M.C., Taylor H.L., Wall M.E., Coggon P. and McPahil A.T., "Plant antitumor agents. V1. Isolation and structure of taxol, a novel antileukemic and antitumor agent from *Taxus brevifolia*". *J. American Chem. Society,* vol. 93, p.p. 2325-2326, 1971.

[22] Francis A.L., "Pharmers market". *The Scientist,* vol. 14, 22 p., 2000.

[23] Goodman J. Walsh V. 2001. "The Story of Taxol. Nature and Politics in the Pursuit of an Anti-cancer Drug". Cambridge Univ. Press, Cambridge, 282 p.

[24 Appendino G., "The phytochemistry of the yew tree". *Natural Product Reports,* vol. 12, p.p. 349-360, 1995.

[25] Baloglu E. and Kingston D.G.I., "The taxane diterpenoids". *J Natural Products,* vol. 62, p.p. 1448 1472, 1999.

[26] Durzan D.J. and Ventimiglia F., "Free taxanes and the release of bound compounds having taxane antibody reactivity by xylanase in female, haploid-derived cell suspension cultures of *Taxus brevifolia*". *In Vitro Plant Cell and Developmental Biology,* vol. 30P, p.p. 219-227, 1994.
[27] Yukimune Y., Tabata H., Higashi Y. and Hara Y., "Methyl jasmonate-induced overproduction of paclitaxel and baccatin III in *Taxus* cell suspension cultures". *Nature Biotechnology,* vol. 14, p.p. 1129-1132, 1996.
[28] Jennewein S. and Croteau R., "Taxol: biosynthesis, molecular genetics, and biotechnological applications". *Applied Microbiology & Biotechnology,* vol. 57, p.p. 13-19, 2001.
[29] Grothaus P., Bignami G.S., O'Malley S., Harada K.E., Byrnes J.B., Waller D.F. and Raybould T.J., "Taxane-specific monoclonal antibodies: Measurement of taxol, baccatin III, and total taxanes in *Taxus brevifolia* extracts by enzyme immunoassay". *J. Natural Products,* vol. 58, p.p. 1003-1004, 1995.
[30] Durzan D.J., Ventimiglia F. and Havel L., "Taxane recovery from cells of *Taxus* in micro and hypergravity". *Acta Astronautica,* vol. 42, p.p. 455-463, 1998.
[31] Durzan D.J., "Gravisensing, apoptosis, and drug recovery in *Taxus* cell suspensions". *Gravitation and Space Biology Bulletin,* vol. 12, p.p. 47-55, 1999.
[32] Obst J.R., "Occurrence of Taxol and Related Taxanes in the Wood of Pacific yew". In: Scher S, Schwarzchild B.S., eds. Yew (Taxus) Conservation Biology and Interactions*. Proc. International Yew Resources Conference*, Univ. California, Berkeley, p. 25, 1993.
[33] Zeyl C., Vanderford T. and Carter M., "An evolutionary advantage of haploidy in large yeast populations". *Science* vol. 299, p.p. 555-559, 2003.
[34] Gamborg O.L., Murashige T., Thorpe T.A. and Vasil I.K., "Plant tissue culture media". *In Vitro Cell and Developmental Biology,* vol. 12, p.p. 473-478, 1976.
[35] Gonda S., "Space bioreactor bioproduct recovery system. MSAD OLMSA NASA HQ and Langley Research Centre". *Advanced Technology Development,* vol. 96, 2 p, 1996.
[36] Albrecht-Buehler G., "The simulation of microgravity conditions on the ground". *American Society Gravitational & Space Biology,* vol. 5 (2), p.p. 3-10, 1992.
[37] Kojima H., Nakatsubo N., Kikuchi K., Kawahara S., Kirono Y., Naogshi H., Hirata Y. and Nagano T., "Detection and imaging of nitric oxide with novel fluorescent indicators: dianminofluoresceins". *Analytical Biochemistry,* vol. 70, p.p. 2446-2453, 1998.
[38] Kojima H., Harridan M., Urana Y., Kikuchi K., Higuchi T. and Nagano T., "Fluorescent indicators for nitric oxide based on rhodamine chromophore". *Tetrahedron Letters,* vol. 41, p.p. 69-72, 2000.
[39] Durzan, D.J., "Automated chromatographic analysis of free monosubstituted guanidines in physiological fluids". *Canadian J. Biochemistry,* vol. 47, p.p. 657-664, 1969b.
[40] Durzan D.J. and Steward F.C., "The nitrogen metabolism of *Picea glauca* (Moench) Voss and *Pinus banksiana* Lamb. as influenced by mineral nutrition". *Canadian J. Botany,* vol. 45, p.p. 695-710, 1967.
[41] Davidoff F., "Effects of guanidines on mitochondrial function. IV. Changes in citric acid cycle intermediates and NADPH". *Bioenergetics,* vol. 3, p.p. 481-498, 1972.
[42] Kollman G., Shapiro B. and Martin D., "Mechanism of radioprotective action of GED against radiation damage to DNA". *Radiation Research,* vol. 31, p.p. 721-731, 1967.
[43] Kirchmann R., Bonotto S. and Bronchart B., « Accumulation des chlorophylles chez les feuilles primordiales de *Phaseolus vulagris* L. irradiées en presence d'AET ou de cystamine. II. Influence de l'AET et de al cystamine sur l'accumulation des chlorophylles ». *Radiation Botany,* vol. 11, p.p. 419-423, 1971
[44] Cseke L.J., Panutich M., Reichenbach D., Fozo P., Ghosheh N.S. and Kaufman P., "Effects of hyper-g and hypo-g stress treatments on taxol and epicuticular wax biosynthesis in Canadian yew (*Taxus canadensis*)". *Plant Physiology,* vol. 108S: abstract 713, p. 137, 1995.
[45] Patel R.M., "Tour de paclitaxel. Biocatalysis for semisynthesis". *Annual Review Microbiology,* vol. 98, p.p. 361-395, 1998.
[46] Namork E. and Heier H.E., "Backscatter electron imaging of double immunogold labeled erythrocytes using two primary monoclonal antibodies". *Microscopy Research and Technique,* vol. 28, p.p. 286-296, 1994.
[47] Driouich A., Jauneau A. and Staehelin A., "7-Dehyrdobrefeldin A, a naturally occurring brefeldin A derivative, inhibits secretion and causes a *cis*-to-*trans* breakdown of Golgi stacks in plant cells". *Plant Physiology,* vol. 113, p.p. 487-492, 1997.
[48] Oparka K.J., Prior D.A.M. and Crawford J.W., "Membrane conservation during plasmolysis". In: "Membranes: specialized functions in plants". ed: Smallwood M, Knox JP, Bowles DJ, Bios Scientific Publishers, Oxford, p.p. 39-56, 1996.
[49] Antosiewicz D.M., Polisensky D.H. and Braam J., "Cellular localization of the Ca^{2+} binding TCH3 protein of *Arabidopsis*". *The Plant Journal,* vol. 8, p.p. 623-636, 1995.

[50] Antosiewicz D.M., Purugganan M.M., Polisensky D.H. and Braam J., "Cellular localization of *Arabidopsis* xyloglucan endotransglycosylase-related proteins during development and after wind stimulation". *Plant Physiology,* vol. 115, p.p. 1319-1328, 1997.
[51] Xu W., Purugganan M.M., Polisensky D.H., Antosiewicz D.M., Fry S.C. and Braam J., "*Arabidopsis TCH4*, regulated by hormones and the environment, encodes a xyloglucan endotransglycosylase". *The Plant Cell,* vol. 7, p.p. 1555-1567, 1995.
[52] Durzan D.J. and Ventimiglia F., "Recovery of taxanes from conifers". *US Patent No. 5,955,621.* September 21. (screening taxanes from Coniferales), 1999b.
[53] Durzan D.J. and Ventimiglia F., "Recovery of taxanes from plant material". *US Patent No. 5,981,777.* November 9. (Use of paramagnetic beads), 1999a.
[54] Klein J., "The interdiffusion of polymers". *Science,* vol. 250, p.p. 640-646, 1990.
[55] Stark C.P., "An invasion percolation model of drainage network evolution". *Nature, vol.* 352, p.p. 423-425, 1991.
[56] Kopelman R., "Fractal reaction kinetics". *Science,* vol. 241, p.p. 1620-1626, 1988.
[57] Pezzuto J., "Taxol production in plant cell culture comes of age". *Nature Biotechnology,* vol. 14, p. 1083, 1996.
[58] Verpoorte R., Van der Deuden R., Ten Hoopen H.J.G. and Memelink J., "Metabolic engineering for the improvement of plant secondary metabolite production". *Plant Tissue Culture and Biotechnology,* vol. 4, p.p. 3-20, 1998.
[59] Son S.H., Choi S.M., Lee Y.H., Choi K.B., Yun S.R., Kim J.K., Park H.J., Kwon O.W., Noh E.W., Seon J.H. and Park Y.G., "Large-scale growth and taxane production in cell cultures of *Taxus cuspidata* (Japanese yew) using a novel bioreactor". *Plant Cell Reports,* vol. 19, p.p. 628-633, 2000.
[60] Choi H.K., Kim S.I., Son J.S., Song J.Y., Hong S.S., Durzan D.J. and Lee H.J., "Localization of paclitaxel in suspension cultures of *Taxus chinensis*". *J. Applied Microbiology & Biotechnology,* vol. 11, p.p. 458-462, 2001.
[61] Durzan D.J., "Metabolic Engineering Plant Cells in a Space Environment". *Biotechnology & Genetic Engineering Reviews,* vol. 17, p.p. 349-383, 2000.
[62] Bringi V., Kadkade P.G., Prince C.L., Schubmehl B.F., Kane E.J. and Roach B., "Enhanced production of taxol and taxanes by cell cultures of *Taxus* species". *U.S. patent No. 5,407,816,* 1995.
[63] Pestchanker L.J., Roberts S.C. and Shuler M., "Kinetics of paclitaxel production and nutrient use in suspension cultures of *Taxus cuspidata* in shake flasks and a Wilson type bioreactor". *Enzyme Microbiology. & Technology,* vol. 19, p.p. 256-260, 1996.
[64] Ketchum R.E.B., Gibson D.M., Croteau R.B. and Shuler M.L., "The kinetics of taxoid accumulation in cell suspension culture of *Taxus* following elicitation with methyl jasmonate". *Biotechnology & Bioengineering,* vol. 62, p.p. 97-105, 1999.
[65] Meijer J.J., Hoopen H.J.G., Luyben K. and Libbenga K.R., "Effects of hydrodynamic stress on cultured plant cells: a literature survey". *Enzyme Microbiology & Technology,* vol. 15, p.p. 234-238, 1993.
[66] Durzan D.J. and Ventimiglia F., "Taxane production in haploid-derived cell cultures". *US Patent No. 5,5547,866.* November 9, 1996.
[67] Bailey J.E., "Toward a science of metabolic engineering". *Science,* vol. 252, p.p. 1275-1279, 1991.
[68] Durzan D.J. and Ventimiglia F., "Cyclodextrins in plant nutrient formulations". *US Patent No. 6,087,176.* July 11, 2000.
[69] Eliseev A.V., "Charged cyclodextrin derivatives and their use in plant cell and tissue culture growth media". *US Patent Application Publication No. 2004/0106199 A1.June 3,* 2004.
[70] Honore S., Kamath K., Braguer D., Horwitz S.B., Wilson L., Briand C. and Jordan M.A., "Synergistic suppression of microtubule dynamics by discodermolide and paclitaxel in non-small carcinoma cells". *Cancer Research,* vol. 64, p.p. 4957-4964, 2004.

COLOR PLATE 1

1.1. *T. brevifolia*. Isolation and culture of an immature female gametophyte released numerous individual egg cells under aseptic conditions. Each protoplast is ca. 200 μ dia and can produce thin cell walls. **1.2.** Ripe egg cells have 8 haploid nuclei. **1.3.** When cells are stressed their amyloplasts produce NO (green fluorescence with DAF-2A). **1.4.** NO is produced in the plasma membrane and around amyloplasts that settle at the plasma membrane. Amyloplasts are responsible for the synthesis of the taxane ring. **1.5.** Antibodies specific to baccatin III (green) are

localized in amyloplasts that dock at the plasmalemma. Baccatin-derived taxanes and taxol are then released into the culture medium or into the cell wall via the plasma membrane. Release sites tend to have the same diameter as the docking amyloplasts (dark shadows beneath the cell surface) (*cf.* Figure 5). Red background is autofluorescence. Nuclei are blue (DAPI). **1.6.** *T. cuspidata*. Taxanes (green, yellow, and red) are processed by the endoplasmic reticulum and Golgi stacks before their release into the culture medium. **1.7**. Surface view of a cell releasing taxol (yellow), baccatin-derived taxanes (green), and taxanes having *N*-benzoyl-3-phenylisoserine side-chain (red). Note the free-floating taxane-bearing materials in the culture medium. **1.8.** *T. brevifolia*. Amyloplasts and membranes release NO (green DAF-2A) in a cell with apoptotic nuclei (TUNEL blue-green nuclei). **1.9.** A fragmenting apoptotic cell releases bound taxol and taxanes (green) into the medium. Fragmenting nucleus (blue, DAPI), autofluorescence (red).

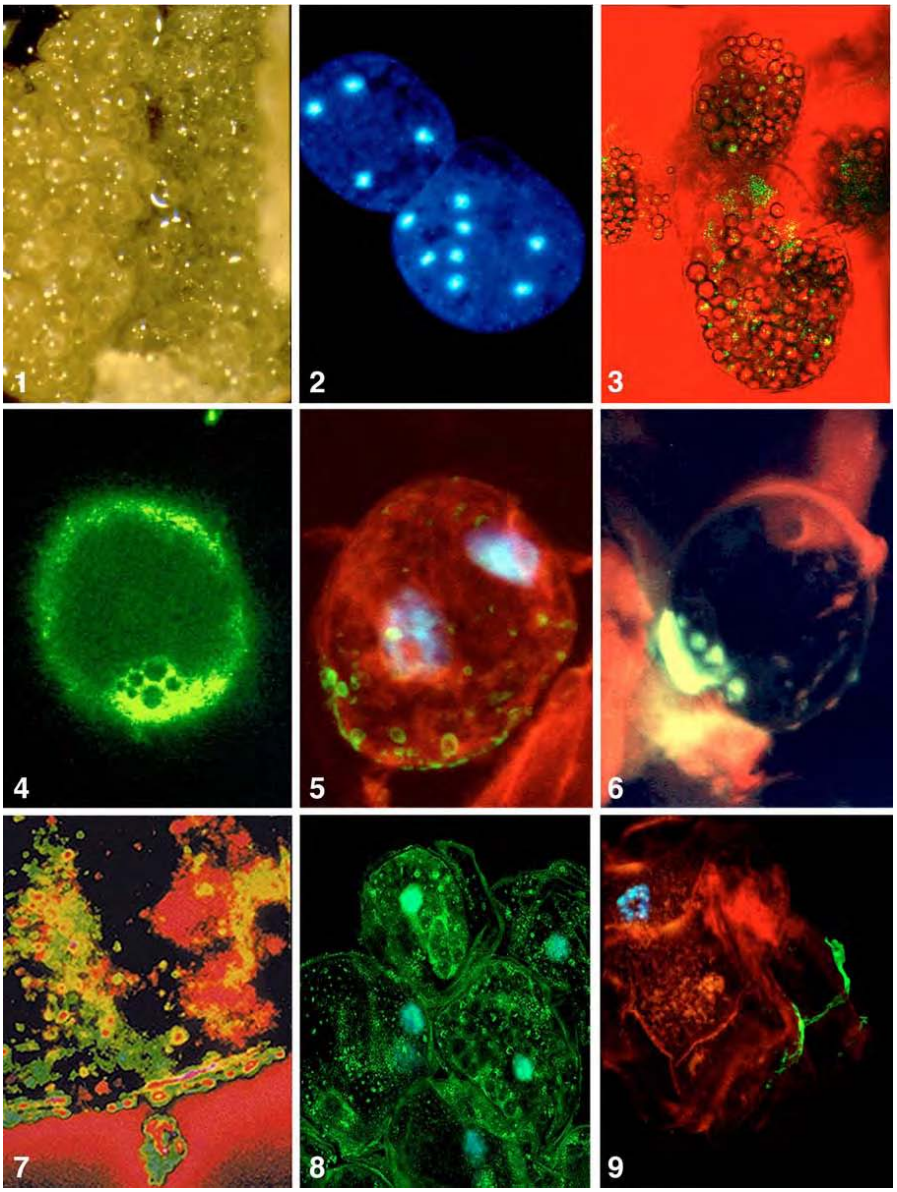

Cell Biology and Instrumentation: UV Radiation, Nitric Oxide and Cell Death in Plants
Y. Blume et al. (Eds.)
IOS Press, 2006

Glutathione-dependent Formaldehyde Dehydrogenase/GSNO Reductase from *Arabidopsis*. Expression Pattern and Functional Implications in Phytoremediation and Pathogenesis

M. Carmen MARTÍNEZ, Maykelis DÍAZ, Hakima ACHKOR and M. Carme ESPUNYA
Departamento de Bioquímica y Biología Molecular. Facultad de Ciencias. Universidad Autónoma de Barcelona. 08193 Bellaterra (Barcelona). Spain

Abstract. The glutathione-dependent formaldehyde dehydrogenase (FALDH) is the main enzyme of the formaldehyde detoxification system in eukaryotes. In *Arabidopsis*, it is coded by a single gene, which is constitutively expressed in the plant tissues. The importance of FALDH has been greatly increased by the discovery of its potent activity toward S-nitrosoglutathione, the condensation product of glutathione and nitric oxide (NO). Due to this activity it has also been named GSNO reductase (GSNOR). We have characterized the *Arabidopsis* FALDH showing that it exhibits kinetic and molecular properties in common with its mammal counterparts. Cloning of the gene encoding *Arabidopsis* FALDH (*ADH2*) and construction of transgenic plants allowed us to investigate the potential applications of FALDH in phytoremediation of formaldehyde. Our results show that overexpression of FALDH in *Arabidopsis* plants results in a 25% increase in their efficiency to eliminate exogenous formaldehyde, whereas plants with reduced levels of FALDH, bearing antisense constructs, exhibit a reduced ability and slower rate in formaldehyde elimination. We have also investigated *ADH2* regulation by signals associated with plant defense, demonstrated that it is responsive to mechanical wounding, jasmonic acid and salicylic acid.

1. Introduction

Glutathione-dependent formaldehyde dehydrogenase (FALDH; EC 1.2.1.1), also known as class III alcohol dehydrogenase, is a widely distributed enzyme and highly conserved medium-chain dehydrogenase reductase. It catalyzes the NAD-dependent formation of S-formylglutathione from S-hydroxymethylglutathione, which forms spontaneously from formaldehyde and glutathione [1]. The high conservation of the enzyme and its universal presence in prokaryotes and eukaryotes suggest a role in basic defense mechanisms of formaldehyde elimination. FALDH has been characterized and sequenced from a few plant species, including pea, maize and *Arabidopsis thaliana* [2, 3, 4, 5]. Structure comparisons and phylogenetic relationships confirm that FALDH, that belongs to the complex family of alcohol dehydrogenases, constitutes a divergent family, common to plants and animals, while the ethanol-active forms from plants (class P) and animals (class I) constitute separate structures [3]. Evolutionary studies positions FALDH as an apparent ancestor from which all members of the ADH family are derived [6].

The importance of FALDH has been greatly increased by the recent discovery of its potent activity toward S-nitrosoglutathione, the condensation product of glutathione and nitric oxide (NO) [7, 8, 9]. NO and NO-related metabolites, such as S-nitrosothiols (SNOs) play a central role in signal transduction and host defence [10, 11, 12]. This positions FALDH as a putative candidate to modulate NO levels and regulate NO-signaling functions.

2. Results

2.1. Molecular properties of Arabidopsis FALDH

Arabidopsis FALDH cDNA *(ADH2,* accession number X82647) was cloned by a PCR-based approach using degenerated oligonucleotides corresponding to conserved regions of the polypeptide chain [2]. Genome blotting on *Arabidopsis* DNA suggested that FALDH is a single-copy gene that was later mapped on chromosome 5 [4]. Amino acid sequence deduced from the full-length cDNA demonstrated that the *Arabidopsis* enzyme exhibits a typical class III structure (69-89% identities with the corresponding forms from humans and pea) while the relationships with the ethanol-active ADHs (class I for mammals and class P for plants) are considerably lower (53-58% identities) (Table I).

The enzyme shows very low expression levels in *Arabidopsis thaliana* plants (5 mu/mg protein, [2]), and thus we used *Saccharomyces cerevisiae* as expression system to produce and characterize the recombinant enzyme [13]. *Arabidopsis* FALDH, purified from *S. cerevisiae* has a molecular mass of 45 kDa, a specific activity of 15 units mg^{-1}, and a K_m value of 7 μM. The FALDH purified from a variety of different sources consists of two identical subunits and is, thus, a homodimer [1]. Based on a dimeric structure for *Arabidopsis* FALDH, we calculated a k_{cat} value of 1351 min^{-1}, and a k_{cat}/K_m of 193,000 mM^{-1} min^{-1}. This last value, which is the catalytic efficiency, is comparable with those of pea and other eukaryotes [3, 14].

Table I. Relationship of plant FALDHs (*Arabidopsis* and pea) to the human FALDH and to the ethanol-active forms (ADH I from humans and class P from plants).

	Arabidopsis FALDH	Pea FALDH	Human FALDH	*Arabidopsis* P	Pea P
Pea FALDH	89				
Human FALDH	69	69			
Arabidopsis P	59	58	54		

Pea P

58
58
51
84

Human ADHI

53
54
62
51
47

2.2 Gene expression and gene regulation.

Northern blot analysis shows that *ADH2* mRNA levels are similar in all plant organs (Figure 1), in analogy with the ubiquitous distribution of the corresponding enzyme in animal tissues. This is also compatible with a constitutive pattern of expression proposed for the animal class III enzyme.

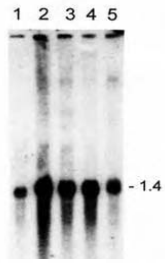

Figure 1. Northern-blot analysis in *Arabidopsis* tissues. 15 µg total RNA from 2-week-old plantlets grown in liquid medium (lane 1), and from flowers (lane 2), leaves (lane 3), roots (lane 4), and 10 µg total RNA from shoots (lane 5) from adult plants were loaded. A radiolabeled probe derived from *Arabidopsis* FALDH cDNA was used. Size of the transcript (kb) is indicated on the right.

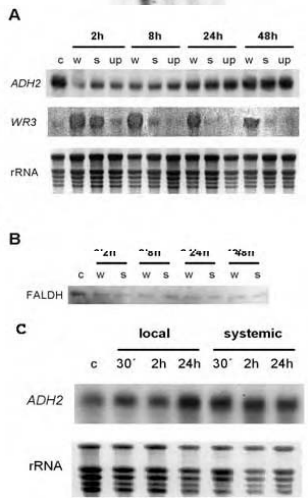

Figure 2. Wound-induced repression of FALDH in *Arabidopsis*. Plants were sampled at the indicated times after wounding. A: 5 µg of total RNA were loaded per lane and blots were hybridized with ^{32}P-labelled probes derived from *ADH2*, or from WR3 (an *Arabidopsis* wound-inducible gene, [16]). Ethidium bromide-stained rRNAs are shown as loading control. B: Western blot analysis using an anti-FALDH antibody. The Coomassie-blue stained membrane is shown as loading control. C: Northern-blot analysis of the wound response in *Arabidopsis coi* mutant (JA-insensitive). Abbreviations: c, control rosette leaves from unwounded plants; w, wounded rosette leaves; s, systemic unwounded rosette leaves from wounded plants; up, cauline leaves from wounded plants

The strong GSNO reductase activity exhibited by FALDH makes this enzyme a strong candidate to modulate intracellular concentrations of GSNO/NO and regulate NO-signaling functions. This prompted us to investigate the response of the *ADH2* gene to wounding and to several hormones that act as signals for biotic and abiotic stress [15]. Our results demonstrate that *ADH2* gene expression is down-regulated by wounding, and that the response is transient and systemic (Figure 2A). A stronger repression is observed in locally injured leaves than in systemic leaves and, in both cases, the expression return to basal levels by 48 hours after wounding. Western blot analysis demonstrate a concomitant decrease in FALDH levels, that is first observed 2 hours after wounding and persisted up to 48 hours (Figure 2B). This repression is abolished in the *coi, Arabidopsis* mutant (Figure 2C), that is jasmonic-insensitive, supporting the idea that JA mediates the wound-induced repression of *ADH2* gene in *Arabidopsis*.

Salicylic acid is also an important signal in plant defense responses. An increase in the intracellular SA levels is necessary for transcriptional activation of defense genes [17, 11] and for the establishment of the systemic acquired resistance (SAR) [18]. Exogenous application of 500 µM SA or 1 mM SA to *Arabidopsis* plantlets provokes a clear increase in FALDH levels that correlate with an increase in *ADH2* mRNA levels (Figure 3). These results strongly suggest a transcriptional up-regulation of *ADH2* gene by SA.

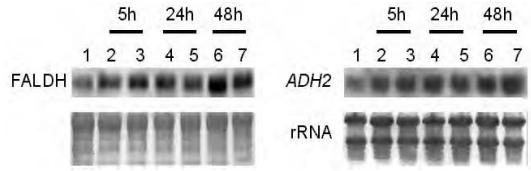

Figure 3. Up-regulation of FALDH by Salicylic acid in *Arabidopsis*. Seedlings were treated with 0.5 mM SA (lanes 2, 4 and 6) or 1 mM SA (lanes 3, 5, and 7) for the indicated times. Samples were analyzed by Western (left panel) or Northern blots (right panel).

2.3 Potential applications of FALDH in the phytoremediation of formaldehyde. Elimination of exogenous formaldehyde by transgenic Arabidopsis plants.

Formaldehyde is a toxic compound produced during plant C1 metabolism, mainly from methanol oxidation [19] and from 5,10-methylene-tetrahydrofolate. It can also have an exogenous origin from industrial waste, being a polluting agent of residual waters and of air [20, 21]. It is one of the main indoor air pollutants that has been classified as a mutagen and suspected carcinogen [5]. Exogenous formaldehyde can be incorporated into the metabolism of photosynthetic cells and be used as a carbon source [21]. Removal of formaldehyde can occur by different *in vivo* pathways [22] but biochemical and genetical studies in several eukaryotes point to the FALDH as the main enzyme responsible for the metabolism of intracellular formaldehyde. To investigate the potential applications of this enzyme in phytoremediation of exogenous formaldehyde we generated transgenic plants by transformation of *Arabidopsis* with either sense or antisense constructs of the *ADH2* gene, and we measured the formaldehyde elimination rate by the different lines.

FALDH cDNA was cloned under the control of the 35SCaMV promoter [13]. Three independent lines, exhibiting from 11- to 18-fold the wild type FALDH activity, were used to test the capacity of plants overexpressing FALDH to eliminate exogenous formaldehyde. We observed an increase in the elimination rate of 25%, both at 2 mM and at 5 mM

formaldehyde (64 ml L^{-1} and 132.5 ml L^{-1}, respectively) (Figure 4). At 2 mM formaldehyde, plants overexpressing FALDH could completely eliminate the exogenous formaldehyde in 48h or less, without any visible damage. To the contrary, antisense lines, with decreased levels of FALDH enzyme, showed a 20% decrease in their ability to eliminate formaldehyde. These results show that the capacity to take up and detoxify high concentrations of formaldehyde is proportionally related to the FALDH activity in the plant, revealing the essential role of this enzyme in formaldehyde detoxification.

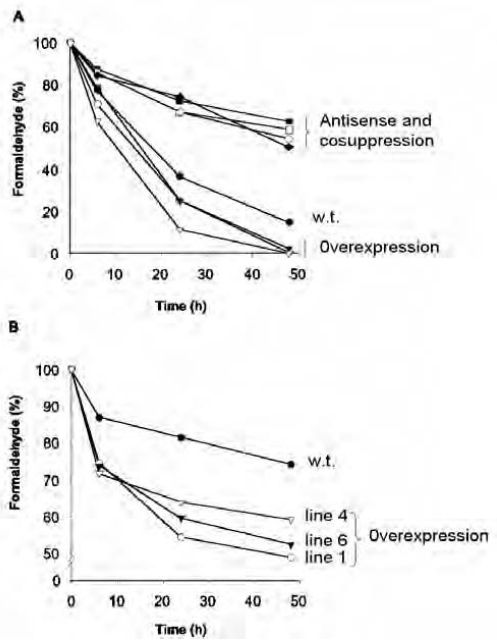

Figure 4. Kinetics of formaldehyde detoxification. Seedlings germinated and grown in liquid medium were subjected to formaldehyde treatment at an initial concentration of 2 mM (A) or 5 mM (B), respectively. Data are shown as % formaldehyde remaining in the liquid culture at different times after inoculation. *Arabidopsis* wild type plants (w.t.) or *Arabidopsis* transgenic lines overexpressing the enzyme (overexpression) or with reduced levels of the enzyme (antisense and co-suppression lines) were used in the experiment.

3. Conclusions

The molecular and kinetic properties of *Arabidopsis* FALDH are remarkably similar to those of other FALDH forms studied in mammals, invertebrates and microorganisms [23], providing evidence of the high degree of structural and functional conservation of this enzyme throughout all life forms. The low Km for S-hydroxymethylglutathione is comparable with the values reported for the FALDH from animals. These values are appropriate for the elimination of the endogenous formaldehyde produced in plants and animals. In contrast, FALDH from yeast and bacteria exhibits a much higher Km,

consistent with a potentially higher level of formaldehyde in the environment of microorganisms [23].

The strong expression of *ADH2* gene in all tissues of *Arabidopsis* adult plants is consistent with the constitutive pattern of expression reported in animal species and suggests a similar role in plants and animals, most probably related to the elimination of endogenous formaldehyde. However, we have demonstrated that *ADH2* is transcriptionally regulated in response to signals associated to plant defense, i.e. wounding, jasmonic acid and salicylic acid. These results have important implications for a role of FALDH in pathogenesis and may be related to the strong GSNO reductase activity exhibited by FALDH. GSNO/NO are signaling molecules in plant defense that can activate plant defense genes [24]. NO production is necessary for the hypersensitive response in plant-pathogen incompatible interactions [11], and there is also a burst of NO after wounding and a subsequent activation of wound-inducible genes [12]. FALDH might play a role in turning off/on NO or GSNO signaling, and in modulating the concentration of intracellular thiol compounds that can generate nitrosative stress.

The up-regulation of the *ADH2* gene in response to SA suggests a role of FALDH in protection against oxidative stress and/or nitrosative stress. In mice and yeast, deletion of the gene encoding FALDH increases the susceptibility of the cells to nitrosative challenge and produces an accumulation of nitrosylated proteins [8]. Although the interrelationship between the NO and ROS signaling pathways in plants is currently unclear, both compounds stimulate the accumulation of SA [25, 26]. One of the consequences of the oxidative stress is lipid peroxidation that might generate formaldehyde and other reactive lipid peroxidation products that can be eliminated by FALDH.

Living plants are very efficient at absorbing contaminants from the environment and, thus, they may provide valuable tools to reduce contamination. Formaldehyde is a ubiquitous chemical found in virtually all indoor environments with important toxic effects in humans. We have achieved a significant reduction in the amount of exogenous formaldehyde by using transgenic plants that overexpress the enzyme FALDH. These plants are able to take up and detoxify formaldehyde without any visible damage, supporting the "green liver" concept of plant xenobiotic metabolism [27].

References

[1] Uotila L. and Koivusalo M., "Glutathione-dependent oxidoreductases: formaldehyde dehydrogenase". In: Coenzymes and cofactors. Glutathione: chemical, biochemical and medical aspects. Vol III, part A (Dolphin D, Poulson R, Avramovic O eds) John Wiley and Sons, New York, p.p. 517-55, 1989.

[2] Martínez M.C., Achkor H., Persson B., Fernández M.R., Shafqat J., Farrés J., Jörnvall H. and Parés X., "*Arabidopsis* formaldehyde dehydrogenase. Molecular properties of plant class III alcohol dehydrogenase provide further insight into the origins, structure and function of plant class P and liver class I alcohol dehydrogenase". Eur. J. Biochem., vol. 241, p.p. 849-85, 1996.

[3] Shafqat J., El-Ahmad M., Danielsson O., Martínez M.C., Persson B., Parés X. and Jörnvall H., "Pea formaldehyde-active class III alcohol dehydrogenase, p.p. common derivation of the plant and animal forms but not of the corresponding ethanol-active forms (classes I and P)". *Proc. Natl. Acad. Sci. USA*, vol. 93, p.p. 5595-5599, 1996.

[4] Dolferus R., Osterman J.C., Peacock W.J. and Dennis E.S., "Cloning of the *Arabidopsis* and rice formaldehyde dehydrogenase genes, p.p. implications of the origin of plant ADH enzymes". *Genetics*, vol. 146, p.p. 1131-1141, 1997.

[5] Wippermann U., Fliegmann J., Bauw G., Langebartels C., Maier K. and Sandermann H. Jr., "Maize glutathione-dependent formaldehyde dehydrogenase: protein sequence and catalytic properties". *Planta*, vol. 208, p.p. 12-18, 1999.

[6] Danielsson O. and Jörnvall H., ""Enzymogenesis": classical liver alcohol dehydrogenase origin from the glutathione-dependent formaldehyde dehydrogenase line". *Proc. Natl. Acad. Sci. USA*, vol. 89, p.p. 9247-9251, 1992.

[7] Jensen D.E., Belka G.K. and Du Bois G.C., "S-Nitrosoglutathione is a substrate for rat alcohol dehydrogenase class III isoenzyme". *Biochem J*., vol. 331, p.p. 659-668, 1998.
[8] Liu L., Hausladen A., Zeng M., Que L., Heitman J. and Stamler J.S., "A metabolic enzyme for S-nitrosothiol conserved from bacteria to humans". *Nature*, vol. 410, p.p. 490-494, 2001.
[9] Sakamoto A., Ueda M. and Morikawa H., "*Arabidopsis* glutathione-dependent formaldehyde dehydrogenase is an S-nitrosoglutathione reductase". *FEBS Lett*., vol. 515, p.p. 20-24, 2002.
[10] Wendehenne D., Pugin A., Kessig D.F. and Durner J., "Nitric oxide, p.p. comparative synthesis and signaling in animal and plant cells". *Trends Plant Sci*., vol. 6, p.p. 177-183, 2001.
[11] Delledonne M., Xia Y., Dixon R.A. and Lamb C., "Nitric oxide functions as a signal in plant disease resistance". *Nature*, vol. 394, p.p. 585-588, 1998.
[12] Huang X., Stettmaier K., Michel C., Hutzler .P, Mueller M.J. and Durner J., "Nitric oxide is induced by wounding and influences jasmonic acid signaling in *Arabidopsis thaliana*". *Planta*, vol. 218, p.p. 938-946, 2003.
[13] Achkor H., Díaz M., Fernández M.R., Biosca J.A., Parés X. and Martínez M.C., "Enhanced formaldehyde detoxification by overexpression of glutathione-dependent formaldehyde dehydrogenase from *Arabidopsis*". *Plant Physiol*, vol. 132, p.p. 2248-2255, 2003.
[14] Fernández M.R., Biosca J.A., Martínez M.C., Achkor H., Farrés J. and Parés X., "Formaldehyde dehydrogenase from yeast and plant. Implications for the general functional and structural significance of class III alcohol dehydrogenase". *Advances in Experimental Medicine and Biology,* vol. 414 (H. Weiner, ed.). Plenum Press, New York, pp. 373-381, 1997.
[15] Díaz M., Achkor H., Titarenko E. and Martínez M.C., "The gene encoding glutathione-dependent formaldehyde dehydrogenase/GSNO reductase is responsive to wounding, jasmonic acid and salicylic acid". *FEBS Lett*, vol. 543, p.p. 136-139, 2003.
[16] Titarenko E., Rojo E., León J. and Sánchez-Serrano J., "Jasmonic acid-dependent and -independent signaling pathways control wound-induced gene activation in *Arabidopsis* thaliana". *Plant Physiol*., vol. 115, p.p. 817-826, 1997.
[17] Vernooij B., Uknes S.J., Ward E. and Ryals J., "Salicylic acid as a signal molecule in plant-pathogen interactions". *Curr. Opin. Cell Biol*., vol. 6, p.p. 275-279, 1994.
[18] Ryals J.A., Neuenschwander U.H., Willits M.G., Molina A., Steiner H.-Y. and Hunt M.D., "Systemic acquired resistance". *Plant Cell*, vol. 8, p.p. 1809-1819, 1996.
[19] Fall R. and Benson A.A., "Leaf methanol - the simplest natural product from plants". *Trends Plant Sci*., vol. 1, p.p. 296-301, 1996.
[20] Wolverton B.C., Johnson A. and Bounds K., "Interior landscape plants for indoor air pollution abatement". Final Report. National Aeronautics and Space Administration*,* John C. Stennis Space Center, Mo, USA, 1989.
[21] Giese M., Bauer-Doranth U., Langebartels C. and Sandermann H. Jr., "Detoxification of formaldehyde by the spider plant (*Chlorophytum comosum* L.) and by soybean (*Glycine max* L.) cell-suspension cultures". *Plant Physiol*., vol. 104, p.p. 1301-1309, 1994.
[22] Hanson A.D. and Roje S., "One-carbon metabolism in higher plants". *Ann. Rev. Plant Physiol. Plant Mol. Biol*., vol. 52, p.p. 119-137, 2001.
[23] Fernández M.R., Biosca J.A., Norin A., Jörnvall H. and Parés X., "Class III alcohol dehydrogenase from *Saccharomyces cerevisiae*, p.p. structural and enzymatic features differ toward the human/mammalian forms in a manner consistent with functional needs in formaldehyde detoxication". *FEBS Lett*., vol. 370, p.p. 23-26, 1995.
[24] Durner J. and Klessig D.F., "Nitric oxide as a signal in plants". *Curr. Opin. Plant Biol*., vol. 2, p.p. 369-374, 1999.
[25] Durner J., Wendehenne D. and Klessing D.F., "Defense gene induction in tobacco by nitric oxide, cyclic GMP, and cyclic ADP-ribose". *Proc. Natl. Acad. Sci. USA*, vol. 95, p.p. 10328-10333, 1998.
[26] Kumar D. and Klessig D.F., "Differential induction of tobacco MAP kinases by the defense signals nitric oxide, salicylic acid, ethylene, and jasmonic acid". *Mol. Plant Microbe Int*., vol. 13, p.p. 347-351, 2000.
[27] Sandermann H., "Plant metabolism of xenobiotics". *Trends Biochem. Sci*., vol. 17, p.p. 82-84, 1992.

This page intentionally left blank

PLANT STRESS AND PROGRAMMED CELL DEATH

This page intentionally left blank

Cell Biology and Instrumentation: UV Radiation, Nitric Oxide and Cell Death in Plants
Y. Blume et al. (Eds.)
IOS Press, 2006

Effect of Chlorsulfuron on Early Embryo Development in Norway Spruce Cell Suspensions

Don J. DURZAN[1], Anne SANTERRE[1], and Ladislav HAVEL[2]
[2]*Department of Plant Science, MS 6, University of California, One Shields Ave. Davis, CA 95616 USA, and* [2] *Department of Botany and Plant Physiology, Mendel University of Agriculture and Forestry, 613-00 Brno, Zemědělská 1, Czech Republic*

Abstract. In diploid parthenogenesis, proembryos developed from binucleate egg-equivalents containing an egg nucleus and an apoptotic ventral canal nucleus. As the axial tier of early embryos formed, the cell regulatory proteins in proembryonal cells were ubiquitinated and turned over as suspensors differentiated. Axial-tier formation was blocked at high levels of chlorsulfuron, an inhibitor of acetolactate synthase. This enzyme is required for the biosynthesis of branched-chain amino acids, which are especially abundant in ubiquitin. The block of acetolactate synthase led to the accumulation of free α-amino-n-butyrate. The overall behavior of branched-chain amino acids revealed rigid and linear relations over all chlorsulfuron levels. The proliferating cell nuclear antigen (PCNA), required for DNA synthesis, was detected in rapidly cycling proembryonal cells. PCNA appeared to serve as a factor maintaining the cell replication typical of rapidly growing early embryos. Less than 0.01% of nuclei reacted with epitopes to anti-p53 and anti-p21 that are commonly associated with cell cycle arrest and DNA damage. The cleavage sites of early embryos involved apoptosis and contributed to their multiplication. Chlorsulfuron contributed to aborted axial-tier development due to disrupted patterns for the ubiquitination of cell regulatory proteins and changes in the soluble amino acid pool.

Introduction

Evidence is provided for the participation of proteins having epitopes that regulate cell division and body-plan development in early embryony in Norway spruce cell suspensions. Second, acetolactate synthase is blocked by the herbicide, chlorsulfuron, to show how axial-tier development in early embryos is altered, and how these changes become evident in the composition of the soluble N pool.

The experimental control of early embryo development in plants under natural and artificial conditions deals with the inception and regulation of basic organization and early body plan (1, 2, 3 and 4). Even so, models of somatic embryogenesis in angiosperms (5, 6, 7), and gymnosperms (8) have not always recognized the importance of the early free nuclear stages, cleavage polyembryony, parthenogenetic alternatives, nor latent diploid parthenogenesis (LDP) (2).

Oogenesis in spruce and pine occurs with the formation of a binucleate egg cell having an egg nucleus and an apoptotic ventral canal nucleus (9). Oogenesis is mimicked in cell bioreactors under artificial conditions where a large binucleate cell appears with nuclei often having similar fates. In the absence of fertilization, the egg equivalent nucleus

can replicate, especially after exposure to colchicine, become parthenogenic, or even die. The ability of these nuclei to form parthenogenetic diploid embryos is latent and expressed under certain controlled but artificial conditions (2). The parthenogenetic egg equivalent nucleus produces a neocytoplasm and a cell wall mimicking the processes in seeds (4, 10). In LDP, this new cell or its cellular derivatives is released from the cytoplasm of the original binucleate cell into the culture medium. The released products are usually called parthenotes.

Darlington (11) used the term 'parthenotes' for the products of parthenogenesis. Recognizing this distinction, and the terminology of Singh (4), we arbitrarily continue use the term 'proembryo', and 'early embryo', rather than 'proparthenote' and 'early parthenote', etc. This choice aims to minimize confusion to readers not familiar with parthenogenetic development and early conifer embryology. The development of an early embryo requires the formation of an axial tier of cells in the body plan. This tier comprises a proembyonal group of cells and embryonal-tube cells that contribute to the formation of the embryonal suspensor. The latter differentiates by apoptosis involving enucleation and nucleolar release to produce the elongated embryonal suspensors (12, 13 and 14). Suspensor formation requires the ubiquitination of cell regulatory proteins and the release of proteinaceous mucilage into the culture medium (15, 16).

The seed development of Norway spruce embryos was classified by Dogra (17) as occurring without cleavage polyembryony (non-cleavage type). In contrast, *Pinus* sp. expressed a cleavage-type polyembryony. Our work with cell suspensions expressing somatic embryogenesis and LDP clearly showed that cleavage polyembryony in Norway spruce was a significant multiplication factor that could be controlled by abscisic acid (18).

First, in describing the physiological gradients of the early embryo, we show that the mucilage released by cells contains a protein with an epitope derived from the proliferating nuclear cell antigen (PCNA). PCNA does not have any enzymatic activity. It is a DNA polymerase δ factor that re-enters dividing cells to maintain the rapid, cell-division rates typical of embryonic cells (19). It does this by binding to mitotic chromosomes to facilitate DNA replication, hence its role as a cell replication 'licensing factor'. PCNA also coordinates DNA replication, DNA repair, epigenetic inheritance, and cell-cycle control.

Second, preliminary evidence is provided for the occurrence of an epitope for a tumor necrosis factor (p53) that stops cell cycle progression in response to chlorsulfuron-dependent DNA damage. In animal cells, p53 activates the *WAF1/Cip1 (p21)* gene, and executes p53-dependent cell death (20). The *WAF1* gene is transcriptionally activated to produce p21 (21, 22). The p21 binds PCNA to stop DNA synthesis (23). Cytochemical evidence is provided to show that in Norway spruce cells having DNA damage at high chlorsulfuron levels, proteins with epitopes for p53 and p21 were detected in nuclei. While this does not prove that the animal cell model can be applied to Norway spruce, the results show that proteins with these conserved epitopes participate in the response to DNA damage and in apoptosis.

Third, the effect of chlorsulfuron on early development and on the composition of the free amino acid pool is evaluated. In plants, chlorsulfuron can usefully and reversibly block the mitotic cycle at G1 and G2 (24, 25). It also inhibits acetolactate synthase required for the synthesis of branched-chain amino acids, leucine, isoleucine, and valine (26). α-Amino-n-butyric acid (AANBA), which is not normally found in the soluble N pool of cells, accumulates when branched-chain amino acid synthesis becomes limited. Chlorsulfuron also restricts the formation of ubiquitin, which is a heat stable, 76-residue polypeptide in all eukaryotic cells. Leucine, isoleucine and valine comprise ca 25% of the molecular weight of ubiquitin (27). Ubiquitination determines the half-lives of normal cell

regulatory proteins whose concentrations change in response to a variety of signals and stresses (14, 28). The unavailability of branched-chain amino acids would limit ubiquitin biosynthesis and its role in regulatory protein turnover, and is predicted to block axial-tier development.

1. Materials and methods

Suspension cultures (cell line KJ1) of Norway spruce (*Picea abies* (L.) Karst.) were established as described by previously (2). Cell populations were fractionated on a Ficoll^{TM} gradient and grown in a 0.5 LP medium in darkness, with or without branched-chain amino acid supplements, and with or without chlorsulfuron. This enabled us to follow their subsequent developmental fates. Since acid casein hydrolysate contained branched-chain amino acids that would overcome chlorsulfuron's block of acetolactate synthase, the casein hydrolysate was omitted from media designated as 'free of branched-chain amino acids'.

Experimental design: Axial-tier development was studied over a range of chlorsulfuron concentrations (nil to 10^{-4} M) using not fewer than triplicated studies, and with the following medium formulations: 1. with casein acid hydrolysate (400 mg L), 2. without casein hydrolysate, but with a reconstituted hydrolysate lacking leucine, isoleucine and valine, and 3. a medium lacking branched-chain amino acids. Cells and tissues were harvested after four subcultures, each 7 to 10-days. Proembryos and early embryos were recovered from the Ficoll^{TM} gradient (2). Percent distributions for the numbers of cells in stained proembryos (Feulgen-Giemsa stained) having size-classes between 2 to 10 cells from chlorsulfuron treatments (> 5000 nM) lacking branched-chain amino acids were determined.

Histo- and immunocytochemical studies: Cells and tissues were fixed in a mixture of 95% ethanol and glacial acetic acid (3:1) for 24 h. This was followed with hydration in 35 and 17.5% ethanol and with water in 2-min. steps, and air-dried before staining with Feulgen and Giemsa (29), acetocarmine (30), or double-stained for apoptosis using DAPI (4'-6-diamidino-2-phenylindole dihydrochloride) and a modified TUNEL reaction (15). In the TUNEL reaction, endonuclease activity was determined by a terminal deoxynucleotidyl transferase (TdT). This enzyme labeled the 3'OH ends of DNA, generated by DNA nicking with biotin-conjugated dUTP, for visualization with sulforhodamine as a fluorescent marker. Nonapoptotic nuclei were TUNEL negative.

Untreated controls of fixed and unfixed cells were examined in not less than three slides for their immunocytochemical reactivity to epitopes of PCNA, p53, p21 (also designated as WAF1/Cip1). Assays were with or without the TUNEL reaction, and counterstained with DAPI. Fluorescent assays using anti-ubiquitin and anti-PCNA were described by Durzan (16) and Havel et al. (31). The p53 epitope (monoclonal) comprised amino acids 371-380 of the human p53 protein. This antibody detected wild-type and mutant p53. The epitope for p21 corresponded to amino acids 1-159 and represented the full length of p21 of mouse origin (Santa Cruz Biotechnology Inc. CA). It was specific for p21 and non cross-reactive with p27. Anti-p21was conjugated either to Cy3 or FITC. Controls for all immunocytochemical experiments included the use of two independent antibodies, control stains, and assays where the first antibody was omitted. Antibody reactivity was visualized using fluorescence of FITC- (green), sulforhodamine- or Cy3-conjugated (red) secondary antibodies. Antibodies were applied to spruce proteins and separated on SDS-Page gels to rule out cross-reactivity in specific protein fractions.

Amino acid determinations: Biomass was ground in a Waring blender and extracted with 80% ethanol until ninhydrin-positive substances were no longer removed.

Extracts were filtered and dried at 20 ^{o}C in a jet of cold air. Dried samples were dissolved in a known volume of pH 2.2, 0.2 M Li citrate buffer to which was added several ml of chloroform to remove pigments and lipids. Known volumes of buffered extract were applied to a Beckman automated amino acid analyzer for physiological fluids (Model 3600). For each study, free amino acids, amides and imino acids were determined in triplicate within ±5% error by the method of Slocum and Cummings (32). For the statistical correlations, a computer-assisted program (33) using the Pearson product-moment method was used (34, Table 1).

Figure 1 Left. Five-celled proembryo exposed to chlorsulfuron (< 50 mM) and stained with Feulgen-Giemsa. This structure released from egg equivalents represented ca 22% of the early developmental patterns found in cell suspensions that developed abnormally. **Figure 2 Right**. At low levels of chlorsulfuron, proembryo development and the differentiation of axial tiers with suspensors also became abnormal (*cf.* Figures 3, 4). Nuclei ca. 10 μm dia.

2. Results

The effect of chlorsulfuron on axial-tier development: The lack of branched-chain amino acids and >50 mM chlorsulfuron in the culture medium severely inhibited or blocked the development of the embryonal axial tier. The provision of branched-chain amino acids (with and without low levels of chlorsulfuron < 50 mM), produced mostly multinucleate egg-equivalents with the release of proembryos (sometimes termed proembryonal leader cells, *cf.* 2) with variable cell numbers. At high chlorsulfuron levels and without branched-chain amino acids, the egg equivalents were collapsed and morphologically apoptotic.

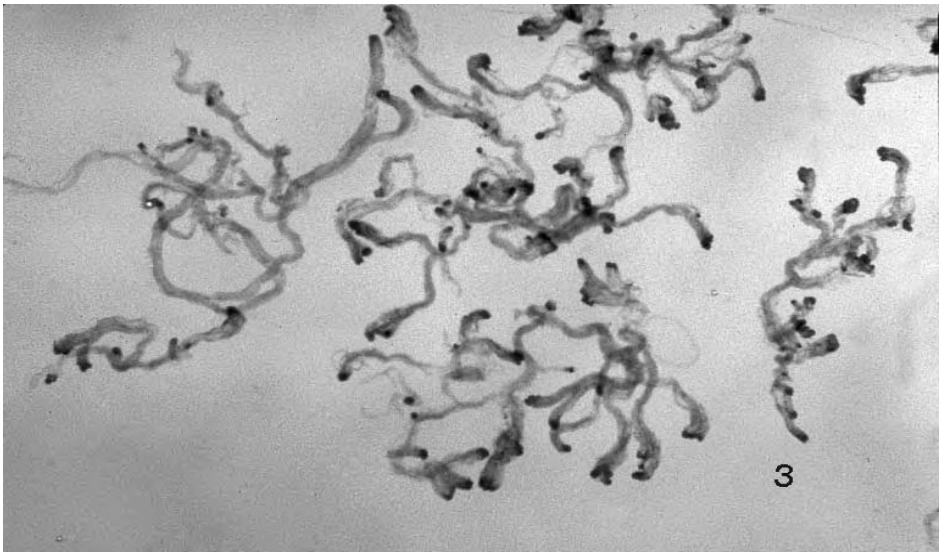

Figure 3. Early embryos in controls without chlorsulfuron showed well-developed and elongated suspensors. The axial tier comprised a darkly stained proembryonal group, the lightly stained embryonal tubes, and the elongated embryonal suspensors. Note cleavage polyembryony in the proembryonal cells. The three components of the axial tier were distinguished by the color and intensity of double-staining with acetocarmine and Evan's blue.

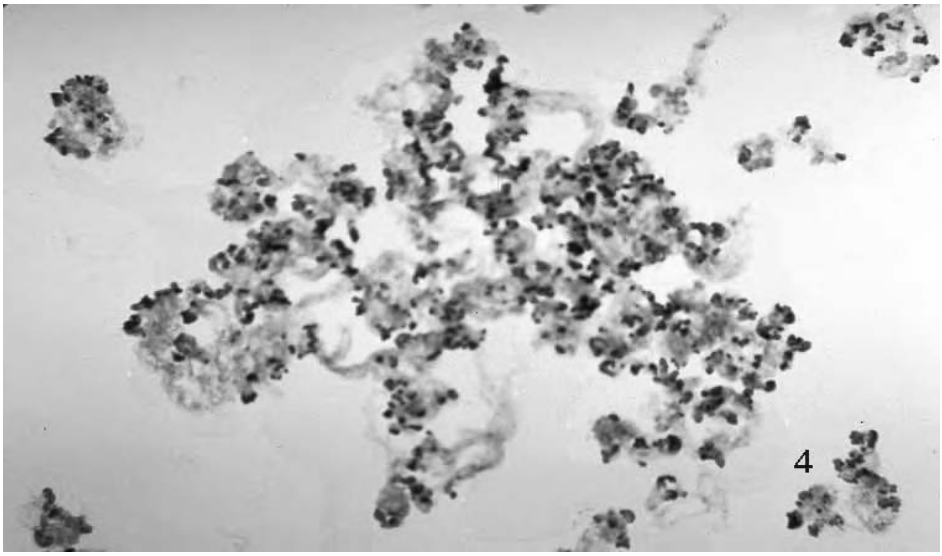

Figure 4. Axial-tier development and cleavage polyembryony was blocked in media with chlorsulfuron, and in media lacking leucine, isoleucine and valine. The proembryonal groups are darkly stained with acetocarmine. The embryonal tubes and a few suspensors are stained lightly with Evans blue.

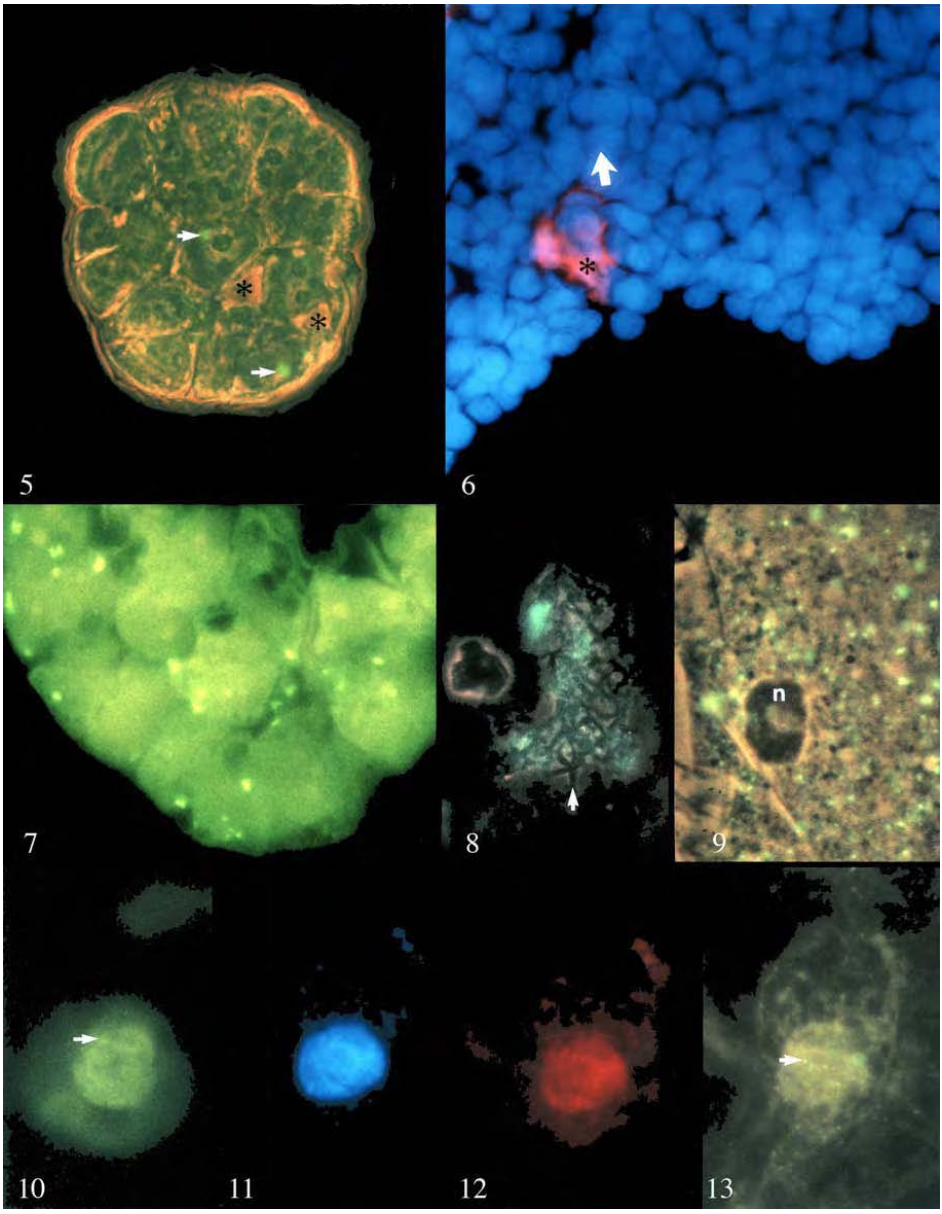

Figure 5. Anti-PCNA, light-green FITC fluorescence) was detected in cells and on the cell surfaces of a proembryo (arrows). Large nucleoli were evident at this stage. Two asterisks identify apoptotic cells possibly initiating cleavage polyembryony. **Figure 6**. Cells reacting pink (rhodamine fluorescence, TUNEL reaction) at the cleavage site in an early embryo were apoptotic, asterisk. DAPI (blue fluorescence) distinguished the nuclei in nonapoptotic cells. Arrow shows the direction of axial-tier development. **Figure 7**. The proembryonal group of an early embryo covered with mucilage having anti-PCNA reactivity (light-green FITC fluorescence). **Figure 8**. Mitotic chromosomes (white arrow) in a rapidly cell cycling proembryo were heavily labeled by anti-PCNA whose green FITC fluorescence lighted up the image. **Figure 9**. Cytoplasm from a tube cell differentiating into a suspensor reacted strongly with anti-ubiquitin (FITC green fluorescence). n=pycnotic nucleus ca. 6 μm dia. **Figure 10**. An apoptotic nucleus (ca. 8 μm dia) in a proembryonal cell reacts with anti-p53 indicating chlorosulfuron-induced DNA damage (arrow, strong FITC

green fluorescence). **Figures 11-13.** An apoptotic nucleus probed for multiple reactions. Nuclear DNA (DAPI Figure 12). The TUNEL reaction (rhodamine fluorescence, Figure 13). Anti-p21 (FITC fluorescence, arrows).

Histo- and immunocytochemical results: FITC-labeled anti-PCNA activity was detected on the outer wall surface of proembyros (arrows Figure 5). A few cells having a brown coloration with collapsed nuclei were evident (asterisk). The TUNEL reaction identified cells that initiated cleavage polyembryony (Figure 6). The PCNA on the surface of proembryos (Figure 7) was also detected in dividing cells where it became bound to chromosomes (Figure 8). The cytoplasm of embryonal tubes reacted strongly to anti-ubiquitin before they differentiated into suspensors (Figure 9). All chlorsulfuron-damaged cells reacted with anti-p53 (Figure 10). The fluorescence pattern for an individual apoptotic nucleus, stained for DAPI (Figure 11), TUNEL (Figure 12) and p21 (Figure 13), shows the predicted concurrence of p53 and p21 epitopes in apoptotic cells.

	Ala	AANB	Glu	Ile	Leu	Thr	Val
Ala	---	-0.495	0.928*	0.897*	0.822*	0.927*	0.880*
AANBA	-0.495	---	-0.449	-0.440	-0.330	-0.401	-0.413
Glu	0.928*	-0.449	---	0.842*	0.767*	0.951*	0.824*
Ile	0.898*	-0.440	0.842*	---	0.983*	0.914*	0.989*
Leu	0.822*	-0.330	0.767*	0.983*	---	0.864*	0.974*
Thr	0.927*	-0.401	0.951*	0.915*	0.864*	---	0.896*
Val	0.880*	-0.413	0.824*	0.989*	0.974*	0.896*	---
* p = 0.001 to 0.0001 n=18							

Table 1. A matrix showing the correlation coefficients among amino acids contributing to the branched-chain amino acid pathway over all chlorsulfuron levels. AANBA α-amino-n-butyric acid. Significant linearity based on 18 observations is indicated by the asterisk.

Effects of chlorsulfuron on amino acid N and growth: Blocking acetolactate synthase and branched-chain amino acid synthesis by chlorsulfuron resulted in a sharp drop in biomass fresh weight (Figure 14). α-Amino-n-butyrate (AANBA) now accumulated (Figure 15) as the free amino acid pool was significantly reduced (Figure 16). In controls, the total soluble N initially consisted mainly of alanine N (25-29%). As levels of added chlorsulfuron increased, glutamine N accumulated (Figure 16). At highest levels of chlorsulfuron, the total branched-chain amino acid N was predictably low as β-alanine N increased (Figure 17).

Correlation coefficients for the decline of tissue biomass and most free amino acids in cells were linear, positive and highly significant (n=18 p .00l to .0001) except for glutamine, β-alanine, and α-amino-n-butyric acid. Branched-chain amino acids are degraded to non N-containing products, *viz*. acetoacetate, acetyl CoA, or propionyl CoA and CO_2 (35).

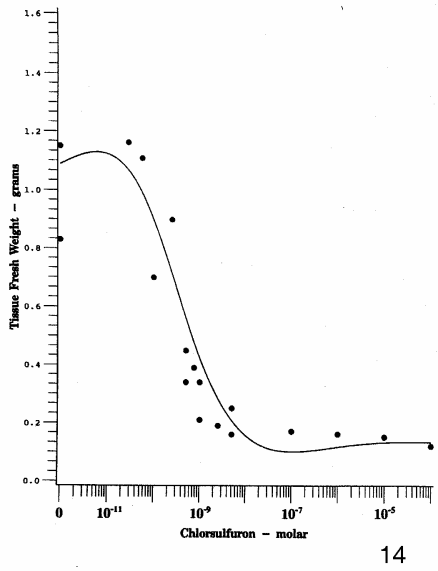

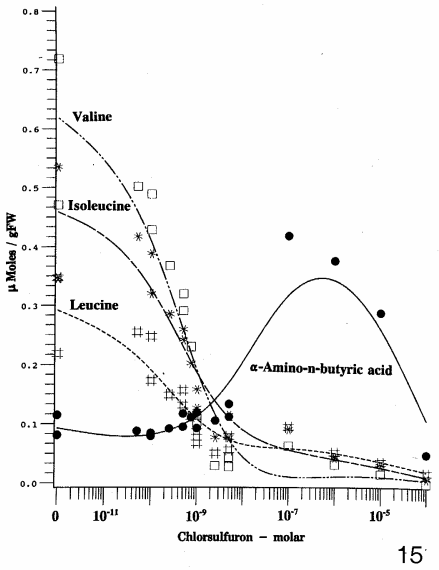

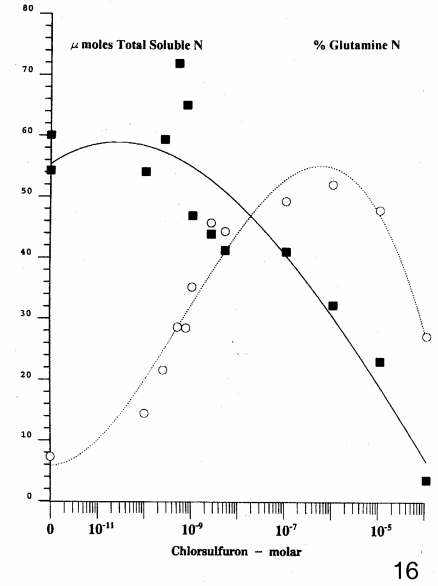

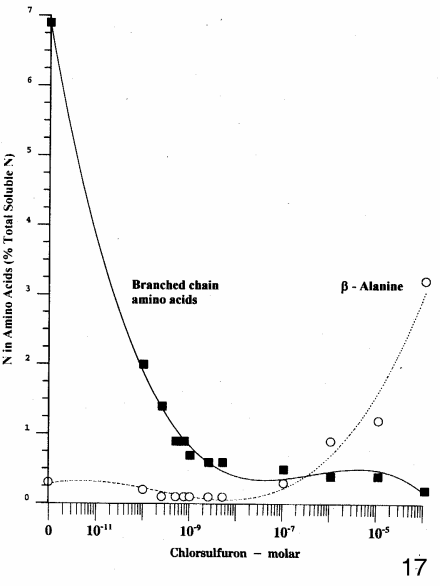

Figures 14. After 7 d in suspension culture at 23 °C in darkness, tissue biomass was significantly reduced with increasing concentrations of chlorsulfuron. **Figure 15.** Levels of leucine, isoleucine, valine were all reduced due to chlorsulfuron's block of acetolactate synthase. The accumulation of α-amino-n-butyric acid is a typical marker for the inhibition of acetolactate synthase activity. **Figure 16.** Glutamine N as a percentage of the total soluble N (circles) increased then decreased as the total soluble N continually decreased (black squares) with higher concentrations of chlorsulfuron. **Figure 17**. Chlorsulfuron reduced the levels of branched-chain amino acids as β-alanine, a product of DNA breakdown and pyrimidine catabolism, increased. Cell populations were now mainly apoptotic.

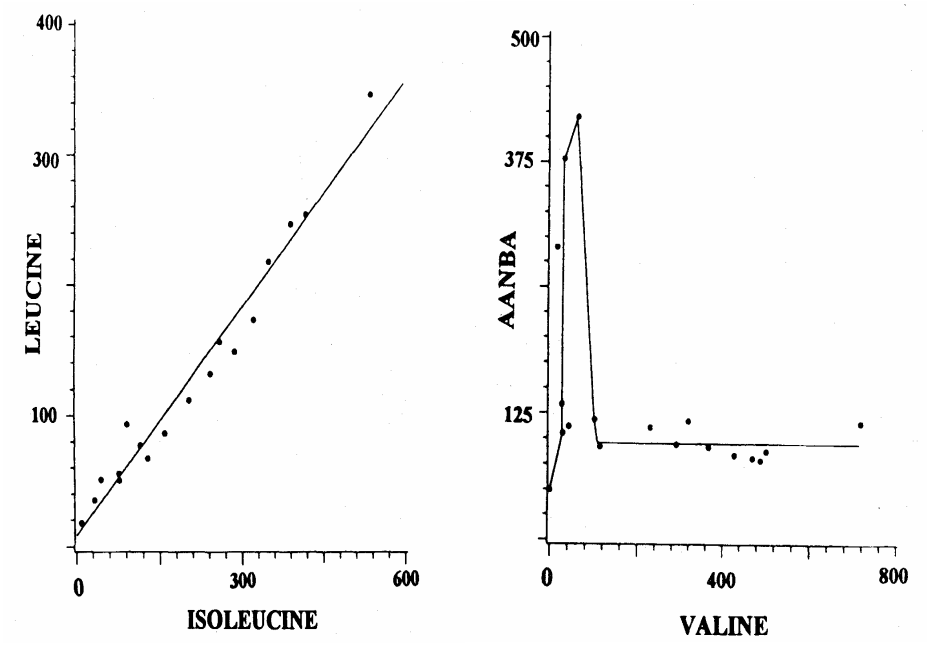

Figure 18. Highly linear relation between leucine and isoleucine was rigidly maintained over all chlorsulfuron levels (*cf.* Table 1). **Figure 19.** The nonprotein amino acid, α-amino-n-butyric acid (AANBA) accumulated at low valine concentrations due to a chlorsulfuron-induced block in acetolactate synthase. Cell cycling was no longer reversible when AANBA declined from its highest to lowest level at low valine concentrations. Cell populations were mainly apoptotic.

Over all chlorsulfuron levels, the metabolites in the branched-chain amino acid pathway showed strong, positive, and rigid linear correlation coefficients (Table 1). Levels of leucine, isoleucine, and valine were strongly and linearly correlated to one another (0.983 to 0.974, *cf.* Figure 18). AANBA was strongly and negatively correlated to all branched-chain amino acids and to their precursors, *viz*. alanine and glutamine, that could provide N for their biosynthesis.

A useful indicator for the inhibition of proembryo development was the relationship between AANBA and valine (Figure 19). The rise in AANBA corresponded to an effective block of the mitotic cycle. Cells at the highest levels of chlorsulfuron became apoptotic.

Discussion

The basal plan for the development of the axial tier of early embryos was readily blocked by the addition of chlorsulfuron to the culture medium (Figures 1 to 4). At least three separate physiological gradients were involved in developing the axial tier. One arises from the linear daughter-cell lineage patterns in the proembryo. Another arose from lateral divisions in the proembryo and early embryo leading to cleavage polyembryony and its variations (Figure 3). The third gradient contributed to axial-tier development involving terminal differentiation and enucleation to produce embryonal suspensors. The

blocking of acetolactate synthase by chlorsulfuron restricted the production of ubiquitin composed of 25% branched-chain amino acids. Ubiquitination-dependent turnover of cell regulatory proteins and the differentiation of the axial tier became inhibited (Figure 4, *cf.*16).

In plant meristems, PCNA is an essential component of the DNA replication and repair machinery (23, 36). PCNA is present at very low levels in non-dividing cells, but as cells enter into the division cycle, the levels of PCNA increased significantly. The detection of anti-PCNA on surfaces and in proembryonal cells at interphase supports the view that PCNA acted as a licensing factor when it became bound chromosomes (Figures 5, 7, 8). As new cells entered G1 the PCNA bound to DNA initiated rapid replication (19, 36). PCNA was also detected in dividing *Cupressus* cells but not in those already undergoing xylogenesis (31).

Plant PCNA has a highly conserved binding site for the p53-inducible gene product $p21^{waf1}$ (37). The C-terminus of $p21^{waf1}$ binds to PCNA preventing DNA synthesis from occurring, but not DNA repair. In normal cells, p53 is a transcription proteins protect the genome when cells are exposed to stressful events. Ubiquitination also regulates the activities and functions of proteins with p53 epitopes (38). In cells with damaged DNA, ubiquitin does not bind to proteins with p53 epitopes. Cell division is therefore stopped to permit DNA repair. However, polyubiquitination of PCNA is needed for DNA repair. If repair fails, or the damage is too great as with high chlorsulfuron, the cells are eliminated by apoptosis. Chlorsulfuron also inhibited the release of mucilage having anti-PCNA activity into the culture medium. In carrot cells, another nuclear antigen is associated with the control of cell division. It is a component of the 26S proteasome in ubiquitination (39).

In animal cells, the p21-gene product is normally transcriptionally activated by p53 in response to DNA damage. This mediates the p53-dependent G1 and G2 arrest and inhibits PCNA activity (21, 23 and 40). $p21^{waf1}$ is also a potent and *reversible* inhibitor of cell-cycle progression at G1 and G2.This may allow DNA repair to be completed. Irreversible arrest at G1 or G2 leads to apoptosis. In Norway spruce controls and over all developmental gradients, proteins with p53 and p21-epitopes were difficult to detect. Only in cells exposed to chlorsulfuron and having irreparable DNA damage were epitopes for p53 and p21 readily detected.

Norway spruce central cells, eggs, and egg equivalents appear to have endoreduplicated DNA (2, 9). In plants undergoing DNA endoreduplication, a retinoblastoma (Rb)-like protein has been reported (41, 42 and 43). In maize, only 28-30% of the amino acids of the Rb protein were the same as in animal cells but the key amino acids required for protein function were conserved (43). Rb activity integrates signals affecting cell division and differentiation. Cell cycle control, mediated by p53 and Rb activity, is integrated with proteins having p21 epitopes. The binding of p21 to cyclin-dependent kinases prevents phosphorylation and the activation of Rb (44). This inhibits cell cycling, cell proliferation, and differentiation. Other regulatory proteins interacting with DNA and controlling cellular processes have a leucine-zipper motif (45). Restriction of the availability of branch-chained leucine residues would limit motif formation, constrain gene-regulatory circuits, and contribute to the developmental patterns observed with exposure to chlorosulfuron.

Regarding cleavage polyembryony, apoptotic cells were observed at the site of cleavage. The apoptotic process is analogous to sculpturing the shape of digits by apoptosis in developing limb buds in vertebrates (46). Structural changes in polyembryonic *Arabidopsis* mutants were due to an altered expression of valyl-tRNA synthetase (47). This mutant would lack the branched-chained amino acid valine for ubiquitin synthesis and for other proteins requiring this amino acid.

Chlorsulfuron's inhibition of acetolactate synthase limited the synthesis of branched-chain amino acids for ubiquitin synthesis in Norway spruce cells. This limitation resulted in linear correlations among metabolites in the branched-chain pathway and in the predicted accumulation of α-amino-n-butyric acid (AANBA, Figure 18 and Table 1).

A reversal of chlorsulfuron-induced blocks would require that glutamine (Figure 16) provide carbon and nitrogen for the synthesis of branched-chain amino acids. Reversal did not occur if internal ratios between α-AANB and valine started to fall after peaking as seen in Figure 19 because apoptosis was already been initiated. Nucleic acid breakdown was indicated by the conversion of pyrimidines to β-alanine (e.g., 48). Purines are also converted to ureides and urea and rapidly re-assimilated into the soluble N pool (49, 50).

The demonstration of linear, rather than nonlinear, relationships are useful in metabolic engineering by characterizing, controlling and predicting metabolite overproduction and batch processing of embryos (51, 52). Coupling this approach to bioreactor process controls that simulate past and future climatic and environmental factors may reveal the latent adaptive plasticity of conifer genomes. This becomes important for understanding reproductive development in tree breeding and under cultural conditions that simulate climatic variables well before angiosperms evolved (53).

Acknowledgments

Authors thank F. Ventimiglia for technical assistance with the amino acid and statistical analyses.

References

[1] Dogra PD. 1984. *The Embryology, Breeding Systems and Seed Sterility in Cupressaceae. A Monograph.* Glimpses in Plant Research. Aspects of Reproductive Biology VI, New Delhi. 1- 126.
[2] Durzan DJ, Jokinen K, Guerra M, Santerre A, Chalupa V, Havel L. 1994. Latent diploid parthenogenesis and parthenote cleavage in egg-equivalents in Norway spruce. *International J Plant Science* **155**, 677-688.
[3] Simak M. 1973. Polyembryonal seeds of *Pinus silvestris* in arctic regions. *Inst. För Skogsföryngring Res Note* **45**, 2-14.
[4] Singh H. 1978. *Embryology of Gymnosperms*. Encyclopedia of Plant Anatomy, Gebrüder, Borntraeger, Berlin. 302 pp.
[5] Kaplan DR, Cooke TJ. 1997. Fundamental concepts in the embryogenesis of dicotyledons: a morphological interpretation of embryo mutants. *The Plant Cell* **9**, 1903-1919.
[6] Komamine A, Kawahara R, Matsumoto M, Sunabori S, Toya T Fujiwara A, Tsukahara M, Smith J, Ito M, Fukuda H, Nomura K, Fujimura T. 1992. Mechanisms of somatic embryogenesis in cell cultures: physiology, biochemistry, and molecular biology. *In Vitro Cell Biology* **28P**, 11-14.
[7] Laux T, Jürgens G. 1997. Embryogenesis: a new start in life. *The Plant Cell* **9**, 989-1000.
[8] Filonova, LH, Bozhkov PV, von Arnold S. 2000. Developmental pathways of somatic embryogenesis in *Picea abies* as revealed by time-lapse tracking. *J. Exptl Bot*any **51**, 249 264.
[9] Håkansson A. 1956. Seed development of *Picea abies* and *Pinus silvestris*. *Med från Statens Skogsforsk* **46**, 1-23.
[10] Camefort H. 1969. Fécondation et proembryogénèse chez les Abiétacées (notion de néocytoplasme). Rev Cytol Biol vég **32**, 253-271.
[11] Darlington CD. 1958. *Evolution of Genetic Systems*. Oliver & Boyd, Edinburgh.
[12] Havel L, Durzan DJ. 1996a. Apoptosis in plants. *Botanica Acta* **109**, 1-10.
[13] Havel L, Durzan DJ. 1996b. Apoptosis during diploid parthenogenesis and early somatic embryony of Norway spruce. *International J Plant Science* **157**, 8-16.
[14] Durzan DJ. 1996a. Protein ubiquitination in diploid parthenogenesis and early embryos of Norway spruce. *International J Plant Science* **157**, 17-26.
[15] Durzan DJ. 1988. Metabolic phenotypes in somatic embryogenesis and polyembryogenesis. In: *Genetic Manipulation of Woody Plants*. Hanover JW, Keathley DE. eds. Plenum Press NY 293-311.

[16] Durzan DJ. 1989. Physiological aspects of somatic polyembryogenesis in suspension cultures of conifers.In: *International Symposium on Forest Tree Physiology.* Ann. Sci. Forestières **46**(suppl.), 101-107.
[17] Dogra PD. 1967. Seed sterility and disturbances in embryogeny of conifers with particular reference to seed testing and tree breeding in Pinaceae. *Studia Forestalia Suecica* **45**, 1-97.
[18] Boulay, M.P., P.K. Gupta, P. Krogstrup and D.J. Durzan. 1988. Development of somatic embryos from cell suspension culture of Norway spruce (*Picea abies* Karst.) *Plant Cell Reports* **7**, 134-137.
[19] Murray A, Hunt T. 1993. *The cell cycle*. WH Freeman, San Francisco.
[20] Gorospe M, Cirielli, C, Wang X, Seth P, Capogrossi MC, Holbrook NJ. 1997.p21$^{Waf1/Cip1}$ protects against p53-mediated apoptosis of human melanoma. *Oncogene* **14**, 929-935.
[21] El-Deiry WS, Tokino T, Waldman T, Oliner JD, Velculescu VE, Burrell M, Hill DE,Healy E, Rees JL, Hamilton SR, Kinzler KW, Vogelstein B. 1995. Topological control of p21$^{waf1/CIP1}$ expression in normal and neoplastic tissues. *Cancer Research* **55**, 2910-2919.
[22] Bayly AC, Roberts RA, Dive C. 1997. Mechanisms in apoptosis. *Advances Molecular Cell Biology* **20**,183-229.
[23] Kelman Z. 1997. PCNA: structure functions and interactions. *Oncogene* **14**, 629-640.
[24] Rost TL. 1984.The comparative cell cycle and metabolic effects of chemical treatments on root tip meristems. III. Chlorsulfuron. *J Plant Growth Regulation* **3**, 51-63.
[25] Rost TL, Reynolds T. 1985. Reversal of chlorsulfuron-induced inhibition of mitotic entry by isoleucine and valine. *Plant Physiology* **77**, 481-482.
[26] Rhodes D, Hogan AL, Deal L, Jamieson GC, Haworth P.1987. Amino acid metabolism of *Lemna minor* L. II. Responses to chlorsulfuron. *Plant Physiology* **84**, 775-780.
[27] Rechsteiner M. 1987. Ubiquitin-mediated pathways for intracellular proteolysis. *Annual Review Cell Biology* **3**, 1-30.
[28] Pollmann L, Wettern M. 1989. The ubiquitin system in higher and lower plants pathways in protein metabolism. *Botanica Acta* **102**, 21-31.
[29] Anamthawat-Jonsson K, Atipanumpa L, Tigerstedt PMA, Tomasson T. 1986. The Feulgen-Giemsa method for chromosomes of *Betula* species. *Hereditas* **104**, 321-322.
[30] Sharma AK, Sharma A. 1980. *Chromosome techniques, theory and practice*. Norfolk: Frankenham Press Ltd p 121.
[31] Havel L, Scarano M-T, Durzan DJ. 1997. Xylogenesis in *Cupressus* callus involves apoptosis. *Adances. Horticultural Science* **11**, 37-40.
[32] Slocum RH, Cummings JG. 1991. *Amino Acid Analysis of Physiological Samples.Techniques in Diagnostic Human Biochemical Genetics. A Laboratory Manual*. Wiley Liss NY pp 87-126.
[33] Knight WE. 1966. A computer method for calculating Kendall's *tau* with ungrouped data. *J American Statistics Assn* **61**, 436-439.
[34] Noether GE. 1967. *Elements of non-parametric statistics*. John Wiley & Sons, New York. 326 pp.
[35] Anderson MD, Che P, Song J, Nikolau BJ, Wurtele ES. 1998. 3-Methylcrotonyl-coenzyme A carboxylase from higher plant mitochondria. *Plant Physiology* **102**, 957-1138.
[36] Kosugi S, Suzuki I, Ohashi Y. 1995. Two of three promoter elements identified in a rice gene for proliferating cell nuclear antigen are essential for meristematic tissue-specific expression. *The Plant Journal* **7**, 877-886.
[37] Ball KL, Lane DP 1996. Human and plant proliferating cell nuclear antigen have a highly conserved binding site for the p53-inducible gene product p21^{waf1}. *European J Biochemistry* **237**, 854-861.
[38] Giles J. 2004. Chemistry Nobel for trio who revealed molecular death-tag. *Nature* **421**, 729.
[39] Smith MW, Ito M, Miyawaki M, Sato S, Yoshikawa Y, Wada S, Maki M, Nakagawa H, Komamine A. 1997. Plant 21D7 protein, a nuclear antigen associated with cell division, is a component of the 26S proteasome. *Plant Physiol*ogy **113**, 281-291.
[40] Agarwal M, Agarwal A, Taylor W, Stark GR. 1995. p53 controls both the G_2/M and the G_1 cell cycle checkpoints and mediates reversible growth arrest in human fibroblasts. *Proc Natl Acad Sci USA* **92**, 8493-8497.
[41] Ach RA, Taranto T, Gruissem W. 1997. A conserved family of WD-40 proteins bind to the retinoblastoma protein in both plants and animals. *The Plant Cell* **9**, 1595-1606.
[42] Murray JAH. 1997. The retinoblastoma protein is in plants! *Trends in Plant Science* **2**, 82-84.
[43] Grafi G, et al 1996. A maize cDNA encoding a member of the retinoblastoma protein family - involvement in endoreduplication. *Proc Natl Acad Sci USA* **93**, 8962-8967.
[44] Harper JW, Adami GR, Wei N, Keyomars K, Elledge SJ. 1993. The p21 ckd interacting protein Cip1 is a potent inhibitor of G1 cyclin-dependent kinases. *Cell* **75**, 817-825.

[45] Alberts B, Johnson A, Lewis L, Raff M, Roberts K, Walter P. 2002. *Molecular Biology of the Cell.* 3rd ed. Garland Pub Inc, NY.
[46] Hurle JM, Ros MR, Climent V. Garcia-Martinez V. 1996. Morphology and significance of programmed cell death in the developing limb bud of the vertebrate embryo. *Microscope Research & Technology* **34**, 236-246.
[47] Zhang JZ, Somerville CR. 1997. Suspensor-derived polyembryony caused by altered expression of valyl-tRNA synthetase in the *twn2* mutant of *Arabidopsis*. *Proc Natl Acad Sci USA* **94**, 7349-7355.
[48] Pitel JA, Durzan DJ. 1975. Pyrimidine metabolism in seeds and seedlings of jack pine (*Pinus banksiana*). *Canadian J Botany* **53**, 137-686.
[49] Pandita ML, Durzan DJ. 1970. Metabolism of guanine-8-^{14}C by germinating jack pine seedlings. *Proc Canadian Soc Plant Physiologists* **10**, 42.
[50] Durzan DJ. 1973. The metabolism of ^{14}C-urea by white spruce seedlings in light and darkness. *Canadian J Botany* **51**, 351-358.
[51] Stephanopoulos G, Vallino J. 1991. Network rigidity and metabolic engineering in metabolite overproduction. *Science* **252**, 1675-1681.
[52] Durzan DJ, Durzan PE. 1991. Future technologies: Model-reference control systems for the scale-up of embryogenesis and polyembryogenesis in cell suspension cultures. In: *Micropropagation*. Debergh PC, Zimmerman RH. Eds. Kluwer Academic, Dordrecht, 389-423.
[53] Durzan DJ. 1996b. Asexual reproductive adaptation to simulated Cretaceous climatic variables by Norway spruce cells in vitro. *Chemosphere* **33**, 1655-1673.

Cell Biology and Instrumentation: UV Radiation, Nitric Oxide and Cell Death in Plants
Y. Blume et al. (Eds.)
IOS Press, 2006

Spruce Embryogenesis – A Model for Developmental Cell Death in Plants

Peter BOZHKOV
Department of Plant Biology and Forest Genetics, Swedish University of Agricultural Sciences, Box 7080, SE-75007 Uppsala, Sweden

Abstract. Programmed cell death (PCD) is indispensable for embryogenesis in animals and plants. Dysregulation of PCD in the embryos often has a lethal effect on the nascent organism. In animals, embryonic PCD has been studied for over a century, with the main breakthrough being the characterization of core cell-death machinery. The basis for this discovery was a powerful developmental model system of *Caenorhabditis elegans*, which has been thoroughly studied at different organization levels to link cell division, cell differentiation and cell-death programmes into the overall scheme of body patterning. The molecular control of PCD during plant development remains obscure. Plant embryogenesis requires PCD for a timely elimination of the terminally-differentiated organ, embryo-suspensor, providing an elegant paradigm for developmental cell death research. In this chapter, I give a brief presentation of a versitile developmental system, somatic embryogenesis of spruce, which is used for studying regulation of PCD at the earliest stages of plant development.

Introduction

As plants grow they not only form new tissues and structures using highly coordinated cell-division and cell-differentiation programmes but also continuously kill many of their own cells through activation of programmed cell death (PCD). The latter is required to ablate surplus and "no longer needed" cells during development (e.g. leaf senescence), to prepare functional cell corpses (e.g. wood formation), as well as to cull damaged cells in response to stresses and pathogens [1]. The earliest functions of PCD in plant ontogenesis are fulfilled during embryogenesis. The plant zygote divides asymmetrically to establish two fundamentally distinct parts - the embryo-proper (or embryonal mass) and suspensor. Embryo-proper gives rise to plant, whereas the terminally-differentiated suspensor transports nutrients and hormones to the embryo and is eventually eliminated by PCD. The developmental programs of embryo-proper and suspensor are tightly coordinated and imbalance causes embryonic defects or lethality [2, 3]. We have developed a model system to address cellular and molecular regulation of embryonic patterning, including the mechanisms of cell-death control. This chapter presents a brief description of the model system (for more in-detail analysis of embryonic PCD in plants see ref. 3).

1. Developmental Pathway – Making an Embryo

Embryogenesis *in planta* takes place under multiple layers of tissues so that its direct observation is obscured. Furthermore, even within the same plant, different ovules develop asynchronously, which hampers collecting embryos at a common developmental

stage for subsequent analyses. To obviate these obstacles to studying cell and molecular mechanisms of plant embryo development we have developed a model system of somatic embryogenesis of a gymnosperm, Norway spruce (*Picea abies*). This system provides a unique opportunity to control the entire pathway of embryo development in laboratory conditions and to isolate large numbers of embryos at common developmental stages. Somatic embryogenesis of spruce includes a stereotyped sequence of developmental stages and corresponding regulatory treatments [4]. Somatic embryos develop from proembryogenic masses (PEMs), which pass through a series of three characteristic stages distinguished by cellular organization and cell number (stages PEM I, PEM II and PEM III). Proembryogenic mass will not differentiate to somatic embryos unless a stage PEM III has been achieved. Plant growth regulators, auxin and cytokinin, stimulate proliferation of PEMs and, in contrast, suppress embryo pattern formation. Consistently, withdrawal of the growth factors triggers the PEM-to-embryo transition, providing a synchronous start of early embryogeny, which is accomplished within approximately seven days in the medium lacking growth factors. Subsequently, early embryos require exogenous abscisic acid to undergo late embryogeny and maturation. Besides a substantial synchronization of embryo development, another significant advantage of this system is that the morphology and anatomy of somatic embryos are similar to those of zygotic embryos, even though embryo origin is different (i.e., somatic cells in PEMs versus zygote; ref. 4).

Programmed cell death is an integral part of the embryo patterning process. The first wave of PCD kills PEM cells at the PEM-to-embryo transition induced by withdrawal of growth factors [5]. Consistently, artificial inhibition of the cell death in PEMs suppresses embryo formation, indicating that PCD in PEMs and normal embryo development are closely interlinked processes [6]. This idea has been strengthened by the experiments with the cell lines composed of PCD-deficient PEMs, which are unable to form embryos regardless of treatment [7, 8] The second wave of PCD affects terminally-differentiated suspensors of early embryos, so that the suspensors are eliminated within a period of three to four weeks [4]. In spruce, as in all gymnosperm species, the suspensor is composed of several layers of terminally-differentiated cells, originating from asymmetric cell divisions in the embryonal mass. Suspensor cells do not proliferate but instead become committed to PCD as soon as they were formed. While the cells in the upper layer of the suspensor (adjacent to the embryonal mass) are in the commitment phase of PCD, the cells in the lower layers exhibit a gradient of successive stages of cell dismantling towards the basal end of the suspensor where the hollow walled cell corpses are located [3, 7]. Thus, successive cell-death processes can be observed simultaneously in a single embryo. Furthermore, position of the cell within the embryo can be used as a marker of the cell-death stage.

2. Cell Dismantling Pathway – Eliminating the Unwanted

How PCD actually proceeds in the embryo-suspensor at the cellular level? We distinguish six major stages of cell dismantling beginning from stage 0, which applies to proliferating cells of the embryonal mass [3, 7]. These cells are small and have isodiametric shape. They contain dense cytoplasm and a rounded nucleus, which occupies a substantial proportion of the protoplast. F-actin and microtubules in these cells form fine networks; microtubule-associated protein MAP-65, known to be essential for cytokinesis [9], is bound to a subset of microtubules.

The cells located in the basal part of embryonal mass divide asymmetrically in the plane perpendicular to the apical-basal axis of the embryo and give rise to two

daughter cells with fundamentally different developmental fates. One daughter cell retains meristematic identity and remains in the embryonal mass (stage 0), whereas its sister cell elongates and undergoes terminal differentiation to lay down the first cellular layer of the suspensor. The cells from this layer are at the commitment stage of PCD (stage I), which is characterised by the formation of autophagosomes from the Golgi and proplastids.

The execution phase of the PCD includes stages II to V corresponding to the successive layers of cells in the suspensor starting already from the first cell layer. During stage II, MAP-65 dissociates from the microtubules and the microtubule network is disrupted, while F-actin forms thick longitudinal bundles. The cells at stage II are much larger than the cells at the previous stages and they expand further as they progress towards stage III. At the same time autophagosomes increase in size and number, which sometimes lead to the formation of small lytic vacuoles. It is during stage III when the earliest nuclear envelope events, nuclear lobing and dismantling of nuclear pore complex, occur. By this stage, several large lytic vacuoles occupy most of the cell volume. No microtubules are left by this stage and only microtubule fragments can be seen in the cytoplasm. In contrast to microtubules, the actin is still preserved in the suspensor cells and forms thick longitudinal cables. By stage IV, the nuclear DNA is fragmented into a chromatin loop-length (50 kbp) and internucleosomal-length (180 bp) fragments, and the nuclei are sometimes segmented. The cells at this stage contain a thin layer of the cytoplasm confined between the plasma membrane and the tonoplast of a large lytic vacuole. Once the vacuole collapses, the remaining cytoplasm is degraded leaving a hollow walled cell corpse (stage V).

Cell dismantling in the suspensor is a slow process; it takes approximately five days for complete autodestruction of an individual suspensor cell. The transition from one stage of the PCD to the next stage takes approximately 24 hours (i.e., the frequency of the addition of the new layers of cells to the suspensor; ref. 4), with the only exception being the transition from the last but one to the last stage (i.e., rupture of the tonoplast and the clearance of the remaining cytoplasm), which is apparently a very rapid process [10].

As in all developmental cell deaths in plants, the pathway of cell dismantling in the embryo-suspensor is executed by autophagic machinery. Inhibiting formation of autophagic vacuoles by an autophagosome-specific inhibitor 3-methyladenine suppresses PCD and disrupts embryogenesis [3]. Despite autophagy is the major mechanism of plant cell disassembly, our recent data suggest that, in addition to vacuolar pathway, another, nucleo-cytoplamic pathway, is also critically involved in the execution of PCD. This pathway encompasses type-II metacaspase mcII-Pa [11], which activates a protease or a group of proteases with a high proteolytic activity on the mammalian caspase-6-specific substrates containing peptide VEID [12]. Hence, autophagic PCD in plants appears to be executed by two cooperating pathways, one pathway activated in the autophagic vacuoles and another pathway acting in the cytoplasm and in the nucleus (see also ref. 13).

3. Conclusion - Why It is Important to Study Programmed Cell Death in Plants?

A knowledge of the mechanisms regulating PCD in plants will provide important clues to the understanding evolution of eukaryotic cell-death machinery. In contrast to animals, plants have not evolved apoptotic type of PCD, which relies on the activation of canonical caspases and pro- and antiapoptotic functions of Bcl-2 family proteins. Furthermore, in apoptosis, cell corpses are cleared by phagocytosis, the phenomenon never occurring in plants and fungi owing to the presence of rigid cell walls. Instead plant and fungal cells dye by autophagy, where one and the same cell commits suicide and cleans itself [3, 14]. The importance of understanding autophagic PCD processes

goes far beyond the areas of plant and fungal biology, because animals too – like plants and fungi – recruit autophagic cell death during development and disease, when apoptosis can not manage with large numbers of cells to be killed [15]. As plants represent one of the oldest phyla of living eukaryotes, they possess ancestral core cell-death machinery (including metacaspases) that was either substantially modified (apoptosis) or conserved (autophagic PCD) by evolutionary younger organisms.

From practical standpoint, expanding our knowledge of the processes of plant PCD has many potential economic benefits. The timing and efficiency of PCD has an important role in determining the yield and pre-harvest quality of many cereal, forage and horticultural crops, as well as wood quality of forest trees. Plant resistance to stresses and pathogens is another area where the role of PCD is difficult to overestimate. Therefore increased knowledge of the plant PCD processes will provide information for plant and forest breeders and biotechnologists to generate crops and trees with improved yield, quality and resistance with benefits for growers, suppliers and consumers. One example of successful implementation of this knowledge is improvement of yield and quality of Norway spruce clonal material through artificial regulation of PCD during somatic embryogenesis [6].

Acknowledgements

Studies of cell death in my group are supported by The Carl Tryggers Foundation, The Swedish Foundation for International Cooperation in Research and Higher Education, The Royal Swedish Academy of Agriculture and Forestry and by The Swedish Institute.

References

[1] Lam E (2004) Controlled cell death, plant survival, and development. Nat. Rev. Mol. Cell Biol. 5, 305-315.
[2] Goldberg RB et al. (1994) Plant embryogenesis: Zygote to seed. Science 266, 605-614.
[3] Bozhkov PV et al. (2005) Programmed cell death in plant embryogenesis. Curr. Top. Dev. Biol. 67, 135-179.
[4] Filonova LH et al. (2000) Developmental pathway of somatic embryogenesis in *Picea abies* as revealed by time-lapse tracking. J. Exp. Bot. 51, 249-264.
[5] Filonova LH et al. (2000) Two waves of programmed cell death occur during formation and development of somatic embryos in the gymnosperm, Norway spruce. J. Cell Sci. 113, 4399-4411.
[6] Bozhkov PV et al. (2002) A key developmental switch during Norway spruce somatic embryogenesis is induced by withdrawal of growth regulators and is associated with cell death and extracellular acidification. Biotehnol. Bioeng. 77, 658-667.
[7] Smertenko AP et al. (2003) Reorganisation of the cytoskeleton during developmental programmed cell death in *Picea abies* embryos. Plant J. 33, 813-824.
[8] van Zyl L et al. (2003) Up, down and up again is a signature global gene expression pattern at the beginning of gymnosperm embryogenesis. Gene Expression Patterns 3, 83-91.
[9] Smertenko A et al. (2000) A new class of microtubule-associated proteins in plants. Nat. Cell Biol. 2, 750-753
[10] Obara K et al. (2001) Direct evodence of active and rapid nuclear degradation triggered by vacuole rupture during programmed cell death in *Zinnia.* Plant Physiol. 125, 615-626.
[11] Suarez MF et al. (2004) Metacaspase-dependent programmed cell death is essential for plant embryogenesis. Curr Biol. 14, R339-R340.
[12] Bozhkov PV et al. (2004) VEIDase is a principal caspase-like activity involved in plant programmed cell death and essential for embryonic pattern formation. Cell Death Differ. 11, 175-182.
[13] Woltering E (2005) Death proteases come alive. Trends Plant Biol.9, 469-472.
[14] Zhivotovsky B (2002) From the nematode and mammals back to the pine tree: On the diversity and evolution of programmed cell death. Cell Death Differ. 9, 867-869.

[15] Baehrecke E (2002) How death shapes life during development. Nat. Rev. Mol. Cell Biol. 3, 779-787.

Cell Biology and Instrumentation: UV Radiation, Nitric Oxide and Cell Death in Plants
Y. Blume et al. (Eds.)
IOS Press, 2006

Cadmium-induced Cell Death in Tomato Suspension Cells is Mediated by Caspase-like Proteases, Oxidative Stress and Ethylene

Elena T. IAKIMOVA[1*], Veneta M. KAPCHINA-TOTEVA[2], Anke J. de JONG[3], and Ernst J. WOLTERING[3]
[1]*AgroBioInstitute,8 Dragan Tzankov Blvd.,1164 Sofia, Bulgaria*
[2]*Faculty of Biology, University of Sofia, Bulgaria*
[3]*Agrotechnology and Food Innovations (A&F), Wageningen University and Research Center, P.O. Box 17, 6700 AA Wageningen, The Netherlands*

Abstract. The ability of cadmium to induce a programmed cell death in tomato (*Lycopersicon esculentum* Mill.) suspension cells, line Msk8, was explored. Using a pharmacological approach with specific inhibitors, we have identified some of the biochemical processes that are involved in the signal transduction. Specific inhibitors of different biochemical steps were tested by simultaneous application with either $CdSO_4$ or topoisomerase-1 inhibitor camptothecin (CPT). Cell viability (FDA staining of the viable cells) after 24 hours and the dynamics of H_2O_2 production were studied. H_2O_2 production was measured by chemiluminescence in a ferricyanide-catalised oxidation of luminol. Both Cd and CPT enhanced the production of hydrogen peroxide. By the application of specific peptide inhibitors we have demonstrated that caspase-like proteases participate in Cd-induced cell death in tomato cells thus giving evidence that the cell death elicited by Cd is most probably a form of programmed cell death. Treatments with ethylene further reduced Cd-inhibited cell viability. The application of ethylene inhibitor AVG restored the cell viability previously diminished in response to the Cd treatment. Also, by application of antioxidants (ascorbic acid, catalase and spermine) and a calcium channel blocker $LaCl_3$ involve oxidative stress and calcium in Cd-stimulated PCD machinery. The cell response to cadmium elicitation and the inhibitors is comparatively discussed to the cell behavior under the administration of CPT. Collectively, the data indicate that by analogy with the CPT effect on cell death, Cd-triggered cell death in plant cells exhibits similarities to HR and cell death induced by known apoptosis-inducing chemicals and to its effect in animal systems.

Introduction

Programmed cell death (PCD) is an active process of cell suicide found throughout the animal and plant kingdoms, aimed at eliminating cells that are harmful, unwanted or misplaced in specific structures and organs during the life cycle of multicellular organisms. PCD is involved in the development and tissue homeostasis and plays an essential role in defensive mechanisms acting against infected or mutated cells. Deregulation of PCD is implicated in various human diseases, including birth defects, ischemic vascular diseases, neurodegenerative diseases (e.g. Alzheimer's and Parkinson's diseases), autoimmune diseases, AIDS, and *Diabetes mellitus* type I.

In animal cells, PCD is often associated with the occurrence of a specific set of cellular morphological features [1] such as condensation of the nucleus and the cytoplasm, fragmentation

of DNA and fragmentation of the cell into membrane confined DNA containing vesicles (apoptotic bodies). According to recent definitions, apoptosis is the caspase-dependent cell death (programmed, physiological, pathological, or inducible in nature) that is associated with apoptotic morphology [2].

1. Role of caspase-like proteases, oxidative stress and ethylene in plant cell death

Caspases are specific cysteine proteases that show a high degree of specificity with an absolute requirement of cleavage an adjacent aspartic acid residue and recognition of sequence of at least four amino acids in N-terminal to this cleavage site [3]. A sequence of caspase-activation cascade involving initiator caspases and down-stream activation of executioner caspases leads to the apoptotic phenotype [4].

In plants, programmed cell death is essential machinery for growth, development, and survival [5-7]. A number of studies have been recently devoted to assess the key steps playing a central role in PCD performance in plants. Cellular suicide is involved in, for example, xylogenesis [8], aerenchyma formation [9], plant reproduction [10], leaf and petal senescence [11], and endosperm cell death during germination [12,13]. Furthermore, PCD plays an important role during a cell death in response to pathogens [14-16], and during responses to various abiotic stresses such as heat shock [17-19], toxic chemicals [20], ozone exposure [20-24], UV radiation [25], and hypoxia [26].

Morphological similarities have been found between animal cells undergoing apoptosis and dying plant cells, including condensation and shrinkage of the cytoplasm and nucleus, DNA and nuclear fragmentation and formation of apoptotic-like bodies [27-29]. Biochemical changes involving formation of reactive oxygen species (ROS) [21,30,31], Ca release [32,33], proteolysis [27,34-36], and ethylene [37-41] were found to actively participate in the signal cascade of PCD in plants.

Although no true structural homologues of animal caspases have yet been identified in plants, there is accumulating evidence that cysteine proteases showing functional similarity to caspases, as in animal systems, participate in the programmed cell death in plants. Caspases can be selectively inhibited by small peptides mimicking the substrate recognition site. Using such pharmacological approach, caspase-like activity has been detected following the infection of tobacco with bacteria and at virus challenge [42,43], and a role of caspase-like proteases has been established at the apoptotic cell death of tomato suspension cells at camptothecin and fumonisin B1 elicitation [27,44]. Camptothecin (CPT) – topoisomerase-1-inhibitor is an anticancer drug. In tomato cells 5 μM CPT caused cell death accompanied by nuclear condensation, the appearance of TUNEL positive niclei and DNA laddering. DNA laddering was also detected in fumonisin B1 treated tomato cells treated by fumonisin B1 [27]. Proteases with caspase-like activity are shown to play a determinative role in shoot selection of pea seedlings [45]. In addition, macromolecular proteins such as cowpox serine proteases inhibitor crmA and the broad-spectrum caspase inhibitor p35 from baculovirus are able to specifically block caspase activity [43,46]. Caspase-3-like protease activation has been observed in tobacco [18] and barley [47].

Metacaspases are candidates to the role of specific plant cysteine proteases [48]. Three-dimensional model of protein structure of metacaspases indicates structure homology to the caspase-hemoglobinase fold of animal caspases [49]. Caspase-like proteolytic activity has been shown for the yeast metacaspase that is activated at hydrogen peroxide stimulation [50], tomato metacaspase *LeMCA1* was induced during infection of tomato leaves with *Botrytis cynerea* [51], and fundamental requirement of plant metacaspase (VEIDase) for embryogenesis has been

recently demonstrated in Norway spruce [52,53]. Caspase-specific CMK-based protease inhibitors have been shown to prevent victorin- and heat-shock-induced proteolysis of Rubisco. Two proteases (SAS-1 and SAS-2), named saspases that are apparently involved in Rubisco proteolytic cascade, have been purified, characterized, and found to exhibit caspase-like hydrolytic activity and to display amino-acid sequences homologues to plant subtilin-like Ser proteases [54].

1.1. ROS are key players in plant cell death

The production of ROS is a key event in plant and animal apoptosis and a sustained oxidative burst is required for induction of the hypersensitive cell death in a plant [30, 31, 55]. ROS are components of the hormonally regulated cell death pathway in barley aleurone cells [56] and an enhanced production of ROS is involved at different cellular stresses such as chilling, ozone, toxic chemicals, hypo-osmotic stress, or drought [57]. The oxidative stress induces cell damage by ROS that are hydroxyl radical, superoxide, hydrogen peroxide, and peroxynitrite. Under normal conditions, ROS are cleared from the cell by the action of superoxide dismutase (SOD), catalase, or glutathione (GSH) peroxidase. ROS enhances the lipid catabolism resulting in the lipid peroxidation of polyunsaturated fatty acids in the cell membranes that in turn leads to structural decomposition and change in permeability and also induces damage by alterations of essential proteins, and DNA. Additionally, the oxidative stress and ROS are implicated in disease states, such as Alzheimer's disease, Parkinson's disease, cancer, and aging [58]. When attacked by incompatible pathogens, plants respond by activating a variety of defense responses, including ROS-generated enzyme complex [59]. Upon pathogen recognition, one of the earlier cell reactions is opening the specific ion channels, and the formation of superoxide and H_2O_2 [60]. Is has been shown that H_2O_2 drives the cross-linking of cell wall structural proteins and functions as a local trigger of PCD in pathogen challenged cells. In addition, H_2O_2 acts as a diffusible signal inducing genes to encode thecellular protectants in adjacent cells [31]. CPT-induced PCD in tomato cell culture is accompanied by a release of ROS into the culture medium. Cell death and accumulation of H_2O_2 were effectively suppressed by addition of NADPH oxidase inhibitor diphenileneiodonium (DPI) and caspase inhibitors [41,61].

1.2. Ethylene is involved in plant programmed cell death

Although the processes of plant PCD share similarity to animal PCD, the control of cell death in plants involves different regulators. In addition to common suicidal cascades, in a number of experimental plant systems it has been demonstrated that the plant hormone ethylene plays an important role in programmed cell death and senescence.

The role of ethylene in pathogen-induced cell death has been evaluated in ethylene-insensitive NR-tomatoes. Following the infection of these mutants, greatly reduced cell death was observed, indicating ethylene involvement in the programmed cell death [39]. Abiotic elicitors, such as ozone (O_3), can also elicit the plant defense reactions. Ozone forms ROS in the apoplast and causes the plant cell itself to produce ROS in an oxidative burst. In sensitive plants this leads to the formation of HR-like lesions. Ozone exposure upregulates ethylene biosynthesis and, if ethylene biosynthesis or perception is blocked, the incidence of lesions is reduced. It was therefore suggested that ROS and ethylene together are involved in the induction of cell death in O_3-exposed plants [22].

Also in a number of other systems ethylene was closely associated with increased cell death. Cell death could be hastened by treatment with ethylene and blocked by ethylene inhibitors [13]. During the aerenchyma formation, cell death shows features of apoptosis and is

dependent on ethylene [9,62]. Maize endosperm development is accompanied by occurrence of DNA ladders and by an increase in ethylene production. Death of epidermal cells at the site of adventitious root emergence in submerged rice seedlings was found to precede the root emergence and to depend on ethylene [63]. Chilling-induced cell death in melon was significantly less in transgenic melons (antisense ACC oxidase) producing only trace amounts of ethylene [64]. Cell death induced by the mycotoxin fumonisin B1 involves ethylene signalling in *Arabidopsis* and tomato [65, 66]. In oat mesophyll cells, the administration of ethylene antagonists, aminooxyacetic acid (AOA) and silver thiosulphate (STS), have effectively inhibited the victorin-induced PCD, involving Rubisco cleavage, DNA laddering, and changes in mitochondrial permeability [67]. Microarray study of AAL-toxin-treated tobacco revealed that genes responsive to ROS, ethylene and a number of proteases, were among the earliest to be upregulated, suggesting that the oxidative burst, production of ethylene and proteolysis, played a role in the activation of the cell death [68]). In *Taxus chinensis* suspension cells, ethylene enhances cell death induced by a fungal elicitor from *Aspergillus niger* [69]. Overproduced ethylene correlates closely with expression of lethal symptoms and apoptotic changes in hybrid tobacco seedlings. The lethality can be suppressed by ethylene synthesis inhibitors AOA and aminoethoxyvinylglycine (AVG) [70].

Additional evidence supporting the role of ethylene in cell death signaling came from the study on *Arabidopsis thaliana* double mutants. Crosses of the lesion mimic mutant *accelerated cell death 5 (acd 5)* and *ethylene insensitive 2 (ein 2)*, in which ethylene signaling is blocked, show decreased cell death [71]. TUNEL positive nuclei and DNA laddering accompany flower petal and ovary senescence. Ethylene treatment induced the senescence and DNA breakdown in petals that could be blocked by ethylene inhibitors [72].

2. Role of cadmium in plant cell death

An extensive research is going for characterisation of PCD in plants at pathogen attack, chemical elicitation and abiotic inducers, but there are still limited reports on the role of heavy metals in PCD induction and little is known about cadmium-triggered signal transduction in plant systems. Contamination of biosphere with heavy metals has hazardous effect on agricultural crops and human health [73, 74].

Cadmium is a toxic trace pollutant originating from industrial sources and phosphate fertilizers [75]. In animal models, cadmium intoxication occurs through apoptosis appearing by activation of endonucleases, DNA laddering, and chromatin condensation. Indirect oxidative stress through inhibition of antioxidant enzymes is involved in the mechanism of Cd action [76]. In HeLa tumour cells Cd can induce apoptosis and oxidative cellular damage [77]. It was demonstrated that in rat C6 glioma cells cadmium is a potent inducer of apoptosis and the apoptotic effect is mediated via generation of oxidative stress [78]. When Cd is in excess in plants, it inhibits respiration, photosynthesis, cell elongation, plant-water relationships, nitrogen metabolism, and mineral nutrition, resulting in poor growth and low biomass [79]. In plant cells, cadmium induces a number of genome-related changes including chromosomal aberrations, decrease of mitotic index in root cells [80], and abnormalities in nuclear structure [80,81]. Symptoms of Cd toxicity include changes in cell membrane integrity and cell ultrastructure; stimulation of ROS production; alterations of antioxidant enzyme system; disturbance of cell ionic equilibrium; triggering of $InsP_3/Ca^{2+}$ transduction processes [82-86]. The accumulation of oxidized proteins and lipid peroxides was observed in shoot and root tissues of pea plants upon the cadmium stress [87,88]. The augmented level of malondialdehyde (MDA) and ion leakage are

markers of the initiated destructive processes and oxidative stress [89]. Increase of MDA content in rice leaves [90] and stimulation of ion leakage in pea plants [91] have been recently reported as a consequence of Cd toxicity.

An increased amount of H_2O_2 was observed in leaves from pea plants grown with 50mM $CdCl_2$. Treatment of leaves from Cd-grown plants with different effectors and inhibitors showed that ROS production was regulated by different processes involving protein phosphatases, Ca^{2+} channels, and cGMP [91]. In rice leaves Cd caused a toxicity associated with the increase in H_2O_2 content, decrease in reduced form glutathione and ascorbic acid contents, and alterations in the specific activities of antioxidant enzymes (superoxide dismutase, glutathione reductase, ascorbate peroxidase, catalase, and peroxidase [90].

Increase of ethylene production was observed in bean leaves under cadmium stress [92, 93]. In barley plants (*H. vulgare* L., cv. CE9704), high concentrations of Cd triggered serious disturbances of the chloroplast membranes and caused an increase of ethylene production whereas the occured a decrease of 18:3 fatty acid content occurred, indicating that Cd mediates the lipid peroxidation in the thylakoids. The enhanced ethylene production is proposed to be used as an early indicator of Cd-induced membrane degradation [94]. Cd-induced superoxide anion and nitric production are known as potential inducers of apoptosis [95], however, in rice leaves, protective effect of nitric oxide against the cadmium toxicity has been established [90].

In this work we have studied the ability of cadmium to induce a programmed cell death in cultured tomato cells and, using a pharmacological approach with specific inhibitors, we have identified some of the biochemical processes involved in the signal transduction cascade. By the administration of specific peptide caspase inhibitors, we have demonstrated for the first time that caspase-like proteases are mediators in the Cd-induced cell death in plants, thus supporting the view that Cd triggered cell death is a form of programmed cell death. Also, by inhibition studies, we have shown that hydrogen peroxide, calcium, and ethylene plays a role in Cd-stimulated PCD machinery. Ethylene was shown to enhance the effect of cadmium on the cell viability reduction. Similar pattern of H_2O_2 stimulation was found in both Cd- and CPT-treated cells. Collectively, the data indicate that, in analogy with CPT effect on cell death, Cd-triggered cell death in plant cells exhibits similarities to HR and cell death, induced by known apoptosis-inducing chemicals, and to the effect in animal systems.

3. Experimental procedure

The experiments were conducted with tomato (*Lycopersicon esculentum* Mill.) suspension cells, line Msk8 grown on a liquid Murashige-Skoog medium, supplemented with 5 μM α-naphtalene acetic acid, 1 μM 6-benzyladenine, 3% (w/v) sucrose, and vitamins. The cells were subcultured every 7 days by 1:4 dilution with fresh medium and kept on a rotary shaker at 25°C. For the experiments, 5 days after subculture 5 ml of the suspension was transferred to 30 ml vials with screw-caps, at sterile conditions. The treatments were provided with $CdSO_4$ or camptothecin (CPT). In order to assess suggested signals involved in cell death pathway, inhibitors of different biochemical steps were tested. Caspase peptide inhibitors, antioxidants, and ethylene blockers were added simultaneously with either $CdSO_4$ or CPT. Parallel control of non-treated suspension cells was subcultured at the same conditions.

For determination of cell viability, 24 h after the treatments with the chemicals, 250 μl from the cell suspension were taken and diluted with 4 ml tap water in small Petri dishes. Fluorescein diacetate (0.002% FDA) was used to stain the viable cells. The cell viability was

calculated as a percentage of living cells to their total number of cells. Data were statistically processed, presented as average values from at least three independent experiments, and compared by SEM.

The amount of hydrogen peroxide was determined by the luminol method as described earlier [96] and measured by chemiluminiscence in a ferricyanide-catalised oxidation of luminol. For details on methodology, see [42, 61].

4. Results and discussion

Tomato suspension culture represents good model system for testing inducers and inhibitors of apoptotic cell death. The suspension cells were treated with a range of $CdSO_4$ concentrations: 10 μM, 100 μM, 1 mM, and 10 mM and the percentage of viable cells was determined by FDA staining. A reduction of cell viability appeared with the increase of Cd dose reaching complete lethality at the application of 10 mM $CdSO_4$ (Fig. 1). In the same set of experiments, the treatment with 5 μM CPT reduced cell viability to 72.5 % (Fig. 2). For further determination of the similarities between cadmium- and CPT-induced cell death, in the experiments with inhibitors, 100 μM $CdSO_4$ was used. Tomato suspension cells showed a gradual restoration of cell viability 48 hrs after the beginning of treatment with 10 and 100 μM $CdSO_4$ (data not shown).

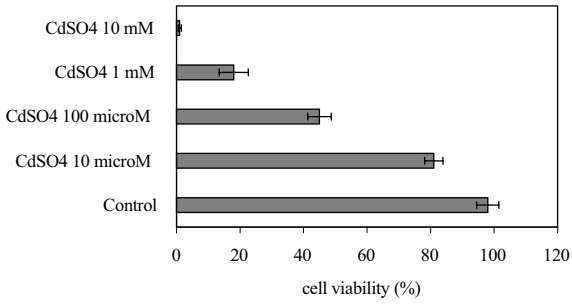

Figure 1. Effect of $CdSO_4$ concentration on cell viability in tomato suspension cells. Percentage of cell viability (FDA staining of viable cells) was scored 24 hrs after the treatments. Data are means of at least three independent experiments. Error bars indicate SEM.

Development of resistant sub-population, sequestrian of Cd to the vacuole or enhanced synthesis of phytochelatins might be a possible explanation. Reversible apoptosis, DNA repair, and 3-days-long lag phase for Cd-induced cell death has been reported for tobacco (TBY-2) cells treated with 50 μM $CdSO_4$ [97]. 150 μM $CaSO_4$ has strongly inhibited the initial growth of tomato cells but the reduced growth rate has been restored after 4 days and these results have been attributed to phytochelatins synthesis in contrast to azuki bean cells that have not survived the high cadmium concentrations [98]. In contrast to Cd-treated cells, CPT-treated cells continued to loose viability after 48 hrs and no living cells were detected after 96 hrs.

To test if the cadmium-induced cell death is apoptotic in nature, caspase-specific inhibitors were administrated simultaneously with 100 μM $CdSO_4$. The human caspase-1

inhibitor Ac-YVAD-CMK and the broad range caspase inhibitor Z-Asp-CH_2-DCB, at concentrations of 100 nM preserved the cell viability of Cd-treated cells at a level close to the control non-treated cells (Fig. 2). This strongly suggests that the cell death pathway, induced by cadmium, employs caspase-like proteases. Similar maintenance of cell viability by the caspase inhibitor Ac-YVAD-CMK was found for CPT treated cells. Inhibitors of human caspases have been shown to suppress plant cell death also in other experimental plant systems. Caspase-3 inhibitor Ac-DEVD-CHO effectively blocked menadione-induced PCD in tobacco protoplasts [20] and co-infiltration of Ac-DEVD-CHO with *Pseudomonas syringae* pv. *tabaci* resulted in a reduced plant cell death [99]. Ac-YVAD-CMK and Z-Asp-CH_2-DCB completely abolished HR lesion formation and significantly reduced H_2O_2 production and malondialdehyde amount in isolated leaves of transgenic and wild type tobacco when applied together with *Pseudomonas syringae* pv. *tabaci* [100]. The inhibition of cell death with specific peptide caspase inhibitors in animal systems [3] and in plants [27,42] is an indication that the cells undergo a cell suicide program. Abiotic stress can induce programmed cell death in plant systems. Heat shock, ethanol, and H_2O_2 have been shown to stimulate cell death in carrot suspension cells but an inhibition of cell death by membrane-permeant ICE inhibitor Z-Val-Ala-Asp-flutomethylketone and by cysteine protease inhibitor leupeptin has not been detected [101].

Here we demonstrate (Fig. 2) that the broad-spectrum caspase inhibitor Z-Asp-CH_2-DCB was able to block the Cd-induced cell death. This gives a reason to assume that in tomato suspension cells Cd-triggered cell death most probably resembles features of the programmed cell death. DNA laddering is a hallmark of animal apoptosis, but in plants the necessity of nucleosomal DNA fragmentation for complete apoptotic phenotype is still controversial. In some cases of plant cell death, the DNA degradation has not been observed [95,102]. No detectable DNA ladder was found in soybean cells undergoing chitosan-induced cell death [33]. Neither TUNEL positive nuclei nor DNA fragmentation have been reported for Cd-treated pea leaves [91]. In contrast, there is the chronic exposure of tobacco cells to cadmium-triggered DNA fragmentation [103]. But in those experiments cadmium concentration was 1000 times higher (100 mM $CdCl_3$)) that that used in this work (100 μM $CdSO_4$). It remains to look for DNA fragmentation in Cd-treated tomato suspension cells.

In the cell death during the HR [31] and following, e.g. CPT treatment of tomato cells, cell death is accompanied by an oxidative burst. At the same time H_2O_2 plays a thought role as signalling molecule in apoptotic machinery [61]. H_2O_2 production was measured in the modified culture medium by chemiluminiscence in a ferricyanide-catalised oxidation of luminol, for 5 hrs following cadmium and CPT treatments. One hour after the application of cadmium, H_2O_2 level increased (Fig. 3), whereas CPT caused a rise of H_2O_2 amount with 30 min delay after cadmium injection. At time points of 1.5 hrs and 3.5 hrs following the beginning of the treatments, the concentration of H_2O_2 was the same in both Cd- and CPT-elicited cells.

After 3.5 hours, the concentration of hydrogen peroxide in Cd-treated cell declined, while in CPT-treated suspension the H_2O_2 amount stayed at high level. Collectively these data indicate that in analogy with CPT effect on cell death, cadmium-induced oxidative burst is integral part of the tomato cells response. To this end cadmium-induced cell death in plant cells exhibits similarities to HR and cell death induced by known apoptosis inducing chemicals and to its effect in animal systems.

To further elucidate the involvement of oxidative stress in Cd-induced reduction of cell viability in the tomato suspension, antioxidants were applied simultaneously with 100 μM $CdSO_4$. The H_2O_2 scavengers (100 μM ascorbic acid, 10 U/ml catalase and 100 μM spermine) were effective stimulators of cell viability of Cd- and CPT-treated cells (Fig. 2).

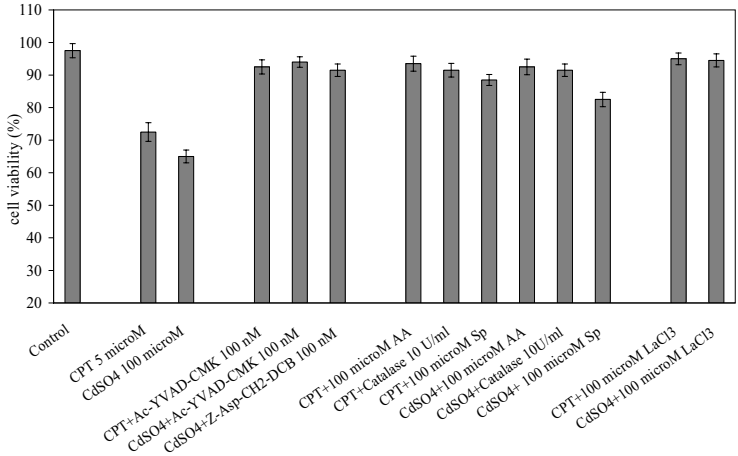

Figure 2. Effect of peptide caspase inhibitors (Ac-YVAD-CMK and Z-Asp-CH2-DCB), antioxidants; ascorbic acid (AA), catalase and spermine (Sp) and calcium channel blocker La Cl_3 on cell viability in tomato suspension cells. Percentage of cell viability (FDA staining of viable cells) was scored 24 hrs after the treatments. Data are means of at least three independent experiments. Error bars indicate SEM.

The inhibition of Cd-induced cell death by ascorbic acid and catalase in tomato suspension is in line with the finding that the same H_2O_2 scavengers prevented H_2O_2 accumulation and reduced the symptoms of Cd toxicity in pea leaves [91]. Our results that antioxidants were able to suppress Cd-induced cell death, suggest that H_2O_2 is responsible for the induction of PCD. Similar cell death inhibition by catalase has been reported in animal cells exposed to Cd. Co-incubation of rat glioma cells with catalase and cadmium did strongly inhibit the Cd-induced DNA ladder formation, indicating the fact of H_2O_2 involvement into apoptotic activity of Cd in animal systems [78].

In parsley cells the scavenging of H_2O_2 by catalase completely abolished detection of H_2O_2 by luminol assay [104]. In addition, TMP (superoxide radical scavenger), DPI, and lanthanum suppressed Cd-induced cell death in pea leaves indicating that the NADPH-oxidase and calcium-fluxes-activated H_2O_2 production are involved [91].

Ascorbic acid (AA) is a major antioxidant in photosynthetic and non-photosynthetic tissues and is utilised as a substrate for ascorbate peroxidase catalised detoxification of H_2O_2 [105]. In tomato suspension cells AA strongly prevented loss of viability of CPT- or Cd-treated cells (Fig. 2). Since it is found that in Cd-stressed pea leaves the level of AA decreases [90], our results are additional indication that Cd is a strong inducer of oxidative stress.

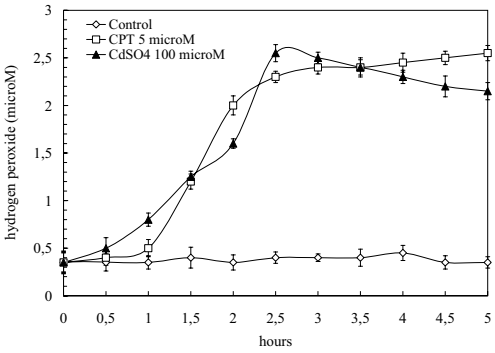

Figure 3. Dynamics of hydrogen peroxide production by tomato suspension cells. At time point 0, cells were treated with either 5 μM CPT or 100 μM $CdSO_4$. Data are means of at least three independent experiments. Error bars indicate SEM.

The administration of 100 μM spermine led to about 50% restoration of Cd-inhibited cell viability and similar stimulation of cell viability was observed at the simultaneous application of CPT and spermine (Fig. 2). Spermine is found to prevent apoptotic cell death in rat cerebellar granule neurons [106]. Spermine is a polyamine and due to positively charged end NH^{2+} groups has a capacity to scavenge ROS [107]. To our knowledge, our data are the first indication that polyamines can be effective inhibitors of Cd-induced cell death in plants.

Ca^{2+} is a second messenger and an important element in elicitor-mediated cell suicide signalling. To study the role of Ca^{2+} in PCD triggering, we assayed the cell viability in the presence of Cd^{2+} and calcium channel blocker La^{3+} applied as $LaCl_3$. A stimulation of the cell viability was determined at the treatment with 1 mM La Cl_3 (Fig. 2).

In mammalian systems elevated levels of intracellular Ca^{2+} can activate programmed cell death and DNA digestion through direct stimulation of endonucleases or via Ca-dependent proteases, phosphatases, and phospholipases [101,108]. In bacteria-elicited tobacco suspension cells the increased Ca^{2+} influx and HR response have been prevented by La^{3+} [109]. La^{3+} has also been reported to completely block the cell condensation and shrinkage of cultured carrot cells triggered by ethanol, heat shock, and H_2O_2 [110]. Other chemical modulators capable of decreasing the cytosolic free Ca^{2+}, such as ruthenium red, W-7 (N-[6-aminohexyl]-5-chloro-1-naphthalenesulfonamide), and Ca^{2+} chelator EGTA, can also inhibit the programmed cell death in plants [37]. Ca^{2+} is also a mediator of signal transduction pathway leading to caspase-3-like dependent cell death following administration of low doses of chitosan [38]. In our experiments with tomato suspension cells, La^{3+}-treatment prevented the Cd-stimulated cell death (Fig. 2) thus indicating that Ca^{2+} is implicated in Cd-triggered signalling. Lanthanum also effectively inhibited Fumonisin B1-induced cell death in tomato cells [100].

It has been demonstrated that the depletion of Ca^{2+} reduces the formation of ROS in cultured spruce cells [96]. Our previous study indicated that La^{3+} decreased H_2O_2 in the tomato suspension treated with CPT [61] and this effect was most probably due to a blockage of Ca channels, thus preventing the activation of enzymes involved in ROS production. This is in line

with the findings that inhibitors of elicitor-stimulated ion fluxes block the oxidative burst [104]. Similar mechanism can be suggested for the effect of lanthanum on Cd-induced cell death.

Ethylene was found to be an important mediator of plant cell death although its mode of action is under investigation. Treatment of the cells with relatively high concentrations of ethylene did not have any effect on viability of the cells (Fig. 4). Concentrations of up to 100 ppm in the headspace, giving about 12 ppm in the liquid phase, were applied during 24 h. Addition of ACC to the nutrient medium, despite its stimulating effect on ethylene production, also did not induce a cell death [41]. This shows that ethylene is not a primary trigger of the cell death in these cells. However, when ethylene was applied to Cd- or CPT-treated cells, a significant decrease in the cell viability was observed as compared to Cd- or CPT-treatments alone (Fig. 4). Experiments with AVG inhibitor of ethylene synthesis, revealed that ethylene is an essential factor mediating the Cd- and CPT-induced cell death. When AVG was administrated simultaneously with either $CdSO_4$ and ethylene or CPT and ethylene, the cell viability could not be restored (Fig. 4).

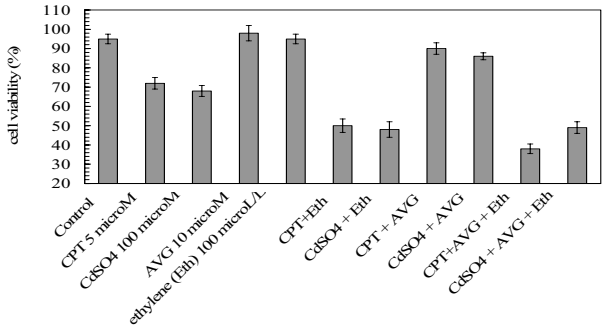

Figure 4. Effect of ethylene and ethylene synthesis inhibitor AVG on cell viability in cadmium- and CPT-treated tomato suspension cells. Percentage of cell viability (FDA staining of viable cells) was scored 24 hrs after the treatments. Data are means of at least three independent experiments. Error bars indicate SEM.

We have reported that the inhibition of ethylene receptor by STS significantly abolishes the cell death triggered by CPT and CPT+ethylene. Ethylene markedly stimulates the amount of hydrogen peroxide produced in response to CPT treatment [41,61]. In addition, AVG and STS blocks the effect of CPT on hydrogen peroxide production [61].

The general proposition can be made that ethylene apparently increases the oxidative stress invoked by the primary stressors (CPT and $CdSO_4$). If we generalise this view, it could explain the stimulatory role of ethylene in the symptom expression in a number of cases where oxidative stress is believed to induce the cell death such as in the effects of temperature extremes, ozone, wounding and pathogen challenge. Ethylene insensitivity in double mutants of *ein 2* and the O_3- sensitive *radical –induced cell death 1 (rcd 1)* blocks ROS accumulation that is required for a lesion propagation, while exogenous ethylene increases the ROS-dependent cell death [22]. Limiting of the spread of pathogen-induced cell death in tomato involves the down-regulation of ethylene [111]. The mechanism of ethylene-enhanced oxidative stress is not known and may vary from case to case. Possible modes of action of ethylene in enhanced ROS levels may be the stimulation of NADPH oxidase activating proteins, the down regulation of ROS scavenging pathways, or interference with mitochondrial functioning.

Cell death in *Taxus chinensis* cell culture treated with fungal elicitor was reported to involve ethylene and polyamines. The addition of ethylene precursor 1-aminocyclopropane-1-carboxylic acid (ACC) has remarkably enhanced the elicitor-induced cell death and diminished the level of endogenous spermine. Exogenous application of spermine, spermidine and putrescine together with the fungal elicitor abolished both the cell death and ethylene production. Addition of ACC synthase inhibitor AVG led to a decrease of ethylene production and reduction of the cell-death-stimulating effect of ACC on elicitor-induced cell death [69].

Biosynthesis of ethylene and polyamines (PA) are linked through a common precursor S-adenosylmethionine (SAM) that may be an explanation of the inhibitory effect of ethylene biosynthesis inhibitors on the cell death. Enhanced PA concentration may decrease the C_2H_4 production because PA can inhibit ACC synthase transcripts [112]. Reduction of ethylene production by administration of PA was also observed in other plant systems [107].

Since in the tomato cells studied here ethylene additionally diminished Cd- and CPT-reduced cell viability and since cell viability was enhanced in response to spermine, we hypothesise that the effect of PA might be attributed not only to their H_2O_2 scavenging properties, but also to the inhibition of C_2H_4 synthesis. Moreover, by laser photoacoustic detection of C_2H_4, Cd was found to significantly stimulate endogenous C_2H_4 production in the tomato cells (Iakimova et al., in preparation). Ethylene and nitric oxide are both integrated in cell death elicitation by pathogenic challenge or abiotic stress [113].

In *Pseudomonas syringae* pv. *tabaci* and *P. s.* pv. *phaselicola* elicited tobacco plants the HR is associated with enhanced NO production as measured by photoacoustics. Treatments with NO donor sodium nitroprusside (SNP) led to increased biphasic ethylene emanation and a model for NO, salicylic acid, C_2H_4, and ROS interplay in the HR is proposed [114]. Antioxidant properties of NO have been found to counteract the Cd-induced oxidative stress, reduce the paraquat toxicity in rice [90,115] and to inhibit the programmed cell death in barley aleurone layers [116]. It is further to be elucidated the involvement of NO in Cd-triggered cell death in tomato suspension cells.

5. Conclusion

Evidence is accumulating that caspase-like cysteine proteases, showing a functional similarity to the animal caspases, participate in the programmed cell death in plants. In addition to discoveries that caspase-like proteases are involved in cell death in response to a pathogen invasion, abiotic stresses, or chemical elicitation, our data show that cell death induced by cadmium is also a form of programmed cell death mediated by caspase-like proteases. We have established a key role of hydrogen peroxide and calcium in the cadmium-induced apoptotic cell death and have demonstrated that oxidative stress is associated with both the cadmium- and camptothecin-triggered cell death. We have also shown that polyamines can effectively preserve the cell viability in the conditions of chemical stress. Ethylene was found to be an important mediator of plant cell death. The finding that ethylene greatly stimulates cadmium-induced cell death, and that cadmium treatment enhances endogenous ethylene production, indicates that ethylene participates in the cadmium-induced cell death in tomato suspension cells.

Collectively, the cell response to cadmium elicitation and the inhibitors indicate that Cd-triggered cell death is analogous to a cell death in response to CPT treatment and involves caspase-like proteases, oxidative stress and ethylene. Cd-induced cell death in plant cells exhibits similarities to HR and cell death induced by known apoptosis-inducing chemicals and to its effect in animal systems.

To assess the complete mechanism of Cd stress in the performance of apoptotic cell death in plants further investigations on nuclear morphological changes and characterization of other biochemical processes are necessary.

Acknowledgements

Elena Iakimova and Veneta Kapchina-Toteva were supported by STSM grants (COST Action 844).

References

[1] Steller H., "Mechanisms and genes of cellular suicide". *Science*, vol. 267, p.p. 1445-1449, 1995.
[2] Zhivotovsky B., "Apotosis, necrosis and between". *Cell Cycle*, vol. 3(1), p.p. 64-66, 2004.
[3] Grütter M.G., "Caspases: key players in programmed cell death". *Curr. Opin. Struct. Biol*., vol. 10, p.p. 649-655, 2000.
[4] Hengartner M.O., "The biochemistry of apoptosis". *Nature*, vol. 407, p.p. 770-776, 2000.
[5] Danon A., Delorme V., Mailhac N. and Gallios P., "Plant programmed cell death: a common way to die". *Plant Physio. Biochem*., vol. 38, p.p. 647-655, 2000.
[6] Jones A.M., "Programmed cell death in development and defense". *Plant Physiol*., vol. 125, p.p. 94-97, 2001.
[7] Lam E., "Controlled cell death, plant survival and development". *Mol. Cell Biol*., vol. 5, p.p. 305-315, 2004.
[8] Fukuda H., "Programmed cell death of tracheary elements as a paradigm in plants". *Plant Mol. Biol*., vol. 44, p.p. 245-253, 2000.
[9] Drew M.C., He I. and Morgan P.W., "Programmed cell death in animals and plants". BIOS Scientific Publishers Ltd., Oxford, pp 183-192, 2000.
[10] Wu H.M. and Cheung A.Y., "Programmed cell death in plant reproduction". *Plant Mol. Biol*., vol. 44, p.p. 267-281, 2000.
[11] Rubinstein B., "Regulation of cell death in flower petals". *Plant Mol. Biol*., vol. 44, p.p. 303-318, 2000.
[12] Fath A., Bethke P., Lonsdale J., Meza-Romero R. and Jones R., "Programmed cell death in cereal aleurone". *Plant Mol. Biol*., vol. 44, p.p. 255-266, 2000.
[13] Young T.E. and Gallie D.R., "Programmed cell death during endosperm development". *Plant Mol. Biol*., vol. 44, p.p. 283-301, 2000.
[14] Greenberg J.T. and Yao N., "The role and regulation of programmed cell death in plant-pathogen interactions". *Cellular Microbiol*., vol. 6(3), p.p. 201-211, 2004.
[15] Heath M.C., "Hypersensitive response-related death". *Plant Mol. Biol*., vol. 44, p.p. 323-334, 2000.
[16] Shirasu K. and Shulze-Lefert P., "Regulation of cell death in disease resistance". *Plant Mol. Biol*., vol. 44, p.p. 371-385, 2000.
[17] McCabe P.F. and Leaver C.J., "Programmed cell death in cell cultures". *Plant Mol. Biol*., vol. 44, p.p. 359-368, 2000.
[18] Tian R.H., Zhang G.Y., Yan C.H. and Dai Y.R., "Involvement of poly (ADP-ribose) polymerase and activatyion of caspase-3-like protease in heat shock-induced apoptosis in tobacco suspension cells". *FEBS Lett*., vol. 474, p.p. 11-15, 2000.
[19] Zhang G.-Y., Zhu R.-Y., Xu Y., Yan Y.-B. and Dai Y.-R., "Increase in methylene resonance signal intensity is associated with apoptosis in plant cells as detected by ^{1}H-NMR". *Acta Bot. Sin*., vol. 46, p.p. 711-718, 2004.
[20] Sun Y.L., Zhao Y., Hong X. and Zhai Z.H., "Cytochrome c release and caspase activation during menadione-induced apoptosis in plants". *FEBS Lett*., vol. 462, p.p. 317-321, 1999.
[21] Moeder W., Barry C.S., Tauriainen A.A., Betz C., Toumainen J., Untriainen M., Gierson D., Sandermann H., Lagebarteles C. and Kangasjarvi J., "Ethyelene synthesis regulated by biphasic induction of 1-aminocyclopropane-1-carboxylic acid synthase and 1-aminocyclopropane-1-carboxylic acid oxidase genes is required for hydrogen peroxide accumulation and cell death in ozone-exposed tomato". *Plant Physiol*., vol. 130, p.p. 1918-1926, 2002.
[22] Overmyer K., Tuominen H., Kettunen R., Betz C. Langebartels C., Sandermann H.Jr. and Kangasjarvi J., "Ozone-sensitive *Arabidopsis* rcd1 mutant reveals opposite roles for ethylene and jasmonate signaling pathways in regulating superoxide- dependent cell death". *Plant Cell*, vol. 12, p.p. 1849-1862, 2000.

[23] Pasqualini S., Piccioni C., Reale L., Ederli L., Della Torre G. and Ferranti F., "Ozone-induced cell death in tobacco cultivar Bel W3 plants. The role of programmed cell death in lesion formation". *Plant Physiol*., vol. 133, p.p. 1122-1134, 2003.

[24] Rao M.V., Koch J.R. and Davis K.R., "Ozone: a tool for probing programmed cell death in plants". *Plant Mol. Biol*., vol. 44, p.p. 345-358, 2000.

[25] Danon A. and Gallois P., "UV-C radiation induces apoptotic-like changes in *Arabidopsis thaliana". FEBS Lett.*, vol. 437, p.p. 131-136, 1998.

[26] Xu C.-J., Chen K.-S. and Ferguson I.B., "Programmed cell death features in apple suspension cells under low oxygen culture". *JZUS*, vol. 5(2), p.p. 137-143, 2004.

[27] De Jong A.J., Yakimova E.T., Hoeberichts F.A., Maximova E. and Woltering E.J., "Chemical-induced apoptotic cell death in tomato cells: Involvement of caspase-like proteases. *Planta*, vol. 211, p.p. 656-662, 2000.

[28] Wang H., Juan L.I., Bostock R.M. and Gilchrist D.G., "Apoptosis: a functional paradigm of programmed cell death induced by a host-selective phytotoxin and invoked during development". *Plant Cell*, vol. 8(3), p.p. 375-391, 1996.

[29] Wang H., Jones C., Ciacci-Zanella J., Holt T., Gilchrist D.G. and Dickman M.B., "Fumonisins and Alternaria alternata lycopersici toxins: sphinganine analog mycotoxins induce apoptosis in monkey kidney cells". *Proc. Natl. Acad. Sci. USA*, vol. 93, p.p. 3461-3465, 1996.

[30] Jabs T., "Reactive oxygen intermediates as mediators of programmed cell death in plants and animals". *Biochem. Pharmacol*., vol. 57, p.p. 231-245, 1999.

[31] Levine A.., Tenhaken R., Dixon R. and Lamb C.J., "H_2O_2 from the oxidative burst orchestrates the plant hypersensitive response". *Cell*, vol. 79, p.p. 583-593, 1994.

[32] Levine A., Pennell R.I., Alvarez M., Palmer R. and Lamb C.J., "Calcium-mediated apoptosis in plant hypersensitive disease resistance response". *Curr. Biol*., vol. 6, p.p. 427-437, 1996.

[33] Zuppini A., Baldan B., Millioni R., Favaron F., Navazio L. and Mariani P., "Chitosan induces Ca^{2+}- mediated programmed cell death in soybean cells". *New Phytol*., vol. 161, p.p. 557-568, 2003.

[34] Beers F.P. and Freeman T.B., "Proteinase activity during tracheary element differentiation in Zinnia mesophyll cultures". *Plant Physiol*., vol. 113, p.p. 873-880, 1997.

[35] Repka V., "Evidence for the involvement of cysteine proteases in the regulation of methyl jasmonate-induced cell death in grapevine". *VITIS*, vol. 41(3), p.p. 115-121, 2002.

[36] Xu F.-X. and Chye M.-L., "Expression of cysteine proteinase during developmental events associated with programmed cell death in brinjal". *Plant J*., vol. 17(3), p.p. 321-327, 1999.

[37] He Ch.-J., Morgan P.W. and Drew M.C., "Transduction of an ethylene signal is required for cell death and lysis in the root cortex of maize during aerenchyma formation induced by hypoxia". *Plant Physiol*., vol. 112, p.p. 463-472, 1996.

[38] Hoeberichts F.A. and Woltering E.J., "Multiple mediators of plant programmed cell death, p.p. interplay of conserved cell death mechanisms and plant-specific regulators". *BioEssays*, vol. 25, p.p. 47-57, 2003.

[39] Lund S.T., Stall E. and Klee H.J., "Ethylene regulates the susceptible response to pathogen infection in tomato". *Plant Cell*, vol. 10, p.p. 371-382, 1998

[40] Spencer M., Ryu Ch.-M., Yang K.-Y., Kim Y.Ch., Kloepper J.W. and Anderson A.J., "Induced defence in tobacco by Pseudomonas chlororaphis strain O6 involves at least the ethylene pathway". *Physiol. Mol. Plant Pathol*, vol. 63, p.p. 27-34, 2003.

[41] Woltering E.J., de Jong A.J., Iakimova E., Kapchina V. and Hoeberichts F.A., "Ethylene: Mediator of oxidative stress and programmed cell death in plants". In: Biology and Biotechnology of the Plant Hormone Ethylene III (Eds. Vendrell et al.) IOS Press, pp.315-323, 2003.

[42] Del Pozo O. and Lam E., "Caspases and programmed cell death in the hypersensitive response of plants to pathogenes". *Curr. Biol*., vol. 8, p.p. 1129-1132, 1998.

[43] Del Pozo O. and Lam E., "Expression of the baculovirus p35 protein in tobacco affects cell death progression and compromises N gene mediated disease resistance response to TMV". *Mol. Plant Microbe Interact*., vol. 16, p.p. 485-494, 2003.

[44] Woltering E.J., van der Bent A. and Hoeberichts F.A., "Do plant caspases exist?". *Plant Physiol*., vol. 130, p.p. 1764-1769, 2002.

[45] Belegni M.V., Fath A., Bathake P.C., Lamttina L. and Jones R.L., "Nitiric oxide acts as an antioxidant and delays programmed cell death in barley aleurine layers". *Plant Physiol*., vol. 129, p.p. 1642-1650, 2002.

[46] Ekert P.G., Silke J. and Vaux D.L., "Caspase inhibitors". *Cell Death and Differ*., vol. 6, p.p. 1081-1086, 1999.

[47] Korthout H.A., Berecki G., Bruin W., van Duijn B. and Wang M., "The presence and subcellular localization of caspase-3-like proteinases in plant cells". *FEBS Lett*., vol. 475, p.p. 139-144, 2000.

[48] Watanabe N, and Lam E., "Recent advance in the study of caspase-like proteases and Bax inhibitor-1 in plants: their possible roles as regulator of programmed cell death". *Mol. Plant Pathol*., vol. 5(1), p.p. 65-70, 2004.
[49] Uren A.G., O'Rourke K., Aravind L., Pisabarro M.T., Seshagiri S., Koonin E.V. and Dixit V.M., "Identification of paracaspases and metacaspases. Two ancient families of caspase-like proteins, one of which plays a key role in MALT lymphoma". *Mol. Cell*, vol. 6, p.p. 961-967, 2000.
[50] Madeo F., Herker E., Maldener C., Wissing S., Lächelt S., Herlan M., Fehr M., Lauber K., Sigrist S.J., Wesselborg S. and Fröhlich K.U., "A caspase-related protease regulates apoptosis in yeast". *Mol. Cell*, vol. 9, p.p. 1-20, 2002.
[51] Hoeberichts F.A., ten Have A. and Woltering E.J., "A tomato metacaspase gene is upregulated during programmed cell death in Botrytis cinerea-infected leaves". *Planta*, vol. 217, p.p. 517-522, 2003.
[52] Bozhkov P.V., Filonova L.H., Suarez M.F., Helmersson A., Smertenko A.P., Zhivotovsky B. and von Arnold S., "VEIDase is a principal caspase-like activity involved in plant programmed cell death and essential for ambryonic pattern formation". *Cell Death and Differ*., vol. 11, p.p. 175-182, 2004.
[53] Suarez M.F., Filonova L.H., Smertenko A., Savenkov E.I., Clapham D.H., von Arnold S., Zhivotovsky B. and Bozhkov P.V., "Metacaspase-dependent programmed cell death is essential for plant embryogenesis". *Curr. Biol*., vol. 14 (9), p.p. 339-340, 2004.
[54] Warren C.C. and Wolpert T.J., "Purification and characterisation of serine proteases that exhibit caspase-like activity and are associated with programmed cell death in Avena sativa". *Plant Cell*, vol. 16, p.p. 857-873, 2004.
[55] Lamb C. and Dixon R.A., "The oxidative burst in plant defense resistance". *Annu. Rev. Plant Physiol*., vol. 48, p.p. 251-275, 1997.
[56] Bethke P.C. and Jones R.L., "Cell death of barley aleurone protoplasts is mediated by reactive oxygen species". *Plant J*., vol. 25(1), p.p. 19-29, 2001.
[57] Foyer C.H., Lopez-Delgado H., Dat J.F. and Scott I.M., "Hydrogen peroxide- and glutathione-associated mechanisms of acclimatory stress tolerance and signaling". *Physiol. Plant*, vol. 100, p.p. 241-254, 1997.
[58] Nicholls. and D.G., Budd S.L., "Mitochondria and neuronal survival". *Physiol. Rev*., vol. 80, p.p. 315-360, 2000.
[59] Bolwell G.P., "Role of active oxygen species and NO in plant defense responses". *Curr. Opin. Plant Biol*., vol. 2, p.p. 287-294, 1999.
[60] Kasparovsky T., Milat M.-L., Humbert C., Blein J.-P., Havel L. and Mikes V., "Elicitation of tobacco cells with ergosterol activates a signal pathway including mobilization of internal calcium". *Plant Physiol. and Biochem*., vol. 41, p.p. 495-501, 2003.
[61] De Jong A.J., Yakimova E.T., Kapchina V.M. and Woltering E.J., "A critical role of ethylene in hydrogen peroxide release during programmed cell death in tomato suspension cells". *Planta*, vol. 214 (4), p.p. 537-545, 2002.
[62] Gunawardena A.H., Pearce D.M., Jackson M.B., Hawes C.R. and Evans D.E., "Characterisation of programmed cell death during aerenchyma formation induced by ethylene or hypoxia in roots of maize (Zea mays L.)". *Planta*, vol. 212, p.p. 205-214, 2001.
[63] Mergemann H. and Sauter M., "Ethylene induces epidermal cell death at the site of adventitious root emergence in rice". *Plant Physiol*., vol. 124, p.p. 609-614, 2000.
[64] Ben-Amor M., Flores M., Latche A., Bouzayen M., Pech J.-C. and Romojaro F., "Inhibition of ethylene biosynthesis by antisense ACC oxidase RNA prevents chilling injury in Charentias cantaloupe melon". *Plant Cell Environ*., vol. 22, p.p. 1579-1586, 1999.
[65] Asai T., Stone J.M., Heard J.E., Kovtun Y., Yorgey P., Sheen J. and Ausubel F.M., "Fumonisin B1-induced cell death in *Arabidopsis* protoplasts requires jasmonate-, ethylene-, and salicylate-dependent signaling pathways". *Plant Cell*, vol. 12, p.p. 1823-1836, 2000.
[66] Moore T., Martineau B., Bostock R.M., Lincoln J.E. and Gilchrist D.G., "Molecular and genetic characterization of ethylene involvement in mycotoxin-induced plant cell death". *Physiol. Mol. Plant Path*., vol. 54, p.p. 73-85, 1999.
[67] Curtis M.J. and Wolpert T.J., "The victorin-induced mitochondrial permeability transition precedes cell shrinkage and biochemical markers of cell death, and shrinkage occurs without loss of membrane integrity". *Plant J*., vol. 38, p.p. 244-259, 2004.
[68] Gechev T.S., Gadjev I.Z. and Hille J., "An extensive microarray analysis of AAL-toxin-induced cell death in *Arabidopsis thaliana* brings new insights into the complexity of programmed cell death in plants". *Cell Mol. Life Sci*., vol. 61, p.p. 1185–1197, 2004.
[69] Qin W.M. and Lan W.Z., "Fungal elicitor-induced cell death in *Taxus chinensis* suspension cells is mediated by ethylene and polyamines". *Plant Sci*., vol. 166, p.p. 989-995, 2004.

[70] Yamada T. and Marubashi W., "Overproduced ethylene causes programmed cell death leading to temperature sensitive lethality in hybrid seedlings from the cross Nicotiana suaveolens x N. Tabaccum". *Planta*, vol. 217, p.p. 690-698, 2003.
[71] Greenberg J.T., Silverman F.P. and Liang J., "Uncoupling salicylic acid-dependent cell death and defense-related responses from disease resistance in the *Arabidopsis* mutant acd 5". *Genetics*, vol. 156, p.p. 341-350, 2000.
[72] Orzaez D. and Granell A., "DNA fragmentation is regulated by ethylene during carpel senescence in Pisum sativum". *Plant J*., vol. 11, p.p. 137-144, 1997.
[73] Freedman L.P., Luisi B.F., Korszun Z.R., Basavappa R., Sigler P.B. and Yamamoto K.R., "The function and structure of the metal coordination sites within the glucocorticoid receptor DNA binding domain". *Nature*, vol. 334, p.p. 543-546, 1988.
[74] Nellessen J.E. and Fletcher J.S., "Assessment of published literature on the uptake, accumulation, and translocation of heavy metals by vascular plants". *Chemosphere*, vol. 9, p.p. 1669-1680, 1993.
[75] Wagner C.J., "Accumulation of cadmium in crop plants and its consequences to human health". *Advances in Agronomy*, vol. 51, p.p. 173-212, 1993.
[76] Hamada T., Tanimoto A. and Sasaguri Y., "Apoptosis induced by cadmium". *Apoptosis*, vol. 2(4), p.p. 359-367, 1997.
[77] Szuster-Ciesielska A., Stachura A., Slotwinska M., Kaminska T., Siniez R., Paduch R., Abramczyk D., Filar J. and Kandefer-Szerszen M., "The inhibitory effect of zinc on cadmium-induced cell apoptosis and reactive oxygen species (ROS) production in cell cultures". *Toxicology*, vol. 145, p.p. 159–171, 2000.
[78] Wetjen W. and Beyersmann D., "Cadmium-induced apoptosis in C6 glioma cells: Influence of oxidative stress". *BioMetals*, vol. 17, p.p. 65-78, 2004.
[79] Di Toppi L.S. and Gabbrielli R., "Response to cadmium in higher plants". *Environ. Exp. Bot*., vol. 41, p.p. 105-130, 1999.
[80] Zhang Y. and Yang X., "The toxic effects of cadmium on cell division and chromosomal morphology of *Hordeum vulgare*". *Mutation Res*., vol. 312, p.p. 121-126, 1994.
[81] Jiang W.S., Liu D.H. and Li M.X., "Effect of Cd2+ on the nucleus in root tip cells of *Allium cepa*". *J. Environ. Sci*., vol. 6, p.p. 382-386, 1994.
[82] Barcelo J., Vazquez M.D. and Poschenrieder Ch., "Structural and ultrastructural disorders in cadmium-treated bush bean plants (Phaseolus vulgaris L.)". *New Phytol*., vol. 108, p.p. 37-49, 1988.
[83] Jones G.J., Nichols P.B., Johns R.S. and Smith J.B., "The effect of mercury and cadmium on the fatty acid and sterol composition of the marine diatom Asterionella glacialis". *Phytochemistry*, vol. 26, p.p. 1343-1348, 1987.
[84] Olmos E., Martinez-Solano J.R., Piqueras A. and Hellin E., "Early steps of the oxidative burt induced by cadmium in cultured tobacco cells (BY-2 line)". *J. Exp. Bot*., vol. 54, p.p. 291-301, 2003.
[85] Stroinski A., "Effect of cadmium on host-pathogen system. V. Effect of exogenous dicyclohexylamine on potato tubers (Solanum tuberosum L.), cadmium and Phytophthora infestans relations". *J. Plant Physiol*., vol. 150, p.p. 178-183, 1997.
[86] Stroinski A., "Some Physiol.ogical and biochemical aspects of plant resistance to cadmium effect. Antioxidative system". *Acta Physiologiae Plantarum*, vol. 21 (2), p.p. 175-188, 1999.
[87] Sandalio L.M., Dalurzo H.C., Gomez M., Romero-Puertas M.C. and del Rio L.A., "Cadmium-induced changes in the growth and oxidative metabolism of pea plants". *J. Exp. Bot*., vol. 52, 2115-2126, 2001.
[88] Romero-Puertas M.C., Zabalza A., Rodríguez-Serrano M., Gómez M., del Río L.A. and Sandalio L.M., "Antioxidative response to cadmium in pea roots". *Free Radical Research*, vol. 37, p. 44, 2003.
[89] Haliwell B. and Gutteridge J., "Role of free radicals and catalytic metal ions in human disease. An overview". *Methods Enzymol*., vol. 186, p.p. 1-85, 1990
[90] Hsu Y.T. and Kao C.H., "Cadmium toxicity is reduced by nitric oxide in rice leaves". *Plant Growth Regulation*, vol. 42, p.p. 227–238, 2004.
[91] Romero-Puertas M.C., Rodrigues-Serrano M., Corpas F.J., Gomez M., del Rio L.A. and Sandalio L.M., "Cadmium-induced subcellular accumulation of O_2·-- and H_2O_2 in pea leaves". *Plant Cell and Environ*. (on line)
[92] Fuhrer J., "Ethylene biosynthesis and cadmium toxicity in leaf tissue of beans (Phaseolus vulgaris L.)". *Plant Physiol*., vol. 70, p.p. 162–167, 1982.
[93] Rodecap K.D., Tingey D.T. and Tibbs J.H., "Cadmium-induced ethylene production in bean plant". *Z. PflanzenPhysiol*., vol. 105, p.p. 65–74, 1981.
[94] Vassilev A., Lidon F., Sciotti P., da Graca M. and Yordanov I., "Cadmium-induced changes in chloroplast lipids and photosystem activities in barley plants". *Biologia Plantarum*, vol. 48 (1), p.p. 153-156, 2004.
[95] Dangl J.L., Dietrich R.A., Richberg M.H., "Death have no mercy: cell death programs in plant-microbe interactions". *Plant Cell*, vol. 8, p.p. 1793-1807, 1996

[96] Schwacke R. and Hager A., "Fungal elicitor induce a transient release of active oxygen species from cultured spruce cells that are dependent on Ca^{2+} and protein-kinase activity". *Planta*, vol. 187, p.p. 136-141, 1992.
[97] Fojtova M., Fulnecekova J., Fajkus J. and Kovarik A., "Recovery of tobacco cells from cadmium stress is accompanied by DNA repair and increased telomerase activity". *J. Exp. Bot*., vol. 53 (378), p.p. 2151-2158, 2002.
[98] Inouhe M., Ito R., Ito S., Sasada N., Tohoyama H. and Joho M., "Azuki bean cells are hypersensitive to cadmium and do not synthesise phytochelatins". *Plant Physiol*., vol. 123, p.p. 1029-1036, 2000.
[99] Richael C., Lincoln J.S., Bostock R.M. and Gilchrist D.G., "Caspase inhibitors reduce symptom development and limit bacterial proliferation in susceptible plant tissues". *Physiol. Mol. Plant Pathol*., vol. 59, p.p. 213-221, 2001.
[100] Iakimova E.T., Batchvarova R., Kapchina-Toteva V.M., Popov T., Atanassov A. and Woltering E.J., "Inhibition of apoptotic cell death induced by Pseudomonas syringae pv. tabaci and mycotoxin Fumonisin B1". *Biotech.&Biotech. Eq*., vol. 18 (2), p.p. 34-46, 2004.
[101] Malviya A.N. and Rogue P.J., ""Tell me where is calcium bred": Clarifying the roles of nuclear calcium". *Cell*, vol. 92, p.p. 17-23, 1998.
[102] Mittler R. and Lam E., "Identification, characterization, and purification of a tovbacco endonuclease activity induced upon hypersensitive response cell death". *Plant Cell*, vol. 7, p.p. 1951-1962, 1995.
[103] Fojtova M. and Kovarik A., "Genotoxic effect of cadmium is associated with apoptotic changes in tobacco cells". *Plant, Cell and Environ*., vol. 23, p.p. 531-537, 2000.
[104] Jabs T., Tschope M., Colling C., Hhlbrock K. and Scheel D., "Elicitor-stimulated ion fluxes and O_2^- from the oxidative burst are essential componrnts in triggering defense gene activation and phytoalexin synthesis in parsley". *Proc. Natl. Acad. Sci. USA*, vol. 94, p.p. 4800-4805, 1997.
[105] Noctor G. and Foyer C.H., "Ascorbate and glutathione: keeping active oxygen under control". *Plant Mol. Biol*., vol. 49, p.p. 249-279, 1998.
[106] Harada J. and Sugimoto M., "Polyamines prevent apoptotic cell death in cultured cerebellar granule neurons". *Brain Res*., vol. 753(2), p.p. 251-259, 1997.
[107] Drolet G., Dumbroff E.B., Legge R.L. and Thompson J.E., "Radical scavenging properties of polyamines". *Phytochem*., vol. 25, p.p. 367-371, 1986.
[108] Nicotera P., Zhivotovsky B. and Orrenius S., "Nuclear calcium transport and the role of calcium in apoptosis". *Cell Calcium*, vol. 16, p.p. 279-288, 1994.
[109] Atkinson M.M., Keppler L.D., Orland E.-W., Baker C.J. and Mischke C.F., "Involvement of plasma membrane calcium influx in bacterial induction of the K^+/H^+ and hypersensitive responses of tobacco". *Plant Physiol*., vol. 92, p.p. 215-221, 1990.
[110] McCabe P.F., Levine A., Meijer P.-J., Tapon N.A. and Pennel R.I., "A programmed cell death pathway activated in carrot cells cultured at low cell density". *Plant J*., vol. 12 (2), p.p. 267-280, 1997.
[111] Ciardi L.A., Tieman D.M., Lund S.T., Jones J.B., Stall R.E. and Klee H.J., "Response to Xanthomonas campestris pv. vbeiscatoria in tomato incolves regulation of ethylene receptor gene expression". *Plant Physiol*., vol. 123, p.p. 81-92, 2000.
[112] Li N., Parsons B.L., Lui D. and Mattoo A.K., "Accumulation of wound inducible ACC synthase transcripts in tomato fruit is inhibited by salicylic acid and polyamines". *Plant Mol. Biol*., vol. 18, p.p. 477-487, 1992.
[113] Neill S.J., Desikan R. and Hancock J.T., "Nitric oxide signaling in plants". *New Phytol*., vol. 159, p.p. 11-35, 2003.
[114] Mur L.A.J., Santosa I.E., Laarhoven L.-J., Harren F. and Smith A.R., "A new partner in the danse macabre, p.p. the role of nitric oxide in the hypersensitive response". *Bulg. J. Plant Physiol*., Special Issue, pp. 110-123, 2003.
[115] Hung K.T., Chang C.J. and Kao C.H., "Paraquat toxicity is reduced by nitiric oxide in rice leaves". *J. Plant Physiol*., vol. 159, p.p. 159-166, 2002.
[116] Belenghi B., Salomon M. and Levine A., "Caspase-like activity in the seedlings of Pisum sativum eliminates weaker shoots during early vegetative development by induction of cell death". *J Exp. Bot*., vol. 55 (398), p.p. 889-897, 2004.

Cell Biology and Instrumentation: UV Radiation, Nitric Oxide and Cell Death in Plants
Y. Blume et al. (Eds.)
IOS Press, 2006

Exploitation of the Daylily Petal Senescence Model as a Source for Novel Proteins that Regulate Programmed Cell Death in Plants

Brandon J. CUTHBERTSON, Joshua RICKEY, Yonnie WU, Gary POWELL, and Jeffrey P. TOMKINS
Proteomics Lab, Clemson University Genomics Institute (CUGI), Department of Genetics, Biochemistry and Life Science Studies, Clemson, SC, 2963, USA

Abstract Daylily (*Hemerocallis* spp.) represents an ideal model system for the study of plant programmed cell death in plants. The progression of petal senescence in the daylily flower is under tight genetic control and progresses over a relatively short period of time. While small-scale studies in expressed gene analysis along with the general assessment of physiological events have been explored, the use of new global analysis technologies has not been applied. This report describes how novel classes of regulatory proteins were discovered using a shotgun proteomics approach applied to senescing daylily petal tissues over three time points. These rare proteins were previously undetected in daylily using conventional molecular biology approaches. All of the information presented here is novel, given that the daylily proteome is relatively unexplored and that none of the proteins we describe match the 33 proteins that have been previously described in this entire genus. A diversity of daylily proteins that exhibit homology to cell signaling molecules from other plant taxa, and signal transduction cascades that are known to be involved in controlling cell death were identified. Our results indicate that a number of the newly identified proteins participating in the cell death process in senescing petals are part of the signal transduction machinery including cell surface and cytoplasmic protein kinases, along with transcription factors. Parallels are implied between the hypersensitive response to pathogens in plants and daylily petal senescence.

Introduction

Senescence and the processes related to genetically programmed cell death in plants have been studied to some extent from a physiological perspective in regard to embryogenesis [1], germination [2], tracheary element formation [3], and leaf and stem morphogenesis [4]. The activation of the plant defense response upon pathogen infection is often accompanied by a rapid process of a local cell death at or around the site of infection [1, 4, 5]. This process is immediately responsive to environmental stimuli (pathogens) and subsequent signal cascade results in host cell death around the infection site to prevent spreading of disease.

Inducible defense response in plants may include the activation of defense genes and proteins [6-9]. For instance the MAPK pathway, implicated as one of the converging points of different cell surface receptor signaling pathways, is sensitive to pathogens and pathogen derived elicitors [10]. Many of these enzymes are serine/threonine kinases and can be either transmembrane proteins (receptor kinases) or cytoplasmic signaling molecules [11]. Functional work using kinase inhibitors and phosphatases revealed that phosophorylation plays a key role in the process of cell death [12, 13].

When NtMEK2 was induced in Nicotiana the result was spontaneous HR type cell death [14]. NtMEK2 is now known to be an upstream regulator for other kinases involved in relaying a signal that ultimately induces cell death in response to plant pathogens [15, 16]. Pathogens are known to induce the expression of receptor kinases that ultimately have a role in regulating the hypersensitive-response [17]. Members of the WRKY transcription factor superfamily control many kinases at the transcriptional level in response to pathogens or salicyclic acid [18, 19].

The WRKY transcription factor superfamily in plants covers a wide molecular weight range with proteins (~17-210kDa) all related by the presence of two domains that contain the Trp-Arg-Lys-Tyr (WRKY) sequence motif adjacent to a zinc-finger motif [20]. In addition to the WRKY superfamily, other types of transcription factors are associated with hypersensitive cell death and senescence such as MYB, GRAS, bZIP, NAC and C2H2 [21,22]. Interestingly the WRKY factors are themselves controlled by MAP kinase signaling [23]. The auto regulatory nature of this type of transcription factor has been well established and was a subject of the recent review of the WRKY superfamily [20]. Furthermore WRKY appears to have a negative regulatory effect on specific modes of plant growth and differentiation [24]. Several types of transcriptional control elements exist in the Arabidopsis genome that are sites for WRKY and MYB factor binding. These cis-acting elements are implicated in the plant immune defense system and responsiveness to stress [25], and can exhibit considerable crosstalk between different types of biological responses.

The rapid and distinct process of senescence in daylily petals provides a key model for studying cell death in plants as it occurs naturally. The process occurs autonomously in an isolated plant organ, rapidly, and synchronously over a 24-hour period thus allowing precise biological correlations. Before flower opening, there is a decrease in activity of protective enzymes such as catalase and ascorbate peroxidase [26]. At about 12 h after opening, lipid peroxidation and increased levels of H_2O_2 are observed [26] which is followed by a loss of differential membrane permeability and ion leakage [27-30]. The activity of hydrolases such as certain wall-based enzymes [29], proteinases [28,31-33], and RNases [29,30] increases markedly during senescence. The ubiquitination, cellular labeling for protease and proteasomal degradation, of specific types of proteins has been correlated with specific senescence stages [33]. Changes in cellular anatomy during the entire senescence process are also well documented [26,29]. Similarly, in other liliaceous species that are insensitive to ethylene (*Alstroemieria*), cysteine protease expression is induced, which correlates with increased protease activity and a decrease in total protein over the senescence period [34]. At the same time in *Hemerocallis* and other lily genera [28,34] the use of cyclohexamide delays the onset of senescence indicating the requirement for de-novo protein synthesis.

We have taken an advanced shotgun proteomics approach to the analysis of the cell death and senescence process in daylily petals. Three stages of senescence were chosen for their distinct reflection of the progression of cell death in daylily petals. Our results indicate that many of the proteins involved in the cell death process have not yet been completely characterized functionally in the context of senescence, and are novel entities at this point. We observed considerable parallels between the cell death processes that function in hypersensitivity to pathogens and the processes that regulate senescence as a normal part of the daylily plant life cycle. In particular, the induced expression of a 70kDa protein with substantial homology to plant serine/threonine kinases at the point of bloom opening is of interest. Furthermore, the detection of daylily proteins with homology to plant transcription factors and senescence associated proteins that are expressed at the same stage as the predicted daylily kinase is indicative of a signal transduction cascade that controls petal senescence, which is very similar to the signal transduction control mechanisms involved in compatible pathogen induced HR cell death.

1. Materials and Methods

1.1 Plant tissue extraction

A diploid daylily variety (Slinky Dink, *Hemerocallis* spp.) was grown and petals at different stages of senescence were collected. Stages for petal harvest were as follows: T_{-12} (12 hours prior to petal opening), T_0 (time of petal opening), and T_{12} (12 hours after petal opening). About 3-5g of petal tissue was collected from each stage and immediately frozen in liquid nitrogen and stored at –80ºC before use. Petals were ground with pestle and mortal in the presence of liquid nitrogen, sepals were excluded, and the resulting powder was extracted in 40ml of ice-cold acidic (pH 5.5) lysis buffer [25mM sodium phosphate, 100mM potassium chloride, 2mM ethylenediaminetetraacetate disodium salt (EDTA), 1.5% polyvinylpolypyrrolidone (PVPP), 1mM phenylmethylsulfonylflouride (PMSF) and 2mM thiourea]. Lysis and solubilization of proteins was carried out at 4ºC while stirring for 2hr. Petal tissue debris were pelleted by centrifugation at 10,000 RCF (4ºC); the supernatant was collected and protein was precipitated with ammonium sulfate at 80% saturation. The resulting protein pellet was dissolved and dialyzed against 2L of Milliq water with two changes and followed by 2L of 10mM ammonium bicarbonate (ambic) in 3kDa cutoff dialysis tubing. The dialyzed material was then concentrated in Speedvac to approximately 1mg/ml as assessed by BCA protein assay (Pierce).

1.2 2D proteome separation and analysis by SDS/PAGE and HPLC

A total of 20µg of total protein from each stage was separated on a 10-20% precasted gel. SDS/PAGE was run at 200 volts in a Protean-2 system (BioRad) until the tracking dye (Bromophenol Blue) ran through the gel. The gel was then stained with 50ml of 0.1% Commasie Briliant Blue in 40% methanol and 10% acetic acid for an hour and destained in 50 ml of 40% methanol and 10% acetic acid for about an hour before equilibrated in water.

Each lane of the gel containing separated petal proteins was sectioned into 35 $1mm^2$ X 4mm bands with a gel slicer, which was sub-sectioned into four individual $1mm^3$ pieces. The four pieces from each band (total of 105 bands) were washed twice in 0.2ml of wash solution [50% acetonitrile, (ACN) 0.2M ambic] by 40 min sonication to remove the Coomassie stain. The washed gel pieces were covered in 100µl of wash solution supplemented with 0.003ml of 45mM DTT (dithiothrietol) for reduction of disulfide bonds at 37ºC for 20min. After cooling at room temperature for 15 min 0.004ml of 100mM IAA (iodoacetamide) was added for alkylation at room temperature for 20min in the dark. The reduction and alkylation solution was removed and the gel pieces were washed for 15min in wash solution. The gel pieces were dried for 15min at 37ºC in an incubator to semi-dry that ensures adsorption of trypsin into gel matrix during rehydration process. Sequence grade modified porcine trypsin (5,000 units/mg) (Promega) was diluted to 0.02mg/0.606ml of 10mM HCl as working solution, the gel pieces were hydrated with 5ml of 0.2M ambic and 0.004ml of the working solution. An additional 20ml of 0.2M ambic was then added to ensure that the gel pieces were covered and the in-gel digest was carried out overnight at 37ºC. The digestion was terminated at 18hr by adding 1.5ml of 0.1% trifluroacetic acid (TFA), the mixture was transferred to a clean tube and the gel cubes were extracted twice with 0.1ml of 60% ACN in 0.1% TFA. The peptide containing fractions were pooled and dried in an Eppendorf tube under vacuum followed by two successive washes to remove residual salt.

The resulting lyophilized tryptic peptides were reconstituted in 0.05ml of injection solution [50% methanol, 0.1% formic acid (FA)], vortexed and centrifuged at 13,000 RPM in a tabletop centrifuge for 5min. An aliquot of 0.045ml supernatant was transferred to a 0.3ml polypropylene injection vial and placed in the sample tray for auto injection. The tryptic peptides from each sample were auto-injected by an auto-sampler into a Waters CapLC system and separated on a C_{18} reverse phase column (Microtech) using 2-40% ACN gradient in 0.1% FA. Peptides from reversed phase chromatography were analyzed in real time by a mass analyzer (Waters Q-ToF micro). Instrumentation was run by Masslynx software.

1.3 Peptide sequencing and identification

Tryptic peptides were subjected to a number of acquisition methods including MS scan which measures peptide ion mass (m/z), retention time and peptide ion counts; a DDA (data dependent acquisition) method, which performs collision induced dissociation to selected ion and produce a series of fragmented ions that can be used for de novo sequencing of the peptide. An external calibrant, glu-fib [glu-fibrinogen peptide (Sigma)] was used to calibrate the mass shift.

MS/MS fragmentation spectra were processed and searched protein databases using Waters ProteinLynx 2.0 Global Server software. Non-redundant, plant protein and SwissProt databases were searched for protein identification. Peptide mapping using tryptic ions searching against the theoretically digested protein databases using GPMAW 6.11 (general protein mass analysis for windows) was done to provide the score for coverage, co-eluting therefore overlapping identification, as well as a second view of all ions present in a single gel band. All mass analysis was done in duplicate. The final protein sequences were double checked for accuracy.

2. Results

2.1 Mass spectrometry analysis of daylily peptides

Analysis of the fragmentation spectra generated from tryptic peptides from each of the three time points produced a total of 1,364 different possible sequences. After repeating the experiment a second time and relying on searches on plant protein database, a total of 430 different possible sequences were obtained and is selected as the focus group of our study. Since so few daylily proteins have been described, the actual number of unique proteins detected may be somewhere between each of these estimates. Many of the protein sequences in the non-redundant and plant protein sequence databases are from predicted proteins, deduced from gene (open reading frame) or transcript based (cDNA) sequences.

2.2 Daylily signal transduction proteins

The middle time point (T_0) chosen in our pilot study of daylily senescence is uniquely characterized by expression of a 70kDa protein with homology to several plant protein kinases. The 70kDa region of the daylily SDS/PAGE gel revealed six unique sequences with some homology to various plant kinases (Table 1). These kinase matching peptides were most abundant at the middle stage of senescence (T_0) and represent the strongest evidence indicative of plant kinase expression during daylily senescence.

Similarly peptide mapping of the daylily proteins using GPMAW 6.11 detected several different kinases with a predicted digest pattern similar to those observed for the

daylily 70kDa protein. [The digested plant protein database identification number recorded by GPMAW is listed after the GPID# prefix.] Comparison to these known and predicted proteins from plants revealed as much as 43.9% sequence coverage for casein kinase I from Arabidopsis (GPID# 9759511) and 35.7% sequence coverage for putative serine/threonine kinase from Arabidopsis (GPID# 2476220). Nine different kinase sequences in the plant protein database detected by tryptic peptide mass searches exhibited 29.4-35.7% sequence coverage when matched against the daylily tryptic peptide masses and all were within the general predicted range of 70-75kDa that we estimate for the daylily protein kinase.

Plant Homologue Identity	Identified Daylily Protein Sequence	e-value	NCBI ID#
Receptor like protein kinase 1*	NLLTGPFPSVSFSKAPELLKAHPPQTR	0.8994	34915202
Serine threonine kinase*	SFSGCGNGGSFKSSSGVSN	1.83783	15810437
Serine threonine kinase*	YNPYTLGRKLRPKVMPRSLTVGNNK	18.9892	12278524
Inositol trisphosphate kinase	SLDLDLSLAEVK	23.3053	5262190
Leucine rich transmembrane kinase*	LKFQMRAEER	28.377	15238872
Thermosensitive gluconokinase	FSSSSGGYNACR	6.34072	7248407

Table 1. de novo sequencing and analysis results using the ProteinLynx Global Server 2.0: Six of the fourteen-kinase MS/MS sequence matches were from the same T_0 70kDa mw range. All but three of the plant kinase matches were from the mid phase time point. NCBI (National Center for Biotechnology) protein ID numbers are listed. Asterisks (*) indicate putative (hypothetical) proteins.

Plant Homologue Identity	Mass (kDa)	Sequence Coverage	GPMAW GPID#
Protein kinase family protein†	77.3	31.6%	7487297
MAP kinase*†	76.3	32.4%	3439522
Transmembrane kinase	74.6	33.7%	3324290
Serine threonine kinase*†	74.5	35.7%	3068546
Serine threonine kinase*†	72.4	33.2%	2019698
Receptor lectin kinase*	70.4	29.4%	1523174
Kinase like protein*†	68.5	40.5%	9759133
Kinase (EC 2.7.1.37) 5 †	64.6	43.9%	421843
Casein kinase I†	53.6	43.9%	9759511

Table 2. Peptide mapping homologues for the daylily kinase observed at the 70kDa range. GPID (plant protein digested database ID) numbers are listed. Asterisks (*) indicate putative (hypothetical) proteins. Crosses (†) indicate more than one similar match in the database.

Daylily proteins from the 40kDa molecular weight range were observed at the T_0 time point which exhibited homology to more than one type of cell signaling molecule including kinases, senescence associated proteins and nuclear factors. A glycine-rich sequence obtained from daylily at T_0 from the 40kDa mass range matched mitogen-activated protein kinase kinase (MEK MAPKK) from *Medicago* (ID# 15528439) (Kiegerl et al. 2000) with an e-value of 0.24. The actual mass of the full-length *Medicago* MEK MAPKK homologue is 40.5kDa including the leader peptide, but minus the 19 residue leader peptide from the protein sequence present in the database the protein is 38.7kDa. Considerable variability in

sequence and molecular weight across plant species is observed for MAPKKs of this type [35].

Hit no.: 27 of 400 Score: 198
Protein: protein kinase family protein [Arabidopsis thaliana]
ID: gi|3068546 Mass (av): 74511.59 Da pI: 8.03 Coverage: 35.7%

mwk**FKPFAQK EPAGLEGRFL EIGNLKVQVR NVIAEGGFSS VYLAQDVNHA SK**qyalk**HMI** 60
CNDEESLELV MKeisvlksl kghpnvvtly ahgildmgrn kkeallamdf cgkslvdvle 120
nrgagyfeek qaltifrdvc navfamhcqs priahrdlk**A ENLLLSSDGQ WKLCDFGSVS** 180
TNHKIFERae emgieednir kyttptyrap emwdlfrrem isekvdiwal gcllfricyf 240
knafdgeskl qilngnyrip espkysvfit dlikemlqas pderpditqi wfrvneqlpa 300
nlqk**SLPDRP PEMQSTGVHD GSSKSATKPS PAPRRSPPPP PPSSGESDSG GPLGAFWATQ** 360
HAKtsvvsed nknmpk**FDEP NSNTSKSERV RVDSHQPKKP SPVR**geargi qr**NKDLETTI** 420
SQKNTTPAAA NNMTRvskdd afnsfvadfd ttkfdngnkp gkeealeaei qrlkdelkqt 480
ksek**AEITAK** feklsaicrs qr**QELQDLK**q tlasksasps psrdssqnqp spgmhsmsst 540
psrdkmegtm welqqdrsnw stgssdtnsw qpfsdeakpv mesaskgnnn tinqsvrtr**S** 600
KPASAAGTQG FEPWGFETES FRaaatsaaa tsasgtqrsm gsgnstsqry gnskmrenqk 660
taqpagwagf 670

Figure 1. Putative serine/threonine kinase from *Arabidopsis*. This GPMAW result from the digested plant protein database gave the highest sequence coverage for a predicted protein in the size range observed for the 70kDa daylily protein from T_0. There is a strong correlation between serine/threonine kinases of this size and the hypersensitive response to pathogens in plants that prevent infection by rapidly induced cell death. Kinases of this type induce immediate early response to pathogens in minutes (15-30) leading to the onset of cell death in a matter of hours . Coverage areas for MS ions obtained from daylily at T_0 are highlighted in bold capital text.

The second tryptic peptide from this band matched to a protein kinase like protein from Arabidopsis (ID# 7270019) with an e-value of 2.56, which has a predicted molecular weight of 46.1kDa including the predicted leader sequence. GPMAW analysis of MS ions from this range revealed few hits for protein kinases. Another daylily protein from this range exhibited homology to a protein sequence that has been named senescence-associated family protein from Arabidopsis (ID# 18398541) with an e-value of 6.20905, which is a peptide (14.9kDa including the leader sequence) predicted by conceptual translation from the Arabidopsis genome. GPMAW analysis of MS ions from this region of the daylily gel revealed 12.9-15.3% tryptic sequencing coverage for each of three different predicted senescence associated proteins from Arabidopsis (GPID# 4257200, 1283689 and 1840848), each of these matches were approximately 46kDa.

Plant Homologue Identity	Identified Daylily Protein Sequence	e-value	NCBI ID#
WRKY transcription factor 24*	SLNNKFASFLDKVR	1.36179	15384231
Putative transcription factor*	NNKFAPHLDKVR	4.79811	41469336
MEK map kinase kinase	SGGGGNGLGSGKER	0.24359	15528439
Protein kinse*	VPNSGSSVSMSVSVAFGHTTLPFGAE	2.56105	7270019
Senescence associated protein*	LSSLHAKELKYEELKRADR	6.20905	18398541

Table 3. de novo sequencing matches from the T_0 40kDa mw range.

Plant Homologue Identity	Mass (kDa)	Sequence Coverage	GPMAW PPID#
Senescence-associated protein*†	45.8	15.3%	1840848
Senescence-associated protein	46.5	12.9%	1283689
Protein kinase	64.9	11.0%	1522146
Putative zinc-finger protein*†	47.4	11.8%	3827552
MYB transcription factor†	42.2	16.3%	4161920

Table 4. Peptide mapping revealed several homologues for signal transduction proteins observed at the 40kDa range. Asterisks (*) indicate putative (hypothetical) proteins. Crosses (†) indicate more than one similar match in the database.

Finally, the 40kDa range of T_0 also contained a daylily protein sequence obtained from MS/MS analysis with homology to WRKY transcription factor from Arabidopsis (ID# 15384231), which are involved in many plant cell processes involving response to pathogens. GPMAW analysis also revealed several hits for putative daylily transcription factors including a putative zinc-finger protein from Oryza and the MYB transcription factor from Arabidopsis (GPID# 3827552 and 4161920). Each of these putative homologues corresponds to the molecular mass range in which the daylily protein sequences were observed.

A large protein (116kDa) in the T_{12} time point sample contained a tryptic peptide with sequence homology to a predicted nuclear protein kinase from Oryza (ID# 23237831). This daylily tryptic peptide matched to the Oryza homologue with an e-value of 2.69. Very few intact proteins were observed at this relatively high molecular weight range in the T_{12} time point. Finally, one of the most obvious hits for a daylily nuclear factor was also observed at T_{12} in the form of a sequence with homology to Anthocyanin 1, a basic helix-loop-helix protein that directly regulates transcription of structural anthocyanin genes [36].

3. Discussion

Detection of a daylily kinase that is induced in the mid-senescence time point (T_0 – time of flower opening) indicates that this type of cell signaling enzyme may function to regulate the senescence process. The T_0 time point is when flower opening occurs and can be viewed as the starting point for petal death, which occurs rapidly in daylily. Plant kinases (including transmembrane and cytoplamsic) are known to participate in the regulation of cell death in response to infection [12,14-16]. Pto is a good example of a serine/threonine kinase [19,37] that directly regulates the hypersensitive cell death response to pathogenic Pseudomonas [38].

Pto can induce cell death in leaves rapidly (less than 24hr) in response to pathogenic stimulation [19,37]. The daylily 70kDa kinase matches closely in function to Pto and is within the molecular weight range of plant serine/threonine kinases. NtACIK1 is a serine/threonine kinase that is very similar to Pto [39], which is observed to be one of the immediate early response genes for disease resistance. This kinase can be induced within 15-30min after pathogen stimulation and subsequently functions to prevent infection. It is possible that the daylily kinase expression is sensitive to environmental queues such as photoperiodicity as the pathogen induced kinases that regulate hypersensitive response cell death. In the case of the hypersensitive response in cell death there are cell surface receptors that are compatible with molecules that certain pathogens produce, which initiate the signal transduction cascades.

It is not at all clear at this point how a putative light based signal could be transduced to the daylily kinase. The loss of chloroplasts in daylily tissues that mature into

petals accompanies the petal senescence process. Since chloroplasts contain photosynthesis machinery it is possible that the degradation or complete absence of such light sensitive biological molecules is connected to the induction and/or activation of the daylily 70kDa kinase. Certainly, the transcriptional regulation of the daylily kinase is of great interest given the induction of expression at T_0. It is possible that the control of this type of cell signaling molecule is a key regulator of daylily petal senescence as well as the plant cell death process in general.

Not only were cytoplasmic signal transduction proteins observed, but also nuclear proteins were expressed at high relative levels in the T_0 time point. The expression of a WRKY type transcription factor at T_0 is another association with the pathogen response in plants since these factors are associated with disease resistance [20-22,25]. Furthermore, the actual MS/MS sequence obtained from T_0 that matched WRKY also matched to other putative proteins described generally as disease resistance proteins deduced from conceptual ORF translation or expressed gene sequences from other plant species. It has been observed recently that receptor-like protein kinases that regulate cell death are under transcriptional control of WRKY transcription factors [17].

In the case of daylily petal senescence the WRKY and disease resistance like proteins are likely regulating the expression of proteins that are important mediators of cell death and the established precedence of association with kinases suggests that there may also be a link between this type of transcription factor and a senescence kinase in daylily. Moreover the auto regulatory nature of members of the WRKY family indicates that that the signaling cascade that the daylily kinase is participating in is further regulating the production of WRKY transcription factors. Since the daylily 70kDa kinase is expressed at the same time point there is a good possibility that we are observing a window into the senescence process that contains both a transcription factor and the proteins encoded by downstream activated target genes, which are functioning to carry out the senescence process. If this is the case then transcriptional regulatory elements that are being utilized to express these proteins may be interesting subjects for future genetic manipulation of plants for the purpose of arresting or altering the onset of senescence.

The final time point examined in our study was characterized by expression of a protein in the 205kDa range that provided an MS/MS sequence with only one plant protein identity for a germ cell specific nuclear protein kinase. The potential exists that this is a large protein that functions during the senescence process in petals that happens to exhibit homology to haploid germ cell specific kinase. Expression of the Anthocyanin1 transcription factor at T_{12} along with a protein that exhibits homology to a kinase indicates the possibility that we are observing the remaining components of a signal transduction cascade that is responsible for pigment production in daylily petals.

It is therefore likely that multiple signal transduction cascades are functioning at the mid to late stages of daylily petal senescence. These results reveal that macromolecule degradation and nutrient reuptake, which are hallmarks of the daylily petal senescence process, are not the only physiological activities that have relevance to the senescence process. More importantly our results provide data from multiple time points during senescence that can be used to examine genomic elements that may control the senescence process. These data have great potential for further exploration and direct application given that genomic tools already exist for daylily [40].

References

[1] Jones A.M. and Dangl J.L., "Logjam at the Styx: programmed cell death in plants". *Trends in Plant Sci.*, vol. 1, p.p. 114-119, 1996.

[2] Brown P.H. and Ho T.-H.D., "Biochemical properties and hormonal regulation of barley nuclease". *Eur. J. Biochem.*, vol. 168, p.p. 357-364, 1987.
[3] Fukuda H., "Xylogenesis: initiation, progression and cell death". *Ann. Rev. Plant Physiol.*, vol. 47, p.p. 299-325, 1996.
[4] Greenberg J.T,. "Programmed cell death: a way of life for plants". *Proc. Nat. Acad. Sci. USA*, vol. 93, p.p. 12094-12097, 1996.
[5] Mittler R. and Lam E., "Sacrifice in the face of foes: pathogen induced programmed cell death in higher plants". *Trends Microbiol*., vol. 4, p.p. 10-15, 1996.
[6] Yang Y., Shah J. and Klessig D.F., "Signal perception and transduction in plant defense responses". *Genes Dev.*, vol. 11, p.p. 1621-1639, 1997.
[7] Scheel D., "Resistance response physiology and signal transduction". *Curr. Opin. Plant Biol.*, vol. 1, p.p. 305–310, 1998.
[8] Somssich I.E. and Hahlbrock K., "Pathogen defence in plants: A paradigm of biological complexity". *Trends Plant Sci.*, vol. 3, p.p. 86–90, 1998.
[9] Martin G.B., "Functional analysis of plant disease resistance genes and their downstream effectors". *Curr. Opin. Plant Biol.*, vol. 2, p.p. 273–279, 1999.
[10] Zhang S. and Klessig D.F., "Resistance gene N-mediated de novo synthesis and activation of a tobacco mitogen-activated protein kinase by tobacco mosaic virus infection". *Proc. Natl. Acad. Sci. USA*, vol. 95, p.p. 7433-7438, 1998.
[11] Zhou J., Loh Y.T., Bressan R.A. and Martin G.B., "The tomato gene Pti1 encodes a serine/threonine kinase that is phosphorylated by Pto and is involved in the hypersensitive response". *Cell*, vol. 83, p.p. 925-935, 1995.
[12] Grosskopf D.G., Felix G. and Boller T., "K-252a inhibits the response of tomato cells to fungal elicitors *in vivo* and their microsomal protein kinase *in vitro*". *FEBS Lett.*, vol. 275, p.p. 177–180, 1990.
[13] Felix G., Grosskopf D.G., Regenass M. and Boller T., "Rapid changes of protein phosphorylation are involved in transduction of the elicitor signal in plant cells". *Proc. Natl. Acad. Sci. USA*, vol. 88, p.p. 8831–8834, 1991.
[14] Yang K.Y., Liu Y. and Zhang S., "Activation of a mitogen-activated protein kinase pathway is involved in disease resistance in tobacco". *Proc. Natl. Acad. Sci. USA*, vol. 98, p.p. 741–746, 2001.
[15] Zhang S, Liu Y., "Activation of salicylic acid-induced protein kinase, a mitogen-activated protein kinase, induces multiple defense responses in tobacco". *Plant Cell*, vol. 13, p.p. 1877-1889, 2001.
[16] Liu Y., Jin H., Yang K.Y., Kim C.Y., Baker B. and Zhang S., "Interaction between two mitogen-activated protein kinases during tobacco defense signaling". *Plant J.*, vol. 34, p.p. 149-160, 2003.
[17] Chen K., Du L. and Chen Z., "Sensitization of defense responses and activation of programmed cell death by a pathogen-induced receptor-like protein kinase in *Arabidopsis*". *Plant Mol Biol.*, vol. 53, p.p. 61-74, 2003.
[18] Du L. and Chen Z., "Identification of genes encoding receptor-like protein kinases as possible targets of pathogen- and salicylic acid-induced WRKY DNA-binding proteins in *Arabidopsis*". *Plant J.*, vol. 24, p.p. 837-847, 2000.
[19] Rocher A., Dumas C. and Cock J.M., "W-box is required for full expression of the SA-responsive gene SFR2". *Gene*, vol. 344, p.p. 181-192, 2005.
[20] Ulker B. and Somssich I.E., "WRKY transcription factors, p.p. from DNA binding towards biological function". *Curr Opin Plant Biol.*, vol. 7, p.p. 491-498, 2004.
[21] Lin J.F. and Wu S.H., "Molecular events in senescing *Arabidopsis* leaves". *Plant J.*, vol. 39, p.p. 612-628, 2004.
[22] Liu Y., Schiff M. and Dinesh-Kumar S.P., "Involvement of MEK1 MAPKK, NTF6 MAPK, WRKY/MYB transcription factors, COI1 and CTR1 in N-mediated resistance to tobacco mosaic virus". *Plant J.*, vol. 38, p.p. 800-809, 2004.
[23] Kim C.Y. and Zhang S., "Activation of a mitogen-activated protein kinase cascade induces WRKY family of transcription factors and defense genes in tobacco". *Plant J.*, vol. 38, p.p. 142-51, 2004.
[24] Zhang Z.L., Xie Z., Zou X., Casaretto J., Ho T.H. and Shen Q.J., "A rice WRKY gene encodes a transcriptional repressor of the gibberellin signaling pathway in aleurone cells". *Plant Physiol.*, vol. 134, p.p. 1500-1513, 2004.
[25] Narusaka Y., Narusaka M., Seki M., Umezawa T., Ishida J., Nakajima M., Enju A. and Shinozaki K., "Crosstalk in the responses to abiotic and biotic stresses in Arabidopsis, p.p. analysis of gene expression in cytochrome P450 gene superfamily by cDNA microarray". *Plant Mol Biol.*, vol. 55, p.p. 327-342, 2004.
[26] Panavas T. and Rubinstein B., "Oxidative events during programmed cell death of daylily (*Hemerocallis* hybrid) petals". *Plant Sci*., vol. 133, p.p. 125-138, 1998.
[27] Bieleski R.L. and Reid M.S., "Physiological changes accompanying senescence in the ephemeral daylily flower". *Plant. Physiol.*, vol. 98, p.p. 1042-1049, 1992.

[28] Stephenson P. and Rubinstein B., "Characterization of proteolytic activity during senescence in daylilies". *Phys. Planta.*, vol. 104, p.p. 463-473, 1998.
[29] Panavas T., Reid P.D. and Rubinstein B., "Programmed cell death of daylily petals, p.p. activities of wall-based enzymes and effects of heat shock". *Plant Physiol. Biochem.*, vol. 36, p.p. 379-388, 1998.
[30] Panavas T., Pikula A., Reid P., Rubinstein B. and Walker E., "Identification of senescence-associated genes from daylily petals". *Plant Mol. Biol*., vol. 40, p.p. 237-248, 1999.
[31] Valpuesta V. Lange N.E., Gurrero C. and Reid M.S., "Up-regulation of a cysteine protease accompanies the ethylene-insensitive senescence of daylily (*Hemerocallis*) flowers". *Plant Mol. Biol*., vol. 28, p.p. 575-582, 1995.
[32] Guerrero C., Calle M., Reid M.S. and Valpuesta V., "Analysis of the expresssion of two thiolprotease genes from daylily (*Hemerocallis* spp.) during flower senescence". *Plant Mol. Biol*., vol. 36, p.p. 565-571, 1998.
[33] Courtney S., Rider C. and Stead A., "Changes in ubiquitination and the expression of ubiquitin-encoding transcripts in daylily petals during floral development and senescence". *Phys Plant*, vol. 91, p.p. 196-204, 1994.
[34] Wagstaff C., Leverentz M., Griffiths G., Thomas B., Chanasut U., Stead A. and Rogers H., "Cysteine protease gene expression and proteolytic activity during senescence of *Alstroemeria* petals". *J Exp Bot.*, vol. 53, p.p. 233-240, 2002.
[35] Kiegerl S., Cardinale F., Siligan C., Gross A., Baudouin E., Liwosz A., Eklof S., Till S., Bogre L., Hirt H. and Meskiene I., "SIMKK, a mitogen-activated protein kinase (MAPK) kinase, is a specific activator of the salt stress-induced MAPK, SIMK". *Plant Cell.*, vol. 12, p.p. 2247-2258, 2000.
[36] Spelt K., Quattrocchio F., Mol J. and Koes R., "Anthocyanin1 of petunia encodes a basic helix-loop-helix protein that directly activates transcription of structural anthocyanin genes". *Plant Cell*, vol. 12, p.p. 1619-1632, 2000.
[37] Martin G.B., Brommonschenkel S.H., Chunwongse J., Frary A., Ganal M.W., Spivey R., Wu T., Earle E.D. and Tanksley S.D., "Map-based cloning of protein kinase gene conferring disease resistance in tomato". *Science*, vol. 262, p.p. 1432–1436, 1993.
[38] Pedley K.F. and Martin G.B., "Molecular basis of Pto-mediated resistance to bacterial speck disease in tomato". *Annu. Rev. Phytopathol*., vol. 41, p.p. 215–243, 2003.
[39] Rowland O., Ludwig A.A., Merrick C.J., Baillieul F., Tracy F.E., Durrant W.E., Fritz-Laylin L., Nekrasov V., Sjolander K., Yoshioka H. and Jones J.D., "Functional Analysis of Avr9/Cf-9 Rapidly Elicited Genes Identifies a Protein Kinase, ACIK1, That Is Essential for Full Cf-9-Dependent Disease Resistance in Tomato". *Plant Cell*, vol. 17, p.p. 295-310, 2005.
[40] Tomkins J.P., "Cloning the daylily genome". *Daylily J.*, vol. 59, p.p. 245-250, 2003.

Cell Biology and Instrumentation: UV Radiation, Nitric Oxide and Cell Death in Plants
Y. Blume et al. (Eds.)
IOS Press, 2006

Changes in the Pattern of HMW-DNA Fragmentation Accompanying the Differentiation and Ageing of Plant Cells

Igor O. ANDREEV, Kateryna V. SPIRIDONOVA, Victor A. KUNAKH, Victor T. SOLOVYAN
Institute of Molecular Biology & Genetics, National Academy of Sciences of Ukraine, Akad. Zabolotnogo str., 150, Kyiv, 03143, Ukraine

Abstract. At the higher level of chromatin compaction, nuclear DNA is arranged into the loop domains by periodical attachment of chromatin fibre to the nuclear matrix. Previously we have demonstrated the regular cleavage of nuclear DNA into ~300 kb and 50-100 kb high molecular weight (HMW) DNA fragments, which represent DNA loop domains or their associates. Here we show that the pattern of excision of DNA loop domains varies in plant tissues differing by the proliferative activity and/or differentiation status. The least HMW-fragmentation was observed in the embryos of dry quiescent seeds, whereas the induction of growth and development was accompanied by the increased excision of DNA loop domains, which was the most prominent in differentiated and senescent tissues. Analysis of the embryos from the aged rye seeds also demonstrated that the loss of germination capacity was accompanied by decreased excision of chromatin loop domains. The results thus demonstrate that the pattern of excision of DNA loop domains possesses a dynamic feature and reflects changes in physiological activity of plant tissues. We hypothesize that excision of DNA loop domains is related to DNA metabolic processes in a cell nuclei and is necessary for maintaining the active physiological status of plant tissues.

Introduction

There are several orders in hierarchy of chromatin structures, which exhibit different degrees of condensation and organization of the genome. The first order chromatin structure is 10-nm chromatin fiber, which represents the nucleosome array. Coiling of the nucleosome array into solenoid-like structures results in 30-nm fiber, which provides the second order chromatin structure. At the higher level of chromatin compaction, nuclear DNA is arranged into the loop domains by periodical attachment of chromatin fiber to the nuclear matrix. Chromatin loops represent the basic structural components of the higher order chromatin folding, which are maintained during the cell cycle and in differentiated cells.

An increasing number of facts suggest existence of the strong relationship between chromatin structure and function in the cell nucleus. Changes in functional state of the cell, such as proliferation arrest, differentiation, or senescence, are accompanied by considerable rearrangements of chromatin structures, which can be related to changes in the activity of DNA metabolism, especially at the level of replication and transcription. Such functional rearrangements in chromatin structures are studied mainly at the level of nucleosome arrays. Numerous facts of evidence suggest, however, that the chromatin rearrangements could involve DNA regions as long as of 100 kb, thus being comparable with the size of individual chromatin loop domains. While chromatin changes at the nucleosomal level are

exhaustively analyzed, the little is known about the changes in chromatin structure at the higher levels of chromatin folding.

Previously we showed that regular DNA cleavage into high molecular weight (HMW) DNA fragments can be induced in intact nuclei, resulting in formation of ~300 kb and 50-100 kb fragments [1]. The pattern of induced HMW-DNA cleavage in isolated nuclei was essentially similar to that found in high-salt-extracted nuclei [2,3], suggesting that HMW-DNA fragments represent DNA loop domains or their associates. In this study we demonstrate the distinct pattern of HMW-DNA cleavage in plant tissues differing by the proliferative activity and differentiation status. We also show that two different types of plant senescence, namely, senescence of coleoptile of developing rye seedling and the loss of viability of the long term stored rye seeds, were also accompanied by changes in HMW-DNA fragmentation pattern.

1. Experimental Procedures

1.1. Preparation of Intact Nuclear DNA Embedded in Agarose

Nuclei were prepared from the various tissues of pea (*Pisum sativum*) and maize (*Zea maize*) seedlings, embryo of dry and moistened seeds, and seedlings of *S. cereale*, and from seedlings and cultured *in vitro* tissues of *C.capillaris*. Fresh plant tissue (0,2-1,5 g) was ground in a prechilled mortar and pestle on ice with 3-5 ml of cold (4°C) nuclei isolation buffer (50 mM Tris HCl, pH 8.0; 0,3 M mannitol, 2,5 mM $MgCl_2$; 0,05 mM β-mercaptoethanol, 0,5 mkM phenylmethylsulphonyl fluoride (PMSF)). Extra buffer was added to bring the final volume to 10-12 ml, and suspension was filtrated through 4 layers of cheesecloth. Nuclei were then pelleted by centrifugation at 1500g at 4°C for 10 min and washed once more. Finally, nuclei were resuspended in the isolation buffer to concentration about 10^6-10^7 nuclei×ml^{-1}, mixed with an equal volume of 1% low melting temperature agarose preheated at 37°C and applied to a mold to form the plugs.

Histone depleted nuclei (nucleoids) were obtained by incubation of agarose-embedded nuclei in extraction buffer (2M NaCl, 10 mM TrisHCl, pH8.0; 1 mM EDTA, 0,5 mkM PMSF) at 4°C twice for 30 min, and then washed 4 times for 25 min with the same buffer without NaCl. Extracted plugs were treated for 1-3 h at 45°C in lysis buffer (10 mM EDTA; 1% SDS) and stored in the same buffer at 4°C.

1.2. Pulsed Field Gel Electrophoresis

Samples were fractionated in 1% agarose gel in 0.5×Tris–borate–EDTA buffer for 18-42 hours at the voltage gradient of 5 V/cm by filed inversion gel electrophoresis (FIGE) with constant (8 sec) or exponentially increasing pulse time (from 1 to 50 sec) and forward/back time ratio 3, p.p. 1. These running parameters allow resolving of fragments with size up to 300 kb in the first case and up to 600 kb – in the second one The gels were stained with ethidium bromide and photographed in UV-light.

To evaluate the residual noncleaved DNA left on the gel start, the agarose blocks were removed from the gel pockets, transferred to microtubes, and incubated at 65°C for 2 h with a presence of 10 mM EDTA, 1% SDS, and 200 mg/ml proteinase K. Then the samples containing melted agarose with the residual DNA were poured into the pockets of a fresh 1% agarose gel and the DNA was fractionated at the constant current under electric field strength of 5–7 V/cm for 2–4 h.

2. Results

2.1. Dynamics of HMW-DNA Fragmentation Patterns in Plant Development

To investigate the possible rearrangements in higher order chromatin structure during the plant development, we examined the patterns of HMW-DNA fragmentation in nuclei prepared from various plant tissues, which differ by age, differentiation level, or proliferative status. We found that the pattern of HMW-DNA fragmentation varies during germination of the seeds (maize or pea) (Fig.1). The efficiency of HMW-DNA cleavage in developing seedlings progressively increased in parallel with increase of the imbibition time. Probably the induction of the physiological activity of the plant tissues is accompanied by enhanced excision of DNA loop domains.

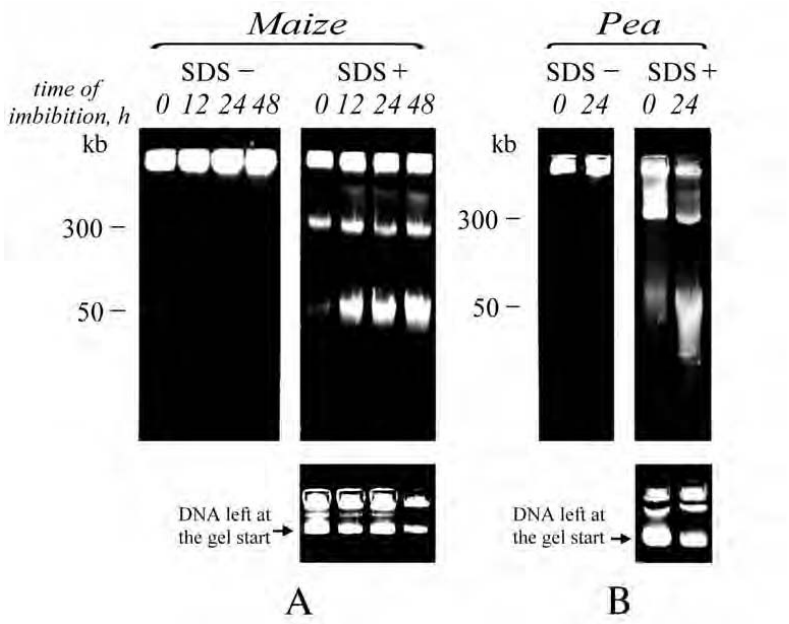

Figure 1. Changes in the pattern of HMW-DNA fragmentation during plant development. Nuclei from the embryos of dried and imbibed for various periods of time maize (panel A) and pea (panel B) seeds were isolated, embedded into agarose and extracted with NaCl to obtain nucleoids. Nucleoids were then treated with SDS (SDS +) followed by fractionation in FIGE. For comparison, as a control, nucleoids were fractionated without SDS treatment (SDS –). Patterns of HMW-DNA cleavage are shown in upper parts. The lower panels show the levels of non-cleaved intact DNA removed with agarose blocks from the wells after FIGE fractionation.

Data in Figure 2 demonstrate differences in the pattern of HMW-DNA fragmentation in the high-salt-extracted nuclei prepared from the apical and the basal part of leaves, as well as in the high-salt-extracted nuclei preparations from the apices and the rest of the roots of the maize seedlings. In both cases the efficiency of excision of DNA loop domains was increased in proliferatively quiescent differentiated tissues as compared to the proliferatively active meristematic cells.

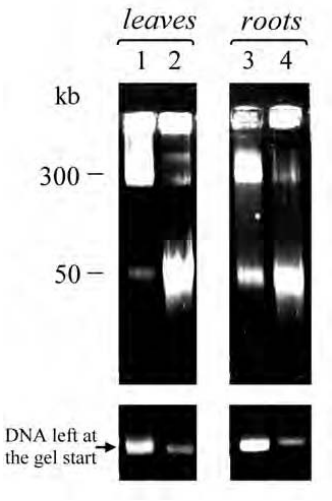

Figure 2. Increase in the efficiency of HMW-DNA fragmentation in proliferatively quiescent differentiated cells of maize seedlings. Nuclei from basal (lane 1) or apical (lane 2) parts of leaves from 10-days-old maize seedlings, and apical (lane 3) and central part (lane 4) of roots from 5-days-old maize seedlings were isolated, embedded in agarose, and extracted with NaCl to obtain nucleoids. Nucleoids were then treated with SDS followed by FIGE-fractionation. The lower panels show the results of re-fractionation of non-cleaved DNA left at the gel start by conventional gel-electrophoresis.

Similarly, marked enhancement of the excision of DNA loop domains was observed in proliferatively quiescent leaf tissue of mature plants as compared to the proliferatively active seedlings (Fig. 3, A) or de-differentiated proliferatively active callus tissue culture of *Crepis capillaris* (Fig. 3, B). The results further suggest the tight relationship between the efficiency of the excision of DNA loop domains and physiological status of the tissues.

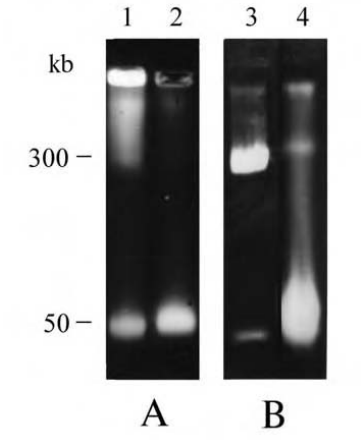

Figure 3. Varying pattern of HMW-DNA fragmentation in tissues differing by proliferative activity. Nuclei from different tissues of C. capillaries were isolated, embedded in agarose and treated with SDS followed by fractionation by FIGE. The patterns of HMW-DNA cleavage were compared in nuclei prepared from 2-days old seedlings and leaves of the mature plant (lanes 1 and 2, respectively),
and in nuclei of the mature plant and *in vitro* cultured rhizogenous callus of *C .capillaris* (lanes 3, 4, respectively).

2.2. Changes in the HMW-DNA Fragmentation Pattern in Senescent Plant Tissues

We analyzed next the changes in the HMW-DNA fragmentation pattern during senescence of plant tissues. Two distinct models were chosen, p.p. coleoptile of developing rye seedlings and rye seeds stored for different periods of time. Coleoptile in cereals is functional for a relatively short period of time at the early stages of ontogenesis, and dies quickly as the seedling grows and develops. Seed ageing is accompanied by the gradual decline in the germination rate as an integral result of many biochemical and physiological events.

We found that an enhanced excision of DNA loop domains accompanies the senescence of rye coleoptile (Fig. 4). Indeed, both the increase of the total level of cleaved DNA and the increased proportion of 50-100 kb DNA fragments, as compared to the 300 kb DNA fragments, were observed in senescent coleoptile (Fig. 4A). It should be noted that enhanced excision of the DNA loop domains was found in the apical part of the same coleoptile as compared to its basal part (Fig. 4B).

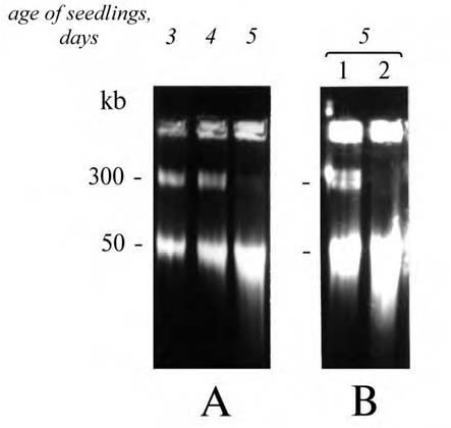

Figure 4. Enhanced excision of loop domains during senescence of rye coleoptile. Panel A. Nuclei prepared from coleoptile of rye seedlings of different age were isolated, embedded in agarose, extracted with NaCl to obtain nucleoids. Nucleoids were then treated with lysis buffer and fractionated by FIGE. Panel B. The results of FIGE fractionation of nucleoids from basal (lane 1) and apical (lane 2) parts of coleoptile from 5-days-old rye seedlings.

Analysis of the aged rye seeds demonstrated also changes in excision of DNA loop domains during rye seed ageing (Fig. 5). We found that after 4 years of seed storage the germination ability of rye seeds dropped to 40%, and less then 10% of seeds remained viable after 7 years of storage (results not shown). The loss of the germination ability of aged rye seeds was accompanied by decrease in excision of loop domains, which was observed as the overall decline in DNA fragmentation in parallel with decrease in amount of 50 kb fragments (Fig. 5A). The further stimulation of endogenous nucleases by incubating the agarose-embedded nuclei in the presence of magnesium ions showed also the decline in the Mg-induced high molecular weight DNA cleavage (Fig.5B).

3. Discussion

Our results demonstrate an ordered disintegration of nuclear DNA into two types of HMW-DNA fragments of about 300 kb and 50 kb. Larger band represents compression region upon pulsed field electrophoresis fractionation [4], it covers all DNA fragments with the size beyond the limits of resolution (results not shown). In contrast to 300 kb fragments, the 50-100 kb DNA fragments were invariably observed in nuclei taken from various species including animals and plants regardless of the methods of DNA fractionation [1,5-9]. Interestingly, essentially similar patterns of HMW-DNA cleavage were observed both in intact and in high-salt-extracted nuclei [2,3]. As high-salt-extracted nuclei comprise nuclear matrix with attached halo of DNA loops which size ranged from 30 to 100 kb [10, 11], one can suggest that observed 50 kb DNA fragments represent excised DNA loop domains.

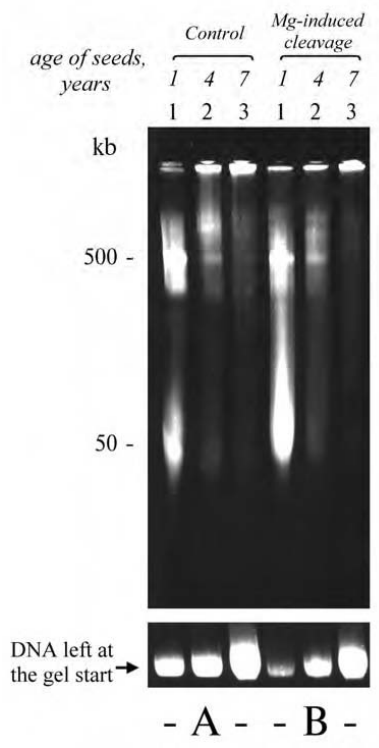

Figure 5. Decreased level of HMW-DNA fragmentation in embryos from aged rye seeds. Panel A. Nuclei were isolated from the embryos of the seeds stored for one (lane 1), four (lane 2), and seven (lane 3) years, treated with lysis buffer followed by FIGE-fractionation. Panel B. The same preparations as in the panel A with exception that HMW-DNA cleavage was induced by additional incubation in Mg^{2+}-containing buffer before the lysis. Patterns of HMW-DNA cleavage are shown in the upper parts. The lower panels show the levels of non-cleaved intact DNA removed from the wells after FIGE fractionation.

Analysis of a number of nuclear preparations revealed no obvious fragments in nuclear DNA after fractionation of deeply salt extracted nuclei by pulsed field gel electrophoresis. Only in the embryos of the non-viable seeds or in senescent coleoptile, some disintegration of nuclear DNA into 50-100 kb fragments have been detected (data not shown). At the same time our results show that the treatment of plant nuclei as well as nucleoids with strong protein denaturants (SDS) results in ordered disintegration of nuclear DNA into HMW fragments. This suggests that ds-DNA breaks leading to the formation of HMW-DNA fragments are clumped by the high-salt-resistant proteins, which the most probably are representing the component of the nuclear scaffold.

Our previous study on DNA fragmentation in nuclei, extracted with 2M NaCl (nucleoids), reveals the nuclease activity resistant to the salt extraction [12, 13]. The properties of this salt extraction-resistant nuclease, namely, i) necessity for protein denaturants for visualization of HMW-DNA fragments, ii) formation of protein-associated DNA breaks, iii) sensitivity of the fragmentation to the topoisomerase II (topoII)-specific poisons (e.g. etoposide and teniposide), and iv) relegation of cleaved DNA fragments into noncleaved DNA under conditions favorable for the topoII-dependent rejoining reaction [2,3,12,13], add an essential credence to the idea for the involvement of scaffold-associated topoII-like activity in the excision of DNA loop domains. This is consistent with the reports showing that topo II is a major component of nuclear scaffold (see for review [14]) and interacts with matrix associated regions (MARs), which comprise the specific class of genome sequences that anchor DNA to the nuclear matrix proteins (see for review [15,16]). DNA topoisomerases form a unique class of enzymes that change the topological state of DNA by breaking and rejoining the phosphodiester backbone of DNA [14]. Thus, changes

in the pattern of HMW-DNA fragmentation may reflect the changes in higher order chromatin organization at the level of chromatin loop domains.

We demonstrate here that the intensity of HMW-fragmentation in geeply salt-extracted nuclei varies in different plant tissues, and apparently is related to physiological activity of plant tissues, namely, their differentiation status and the level of senescence. The lowest intensity of DNA loop excision was observed in low-active nuclei from embryo of dry seeds and, interestingly, the loss of viability of aged seeds was paralleled by decrease in the capacity to excise DNA loop domains. Germination and development of seedlings was accompanied by the progressive increase in HMW-DNA fragmentation, and the most intensive level of HMW-DNA fragmentation was observed in differentiated tissues, such as mature leaves and roots, or senescent tissues, e.g. coleoptile of rye seedlings. The data thus suggest that chromatin organization at the level of loop domains possesses dynamic feature, and reflects changes in physiological status of the plant tissues.

Taken together, our data demonstrate that changes in the physiological status of the plant tissues are accompanied by the changes in the pattern excision of DNA loop domains. This suggests that higher order chromatin structure possess a dynamic feature, which varies during development and correlates with the overall metabolic activity of plant tissues. Whether the dynamic feature of the loop domain reflects changes in chromatin accessibility to nuclease, or results from the increase in the enzymatic activity of matrix-associated nucleases needs further elucidation.

Acknowledgements

This work has been partially supported by the grants from INTAS-Ukraine (No. 95-0092) and the Governmental Fund of Fundamental Researches of Ministry of Education and Science of Ukraine (No. 05.07/00219).

References

[1] Solov'yan V.T. and Kunakh V.A., "Fractionation of DNA from eukariotes by pulsed field gel electrophoresis. I. Detection and properties of discrete DNA fragments". *Mol. Biol.* (Moscow), vol. 25(4), p.p. 844-851, 1991.

[2] Solovyan V.T., Andreev I.O. and Kunakh V.A., "Functional organization of plant nuclear DNA. I. Evidence for a DNA-topoisomerase II complex". *Mol. Biol*. (Moscow), vol. 27(6), p.p. 770-774, 1993.

[3] Solovyan V.T. and Andreev I.O., "Structural domains of plant DNA as a constitutive component of the topoisomerase II/DNA complex". *Acta Biochim. Polon*., vol. 42(2), p.p. 201–204, 1995.

[4] Heller C. and Pohl F.M., "Field inversion gel-electrophoresis with different pulse time ramps". *Nucleic Acids Res*., vol. 18(21), p.p. 6299–6304, 1990.

[5] Szabo G., Boldog F. and Wikonkal N., "Disassembly of chromatin into 50 kb units by detergent". *Biochem. Biophys. Res. Commun*., vol. 169(1), p.p. 706-712, 1990.

[6] Filipski J., Leblanc J., Youdale T., Sicorska M. and Walker P.R., "Periodicity of DNA folding in higher order chromatin structure". *EMBO J*., vol. 9(4), p.p. 1319-1327, 1990.

[7] Espinas M.L. and Carballo M., "Pulsed-field gel electrophoresis analysis of higher order chromatin structures of Zea mays. Highly methylated DNA in the 50 kb chromatin structure". *Plant Mol. Biol*., vol. 21, p.p. 847-857, 1993.

[8] Gromova I.I., Nielsen O.F. and Rasin S.V., "Long-range fragmentation of the eukaryotic genome by exogenous and endogenous nucleases proceeds in a specific fashion via preferential DNA cleavage at matrix attachment sites". *J. Biol. Chem*., vol. 270(31), p.p. 18685-18690, 1995.

[9] Paul A.L. and Ferl R.J., "Higher-order chromatin structure: looping long molecules". *Plant Mol Biol*., vol. 41(6), p.p. 713-720, 1999.

[10] Cook P.R. and Brazell I.A., "Conformational constraints in nuclear DNA". *J. Cell Sci*., vol. 22(2), p.p. 287-302, 1976.

[11] Jackson D.A., McCready S.J. and Cook P.R., "Replication and transcription depend on attachment of DNA

to the nuclear cage". *J. Cell Sci. Suppl*., vol. 1, p.p. 59-79, 1984.
[12] Andreev I.O., Spiridonova K.V., Solovyan V.T. and Kunakh V.A., "The endogenous cleavage of nuclear DNA into HMW-DNA fragments during early stages of maize seedlings growth". *Proc. Natl. Acad. Sci. Ukraine*, vol. 1, p.p. 173-177, 2000.
[13] Andreev I.O., Spiridonova K.V., Kunakh V.A. and Solovyan V.T., "Aging and loss of germination in rye seeds is accompanied by a decreased fragmentation of nuclear DNA at loop domain boundaries". *Rus. Journ. Plant Physiol*., vol. 51(2), p.p. 241-248, 2004.
[14] Wang J.C., "DNA Topoisomerases". *Annu. Rev. Biochem*., vol. 65, p.p. 635-692, 1996.
[15] Boulikas T., "Chromatin domains and prediction of MAR sequences". *Int. Rev. Cytol*., vol. 162A, p.p. 279-388, 1995.
[16] Bode J., Stengert-Iber M., Kay V., Schlake T. and Dietz-Pfeilstetter A., "Scaffold/Matrix-attached regions: topological switches with multiple regulatory functions". *Crit. Rev. Eukaryot. Gene*, vol. 6, p.p. 115-138, 1996..

Cell Biology and Instrumentation: UV Radiation, Nitric Oxide and Cell Death in Plants
Y. Blume et al. (Eds.)
IOS Press, 2006

Maintenance of Stomata Function is Required for Containment of Hypersensitive Response

Per MÜHLENBOCK
Department of Botany, Stockholm University,
10405, Stockholm, Sweden

Abstract. Using artificial restriction of gas exchange and pathogen infection we have set out to investigate the role of stomata in biotic stress. Stomata function is imperative for the plant's interaction with its environment. This is widely accepted for abiotic interactions but the stomata functions in biotic interactions are only starting to elucidate. Many plant - pathogen interactions involve a defence system termed the hypersensitive response a kind of programmed cell that increases the plant's resistance against another pathogen attack. Stomata close in response to elicitors and to avirulent bacterial infection. By artificially restricting gas exchange we aim to mimic the effects of closing stomata and to study its effects on development of disease symptoms.

Introduction

Plants have evolved several different strategies to be able to cope with biotic stress. One of these is the development of the hypersensitive response (HR) [1-3]. This programmed cell death response is one of the more efficient of the plant defences against pathogen infection. In the light of a previous study were we investigated the spread of uncontrolled HR in the *lsd1* mutant of *Arabidopsis thaliana*, we hypothesized that stomata conductance is pivotal in the control of the HR integrity. The studies of the cell death mutants *lsd1*, *eds1* and *pad4* had shown that the Runaway Cell Death (RCD) phenotype was associated with a simultaneous decrease in stomata conductance and increase in levels of ROS. [4]

To mimic the effects of closed stomata we devised a simplified approach of restricting stomata gas exchange by blocking stomata openings with inert lanolin wax that proved to induce RCD in the lsd1 mutant together with increased amounts of ROS.

We reasoned that restriction in gas exchange was able to overflow the photorespiration [4] and thereby contributed to an increased sensitivity to the induction and spread of RCD. To assess whether the artificial restriction of gas exchange had an effect on the cell viability in *Arabidopsis thaliana* wild type plants and if gas exchange plays a role in HR we conducted a series of simple experiments based on artificial reduction of gas exchange and *Pseudomonas syringae* infection.

Our preliminary data, presented here, indicate a role of stomata regulation during the hypersensitive response.

For all experiments we grew *Arabidopsis thaliana* plant in SD conditions (8h, 100 μE light and 16 darkness in 21ºC) for 4 to 6 weeks.

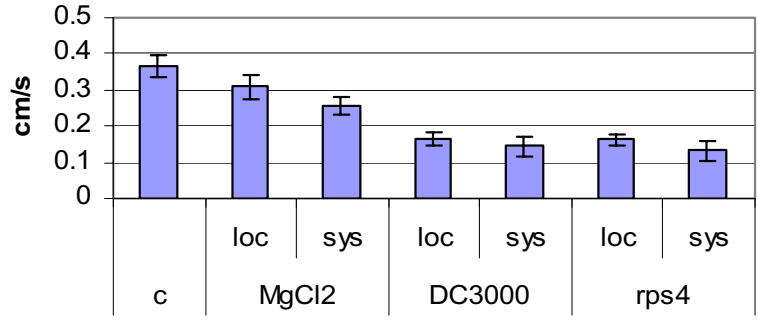

Figure.1. Pathogen infection induces stomata closure in *Arabidopsis*

1. Pathogen infection causes stomata closure

We infected *Arabidopsis thaliana* plants with *Pseudomonas syringae* strains (DC3000 10^5 cfu, avrRPS4 10^6 cfu), as described in Rusterucci *et al,*. 2001. [5-7] 10mM MgCl2 was used as control solution.

Plants infected with virulent (DC3000) and avirulent strains (avrRPS4) of *Pseudomonas syringae* reduced stomata conductance by 50% after 48 hours compared to uninfected plants and reduced stomata conductance significantly compared to plants treated with the control solution containing 10mM $MgCl_2$ (Fig1). The reduction was seen both in infected leaves (local) and in uninfected leaves of the same plant (systemic). Stomata conductance was measured using an AP4 porometer (Delta-T Devices, Cambridge, UK).

2. Reduced gas exchange causes HR-like necrosis

Artificial blocking of stomata openings caused cell death in several focused areas after 48h in *Arabidopsis thaliana* leaves (Fig 2). The lesions, shown here by trypan blue staining, bore a phenotypical resemblance to the hypersensitive cell death like lesions described in Rusterucci *et al*., 2001. [5] Cell necrosis was detected as described in Koch and Suslarenko, 1990. [8] Artificial restriction of gas exchange was achieved by adhering strips of semitransparent tape to abaxial sides of 6 week old *Arabidopsis thaliana* (Col) leaves directly after infection.

3. Reduced gas exchange promotes accumulation of ROS and the spreading of cell death in infected plants

At 48h post infection, combined with restriction of gas exchange there was a clear development of focused lesions in plants infected with the virulent *Pseudomonas syringae*, DC3000 and an uncontrolled spreading of lesions in the avirulent (RPS4) infection (Fig 3). In both cases the phenotype was associated with an increased accumulation of ROS. Detection of Reactive Oxygen Species was performed as described in Mateo et al. 2004, using H_2DCF-DA (Sigma). [4]

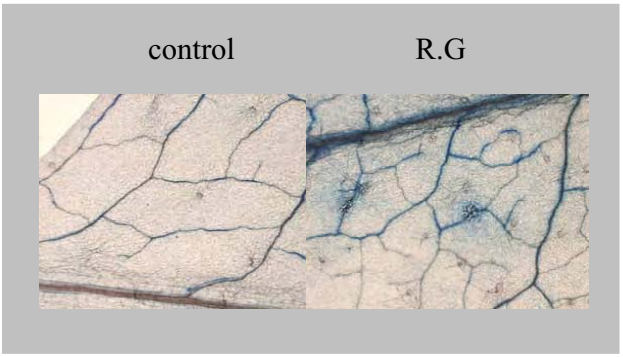

Figure 2. Cell death specific Trypan Blue stain. After 48h of artificially blocking gas exchange focused lesion can be detected.

Our data indicate that when plants induce hypersensitive response, a sufficient amount of gas exchange is important in order to prevent further spread of lesions. We have assessed that stomata closure is induced upon pathogen infection. We observed no difference in stomata conductance between the compatible DC3000 strains and the incompatible (giving rise to HR) RPS4 strains. Restricting gas exchange after infection leads to formation of spot like lesions in the compatible interaction and runaway cell death like lesions in the incompatible interaction. We propose that three things may be happening in the subdermal tissues when plants are exposed to the artificial restriction of gas exchange. Due to rising levels of oxygen and decreased levels of carbon dioxide, photorespiration is overflowed, followed by increased levels of ROS. [4] This is supported by our observation that wild type forms spot like microlesions when gas exchange is limited.

It has been shown that the early phases of the incompatible interaction is preceeded by localized temperature increases and that temperature differences of that magnitude are probable to be the effect of closing stomata. [9] Furthermore it has been proven that in defence responses, plants produce a range of gaseous compounds that serve as either systemic signals or as antimicrobial agents like e.g. NO. [10] We propose that we are not only dealing with the trapping of metabolic substances, such as oxygen and carbon dioxide but also with the trapping of gaseous signals, such as NO or Me JA. It has been shown that NO is required for the development of HR. [3]

In a previous study, presented by Samuilov *et al.,* 2003, it was shown that chloroplasts are involved in CN induced PCD and that the effects of light largely contributes to the spreading of the cell death. In Mateo et al., 2004 we proposed that the mechanism of this function lies in the chloroplasts contribution to ROS signalling. [4, 11]

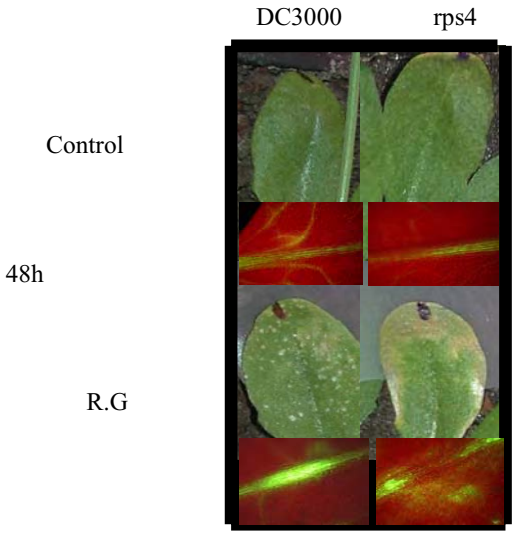

Figure 3. 48 h after infection no visible lesions were detected on infected leaves. When additionally restricting gas (R.G.) exchange lesion formation was clearly detected, accompanied by an increase in ROS formation (H2DCF-DA staining).

The role of light in the regulation of stomata conductance is a widely accepted concept and has contributed to a great deal of the understanding of the physiology behind abiotic stress regulation e.g. senescence and cold acclimation. We will continue this study by analysing the significance and regulation of stomata conductance in biotic interactions. This study suggests that in the combination of abiotic and biotic stress situations, were stomata conductance is known to be affected, a tight control of stomata is required in order to prevent detrimental effects.

Acknowledgments

Acknowledgments are extended to all associates of Professor Stanislaw Karpinski's group at the department of botany, Stockholm University.

References

[1] Dangl J.L. et al., "Death Don't Have No Mercy: Cell Death Programs in Plant-Microbe Interactions". Plant Cell, vol. 8, p.p. 1793-1807, 1996

[2] Hammond-Kosack K.E. and Parker J., "Deciphering plant-pathogen communication: fresh perspectives for molecular resistance breeding". *Curr. Opin. Biotech*., vol. **14,** p.p. 177-193

[3] Lamb C. and Dixon R.A. (1997) The oxidative burst in plant disease resistance. *Annu. Rev. Plant Phys. Plant Mol. Biol.*, vol. 48, p.p. 251-275

[4] Mateo *et al*. "Lesion simulating disease 1 is required for acclimation to conditions that promote excess excitation energy". *Plant Physiol*., vol. 136, p.p. 2818-2830, 2004.

[5] Rustérucci C., Aviv D.H., Holt B.F., Dangl J.L. and Parker J.E., "the disease resistance signaling components EDS1 and PAD4 are essential regulators of the cell death pathway controlled by LSD1 in *Arabidopsis*". *Plant Cell*, vol. 13, p.p. 2211-2224, 2001.
[6] Lee S. et al., "Oligogalacturonic acid and chitosan reduce stomatal aperture by inducing the evolution of reactive oxygen species from guard cells of tomato and *commelina communis*". *Plant Physiol*., vol. 121, p.p. 147-152, 1999.
[7] McDonald K. and Cahill D., "Evidence for a transmissible factor that causes rapid stomatal closure in soybean at sites adjacent to and remote from hypersensitive cell death induced by Phytophthora sojae". *Phys. and Mol. Plant Path.*, vol. 55, p.p. 197-203, 1999.
[8] Koch E. and Suslarenko A., "*Arabidopsis* is susceptible to infection by a downy mildew fungus". *Plant Cell*, vol. 2, p.p. 437-445, 1990.
[9] Chaerle L. et al. "Thermal and chlorophyll-fluorescence imaging distinguish plant-pathogen interactions at an early stage". *Plant Cell Physiol*., vol. 7, p.p. 887-896, 2004.
[10] Delledonne M. et al., "Reactive oxygen intermediates modulate nitric oxide signalling in the plant hypersensitive disease-resistance response". *Plant Physiol. Biochem*., vol. 40, p.p. 605-610, 2002.
[11] Samuilov et al., "Role of chloroplast photosystems II and I in apoptosis of pea guard cells". *Biochemistry* (Moscow), vol. 8, p.p. 912-917, 2003.

Cell Biology and Instrumentation: UV Radiation, Nitric Oxide and Cell Death in Plants
Y. Blume et al. (Eds.)
IOS Press, 2006

High-Scale Analysis of Pathogenicity Determinants of *Potato mop-top virus*

Andrey A. ZAMYATNIN[1,2], Natasha E. YELINA[3], Nina I. LUKHOVITSKAYA[3], Andrey G. SOLOVYEV[3], Anna GERMUNDSSON[2], Maria SANDGREN[2], Sergey Yu. MOROZOV[3], Jari P. T. VALKONEN[2], Eugene I. SAVENKOV[2]
[1] *Natural Sciences Center of A.M.Prokhorov General Physics Institute, Russian Academy of Sciences, Vavilov Str, 38, Bld. L-2, Moscow 119991, Russia*
[2] *Department of Plant Biology and Forest Genetics, Genetics Centre, SLU, S-750 07 Uppsala, Sweden*
[3] *A. N. Belozersky Institute of Physico-Chemical Biology and Department of Virology, Moscow State University, Moscow 119899, Russia*

Abstract. *Potato mop-top virus* (PMTV) is the type member of the genus *Pomovirus* characterized by a tripartite, single-stranded, positive-sense RNA genome. However, PMTV differs from the other pomoviruses by having an open reading frame (ORF) for a 8-kDa cysteine-rich protein (CRP) on RNA 3, downstream the triple gene block. Site-directed mutagenesis of infectious cDNA clones of PMTV showed that the CRP ORF is not needed for the systemic infection in *Nicotiana benthamiana* and several other hosts. CRP of PMTV was not capable of RNA silencing suppression in agroinfiltration tests. However, the expression of CRP using vectors based on *Potato virus X* (PVX) or *Tobacco mosaic virus* (TMV) resulted in necrotic symptoms on *N. benthamiana* and tobacco plants, respectively. Sequencing of PMTV isolates obtained from the field revealed significant sequence variability of the CRP. These data suggest that the functions of CRP may be expressed only in certain hosts or at certain phases of the PMTV infection cycle.

Introduction

Potato Mop-Top Virus (PMTV) is one of the causative agents of potato 'spraing' disease worldwide and induces spraing symptoms (brown rings and arcs) in potato tuber flash [1]. The molecular basis for this type of symptoms has not been identified. There are indications of variation in virulence/pathogenesis between PMTV isolates as tested in indicator plants [2], but molecular basis for that is not understood.

PMTV, a type member of genus *Pomovirus*, consists of tripartite single-stranded RNA genome of positive polarity, organised into 8 ORFs. RNA 1 and RNA 2 encode viral replication and encapsidation/transmission functions, respectively [3, 4]. RNA 3, the smallest RNA in PMTV genome, encodes a triple gene block (TGB) involved in cell-to-cell movement of the virus [5] and a 8K cyctein-rich protein (CRP, ORF4) that in earlier study was reported not to function in virus replication, accumulation, movement or virulence in *Nicotiana benthamiana* host [6]. However, there is no conclusive evidence

that this protein is expressed in infected plants. Another pomovirus *Broad Bean Necrosis Virus* (BBNV) also carry ORF for a small 6K protein [7]. However, this protein does not contain cysteine/histidine motifs resembling zinc-binding domains characteristic for 'zinc-finger' proteins and some regulatory proteins including many viral proteins and transcription factors. Moreover, there is no sequence similarity between BBNV 6K glycin-rich protein and PMTV 8K CRP [7, 8]. Two other pomoviruses BSBV and BVQ do not carry ORF4 on RNA 3 and do not encode CRP similar to the PMTV 8K.

Analysis of the sequences for PMTV CRP from several isolates revealed considerable sequence variability at amino acid level [2] with amino acid sequence identity being as low as 88% when compared Danish and Swedish isolates. However, sequences of CRP from Swedish and Todd (Scottish) isolates appeared to be identical. One of the characteristic features of all sequenced Danish isolates appeared to be the replacement of the AUG start codon of the CRP ORF by GUG start codon. Thus, based on the sequence comparison of different isolates, PMTV CRP can be divided into two groups: Danish type and Swedish type of CRP.

In several virus genera including *Hordei-*, *Peclu-*, *Beny-*, *Furo-* and *Tobraviruses* CRPs were shown to be pathogenesity determinants and appeared to be effective suppressors of host defense mechanism against invading nucleic acids known as RNA silencing [9-11]. However, PMTV CRP has no statistically significant similarity to the aforementioned CRPs.

Despite of the worldwide distribution of PMTV and its high economical impact on modern agriculture, little information is available on virulence variation between isolates and virus pathogenesity determinants. In this study we have shown that the PMTV CRP is a candidate virulence factor of the virus.

1. Sequence analysis of PMTV CRP

Previous amino acid sequence analysis revealed that the CRP is the least conserved PMTV protein [2; our unpublished data]. Alignment of the PMTV CRP sequences available for six virus isolates, Swedish (Sw), Todd and four Danish isolates (D, D54-10, D54-15 and D54-19) [2; our unpublished data], revealed identity of the Sw and Todd isolates and a close relation of the four Danish isolates, which were distant from the Sw and Todd isolates. The most remarkable feature of the Danish isolates is an absence of the CRP initiator AUG codon replaced with GUG encoding Val [2].

To predict probable properties of PMTV CRP, we further analysed its sequence. The central region of the protein was found to be highly hydrophobic, indicating that PMTV CRP could interact with cell membranes.

2. CRP is not essential for PMTV virulence, accumulation, and systemic movement in several hosts.

Re-examination of the pPMTV-3 [6] sequence revealed that ORF for 8K CRP starts with GUG codon instead of AUG and bears Danish type of the CRP. To test whether the type of the CRP influence PMTV infection phenotype in *N. bentamiana*, we obtained recombinant PMTV carrying Swedish type of the CRP by replacing the 8K gene in

pPMTV-3 clone with corresponding sequence from a clone for Swedish isolate using convenient restriction sites. *N. bentamiana* plants inoculated with *in vitro* synthesized RNAs transcribed from the full-length infectious PMTV cDNA clones for RNA1, RNA 2 [6] and new clone for RNA 3 (pPMTV-3-Sw8K) developed symptoms undistinguishable from those induced by a wt inocolum at 14 dpi. DAS-ELISA and Northern blot analysis did not reveal any differences in accumulation of the virus and viral RNA in two types of samples analyzed both in inoculated and systemically infected leaves. Thus, the type of the 8K gene in PMTV genome does not have any effect on virulence, accumulation, and long-distance movement of the virus in *N. bentamiana*.

Previously, it was reported that the presence of CRP ORF is dispensable for systemic virus movement in *N. benthamiana* [6]. To address the possible role of the CRP in systemic virus movement and symptom expression in the hosts other than *N. benthamiana*, PMTV mutant carrying the deletion of CRP cistron [6] was used for inoculation of *Nicotiana debneyi, Nicotiana tabacum* cv. Samsun *and Nicandra physalode.* However, in all experiments no significant differences were found in systemic virus movement and symptom expression of PMTV deletion mutant in comparison to wt virus.

3. PMTV CRP influence on TMV and PVX symptom expression

To study whether PMTV CRP could have an effect on infection phenotypes of representatives of two other plant viral genera, the CRP gene was inserted into engineered cDNAs of *Tobacco mosaic virus* (TMV, genus *Tobamovirus*) and *Potato virus X* (PVX, genus *Potexvirus*).

A TMV-based expression vector TMV30B [12] was modified to give TMV30B[PMTV-CRP] carrying the PMTV CRP gene under control of a subgenomic RNA promoter. As it was reported previously [12], the parental construct TMV30B caused no visible symptoms on the inoculated leaves of *N. benthamiana* and displayed mild mosaic on the systemically infected leaves. TMV30B[PMTV-CRP] was also able to infect *N. benthamiana* leading to the development of localized necroses about 2 mm in diameter on the inoculated leaves at 4 dpi. Later on, these necroses expanded to cover substantial part of the leaf surface. At 7-9 dpi TMV-30B-8K developed mild systemic mosaic closely resembling that caused by TMV-30B. Dot-blot RNA analysis with a PMTV CRP probe failed to detect CRP gene in leaves systemically infected with TMV30B[PMTV-CRP], suggesting that the CRP gene was eliminated from the recombinant viral genome during the viral infection. When the PMTV CRP gene with a translation termination codon six nucleotides downstream of the CRP start codon was introduced into TMV-30B similarly to the native gene, the resulting virus had an infection phenotype similar to that of the parental vector TMV-30B (data not shown), indicating that the observed necrotization of *N. benthamiana* leaves inoculated with TMV30B[PMTV-CRP] resulted from expression of PMTV CRP. To test if the PMTV CRP effect on the recombinant TMV was host-specific, we compared infection patterns of TMV30B and TMV30B[PMTV-CRP] in another tobacco species, *N. tabacum* cv. Samsun (nn). Infection of this host with TMV30B causes mild systemic mosaic [13]. In control plants infected with TMV30B, TMV-specific RNA was readily detected in both the symptomless inoculated leaves and systemic leaves showing mosaic symptoms. In

contrast to TMV30B, leaves inoculated with TMV30B[PMTV-CRP] displayed small necrotic lesions about 1-2 mm in diameter at 4 dpi. RNA blot analysis revealed that TMV30B[PMTV-CRP] is accumulated in the inoculated leaves to lower levels than TMV30B. The upper non-inoculated leaves remained symptomless in most of TMV30B[PMTV-CRP]-infected plants, and TMV RNA was not detected in these leaves. In 20% of plants (4 out of 20 inoculated plants in two repeated experiments), systemic symptoms were observed similar to those produced by TMV30B. In these leaves, TMV was readily detected by RNA blotting, however a CRP-specific probe failed to detect the presence of CRP gene, pointing to its elimination from the recombinant genome during the virus multiplication.

The PMTV CRP gene was inserted into an engineered PVX cDNA to yield a PVX[PMTV-CRP] chimera. This construct was inoculated onto *N. benthamiana* plants, along with PVX used as a control. Systemic infection with PVX caused mild mosaic symptoms on the upper non-inoculated leaves at 7 dpi while the inoculated leaves remained symptomless. In contrast, PVX-8K caused localized necroses on the inoculated *N. benthamiana* leaves at 5 dpi, followed by the development of severe necroses and wilting of the whole upper non-inoculated leaves 9 to 10 dpi. 2 to 3 days later these plants died. This finding suggests that PMTV CRP expressed in the PVX genome dramatically enhances the symptom severity of PVX.

Being considered in total, our data show that despite the PMTV CRP is not capable of RNA silencing suppression in agroinfiltration and cross-protection tests [our unpublished data], it induces necrotization of virus-infected tissues when expressed in the background of PVX and TMV genomes. Our findings as a whole suggest that PMTV CRP is a determinant of viral virulence and this conclusion could not be simply drown from analysis of the PMTV CRP knockouts in *N. benthamiana, N. debneyi, N. tabacum and N. physalode* but rather by conducting comprehensive analysis of the phenotypes induced by expression of the protein from heterologous viruses. Therefore, further studies in potato, a natural host of PMTV, are needed to determine the role of the PMTV 8K CRP in the virus life cycle.

Acknowledgements

Financial support from INTAS (grant 01-2379), the Royal Swedish Academy of Sciences (KVA), the Swedish Research Council for Environment, Agricultural Sciences and Spatial Planning (FORMAS, grant 22.0/2003-0859); Carl Tryggers Stiftelse, Russian Foundation for Basic Research (grant 04-04-49356), and Grant of the President of Russian Federation (MD-130.2003.04) is gratefully acknowledged.

References

[1] Sandgren M., "*Potato mop-top virus* (PMTV): Distribution in Sweden, development of symptoms during storage and cultivar trials in field and glasshouse". *Potato Res*., vol. 38, p.p. 379-389, 1995.

[2] Pečenková T. et al., "Extended sequence analysis of three Danish *Potato mop-top virus* (PMTV) isolates". *Virus Genes*, vol. 29, p.p. 249-255, 2004.

[3] Savenkov E.I. et al,. "Complete sequence of RNA 1 and the presence of tRNA-like structures in all RNAs of *Potato mop-top virus*, genus *Pomovirus*". *J. Gen. Virol*., vol. 80, p.p. 2779-2784, 1999.

[4] Sandgren M. et al. "The readthrough region of *Potato mop-top virus* (PMTV) coat protein encoding RNA, the second largest RNA of PMTV genome, undergoes structural changes in naturally infected and experimentally inoculated plants". *Arch. Virol*., vol. 146, p.p. 467-477, 2001.
[5] Zamyatnin A.A. et al., "Transient coexpression of individual genes encoded by the triple gene block of *Potato mop-top virus* reveals requirements for TGBp1 trafficking". *Mol. Plant-Microbe. Interact*., vol. 17, p.p. 921-930, 2004.
[6] Savenkov E.I. et al., "*Potato mop-top virus*: the coat protein-encoding RNA and the gene for cysteine-rich protein are dispensable for systemic virus movement in *Nicotiana benthamiana*". *J. Gen. Virol*., vol. 84, p.p. 1001-1005, 2003.
[7] Lu X. et al., "The genome organization of the *Broad bean necrosis virus* (BBNV)". *Arch. Virol*., vol. 143, p.p. 1335-1348, 1998.
[8] Savenkov E.I., "Genus *Pomovirus*". In: *The Springer Index of Viruses*, Edited by C.A. Tidona & G. Darai. Heidelberg, Germany: Springer-Verlag, p.p. 1297-1301.
[9] Donald R.G.K. et al., "The *Barley stripe mosaic virus* gamma b gene encodes a multifunctional cysteine-rich protein that affects pathogenesis". *Plant Cell*, vol. 6, p.p. 1593-1606, 1994.
[10] Yelina N.E. et al., "Long-distance movement, virulence, and RNA silencing suppression controlled by a single protein in hordei- and potyviruses: Complementary functions between virus families". *J. Virol*., vol. 76, p.p. 12981-12991, 2002.
[11] Dunoyer P. et al., "Identification, subcellular localization and some properties of a cysteine-rich supressor of gene silencing encoded by *Peanut clump virus*". *Plant J*., vol. 29, p.p. 555-567, 2002.
[12] Shivprasad S. et al., "Heterologous sequences greatly affect foreign gene expression in *Tobacco mosaic virus*-based vectors". *Virology*, vol. 255, p.p. 312-323, 1999.
[13] Li H.W. et al., "Strong host resistance targeted against a viral suppressor of the plant gene silencing defence mechanism". *EMBO J*., vol. 18, p.p. 2683-2691, 1999.

Cell Biology and Instrumentation: UV Radiation, Nitric Oxide and Cell Death in Plants
Y. Blume et al. (Eds.)
IOS Press, 2006

Nitrotyrosination of α-Tubulin: Structural Analysis of Functional Significance in Plants and Animals

Yaroslav B. BLUME, Alexey NYPORKO, Alla YEMETS

Department of Genomics and Biotechnology,
Institute of Cell Biology and Genetic Engineering, National Academy of Sciences of Ukraine, Zabolotnogo str., 148, Kiev, 03143, Ukraine
e-mail address: cellbio@cellbio.freenet.viaduk.net

Abstract. Nitric oxide (NO) is a precursor of reactive nitrating species, peroxynitrite and nitrogen dioxide, which modify proteins to generate oxidized species such as 3-nitrotyrosine that has been used as a hallmark of peroxynitrite-mediated oxidative stress on proteins. A growing body of evidences indicates that NO also regulates a myriad of physiologic responses by modifying tyrosine residues. As a result of these investigations, the cytoskeleton becomes the main cellular fraction containing nitrotyrosinated proteins, and α-tubulin is the major target. 3-Nitrotyrosine is posttranslational incorporated into the carboxyl terminus of the α-tubulin molecule by tubulin-tyrosine ligase. Incorporation is similar to the unmodified tyrosine residue, but is irreversible in comparison to tyrosination/detyrosination. Nitration can occur on animal α-tubulin at sites other than the C-terminus. We positively identify Tyr-161 and Tyr-357 as two specific amino acids endogenously nitrated. Regarding the nitrotyrosination of α--tubulin, we reconstructed the spatial structure of nitrotyrosinated plant α-tubulin isoforms and modeled the possible mechanisms of this posttranslational modification on cellular processes. Reconstruction of α-tubulin from goosegrass, and the redistribution of surface electrostatic charge, revealed that the nitration of Tyr-161 increases the negative electrostatic potential in the lateral contact interface of the molecule (H4-S5 region). The nitration of Tyr-357 results in more significant reorganizations of the molecular surface structure in comparison with nitration of Tyr-161. We can predict the influence of Tyr-357 nitration on the interaction with GTP molecule that is attached to β-tubulin of next dimer. We also assume that nitration of Tyr-161 and 357 can increase their ability to undergo phosphorylation. The results of reconstruction the spatial structure goosegrass α-tubulin with detyrosinated, tyrosinated and nitrotyrosinated C-termini testify that these modifications change substantially the flexibility of the α-tubulin C-terminal domain. The tyrosination increases substantially the mobility of the C-terminus. The breakdown of the tyrosination/detyrosination cycle due to incorporation the nitrotyrosine into C-terminus should resulted in the predominance of short-time living microtubules over long-time living microtubules. The modelling of α-tubulin interaction with MT-binding domain of dynein heavy chain allows us to speculate that nitrotyrosination can influence tubulin-MAP recognition and interaction.

Introduction

Nitric oxide (NO) is one of the 10 smallest molecules in nature and has been a favorite subject of research for chemists, beginning with it s discovery more than 200 years ago. In spite of the intense interest in the biological roles of the nitrogen oxides, it came as a great surprise in the 1980s when a number of investigators demonstrated that not only was NO formed in mammalian cells, but it was involved in an astonishingly large number of

critically important physiological and pathophysiological processes in mammals [5, 10]. These findings prompted researchers to look for the presence of NO in other organisms , and found NO to be a ubiquitous signalling molecule in all living organisms, including bacteria, yeast, and plants [56].

This a highly diffusive gaseous free radical that has been reported to play a key role in plant ethylene emission [26, 34], senescence [9, 22, 35], plant response to drought stress [35], plant disease resistance [11, 12, 15, 16, 20, 21, 33, 46, 57] and plant stress in general [32, 40]. NO was able to reduce the oxidative injury of plants produced by UV-B radiation [38, 54] and it might function as a signalling molecule of ultraviolet-B inhibiting plant growth to carry out stress-signalling transduction [1, 60]. A number of new exciting reports on NO function in germination, growth and reproduction support the view that NO is a "do it all" molecule that plays a crucial role during the entire lifespan of the plant [11, 13].

Recent evidences suggest that key components of animal NO signaling are also operating in plants [11, 12, 15, 16 57, 58]. Plants not only respond to atmospheric nitric oxide, but also possess the capacity to produce nitric oxide enzymatically [17, 32]. Initial investigations into nitric oxide functions suggested that plants use nitric oxide as a signalling molecule via pathways remarkably similar to those found in mammals. These findings complement an emerging body of evidence indicating that many signal transduction pathways are shared between plants and animals. NO can be produced in plants by non-enzymatic and enzymatic systems. The NO-producing enzymes identified in plants are nitrate reductase, and several nitric oxide synthase-like activities, including one localized in peroxisomes which has been biochemically characterized [13, 32]. Recently, two genes of plant proteins with NOS activity have been isolated and characterized for the first time, and both proteins do not have sequence similarities to any mammalian NOS isoform. However, different evidence available indicate that there are other potential enzymatic sources of NO in plants, including xanthine oxidoreductase, peroxidase, cytochrome P450, and some hemeproteins [13]. In plants, the enzymatic production of the signal molecule NO, either constitutive or induced by different biotic/abiotic stresses, may be a much more common event than was initially thought.

Nitric oxide and protein post-translational modifications

In animals, NO functioning as an intra- and intercellular messenger, being involved in several pathophysiological processes including programmed cell death [8, 36, 42, 44, 45, 53], involving signalling via microtubules [24, 25, 31, 51, 59] as important constituent part of cytoskeleton. It was shown that nitric oxide leads to irreversible DNA fragmentation and plant cell death under stressful conditions (mechanical stress), and that its effect can be prevented by inhibitors of NO-synthase [48-50]. Moreover, NO appears to be involved in the pathway(s) leading to the accumulation of transcripts encoding the heat shock proteins, the ethylene-forming enzymes, and cell death.[13, 33].

The pathophysiological actions of NO congeners are primarily rooted in their capacity to alter the function of biological macromolecules through covalent modifications. The formation of nitric oxide in biological systems has led to the discovery of new post-translational protein modifications that could regulate protein functions or potentially be utilized as transducers of nitric oxide signalling. Principal among the nitric oxide-mediated protein modifications are: the nitric oxide-iron heme binding, the S-nitrosylation of reduced cysteine residues, and the C-nitration of tyrosine and tryptophan residues [28]. With the exception of the nitric oxide binding to heme iron proteins, the other two modifications appear to require secondary reactions of nitric oxide and the formation of nitrogen oxides. The most known metabolite generally reflecting *in vivo* production of reactive nitrogen intermediates is the amino acid derivative 3-nitrotyrosine (NO_2Tyr). The significance of

NO_2Tyr *in vivo* was highlighted during last years by observations that protein-linked NO_2Tyr is markedly elevated in a broad range of human diseases and clinical disorders [27, 28].

Analyses of NO-dependent processes in animal systems have demonstrated protein S-nitrosylation of cysteine and C-nitration of tyrosine residues to be placed among of the dominant regulation mechanisms for many animal proteins. The rapid development of analytical and immunological methodologies has allowed for the quantification of S-nitrosylated and C-nitrated proteins in vivo revealing an apparent selectivity and specificity of the proteins modified [27, 28]. S-nitrosylated [37] and C-nitrated [30] proteins were found recently in plant material even among cytoskeletal proteins (actin). The results imply that the varied nitration of tyrosine residues in proteins/enzymes may occur as a post-translational modification in vivo, and such discriminative nitration may be vital in PN/NO-regulated signal transduction cascade. The functional consequences of protein nitration are manifold: the impact is mainly on the structural and conformational properties and catalytic activity but noticeable effects include a decreased effectiveness as tyrosine kinase substrates [41].

Although protein tyrosine nitration is a low-yield process in vivo, 3-nitrotyrosine has been revealed as a relevant biomarker of NO-dependent oxidative stress; additionally, site-specific nitration focused on particular protein tyrosines may result in modification of function and promote a biological effect [52]. Tissue distribution and quantitation of nitrated proteins, recognition of their functional role at different functional states can open new avenues for the understanding and treatment of different pathologies. It was shown that free NO_2Tyr is taken up by mammalian cells and irreversibly incorporated into α-tubulin - but no other protein - via a posttranslational mechanism catalyzed by tubulin-tyrosine ligase, a process that alters microtubule function [18]. Later was shown that the in vivo tyrosine nitration of such cytoskeletal proteins as actin and α-tubulin is most common for animal tissues [9] and α-tubulin can be identified as as the major target of nitration [6].

Nitrotyrosination of α-tubulin: prediction of potential functional role based on structural modelling

Although it was shown firstly that free NO_2Tyr is incorporated into C-terminus of α-tubulin [18] via irreversible posttranslational mechanism catalyzed by tubulin-tyrosine ligase [29], the results about reversibility and not detrimental role to dividing cells were obtained [2]. Quite later using Western blotting and matrix-assisted laser desorption/ionization-time of flight analysis, was shown, both in vivo and in vitro, that nitration can occur on α-tubulin at sites other than the C-terminus: at Tyr-161 and Tyr-357 [55].

Comparative alignment of α-tubulin sequences from different plants and animals has shown the high conservativity of tyrosine residues in 161 and 357 positions and amino acid motives which contain these residues (Fig. 1). Consequently, we can assume the existence of common mechanisms for tyrosine nitration for α-tubulins from plants as well as animals. To investigate potential spatial effects of nitrotyrosination of these residues we used 3-D model of α-tubulin from goosegrass (*Eleusine indica* (L.) Gaerth.) [4] with introduction of nitrogroups in respective positions (Fig. 2). It is obviously that Tyr-161 is localized on the lateral contact interface of α-tubulin (H4-S5 region). The nitration of the residue results in increase of negative electrostatic potential in this area and, accordingly, can modify processes of interaction between tubulin protofilaments. Tyr-357 is located in immediate proximity to interdimer contact residues Ala-247, Val-324, Pro-325. The nitration of Tyr-357 results in more significant reorganizations of molecular surface structure in comparison with nitration of Tyr-161. Moreover such reorganization does not disrupt of interdimer

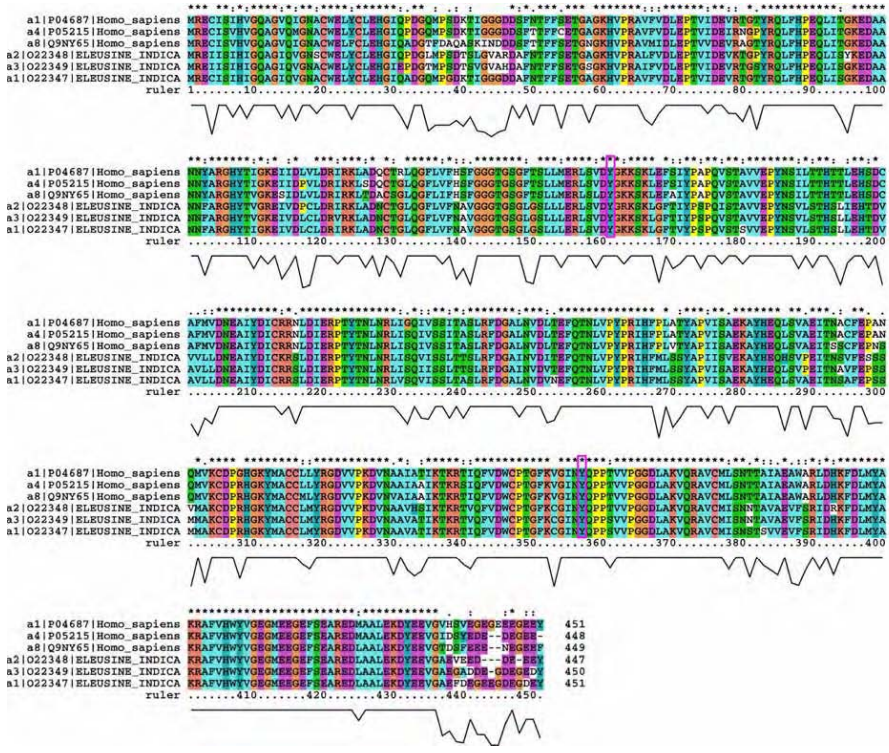

Figure 1. Alignment of α-tubulin sequences from human and goosegrass (*Eleusine indica*)

surface structure. However, we can predict the influence of the nitration of Tyr-357on the interaction with GTP molecule that is attached to β-tubulin of next dimer, because of above mentioned contact residues are involved in this interactive process. Also we can assume that nitration of Tyr161 and 357 can increase their ability to undergo a phosphorylation. Respectively the nitration of these two residues can have impact on assembly of microtubules and dynamics of microtubules, including, for example degradation of tubulin [47]. For example, it was proposed that nitric oxide-mediated α-tubulin posttranslational nitrotyrosination may be a major mechanism through which cytokine, TNF-alpha, exerts its tumor-selective cytotoxic effects in certain cancers [24]. It was shown, too, that motor neuron apoptosis might be induced by free 3-nitro-L-tyrosine via incorporation into α-tubulin [51] as well as apoptosis in colorectal carcinoma cells [31] and this modification can be considered as “last check point” apoptotic step [25].

However, α-tubulin C-terminal nitrotyrosination results in an appearance of some changes in animal cell morphology and their microtubule organization, a loss of some cellular functions, and in intracellular redistribution of cytoplasmic dynein [18]. As it was mentioned above incorporation of 3-nitrotyrosine into the C-terminus of α-tubulin is not detrimental to dividing cells [2]. In animal cells alteration of the C-terminal amino acid of α-tubulin via nitrotyrosination specifically inhibits myogenic differentiation [7]. Our results on reconstruction of the spatial tubulin structure demonstrate that substitution of C-terminal tyrosine by 3-nitrotyrosine has very specific effects on conformation and flexibility of C-

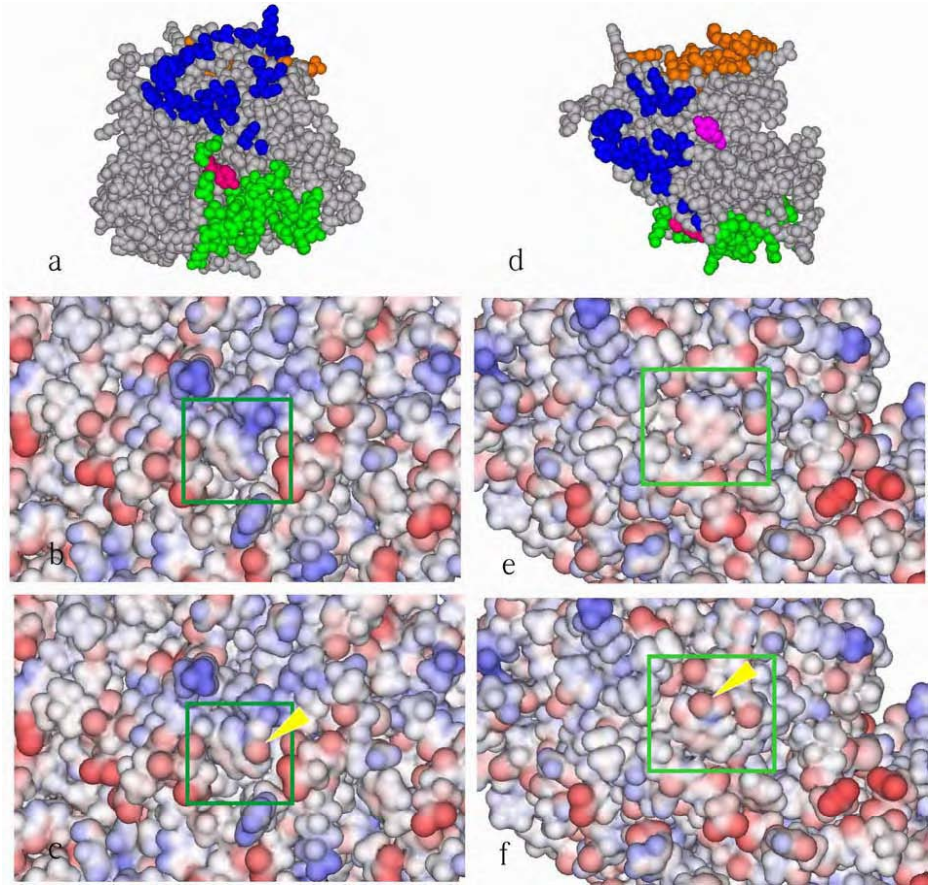

Figure 2. View of goosegrass α-tubulin molecule from surface location of Tyr-161 (a-c) and Tyr-357 (d-**f):**
a, d – Whole molecule models with marked location of Tyr-161 (red) and Tyr-357 (pink). Amino acid residues involved in lateral contacts are indicated as green, involved in interdimer contacs are indicated as blue, involved in GTP interaction are indicated as brown;
b, e – Distribution of electrostatic charges on α-tubulin surface (positive charge – blue, negative – red) near Tyr-161 and Tyr-357, respectively (location of the residues is marked by a frames);
c, f - Redistribution of electrostatic charges on α-tubulin surface after nitration of Tyr-161 and Tyr-357, respectively (NO_2Tyr are indicated by yellow arrows).

terminal part of investigated molecule [3]. The results of reconstruction the spatial structure of detyrosinated, tyrosinated and nitrotyrosinated goosegrass (*Eleusine indica* (L.) Gaerth.) α-tubulin forms, and of their behavior investigations, testify that these modifications change substantially the level of mobility of flexible α-tubulin C-terminal domain (Fig. 3). The last 10-12 amino acid residues of α-tubulin C-terminal region, unlike the main part of the molecule, form a free oscillating tail that can be considered as individual structural domain. Respectively, it was found that tyrosination increases substantially the mobility of C-terminus of goosegrass α-tubulin (Fig. 1b).

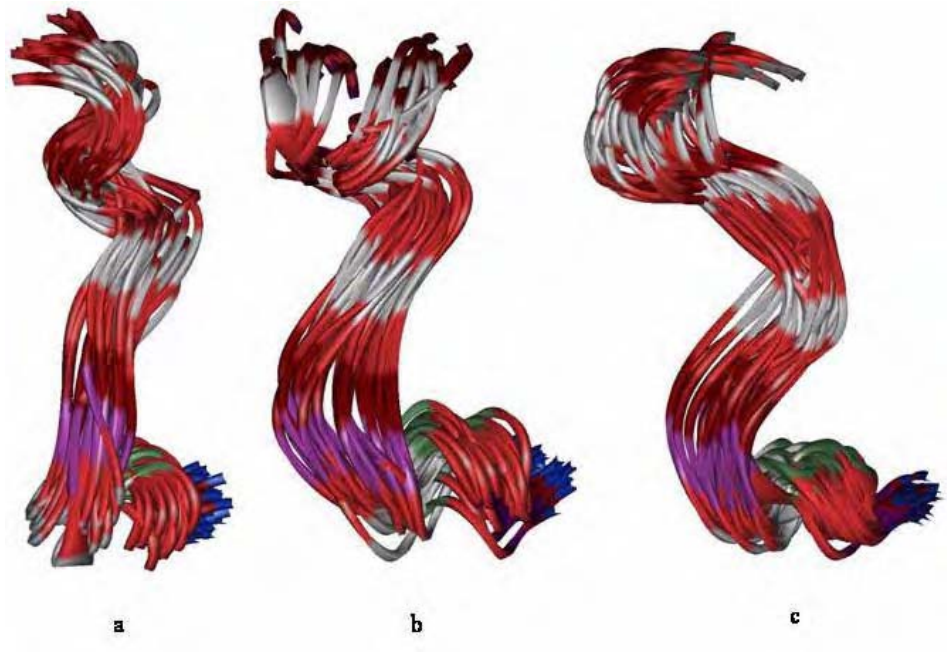

Figure 3. Modelling of different allowed conformation of C-terminal tails of α-tubulin from goosegrass: a - Detyrosinated molecule; b - Tyrosinated molecule; c - Nitrotyrosinated molecule

The root mean square deviation (RMSD) in coordinates of amino acid residues composing this region grows from 0.48 A for detyrosinated form, to 0.55 A for tyrosinated α-tubulin as was calculated on the basis of molecular fluctuations trajectory in 500 psec interval. These results correlate with data about predomination of detyrosinated α-tubulin in long-time living microtubules and *vice versa* [7]. The breakdown of tyrosination/detyrosination cycle due to incorporation the nitrotyrosine into C-terminus should be resulted in predomination of short-time living microtubules over long-time living microtubules. It is necessary to note that mobility of nitrotyrosinated terminus is lower than tyrosinated one, but it is higher than detyrosinated. In last case RMSD consists 0.52 A. It can lead to appearance of microtubules with certain "intermediate" life-time and, as consequence, to modifying of the microtubules organization in living cells.

It is known that tubulin C-terminal region is responsible for interactions with structural and motor MAPs (dynein and kinesin) [43]. In combination with the above mentioned data about redistribution of cytoplasmic dynein after nitrotyrosination of α-tubulin [18] we can speculate that nitrotyrosination can influence on processes of tubulin-MAP recognition and interaction. This assumption is confirmed by our results on modeling of α-tubulin interaction with MT-binding domain of dynein heavy chain [3]. The high content of dicarboxy amino acid residues, especially glutamate residues, is the hallmark of flexible C-terminal region of both tubulin subunits. It has to be correlated with necessity of presence a surface enriched with diamino acid residues in dynein MT-binding domain structure. The surface of dynein MT-binding domain formed by residues Lys-148, Lys-151, Lys-154, Lys-155, Arg-162, Lys-287, Lys-300, Arg-327, Lys-328 is correspondent to this factor. The surface is flanked by residues Asp-144, Asp-146 and Asp-320, Asp-321 from both sides. The nitrogroup, included into nitrotyrosine, possesses an additional negative

charge, that is not typical for dynein-tubulin interaction, and locates closely to flanking residues. This location results in strong decreasing of the affinity between dynein contact surface and α-tubulin C-terminal region. These results support the idea that nitrotyrosination of C-terminus of α-tubulin can change the effectiveness of tubulin interaction with motor proteins and with structural MAPs.

Concluding remarks

Up to now it was found that both in vivo and in vitro, that nitration can occur on α-tubulin at sites other than the C-terminus and Tyr 161 and Tyr 357 were positively identified as two specific amino acids endogenously nitrated in animal cells. Taking into account the conservativity of the parts of tubulin molecules with nitrotyrosinated sites in plant and animals, the results of reconstruction the spatial structure of α-tubulin from goosegrass and redistribution of surface electrostatic charge revealed that the nitration of Tyr-161 increases negative electrostatic potential in the lateral contact interface of the molecule (H4-S5 region). The nitration of Tyr-357 results in more significant reorganizations of molecular surface structure in comparison with nitration of Tyr-161.

We can suppose the influence of Tyr-357 nitration on the interaction with GTP molecule that is attached to β-tubulin of next dimer. Also it is possible to assume, that nitration of Tyr-161 and 357 can increase their ability to undergo a phosphorylation. The results of reconstruction the spatial structure goosegrass α-tubulin with detyrosinated, tyrosinated and nitrotyrosinated C-termini testify that these modifications change substantially the level of flexibility of α-tubulin C-terminal domain. The tyrosination increases substantially the mobility of C-terminus. The breakdown of tyrosination/detyrosination cycle due to incorporation the nitrotyrosine into C-terminus should resulted in predomination of short-time living microtubules over long-time living microtubules. The modelling of α-tubulin interaction with MT-binding domain of dynein heavy chain allows us to speculate that nitrotyrosination can influence tubulin-MAP recognition and interaction. Overall, these results point to a novel potential physiologic role of NO and free 3-nitrotyrosine in the control of the α-tubulin molecular properties.

References

[1] An L, Liu Y, Zhang M, Chen T, Wang X (2005) Effects of nitric oxide on growth of maize seedling leaves in the presence or absence of ultraviolet-B radiation. J Plant Physiol 162: 317-326

[2] Bisig CG, Purro SA, Contin MA, Barra HS, Arce CA (2002) Incorporation of 3-nitrotyrosine into the C-terminus of alpha-tubulin is reversible and not detrimental to dividing cells. Eur J Biochem 269: 5037-5045

[3] Blume YaB, Nyporko A, Demchuk O (2005) Nitrotyrosination of plant α-tubulin: potential mechanisms of influence on cellular processes. BMC Plant Biol 5 (Suppl 1): S26 doi:10.1186/1471-2229-5-S1-S26

[4] Blume YaB, Nyporko AYu, Yemets AI, Baird WV (2003). Structural modeling of plant alpha-tubulin interaction with dinitroanilines and phosphoroamidates. Cell Biol Intl 27: 171-174.

[5] Bredt DS, Snyder SH (1994) Nitric oxide: a physiologic messenger molecule. Annu Rev Biochem 63: 175-195

[6] Cappelletti G, Maggioni MG, Tedeschi G, Maci R. (2003) Protein tyrosine nitration is triggered by nerve growth factor during neuronal differentiation of PC12 cells. Exp Cell Res. 288: 9-20

[7] Chang W, Webster DR, Salam AA, Gruber D, Prasad A, Eiserich JP, Bulinski JC (2002) Alteration of the C-terminal amino acid of tubulin specifically inhibits myogenic differentiation. J Biol Chem. 277: 30690-30698

[8] Cheng A, Chan SL, Milhavet O, Wang S, Mattson MP (2001) p38 MAP kinase mediates nitric oxide-induced apoptosis of neural progenitor cells. J Biol Chem 276: 43320-43327

[9] Corpas FJ, Barroso JB, Carreras A, Quiros M, Leon AM, Romero-Puertas MC, Esteban FJ, Valderrama R, Palma JM, Sandalio LM, Gomez M, del Rio LA (2004) Cellular and subcellular localization of endogenous nitric oxide in young and senescent pea plants. Plant Physiol 136: 2722-2733

[10] Davis KL, Martin E, Turko IV, Murad F (2001) Novel effects of nitric oxide. Annu Rev Pharmacol Toxicol 41: 203 - 236
[11] Delledonne M (2005) NO news is good news for plants. Curr Opin Plant Biol 8: 390-396
[12] Delledonne M, Xia Y, Dixon RA, Lamb C (1998) Nitric oxide functions as a signal in plant disease resistance. Nature. 394: 585-588
[13] del Rio LA, Corpas FJ, Barroso JB (2004) Nitric oxide and nitric oxide synthase activity in plants. Phytochemistry 65: 783-792
[14] Durner J, Gow AJ, Stamler JS, Glazebrook J. (1999) Ancient origins of nitric oxide signaling in biological systems. Proc Natl Acad Sci USA. 96: 14206-14207
[15] Durner J, Klessig DF. (1999) Nitric oxide as a signal in plants. Curr Opin Plant Biol 2: 369-374
[16] Durner J, Wendehenne D, Klessig DF (1998) Defense gene induction in tobacco by nitric oxide, cyclic GMP, and cyclic ADP-ribose. Proc Natl Acad Sci USA. 95: 10328-10333
[17] Durzan DJ, Pedroso MC (2002) Nitric oxide and reactive nitrogen oxide species in plants. Biotechnol Genet Eng Rev 19: 293-337
[18] Eiserich JP, Estevez AG, Bamberg TV, Ye YZ, Chumley PH, Beckman JS, Freeman BA (1999) Microtubule dysfunction by posttranslational nitrotyrosination of alpha-tubulin: a nitric oxide-dependent mechanism of cellular injury. Proc Natl Acad Sci USA 96: 6365-6370
[19] Giannopoulou E, Katsoris P, Polytarchou C, Papadimitriou E (2002) Nitration of cytoskeletal proteins in the chicken embryo chorioallantoic membrane. Arch Biochem Biophys. 400: 188-198
[20] Gilchrist DG (1998) Programmed cell death in plant disease: the purpose and promise of cellular suicide. Annu Rev Phytopathol 36:393-414
[21] Hausladen A, Stamler JS (1998) Nitric oxide in plant immunity. Proc Natl Acad Sci USA. 95: 10345-10347
[22] Hung KT, Kao CH (2003) Nitric oxide counteracts the senescence of rice leaves induced by abscisic acid. J Plant Physiol 160: 871-879
[23] Hung KT, Kao CH (2004) Nitric oxide acts as an antioxidant and delays methyl jasmonate-induced senescence of rice leaves. J Plant Physiol 161: 43-52
[24] Idriss HT (2000) Do TNF-alpha-insensitive cancer cells escape alpha-tubulin nitrotyrosination? Nitric Oxide 4: 1-3
[25] Idriss HT (2004) Three steps to cancer: how phosphorylation of tubulin, tubulin tyrosine ligase and P-glycoprotein may generate and sustain cancer. Cancer Chemother Pharmacol 54: 101-104
[26] Igamberdiev AU, Baron K, Manac'h-Little N, Stoimenova M, Hill RD (2005) The haemoglobin/nitric oxide cycle: involvement in flooding stress and effects on hormone signalling. Ann Bot Jul 18
[27] Ischiropoulos H (1998) Biological tyrosine nitration: a pathophysiological function of nitric oxide and reactive oxygen species. Arch Biochem Biophys 356:1-11
[28] Ischiropoulos H (2003) Biological selectivity and functional aspects of protein tyrosine nitration. Biochem Biophys Res Commun 305: 776-783
[29] Kalisz HM, Erck C, Plessmann U, Wehland J (2000) Incorporation of nitrotyrosine into α-tubulin by recombinant mammalian tubulin-tyrosine ligase. Biochim Biophys Acta 1481: 131-138
[30] Kuo WN, Kreahling JM, Shanbhag VP, Shanbhag PP, Mewar M (2000) Protein nitration. Mol Cell Biochem 214: 121-129
[31] Laguinge LM, Lin S, Samara RN, Salesiotis AN, Jessup JM (2004) Nitrosative stress in rotated three-dimensional colorectal carcinoma cell cultures induces microtubule depolymerization and apoptosis. Cancer Res 64: 2643-2648
[32] Lamattina L, Garcia-Mata C, Graziano M, Pagnussat G (2003) Nitric oxide: the versatility of an extensive signal molecule. Annu Rev Plant Biol 54: 109-136
[33] Lamotte O, Gould K, Lecourieux D, Sequeira-Legrand A, Lebrun-Garcia A, Durner J, Pugin A, Wendehenne D (2004) Analysis of nitric oxide signaling functions in tobacco cells challenged by the elicitor cryptogein. Plant Physiol. 135: 516-529
[34] Leshem YY, Haramathy E (1996) The characterization and contrasting effects of the nitric oxide free radical in vegetative stress and senescence of *Pisum sativum* Linn. foliage. J Plant Physiol 148: 258-263
[35] Leshem YY, Wills RBH, Ku VVV (1998) Evidence for the function of the free radical gas - nitric oxide - as an endogenous maturation and senescence regulating factor in higher plants. Plant Physiol Biochem 36: 825-833
[36] Li CQ, Trudel LJ, Wogan GN (2002) Nitric oxide-induced genotoxicity, mitochondrial damage, and apoptosis in human lymphoblastoid cells expressing wild-type and mutant p53. Proc Natl Acad Sci USA 99: 10364-10369
[37] Lindermayr C, Saalbach G, Durner J (2005) Proteomic identification of S-nitrosylated proteins in *Arabidopsis*. Plant Physiol. 137: 921-930
[38] Mackerness SAH, John CF, Jordan B, Thomas B (2001) Early signaling components in ultraviolet-B responses : distinct roles for different reactive oxygen species and nitric oxide. FEBS Lett 489: 237-242
[39] Magalhaes JR, Monte DC, Durzan DJ (2000) Nitric oxide and ethylene emission in *Arabidopsis thaliana*. Physiol Mol Biol Plants 6: 117-127

[40] Magalhaes JR, Pedroso MC, Durzan DJ (1999) Nitric oxide, apoptosis and plant stresses. Physiol Plant Mol Biol 5: 115-125
[41] Martin BL, Wu D, Jakes S, Graves DJ (1990) Chemical influences on the specificity of tyrosine phosphorylation. J Biol Chem. 265: 7108-7111
[42] McLaughlin LM, Demple B (2005) Nitric oxide-induced apoptosis in lymphoblastoid and fibroblast cells dependent on the phosphorylation and activation of p53. Cancer Res 65: 6097-6104
[43] Mizuno N, Toba S, Edamatsu M, Watai-Nishii J, Hirokawa N, Toyoshima YY, Kikkawa M (2004) Dynein and kinesin share an overlapping microtubule-binding site. EMBO J 23: 2459-2467
[44] Moncada S, Erusalimsky JD (2002) Does nitric oxide modulate mitochondrial energy generation and apoptosis? Nat Rev Mol Cell Biol 3: 214-220
[45] Murphy MP (1999) Nitric oxide and cell death. Biochim Biophys Acta. 1411: 401-414
[46] Orozco-Cárdenas ML, Ryan CA (2002) Nitric oxide negatively modulates wound signaling in tomato plants. Plant Physiol 130: 487-493
[47] Palumbo A, Fiore G, Di Cristo C, Di Cosmo A, d'Ischia M (2002) NMDA receptor stimulation induces temporary alpha-tubulin degradation signaled by nitric oxide-mediated tyrosine nitration in the nervous system of *Sepia officinalis*. Biochem Biophys Res Commun. 293: 1536-1543
[48] Pedroso MC, Durzan DJ (2000) Effect of different gravity environments on DNA fragmentation and cell death in *Kalanchoe* leaves. Ann Bot (Lond) 86: 983-994
[49] Pedroso MC, Magalhaes JR, Durzan D (2000) A nitric oxide burst precedes apoptosis in angiosperm and gymnosperm callus cells and foliar tissues. J Exp Bot. 51: 1027-1036
[50] Pedroso MC, Magalhaes JR, Durzan D (2000) Nitric oxide induces cell death in *Taxus* cells. Plant Sci 157: 173-180
[51] Peluffo H, Shacka JJ, Ricart K, Bisig CG, Martinez-Palma L, Pritsch O, Kamaid A, Eiserich JP, Crow JP, Barbeito L, Estevez AG (2004) Induction of motor neuron apoptosis by free 3-nitro-L-tyrosine. J Neurochem 89: 602-612
[52] Radi R (2004) Nitric oxide, oxidants, and protein tyrosine nitration. Proc Natl Acad Sci USA 101: 4003-4008
[53] Sarker KP, Biswas KK, Rosales JL, Yamaji K, Hashiguchi T, Lee KY, Maruyama I (2003) Ebselen inhibits NO-induced apoptosis of differentiated PC12 cells via inhibition of ASK1-p38 MAPK-p53 and JNK signaling and activation of p44/42 MAPK and Bcl-2. J Neurochem 87: 1345-1353
[54] Shi S, Wang G, Wang Y, Zhang L, Zhang L (2005) Protective effect of nitric oxide against oxidative stress under ultraviolet-B radiation. Nitric Oxide 13: 1-9
[55] Tedeschi G, Cappelletti G, Negri A, Pagliato L, Maggioni MG, Maci R, Ronchi S (2005) Characterization of nitroproteome in neuron-like PC12 cells differentiated with nerve growth factor: identification of two nitration sites in alpha-tubulin. Proteomics 5: 2422-2432
[56] Torreilles J (2001) Nitric oxide: one of the more conserved and widespread signaling molecules. Front Biosci 6: D1161-1172
[57] Van Camp W, Van Montagu M, Inze D (1998) H_2O_2 and NO: redox signals in desease resistance. Trends Plant Sci. 3: 330-334.
[58] Wendehenne D, Pugin A, Klessig DF, Durner J (2001) Nitric oxide: comparative synthesis and signaling in animal and plant cells. Trends Plant Sci 6: 177-183
[59] Zedda M, Lepore G, Gadau S, Manca P, Farina V (2004) Morphological and functional changes induced by the amino acid analogue 3-nitrotyrosine in mouse neuroblastoma and rat glioma cell lines. Neurosci Lett 363: 190-193
[60] Zhang M, An L, Feng H, Chen T, Chen K, Liu Y, Tang H, Chang J, Wang X (2003) The cascade mechanisms of nitric oxide as a second messenger of ultraviolet B in inhibiting mesocotyl elongations. Photochem Photobiol 77: 219-225

This page intentionally left blank

Cell Biology and Instrumentation: UV Radiation, Nitric Oxide and Cell Death in Plants
Y. Blume et al. (Eds.)
IOS Press, 2006

Subject Index

This page intentionally left blank

Cell Biology and Instrumentation: UV Radiation, Nitric Oxide and Cell Death in Plants
Y. Blume et al. (Eds.)
IOS Press, 2006

Author Index

This page intentionally left blank

This page intentionally left blank